MOLECULAR NETWORK STUDY OF PITUITARY ADENOMAS

EDITED BY: Xianquan Zhan and Dominic M. Desiderio
PUBLISHED IN: Frontiers in Endocrinology

frontiers Research Topics

frontiers

ISSN 1664-8714
ISBN 978-2-88963-602-0
DOI 10.3389/978-2-88963-602-0

About Frontiers

Frontiers is more than just an open-access publisher of scholarly articles: it is a pioneering approach to the world of academia, radically improving the way scholarly research is managed. The grand vision of Frontiers is a world where all people have an equal opportunity to seek, share and generate knowledge. Frontiers provides immediate and permanent online open access to all its publications, but this alone is not enough to realize our grand goals.

Frontiers Journal Series

The Frontiers Journal Series is a multi-tier and interdisciplinary set of open-access, online journals, promising a paradigm shift from the current review, selection and dissemination processes in academic publishing. All Frontiers journals are driven by researchers for researchers; therefore, they constitute a service to the scholarly community. At the same time, the Frontiers Journal Series operates on a revolutionary invention, the tiered publishing system, initially addressing specific communities of scholars, and gradually climbing up to broader public understanding, thus serving the interests of the lay society, too.

Dedication to Quality

Each Frontiers article is a landmark of the highest quality, thanks to genuinely collaborative interactions between authors and review editors, who include some of the world's best academicians. Research must be certified by peers before entering a stream of knowledge that may eventually reach the public - and shape society; therefore, Frontiers only applies the most rigorous and unbiased reviews.
Frontiers revolutionizes research publishing by freely delivering the most outstanding research, evaluated with no bias from both the academic and social point of view. By applying the most advanced information technologies, Frontiers is catapulting scholarly publishing into a new generation.

What are Frontiers Research Topics?

Frontiers Research Topics are very popular trademarks of the Frontiers Journals Series: they are collections of at least ten articles, all centered on a particular subject. With their unique mix of varied contributions from Original Research to Review Articles, Frontiers Research Topics unify the most influential researchers, the latest key findings and historical advances in a hot research area! Find out more on how to host your own Frontiers Research Topic or contribute to one as an author by contacting the Frontiers Editorial Office: researchtopics@frontiersin.org

MOLECULAR NETWORK STUDY OF PITUITARY ADENOMAS

Topic Editors:
Xianquan Zhan, Shandong First Medical University, China; Xiangya Hospital, Central South University, China
Dominic M. Desiderio, University of Tennessee Health Science Center (UTHSC), United States

Citation: Zhan, X., Desiderio, D. M., eds. (2020). Molecular Network Study of Pituitary Adenomas. Lausanne: Frontiers Media SA. doi: 10.3389/978-2-88963-602-0

Table of Contents

frontiers in Endocrinology

EDITORIAL
published: 18 February 2020
doi: 10.3389/fendo.2020.00026

Editorial: Molecular Network Study of Pituitary Adenomas

Xianquan Zhan [1,2,3,4,5]* *and Dominic M. Desiderio* [6]

[1] University Creative Research Initiatives Center, Shandong First Medical University, Shandong, China, [2] Key Laboratory of Cancer Proteomics of Chinese Ministry of Health, Xiangya Hospital, Central South University, Changsha, China, [3] State Local Joint Engineering Laboratory for Anticancer Drugs, Xiangya Hospital, Central South University, Changsha, China, [4] Department of Oncology, Xiangya Hospital, Central South University, Changsha, China, [5] National Clinical Research Center for Geriatric Disorders, Xiangya Hospital, Central South University, Changsha, China, [6] The Charles B. Stout Neuroscience Mass Spectrometry Laboratory, Department of Neurology, College of Medicine, University of Tennessee Health Science Center, Memphis, TN, United States

Keywords: pituitary adenoma, signaling pathway, molecular network, multi-omics, personalized medicine, precision medicine, therapeutic target, molecule-panel biomarker

Editorial on the Research Topic

Molecular Network Study of Pituitary Adenomas

Pituitary adenoma is a common intracranial tumor that occurs in the pituitary gland that seriously affects the hypothalamus–pituitary–targeted organ axis system (1–3), and it is also a chronic, complex, and whole-body disease, with multiple causing factors, multiple processes, and multiple consequences (4, 5). It is very difficult to use any single molecule as biomarker to clarify its molecular mechanisms, and to predict, prevent, diagnose, and treat a pituitary adenoma (5–9). Rapidly developed multi-omics and systems biology affect treatment of pituitary adenomas and change the paradigms from the traditional single-factor strategy to a multi-parameter systematic strategy (5, 9–11). A series of molecular alterations at different levels of genes (genome), RNAs (transcriptome), proteins (proteome), peptides (peptidome), metabolites (metabolome), and imaging characteristics (radiome) that resulted from exogenous and endogenous carcinogens are involved in pituitary tumorigenesis, and mutually associate and function in a molecular network system (4, 5, 10, 11). Molecular network alterations are the hallmark of, and play central roles in, pituitary pathogenesis (12, 13). A key molecule-panel biomarker that is derived from a molecular network is necessary for accurate clinical practice of a pituitary adenoma (13). The modern multi-omics, computation biology, and systems biology technologies lead to the possibility of recognizing really reliable molecular-panel biomarkers for research and clinical practice in pituitary adenomas.

This present issue mainly focuses on the molecular network study of pituitary adenomas, which contains 14 topics: (i) The first topic addressed the idea that a tyrosine kinase inhibitor, imatinib, inhibited growth hormone (GH) secretion signaling via the PDGFR-β pathway, but did not affect cell viability and apoptosis, which might be used as an adjunct therapy to treat GH-secreting pituitary adenomas (Gupta et al.). These data clearly demonstrate the importance of GH signaling pathway-based therapeutic treatment in GH-secreting pituitary adenomas. (ii) The second topic addressed the notion that the pattern change of six prolactin (PRL) proteoforms existed among five subtypes of pituitary adenomas, and different hPRL proteoforms might function in different PRL receptor-signaling pathways, which clearly demonstrates the importance and clinical value of PRL receptor-signaling pathway-based PRL proteoform pattern study in human pituitaries and pituitary adenomas (Qian, Yang et al.). (iii) The third topic addressed the integration of proteomics and metabolomics to reveal metabolite–protein networks in adrenocorticotropic hormone (ACTH)-secreting pituitary adenomas (Feng et al.). Proteomic and metabolomic variations are a precious resource to clarify disease mechanisms and determine effective biomarkers

OPEN ACCESS

Edited and reviewed by:
Maria Fleseriu,
Oregon Health & Science University, United States

***Correspondence:**
Xianquan Zhan
yjzhan2011@gmail.com

Specialty section:
This article was submitted to Pituitary Endocrinology, a section of the journal Frontiers in Endocrinology

Received: *09 December 2019*
Accepted: *14 January 2020*
Published: *18 February 2020*

Citation:
Zhan X and Desiderio DM (2020) Editorial: Molecular Network Study of Pituitary Adenomas. Front. Endocrinol. 11:26. doi: 10.3389/fendo.2020.00026

(14). This topic emphasized the importance of the protein–metabolite joint pathway analysis and revealed glycolysis/gluconeogenesis, pyruvate metabolism, citrate cycle (TCA cycle), fatty acid metabolism, and Myc signaling pathways in ACTH-secreting pituitary adenomas. (iv) The fourth topic addressed estrogen signaling pathway-mediated sex difference in lactotroph tumor aggressiveness and discovered a number of estrogen receptor (ER)-related candidate genes as target molecules for sex-specific aggressive behavior in male lactotroph tumors (Wierinckx et al.). (v) The fifth topic addressed metabolomics as a promising approach to pituitary adenomas (Pînzariu et al.). Pituitary adenoma is an endocrine- and metabolic-related disease. Some metabolites have been studied; however, real metabolomics has not been extensively carried out in pituitary adenomas. (vi) The sixth topic addressed the new progress on different pathway mechanisms of dopamine and dopamine agonists (BRC and CAB) in prolactinomas (Liu et al.), which will provide new evidence for dopamine signaling pathway-based personalized and precise treatment of prolactinomas. (vii) The seventh topic addressed the molecular network basis of invasive pituitary adenomas, namely, the invasiveness-related molecules, including pituitary tumor transforming gene (PTTG), vascular endothelial growth factor (VEGF), hypoxia-inducible factor-1a (HIF-1a), fibroblast growth factor-2 (FGF-2), and matrix metalloproteinases (MMPs, mainly MMP-2, and MMP-9), which interact in a complex molecular network and are responsible for the invasiveness of pituitary adenomas (Yang and Li). Of course, the mechanism of the invasiveness of pituitary adenomas is very complex. Multiomics-based molecular network investigation might provide novel insights into the molecular mechanisms and therapeutic targets of pituitary adenoma invasiveness (5, 11). (viii) The eighth topic addressed the roles of phosphodiesterases (PDEs) and cAMP pathway in pituitary adenomas, which emphasizes that the unique disturbance of the cAMP-PDE pathway in most AIP-mutation positive pituitary adenomas could contribute to poor response to somatostatin analogs for personalized treatment of pituitary adenomas (Bizzi et al.). (ix) The ninth topic addressed the epigenomics of pituitary adenomas, focusing on DNA methylation, histone modification, and transcript modification (Hauser et al.). In-depth investigation of the relationship between tumor epigenetics-related molecular pathways and clinical pathological characteristics might serve for clinical decision-making. (x) The 10th topic addressed the first ubiquitinomic profile and ubiquitination-involved signaling pathway network alterations, including ribosome, hippo signaling pathway, PI3K-AKT signaling pathway, and nucleotide excision repair pathway, in human pituitary adenomas (Qian, Zhan et al.). (xi) The 11th topic addressed mitogen-activated protein kinases (MAPKs; including ERK, p38, and JNK) pathway-based drug therapeutic targets in pituitary adenomas (Lu et al.), which in detail discussed the advances in understanding the role of MAPK signaling in pituitary tumorigenesis, and the MAPK pathway-based potential therapeutic drugs for pituitary adenomas. (xii) The 12th topic addressed biological roles and mechanisms of mitochondrial dysfunction pathway network and mitochondrial dynamics in pituitary adenomas, and current status of mitochondria-based biomarkers and targeted drugs for effective treatment of pituitary adenomas (Li and Zhan). (xiii) The 13th topic described the large-scale quantitative proteomic profile (n = 6,076 proteins) and the protein molecular pathway network profile of non-functional pituitary adenomas, which were combined with transcriptomic data (n = 3,598 differentially expressed genes) to reveal 52 statistically significant pathways, including cGMP-PKG pathway, focal adhesion, and platelet activation signaling pathways (Cheng et al.). (xiv) The 14th topic addressed multiomics-based signaling pathway network alterations in non-functional pituitary adenomas (Long et al.), which analyzed nine sets of omics data, and provided a comprehensive and large-scale pathway network data for non-functional pituitary adenomas to understand the accurate molecular mechanisms and discover effective biomarkers for diagnosis, prognosis, and determination of therapeutic targets for pituitary adenomas.

Molecular networks are an effective approach to annotate the interactome in pituitary adenomas for in-depth insight into its molecular mechanisms and discovery of effective biomarkers and therapeutic targets (12, 13). (i) This special issue covers several single signaling pathways and their targeted therapeutic drugs. These single signaling pathways include the MAPK (ERK, p38, and JNK) signaling pathway (Lu et al.), mitochondrial dysfunctional pathway (Li and Zhan), GH-PDGFR-β signaling pathway (Gupta et al.), estrogen signaling pathway (Wierinckx et al.), cAMP-PDE pathway (Bizzi et al.), and dopamine signaling pathway (Liu et al.). Based on these given signaling pathways, some therapeutic targets and drugs have been discovered and FDA-approved for pituitary adenomas. However, one must realize that although many advances have been made, these signaling pathways have not been fully clarified in pituitary adenomas, and in-depth exploring diversity of each of these pathways might discover great potentials of these pathways for pituitary adenomas. Also, from a systematic viewpoint, the multi-target combination treatment within each pathway or with combining each pathway with other pathways will be superior to the single-target treatment. (ii) Multiomics has driven molecular network study in pituitary adenoma. This special issue involved in egigenomics (Hauser et al.), transcriptomics, proteomics (Cheng et al.), ubiquitinomics (Qian, Zhan et al.), nitroproteomics, phosphoproteomics, metabolomics (Pînzariu et al.; Feng et al.), and multiomics-based integrative study (Long et al.) in pituitary adenomas, including GH-secreting adenoma, ACTH-secreting adenoma, PRL-secreting adenoma, and non-functional pituitary adenomas. Omics-based molecular network analysis has made significant advances in pituitary adenomas. Until now, transcriptomics and proteomics have been extensively studied in pituitary adenomas (Cheng et al.) (15–19); epigenomics, ubiquitinomics, phosphoproteomics, nitroproteomics (20–23), and metabolomics have been initiated but not extensively studied in pituitary adenomas. However, one must note that post-transcriptional modifications/post-translational modifications (PTMs) are very complex up to several hundreds of PTMs in the human body (14), and PTM-mediated molecular network alterations play important roles in pituitary adenomas. However, PTM-omics has not been extensively studied in pituitary adenomas. Therefore,

we would emphasize the scientific importance of PTM-omics, including DNA modifications, RNA modifications, and protein modifications, in pituitary adenomas. PTM-based omics and molecular network studies will bring the big promise for insight into the novel molecular mechanism, discovery of novel effective therapeutic targets and drugs, and determination of effective and reliable biomarkers for patient stratification, diagnosis, and prognostic assessment of pituitary adenoma patients. (iii) Pituitary adenoma invasiveness is a big clinical challenge. This special issue has one topic to address the molecular network basis of invasive pituitary adenoma based on several invasiveness-related molecules (PTTG, VEGF, HIF-1a, FGF-2, and MMPs such as MMP-2, and MMP-9) and their interacted complex molecular network (Yang and Li). However, one must note that these invasiveness-related molecules are derived from previous traditional studies and do not represent at all the entire molecule world of the invasive characteristics of pituitary adenomas. Indeed, the molecule world of invasive pituitary adenomas is very complex. We strongly recommend the use of multiomics to study pituitary adenoma invasiveness, which might be the right way to resolve its clinical invasiveness challenge for clarification of its molecular mechanisms, discovery of effective therapeutic targets, and determination of effective biomarkers for diagnosis and prognostic assessment. Some proteomics and transcriptomics between invasive and non-invasive pituitary adenomas have been performed to understand molecular mechanism and discover biomarkers of pituitary adenoma invasiveness (24–26). (iv) Proteome is the final functional performer of genome and transcriptome. However, proteome complexity is significantly influenced by RNA splicing, PTMs, and many other factors (14). The concept development of proteoform/protein species significantly enriches the content of proteome; a protein is an umbrella term of proteoform encoded by the same gene, and a proteoform is defined as its amino acid sequence + PTMs + spatial conformation + cofactors + binding partners + localization + a function, and thus proteoform is the basic unit of proteome (27, 28). Clarification of proteoforms and proteoform-mediated signaling pathway networks will precisely help understand the molecular mechanism, directly identify reliable biomarkers for precise diagnosis and prognostic assessment, and precisely determine therapeutic treatment of pituitary adenoma (28, 29). For pituitary adenoma, we have studied hormone proteoforms and their involved signaling pathway alterations (30), including GH proteoforms (31), and prolactin proteoforms (Qian, Yang et al.). Also, dopamine receptor proteoforms (Liu et al.), PDE proteoforms (Bizzi et al.), and their involved molecular signaling pathways are discussed in this special issue. Proteoform studies will need in-depth insights into a proteome, which is the future direction of proteomics. We recommend the strengthening of proteoform-mediated molecular signaling pathway network studies in pituitary adenomas for precise treatment in the future.

In summary, molecular network studies of pituitary adenoma have achieved significant advances. However, one must realize that this special issue contains only a fraction of the very important molecular network study of pituitary adenomas. This Research Topic serves as a spur to stimulate and encourage researchers who study molecular networks to come forward with its scientific merits to research and clinical practice of pituitary adenomas. Future issues will collect more multiomics-based molecular network studies with large-scale clinical information for basic research, translational research, and clinical practice in pituitary adenomas. We strongly believe that multiomics-based molecular network studies, molecular network-based therapeutic target and drug studies, and molecular network-based pattern biomarker studies (5, 10, 11, 13, 32–37) will bring a brighter future for pituitary adenoma patients through the realization of personalized and precision medicine.

AUTHOR CONTRIBUTIONS

XZ conceived the concept, designed manuscript, wrote and critically revised the manuscript, and was responsible for its financial supports and the corresponding works. DD participated in the development of concept and critically revised the manuscript. All authors approved the final manuscript.

FUNDING

This work was supported by grants from the Shandong First Medical University Talent Introduction Funds (to XZ) and the Hunan Provincial Hundred Talent Plan (to XZ).

REFERENCES

1. Melmed S. Pituitary tumors. *Endocrinol Metab Clin North Am.* (2015) 44:1–9. doi: 10.1016/j.ecl.2014.11.004
2. Melmed S. Pathogenesis of pituitary tumors. *Nat Rev Endocrinol.* (2011) 7:257–66. doi: 10.1038/nrendo.2011.40
3. Melmed S. Mechanisms for pituitary tumorigenesis: the plastic pituitary. *J Clin Invest.* (2003) 112:1603–18. doi: 10.1172/JCI20401
4. Grech G, Zhan X, Yoo BC, Bubnov R, Hagan S, Danesi R, et al. EPMA position paper in cancer: current overview and futu4re perspectives. *EPMA J.* (2015) 6:9. doi: 10.1186/s13167-015-0030-6
5. Cheng T, Zhan X. Pattern recognition for predictive, preventive, and personalized medicine in cancer. *EPMA J.* (2017) 8:51–60. doi: 10.1007/s13167-017-0083-9
6. Hood L, Tian Q. Systems approaches to biology and disease enable translational systems medicine. *Genomics Proteomics Bioinformatics.* (2012) 10:181–5. doi: 10.1016/j.gpb.2012.08.004
7. Aderem A. Systems biology: its practice and challenges. *Cell.* (2005) 121:511–3. doi: 10.1016/j.cell.2005.04.020
8. Hood L. Systems biology: integrating technology, biology, and computation. *Mech Ageing Dev.* (2003) 124:9–16. doi: 10.1016/S0047-6374(02)00164-1
9. Zhan X, Desiderio DM. The use of variations in proteomes to predict, prevent, personalize treatment for clinically non-functional pituitary adenomas. *EPMA J.* (2010) 1:439–59. doi: 10.1007/s13167-010-0028-z
10. Hu R, Wang X, Zhan X. Multi-parameter systematic strategy for predictive, preventive, and personalized medicine in cancer. *EPMA J.* (2013) 4:2. doi: 10.1186/1878-5085-4-2

11. Lu M, Zhan X. The crucial role of multiomic approach in cancer research and clinically relevant outcomes. *EPMA J.* (2018) 9:77–102. doi: 10.1007/s13167-018-0128-8
12. Zhan X, Desiderio DM. Editorial: systems biological aspects of pituitary tumors. *Front Endocrinol.* (2016) 7: 86. doi: 10.3389/fendo.2016.00086
13. Zhan X, Long Y. Exploration of molecular network variations in different subtypes of human nonfunctional pituitary adenomas. *Front Endocrinol.* (2016) 7:13. doi: 10.3389/fendo.2016.00013
14. Zhan X, Long Y, Lu M. Exploration of variations in proteome and metabolome for predictive diagnostics and personalised treatment algorithms: innovative approach and examples for potential clinical application. *J Proteomics.* (2018) 188:30–40. doi: 10.1016/j.jprot.2017.08.020
15. Zhan X, Desiderio DM. Comparative proteomics analysis of human pituitary adenomas: current status and future perspectives. *Mass Spectrom Rev.* (2005) 24:783–813. doi: 10.1002/mas.20039
16. Moreno CS, Evans CO, Zhan X, Okor M, Desiderio DM, Oyesiku NM. Novel molecular signaling in human clinically non-functional pituitary adenomas identified by gene expression profiling and proetomic analyses. *Cancer Res.* (2005) 65:10214–22. doi: 10.1158/0008-5472.CAN-05-0884
17. Zhan X, Wang X, Long Y, Desiderio DM. Heterogeneity analysis of the proteomes in clinically nonfunctional pituitary adenomas. *BMC Med Genomics.* (2014) 7:69. doi: 10.1186/s12920-014-0069-6
18. Zhan X, Wang X, Cheng T. Human pituitary adenoma proteomics: new progresses and perspectives. *Front Endocrinol.* (2016) 7:54. doi: 10.3389/fendo.2016.00054
19. Evans CO, Moreno CS, Zhan X, McCabe MT, Vertino PM, Desiderio DM, et al. Molecular pathogenesis of human prolactinomas identified by gene expression profiling, RT-qPCR, and proteomic analyses. *Pituitary.* (2008) 11:231–45. doi: 10.1007/s11102-007-0082-2
20. Zhan X, Wang X, Desiderio DM. Mass spectrometry analysis of nitrotyrosine-containing proteins. *Mass Spectrom Rev.* (2015) 34:423–48. doi: 10.1002/mas.21413
21. Zhan X, Desiderio DM. Nitroproteins from a human pituitary adenoma tissue discovered with a nitrotyrosine affinity column and tandem mass spectrometry. *Anal Biochem.* (2006) 354:279–89. doi: 10.1016/j.ab.2006.05.024
22. Zhan X, Desiderio DM. The human pituitary nitroproteome: detection of nitrotyrosyl-proteins with two-dimensional Western blotting, and amino acid sequence determination with mass spectrometry. *Biochem Biophys Res Commun.* (2004) 325:1180–6. doi: 10.1016/j.bbrc.2004.10.169
23. Zhan X, Desiderio DM. Linear ion-trap mass spectrometric characterization of human pituitary nitrotyrosine-containing proteins. *Int J Mass Spectrom.* (2007) 259:96–104. doi: 10.1016/j.ijms.2006.06.009
24. Zhan X, Desiderio DM, Wang X, Zhan X, Guo T, Li M, et al. Identification of the proteomic variations of invasive relative to noninvasive nonfunctional pituitary adenomas. *Electrophoresis.* (2014) 35:2184–94. doi: 10.1002/elps.201300590
25. Wang X, Guo T, Peng F, Long Y, Mu Y, Yang H, et al. Proteomic and functional profiles of a follicle-stimulating hormone-positive human nonfunctional pituitary adenoma. *Electrophoresis.* (2015) 36:1289–304. doi: 10.1002/elps.201500006
26. Wang Y, Cheng T, Lu M, Mu Y, Li B, Li X, et al. TMT-based quantitative proteomics revealed follicle-stimulating hormone (FSH)-related molecular characterizations for potentially prognostic assessment and personalized treatment of FSH-positive non-functional pituitary adenomas. *EPMA J.* (2019) 10:395–414. doi: 10.1007/s13167-019-00187-w
27. Zhan X, Li B, Zhan X, Schlüter H, Jungblut PR, Coorssen JR. Innovating the concept and practice of two-dimensional gel electrophoresis in the analysis of proteomes at the proteoform level. *Proteomes.* (2019) 7:36. doi: 10.3390/proteomes7040036
28. Zhan X, Li N, Zhan X, Qian S. Revival of 2DE-LC/MS in proteomics and its potential for large-scale study of human proteoforms. *Med ONE.* (2018) 3:e180008. doi: 10.20900/mo.20180008
29. Zhan X, Yang H, Peng F, Li J, Mu Y, Long Y, et al. How many proteins can be identified in a 2-DE gel spot within an analysis of a complex human cancer tissue proteome? *Electrophoresis.* (2018) 39:965–80. doi: 10.1002/elps.201700330
30. Zhan X, Zhou T. Application of two-dimensional gel electrophoresis in combination with mass spectrometry in the study of hormone proteoforms. In: Kamble GS, editor. *Mass Spectrometry—Future Perceptions and Applications*. London: InTech - Open science publisher (2019). doi: 10.5772/intechopen.82524
31. Zhan X, Giorgianni F, Desiderio DM. Proteomics analysis of growth hormone isoforms in the human pituitary. *Proteomics.* (2005) 5:1228–41. doi: 10.1002/pmic.200400987
32. Putignani L, Gasbarrini A, Dallapiccola B. Potential of multiomics technology in precision medicine. *Curr Opin Gastroenterol.* (2019) 35:491–8. doi: 10.1097/MOG.0000000000000589
33. Khatri VP, Petrelli NJ. Precision medicine. *Surg Oncol Clin N Am.* (2020) 29:xv–xvi. doi: 10.1016/j.soc.2019.10.001
34. Olivier M, Asmis R, Hawkins GA, Howard TD, Cox LA. The need for multi-omics biomarker signatures in precision medicine. *Int J Mol Sci.* (2019) 20:E4781. doi: 10.3390/ijms20194781
35. Hawe JS, Theis FJ, Heinig M. Inferring interaction networks from multi-omics data. *Front Genet.* (2019) 10:535. doi: 10.3389/fgene.2019.00535
36. Yoo BC, Kim KH, Woo SM, Myung JK. Clinical multi-omics strategies for the effective cancer management. *J Proteomics.* (2018) 188:97–106. doi: 10.1016/j.jprot.2017.08.010
37. Zhan X, Zhou T, Cheng T, Lu M. Recognition of multiomics-based molecule-pattern biomarker for precise prediction, diagnosis and prognostic assessment in cancer. In: Samadikuchaksaraei A, editor. *Bioinformatics Tools for Detection and Clinical Interpretation of Genomic Variations*. London: InTech - Open science publisher (2019). doi: 10.5772/intechopen.84221

Conflict of Interest: The authors declare that the research was conducted in the absence of any commercial or financial relationships that could be construed as a potential conflict of interest.

frontiers in Endocrinology

ORIGINAL RESEARCH
published: 27 August 2018
doi: 10.3389/fendo.2018.00453

Imatinib Inhibits GH Secretion From Somatotropinomas

*Prakamya Gupta[1], Ashutosh Rai[1], Kanchan Kumar Mukherjee[1], Naresh Sachdeva[2], Bishan Das Radotra[3], Raj Pal Singh Punia[4], Rakesh Kumar Vashista[3], Debasish Hota[5], Anand Srinivasan[5], Sivashanmugam Dhandapani[1], Sunil Kumar Gupta[1], Anil Bhansali[2] and Pinaki Dutta[2]**

[1] Department of Neurosurgery, Postgraduate Institute of Medical Education and Research, Chandigarh, India, [2] Department of Endocrinology, Postgraduate Institute of Medical Education and Research, Chandigarh, India, [3] Department of Histopathology, Postgraduate Institute of Medical Education and Research, Chandigarh, India, [4] Department of Histopathology, Government Medical College and Hospital, Chandigarh, India, [5] Department of Pharmacology, Postgraduate Institute of Medical Education and Research, Chandigarh, India

OPEN ACCESS

Edited by:
Xianquan Zhan,
Central South University, China

Reviewed by:
Luiz Eduardo Armondi Wildemberg,
Instituto Estadual do Cérebro Paulo Niemeyer, Brazil
Leandro Kasuki,
Instituto Estadual do Cérebro Paulo Niemeyer, Brazil

***Correspondence:**
Pinaki Dutta
pinaki_dutta@hotmail.com

Specialty section:
This article was submitted to Pituitary Endocrinology, a section of the journal Frontiers in Endocrinology

Received: *15 May 2018*
Accepted: *24 July 2018*
Published: *27 August 2018*

Citation:
Gupta P, Rai A, Mukherjee KK, Sachdeva N, Radotra BD, Punia RPS, Vashista RK, Hota D, Srinivasan A, Dhandapani S, Gupta SK, Bhansali A and Dutta P (2018) Imatinib Inhibits GH Secretion From Somatotropinomas. Front. Endocrinol. 9:453. doi: 10.3389/fendo.2018.00453

Background: Imatinib, a tyrosine kinase inhibitor, causes growth failure in children with chronic myeloid leukemia probably by targeting the growth hormone (GH)/insulin like growth factor-1 (IGF-1) axis. We aim to explore the imatinib targets expression in pituitary adenomas and study the effect of imatinib on GH secretion in somatotropinoma cells and GH3 cell line.

Materials and Methods: The expression pattern of imatinib's targets (c-kit, VEGF, and PDGFR-α/β) was studied using immunohistochemistry and immunoblotting 157 giant (≥4 cm) pituitary adenomas (121 non-functioning pituitary adenomas, 32 somatotropinomas, and four prolactinomas) and compared to normal pituitary ($n = 4$) obtained at autopsy. The effect imatinib on GH secretion, cell viability, immunohistochemistry, electron microscopy, and apoptosis was studied in primary culture of human somatotropinomas ($n = 20$) and in rat somato-mammotroph GH3 cell-line. A receptor tyrosine kinase array was applied to human samples to identify altered pathways.

Results: Somatotropinomas showed significantly higher immunopositivity for c-kit and platelet-derived growth factor receptor-β (PDGFR-β; $P < 0.009$ and $P < 0.001$, respectively), while staining for platelet-derived growth factor receptor-α (PDGFR-α) and vascular endothelial growth factor (VEGF) revealed a weaker expression ($P < 0.001$) compared to normal pituitary. Imatinib inhibited GH secretion from both primary culture ($P < 0.01$) and GH3 cells ($P < 0.001$), while it did not affect cell viability and apoptosis. The receptor tyrosine kinase array showed that imatinib inhibits GH signaling via PDGFR-β pathway.

Conclusion: Imatinib inhibits GH secretion in somatotropinoma cells without affecting cell viability and may be used as an adjunct therapy for treating GH secreting pituitary adenomas.

Keywords: growth hormone, imatinib, somatotropinoma, c-kit, VEGF, PDGFR-α/β

INTRODUCTION

The tyrosine kinase inhibitor (TKI) imatinib is the first-line treatment for chronic myeloid leukemia (CML) and gastrointestinal stromal tumors (GIST). Growth failure or growth retardation has been observed in children treated for breakpoint cluster region-Abelson (BCR-ABL)-positive leukemia, especially if treated before the onset of puberty (1–5). The mechanism of action leading to inhibition of the GH-IGF-1 axis remains undeciphered.

Hypersecretion of growth hormone (GH) causes acromegaly and is invariably due to somatotropinoma. Although the past few decades have seen tremendous improvement in the management of somatotropinomas by the use of somatostatin and dopamine agonists and GH receptor antagonists. The limitations imposed by their cost and efficacy indicate the need for alternative drugs. The present study was designed to study the imatinib's targets (c-kit, VEGF, and PDGFR-α/β) expression in pituitary adenoma subtypes and elucidate the effects of imatinib on cultured human somatotropinoma cells and the rat somato-mammotroph GH3 cell-line and explore the plausible mechanism of action.

MATERIALS AND METHODS

Tissue Microarray Construction, Staining, and Image Analysis

Following approval from Institute Ethics Committee of PGIMER, Chandigarh (Ref No INT/IEC/2016/2724), 157 cases of giant (maximum diameter ≥4 cm) pituitary adenomas [121 non-functioning pituitary adenomas (NFPA), 32 somatotropinomas, and four prolactinomas] were used for tissue microarray (TMA) construction. After-surgery, the cure rate of giant adenomas is less as compared to smaller adenomas and may require multi-modality treatment. None of the patients with prolactinomas had abnormalities of GH/IGF-1. Hematoxylin & eosin (H&E) staining was performed on paraffin section and the region of interest was identified. Two 3 millimeter cores were punched from each tumor and placed into a recipient block. Four non-adenomatous pituitary glands were taken at autopsy (within 4 h of death), from adult patients who died of non-endocrine disorders. Their sections were taken as control separately. None of the cases used in the study were known to harbor familial tumors or showed signs of syndromic disorder.

Both TMA and controls were stained simultaneously. The slides were deparaffinized in xylene, gradually rehydrated through a series of decreasing alcohols (100–70%) to distilled water and microwaved in 0.01 M sodium citrate buffer. Staining was performed with anti-PDGFR-α/β, anti-VEGF-A, anti-c-kit (Santa Cruz Biotech, California, USA), Ki-67, and anti-p53 (DAKO, USA) antibodies. Following washes in phosphate buffer saline (PBS), sections were incubated with the secondary antibody (anti-rabbit HRP conjugate, Santa Cruz). Staining was developed using the chromogen substrate diaminobenzidine (Liquid DAB, Dako K3468) followed by counterstaining with hematoxylin and rinsed in water. The brown signal obtained was visualized and scored under light microscopy. The stained slides were independently reviewed by three pathologists who were blinded for clinical and radiological details. Staining intensity and domain were scored as 0 (no staining), 1 (weak staining), 2 (moderate staining), and 3 (strong staining) according to a scoring system described previously by Tohti et al. (6).

TABLE 1 | Patient characteristics for primary culture of somatotropinoma.

Parameters	Value
Gender (M:F)	10:10
Mean age (years)	33.1 ± 13
Mean tumor volume (mm^3)	10672.82
Mean pre op GH (ng/ml)	25.09 ± 22.68
Mean pre op IGF-1 (ng/ml)	872.09 ± 352.22
IMMUNOHISTOCHEMISTRY	
GH+	13
GH+ Prl+	7

Double-Immunofluorescence

Paraffin-embedded samples were sectioned at 7 μm thickness for histochemical evaluation. Double immunofluorescence was performed by deparaffinization of the sections followed by rehydration through decreasing ethanol dilutions. Heat-induced antigen retrieval was performed in 10 mM sodium citrate buffer (pH 6) with a microwave. Sections were left to cool down at room temperature and incubated for 1 h in blocking buffer [1X PBS, 0.1% Triton X-100, 5% Normal Goat Serum (Vector Laboratories, UK)]. Endogenous hPDGFR-α and hPDGFR-β were detected by staining the tissues overnight with a primary mouse monoclonal antibody against hPDGFR-α (Santa Cruz; sc-398206; 1:100) or PDGFR-β (Abcam; ab69506; 1:100). Staining against hGH was performed by incubating the tissues overnight with a primary rabbit polyclonal antibody against hGH. Overnight incubations with the primary antibodies were followed by 1 h incubation of the tissues with a secondary goat anti-mouse Alexa Fluor 488 antibody (Life Technologies; A11001; 1:200) in order to detect hPDGFR-α or hPDGFR-β. For the detection of hGH, tissues were incubated for 1 h with a secondary biotinylated goat anti-rabbit antibody (Vector Laboratories; BA-1000; 1:300) followed by DyLight 549 Streptavidin (Vector Laboratories; SA-5549; 1:300). Cell nuclei were stained with DAPI [4′,6-diamidino-2-phenylindole (VECTASHIELD Antifade Mounting Medium with DAPI; H-1200)]. Images were acquired using a confocal microscope (ZEISS LSM 880 with Airyscan) and figures were done using Adobe Photoshop CS6.

Western Blotting

Somatotropinoma ($n = 27$), NFPA ($n = 27$), prolactinomas ($n = 4$), and normal pituitary ($n = 9$) were homogenized in 1 ml of ice-cold PBS buffer containing 60 mM Tris–HCl, 1 mM EDTA (pH 6.8), and protease inhibitors. The lysate was then centrifuged at 10,000 × g for 10 min at 4°C. An aliquot of supernatant was taken to quantify proteins by the Pierce BCA protein assay kit (Thermofisher Scientific, MA, USA). Lysates (20 μg protein per sample) were resolved in 10% SDS-PAGE. The gel was then blotted onto a nitrocellulose

membrane (Amersham, Aylesbury, UK) and probed with the corresponding primary antibody (VEGF 1:250, PDGFR-α 1:250, PDGFR-β 1:250, c-kit 1:250, Santa Cruz) followed by secondary antibody (bovine anti rabbit, Santa Cruz). Actin expression was evaluated to confirm equivalent total protein loading (rabbit anti-actin, 1:5,000, Sigma, Missouri, USA). Immunoreactive proteins were detected by electro chemoluminiscence (Amersham) using chemiluminescent imaging (FluorChem, Protein Simple, CA, USA). Intensity of the band was normalized to the corresponding actin intensity. The final data were subjected to gray-scale scanning and semi-quantitative analysis using Image J (National Institute of Mental Health, Maryland, USA). All samples were run in triplicates.

Primary Culture of Human Somatotropinoma and GH3 Cell-Line

Pituitary samples from 20 treatment-naïve acromegaly patients were used for this part of the study. The tumors were washed thoroughly with PBS (pH 7.4) until supernatant was clear and most red blood cells removed. The cells were dispersed using enzymatic (2.5% Trypsin, Gibco, USA) and mechanical dispersion procedure. Cells were washed with complete media and seeded in 24 and/or 96 well culture plate (Corning costar, USA). The primary culture was performed in Dulbecco Modified Eagle Media (DMEM, Gibco, USA) containing fetal calf serum (FCS, Gibco, USA), penicillin and streptomycin soon after transsphenoidal resection of the tumor. GH3 cells were obtained from American Type Culture Collection (ATCC, USA). These cells were grown in DMEM-F12 media (Gibco, USA) containing FCS. The cells were trypsinized and split once the confluence reached 80%. GH3 cells from the third passage were used for all experimental purpose. The cells were grown in complete media (DMEM + FCS + antibiotics) at 37°C and 5% CO_2.

Imatinib Treatment

The stock solution of 50 mM of imatinib (Novartis Basel, Switzerland) were prepared by dissolving the compound in double distilled water and stored at −20°C until use. Cells were plated 12 h before imatinib was added at 0.25, 0.5, 1, 2.5, 5, and 10 μM concentrations. Effective dose 50 (ED_{50}) was calculated by measuring the concentration of GH in culture supernatant. E-max method (four parametric logistic regression) was used to construct the dose-response curve and ED_{50} was calculated using the model built by substituting the dependent variable with half maximum value of GH. The effect of imatinib was compared to somatostatin analogs octreotide (0.1 μM; primarily SSTR2 agonist) and pasireotide (10 μM; SSTR1, 2, 3, and 5 agonist) with or without GHRH stimulation (0.5 μM) treated for 48 h.

Growth Hormone Assay

Growth hormone was assessed from the primary culture supernatant using electro-chemiluminiscence immunoassay (COBAS, e601, Roche-Hitachi, USA) with lowest detection limit of 0.03 ng/ml and the inter and intra-assay coefficient of variation was <2.5%. The human growth hormone differs structurally from the rat growth hormone. GH from GH3 cell line supernatant was measured using ELISA (Cloud-Clone Corp, SEA044Ra, Hubei, China).

Immunocytochemistry

For immunocytochemistry, cells were cyto-spun onto poly-lysine double-coated slides at 1,000 rpm for 15 min and fixed with 4% paraformaldehyde. Excess formaldehyde was washed with PBS and the cells were exposed to rabbit anti-hGH antibody (1:400; DAKO) for 1 h and conjugated anti-rabbit anti-mouse secondary antibody (DAKO) for 30 min at room temperature. Thereafter cells were washed with PBS and incubated with DAB for 2 min followed by hematoxylin staining.

Apoptosis and Cell Viability

Apoptosis was determined in untreated and imatinib treated GH3 cells by staining with annexinV-FITC antibody and propidium iodide (Molecular Probes, Life Technologies, USA) followed by flow cytometric analysis, measuring emission at 530 nm (FL1) and 575 nm (FL3).

The cell viability was measured by cellular uptake of 3-[4,5-dimethylthiazol-2-yl]-2,5-diphenyltetrazolium bromide (MTT). Cells were seeded at 4×10^3 per well in 96 well plate containing 100 μl of culture medium with 10% FBS and cultured overnight. All analysis were performed in quadruplets. Prior to imatinib treatment, media was removed and fresh media was added. Subsequently, cells were exposed to imatinib. After 48 h of induction, 20 μl of MTT (0.05 g/ml, Himedia) was added to each well and incubated at 37°C for 4 h. After 48 h, the medium was removed, MTT solution was added and left for 4 h at 37°C. The medium was aspirated and DMSO was added to each well. The color development was measured at 570 and 630 nm (Infinite M200 pro, Tecan, Austria). The absorbance was proportional to the number of viable cells.

% Cell Viability = Optical density of imatinib treated cells/Optical density of untreated cells × 100.

Electron Microscopy

Both treated and control GH3 cells were harvested in 2.5% glutaraldehyde and were washed with Sorenson buffer, millonin buffer and 1% osmium tetroxide. Thereafter, cells were dehydrated in graded series of ethanol, processed through propylene oxide, and embedded in an Epon-araldite mixture (Epon 812, Sigma, USA). Ultrathin sections were stained with uranyl acetate lead citrate and viewed under the electron microscope (JEM 1400 Flash, JEOL, USA).

Receptor Tyrosine Kinase Array

To investigate the mechanism of GH inhibition by imatinib we used human phospho-receptor tyrosine kinase (RTK) array to screen 49 different phospho-RTKs for differentially activated kinase in response to imatinib treatment in somatotropinoma cells. Cell lysate from both treated and control somatotropinoma cultured cells were extracted and subjected to receptor tyrosine kinase array (R&D Systems, MN, USA) according to manufacturer's protocol. The kit is specifically designed to screen relative level of phosphorylation of 49 different RTK. Phosphorylation status was determined by chemiluminescence

and analyzed using Image J software (National Institute of Mental Health, Maryland, USA).

Statistical Analysis

The statistical analysis was performed using SPSS version 16. For two group comparisons Student's *t*-test or Mann–Whitney *U*-test and for multiple comparison one-way ANOVA (followed by Bonferroni *post-hoc* test) or Kruskal–Wallis test (followed by Dunn's test) was used depending of the normal distribution of the data. Spearman's test was used for correlations. *P*-value of <0.05 was considered as significant.

RESULTS

Low Dose of Imatinib Attenuates GH Secretion Without Affecting Cell Number and Viability

To assess the effect of imatinib treatment of GH secretion, primary cultured cells from 20 somatotropinomas were tested (patient characteristics are shown in **Table 1**). Cells were treated with increasing concentrations of imatinib (0.5–10 μM) and levels of GH measured using electrochemoluminiscence, cell viability was measured using MTT assay (**Supplementary Figure 1**). The maximum reduction in GH was observed at concentration of 0.5 μM of imatinib, with statistically significant reduction at higher doses (1–10 μM). The mean GH measured from the 20 different somatotropinoma primary cultures treated with 0.5 μM of imatinib showed 20% reduction in GH compared to controls ($p < 0.001$; **Figure 1a**). To further assess the inhibitory effect on GH secretion, pituitary rat tumor cells line GH3 (GH and PRL secreting) were treated with 0.5 μM imatinib. After treatment, 88% reduction of GH secretion was observed ($p < 0.001$; **Figure 1d**). These results were further confirmed by immunostaining against GH in both primary tumor and GH3 cultured cells. 0.5 μM imatinib treated cells exhibited negligible GH staining in both primary culture and GH3 cells (**Figures 1b,c,e,f**, respectively). We then assessed if the imatinib treatment had and effect on cell proliferation, viability, and apoptosis of GH3 cells. Cell viability was studied post imatinib treatment using cellular uptake of MTT. No significant differences in cell viability or proliferation ($p < 0.88$) were observed between treated and untreated cells (**Supplementary Figure 2**). Moreover, the viability analysis at

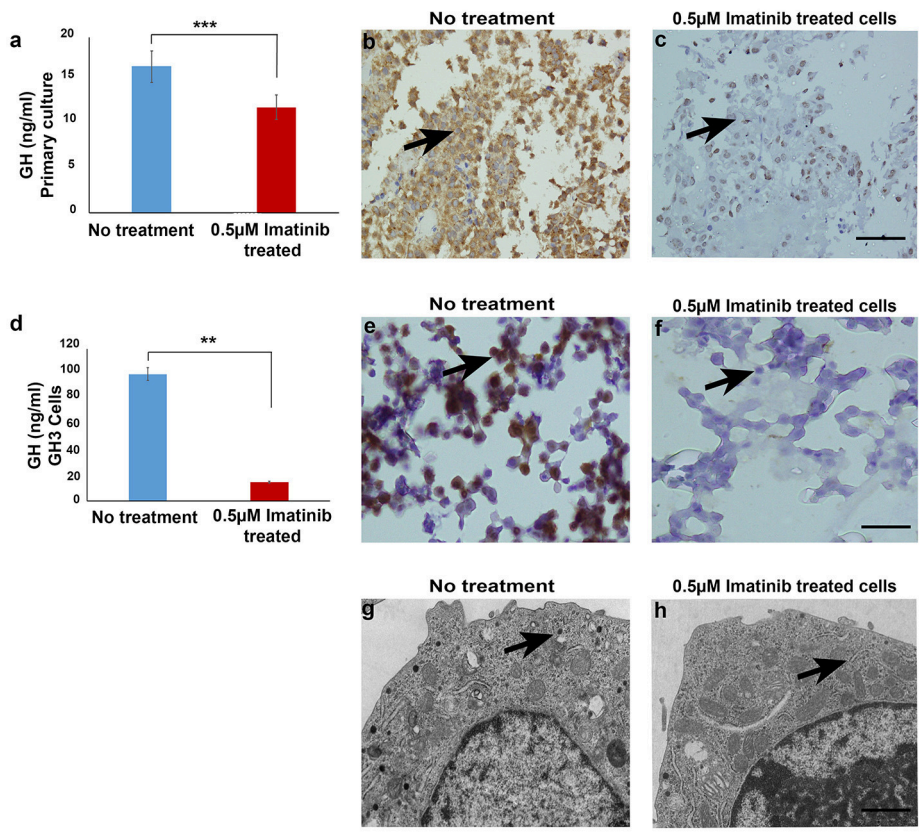

FIGURE 1 | (a) Bar diagram showing reduction in growth hormone levels in culture media after treatment with 0.5 μM imatinib in primary culture of somatotropinoma cells ($P < 0.0001$). **(b,c)** Representative image of immunohistochemistry with anti-GH antibody on treated and untreated primary somatotropinoma culture. **(d)** Bar diagram showing reduction in GH levels in culture media of GH3 cell line after treatment with 0.5 μM imatinib ($P < 0.01$). **(e,f)** IHC of GH3 cells showing intense GH positivity in untreated and no GH staining in treated cells (20X). **(g,h)** Ultra-structural analysis of GH granules using electron microscopy between treated and untreated GH3 cells (6000X). $^{**}P < 0.01$; $^{***}P < 0.0001$.

0, 24, and 48 h also showed no change in somatotropinoma viability. To assess if imatinib leads to inhibition of GH secretion due to reduced *GH* and *Pit-1* transcription we used real time PCR from primary somatotropinoma cultures. Treatment with imatinib did not affect *GH* or *Pit-1* transcripts (**Supplementary Figure 3**). This prompted us to study if the secretion of GH vesicles was affected in GH3 tumor cells after imatinib treatment using transmission electron microscopy (TEM). Interestingly, untreated cells showed secretory granules of 122–150 nm localized to Golgi region and the periphery, whilst cells treated with 0.5 μM imatinib showed marked reduction in granularity of secretory vesicles (**Figures 1g,h**). Due to paucity of the cells, similar results could not be reproduced in imatinib-treated cells from primary culture. Together this data indicates that imatinib reduces GH secretion by reducing the secretory granules.

Expression of Imatinib Targets (c-Kit, PDGFR-α, PDGFR-β, and VEGF) in Pituitary Adenomas Using Immunostaining

Imatinib has been shown to inhibit tyrosine kinases activity in several tumors (7). In particular it has been shown to inhibit the tyrosine kinase c-Kit, PDGFR-α, PDGFR-β, and VEGF. The differential expression of imatinib targets were analyzed in a cohort of 157 patients with giant pituitary adenomas (>4 cm). The patient characteristics are shown in **Table 2**. c-Kit was expressed in a large proportion of pituitary adenomas (100% in somatotropinomas and prolactinomas and 97% in NFPAs; **Figures 2**, **3**). In patients with somatotropinomas, moderate to strong positivity was much more frequent as compared to NFPAs (88 vs. 55%, $P = 0.009$). No difference was found when compared to normal pituitary for both adenomas. PDGFR-α positivity was observed in all controls, 79% NFPA, 50% prolactinomas and only 35% somatotropinomas (**Figures 2**, **3**). The PDGFR-α cytoplasmic staining showed significant increase in NFPA, compared to somatotropinoma ($P < 0.001$). As compared to the controls, the PDGFR-α was poorly expressed in somatotropinoma (100 vs. 35%, $P = 0.03$). The PDGFR-β was expressed in all adenoma subtypes as well as controls, with somatotropinomas showing higher expression compared to NFPA or control (59 vs. 20%, $P < 0.001$; **Figures 2**, **3**). Strong PDGFR-β positivity was observed in somatotropinomas as compared to control. VEGF expression was observed in both normal (100%) and adenomatous pituitaries. Overall, VEGF positivity was identified in 96% NFPA, 82% somatotropinomas and 50% prolactinomas (**Figures 2**, **3**). However, strong VEGF positivity was observed in NFPA more often than somatotropinomas (19 vs. 0%, $P < 0.003$) but no difference was observed when compared to the controls.

Comparison between various tyrosine kinase pathway members in different pituitary adenomas are enlisted in **Figure 3**. Though all patients had giant pituitary adenoma, they were not overtly proliferative (Ki-67 <3% in all). There was no correlation between TK pathway members expression (VEGF, c-kit, PDGFR-α/β), immuno-positivity to pituitary adenoma subtypes and Ki-67, p53, age, gender, recurrent, or residual lesion (data not shown).

TABLE 2 | Patient characteristics for tissue microarray staining.

	NFPA ($n = 121$)	Somatotropinoma ($n = 32$)	Prolactinoma ($n = 4$)
Gender (Males: Females)	74 (61.1%): 47 (38.8%)	20 (62.5%): 12 (37.5)	3 (75%): 1 (25%)
Mean age (years)	43.1 (±12.6)	33.2 (±11.1)	33.0 (±17.1)
Complete resection	47	9	4
Residual lesion	74	23	0
Underwent second surgery	21	5	0
Post-op radiotherapy/gamma knife	18	12	0
IMMUNOHISTOCHEMISTRY			
Non-functioning adenoma (all six negative)*	95.9%	3.1%**	0
LH/FSH POSITIVE			
GH +ve	1.7%	65.6%	0
GH and PRL+ve	2.4%	31.2%	100%

**They were not stained for α-subunit of gonadotropin.*
***Negative for GH, LH, FSH, ACTH, and PRL staining.*

Co-localization of GH and PDGFR-α/β in Somatotropinomas and Normal Pituitary

In order to determine which cell type expresses imatinib targets, double immunofluorescence staining was performed with anti-GH, anti-PDGFR-α, and PDGFR-β on somatotropinoma and normal pituitary tissues. Colocalization between GH and both PDGFR-α/β was observed in both normal pituitary and somatotropinoma cells. There was loss of PDGFR-α and gain of PDGFR-β in somatotropinomas (**Figure 4**). This data shows that GH cells express the imatinib target PDGFR-α/β.

Quantitative Analysis of c-Kit, PDGFR-α, PDGFR-β, and VEGF

To quantify the differential expression between tumor subtypes and imatinib targets, we evaluated protein expression of c-Kit VEGF, PDGFR-α, and PDGFR-β in somatotropinomas ($n = 27$), NFPA ($n = 27$), prolactinomas ($n = 4$), and normal pituitaries ($n = 9$) using western blotting (**Figure 5**). As compared to normal pituitaries, c-Kit protein expression was found to be significantly higher in somatotropinomas (224.3%, $P < 0.05$) and NFPA (193.5%, $P < 0.05$). Notably, somatotropinoma cells exhibited higher expression of PDGFR-β protein when compared to normal pituitary tissue (195.8 vs. 100%, $P < 0.05$). Compared to normal pituitary, the relative expression of PDGFR-α was found to be lower in somatotropinomas (37.1%, $P < 0.05$) and NFPA (81.4%, $P = 0.08$). Hence, these data indicate a relative over expression of PDGFR-β and under expression of PDGFR-α in somatotropinomas. VEGF was differentially expressed between somatotropinomas and NFPA (68.2 vs. 104.7%, $P < 0.03$), compared to normal pituitary (100%). However, no correlation was observed between TKs protein expression in both adenomas. Our quantification studies indicate that PDFGR-β is unregulated in somatotropinaomas compared to both NFPAs and normal pituitary.

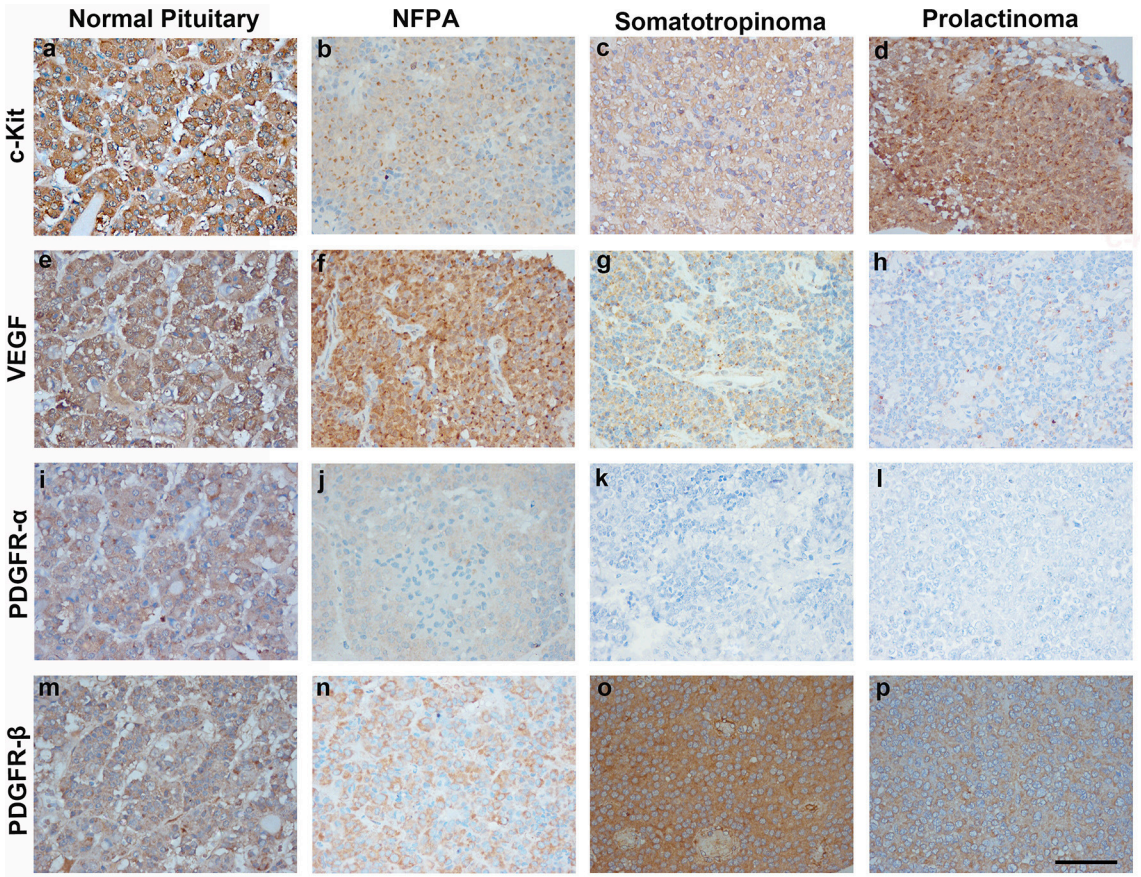

FIGURE 2 | Immunohistochemistry (IHC) of pituitary adenoma shows differential expression of tyrosine kinases (c-kit, VEGF, and PDGFR-α/β). Cytoplasmic immunopositivity for c-Kit was high in somatotropinoma followed by NFPA, prolactinoma, and normal pituitary **(a–d)**. Strong cytoplasmic expression for VEGF was observed in NFPA as compared to somatotropinomas, prolactinomas and normal pituitaries **(e–h)**. PDGFR-α expression was weakly positive in NFPA as compared to normal pituitary while it was negative for somatotropinoma and prolactinomas. **(i–l)**, PDGFR-β expression was strongly positive in somatotropinomas as compared to normal pituitary while it was weakly positive in NFPA and prolactinomas **(m–p)**.

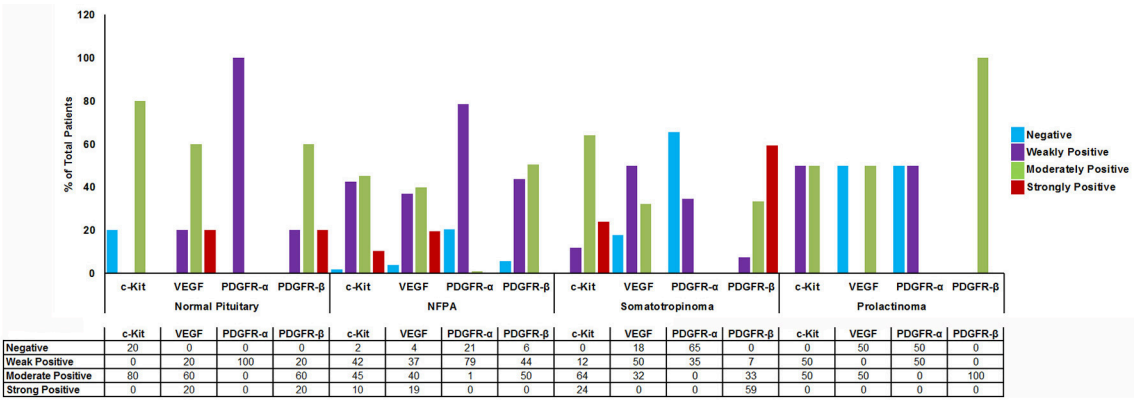

	c-Kit	VEGF	PDGFR-α	PDGFR-β	c-Kit	VEGF	PDGFR-α	PDGFR-β	c-Kit	VEGF	PDGFR-α	PDGFR-β	c-Kit	VEGF	PDGFR-α	PDGFR-β
Negative	20	0	0	0	2	4	21	6	0	18	65	0	0	50	50	0
Weak Positive	0	20	100	20	42	37	79	44	12	50	35	7	50	0	50	0
Moderate Positive	80	60	0	60	45	40	1	50	64	32	0	33	50	50	0	100
Strong Positive	0	20	0	20	10	19	0	0	24	0	0	59	0	0	0	0

FIGURE 3 | Graph showing percentage of cytoplasmic TK (c-Kit, VEGF, PDGFR-α/β) immunostaining in normal pituitary ($n = 4$), NFPAs ($n = 121$), somatotropinomas ($n = 32$), and prolactinomas ($n = 4$). c-Kit showed moderate to strong positivity in somatotropinomas. VEGF showed higher percentage of positivity in NFPA. PDGFR-β was strongly positive in maximum number of somatotropinomas (59%), whereas PDGFR-α was negative (65%).

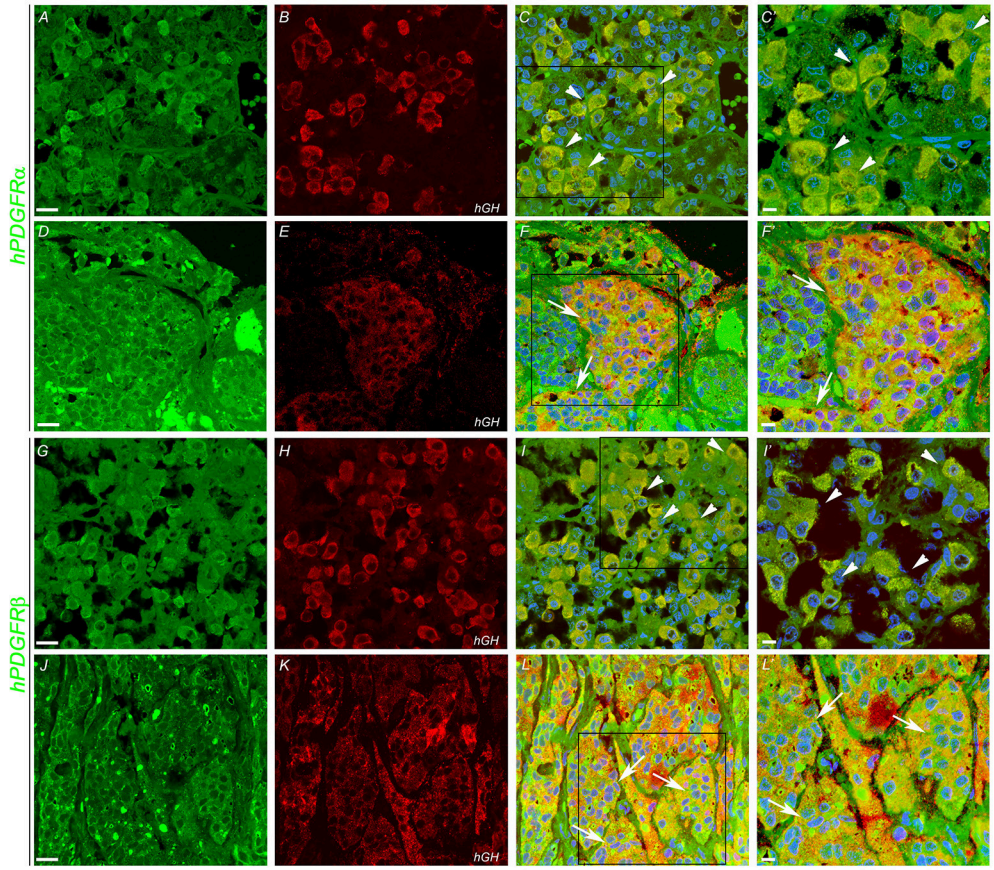

FIGURE 4 | Double immunofluoroscence showing co-expression (arrows) of PDGFR-α and PDGFR-β (green) and of hGH (red) in normal pituitary gland **(A,B,G,H)** and in somatotropinoma **(D,E,J,K)**. Overlays of the green and red channels are shown in the third column. **(C′,F′,I′,L′)** are the magnified views of the boxes marked in **(C,F,I,L)** respectively. Scale bar = 100 μm **(A–L)**, 50 μm **(C′,F′,I′,L′)**.

Efficacy of Imatinib Compared to Gold Standard Drugs—Octreotide and Pasireotide

The somatotropinoma cells were exposed to different concentration of GHRH (0–10 μM), octreotide (0–10^{-9} M) and pasireotide (0–20 μM). After standardization, the effect of imatinib on somatotropinomas was compared with octreotide (0.1 μM), pasireotide (10 μM), and GHRH (0.5 μM). It was observed that, compared to vehicle-treated controls, GHRH stimulation enhances GH synthesis (125%, $P < 0.01$) whereas pasireotide and octreotide cause significant decrease in GH (39 and 45.8%, $P < 0.0001$ and $P < 0.003$, respectively; **Supplementary Figure 2**). Although imatinib causes GH reduction in somatotropinoma cells (30%, $P < 0.01$), it was found to be less efficient than pasireotide (54%, $P < 0.01$) and octreotide (64%, $P < 0.01$; **Supplementary Figure 4**).

Mechanism of Imatinib Inhibition of GH Secretion

Our data indicates that imatinib has inhibitory effect on GH secretion in somatotropinomas. In order to understand the mechanism of action of imatinib in GH reduction in somatotropinoma cells we employed a tyrosine kinase (RTK) array. Cell lysates from somatotropinomas were subjected to tyrosine kinase array. Importantly we identified that PDGFR-beta was significantly decreased in the imatinib treated cell compared to the untreated cells. Importantly, this suggests that imatinib-mediated inhibition of GH release is mediated through PDGFR-β activation and the array detect phosphorylation status of the receptors (**Figure 6**).

DISCUSSION

In this study, we have demonstrated the differential expression of imatinib targets (c-kit, PDGFR-α/β, and VEGF) in different pituitary adenomas subtypes and we have shown that imatinib decreases GH secretion in cultured somatotropinoma cells and GH3 cell line acting through PDGFR-β pathway.

In the present study, we found differential expression of TK pathway members (c-kit, VEGF and PDGFR-α/β) on a large cohort of pituitary adenoma subtypes compared with normal pituitary samples. We have shown that in somatotropinomas and prolactinomas there is increased positivity of c-kit and PDGFR-β, whereas in NFPAs exhibit higher VEGF and PDGFR-α positivity. Thus, it was speculated that prolactinomas and

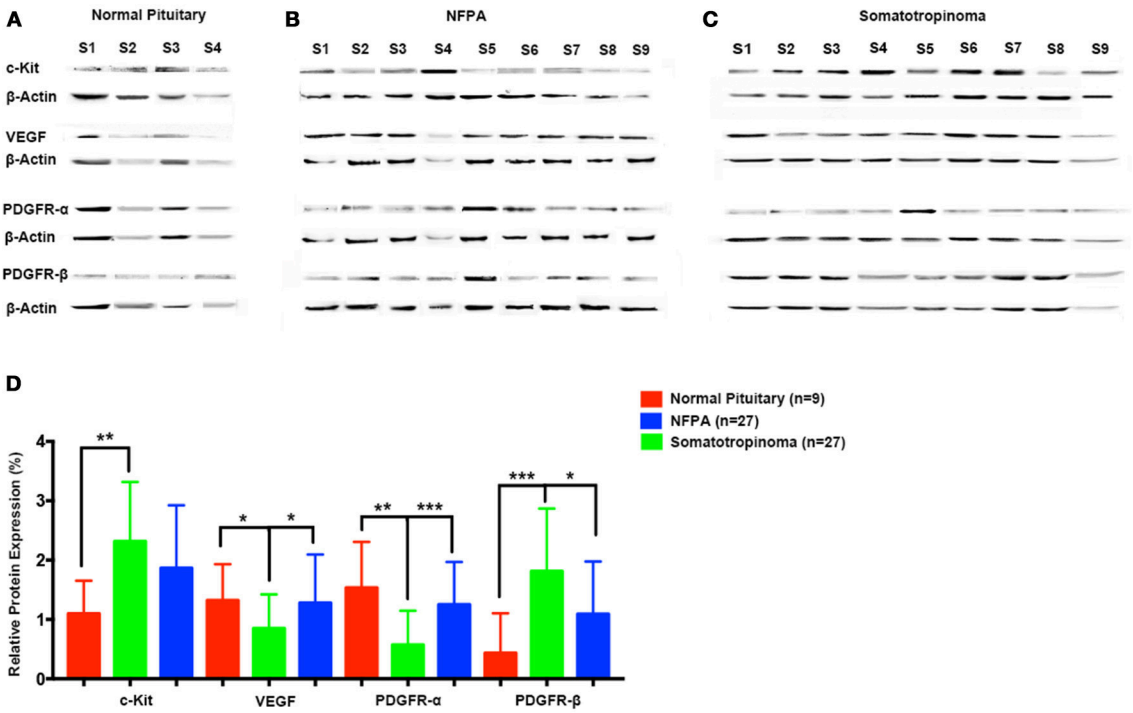

FIGURE 5 | Quantification of tyrosine kinases (c-Kit, VEGF, PDGFR-α, and PDGFR-β) using western blot in **(A)** normal pituitary ($n = 9$), **(B)** NFPA ($n = 27$), and **(C)** somatotropinomas ($n = 27$). Data were normalized to β-Actin and compared to expression in normal pituitary. **(D)** Similar to IHC findings, PDGFR-β and c-Kit was overexpressed in somatotropinoma ($P < 0.01$) compared to normal pituitary whereas PDGFR-α was under expressed in somatotropinoma ($P < 0.05$). $^{*}P < 0.05$; $^{**}P < 0.01$ and $^{***}P < 0.001$.

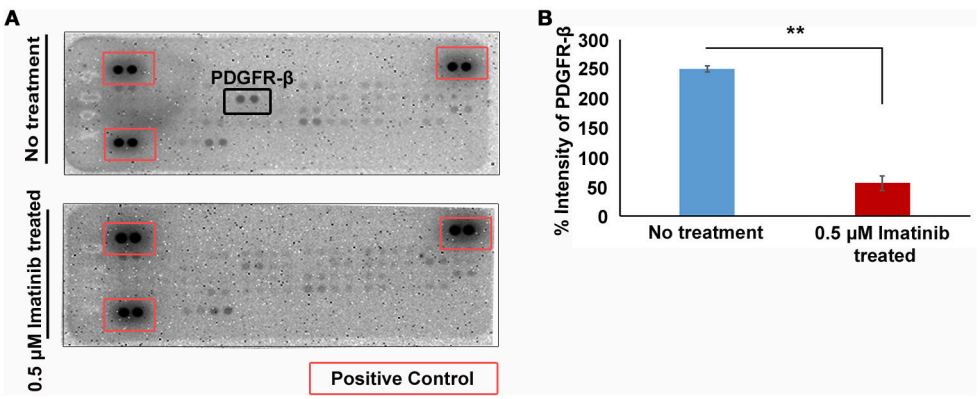

FIGURE 6 | Phospho-tyrosine profiling of somatotropinomas treated and untreated with 0.5 μM Imatinib. $^{**}P < 0.01$. **(A)** Phospho-tyrosine profiling of somatotropinomas treated and untreated with 0.5 μM Imatinib. Note the absence of PDGFR-β after imatinib treatment **(B)** Bar diagram showing reduction in PDGFR-β levels after treatment with 0.5 μM imatinib in primary culture of somatotropinoma cells ($P < 0.01$).

somatotropinomas lose PDGFR-α and acquire PDGFR-β. This result could have potentials for more precise mechanistic insights and therapeutic approaches.

La Rosa et al. have evaluated c-kit expression in normal human pituitary and 62 well characterized pituitary adenomas. In their study, c-kit expression was predominantly found in corticotropinomas followed by NFPA. However, it was absent in prolactinomas and somatotropinomas (8). Unlike their study, we found predominant expression of c-kit in NFPA and somatotropinomas, though we have not examined any patient with corticotropinoma and the intensity of positivity varied from tumor subtypes. Similar to our study, Casar et al. found cytoplasmic c-kit positivity in 52.4% and membranous positivity in 8.3% (9). Usually it is believed that the mutated protein translocates into the nucleus and gives nuclear positivity. However, neither our study nor Casar et al. had identified any

mutations in c-kit (10). We did whole exome sequencing in both in blood and tumor tissue in 11 patients with acromegaly and didn't find any mutation of c-kit (data not shown). Platelet-derived growth factor (PDGF) is a potent mitogen known to stimulate tumor growth in a number of human tumors through autocrine and/or paracrine loops (11). PDGF receptor and its ligand are believed to be expressed predominantly in folliculo stellate cells of the pituitary gland and regulate VEGF expression and activity (12). In a study by Sullivan et al. PDGF has been reported to stimulate GH secretion in somatotrophs and inhibit prolactin release from lacto-somatotroph GH4C1 and GH3 cell-lines (13). However, little is known about the expression of PDGFR in pituitary adenomas. In our study, the expression of PDGFR isoforms varied greatly between the pituitary tumor subtypes. Our results showed that PDGFR-α was over-expressed in NFPA compared to somatotropinomas, whereas PDGFR-β was increased in somatotropinomas as compared to NFPA. Double immunofluorescence confirmed reduced expression of PDGFR-α and increased expression of PDGFR-β. However, quantification by western blot showed definite increase in PDGFR-β levels.

The VEGF family consists of five glycoproteins (VEGF A-D) as well as placental growth factor. Of these, VEGF-A is the best characterized and commonly referred to as VEGF in humans (14). There have been contradicting reports about VEGF expression in pituitary adenomas. A study from McCabe et al. has shown that VEGF mRNA expression is higher in pituitary adenomas compared to the normal pituitary gland, probably due to PTTG action (15). Lloyd et al. have reported stronger VEGF expression in normal pituitary as compared to pituitary adenomas (16). Moreover, another report showed no significant difference in VEGF immunostaining between normal and adenomatous pituitary gland (17). However, decreased VEGF expression in pituitary adenomas has also been reported by Raica et al. (18). Anti-angiogenic therapy can sensitize tumor stem cells to radio- and chemo-therapy. Inhibition of the VEGF pathway can be achieved via neutralizing antibodies against VEGF (19). The VEGF receptor (VEGFR) expression is poorly studied in normal and adenomatous pituitary. VEGFR-2 expression analyzed on rodent showed elevated expression of VEGFR-2 after estrogen treatment (20). In our cohort, we observed significantly high expression of VEGF in NFPA as compared to somatotropinomas. Consistent with the results from previous study by McCabe et al. (15). VEGF was found to be differentially expressed in adenomatous pituitary in our cohort also (18). Like in our study, the work done by Cristina et al., showed that all our patients with prolactinoma (though small in number) were VEGF positive (21). Further, they have also shown that expression of above mentioned TK pathway members were not influenced by gender, age and Ki-67 index (21).

In vitro samples of primary cultures of somatotropinoma and rat pituitary adenoma cell line (GH3) showed that imatinib, a drug that causes growth failure in CML probably targeting GH or IGF-1 axis, inhibited GH secretion in a dose-independent manner and without affecting cell viability. GH lowering response was much robust in GH3 cell line, compared to primary culture. This could be because of pure cell population in case of commercial cell line. Our results also shed light on the mechanism of action of imatinib, which acts by inhibiting GH signaling via PDGFR-β/PKC pathway. However, it does not causes apoptosis. Further, real time PCR for *Pit-1* and *GH1* genes showed that imatinib does not affect GH synthesis but inhibits GH secretion, which is also corroborated by electron microscopic findings of loss of GH secretory granules in imatinib-treated GH3 cells. Similar to our cell viability results, a previous study by Venalis et al. have also shown that imatinib does not affect proliferation, viability, migration and metabolic activity of endothelial cells (22). At low concentration, it has relatively similar inhibition of BCR-ABL and c-kit in various malignancies. In patients with CML treated with 400–600 mg imatinib per day, the plasma concentration of 0.17–5.68 μM shows cytogenetic and hematologic response. The ED50 of imatinib calculated from our experiment was 0.015 μM, which is lower than the clinically relevant plasma concentrations (**Supplementary Figure 5**). Therefore, the plasma concentrations that can be achieved are likely to inhibit GH synthesis enough to be beneficial in patients with somatotropinoma. The maximum achievable plasma levels of imatinib in patients are not higher than 6.7 μM at maximum administered dose of 600 mg per day. Higher level of plasma concentration of imatinib is difficult to achieve because of adverse side effects of the drug. However, extrapolation of the data obtained from *in vitro* model to real life situation in patients with acromegaly needs long term trials. Although octreotide and pasireotide are more efficacious, imatinib could be used as an inexpensive alternative therapy or as an adjunct.

Patients with childhood CML who are on imatinib (targets-c-kit, PDGFR-α/β, and VEGF) and are in remission have growth retardation by affecting GH/IGF-1 axis, probably acting on somatotrophs (5). Previously we have shown a close association in common pathogenic mechanism in acromegaly and hematological disorders (23). Our observation of use of anti-VEGF therapy in childhood somatotropinomas demonstrated that it was very effective (24). Similarly, Ortiz et al. have successfully used the anti-VEGF antibody in a patient with silent corticotroph carcinoma with successful outcome (25). So, it could be a therapeutic option in selected subgroup of aggressive pituitary adenoma with or without other TKIs. Increased expression of VEGF in tumors that undergo apoplexy is well-known (26). We presume that this can be tried in future as a therapeutic option in patients with pituitary apoplexy who are poor surgical candidates, akin to vitreous hemorrhage in patients with diabetic retinopathy. A previous study by Fukuoka et al. have shown successful use of gefitinib, an epidermal growth factor receptor (EGFR) tyrosine kinase inhibitor in human and canine cultured corticotropinoma (27). They also reported that in mice, gefitinib treatment decreased both tumor size and cortisol level. However, mere expression of receptor in a tumor seen on IHC does not necessarily mean response to therapies targeting these receptors. Thus, NFPA express somatostatin receptor type 2 (SSTR2) and somatostatin receptor type 5 (SSTR5), they poorly responded to somatostatin analogs (28).

The cross-talk between different hormones, cytokines, receptors and growth factors play an important role in regulating cellular response. The GH receptor and the downstream pathways share a complex relationship with other receptor

and signaling pathway members. A variety of signaling pathways, including the Src, Grb2, MEK/MAP kinase, the phosphatidylinositol 3 (PI-3)-kinase, and the protein kinase C (PKC) pathways has been shown to be activated by both GH and PDGF. GH has been shown to interact with the IGF-1 receptor and downstream members of IGF-1 signaling pathways (29). A study by Rui et al. has reported that PDGF down regulate GH signaling via PKC dependent pathway. Further, they have shown that PDGF significantly reduces the tyrosyl phosphorylation of GHR (by 90%) and the amount of both total cellular GHR (by 80%) and GH binding (by 70%) (30). In somatotropinomas, both GH/GHR and PDGF/PDGFR can synergize the signal transduction that they elicit, at least in part by virtue of GH's ability to potentiate and sustain GH signaling. We hypothesize that imatinib might inhibit PDGFR-β preventing the binding of PDGF to PDGFR-β, thereby increasing the extracellular concentration of PDGF which further inhibits GH signaling pathway. In future we need to prove by adding PDGFR beta ligand to primary culture and see that GH is stimulated. On the other way PDGFR-β can be absorbed with an antibody and the cells can be thwart with this mixture to show that the antibody takes away the release effect of PDGFR-β. The somatostatin receptor ligands also inhibits GH through PKC and downstream pathway. In pediatric CML cases, growth retardation due to imatinib could be through this pathway.

The strength of our study is large sample size for validation through IHC, *in vitro* culture using both somatotropinoma cells and GH3 cell line. Four tire validation of protein expression doing IHC, western blot, RTK array, co-localization using double immunofluorescence and negative and positive controls using brain, tonsilar and placental tissue to exclude non-specific antibody binding (**Supplementary Figure 6**).

The limitations of our study are use of TMA which can sometimes not represent the expression of the whole sample due to heterogeneity. The second limitation is we had not looked for the impact of imatinib in densely and sparsely granulated somatototroph adenomas of variable sizes. We would have been wiser looking at the combined effect of imatinib and octreotide/pasireotide to look for augmented effect if any. Last but not the least data on PDGF stimulation and inhibition could have strengthened the study.

In conclusion, Imatinib targets (c-kit, VEGF, PDGFR-α/β) are differentially expressed between various giant pituitary adenoma subtypes and can serve as potential biomarkers. PDGFR-β was found to be over-expressed in giant somatotropinomas and possibly be used as selective target. Imatinib reduces GH secretion both in GH3 cell line and cultured somatotropinoma cell *in vitro* without affecting cell number. Therefore, it could be used as an adjunct for treating GH secreting pituitary adenoma.

Way forward: A clinical trial in a large cohort showing the response of somatotropinoma of variable sizes both in sparsely and coarsely granulated tumors to imatinib is required. Similarly, we have to weigh the risk and benefits of this drug because of potential side effects before it can be recommended for clinical use. Multi-targeted TKIs might be a suitable alternative treatment for these tumors in desperate cases.

ETHICS STATEMENT

The Study was carried out in accordance with the recommendations of Institute Ethics Committee of Postgraduate Institute of Medical Education and Research (PGIMER), Chandigarh, India. All subjects gave written informed consent in accordance with the Declaration of Helsinki. The protocol was approved by Institute Ethics Committee of PGIMER, Chandigarh, India (Ref No INT/IEC/2016/2724).

AUTHOR CONTRIBUTIONS

All authors listed have made a substantial, direct and intellectual contribution to the work, and approved it for publication.

FUNDING

The study was funded by an intramural research grant of the Postgraduate Institute of Medical Education and Research (71/6-Edu/13/3314) to KM. We would like to thank Indian Council of Medical Research (ICMR), Government of India for providing research fellowship for PG.

ACKNOWLEDGMENTS

We are thankful to Dr. Marta Korbonits, Prof. and Head, Department of Endocrinology, and Dr. Carles Gaston Massuet, senior lecturer, Department of Endocrinology, QMUL, London for their constructive comments. We are also thankful to them for providing culture protocol. We are deeply indebted to Dr. C S Rayat, Dept. of Histopathology, PGIMER Chandigarh for helping us with electron microsopy. We extend our gratitude to Dr. Manish Mistry, medical director, Novartis India Ltd. for generously gifting us crude salts of imatinib mesylate.

TRIBUTE

We are deeply saddened to inform the sudden, untimely and tragic demise of Prof. K.K. Mukherjee, Department of Neurosurgery, PGIMER, Chandigarh at the end of the study before publication could see the light. He was our dear friend, senior colleague and mentor. May his soul rest in peace and we wish that his legacy would continue.

SUPPLEMENTARY MATERIAL

The Supplementary Material for this article can be found online at: https://www.frontiersin.org/articles/10.3389/fendo.2018.00453/full#supplementary-material

REFERENCES

1. Hobernicht SL, Schweiger B, Zeitler P, Wang M, Hunger SP. Acquired growth hormone deficiency in a girl with chronic myelogenous leukemia treated with tyrosine kinase inhibitor therapy. *Pediatr Blood Cancer* (2011) 56:671–3. doi: 10.1002/pbc.22945
2. Shima H, Tokuyama M, Tanizawa A, Tono C, Hamamoto K, Muramatsu H, et al. Distinct impact of imatinib on growth at prepubertal and pubertal ages of children with chronic myeloid leukemia. *J Pediatr.* (2011) 159:676–81. doi: 10.1016/j.jpeds.2011.03.046
3. Bansal D, Shava U, Varma N, Trehan A, Marwaha RK. Imatinib has adverse effect on growth in children with chronic myeloid leukemia. *Pediatr Blood Cancer* (2012) 59:481–4. doi: 10.1002/pbc.23389
4. Rastogi MV, Stork L, Druker B, Blasdel C, Nguyen T, Boston BA. Imatinib mesylate causes growth deceleration in pediatric patients with chronic myelogenous leukemia. *Pediatr Blood Cancer* (2012) 59:840–5. doi: 10.1002/pbc.24121
5. Narayanan KR, Bansal D, Walia R, Sachdeva N, Bhansali A, Varma N, et al. Growth failure in children with chronic myeloid leukemia receiving imatinib is due to disruption of GH/IGF-1 axis. *Pediatr Blood Cancer* (2013) 60:1148–53. doi: 10.1002/pbc.24397
6. Tohti M, Li J, Ma C, Li W, Lu Z, Hu Y. Expression of AGR2 in pituitary adenomas and its association with tumor aggressiveness. *Oncol Lett.* (2015) 10:2878–82. doi: 10.3892/ol.2015.3734
7. Broekman F, Giovannetti E, Peters GJ. Tyrosine kinase inhibitors: multi-targeted or single-targeted? *World J Clin Oncol.* (2011) 2:80–93. doi: 10.5306/wjco.v2.i2.80
8. La Rosa S, Uccella S, Dainese L, Marchet S, Placidi C, Vigetti D, et al. Characterization of c-kit (CD117) expression in human normal pituitary cells and pituitary adenomas. *Endocr Pathol.* (2008) 19:104–11. doi: 10.1007/s12022-008-9032-4
9. Casar-Borota O, Fougner SL, Bollerslev J, Nesland JM. KIT protein expression and mutational status of KIT gene in pituitary adenomas. *Virchows Arch.* (2012) 460:171–81. doi: 10.1007/s00428-011-1185-8
10. Mukherjee KK, Rai A, Gupta P, Dutta P, Walia R, Bhansali A. Exome sequencing of acromegaly and cushing–what's new? In: *15th International Pituitary Congress*, Orlando, FL (2017). p. P46.
11. Klinghoffer RA, Mueting-Nelsen PF, Faerman A, Shani M, Soriano P. The two PDGF receptors maintain conserved signaling *in vivo* despite divergent embryological functions. *Mol Cell* (2001) 7:343–54. doi: 10.1016/S1097-2765(01)00182-4
12. Kowarik M, Onofri C, Colaco T, Stalla GK, Renner U. Platelet-derived growth factor (PDGF) and PDGF receptor expression and function in folliculostellate pituitary cells. *Exp Clin Endocrinol Diabetes* (2010) 118:113–20. doi: 10.1055/s-0029-1202832
13. Sullivan NJ, Tashjian AH Jr. Platelet-derived growth factor selectively decreases prolactin production in pituitary cells in culture. *Endocrinology* (1983) 113:639–45.
14. Ellis LM, Hicklin DJ. VEGF-targeted therapy: mechanisms of anti-tumour activity. *Nat Rev Cancer* (2008) 8:579–91. doi: 10.1038/nrc2403
15. McCabe CJ, Boelaert K, Tannahill LA, Heaney AP, Stratford AL, Khaira JS, et al. Vascular endothelial growth factor, its receptor KDR/Flk-1, and pituitary tumor transforming gene in pituitary tumors. *J Clin Endocrinol Metab.* (2002) 87:4238–44. doi: 10.1210/jc.2002-020309
16. Lloyd RV, Scheithauer BW, Kuroki T, Vidal S, Kovacs K, Stefaneanu L. Vascular endothelial growth factor (VEGF) expression in human pituitary adenomas and carcinomas. *Endocr Pathol.* (1999) 10:229–35.
17. Viacava P, Gasperi M, Acerbi G, Manetti L, Cecconi E, Bonadio AG, et al. Microvascular density and vascular endothelial growth factor expression in normal pituitary tissue and pituitary adenomas. *J Endocrinol Invest.* (2003) 26:23–8. doi: 10.1007/BF03345118
18. Raica M, Coculescu M, Cimpean AM, Ribatti D. Endocrine gland derived-VEGF is down-regulated in human pituitary adenoma. *Anticancer Res.* (2010) 30:3981–6.
19. Krause DS, Van Etten RA. Tyrosine kinases as targets for cancer therapy. *N Engl J Med.* (2005) 353:172–87. doi: 10.1056/NEJMra044389
20. Banerjee SK, Sarkar DK, Weston AP, De A, Campbell DR. Over expression of vascular endothelial growth factor and its receptor during the development of estrogen-induced rat pituitary tumors may mediate estrogen-initiated tumor angiogenesis. *Carcinogenesis* (1997) 18:1155–61.
21. Cristina C, Perez-Millan MI, Luque G, Dulce RA, Sevlever G, Berner SI, et al. VEGF and CD31 association in pituitary adenomas. *Endocr Pathol.* (2010) 21:154–60. doi: 10.1007/s12022-010-9119-6
22. Venalis P, Maurer B, Akhmetshina A, Busch N, Dees C, Sturzl M, et al. Lack of inhibitory effects of the anti-fibrotic drug imatinib on endothelial cell functions *in vitro* and *in vivo*. *J Cell Mol Med.* (2009) 13:4185–91. doi: 10.1111/j.1582-4934.2008.00492.x
23. Gupta P, Dutta P. Co-occurrence of acromegaly and hematological disorders: a myth or common pathogenic mechanism. *Integr Med Int.* (2017) 4:94–100. doi: 10.1159/000478932
24. Korbonits M, Dutta P, Reddy KS, Bhansali A, Gupta P, Rai A, et al. Exome sequencing reveals double hit by AIP gene mutation and copy loss of chromosome 11 but negative X-LAG in a pituitary adenoma of a 4 yrs child with gigantism treated with multimodal therapy. In: *Endocrine Society's 98th Annual Meeting and Expo*, April 1–4, 2016. Boston, MA (2016).
25. Ortiz LD, Syro LV, Scheithauer BW, Ersen A, Uribe H, Fadul CE, et al. Anti-VEGF therapy in pituitary carcinoma. *Pituitary* (2012) 15:445–9. doi: 10.1007/s11102-011-0346-8
26. Lee JS, Park YS, Kwon JT, Nam TK, Lee TJ, Kim JK. Radiological apoplexy and its correlation with acute clinical presentation, angiogenesis and tumor microvascular density in pituitary adenomas. *J Korean Neurosurg Soc.* (2011) 50:281–7. doi: 10.3340/jkns.2011.50.4.281
27. Fukuoka H, Cooper O, Ben-Shlomo A, Mamelak A, Ren SG, Bruyette D, et al. EGFR as a therapeutic target for human, canine, and mouse ACTH-secreting pituitary adenomas. *J Clin Invest.* (2011) 121:4712–21. doi: 10.1172/JCI60417
28. Colao A, Filippella M, Di Somma C, Manzi S, Rota F, Pivonello R, et al. Somatostatin analogs in treatment of non-growth hormone-secreting pituitary adenomas. *Endocrine* (2003) 20:279–83. doi: 10.1385/ENDO:20:3:279
29. Huang Y, Kim SO, Yang N, Jiang J, Frank SJ. Physical and functional interaction of growth hormone and insulin-like growth factor-I signaling elements. *Mol Endocrinol.* (2004) 18:1471–85. doi: 10.1210/me.2003-0418
30. Rui L, Archer SF, Argetsinger LS, Carter-Su C. Platelet-derived growth factor and lysophosphatidic acid inhibit growth hormone binding and signaling via a protein kinase C-dependent pathway. *J Biol Chem.* (2000) 275:2885–92. doi: 10.1074/jbc.275.4.2885

Conflict of Interest Statement: The authors declare that the research was conducted in the absence of any commercial or financial relationships that could be construed as a potential conflict of interest.

frontiers in Endocrinology

ORIGINAL RESEARCH
published: 28 August 2018
doi: 10.3389/fendo.2018.00468

Prolactin Variants in Human Pituitaries and Pituitary Adenomas Identified With Two-Dimensional Gel Electrophoresis and Mass Spectrometry

Shehua Qian[1,2,3], *Yongmei Yang*[4], *Na Li*[1,2], *Tingting Cheng*[1,2,3], *Xiaowei Wang*[1,2,3], *Jianping Liu*[5], *Xuejun Li*[6], *Dominic M. Desiderio*[7] *and Xianquan Zhan*[1,2,3,8]*

[1] Key Laboratory of Cancer Proteomics of Chinese Ministry of Health, Xiangya Hospital, Central South University, Changsha, China, [2] Hunan Engineering Laboratory for Structural Biology and Drug Design, Xiangya Hospital, Central South University, Changsha, China, [3] State Local Joint Engineering Laboratory for Anticancer Drugs, Xiangya Hospital, Central South University, Changsha, China, [4] Geriatric Department of Cadre's Ward, Baoji Traditional Chinese Medicine Hospital, Baoji, China, [5] Bio-Analytical Chemistry Research Laboratory, Modern Analytical Testing Center, Central South University, Changsha, China, [6] Department of Neurosurgery, Xiangya Hospital, Central South University, Changsha, China, [7] The Charles B. Stout Neuroscience Mass Spectrometry Laboratory, Department of Neurology, College of Medicine, University of Tennessee Health Science Center, Memphis, TN, United States, [8] The Laboratory of Medical Genetics, Central South University, Changsha, China

OPEN ACCESS

Edited by:
Corin Badiu, Carol Davila University of Medicine and Pharmacy, Romania

Reviewed by:
Mark S. Roberson, Cornell University, United States
Leila Warszawski, Instituto Estadual de Diabetes e Endocrinologia Luiz Capriglione, Brazil

***Correspondence:**
Xianquan Zhan
yjzhan2011@gmail.com

Specialty section:
This article was submitted to Pituitary Endocrinology, a section of the journal Frontiers in Endocrinology

Received: *28 April 2018*
Accepted: *30 July 2018*
Published: *28 August 2018*

Citation:
Qian S, Yang Y, Li N, Cheng T, Wang X, Liu J, Li X, Desiderio DM and Zhan X (2018) Prolactin Variants in Human Pituitaries and Pituitary Adenomas Identified With Two-Dimensional Gel Electrophoresis and Mass Spectrometry. Front. Endocrinol. 9:468. doi: 10.3389/fendo.2018.00468

Human prolactin (hPRL) plays multiple roles in growth, metabolism, development, reproduction, and immunoregulation, which is an important protein synthesized in a pituitary. Two-dimensional gel electrophoresis (2DE) is an effective method in identity of protein variants for in-depth insight into functions of that protein. 2DE, 2DE-based PRL-immunoblot, mass spectrometry, and bioinformatics were used to analyze hPRL variants in human normal (control; $n = 8$) pituitaries and in five subtypes of pituitary adenomas [NF^- ($n = 3$)-, FSH^+ ($n = 3$)-, LH^+ ($n = 3$)-, FSH^+/LH^+ ($n = 3$)-, and PRL^+ ($n = 3$)-adenomas]. Six hPRL variants were identified with different isoelectric point (*p*I)-relative molecular mass (M_r) distribution on a 2DE pattern, including variants V1 (*p*I 6.1; 26.0 kDa), V2 (*p*I 6.3; 26.4 kDa), V3 (*p*I 6.3; 27.9 kDa), V4 (*p*I 6.5; 26.1 kDa), V5 (*p*I 6.8; 25.9 kDa), and V6 (*p*I 6.7; 25.9 kDa). Compared to controls, except for variants V2-V6 in PRL-adenomas, V2 in FSH^+-adenomas, and V3 in NF^--adenomas, the other PRL variants were significantly downregulated in each subtype of pituitary adenomas. Moreover, the pattern of those six PRL variants was significantly different among five subtypes of pituitary adenomas relative to control pituitaries. Different hPRL variants might be involved in different types of PRL receptor-signaling pathways in a given condition. Those findings clearly revealed the existence of six hPRL variants in human pituitaries, and the pattern changes of six hPRL variants among different subtypes of pituitary adenomas, which provide novel clues to further study the functions, and mechanisms of action, of hPRL in human pituitary and in PRL-related diseases, and the potential clinical value in pituitary adenomas.

Keywords: prolactin variants, human pituitary, post-translational modifications, mass spectrometry, variant pattern

INTRODUCTION

Prolactin (PRL) is a four long α-helix protein hormone, which was discovered in mammals in the 1930s by Oscar Riddle, and in humans in the 1970s by Friesen et al. (1). The PRL-encoded gene is located on chromosome 6 in the human, and consists of five exons and four introns (2). The hPRL cDNA consists of 914 nucleotides and includes a 681-nucleotide open-reading frame that encodes the PRL prohormone with 227 amino acids (positions 1–227), 25.9 kDa, which contains a signal peptide in amino acid positions 1-28 (**Table 1**). Mature hPRL contains 199 amino acids (positions 29–227), 22.9 kDa, which removed the signal peptides (positions 1–28). PRL was originally named because of the fact that it promotes lactation in rabbit (3). PRL is a polypeptide hormone with complex function, and is synthesized and secreted in the anterior pituitary gland, but also in other tissues and organs, such as skin, prostate, and the immune system. Pituitary PRL secretion is regulated by a series of factors that are derived from the external environment and internal milieu. In mammals, hypothalamic regulation of pituitary PRL secretion is largely inhibitory. The physiological stimuli include suckling, stress, and increased levels of ovarian steroids; primary estrogen can elevate pituitary PRL secretion. PRL is produced in autocrine/paracrine and endocrine systems. After secretion, PRL transports to the target tissues mammary gland, prostate, liver, and ovary via the blood circulation to bind to two different types of short or long PRL receptors (PRLRs) to activate signal pathways, which include JaK2 activation, Ras-Raf-MAPK pathway, modulatory pathways, PI3K and downstream pathways, and stats (4). PRLs that interact with different short or long PRLRs must be different PRL variants.

Protein variants are mainly due to alternative splicing, post-translational modifications (PTMs), translocation, re-distribution, and spatial conformation alteration (5). Normal hPRL is 25.9 kDa with 227 amino acid residues for PRL prohormone in the pituitary gland or 22.9 kDa with 199 amino acid residues for mature PRL secreted into body fluid. However, PRL variants have been found in many mammals, which are derived from proteolytic cleavage, alternative splicing, and other PTMs such as phosphorylation, glycosylation, and polymerization in amino acid residues to result in changes in their *p*I and M_r. Further studies found that the main source of PRL variants in mammals is not alternative splicing, but cleavage of PRL, and those variants were 14-, 16-, and 22-kDa (6). Liu et al. found one variant of hPRL with a sperm-penetration assay to be relative to breast cancer (7). Sohm et al. discovered two variants of PRL in the tilapia species Oreochromis niloticus and in fish (8). Although PRL is involved in osmotic regulation, PRL variants contribute to an osmotic adjustment disorder. Bollengier et al. indicated four variants of rat PRL in the pituitary cell with two-dimensional gel electrophoresis (2DGE), and also found that those variants were derived from different PTMs (9). Most of publications are involved in the studies of non-human PRL variants with identity of only a few non-human PRL variants (10–12). Some studies also found hPRL variants ($n = 3$–4) (13). However, until now 2DGE has not been used to study the hPRL variants.

TABLE 1 | The amino acid sequence of hPRL prohormone (Swiss-Prot No.: P01236; position 1–227; 227 amino acids long, and 25.9 kDa), and mature PRL (position 29-227; 199 amino acids long, 22.9 kDa).

10	20	30	40	50
MNIKGSPWKG	**SLLLLLVSNL**	**LLCQSVAP**LP	ICPGGAARCQ	VTLRDLFDRA
60	70	80	90	100
VVLSHYIHNL	SSEMFSEFDK	RYTHGRGFIT	KAINSCHTSS	LATPEDKEQA
110	120	130	140	150
QQMNQKDFLS	LIVSILRSWN	EPLYHLVTEV	RGMQEAPEAI	LSKAVEIEEQ
160	170	180	190	200
TKRLLEGMEL	IVSQVHPETK	ENEIYPVWSG	LPSLQMADEE	SRLSAYYNLL
210	220			
HCLRRDSHKI	DNYLKLLKCR	IIHNNNC		

Signal peptide is position 1–28 in the underlined bold letters.

2DGE is an effective method to separate proteins according to different *p*I values in the isoelectric focusing (IEF) direction, and different M_r values in the sodium dodecyl sulfate-polyacrylamide gel electrophoresis (SDS-PAGE) direction (14). *p*I and M_r are the basic properties of a protein variant. 2DGE-based Western blotting coupled with antibody of a given protein can also be used to detect the variants of that protein. Therefore, 2DGE is able to array PRL variants with different *p*I and M_r. Mass spectrometry (MS) is an effect method to characterize the isolated PRL variants and identify PTMs with an analysis of amino acid sequence and determination of PTM sites. These types of MS have been used to study the 2DGE-separated pituitary proteins, including matrix-assisted laser desorption/ionization time-of-flight MS (MALDI-TOF MS) peptide fingerprint (PMF), MALDI-TOF-TOF MS and tandem mass spectrometry (MS/MS), and liquid chromatography-electrospray ionization-quadruple-ion trap MS (LC-ESI-Q-IT MS) MS/MS analysis (15–18).

This present study used 2DGE, 2DGE-based Western blotting, and MS to detect and identify hPRL variants in human pituitaries and differentially expressed profiles of hPRL variants among different subtypes of pituitary adenomas relative to controls, which will provide novel clues to further study the functions, and mechanisms of action, of hPRL in human pituitary and in PRL-related diseases, and the potential clinical value in pituitary adenomas.

MATERIALS AND METHODS

Tissue Samples

Human control pituitary glands were post-mortem tissues obtained from the National Disease Research Interchange ($n = 1$) and the Memphis Regional Medical Center ($n = 7$), which

Abbreviations: 2DGE, two-dimensional gel electrophoresis; BSA, bovine serum albumin; ddH_2O, deionized distilled water; DTT, dithiothreitol; ESI, electrospray ionization; FSH, follicle-stimulating hormone; hPRL, human prolactin; IEF, isoelectric focusing; IPG, immobilized pH gradient; LC, liquid chromatography; LH, leuteinizing hormone; MALDI, matrix-assisted laser desorption ionization; MS, Mass spectrometry; M_r, relative molecular mass; PBS, phosphate-buffered saline; pI, isoelectric point; PRL, prolactin; PRLR, prolactin receptor; PTMs, post-translational modifications; PVDF, polyvinylidene fluoride; SDS-PAGE, sodium dodecyl sulfate-polyacrylamide gel electrophoresis; TOF, time-of-flight.

were approved by University of Tennessee Health Science Center (UTHSC) Internal Review Board (IRB). Human pituitary adenoma tissues were obtained from the Emory University Hospital, which were approved by Emory University Hospital IRB, and Department of Neurosurgery of Xiangya Hospital, which were approved by the Xiangya Hospital Medical Ethics Committee of Central South University, China. Consent was obtained from each patient or the family of control pituitary subject after full explanation of the purpose and nature of all procedures used. All tissues were removed, frozen immediately in liquid nitrogen, and stored at −80°C until processing. The clinical information of pituitary adenoma and control samples is summarized in **Table 2**.

Protein Extraction

Tissue processing and protein extraction of pituitary control and adenoma tissues have been previously described (17, 19). Briefly, each tissue sample (∼600 mg) was washed with 0.9% NaCl (3 ml, 5×) to thoroughly remove blood, and was finely ground in liquid nitrogen. A volume (5 ml) of protein extraction buffer that contained 2 mol/L thiourea, 7 mol/L urea, 40 g/L CHAPS, 100 mmol/L dithiothreitol (DTT), 5 mol/L immobilized pH gradient (IPG) buffer pH 3-10 NL, and a trace of bromphenol blue was added, and the mixture was thoroughly mixed. The mixture was vortexed (2 h) on ice and was centrifuged (15,000 × g, 15 min, 4°C). The supernatant was collected, and its protein concentration was determined with a Bio-Rad 2D Quant kit (Bio-Rad). The supernatant was the "protein sample solution."

2DGE and Western Blot

First Dimension—IEF

IEF was performed with precast IPG strips (pH 3-10 NL, 180 × 3 × 0.5 mm) and 18 cm IPG strip holder on an IPGphor instrument (GE Healthcare). Before IEF, an aliquot (350 μl) of protein sample solution was loaded onto an IPG strips. The IPG strip was rehydrated about 18 h. IEF was performed at 25°C with the following parameters: a gradient 250 V and 1 h for 125 Vh, a gradient at 1000 V and 1 h for 500 Vh, a gradient at 8000 V and 1 h for 4000 Vh, a step-and-hold at 8000 h and 4 h for 32000 Vh, a step-and-hold at 500 V and 0.5 h for 250 Vh to achieve a total of 36,875 Vh and ∼7.5 h analysis. The IPG strip was removed and laid on its plastic back to blot off mineral oil. After IEF, IPG strips were processed with SDS-PAGE.

Second Dimension—SDS-PAGE

After IEF, an Ettan DALT II system (GE Healthcare, up to 12 gels at a time) was used. An Ettan DALTsix multiple casters (GE Healthcare) was used to cast the 12% PAGE resolving gel (250 × 215 × 1.0 mm). The resolving-gel solution was made by mixing 75 ml of 1.5 mol/L Tris-HCl pH 8.8, 90 ml of 400 g/L acrylamide/bis-acrylamide (29:1 = weight:weight, cross-linking ratio = 3.3%), 3 ml of 10% ammonium persulfate, 150 ml deionized distilled water (ddH_2O), and 50 μl of tetramethylethylenediamine. The IPG strip was equilibrated in 15 ml of reducing equilibration buffer (15 min) that consisted of a trace of bromphenol blue, 375 mmol/L Tris-HCl pH 8.8, 2% w/v SDS, and 20% v/v glycerol. The IPG strip was equilibrated in 15 ml of alkylation equilibrium solution (15 min) that consisted of 2.5% w/v iodoacetamide instead of 2% w/v DTT. A boiled solution that consisted of 1% w/v agarose solution was used to seal the equilibrated IPG strip onto the top of the resolving gel. 2DGE was performed in 25 L of Tris-glycine-SDS electrophoresis buffer that consisted of 192 mmol/L glycine, 25 mmol/L Tris-base, and 0.1 % w/v SDS at 25°C with a constant voltage (250 V, 360 min).

2DGE-Based Western Blot With Anti-hPRL Antibody

After electrophoresis, the 2D gel was removed, and proteins in the 2D gel were transferred to a polyvinylidene fluoride (PVDF) membrane (0.8 mA/cm^2 for 1 h 20 min) with an Amersham Pharmacia Biotech Nova Blot semi-dry transfer instrument. The proteins on the PVDF membrane were blocked for 1 h at room temperature with a solution (100 ml) of 0.3% bovine serum albumin/phosphate-buffered saline (BSA/PBS) with 0.2% Tween 20 and 0.1% sodium azide (PBST). The proteins on the PVDF membrane were incubated for 1 h at room temperature with rabbit anti-hPRL antibodies that were diluted (v:v = 1:1000) in a 0.3% BSA/PBST solution. After incubation with the primary antibody, the PVDF membrane was washed with 200 ml PBST solution (15 min × 4) and rinsed twice with ddH_2O. The secondary antibody, goat anti-rabbit alkaline phosphtase-conjugated IgG was diluted (v:v = 1:4000) in a 0.3% BSA/PBST solution. The solution was added to the blots for 1 h at room temperature. The membrane was washed with 200 ml PBST solution (15 min × 4), and proteins were visualized with 5-bromo-4-chloro-3-indolyl phosphate.

Protein Staining and Image Analysis

All 2DGE-separated proteins were visualized with silver-staining (20). The silver-stained 2D gel was digitized and analyzed with Discovery Series PDQuest 2D Gel Analysis software (15, 21).

MS Analysis and Database Searching

MALDI-TOF MS

MALDI-TOF MS was used to analyze each protein that was digested with trypsin. Experiments were performed on a Perseptive Biosystems MALDI-TOF Volyager DE-RP MS (Framingham, MA, USA). The parameters of the instrument were described (15). The protonated molecule ion $[M+H]^+$ was produced with MALDI-TOF MS. Data-processing software (DataExplore) was used to obtain accurate masses. Blank-gel experiments were conducted simultaneously to remove masses from known contaminants (usually keratin), matrix, trypsin, and other unknown contaminants. Each protein was identified by using the data obtained from MALDI-TOF MS PMF by searching the Swiss-Prot database 091215 (513877 sequences; 180750753 residues; January 19, 2015) with PeptIdent software.

LC-ESI-Q-IT MS

Proteins in 2D gel-spots that corresponded to each positive Western blot were excised and digested in the gel with trypsin. According to the manufacturer's method recommendations, the mixture of tryptic peptides was purified with a ZipTipC18 microcolumn. Purified tryptic peptides were analyzed with an

TABLE 2 | Clinical information of human pituitaries and pituitary adenomas.

Groups	Samples ID	Sex/Age	Clinical information	Immuno-histochemistry
Control pituitary	C4	M/45	White, Drowning. Blood alcohol = 3.1 g/L; no other drugs detected. Blood: HepBb (+), HepC (+), HIV (–)	DNT
	C2	M/27	Black, none	DNT
	C3	F/40	White, Multiple toxic compounds. Blood: HepB (+), HepC (+), HIV (–)	DNT
	C5	M/36	White, Multiple toxic materials. Blood alcohol = 0.5g/L. Blood: HepB (+), HepC (–), HIV (–)	DNT
	C7	F/34	Black, Gunshot wound to chest. Blood alcohol =0.3g/L; no drugs. Blood: HepB (+), HepC (–), HIV (–)	DNT
	C8	F	White, 15 h gunshot wound to head. No drugs or alcohol. Blood: HepB (–), HepC (–), HIV (–)	DNT
	C9	M/55	White, 12 h gunshot wound to chest. No alcohol or drugs. Blood: HepB (–), HepC (–), HIV (–)	DNT
	C10	F/47	White, smoke inhalation. No drugs or alcohol. Numerous amylacea present in brain. Early autolytic changes to brain. Blood: HepB (–), HepC (+), HIV (–)	DNT
Prolactinoma (PRL-PA)	T237	M/36	Prolactinoma, 1.918ng/ml, 2.0 × 2.1 × 2.5 cm	PRL3+
	T192	M/41	Prolactinoma,1.176ng/ml, 3 × 2.5 ×2.0 cm	PRL3+
	T131	F/52	Prolactinoma,359ng/ml, 2.5 × 3.5 ×2.8 cm	PRL3+
	T87	M/48	Prolactinoma with calcilication,	PRL+
	T914933	F/45	Prolactinoma, with active cell growth, invasive tumor	PRL++
NF-NFPA	T219	M/68	Non-functional, 1.9 × 2.3 × 2.2 cm, invasion of the right cavernous sinus	Neg.
	T164	M/35	Non-functional, visual loss, 3 × 3.5 × 4 cm. Partial hypopituitarism	Neg.
	T217	M/39	Non-functional	Neg.
LH-NFPA	T208	F/47	Non-functional, 2 × 2 × 2 cm	LH 1–2+
	T204	M/47	Non-functional	LH 3+
	T237	F/40	Non-functional, right cavernous sinus extension	LH 2+
LH/FSH-NFPA	T65	F/54	Non-functional, 4 × 4 × 4 cm, cavernous sinus invasion	LH 2+, FSH 1+
	T138	M/60	Non-functional, 2.9 × 3.1 × 3.5 cm	LH 2+, FSH 2+
	T185	M/66	Non-functional, 2.8 ×, 2 × 2.4 cm. Bilateral cavernous sinus invasion	LH 2-3+, FSH 2-3+
FSH-NFPA	T57	F/59	Non-functional, 2 × 3 cm	FSH 1+
	T89	M/62	Non-functional, 2 × 2.3 × 2.3 cm	FSH 2+
	T77	M/67	Non-functional, 2 × 2.2 × 2.4 cm, questionable cavernous sinus	FSH 2+

Neg, Immunohistochemical stains for ACTH, LH, FSH, PRL, GH, and TSH were negative. LH^+, nonfunctional pituitary adenoma that expressed leuteinizing hormone, or lutropin; FSH^+, nonfunctional pituitary adenoma that expressed follicle-stimulating hormone, or follitropin; FSH^+ and LH^+, nonfunctional pituitary adenoma that expressed both follicle-stimulating hormone and leuteinizing hormone. Adenomas were graded blindly by a neuropathologist (from 0 to 4) for the intensity of staining for each peptide hormone. NFPA, nonfunctional pituitary adenoma. DNT, Do not know.

LCQ^{Deca} mass spectrometer (Thermo-Finnigan, San Jose, CA, USA). The instrument parameters were: electron multiplier-900 V, ESI voltage 2.0 kV, and capillary probe temperature 110°C. The detailed experimental steps have been described (15). Data from LC-ESI-Q-IT MS were used to identify the protein with Swiss-Prot database.

MALDI-TOF-TOF MS

Proteins in the 2D gel-spots that corresponded to the positive Western blot were excised and digested in the gel with trypsin. For Perspective Biosystems MALDI-TOF-TOF MS analysis, the tryptic peptide extraction was eluted directly from a liquid chromatography microcolumn onto a MALDI plate with a matrix that contained 3 mg/ml saturated α-cyano-4-hydroxycinnamic acid solution. The purified tryptic peptide mixture was analyzed ($n = 5$). Tryptic peptides were analyzed with MALDI-TOF-TOF MS that operated in the reflective mode at an acceleration voltage of 25 kV over m/z 800-4000. Precursor ions close to the theoretical m/z were selected for TOF-TOF [UltraFlex III MALDI-TOF-TOF (Bruker Daltonics)] MS analysis. After automatic analysis, any remaining unidentified ions were manually analyzed. In the results obtained from MS, data

compared to the theoretical values from the database were used to determine whether these peptides had undergone PTMs.

Bioinformatics Analysis

NetPhos 3.1 Server (http://www.cbs.dtu.dk/services/NetPhos) (22, 23), NetNGlyc 1.0 Server (http://www.cbs.dtu.dk/services/NetNGlyc) (24), and NetOGlyc 4.0 Server (http://www.cbs.dtu.dk/services/NetOGlyc) (25) were used to predict phosphorylation sites, N-glycosylation sites, and O-glycosylation sites in the hPRL in human pituitaries, respectively.

Statistical Analysis

The Chi-square test included in SPSS 22 software was used to analyze the difference in proportional ratio of PRL variants among five subtypes of pituitary adenomas, with a significance level of $p = 0.05$.

RESULTS

2DGE Pattern of Six Human Pituitary PRL Variants and Their Differential Expression Changes Among Different Subtypes of Pituitary Adenomas

Approximately 1,200 protein spots were detected in each silver-stained 2D gel. Six protein spots were found to contain PRL (Swiss-Prot No. P01236) (**Figure 1**). Six 2D gel spots were MS-identified to contain hPRL with a different *p*I-*Mr* pattern, including hPRL variants v1 (*p*I 6.1; 26.0 kDa), v2 (*p*I 6.3; 26.4 kDa), v3 (*p*I 6.3; 27.9 kDa), v4 (*p*I 6.5; 26.1 kDa), v5 (*p*I 6.8; 25.9 kDa), and v6 (*p*I 6.7; 25.9 kDa).

The MS-identification of hPRL in spot v6 will be used here as a representative example. The tryptic peptides from spot v6 were analyzed with MALDI-TOF MS or MALDI-TOT-TOF MS. The PMF data were obtained from spot V6 (**Figure 2**), and four peptides were significantly matched to hPRL (P01236) in the Swiss-Prot human database. Moreover, the tryptic peptides from spot V6 were also analyzed with MALDI-TOF-TOF MS/MS or LC-ESI-Q-IT MS/MS. Three peptides from spot V6 were sequenced with MS/MS data, including ^{72}YTHGRGFITK^{81}, ^{118}SWNEPLYHLVTEVR^{131}, and ^{171}ENEIYPVWSGLPSLQMADEESR^{192}, to significantly match with hPRL (P01236) in the Swiss-Prot human database. The MS/MS spectrum of the tryptic peptide ^{118}SWNEPLYHLVTEVR^{131} contained a robust product-ion series that included b8, b9, b12, b13, y1, y2, y5, y6, y7, y10, y11, and y12 ions (**Figure 3**). Similarly, the hPRL in the other spots v1-v5 were identified (**Figure 1** and **Table 3**).

In the non-hormone expressed nonfunctional pituitary adenoma (NF-NFPA) group relative to controls (**Table 3**), hPRL was downregulated by 8.3-fold in spot v1 and 4.9-fold in spot v2, was not changed in spot v3, and was lost in spots v4, v5, and v6. In the leuteinizing hormone (LH)-positive NFPAs relative to controls, hPRL was downregualted by 12.6-fold in spot v1, 4.1-fold in spot v2, 26.2-fold in spot v3, 20.1-fold in spot v4, 36.7-fold in spot v5, and 33.6-fold in spot v6. In the follicle-stimulating hormone (FSH)-positive NFPAs relative to controls, hPRL was not changed in spot v2, lost in spot v5, and was downregulated by 46.2-fold in spot v1, 14.6-fold in spot v3, 17.6-fold in spot v4, and 11.3-fold in spot v6. In FSH/LH-positive NFPAs relative to controls, hPRL in all spots was downregulated by 99.9-, 3.8-, 12.3-, 19.0-, 19.7-, and 32.6-fold, respectively. However, for prolactinomas (PRL-adenomas) relative to controls, hPRL was downregulated in only spot v1 by 3.4-fold, and not changed in the other spots. Moreover, the overall proportional ratio of six PRL variants was significantly different among the five subtypes of pituitary adenomas (NF^-, FSH^+-, LH^+-, FSH^+/LH^+-, and PRL^+-adenomas) analyzed here with the Chi-square test performed with SPSS 22 software ($p < 0.05$) (**Figure 4**). The Chi-square tests carried out between every two subtypes of pituitary adenomas indicated that the proportional ratio of six hPRL variants was significantly different between every two subtypes of pituitary adenomas ($p < 0.05$), except for no significant difference between subtypes FSH^+/LH^+ and PRL^+, and between subtypes FSH^+ and PRL^+.

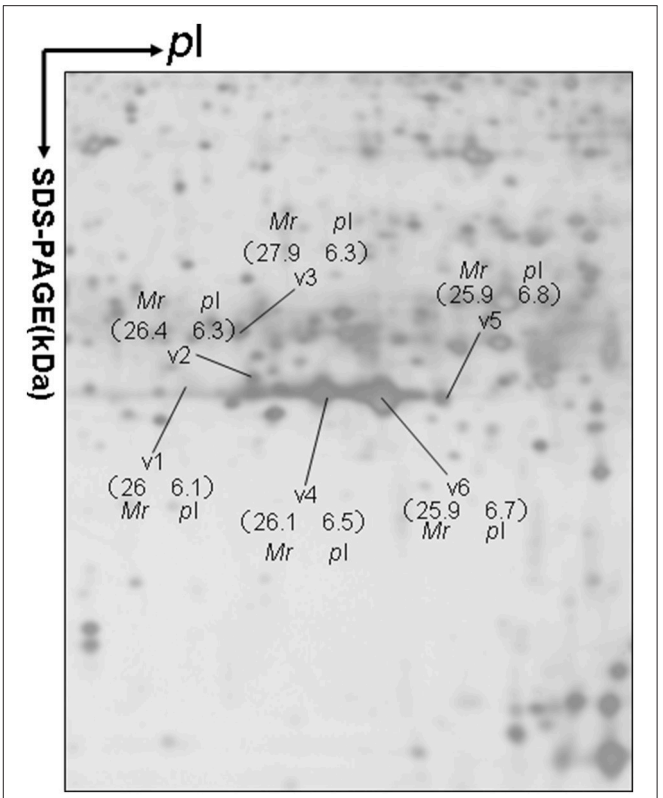

FIGURE 1 | A representative 2DGE image (master gel image from a control) between a comparison between 8 control tissues and 16 human pituitary adenoma tissues. IEF was done with an 18-cm IPG strip (pH 3–10, nonlinear), and vertical SDS-PAGE was done with a 12% polyacrylamide gel.

Validation of hPRL Variants With 2DGE-Based PRL Immunoaffinity Blot

2DGE-based Western blot coupled with anti-hPRL antibody and MS was an effective method to validate hPRL variants in human pituitaries. Four hPRL variants in human pituitary, including variants v1, v4, v5, and v6, were detected with an hPRL

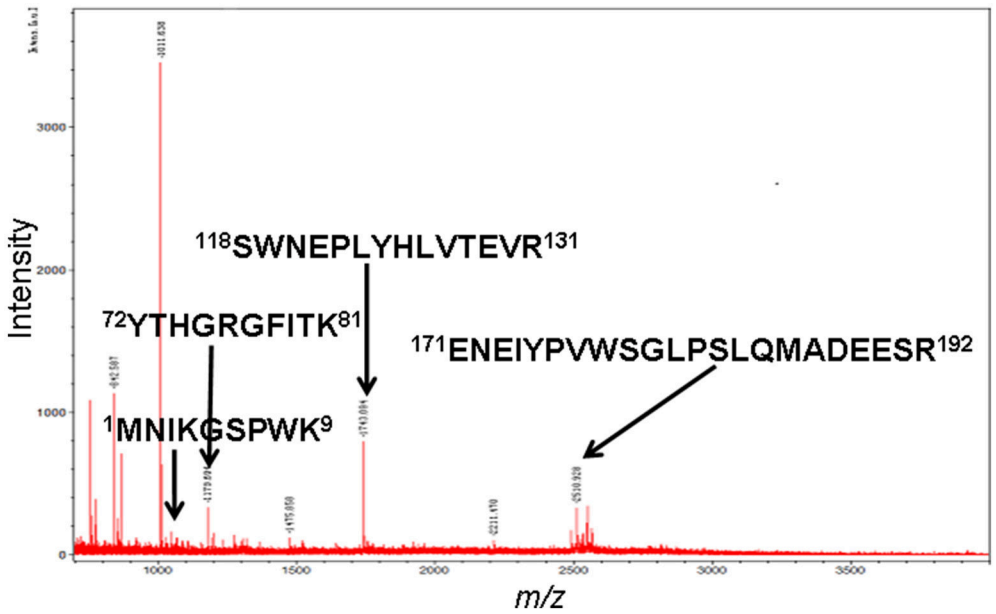

FIGURE 2 | MS spectrum of hPRL that was contained in spot v6.

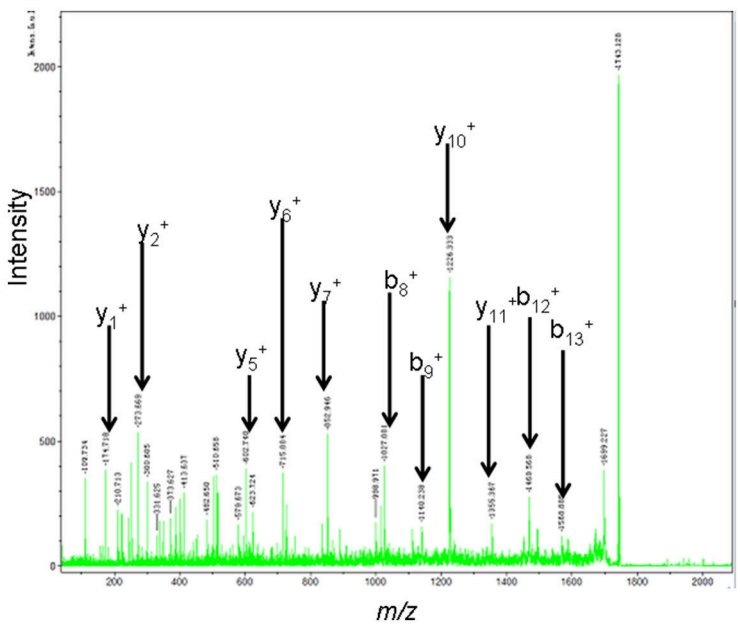

Seq	b#	b+	y+	y#
S	1	88.04	---	14
W	2	274.12	1655.85	13
N	3	388.16	1469.78	12
E	4	517.20	1355.73	11
P	5	614.26	1226.69	10
L	6	727.34	1129.64	9
Y	7	890.40	1016.55	8
H	8	1027.46	853.49	7
L	9	1140.55	716.43	6
V	10	1239.62	603.35	5
T	11	1340.66	504.28	4
E	12	1469.71	403.23	3
V	13	1568.77	274.19	2
R	14	---	175.12	1

FIGURE 3 | MS/MS spectrum of the tryptic peptide ^{118}SWNEPLYHLVTEVR^{131} that was derived from hPRL in spot v6. The upper right corner is the theoretically calculated b- and y-ions for this analyzed tryptic peptide. The corresponding observed b- and y-ions were labeled in the MS/MS spectrum.

Western blot-immunopositive reaction (**Figure 5**). Furthermore, the protein in each immunopositive spot (v1, v4, v5, and v6) was identified as PRL (Swiss-Prot No. P01236) with MALDI-TOF-MS PMF data and MALDI-TOF-TOF MS/MS. The PMF data (calculated; observed) of those four validated hPRL variants are collected in **Table 4**. Two tryptic peptides were obtained in spot v1, including ^{72}YTHGRGFITK^{81} with a $[M+H]^+$ ion at *m/z* 1179.7 and ^{118}SWNEPLYHLVTEVR^{131} with a $[M+H]^+$ ion at *m/z* 1743.0. Two tryptic peptides that is the same as spot v1 were also identified in spot v4. Compared to spots v1 and v4, one more tryptic peptide ^{171}ENEIYPVWSGLPSLQMADEESR^{192} with a $[M+H]^+$ ion at *m/z* 2550.6 was identified in spot v6. The tryptic peptide ^{118}SWNEPLYHLVTEVR^{131} of PRL in spot v6 was also analyzed with MALDI-TOF-TOF MS/MS.

TABLE 3 | Prolactin variants changed in different subtypes of pituitary adenomas relative to control pituitaries.

Variant No.	SSP No.	Protein description	Swiss-prot No.	*p*I	M_r	Ratio (NF^-: Con)	Ratio (FSH^+/LH^+: Con)	Ratio (FSH^+: Con)	Ratio (LH^+: Con)	Ratio (PRL: Con)
V1	4106	Chain1:prolactin	P01236	6.1	26.0	−8.3	−99.9	−46.2	−12.6	−3.4
V2	4215[a)]	Prolactin precursor	P01236	6.3	26.4	−4.9	−3.8	1	−4.1	1
V3	4216	Chain1:prolactin	P01236	6.3	27.9	1	−12.3	−14.6	−26.2	1
V4	5114[b)]	Chain1:prolactin	P01236	6.5	26.1	−100	−19.0	−17.6	−20.1	1
V5	6109	Chain1:prolactin	P01236	6.8	25.9	−100	−19.7	−100	−36.7	1
V6	6119	Chain1:prolactin	P01236	6.7	25.9	−100	−32.6	−11.3	−33.6	1

[a)]characterized with LC-ESI MS/MS; [b)]characterized with LC-ESI-MS/MS and MALDI-TOF PMF; all other proteins were characterized with MALDI-TOF PMF. LH^+, NF that expressed leuteinizing hormone, or lutropin; FSH^+, NF that expressed follicle-stimulating hormone, or follitropin; FSH^+ and LH^+, NF that expressed both follicle-stimulating hormone and leuteinizing hormone; NF-, NF that had negative immunohistochemical stains for ACTH, FSH, GH, LH, prolactin, and TSH. Each adenoma was graded blindly by a neuropathologist from 0 to 4 for intensity of staining for each peptide hormone. Con, control; -, decreased relative to controls;−100, lost relative to controls; 1, no change relative to controls; M_r, kDa

A Proportional ratio of hPRL variants among five subtypes of pituitary adenomas (PAs)

Variant	NF^-	FSH^+/LH^+	FSH^+	LH^+	PRL^+
V1	2.64%	53.34%	24.24%	9.45%	40.48%
V2	1.56%	2.03%	0.52%	3.08%	11.90%
V3	0.31%	6.57%	7.66%	19.65%	11.91%
V4	31.83%	10.14%	9.18%	15.08%	11.90%
V5	31.83%	10.52%	52.47%	27.53%	11.91%
V6	31.83%	17.40%	5.93%	25.21%	11.90%
Total	100.00%	100.00%	100.00%	100.00%	100.00%

*χ^2=360.606, p = 0.000 (p < 0.01), among five subtypes of pituitary adenomas

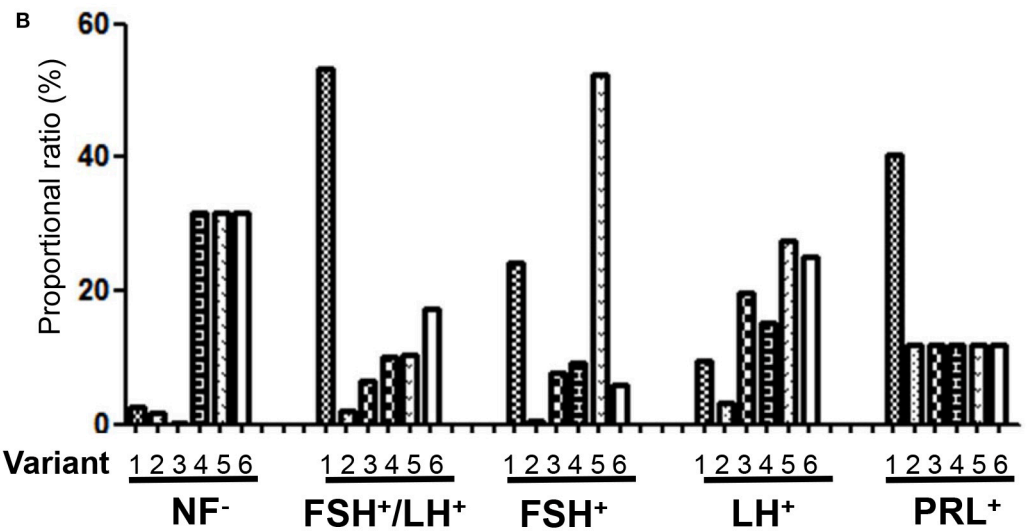

FIGURE 4 | Comparison of the proportional ratio of PRL variants among different subtypes of pituitary adenomas.

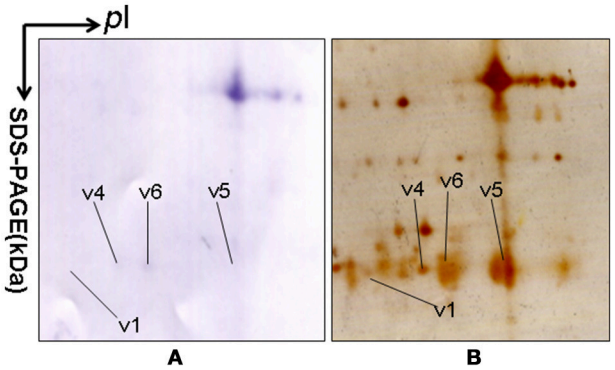

FIGURE 5 | 2DGE-based Western blot confirmed hPRL variants in pituitary tissues. IEF was done with an 18-cm IPG strip (pH 3-10, nonlinear), and vertical SDS-PAGE was done with a 12% polyacrylamide gel. The primary antibody was rabbit anti-hPRL antibody. The second antibody was goat anti-rabbit alkaline phosphtase-conjugated IgG. **(A)** Western blot image of anti-hPRL proteins (rabbit anti-hPRL antibodies + goat anti-rabbit alkaline phosphtase-conjugated IgG). **(B)** Silver-stained image on a 2D gel after transfer of protein to a PVDF membrane.

TABLE 4 | Tryptic peptides of prolactin identified with mass spectrometry.

Variant No.	Tryptic peptide	Calculated $[M+H]^+$ ion (m/z)	Observed $[M+H]^+$ ion (*m/z*)
V1	^{72}YTHGRGFITK^{81}	1178.6	1179.7
	^{118}SWNEPLYHLVTEVR^{131}	1741.9	1743.0
V4	^{72}YTHGRGFITK^{81}	1178.6	1179.7
	^{118}SWNEPLYHLVTEVR^{131}	1741.9	1743.0
V6	^{72}YTHGRGFITK^{81}	1178.6	1179.7
	^{118}SWNEPLYHLVTEVR^{131}	1741.9	1743.1
	^{171}ENEIYPVWSGLPSLQMADEESR^{192}	2549.2	2550.6
V5	^{118}SWNEPLYHLVTEVR^{131}	1741.9	1743.0
	^{171}ENEIYPVWSGLPSLQMADEESR^{192}	2549.2	2550.2

The calculated $[M+H]^+$ ion of each PRL tryptic peptide was obtained with the EXPASY-PeptideMass tool (https://web.expasy.org/peptide_mass/). The observed $[M+H]^+$ ion in each MALDI-TOF PMF spectrum was compared to the calculated $[M+H]^+$ ion to determine the status of PRL variant in each 2-D gel spot.

Those two tryptic peptides ^{118}SWNEPLYHLVTEVR^{131} and ^{171}ENEIYPVWSGLPSLQMADEESR^{192}, were also identified at spot v5, with $[M+H]^+$ ions at *m/z* 1743.0 and 2550.2, respectively.

2DGE-based Western blot coupled with anti-hPRL antibody and MS clearly confirmed hPRL variants that were contained in spots v1, v4, v5, and v6 (**Figure 1** vs. **Figure 5**). However, the hPRL variants in spots v2 (*p*I 6.3; 26.4 kDa) and v3 (*p*I 6.3; 27.9 kDa) were not confirmed; that finding might be due to several factors: (i) the PRL antibody was a general antibody, not specific to a given variant, and (ii) the M_r of hPRL in the spots v2 and v3 was larger than the M_r (25.9 kDa) of hPRL, obviously some adducts were added to the hPRL, which could be result in its non-reaction with the hPRL antibody. Whether the hPRL was detected with an immunoblot or not the hPRL in spots v2 and v3 was unequivocally identified with MS and MS/MS (**Figure 1**). Therefore, hPRL in spots v2 and v3 is still recognized as the hPRL variants in human pituitaries.

Determination of Signal Peptide (Position 1-28) Contained in Each hPRL Variant in Human Pituitaries

PRL in human Swiss-Prot database contains 227 amino acids (position 1–227) with a signal peptide (position 1-28) (**Table 1**), which is a prohormone of hPRL with a molecular weight of 25.9 kDa, whereas mature hPRL contains 199 amino acids (position 29–227) with a removal of the signal peptide (position 1–28), with a molecular weight of 22.9 kDa. Therefore, it is necessary to determine whether those identified six hPRL variants are derived from hPRL prohormone or mature hPRL. With the theoretical calculation using PeptideMass Cleavage software (**Table 5**), there are seven characteristic tryptic peptides (positions 1–4, 1–9, 1–38, 5–9, 5–38, 10–38, and 10–44) derived from hPRL prohormone (position 1–227) that can be used to determine the signal peptide (position 1–28) in the identified hPRL variants, and there are three characteristic tryptic peptides (positions 29–38, 29–44, and 29–49) derived from mature hPRL (position 29–227) that can be used to determine the removal of signal peptide (position 1–28) in the identified hPRL variants. Comprehensive analysis of all MS data and MS/MS data of hPRL in spots v1–v6, demonstrated that three characteristic tryptic peptides (positions 29–38, 29–44, and 29–49) were not found (**Table 5**), and that one characteristic tryptic peptide (position 1–9, MNIKGSPWK, $[M+H]^+$ *m/z* 106.5608) was identified (**Table 5** and **Figure 2**). Two small characteristic tryptic peptides (position 1-4, MNIK, $[M+H]^+$ *m/z* 505.2803; position 5–9, GSPWK, $[M+H]^+$ *m/z* 574.2983) were not detected because they were out of the range of MS acquisition (**Figure 2**). Moreover, from the 2DGE pattern of six hPRL variants (**Figure 1**), it is clear that variants v1, v4, v5, and v6 had the corresponding M_r of 26.0 kDa, 26.1 kDa, 25.9 kDa, and 25.9 kDa, respectively, which are very close to the molecular weight of hPRL prohormone 25.9 kDa; and that the variants v2 and v3 have the corresponding M_r of 26.4 kDa, and 27.9 kDa, which is a bit larger than the molecular weight of hPRL prohormone 25.9 kDa. Therefore, according to MS data and 2DGE pattern, the identified six hPRL variants in human pituitary tissue should be derived from hPRL prohormone (position 1–227), but not from mature hPRL (position 29–227).

Bioinformatic Prediction of Potential Factors to Result in hPRL Variants

Alternative splicing and PTMs are two main factors to result in protein variants. From the analysis in the section determination of signal peptide (position 1–28) contained in each hPRL variant in human pituitaries, six identified hPRL variants were not from splicing and truncation. Thus, PTMs might be the main factor to result in six hPRL variants. In the 2DGE map of hPRL variants (**Figure 1**), variants v1, v4, v5, and v6 had the very similar M_r, but with obviously measurably different p*I*. The deamidation of an asparagine (N) residue to aspartate (D) and of glutamine (Q)

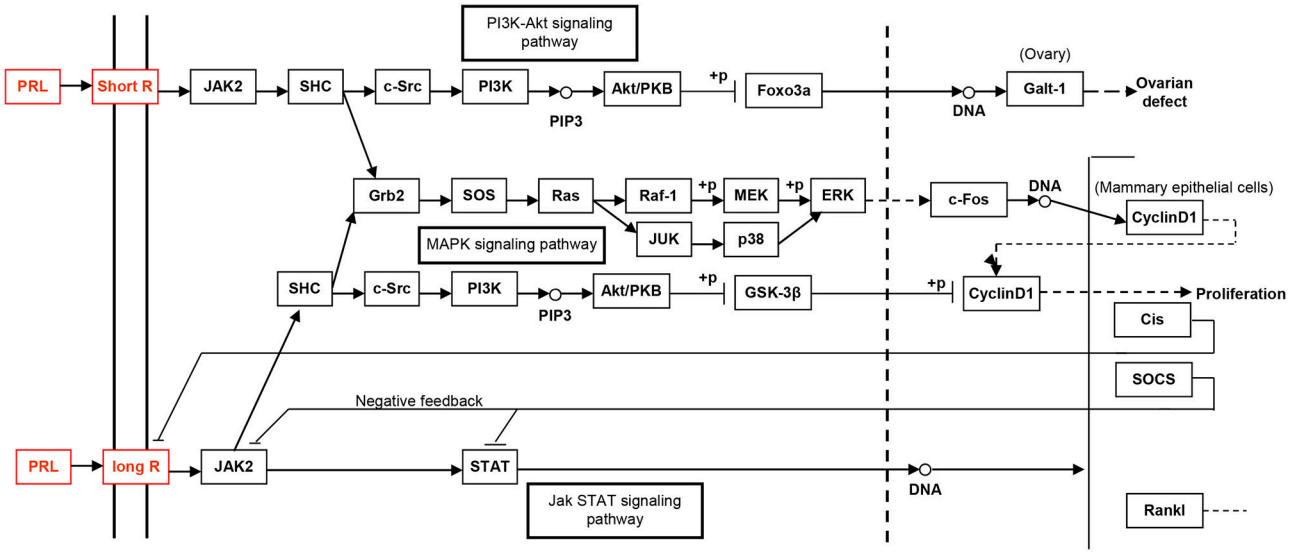

FIGURE 6 | The PRL-driven signaling pathways via the short or long PRL receptors, which was achieved from KEGG pathway database.

TABLE 5 | Characteristic tryptic peptides to determine signal peptide (position 1–28) within the identified hPRL variants.

Calc. $[M+H]^+$	Position	Characteristic tryptic peptide sequence	Observed $[M+H]^+$
505.2803	1–4	MNIK	–
1060.5608	1–9	MNIKGSPWK	+
3930.1893	1–38	MNIKGSPWKGSLLLLLVSNL LLCQSVAPLPICPGGAAR	–
574.2983	5–9	GSPWK	–
3443.9268	5–38	GSPWKGSLLLLLVSNLLLCQ SVAPLPICPGGAAR	–
2888.6463	10–38	GSLLLLLVSNLLLCQSVAPL PICPGGAAR	–
3589.0154	10–44	GSLLLLLVSNLLLCQSVAPL PICPGGAARCQVTLR	–
954.5189	29–38	LPICPGGAAR	–
1654.8879	29–44	LPICPGGAARCQVTLR	–
2301.1954	29–49	LPICPGGAARCQVTLRDLFD R	–

+, this peptide ion was observed with mass spectrometry in each MS spectrum. -, this peptide was not observed with mass spectrometry.

residue to glutamate (E) is an effect of protein aging, and is often observed in 2-D gels (26–29). Deamidation results in a series of spots with the same M_r values but measurably different *p*I values (30), with an increase of 1 Da in peptide mass and a decrease in the apparent p*I* from the uncharged amide to a negatively charged carboxylate anion at pH 7.4. Moreover, deamidation might be produced under the basic conditions for storing samples (30).

In the 2DGE map of hPRL variants (**Figure 1**), variants v2 and v3 had the same apparent p*I* but obviously measurably different M_r, and their M_r 26.4 kDa and 27.9 kDa were a bit larger than hPRL prohormone (25.9 kDa). This phenomenon might arise from some PTMs with a relatively larger chemical group, such as glycosylation or phosphorylation. Glycosylation means that the protein contains one or more covalently linked carbohydrates of various types from monosaccharides to branched polysaccharides. Phosphorylation means that the protein is modified by the attachment of either a single phosphate group, or of a complex molecule such as 5'-phospho-DNA through a phosphate group at the targeted serine, threonine, or tyrosine residues. The annotation page of hPRL in the UniProt database (https://www.uniprot.org/uniprot/P01236); P01236, or PRL_HUMAN) clearly demonstrates the hPRL is a glycoprotein or phosphoprotein. Moreover, multiple phosphorylated sites at the serine (S), threonine (T), and tyrosine (Y) residues were significantly predicted by NetPhos 3.1 Server, including 14 pS sites, 5 pT sites, and 3 pY sites in the hPRL (**Table 6**). Ten significantly N-glycosylated sites were predicted by NetNGlyc 1.0 Server in the hPRL (**Table 7**), and six significantly O-glycosylated sites were predicted by NetOGlyc 4.0 Server in the hPRL (**Table 8**).

DISCUSSION

Biological Functions of PRL in Different Physiological and Pathological Conditions

PRL plays an extremely important role in different vertebrate species and organ systems, such as growth, metabolism, development, reproduction, immunoregulation (31), behavior and brain (6), water and balance (32), stress response, and suppression of (33–35) and regulation of firing of oxytocin neurons (36, 37). As it is named, PRL exerts multiple effects that include development (mammogenesis) and stimulation of mammary gland growth, synthesis of milk (lactogenesis), and maintain the secretion of milk (galactopoiesis) on the mammary gland (38). Moreover, PRL affects reproduction of

TABLE 6 | Prediction of phosphorylation sites in hPRL (position 1–227) with NetPhos 3.1 Server with a score more than 0.5.

Sequence	#	x	Context	Score	Kinase	Answer
Sequence	6	S	NIKGSPWKG	0.779	unsp	YES
Sequence	11	S	PWKGSLLLL	0.848	PKA	YES
Sequence	18	S	LLLVSNLLL	0.523	cdc2	YES
Sequence	42	T	RCQVTLRDL	0.891	unsp	YES
Sequence	61	S	IHNLSSEMF	0.718	unsp	YES
Sequence	62	S	HNLSSEMFS	0.553	unsp	YES
Sequence	66	S	SEMFSEFDK	0.991	unsp	YES
Sequence	72	Y	FDKRYTHGR	0.503	INSR	YES
Sequence	73	T	DKRYTHGRG	0.557	unsp	YES
Sequence	90	S	CHTSSLATP	0.585	DNAPK	YES
Sequence	93	T	SSLATPEDK	0.737	unsp	YES
Sequence	110	S	KDFLSLIVS	0.507	PKA	YES
Sequence	118	S	SILRSWNEP	0.749	unsp	YES
Sequence	124	Y	NEPLYHLVT	0.956	unsp	YES
Sequence	142	S	EAILSKAVE	0.517	CKII	YES
Sequence	151	T	IEEQTKRLL	0.983	unsp	YES
Sequence	163	S	ELIVSQVHP	0.623	ATM	YES
Sequence	169	T	VHTEPKENE	0.541	CKII	YES
Sequence	175	Y	ENEIYPVWS	0.804	unsp	YES
Sequence	191	S	ADEESRLSA	0.576	cdc2	YES
Sequence	194	S	ESRLSAYYN	0.982	unsp	YES
Sequence	207	S	LRRDSHKID	0.993	unsp	YES

MNIKGSPWKGSLLLLLVSNLLLCQSVAPLPICPGGAARCQVTLRDLFDRA	#	50
VVLSHYIHNLSSEMFSEFDKRYTHGRGFITKAINSCHTSSVTLRDLFDRA	#	100
QQMNQKDFLSLIVSILRSWNEPLYHLVTEVRGMQEAPEAILSKAVEIEEQ	#	150
TKRLLEGMELIVSQVHPETKENEIYPVWSGLPSLQMADEESRLSAYYNLL	#	200
HCLRRDSHKIDNYLKLLKCRIIHNNNC	#	250
.....S....S.....S.....T.....	#	50
.....SS...S.....YT.....S..T.....	#	100
.....S.....S.....Y.....S.....	#	150
.....S.....T.....Y.....S..S.....	#	200
.....S.....		

the mammalian species. During pregnancy, PRL concentrations are high. During pregnancy, low immunity might be associated with PRL. Decreased serum PRL might cause anxiety in the first trimester of pregnancy (39). PRL induces and maintains maternal behaviors in rabbit, rat, hamsters, and sheep (40). These maternal behaviors include cleaning, nesting, grouping, and nursing of the baby by the mother (41, 42). Aside from the effects of PRL on reproductive processes, PRL also plays a significant role to maintain homeostasis of the body's environment by development of blood vessels (angiogenesis), regulation of the immune systems, and osmotic balance (3). PRL is also involved in the synthesis and secretion of milk, and the major ions in milk are sodium, potassium, and chloride ions. The levels of chloride and sodium ions in milk are low, and potassium is high (43). PRL might maintain low levels of sodium in milk because it can promote sodium retention in the mammary gland.

Moreover, PRL is involved in some endocrine-related cancers. PRL plays a vital role in the regulation of the immune responses; it interferes with inhibiting apoptosis, induces B-cell tolerance, increases antibody secretion, enhances antigen presentation, and upregulates cytokine production (44). PRL has different functions in the immune system of healthy people, including Treg cell inhibitory factor and inhibition of cell secretion (45). PRL contributes to the inflammatory microenvironment by reducing the inhibitory effect of Treg cells on T cells (45, 46). The proteolytic fragments of native PRL inhibit angiogenesis. Anti-angiogenic activity is achieved by the interaction between the 16 kDa N-terminal fragment of PRL and a specific receptor (47). Under normal conditions, PRL can promote the growth and development of the mammary gland, and the 16 kDa fragment of PRL can inhibit angiogenesis. Dilatation and regression of blood vessels seriously affect the normal growth and degeneration of breast cancer. However, angiogenesis disorders are the characteristics of growth and metastasis of breast cancer. That is not given physiological significance. It seems possible that the 16-kDa fragment of PRL plays a pathological role to inhibit angiogenesis or a local inhibitor of tumorigenesis.

TABLE 7 | Prediction of N-glycosylation sites in hPRL (position 1–227) with NetNGlyc 1.0 Server with score more than 0.5.

MNIKGSPWKGSLLLLLVSNLLLCQSVAPLPICPGGAARCQVTLRDLFDRAVVLSHYIHNLSSEMFSEFDKRYTHGRGFIT	80
KAINSCHTSSVTLRDLFDRAQQMNQKDFLSLIVSILRSWNEPLYHLVTEVRGMQEAPEAILSKAVEIEEQTKRLLEGMEL	160
IVSQVHPETKENEIYPVWSGLPSLQMADEESRLSAYYNLLHCLRRDSHKIDNYLKLLCRIHNNNC	
. n . . . . . n . . . . . N	80
. . . n . . . . . n . . . . . n	160
. . . . . n . . . . . n . . . . . n . . . . . n . . .	

SeqName	Position	Potential	Jury Agreement	N-Glyc result	
Sequence	2 NIKG	0.7530	(9/9)	+ + +	
Sequence	19 NLLL	0.7151	(9/9)	++	
Sequence	59 NLSS	0.7380	(9/9)	++	
Sequence	84 NSCH	0.7312	(8/9)	+	
Sequence	104 NQKD	0.6020	(7/9)	+	SEQUON
Sequence	120 NEPL	0.6051	(6/9)	+	ASN-XAA-SER/THR.
Sequence	172 NEIY	0.5346	(5/9)	+	
Sequence	198 NLLH	0.5642	(5/9)	+	
Sequence	212 NYLK	0.6726	(8/9)	+	
Sequence	224 NNNC	0.5146	(5/9)	+	
Sequence	225 NNC-	0.3576	(8/9)	–	
Sequence	226 NC–	0.3351	(9/9)	–	

Asn-Xaa-Ser/Thr sequons in the sequence are highlighted in blue. Asparagines predicted to be N-glycosylated are highlighted in red.

TABLE 8 | Prediction of O-glycosylation sites in hPRL (position 1–227) with NetOGlyc 4.0 Server with score more than 0.5.

#Seq name	Source	Feature	Start	End	Score	Strand	Frame	Comment
SEQUENCE	netOGlyc-4.0.0.13	CARBOHYD	25	25	0.134588	.	.	
SEQUENCE	netOGlyc-4.0.0.13	CARBOHYD	42	42	0.190888	.	.	
SEQUENCE	netOGlyc-4.0.0.13	CARBOHYD	54	54	0.194926	.	.	
SEQUENCE	netOGlyc-4.0.0.13	CARBOHYD	66	66	0.176466	.	.	
SEQUENCE	netOGlyc-4.0.0.13	CARBOHYD	73	73	0.111052	.	.	
SEQUENCE	netOGlyc-4.0.0.13	CARBOHYD	80	80	**0.613645**	.	.	#POSITIVE
SEQUENCE	netOGlyc-4.0.0.13	CARBOHYD	85	85	**0.618483**	.	.	#POSITIVE
SEQUENCE	netOGlyc-4.0.0.13	CARBOHYD	88	88	**0.602886**	.	.	#POSITIVE
SEQUENCE	netOGlyc-4.0.0.13	CARBOHYD	89	89	**0.717093**	.	.	#POSITIVE
SEQUENCE	netOGlyc-4.0.0.13	CARBOHYD	90	90	**0.928857**	.	.	#POSITIVE
SEQUENCE	netOGlyc-4.0.0.13	CARBOHYD	93	93	**0.778272**	.	.	#POSITIVE
SEQUENCE	netOGlyc-4.0.0.13	CARBOHYD	128	128	0.181904	.	.	
SEQUENCE	netOGlyc-4.0.0.13	CARBOHYD	151	151	0.11243	.	.	
SEQUENCE	netOGlyc-4.0.0.13	CARBOHYD	163	163	0.424529	.	.	
SEQUENCE	netOGlyc-4.0.0.13	CARBOHYD	169	169	0.122664	.	.	
SEQUENCE	netOGlyc-4.0.0.13	CARBOHYD	179	179	0.380532	.	.	
SEQUENCE	netOGlyc-4.0.0.13	CARBOHYD	183	183	0.309982	.	.	
SEQUENCE	netOGlyc-4.0.0.13	CARBOHYD	191	191	0.1589	.	.	
SEQUENCE	netOGlyc-4.0.0.13	CARBOHYD	194	194	0.249957	.	.	

The bold values mean statistical significantly positive results.

Determination of the Number of hPRL Variants in Human Pituitaries

The pituitary proteome was separated with 2DGE, followed by MS identification. Six 2D gel spots were found to contain hPRL with MS-identification, which represents six hPRL variants in human pituitaries. Of them, four hPRL variants (v1, v4, v5, and v6) were confirmed with 2DGE-based Western blotting in combination with anti-hPRL antibodies and followed by MS identification. However, two hPRL variants (v2 and v3) was not detected with 2DGE-based Western blotting in combination with anti-hPRL antibodies, which is due to the factors: (i) anti-hPRL antibody was not a variant-specific antibody, and (ii) those two hPRL variants might have different properties including different PTMs and unknown factors to cause its no-reaction

with anti-hPRL antibody. Anyway, this present study directly MS-identified the hPRL in six different 2D gel spot with different *p*I and M_r. Therefore, the present study still used the six hPRL variants to study their differential expression profile among different subtypes of pituitary adenomas.

Formation of hPRL Variants in Human Pituitaries

There are many factors that might produce protein variants: (i) Estimates of DNA level variation. Major sources of human protein variation include the encoding of single nucleotide polymorphisms and mutations. (ii) The main source of RNA level variation. Alternative splicing is a key factor in transcriptome complexity and regulating complex human characteristics. (iii) Errors in translation. Errors in protein translation provide a very large potential source of proteome expansion, especially in stressed or aging cells. (iv) PTMs. Due to PTMs, the potential number of proteoforms can increase exponentially (48). PTMs might have a certain influence on the structure and function of the protein; for example, PTMs of α-synuclein are major regulators of their function, structure, degradation, and toxicity (49). PTMs of the FUS protein might affect its associated pathology and serve as a therapeutic target (50). Currently, different types of PTMs have been found in the human, including glycosylation, phosphorylation, acetylation, ubquitination, methylation, deamidation, and nitration (27, 28, 51). These factors could also produce hPRL variants.

The present study found that six PRL variants that are derived from the same PRL gene in human pituitaries were not due to alternative splicing, but rather to PTMs, including deamidation, glycosylation, and phosphorylation. The hPRL variants v1, v4, v5, and v6 on the 2DGE map had a very similar M_r but obviously different p*I*, which might be mainly due to deamidaton. The hPRL variants v2 and v3 with a slightly larger M_r relative to hPRL (position 1–227) might be mainly due to the glycosylation and phosphorylation. Therefore, PTMs might be the main reason to produce hPRL variants. Furthermore, we confirmed that the amino acid sequence of six identified hPRL variants in human pituitaries contained the signal peptide (position 1–28), which is the hPRL prohormone (position 1–227), but not the mature PRL (position 29–227).

Potential Molecular Mechanisms of Action of hPRL Variants Elucidated by Signaling Pathway Networks

The study of the hPRL signaling pathway network is helpful to understand its functions; explore molecular mechanism of PRL-related tumors such as pituitary adenomas, including prolactinomas; develop effective therapeutic drugs; and discover tumor biomarkers (52). Only after the interaction between PRL and its receptors can PRL play a corresponding function. For example, for the secretion of milk, the binding of PRL and PRL receptor (PRLR) does not activate cell membrane binding enzyme, but phospholipase A. The signaling pathway map of hPRL is complex (**Figure 6**). There are two types of PRLRs: long-PRLR and short-PRLR. PRL binding to different receptors can cause different physiological functions. The signaling pathways activated by PRL binding to different receptors are specific and exhibit crossover. PRL binding to short receptors activates the PI3K/Akt signaling pathway, whereas PRL binding to long receptors activates the JAK2/STAT signaling pathway. The cross-signaling pathway activated by the binding of PRL to long or short receptors is a MAPK signaling pathway that activates cell cycle regulators and thus affects cell proliferation. The different short or long PRLRs should bind different hPRL variants v1–v6 to activate different signaling pathways and produce different biological effects in different physiological and pathological conditions. Furthermore, the significantly differential expression of six hPRL variants (**Table 3**) might result in different signaling pathway alteration. The further studies on the association of different hPRL variants and PRLR signaling pathway might have important scientific merits and clinical significance.

STRENGTH AND LIMITATION

The present study clearly demonstrated the existence of six hPRL variants in human pituitaries with 2DGE and MS analyses, and its differential expression profile of six hPRL variants among different subtypes of pituitary adenomas; and confirmed that those six hPRL variants in human pituitary tissues were derived from hPRL prohormone with 227 amino acids (position 1–227), but not from mature hPRL with 199 amino acids (position 29–227).

However, mature PRL is secreted by prolactotroph cells concentrated on both sides of the posterior pituitary gland and enters the bloodstream after secretion. After blood transport, PRL will bind to its specific receptor before it can play a corresponding physiological role. PRL in pituitary tissue is difficult to detect with routine examinations, but PRL in blood is relatively easy to detect. Under normal circumstances, the level of PRL in the blood plays its role in a certain range. The abnormal secretion of PRL is related to many diseases, such as hyperprolactinemiaemia, tumor, and autoimmune diseases. Studies have shown that PRL has a direct or indirect relationship with many diseases. Whether these diseases are associated with serum PRL variants remains unknown. Therefore, it is necessary in our future studies to in-depth investigate the mechanisms and function of different PRL variants and the status of serum PRL variants. The present study provides the basis for us to in-depth study serum PRL variants and their functions.

CONCLUSION

2DGE, 2DGE-based Western blot coupled with anti-hPRL antibody, MS, and bioinformatics were used to identify hPRL variants in human pituitaries, and their differential expression profiles among different pituitary adenomas. Six hPRL variants in human pituitaries were identified, including two hPRL variants that were not detected by Western blotting. The differential expression patterns of six hPRL variants were significantly different among five subtypes of pituitary adenomas (NF^-, FSH^+-, LH^+-, FSH^+/LH^+-, and PRL^+-adenomas). Moreover,

six hPRL variants in human pituitaries derived from hPRL prohormone (position 1–227) with different PTMs such as deamidation, glycosylation, and phosphorylation, but not from mature hPRL (position 29–227). Those findings provide novel insights into the functions, and mechanisms of action, of hPRL in human pituitary and in PRL-related diseases, and into the potential clinical value in pituitary adenomas. Furthermore, the hPRL variants involved signaling pathways that might clarify the biological functions of different PRL variants and their potential clinical significance, and contribute to the development of drugs that block the PRL signaling pathway for clinical treatment.

AUTHOR CONTRIBUTIONS

SQ analyzed data, prepared figures and tables, designed, and wrote the manuscript. YY collected tissue samples, performed clinical explanation, and carried out bioinformatics analysis and partial revision of manuscript. NL, TC, XW, and JL participated in experiments and partial data analysis. XL collected tissue samples and performed clinical diagnosis. DD participated in design, instructed, and critically revised manuscript. XZ conceived the concept, designed experiments, and manuscript, instructed experiments and data analysis, supervised results, coordinated, critically revised/wrote manuscript, and was responsible for its financial supports and the corresponding works. All authors approved the final manuscript.

ACKNOWLEDGMENTS

This work was supported by the grants from the China 863 Plan Project (Grant No. 2014AA020610-1 to XZ), National Natural Science Foundation of China (Grant No. 81572278, 81272798, and 81770781), SCIBP Supported Projects (Grant No. SCIBP2018060008), the Xiangya Hospital Funds for Talent Introduction (to XZ), and the Hunan Provincial Natural Science Foundation of China (Grant No. 14JJ7008 to XZ).

REFERENCES

1. Cabrera-Reyes EA, Limon-Morales O, Rivero-Segura NA, Camacho-Arroyo I, Cerbon M. Prolactin function and putative expression in the brain. *Endocrine* (2017) 57:199–213. doi: 10.1007/s12020-017-1346-x
2. Owerbach D, Rutter WJ, Cooke NE, Martial JA, Shows TB. The prolactin gene is located on chromosome 6 in humans. *Science* (1981) 212:815–6. doi: 10.1126/science.7221563
3. Binart N, Bachelot A, Bouilly J. Impact of prolactin receptor isoforms on reproduction. *Trends Endocrinol Metab.* (2010) 21:362–8. doi: 10.1016/j.tem.2010.01.008
4. Clevenger CV, Furth PA, Hankinson SE, Schuler LA. The role of prolactin in mammary carcinoma. *Endocr Rev.* (2003) 24:1–27. doi: 10.1210/er.2001-0036
5. Zhan X, Long Y, Lu M. Exploration of variations in proteome and metabolome for predictive diagnostics and personalized treatment algorithms: Innovative approach and examples for potential clinical application. *J Proteomics* (2017). doi: 10.1016/j.jprot.2017.08.020. [Epub ahead of print].
6. Freeman ME, Kanyicska B, Lerant A, Nagy G. Prolactin: structure, function, and regulation of secretion. *Physiol Rev.* (2000) 80:1523–631. doi: 10.1152/physrev.2000.80.4.1523
7. Liu Y, Gong W, Breinholt J, Norskov-Lauritsen L, Zhang J, Ma Q, et al. Discovery of the improved antagonistic prolactin variants by library screening. *Protein Eng Des Sel.* (2011) 24:855–60. doi: 10.1093/protein/gzr047
8. Sohm F, Pezet A, Sandra O, Prunet P, De Luze A, Edery M. Activation of gene transcription by tilapia prolactin variants tiPRL188 and tiPRL177. *FEBS Lett.* (1998) 438:119–23. doi: 10.1016/S0014-5793(98)01285-X
9. Bollengier F, Velkeniers B, Hooghe-Peters E, Mahler A, Vanhaelst L. Multiple forms of rat prolactin and growth hormone in pituitary cell subpopulations separated using a Percoll gradient system: disulphide-bridged dimers and glycosylated variants. *J Endocrinol.* (1989) 120:201–6. doi: 10.1677/joe.0.1200201
10. Mittra I. A novel "cleaved prolactin" in the rat pituitary: part I. Biosynthesis, characterization and regulatory control. *Biochem Biophys Res Commun.* (1980) 95:1750–9. doi: 10.1016/S0006-291x(80)-80101-X
11. Oetting WS, Walker AM. Differential isoform distribution between stored and secreted prolactin. *Endocrinology* (1986) 119:1377–81. doi: 10.1210/endo-119-3-1377
12. Asawaroengchai H, Russell SM, Nicoll CS. Electrophoretically separable forms of rat prolactin with different bioassay and radioimmunoassay activities. *Endocrinology* (1978) 102:407–14. doi: 10.1210/endo-102-2-407
13. Pansini F, Bergamini CM, Malfaccini M, Cocilovo G, Linciano M, Jacobs M, et al. Multiple molecular forms of prolactin during pregnancy in women. *J Endocrinol.* (1985) 106:81–5. doi: 10.1677/joe.0.1060081
14. Zhan X, Yang H, Peng F, Li J, Mu Y, Long Y, et al. How many proteins can be identified in a 2DE gel spot within an analysis of a complex human cancer tissue proteome? *Electrophoresis* (2018) 39:965–80. doi: 10.1002/elps.201700330
15. Zhan X, Desiderio DM. A reference map of a human pituitary adenoma proteome. *Proteomics* (2003) 3:699–713. doi: 10.1002/pmic.200300408
16. Zhan X, Wang X, Desiderio DM. Pituitary adenoma nitroproteomics: current status and perspectives. *Oxid Med Cell Longev* (2013) 2013:580710. doi: 10.1155/2013/580710
17. Moreno CS, Evans CO, Zhan X, Okor M, Desiderio DM, Oyesiku NM. Novel molecular signaling and classification of human clinically nonfunctional pituitary adenomas identified by gene expression profiling and proteomic analyses. *Cancer Res.* (2005) 65:10214–22. doi: 10.1158/0008-5472.can-05-0884
18. Zhan X, Wang X, Desiderio DM. Mass spectrometry analysis of nitrotyrosine-containing proteins. *Mass Spectrome Rev.* (2015) 34:423–48. doi: 10.1002/mas.21413
19. Evans CO, Moreno CS, Zhan X, Mccabe MT, Vertino PM, Desiderio DM, et al. Molecular pathogenesis of human prolactinomas identified by gene expression profiling, RT-qPCR, and proteomic analyses. *Pituitary* (2008) 11:231–45. doi: 10.1007/s11102-007-0082-2
20. Zhan X, Desiderio DM. Mass spectrometric identification of *in vivo* nitrotyrosine sites in the human pituitary tumor proteome. *Methods Mol Biol.* (2009) 566:137–63. doi: 10.1007/978-1-59745-562-6_10
21. Peng F, Li J, Guo T, Yang H, Li M, Sang S, et al. Nitroproteins in human astrocytomas discovered by gel electrophoresis and tandem mass spectrometry. *J Am Soc Mass Spectrom.* (2015) 26:2062–76. doi: 10.1007/s13361-015-1270-3
22. Blom N, Gammeltoft S, Brunak S. Sequence and structure-based prediction of eukaryotic protein phosphorylation sites. *J Mol Biol.* (1999) 294:1351–62. doi: 10.1006/jmbi.1999.3310
23. Blom N, Sicheritz-Ponten T, Gupta R, Gammeltoft S, Brunak S. Prediction of post-translational glycosylation and phosphorylation of proteins from the amino acid sequence. *Proteomics* (2004) 4:1633–49. doi: 10.1002/pmic.200300771
24. Gupta R, Brunak S. Prediction of glycosylation across the human proteome and the correlation to protein function. *Pac Symp Biocomput.* (2002) 2002:310–22. doi: 10.1142/9789812799623_0029
25. Steentoft C, Vakhrushev SY, Joshi HJ, Kong Y, Vester-Christensen MB, Schjoldager KT, et al. Precision mapping of the human O-GalNAc glycoproteome through SimpleCell technology. *EMBO J.* (2013) 32:1478–88. doi: 10.1038/emboj.2013.79

26. Zhan X, Giorgianni F, Desiderio DM. Proteomics analysis of growth hormone isoforms in the human pituitary. *Proteomics* (2005) 5:1228–41. doi: 10.1002/pmic.200400987
27. Tsai PK, Bruner MW, Irwin JI, Ip CC, Oliver CN, Nelson RW, et al. Origin of the isoelectric heterogeneity of monoclonal immunoglobulin h1B4. *Pharm Res* (1993) 10:1580–6.
28. Sarioglu H, Lottspeich F, Walk T, Jung G, Eckerskorn C. Deamidation as a widespread phenomenon in two-dimensional polyacrylamide gel electrophoresis of human blood plasma proteins. *Electrophoresis* (2000) 21:2209–18. doi: 10.1002/1522-2683(20000601)21:11<2209::aid-elps2209>3.0.co;2-t
29. Gianazza E. Isoelectric focusing as a tool for the investigation of post-translational processing and chemical modifications of proteins. *J Chromatogr A* (1995) 705:67–87. doi: 10.1016/0021-9673(94)01251-9
30. Karty JA, Ireland MM, Brun YV, Reilly JP. Artifacts and unassigned masses encountered in peptide mass mapping. *J Chromatogr B Analyt Technol Biomedl Life Sci.* (2002) 781:363–83. doi: 10.10016/S1570-0232(02)00550-0
31. Kelley KW, Weigent DA, Kooijman R. Protein hormones and immunity. *Brain Behav Immun.* (2007) 21:384–92. doi: 10.1016/j.bbi.2006.11.010
32. Sakamoto T, Oda A, Narita K, Takahashi H, Oda T, Fujiwara J, et al. Prolactin: fishy tales of its primary regulator and function. *Ann N Y Acad Sci.* (2005) 1040:184–8. doi: 10.1196/annals.1327.023
33. Carter DA, Lightman SL. Oxytocin responses to stress in lactating and hyperprolactinaemic rats. *Neuroendocrinology* (1987) 46:532–7. doi: 10.1159/000124876
34. Donner N, Bredewold R, Maloumby R, Neumann ID. Chronic intracerebral prolactin attenuates neuronal stress circuitries in virgin rats. *Eur J Neurosci.* (2007) 25:1804–14. doi: 10.1111/j.1460-9568.2007.05416.x
35. Torner L, Toschi N, Pohlinger A, Landgraf R, Neumann ID. Anxiolytic and anti-stress effects of brain prolactin: improved efficacy of antisense targeting of the prolactin receptor by molecular modeling. *J Neurosci.* (2001) 21:3207–14. doi: 10.1523/JENUROSCI.21-09-03207.2001
36. Kokay IC, Bull PM, Davis RL, Ludwig M, Grattan DR. Expression of the long form of the prolactin receptor in magnocellular oxytocin neurons is associated with specific prolactin regulation of oxytocin neurons. *Am J Physiol Regul Integr Comp Physiol.* (2006) 290:R1216–25. doi: 10.1152/ajpregu.00730.2005
37. Townsend J, Cave BJ, Norman MR, Flynn A, Uney JB, Tortonese DJ, et al. Effects of prolactin on hypothalamic supraoptic neurones: evidence for modulation of STAT5 expression and electrical activity. *Neuro Endocrinol Lett.* (2005) 26:125–30
38. Trott JF, Schennink A, Petrie WK, Manjarin R, Vanklompenberg MK, Hovey RC. Triennial Lactation Symposium: Prolactin: The multifaceted potentiator of mammary growth and function. *J Anim Sci.* (2012) 90:1674–86. doi: 10.2527/jas.2011-4682
39. Larsen CM, Grattan DR. Prolactin, neurogenesis, and maternal behaviors. *Brain Behav Immun.* (2012) 26:201–9. doi: 10.1016/j.bbi.2011.07.233
40. Bridges RS, Numan M, Ronsheim PM, Mann PE, Lupini CE. Central prolactin infusions stimulate maternal behavior in steroid-treated, nulliparous female rats. *Proc Nat Acad Sci USA*. (1990) 87:8003–7. doi: 10.1073/PNAS.87.20.8003
41. Bridges RS, Dibiase R, Loundes DD, Doherty PC. Prolactin stimulation of maternal behavior in female rats. *Science* (1985) 227:782–4. doi: 10.1126/science.3969568
42. Sakaguchi K, Tanaka M, Ohkubo T, Doh-Ura K, Fujikawa T, Sudo S, et al. Induction of brain prolactin receptor long-form mRNA expression and maternal behavior in pup-contacted male rats: promotion by prolactin administration and suppression by female contact. *Neuroendocrinology* (1996) 63:559–68. doi: 10.1159/000127085
43. Shiu RP, Friesen HG. Mechanism of action of prolactin in the control of mammary gland function. *Annu Rev Physiol.* (1980) 42:83–96. doi: 10.1146/annurev.ph.42.030180.000503
44. Shelly S, Boaz M, Orbach H. Prolactin and autoimmunity. *Autoimmun Rev.* (2012) 11:A465–70. doi: 10.1016/j.autrev.2011.11.009
45. Legorreta-Haquet MV, Chavez-Rueda K, Chavez-Sanchez L, Cervera-Castillo H, Zenteno-Galindo E, Barile-Fabris L, et al. Function of treg cells decreased in patients with systemic lupus erythematosus due to the effect of prolactin. *Medicine* (2016) 95:e2384. doi: 10.1097/md.0000000000002384
46. Legorreta-Haquet MV, Chavez-Rueda K, Montoya-Diaz E, Arriaga-Pizano L, Silva-Garcia R, Chavez-Sanchez L, et al. Prolactin down-regulates CD4+CD25hiCD127low/-regulatory T cell function in humans. *J Mol Endocrinol.* (2012) 48:77–85. doi: 10.1530/jme-11-0040
47. Clapp C, Torner L, Gutierrez-Ospina G, Alcantara E, Lopez-Gomez FJ, Nagano M, et al. The prolactin gene is expressed in the hypothalamic-neurohypophyseal system and the protein is processed into a 14-kDa fragment with activity like 16-kDa prolactin. *Proc Natl Acad Sci USA*. (1994) 91:10384–8. doi: 10.10731/pnas.91.12.10384
48. Aebersold R, Agar JN, Amster IJ, Baker MS, Bertozzi CR, Boja ES, et al. How many human proteoforms are there? *Nat Cheml Biol.* (2018) 14:206–14. doi: 10.1038/nchembio.2576
49. El TF, De GE, Guilliams T, Fauvet B, Hejjaoui M, Di TJ, et al. Exploring the role of post-translational modifications in regulating alpha-synuclein interactions by studying the effects of phosphorylation on nanobody binding. *Protein Sci.* (2018) 27:1262–74. doi: 10.1002/pro.3412
50. Rhoads SN, Monahan ZT, Yee DS, Shewmaker FP. The role of post-translational modifications on prion-like aggregation and liquid-phase separation of FUS. *Int J Mol Sci.* (2018) 19:3. doi: 10.3390/ijms19030886
51. Zhan X, Qian S, Huang Y. The untapped potential of nitroproteomics for medicine. *Med One* (2017) 2:e170027. doi: 10.20900/mo.20170027
52. Zhan X, Long Y, Mu Y. Consideration of statistical vs. biological significances for data-based pathway network analysis. *Med One* (2017) 1:e170002. doi: 10.20900/mo.20170002

Conflict of Interest Statement: The authors declare that the research was conducted in the absence of any commercial or financial relationships that could be construed as a potential conflict of interest.

frontiers in Endocrinology

ORIGINAL RESEARCH
published: 23 November 2018
doi: 10.3389/fendo.2018.00678

Integration of Proteomics and Metabolomics Revealed Metabolite–Protein Networks in ACTH-Secreting Pituitary Adenoma

Jie Feng[1,2,3†], *Qi Zhang*[4†], *Yang Zhou*[5], *Shenyuan Yu*[1], *Lichuan Hong*[1], *Sida Zhao*[1], *Jingjing Yang*[1], *Hong Wan*[1], *Guowang Xu*[5], *Yazhuo Zhang*[1,2,3] *and Chuzhong Li*[1,2,3*]

[1] Beijing Neurosurgical Institute, Beijing Tiantan Hospital, Capital Medical University, Beijing, China, [2] Beijing Institute for Brain Disorders, Brain Tumor Center, Capital Medical University, Beijing, China, [3] China National Clinical Research Center for Neurological Diseases, Beijing Tiantan Hospital, Capital Medical University, Beijing, China, [4] Department of Hepatobiliary and Pancreatic Surgery, The Second Affiliated Hospital, Zhejiang University School of Medicine, Hangzhou, China, [5] CAS Key Laboratory of Separation Science for Analytical Chemistry, Dalian Institute of Chemical Physics, Chinese Academy of Sciences, Dalian, China

OPEN ACCESS

Edited by:
Xianquan Zhan, Central South University, China

Reviewed by:
Odelia Cooper, Cedars-Sinai Medical Center, United States
Jianbo Pan, Johns Hopkins Medicine, United States

***Correspondence:**
Chuzhong Li
lichuzhong@163.com

[†]*These authors have contributed equally to this work*

Specialty section:
This article was submitted to Pituitary Endocrinology, a section of the journal Frontiers in Endocrinology

Received: *22 June 2018*
Accepted: *29 October 2018*
Published: *23 November 2018*

Citation:
Feng J, Zhang Q, Zhou Y, Yu S, Hong L, Zhao S, Yang J, Wan H, Xu G, Zhang Y and Li C (2018) Integration of Proteomics and Metabolomics Revealed Metabolite–Protein Networks in ACTH-Secreting Pituitary Adenoma. Front. Endocrinol. 9:678. doi: 10.3389/fendo.2018.00678

An effective treatment for the management of adrenocorticotropic hormone-secreting pituitary adenomas (ACTH-PA) is currently lacking, although surgery is a treatment option. We have integrated information obtained at the metabolomic and proteomic levels to identify critical networks and signaling pathways that may play important roles in the metabolic regulation of ACTH-PA and therefore hopefully represent potential therapeutic targets. Six ACTH-PAs and seven normal pituitary glands were investigated via gas chromatography-mass spectrometry (GC-MS) analysis for metabolomics. Five ACTH-PAs and five normal pituitary glands were subjected to proteomics analysis via nano liquid chromatography tandem-mass spectrometry (nanoLC-MS/MS). The joint pathway analysis and network analysis was performed using MetaboAnalyst 3.0. software. There were significant differences of metabolites and protein expression levels between the ACTH-PAs and normal pituitary glands. A proteomic analysis identified 417 differentially expressed proteins that were significantly enriched in the Myc signaling pathway. The protein–metabolite joint pathway analysis showed that differentially expressed proteins and metabolites were significantly enriched in glycolysis/gluconeogenesis, pyruvate metabolism, citrate cycle (TCA cycle), and the fatty acid metabolism pathway in ACTH-PA. The protein–metabolite molecular interaction network identified from the metabolomics and proteomics investigation resulted in four subnetworks. Ten nodes in subnetwork 1 were the most significantly enriched in cell amino acid metabolism and pyrimidine nucleotide metabolism. Additionally, the metabolite–gene–disease interaction network established nine subnetworks. Ninety-two nodes in subnetwork 1 were the most significantly enriched in carboxylic acid metabolism and organic acid metabolism. The present study clarified the pathway networks that function in ACTH-PA. Our results demonstrated the presence of downregulated glycolysis and fatty acid synthesis

in this tumor type. We also revealed that the Myc signaling pathway significantly participated in the metabolic changes and tumorigenesis of ACTH-PA. This data may provide biomarkers for ACTH-PA diagnosis and monitoring, and could also lead to the development of novel strategies for treating pituitary adenomas.

Keywords: metabolite–protein networks, proteomics, metabolomics, ACTH, pituitary adenoma

INTRODUCTION

Adrenocorticotropic hormone (ACTH)-secreting pituitary adenoma (ACTH-PA), also known as Cushing disease, is a monoclonal functioning pituitary adenoma that secretes excessive ACTH, which can cause multisystem symptoms, including central obesity, diabetes, hypertension, and psychiatric consequences. Although the majority of ACTH-PAs are benign, they are usually associated with high morbidity and mortality (1, 2). To date, tumor radiation and/or medical suppression of cortisol production have been used to treat this disease, but the efficacy is remains debatable. Surgery is the predominant treatment option, yet patients may suffer from recurrence. Unfortunately, an alternative treatment for the adequate management of ACTH-PA is currently lacking. A deeper understanding of the molecular mechanisms of ACTH-PA initiation and progression is warranted to develop novel strategies to treat this disease.

Tumor metabolic reprogramming has been considered a hallmark of cancer (3). Many oncogenes and suppressor genes play key roles in regulating the metabolism of tumor cells in order to support their growth and survival. These genes include but are not limited to, *Ras*, *Myc*, *HIF1A,* and *Tp53* (4). Tumors generally utilize glycolysis for energy production, which meet the requirements of both rapid growth and macromolecule biosynthesis. Many glycolytic enzymes are upregulated in tumors because of elevated c-Myc and HIF-1α transcriptional activities. In contrast, p53 is known to suppress glucose uptake by directly inhibiting the transcription of glucose transporters Glut1 and Glut4 and by suppressing the expression of Glut3 (4–6). An increase in lipid metabolism is another prominent feature of cancer metabolism. Lipid synthesis is a multistep process involving several enzymes, such as ATP citrate lyase (ACLY), fatty acid synthase (FASN), and stearoyl-CoA desaturase (SCD). FASN is a target gene of HIF-1α and is frequently upregulated by hypoxia (7). In addition, several studies have demonstrated that c-Myc promotes both glutamine uptake and the catabolic process of glutamine (4).The activity of glucose-6-phosphate dehydrogenase (G6PD), a critical enzyme participating in the pentose phosphate pathway, was reported to be increased in cancer cells. In fact, G6PD function is tightly controlled by p53. However, to date, the mechanism of abnormal metabolism in ACTH-PA is yet to be understood. Therefore, we have focused on ACTH-PA to investigate the metabolic and protein changes related to tumorigenesis.

Tumor is a complex disease and many high-throughput "-omic" technologies (genomics, transcriptomics, proteomics, and metabolomics) have been applied to tumors to study large-scale biological processes (BP) (8–10). The data generated from "-omic" studies have also driven the rapid development of integrative omics, whose aim is to integrate the information obtained from different levels of omic experiments into one unified model and to address the network of interactions and regulatory events that characterize the essential underlying biology.

In the present study, through gas chromatography-mass spectrometry (GC-MS) analysis and nano liquid chromatography tandem-mass spectrometry (nanoLC-MS/MS), we describe and integrate the data from the metabolomic and proteomic levels to identify critical networks and signaling pathways that may play important roles in the metabolic regulation of ACTH-PA, and therefore hope to elucidate potential therapeutic targets.

MATERIALS AND METHODS

Patients and Specimens

All six patients without preoperative treatment suffered from hypercortisolemia with Cushing disease. The cortisol level of each patient is listed in **Supplementary Table 1**. The diagnosis of ACTH-PA was based on pathological and electron microscopic examination, as previously described. The low/high dose dexamethasone suppression tests supported the diagnosis. All six patients were diagnosed with functioning ACTH-PA and received trans-sphenoidal surgery at Beijing Tiantan Hospital. Fresh tumor tissue samples from these patients were frozen and stored in liquid nitrogen. Patients who had previously received radiation therapy or experienced tumor recurrence were not included in this study. All six functioning ACTH-PAs were used for metabolomic analysis, and five of them were used for proteomic analysis.

Seven healthy pituitary glands were used as controls. All control donors died from accidents and their pituitary glands had not been damaged. Written informed consent for the healthy donors was obtained from the next of kin. All seven pituitary glands were used for metabolomic analysis, and five of them were used for proteomic analysis.

This study was approved by the ethics committees of the Beijing Tiantan Hospital (KY2013-015-02). Informed consent was obtained from all of the enrolled subjects, and the study was performed in full compliance with all principles of the Helsinki Declaration.

Protein Preparation and NanoLC-MS/MS Analysis

The workflow of the protein preparation and nanoLC-MS/MS analysis are shown in **Figure 1A**. The proteins were extracted using a total protein extraction kit (2140, Millipore, Billerica, MA, USA). The protein concentrations were measured using a

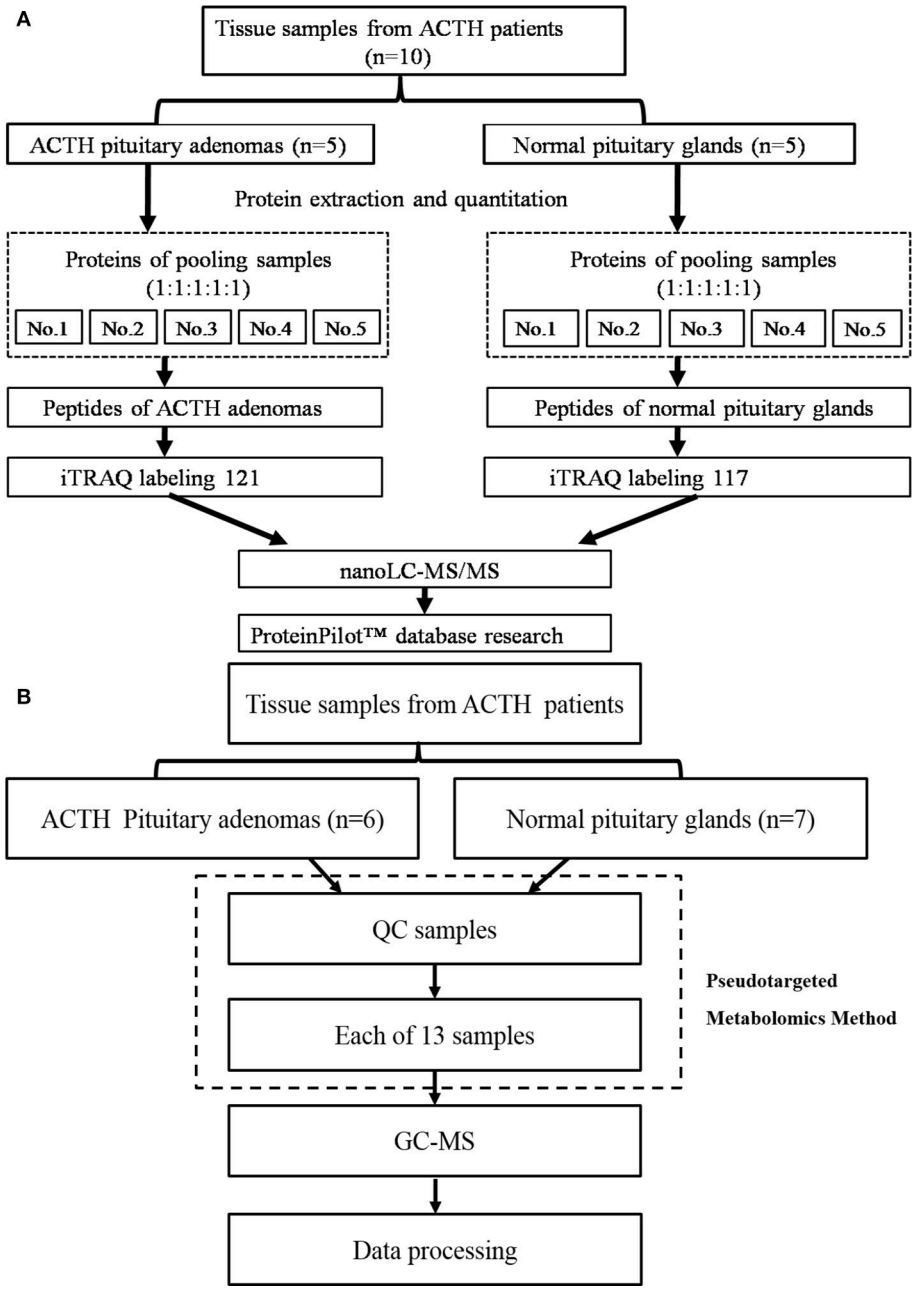

FIGURE 1 | (A) The workflow of the protein preparation and nano LC-MS/MS analysis, **(B)** The workflow of the metabolomics analysis.

bicinchoninic acid protein assay kit (23225, Pierce, Rockford, IL, USA).

The proteins from five ACTH-PAs or five healthy pituitary glands were equally combined into a single pool, as previously described (11). The pooling of samples in proteomics should reduce the measured biological variation giving increased power to detect treatment differences (12, 13). A total of 100 μg of each pooled sample was denatured, reduced, and alkylated, as described in the iTRAQ protocol (Applied Biosystems Sciex, USA) and digested overnight with 0.1 μg/μL trypsin solution at 37°C. The digested ACTH-PA and healthy pituitary gland pooled samples were labeled with 121 and 117 iTRAQ tags, respectively, according to the manufacturer's protocol (Applied Biosystems Sciex, USA). The tagged peptides were dried via vacuum centrifugation and combined in one tube. Strong cation-exchange (SCX) chromatography was performed according to a previously described method (11). Briefly, the pooled sample was separated on an apoly-LC SCX column (4.6 × 250 mm,

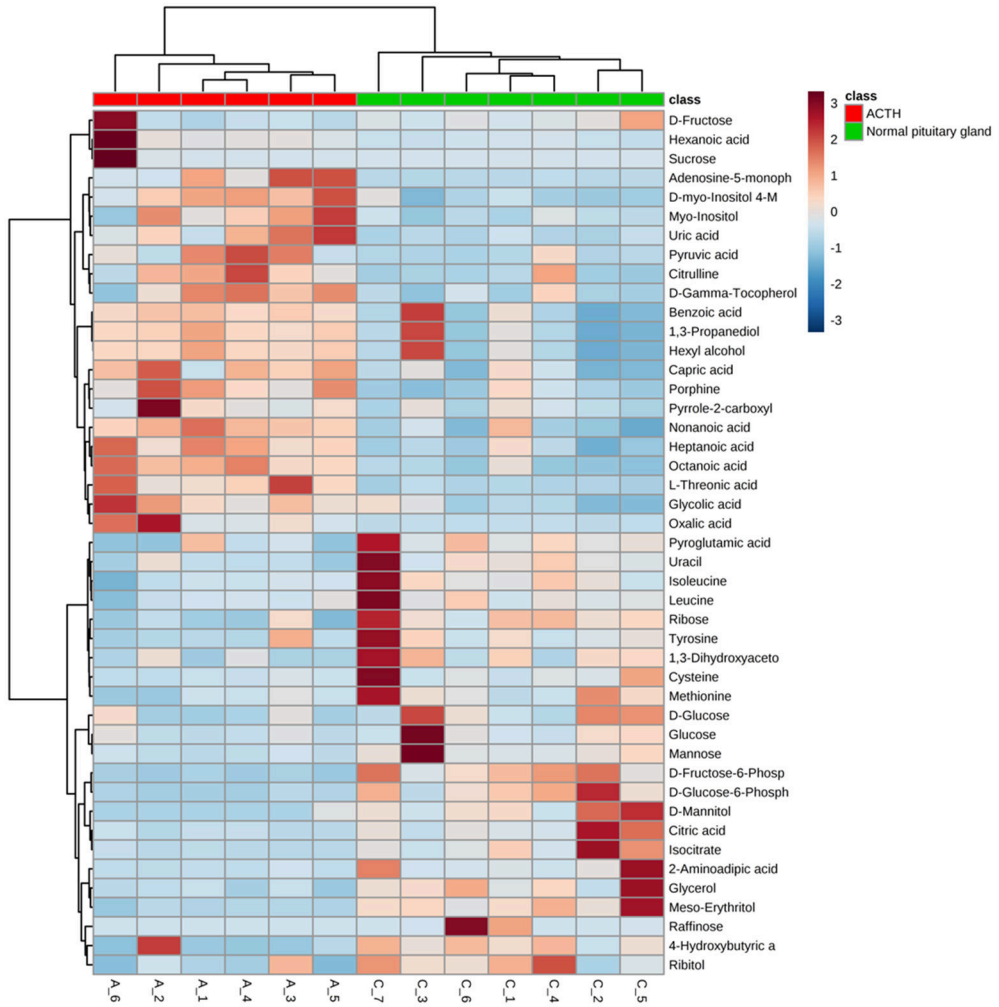

FIGURE 2 | A heatmap illustrating that the 37 metabolites clearly segregate patients with ACTH-PAs and normal pituitary glands. Each colored cell on the map corresponds to a concentration value in the data table, with samples in rows and features/compounds in columns. The heatmap was used to identify samples/features that are unusually high/low.

5 μm, 100 Å) using an LC 100 instrument (Eksigent, Dublin, CA, USA), and the labeled peptides were detected by ultraviolet radiation using an SPD-20 (Shimadzu, Japan). In this study, a total of 48 fractions were collected, dried by speed vacuum centrifugation, and combined into 10 fractions according to the SCX chromatogram. Each fraction was injected onto a desalting column (350 μm × 0.5 mm, 3 μm C18, 120 Å) and separated on an analytical column (75 μm × 150 mm, 3 μm C18, 120 Å) using an Eksigent nanoLC instrument (Eksigent, Dublin, CA, USA). The samples were separated via capillary high-performance liquid chromatography and were subsequently analyzed using a Triple TOF 5600 system (Applied Biosystems Sciex, USA).

Protein identification and differentially expression were performed using the ProteinPilot software package (Applied Biosystems Sciex, USA) and searched against the SwissProt database (March 2013) using the Mascot 2.2 search engine (Matrix Science, London, UK). The following search parameters were utilized to analyze the MS/MS data: trypsin as the digestion enzyme, with a maximum of two missed cleavages allowed; fixed modifications of carbamidomethyl (C) and iTRAQ Plex (K and N-terminus); variable modifications of oxidation (M); peptide mass tolerance of ±20 ppm; fragment mass tolerance of ± 0.1 Da; and peptide FDR ≤0.01.

Metabolomics and GC-MS Analysis

The workflow of metabolomics analysis is shown in **Figure 1B**. For GC-MS analysis, tissue samples were mixed with 600 μl of a methanol/water (v/v 4:1) solution containing internal standards and homogenate. Supernatants were lyophilized for subsequent oximation and silylation reactions. A QP 2010 GC-MS system (Shimadzu, Japan) with a DB-5 MS fused-silica capillary column (30 m × 0.25 mm × 0.25 μm, Agilent Technologies, Santa Clara, CA, USA) was used for metabolic profiling. A pseudotargeted GC-MS metabolomics method

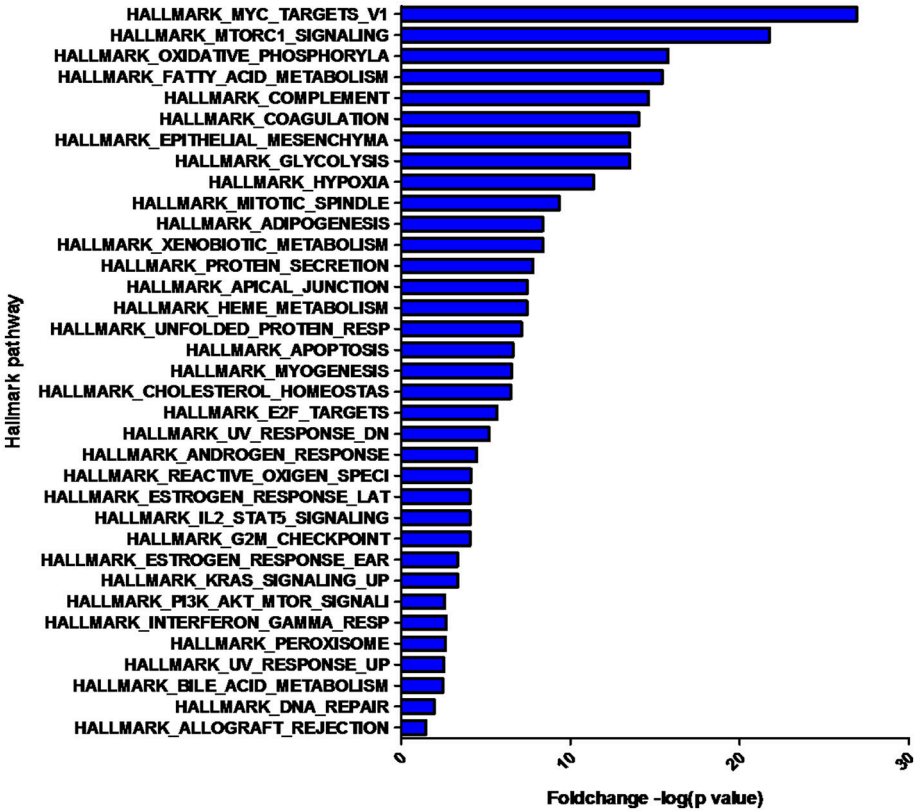

FIGURE 3 | Hallmark pathways enriched by the differentially expressed proteins. The significant pathways are displayed along the X-axis. The Y-axis displays the –log of the *p*-value.

was established elsewhere (14–16). The ion peak area of the metabolite was normalized to the internal standard and multiplied by 1×10^6, then utilized for following data processing. A total of 288 features assigned to 32 groups were defined for data collection and quantification. The system parameter settings have previously been described (16). Metabolite identities were determined based on commercial libraries (Mainlib, NIST, Wiley, and Fiehn) and an internal metabolite library.

Bioinformatic Analysis and Statistics

Student's *t*-test and SAM were performed to calculate the differential expression and false discovery rate (FDR) between ACTH-PAs and normal pituitary glands. Filtering was performed to identify metabolites that were either overexpressed or underexpressed by at least 2.0-fold and to determine *q*-values of <5% in ACTH-PAs compared with normal pituitary glands. Comprehensive metabolomic data analysis was performed by using MetaboAnalyst 3.0 (http://www.metaboanalyst.ca/faces/home.xhtml).

Hierarchical cluster analysis was performed to create a heatmap of the differentially expressed metabolites using MetaboAnalyst 3.0. Protein enrichment pathway analysis was used based on the hallmark gene set database determined by Gene Set Enrichment Analysis software (GSEA, http://software.broadinstitute.org/gsea/msigdb/index.jsp). The joint pathway analysis conducted using MetaboAnalyst 3.0 enabled the visualization of significant genes and metabolites that were enriched in a particular pathway. Network analysis was performed by MetaboAnalyst 3.0 in three different modes: gene-metabolite interaction network, metabolite–disease interaction network, and metabolite–gene–disease interaction network. Functional annotation databases were utilized based on the BP determined by gene ontology (GO).

RESULTS

Hierarchical Clustering of Metabolic Profiling in ACTH-PA

Significant differences of metabolites between ACTH-PAs ($n = 6$) and normal pituitary glands ($n = 7$) were observed. A total of 192 metabolites were identified among the ACTH-PAs and normal pituitary glands, and 37 of these metabolites were diversely expressed between the two groups (P-value < 0.05, with a fold change >2 or <0.5). Specifically, 17 metabolites were upregulated and 20 were downregulated in ACTH-PA samples. A heatmap with two-dimensional hierarchical clustering (**Figure 2**) illustrated that the analyzed metabolites clearly segregated the samples into

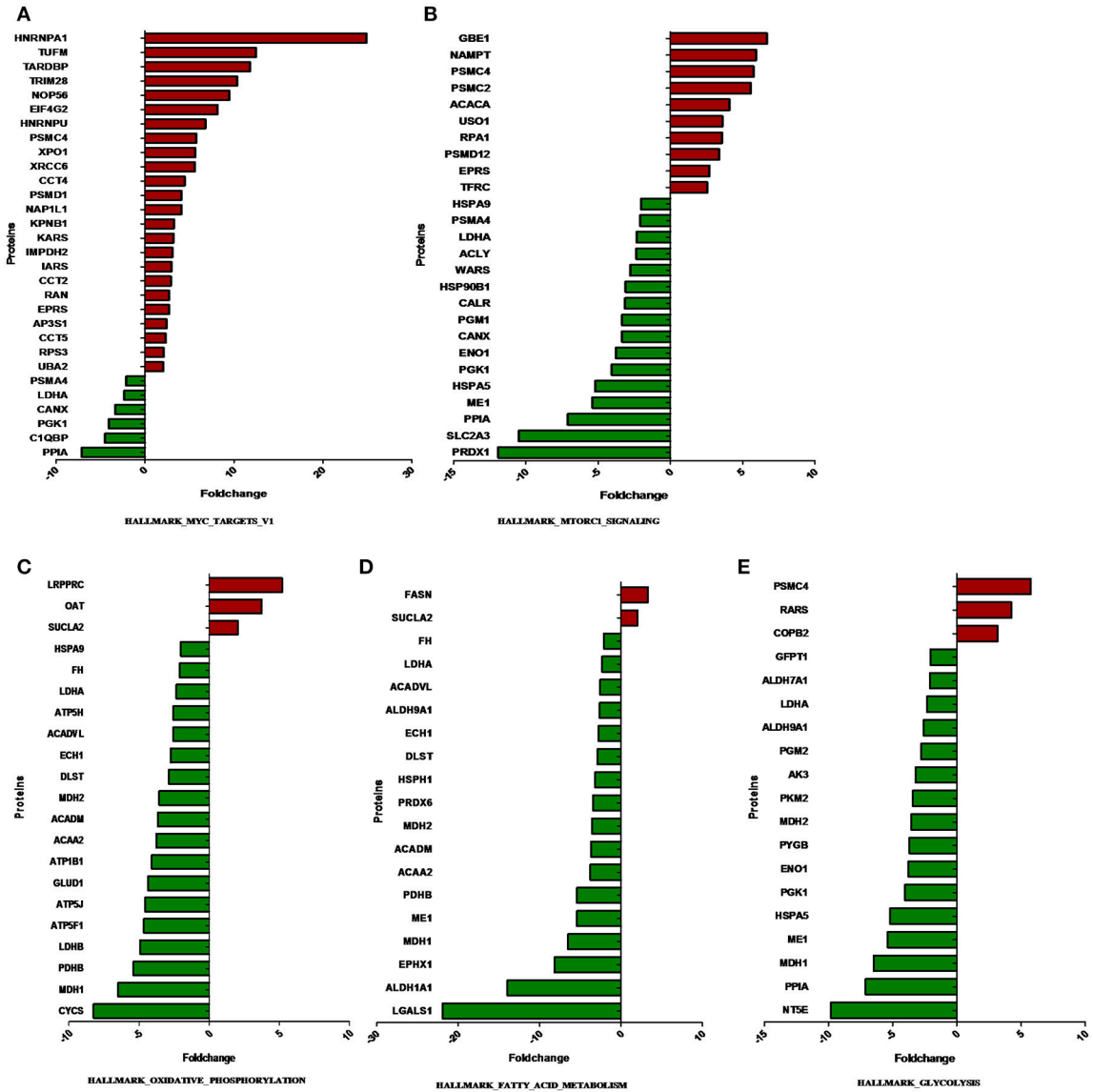

FIGURE 4 | The expression of proteins in metabolism-related hallmark pathways. The proteins differentially expressed between ACTH-PAs and normal pituitary glands are displayed along the X-axis. The Y-axis displays the –log of the *p*-value. **(A)** Proteins in HALLMARK_MYC_TARGETS_V1, **(B)** Proteins in HALLMARK_MTORC1_SIGNALING, **(C)** Proteins in HALLMARK_OXIDATIVE_PHOSPHORYLATION, **(D)** Proteins in HALLMARK_FATTY_ACID_METABOLISM, **(E)** Proteins in HALLMARK_GLYCOLYSIS.

two groups and was consistent with the clinical diagnosis of the patients.

Protein Enrichment Pathway Analysis in ACTH-PA

We next explored the proteins that were differentially expressed between ACTH adenomas ($n = 5$) and normal pituitary glands ($n = 5$). A proteomic analysis identified 48,391 peptides that were mapped to 4,568 proteins in this study. A total of 417 differentially expressed proteins were further identified ($P < 0.05$; FDR < 0.01; iTRAQ ratio >2 or <0.5). Of these proteins, 218 and 199 were upregulated and downregulated in ACTH-PAs, respectively, compared to the normal pituitary glands.

The overlap computing tool of GSEA evaluates the overlap of a provided differentially expression protein/gene set with hallmark gene sets from MSigDB and estimates the statistical significance. The protein/gene sets with a *P*-value < 0.05 and an FDR *q*-value < 0.05 are shown in **Figure 3**. These hallmark pathways were closely related to tumor metabolism and included HALLMARK_MYC_TARGETS_V1, HALLMARK_MTORC1_SIGNALING, HALLMARK_OXIDATIVE_ PHOSPHORYLATION, HALLMARK_FATTY_ACID_METABOLISM, and HALLMARK_GLYCOLYSIS. The

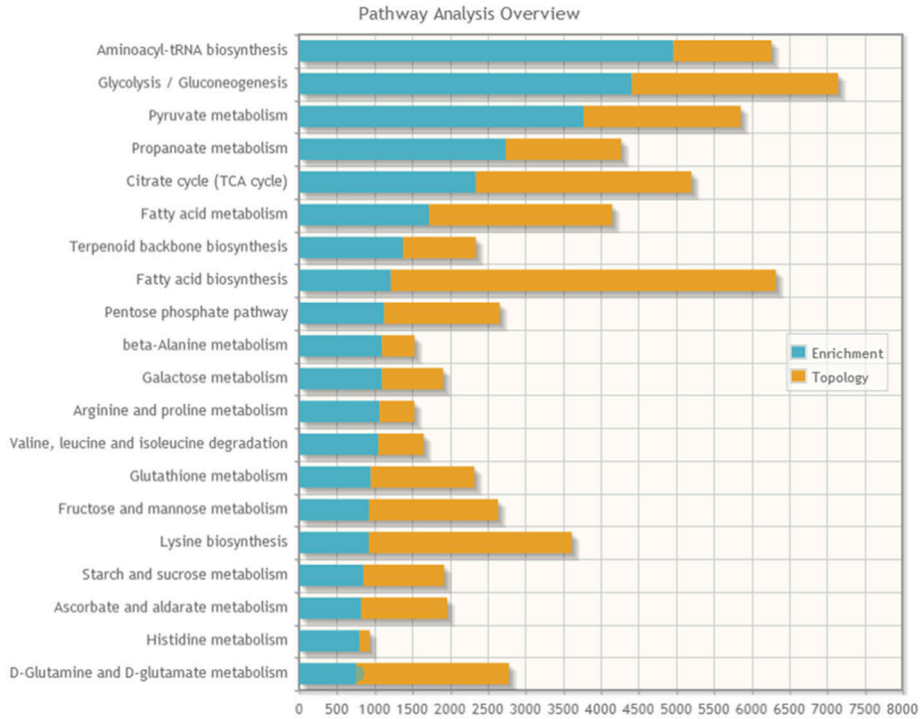

FIGURE 5 | The stacked bars below show a summary of the protein–metabolite joint evidence from enrichment analysis and topology analysis.

expression of proteins in metabolism-related hallmark pathways is listed (**Figure 3**). Intriguingly, the majority of proteins in the HALLMARK_OXIDATIVE_PHOSPHORYLATION, HALLMARK_FATTY_ACID_METABOLISM, and HALLMARK_GLYCOLYSIS pathways were found to be downregulated (**Figures 4C–E**).

Protein–Metabolite Joint Pathway Analysis

A joint pathway analysis was performed using the enrichment analysis and the topology analysis. The enrichment analysis showed the identified proteins and metabolites that were significantly enriched in a particular pathway ($P < 0.05$; **Figure 5**), including aminoacyl-tRNAbiosynthesis, glycolysis/gluconeogenesis, pyruvate metabolism, propanoate metabolism, citrate cycle (TCA cycle), fatty acid metabolism, terpenoid backbone biosynthesis, fatty acid biosynthesis, pentose phosphate pathway, beta-alanine metabolism, and galactose metabolism. The topology analysis showed the identified genes or metabolites that probably play an important role in pathways based on their positions within these pathways.

Protein–Metabolite Interaction Network

The protein–metabolite interaction network provides visible interactions between functionally related metabolites and proteins. The metabolites and proteins identified from proteomics and metabolomics were mapped to the protein–metabolite molecular interaction network to create four subnetworks (**Figure 6**).

Subnetwork 1 includes 10 nodes (proteins, metabolites), and two of them were upregulated, including EPRS and adenosine monophosphate (AMP) **(Figure 6A)**. The nodes (proteins, metabolites) in subnetwork 1 were the most significantly enriched in cell amino acid metabolism and pyrimidine nucleotide metabolism based on the GO:BP database (**Table 1**).

Subnetwork 2 includes seven nodes (proteins, metabolites), and two of them were upregulated, including SND1 and pyruvate acid (**Figure 6B**). The nodes in subnetwork 2 were the most significantly enriched in cellular carbohydrate metabolism and aerobic respiration based on the GO:BP database (**Table 2**).

Subnetwork 3 includes six nodes (proteins, metabolites), and only uric acid was upregulated (**Figure 6C**). The nodes in subnetwork 3 were the most significantly enriched in protein import into the nucleus and nuclear import based on the GO:BP database (**Table 3**).

Subnetwork 4 includes five nodes (proteins, metabolites), two of which were upregulated, including MPG and FASN (**Figure 6D**). The nodes in subnetwork 4 were the most significantly enriched in base-excision and the DNA catabolic process based on the GO:BP database (**Table 4**).

Metabolite–Disease Interaction Network

The metabolite–disease interaction network provides an exploration of disease-related metabolites. The metabolites identified from metabolomics were mapped to the metabolite–disease interaction network to create two subnetworks (**Figure 7**).

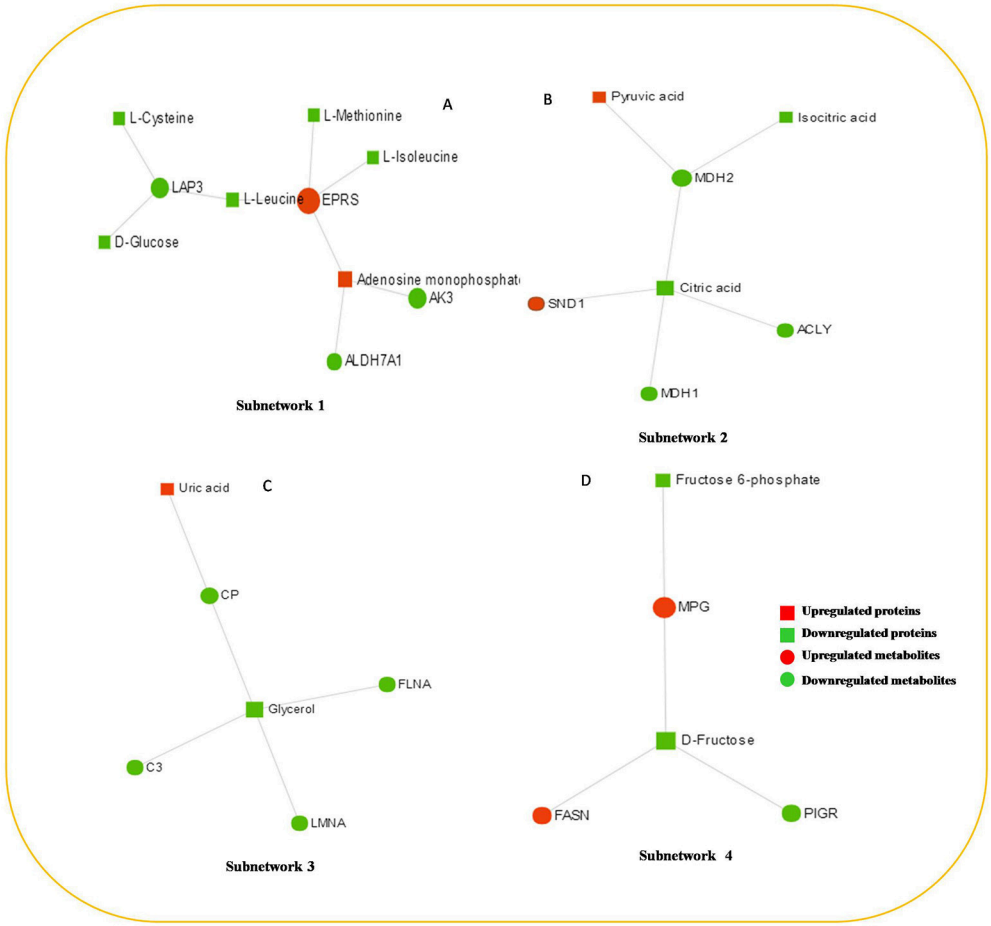

FIGURE 6 | The protein–metabolite interaction network provides a visualization of the interactions between functionally related metabolites and genes (proteins) identified from proteomics and metabolomics. **(A)** Subnetwork 1, **(B)** Subnetwork 2, **(C)** Subnetwork 3, **(D)** Subnetwork 4.

Subnetwork 1 includes 48 nodes (metabolites, connected proteins, and target diseases), and 14 of them were metabolites identified from the present study. In detail, 3 of the 14 metabolites were upregulated: uric acid, citrulline, and glycolic acid (**Figure 7**).

Metabolite–Protein–Disease Interaction Network

The metabolite–protein–disease interaction network provides a global view of potentially functional relationships between metabolites, connected proteins, and target diseases. The metabolites and proteins identified from the metabolomics and proteomics analyses were mapped to the metabolite–gene–disease interaction network and successfully created nine subnetworks.

Subnetwork 1 includes 92 nodes (metabolites, connected proteins, and target diseases), and 36 of them were metabolites and proteins identified from the present study. Five of the 36 metabolites and proteins were upregulated: uric acid, EPRS, AMP, glycolic acid, and FASN (**Figure 8A**). **Figure 8A** indicates the potentially functional relationships between metabolites such as D-glucose, L-cysteine, L-tyrosine, L-leucine, mannitol, and Alzheimer's disease.

Subnetwork 2 includes six nodes, and three of them were proteins identified from the present study. FGB was indicated to be upregulated (**Figure 8B**). Subnetwork 2 showed potential functional relationships between proteins FGB, FGA, APOA1, and afibrinogenemia congenital, amyloidosis familial visceral, and hypoalphalipoproteinemia.

The other 7 subnetworks (3–9) are also shown in **Figure 8**. Subnetwork 3 and subnetwork 4 include four nodes, and one node consisted of proteins identified from the current study. CHD1 in subnetwork 3 was indicated to have a potentially functional relationship with tumors such as breast cancer, gastric cancer, and prostate cancer. DCTN1 in subnetwork 4 was shown to have a potentially functional relationship with neuronopathy distal hereditary motor, Perry syndrome, and amyotrophic lateral sclerosis 1.

Subnetworks 5–9 include three nodes, one of which was a protein or metabolite identified from our study. The metabolite

TABLE 1 | Pathways enriched by proteins and metabolites in subnetwork 1 of the protein–metabolite interaction network based on the GO:BP database.

Pathway	Total	Expected	Hits	*P*-value
Cellular amino acid metabolic process	670	0.188	2	0.0124
Pyrimidine nucleotide metabolic process	50	0.014	1	0.0139
Negative regulation of translation	70	0.0196	1	0.0195
Cellular modified amino acid biosynthetic process	71	0.0199	1	0.0197
Carboxylic acid metabolic process	1,270	0.357	2	0.0422
Cellular amino acid catabolic process	166	0.0465	1	0.0457
Cellular biogenic amine metabolic process	167	0.0468	1	0.0459
tRNA metabolic process	173	0.0484	1	0.0476
Organic acid metabolic process	1,430	0.4	2	0.0522

TABLE 2 | Pathways enriched by proteins and metabolites in subnetwork 2 of the protein–metabolite interaction network based on the GO:BP database.

Pathway	Total	Expected	Hits	*P*-value
Cellular carbohydrate metabolic process	259	0.0725	3	2.32*E*−05
Aerobic respiration	61	0.0171	2	0.000107
Energy derivation by oxidation of organic compounds	437	0.122	3	0.000111
Generation of precursor metabolites and energy	603	0.169	3	0.00029
Carbohydrate biosynthetic process	203	0.0568	2	0.00118
Carbohydrate metabolic process	1,040	0.291	3	0.00145
Cellular respiration	236	0.0661	2	0.00159
Coenzyme metabolic process	266	0.0745	2	0.00202
Glucose metabolic process	290	0.0812	2	0.0024
Carboxylic acid metabolic process	1,270	0.357	3	0.00264
Cofactor metabolic process	331	0.0927	2	0.00311
Organic acid metabolic process	1,430	0.4	3	0.00369
Gene silencing	99	0.0277	1	0.0274
Nucleotide metabolic process	1,040	0.292	2	0.0289
Triglyceride metabolic process	126	0.0353	1	0.0348
Coenzyme biosynthetic process	133	0.0372	1	0.0367

pyroglutamic acid in subnetwork 5 has a potentially functional relationship with diseases such as glutathione synthetase deficiency and 5-oxoprolinase deficiency. NRAS in subnetwork 7 was indicated to have a potentially functional relationship with colorectal cancer and thyroid cancer. HSPB1 in subnetwork 6, EPHX1 in subnetwork 8, and TPM2 in subnetwork 9 were indicated to have potentially functional relationships with diseases such as neuronopathy distal hereditary motor, Charcot-Marie-Tooth disease axonal, hypercholanemia familial, preeclampsia/eclampsia 1, and arthrogryposis distal.

TABLE 3 | Pathways enriched by proteins and metabolites in subnetwork 3 of the protein–metabolite interaction network based on the GO:BP database.

Pathway	Total	Expected	Hits	*P*-value
Protein import into nucleus	228	0.0638	2	0.00149
Nuclear import	232	0.0649	2	0.00154
Protein import	272	0.0761	2	0.00211
Microtubule cytoskeleton organization	337	0.0943	2	0.00323
Nucleocytoplasmic transport	388	0.109	2	0.00426
Nuclear transport	392	0.11	2	0.00434
Cellular membrane organization	471	0.132	2	0.00623
Microtubule-based process	516	0.144	2	0.00744
Regulation of protein metabolic process	1,820	0.511	3	0.00753
Protein targeting	545	0.153	2	0.00828

TABLE 4 | Pathways enriched by proteins and metabolites in subnetwork 4 of the protein–metabolite interaction network based on the GO:BP database.

Pathway	Total	Expected	Hits	*P*-value
Base-excision repair	45	0.0063	1	0.00629
DNA catabolic process	72	0.0101	1	0.0101
DNA modification	83	0.0116	1	0.0116
Vitamin metabolic process	115	0.0161	1	0.016
Triglyceride metabolic process	126	0.0176	1	0.0176
Coenzyme biosynthetic process	133	0.0186	1	0.0185
Fatty acid biosynthetic process	151	0.0211	1	0.021
Cofactor biosynthetic process	185	0.0259	1	0.0257
Energy reserve metabolic process	199	0.0279	1	0.0277
Cellular modified amino acid metabolic process	241	0.0337	1	0.0335
Coenzyme metabolic process	266	0.0372	1	0.0369
Cofactor metabolic process	331	0.0463	1	0.0458

DISCUSSION

The present study, for the first time, used integrative omic analysis from proteomics and metabolomics to reveal the significant molecular signaling pathways and networks that have potentially functional relationship with ACTH-PA. Among the complicated pathway networks described above, several protein–metabolite joint pathways and networks were found to be significantly associated with the abnormal metabolism in ACTH-PA.

Glycolysis/Gluconeogenesis

It is well-known that tumor cells preferentially use glycolysis for their energy supply. The majority of glycolytic enzymes were markedly elevated in most tumors. In addition to their metabolic

FIGURE 7 | The metabolite–disease interaction network provides a visualization of the disease-related metabolites identified from metabolomics.

functions, glycolytic enzymes also play important roles in cell survival, metastasis, invasion, chromatin remodeling, regulation of gene expression, and other essential cellular processes (4, 17). In addition, glycolysis provides cancer cells not only with energy but also with the necessary precursors for biosynthesis. For example, several glycolytic metabolites, such as glucose-6-phosphate and pyruvate, could be diverted into other metabolic pathways. Furthermore, lactate not only is taken up by other cancer cells in the tumor microenvironment to enhance TCA flux but also lowers the pH of the extracellular microenvironment, facilitating the activity of metalloproteases for tumor invasion (4, 18).

Notably, most of the proteins involved in glycolysis and glucogenesis, including LDHA, HK1, and PKM2, showed lower levels in ACTH-PAs than in normal pituitary glands (**Figure 4**). Some metabolites, such as glucose-6-phosphate, which is used for the synthesis of nucleotides and NADPH, were reduced in ACTH-PAs (**Supplementary Tables 2**, **3**). These phenomena are markedly different from the Warburg effect seen in most tumors.

Furthermore, pyruvate was found to be significantly higher in ACTH-PAs compared to normal pituitary glands, but it appeared to not be diverted into mitochondrial TCA and lactate metabolism. We speculate that pyruvate was detoured into alanine metabolism.

Fatty Acid Metabolism

An increase in fatty acid metabolism is another remarkable feature of tumor metabolism. Tumor cells upregulate fatty acid synthesis to meet their requirements for fatty acid. Fatty acid synthesis is a multistep process involving several critical enzymes. Fatty acid synthase (FASN) was reported to be elevated in many cancers, including breast, prostate and other types of cancer. However, fatty acid catabolic metabolism, including fatty acid oxidation, still remains a poorly understood metabolic pathway.

In the present study, FASN was shown to be upregulated in ACTH-PAs, which was similar to other types of cancer (4, 19), while enzymes related to fatty acid catabolic metabolism,

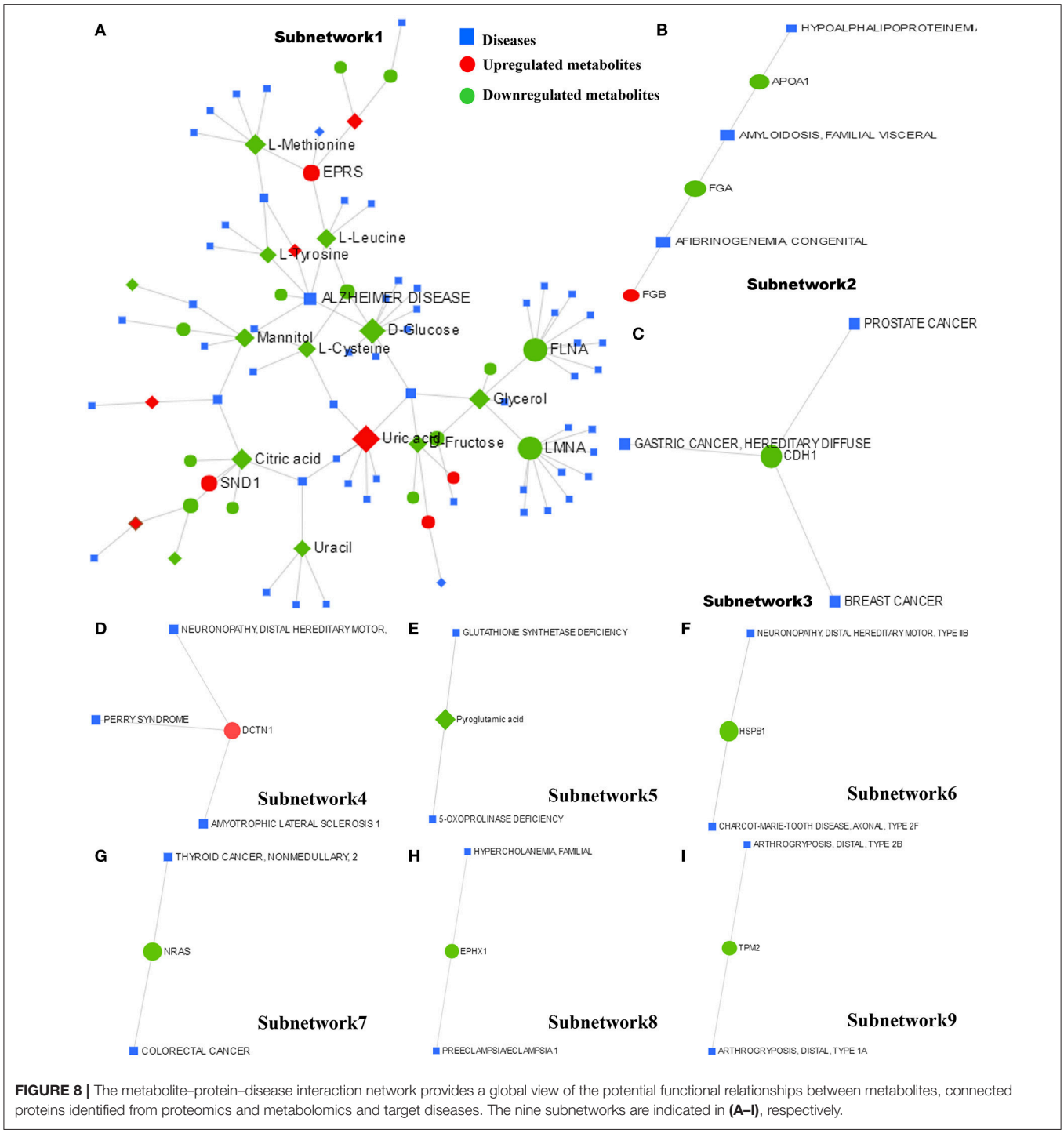

FIGURE 8 | The metabolite–protein–disease interaction network provides a global view of the potential functional relationships between metabolites, connected proteins identified from proteomics and metabolomics and target diseases. The nine subnetworks are indicated in **(A–I)**, respectively.

such as ACADVL, ACADM, and ACAA2, were downregulated in ACTH-PAs (**Figure 4**). A limited number of metabolites from fatty acid metabolism were identified due to the GC-MS methods. Additionally, short chain fatty acids, such as capric acid, hexanoic acid, heptanoic acid, nonanoic acid, and octanoic acid, were found to be increased in ACTH-PAs (**Table 5**).

Mitochondrial Metabolism

Another major change in cancer metabolism is the abnormal mitochondrial biogenesis and metabolism. Mitochondria play essential roles in cancer cells because mitochondria are not only involved in energy production but also in the synthesis of many indispensable molecules for cellular biosynthesis, growth, and proliferation (20). In contrast to normal cells that use

TABLE 5 | The differentially expressed level of metabolites between ACTH-PAs and normal pituitary glands.

Name	*P*-value	Fold change
Capric acid	0.010	1.65
Heptanoic acid	0.007	2.20
Hexanoic acid	0.003	2.26
Nonanoic acid	0.015	1.72
Octanoic acid	0.003	2.05
D-Glucose-6-phosphate	0.003	0.14

mitochondrial TCA and oxidative phosphorylation for energy production, tumor cells preferentially use glycolysis for energy production (4), which was similar to our results. Our data also showed that the proteins and metabolites involved in mitochondrial TCA and oxidative phosphorylation, such as MDH1, MDH2, FH, CYCS, ATP5H, ATP5J, ATP5F1, ATP1B1, citrate, and isocitrate, were reduced in ACTH-PAs (**Figures 4**, **5**). Alternatively, mitochondrial biogenesis was increased in tumors. TUFM is a Tu translation elongation factor that participates in protein translation in mitochondria. In the present study, the expression of TUFM, which is indispensable for mitochondrial biogenesis, was shown to be increased in ACTH-PAs. Therefore, our results suggested enhanced mitochondrial biogenesis in ACTH-PA.

Myc Signaling Pathway and Metabolism

Our proteomic profiling results further indicated that Myc signaling was deeply involved in the altered metabolism of ACTH-PA. In the previous study, Myc as the master inducer of tumor glycolysis, promoted the expression of key glycolytic enzymes (21). Most glycolytic gene promoter areas contain consensus Myc-binding motifs. However, the expression of glycolytic enzymes such as LDHA and PGK1 in the Myc signaling pathway was decreased in ACTH-PA, which was consistent with the reduced glycolysis observed in this tumor type. It is thus possible that the Myc signaling pathway takes part in regulating the glycolysis of ACTH-PAs.

In addition, Myc upregulates glutaminolysis in tumor cells. Many studies have demonstrated that Myc promotes both glutamine uptake and the catabolic process of glutamine. Myc also participates in mitochondrial biogenesis and metabolism (22). This is associated with the transcriptional induction of TFAM, the proteins of the complex I subunits, uncoupling proteins, mitochondrial membrane proteins, and the proteins involved in intermediary metabolism (20). Although we did not find any proteins of the Myc signaling pathway related to glutaminolysis in ACTH-PA, we did notice that some proteins in the Myc signaling pathway that were associated with mitochondrial biogenesis (such as TUFM) were increased in ACTH-PA.

It has been reported that the Myc signaling pathway is often activated during tumorigenesis. Consistently, our proteomic profiling revealed that Myc signaling pathway proteins that are involved in protein and nucleotide synthesis, such as PSMC2, PSMC4, EIF4G2, and IMPDH2, had increased expression in ACTH-PA (**Figure 4**).

CONCLUSIONS

The present study clarified pathway networks that function in ACTH-PA. Our results demonstrated a downregulated glycolysis and fatty acid synthesis in ACTH-PA. We also revealed that the Myc signaling pathway significantly participates in the metabolic changes and tumorigenesis of ACTH-PAs. Further experimental investigations are required to elucidate the biological consequences of these pathway networks and their relevance to the tumorigenesis of ACTH-PAs. The data from the current study may provide biomarkers for ACTH-PA diagnosis and monitoring, and possibly lead to the development of novel strategies to treat the tumors.

AUTHOR CONTRIBUTIONS

CL and JF conceived the idea. CL and YazZ collected the samples. JF, SY, JY, and LH performed the proteomic analyses. YanZ and GX performed the metabolomic analysis. JF, HW, CL, and YazZ interpreted the data. QZ and JF aided in the data analysis and wrote the manuscript. All authors approved the submission.

ACKNOWLEDGMENTS

YazZ is supported by the Research Special Fund for Public Welfare Industry of Health (201402008) and the National High Technology Research and Development Program of China (2014AA020610). JF is supported by the Beijing Municipal Administration of Hospitals Youth Program (QML20160506) and the National Natural Science Foundation of China (81702455).

SUPPLEMENTARY MATERIAL

The Supplementary Material for this article can be found online at: https://www.frontiersin.org/articles/10.3389/fendo.2018.00678/full#supplementary-material

REFERENCES

1. Sharma ST, Nieman LK, Feelders RA. Comorbidities in Cushing's disease. *Pituitary* (2015) 18:188–94. doi: 10.1007/s11102-015-0645-6
2. Zhou YZ, Li CZ, Gao H, Zhang YZ. The effects of Smad3 on ACTH-Secreting Pituitary Adenoma development, cell proliferation, apoptosis, and hormone secretion. *World Neurosurg.* (2018) 114:e329–37. doi: 10.1016/j.wneu.2018.02.181
3. Hanahan D, Weinberg RA. Hallmarks of cancer: the next generation. *Cell* (2011) 144:646–74. doi: 10.1016/j.cell.2011.02.013
4. Phan LM, Yeung SC, Lee MH. Cancer metabolic reprogramming: importance, main features, and potentials for precise targeted anti-cancer therapies.

Cancer Biol Med. (2014) 11:1–19. doi: 10.7497/j.issn.2095-3941.2014.01.001
5. Kawauchi K, Araki K, Tobiume K, Tanaka N. p53 regulates glucose metabolism through an IKK-NF-kappaB pathway and inhibits cell transformation. *Nat Cell Biol.* (2008) 10:611–8. doi: 10.1038/ncb1724
6. Schwartzenberg-Bar-Yoseph F, Armoni M, Karnieli E. The tumor suppressor p53 down-regulates glucose transporters GLUT1 and GLUT4 gene expression. *Cancer Res.* (2004) 64:2627–33. doi: 10.1158/0008-5472.CAN-03-0846
7. Furuta E, Pai SK, Zhan R, Bandyopadhyay S, Watabe M, Mo YY, et al. Fatty acid synthase gene is up-regulated by hypoxia via activation of Akt and sterol regulatory element binding protein-1. *Cancer Res.* (2008) 68:1003–11. doi: 10.1158/0008-5472.CAN-07-2489
8. Liu X, Guo Z, Sun H, Li W, Sun WJ. Comprehensive map and functional annotation of human pituitary and thyroid proteome. *Proteome Res.* (2017) 16:2680–91. doi: 10.1021/acs.jproteome.6b00914
9. Jarmusch AK, Pirro V, Baird Z, Hattab EM, Cohen-Gadol AA, Cooks RG. Lipid and metabolite profiles of human brain tumors by desorption electrospray ionization-MS. *Proc Natl Acad Sci USA*. (2016) 113:1486–91. doi: 10.1073/pnas.1523306113
10. Zhan X, Wang X, Cheng T. Human pituitary adenoma proteomics: new progresses and perspectives. *Front Endocrinol.* (2016) 7:54. doi: 10.3389/fendo.2016.00054
11. Feng J, Yu SY, Li CZ, Li ZY, Zhang YZ. Integrative proteomics and transcriptomics revealed that activation of the IL-6R/JAK2/STAT3/MMP9 signaling pathway is correlated with invasion of pituitary null cell adenomas. *Mol Cell Endocrinol.* (2016) 436:195–203. doi: 10.1016/j.mce.2016.07.025
12. Diz AP, Truebano M, Skibinski DO. The consequences of sample pooling in proteomics: an empirical study. *Electrophoresis* (2009) 30:2967–75. doi: 10.1002/elps.200900210
13. Karp NA, Lilley KS. Design and analysis issues in quantitative proteomics studies. *Proteomics* (2007) 7(Suppl. 1):42–50. doi: 10.1002/pmic.200700683
14. Ye G, Liu Y, Yin P, Zeng Z, Huang Q, Kong H, et al. Study of induction chemotherapy efficacy in oral squamous cell carcinoma using pseudotargeted metabolomics. *J Proteome Res.* (2014) 13:1994–2004. doi: 10.1021/pr4011298
15. Li Y, Ruan Q, Ye G, Lu X, Lin X, Xu G. A novel approach to transforming a non-targeted metabolic profiling method to a pseudo-targeted method using the retention time locking gas chromatography/mass spectrometry-selected ions monitoring. *J Chromatogr A* (2012) 1255:228–36. doi: 10.1016/j.chroma.2012.01.076
16. Zhou Y, Song R, Zhang Z, Lu X, Zeng Z, Hu C, et al. The development of plasma pseudotargeted GC-MS metabolic profiling and its application in bladder cancer. *Anal Bioanal Chem.* (2016) 408:6741–9. doi: 10.1007/s00216-016-9797-0
17. Kim JW, Dang CV. Multifaceted roles of glycolytic enzymes. *Trends Biochem Sci.* (2005) 30:142–50. doi: 10.1016/j.tibs.2005.01.005
18. Bonuccelli G, Tsirigos A, Whitaker-Menezes D, Pavlides S, Pestell RG, Chiavarina B, et al. Ketones and lactate "fuel" tumor growth and metastasis: evidence that epithelial cancer cells use oxidative mitochondrial metabolism. *Cell Cycle* (2010) 9:3506–14. doi: 10.4161/cc.9.17.12731
19. Santos CR, Schulze A. Lipid metabolism in cancer. *FEBS J.* (2012) 279:2610–23. doi: 10.1111/j.1742-4658.2012.08644.x
20. Wallace DC. Mitochondria and cancer. *Nat Rev Cancer* (2012) 12:685–98. doi: 10.1038/nrc3365
21. Yeung SJ, Pan J, Lee MH. Roles of p53, MYC and HIF-1 in regulating glycolysis—the seventh hallmark of cancer. *Cell Mol Life Sci.* (2008) 65:3981–99. doi: 10.1007/s00018-008-8224-x
22. Li F, Wang Y, Zeller KI, Potter JJ, Wonsey DR, O'Donnell KA, et al. Myc stimulates nuclearly encoded mitochondrial genes and mitochondrial biogenesis. *Mol Cell Biol.* (2005) 25:6225–34. doi: 10.1128/MCB.25.14.6225-6234.2005

Conflict of Interest Statement: The authors declare that the research was conducted in the absence of any commercial or financial relationships that could be construed as a potential conflict of interest.

frontiers in Endocrinology

ORIGINAL RESEARCH
published: 30 November 2018
doi: 10.3389/fendo.2018.00706

Sex-Related Differences in Lactotroph Tumor Aggressiveness Are Associated With a Specific Gene-Expression Signature and Genome Instability

Anne Wierinckx[1,2,3†], Etienne Delgrange[4†], Philippe Bertolino[2], Patrick François[5], Philippe Chanson[6,7], Emmanuel Jouanneau[8,9], Joël Lachuer[1,2,3], Jacqueline Trouillas[1,9] and Gérald Raverot[2,9,10]*

[1] Institut Universitaire de Technologie, Université Lyon 1, Université de Lyon, Lyon, France, [2] Centre de Recherche en Cancérologie de Lyon (CRCL), INSERM U1052, CNRS UMR5286, Université de Lyon, Lyon, France, [3] ProfileXpert, SFR-Est, CNRS UMR-S3453, INSERM US7, Lyon, France, [4] Service d'Endocrinologie, CHU UCL Namur, Université catholique de Louvain, Ottignies-Louvain-la-Neuve, Belgium, [5] Service de Neurochirurgie, CHU de Tours, Tours, France, [6] Service d'Endocrinologie et des Maladies de la Reproduction, Assistance Publique-Hôpitaux de Paris, Centre de Référence des Maladies Rares de l'Hypophyse, Hôpital Bicêtre, Le Kremlin-Bicêtre, France, [7] Faculté de Médecine Paris-Sud, UMR S-1185, Université Paris-Sud, Université Paris-Saclay, Le Kremlin-Bicêtre, France, [8] Service de Neurochirurgie Groupement Hospitalier Est, Hospices Civils de Lyon, Bron, France, [9] Faculté de Médecine Lyon-Est, Université Lyon 1, Université de Lyon, Lyon, France, [10] Département d'Endocrinologie, Centre de Référence pour les Maladies Hypophysaires Rares (HYPO), Groupement Hospitalier EST, Hospices Civils de Lyon, Université de Lyon, Lyon, France

OPEN ACCESS

Edited by:
Hidenori Fukuoka,
Kobe University, Japan

Reviewed by:
Giampaolo Trivellin,
National Institutes of Health (NIH), United States
Haruhiko Kanasaki,
Shimane University, Japan
Odelia Cooper,
Cedars-Sinai Medical Center, United States

***Correspondence:**
Anne Wierinckx
anne.wierinckx@univ-lyon1.fr

[†]These authors have contributed equally to this work

Specialty section:
This article was submitted to Pituitary Endocrinology, a section of the journal Frontiers in Endocrinology

Received: 24 September 2018
Accepted: 09 November 2018
Published: 30 November 2018

Citation:
Wierinckx A, Delgrange E, Bertolino P, François P, Chanson P, Jouanneau E, Lachuer J, Trouillas J and Raverot G (2018) Sex-Related Differences in Lactotroph Tumor Aggressiveness Are Associated With a Specific Gene-Expression Signature and Genome Instability. Front. Endocrinol. 9:706. doi: 10.3389/fendo.2018.00706

Sex-related differences have been reported in various cancers, in particular men with lactotroph tumors have a worse prognosis than women. While the underlying mechanism of this sexual dimorphism remains unclear, it has been suggested that a lower estrogen receptor alpha expression may drive the sex differences observed in aggressive and malignant lactotroph tumors that are resistant to dopamine agonists. Based on this observation, we aimed to explore the molecular importance of the estrogen pathway through a detailed analysis of the transcriptomic profile of lactotroph tumors from 20 men and 10 women. We undertook gene expression analysis of the selected lactotroph tumors following their pathological grading using the five-tiered classification. Chromosomic alterations were further determined in 13 tumors. Functional analysis showed that there were differences between tumors from men and women in gene signatures associated with cell morphology, cell growth, cell proliferation, development, and cell movement. Hundred-forty genes showed an increased or decreased expression with a minimum 2-fold change. A large subset of those genes belonged to the estrogen receptor signaling pathway, therefore confirming the potent role of this pathway in lactotroph tumor sex-associated aggressiveness. Genes belonging to the X chromosome, such as *CTAG2, FGF13,* and *VEGF-D*, were identified as appealing candidates with a sex-linked dysregulation in lactotroph tumors. Through our comparative genomic hybridization analyses (CGH), chromosomic gain, in particular chromosome 19p, was found only in tumors from men, while deletion of chromosome

11 was sex-independent, as it was found in most (5/6) of the aggressive and malignant tumors. Comparison of transcriptomic and CGH analysis revealed four genes (*CRB3, FAM138F, MATK, and STAP2*) located on gained regions of chromosome 19 and upregulated in lactotroph tumors from men. MATK and STAP2 are both implicated in cell growth and are reported to be associated with the estrogen signaling pathway. Our work confirms the proposed involvement of the estrogen signaling pathway in favoring the increased aggressiveness of lactotroph tumors in men. More importantly, we highlight a number of ER-related candidate genes and further identify a series of target molecules with sex-specific expression that could contribute to the aggressive behavior of lactotroph tumors in men.

Keywords: pituitary tumors, gene expression, estrogen signaling, sexual dimorphism, chromosome, aggressiveness

INTRODUCTION

Epidemiological data indicates that tumors such as lung cancer, hepatocarcinoma, and melanoma have a worse prognosis in men than in women. This observation is also true for both metastatic and primary brain tumors including gliomas, meningiomas, and a subset of pituitary tumors that produce prolactin. These latter tumors, defined as pituitary lactotroph tumors, are larger in men than in women (1), less sensitive to dopamine agonists (2), and their proliferative activity is reported to be higher in men and older women (>40 years of age) than in young women (3). The longer diagnostic delay in men cannot solely explain the sex-related differences in lactotroph tumors. Indeed, in a large surgical series of patients with lactotroph tumors, we previously demonstrated the increased aggressiveness of this type of tumor related to a higher proliferative index among men (2). More recently, we confirmed the sexual dimorphism that exists in lactotroph pituitary tumors by demonstrating that low expression of estrogen receptor alpha (ERα) is more frequently observed in men and further associated in both sexes with high-grade lactotroph tumors that are resistant to therapeutic treatments (4). Besides the sex specificity that exists in terms of hormone regulation and secretion, the most evident differences between men and women lie in their epigenome and the existence of X and Y sex chromosomes. Among X located genes, the androgen receptor (AR), glucose metabolic enzymes, proteins of the apoptotic cascade are expressed in normal tissues and modified in various tumors. Moreover, other X-located genes as cancer-testis antigens are expressed in numerous tumors, while in normal tissues, the expression of most of them remains restricted within the testis and the placenta (5). Expression of cancer-testis antigens is regulated by epigenetic mechanisms and could be associated with tumor progression (6). Increasing data also support the role of genes located on the Y chromosome, such as the candidate tumor suppressor *TMSB4Y* (7), a hypothesis further confirmed by the loss of the Y chromosome that is observed in cancers (8, 9). Surprisingly, little is known about the molecular mechanisms that drives the sexual dimorphism observed in pituitary lactotroph tumors, and studies comparing gene expression between tumors in men and women are lacking.

Here, we addressed these questions in order to delineate the mechanisms and identify genes that drive the sex specificity that exists in aggressive lactotroph tumors. While our data confirm the implication of estrogen signaling in the sexual dimorphism observed in these tumors, it further highlights a number of candidate genes and pathways that could represent appealing targets contributing to sex-related differences in lactotroph tumors.

MATERIALS AND METHODS

Human Pituitary Tumors

Thirty frozen tumors stored at the Neurobiotec Bank (Lyon, France) were selected from a series of 89 lactotroph pituitary tumors we had previously used to report the existence of ERα-associated sex-related differences among men and women (4). All included tumors were resected between 1989 and 2005 by the transsphenoidal route and were further shown to be positive for prolactin expression by immunohistochemistry. Their grading was carried out according to the clinicopathological classification we have previously established (10). Briefly, they were classified into five grades (grades 1a, 1b, 2a for non-aggressive tumors, grade 2b for aggressive, and grade 3 for malignant tumors). The expression of ERα in those tumors was quantified as previously reported (4). The surrounding normal pituitary of each non-invasive microadenoma was macroscopically discarded by manual dissection to avoid any potent contamination that could interfere with our gene expression analysis. A subsequent qRT-PCR was also performed on the 30 selected tumors to address prolactin (*PRL*), growth hormone (*GH*), proopiomelanocortin (*POMC*), and luteinizing hormone *LHβ* in order to exclude PRL/GH co-producing tumors and normal tissues that co-express POMC/LHβ. Note that although normal pituitary tissues are not representative of normal lactotroph cells, we used a pool of normal pituitary from men and women as control references (data not shown). Microarray data for transcriptomic analysis were obtained from patients participating to the HYPOPRONOS (Programme Hospitalier de Recherche Clinique National 27-43) study, and genotyping and copy number alteration (CNA)

analysis from patients included in the PITUIGENE study PHRC-INCa 2012 (ClinicalTrials.gov Identifier: NCT01903967). These studies were approved by the ethics committee of Lyon, and informed consent was obtained from each patient according to French law.

Transcriptomic Analysis

Total RNA was extracted from pituitary tumors using Trizol (Invitrogen), according to the manufacturer's protocol (Invitrogen, Carlsbad, California, USA). For qRT-PCR, total RNA was subjected to DNAse treatment using an RNeasy minikit (Qiagen, Hilden, Germany) according to the manufacturer's protocol. Total RNA yield was measured by the OD260, the purity was checked by a A260/A280 ratio of 1.9-2.1, and the quality was evaluated on nanochips with the Agilent 2100 Bioanalyzer (Agilent Technologies, Palo Alto, CA, USA) according to the manufacturer's protocol.

RNA Amplification

Total RNA (2 μg) was amplified and biotin-labeled by a round of *in vitro* transcription with a Message Amp aRNA kit (Ambion, Austin, Texas, USA) following the manufacturer's protocol. Before amplification, spikes of synthetic mRNA at different concentrations were added to all samples; these positive controls were used to ascertain the quality of the process. aRNA yield was measured using a UV spectrophotometer and the quality on nanochips with the Agilent 2100 Bioanalyzer (Agilent).

Array Hybridization and Processing

Ten micrograms of biotin-labeled aRNA was fragmented using 5 μl of fragmentation buffer in a final volume of 20 μl and was then mixed with 240 μl of Amersham hybridization solution (GE Healthcare Europe GmbH, Freiburg, Germany) and injected onto CodeLink Uniset Human Whole Genome bioarrays containing 5,5000 human oligonucleotide gene probes (GE Healthcare Europe GmbH, Freiburg, Germany) as described previously (11). Arrays were hybridized overnight at 37°C at 300 rpm in an incubator. The slides were washed in stringent TNT buffer at 46°C for 1 h, then a streptavidin-cy5 (GE Healthcare) detection step was performed. Each slide was incubated for 30 min in 3.4 ml of streptavidin-cy5 solution, was then washed four times in 240 ml of TNT buffer, rinsed twice in 240 ml of water containing 0.2%Triton X-100, and dried by centrifugation at 600 rpm. The slides were scanned using a Genepix 4000B scanner (Axon, Union City, USA) and Genepix software, with the laser set at 635 mm, the laser power at 100%, and the photomultiplier tube voltage at 60%. The scanned image files were analyzed using CodeLink expression software, version 4.0 (GE Healthcare), which produces both a raw and normalized hybridization signal for each spot on the array. Transcriptomic data have been deposited in Gene Expression Omnibus under the accession number GSE120350.

Microarray Data Analysis

The relative intensity of the raw hybridization signal on arrays varies in different experiments. CodeLink software was therefore used to normalize the raw hybridization signal on each array to the median of the array (median intensity is 1 after normalization) for better cross-array comparison. The threshold of detection was calculated using the normalized signal intensity of the 100 negative control samples in the array; spots with signal intensities below this threshold are referred to as "absent." Quality of processing was evaluated by generating scatter plots of positive signal distribution. Signal intensities were then converted to log base 2 values. Differential expression analysis was performed using RStudio (http://www.rstudio.org) to isolate differentially expressed mRNAs between men and women lactotroph tumors. A mRNA transcript was considered differentially expressed if the difference gave a $p \leq 0.05$ with the Student's *t*-test, and showed a minimal 2-fold variation. Functional Analysis were created with Ingenuity Pathway Analysis software (IPA®, QIAGEN Redwood City, www.qiagen.com/ingenuity).

Quantitative Gene Expression Analysis Through qRT-PCR

Total RNA (0.5 μg) was reverse transcribed using MMLV reverse transcriptase (Invitrogen). The absence of contaminating genomic DNA in the RT reactions was checked by qRT-PCR directly on total RNA. The cDNA synthesized was measured using qRT-PCR (SYBR Green PCR, LightCycler, Roche Diagnostics Indianapolis, USA) following manufacturer's recommendations. The LightCycler experimental run consisted of an initial Taq activation at 95°C for 10 min and 45 cycles of the amplification and quantification program (95°C for 15 s, 60°C for 5 s, and 72°C for 10 s, with a single fluorescence measurement). The specificity of PCR amplification was always analyzed with a melting curve program (69–95°C) with a heating rate of 0.1°C per second and continuous fluorescence measurement. Primers were designed using Primer3 software (Whitehead Institute/MIT, USA) to insure their respective Tm were between 59 and 61°C and their use produces amplicons between 100 and 150 bp.

Comparative Genomic Hybridization (CGH) Analysis

Genomic DNA was isolated from 13 tumoral and 1 pool of normal pituitary frozen fragments using the QIAamp DNA micro kit (Qiagen, Hilden, Germany), quantified with nanodrop (NanoDrop, Wilmington, DE, USA), and quality verified on agarose gel. Genotyping and CNA analysis was performed using the Affymetrix Genome-wide human SNP array 6.0 chip following manufacturer protocol (Affymetrix, Santa Clara, CA, USA). Briefly, 250 ng of genomic DNA was digested by the nsp/sty enzyme, adaptor ligated and PCR amplified using a single primer with titanium Taq polymerase (Invitrogen, Carlsbad, California, USA). Amplified PCR products were pooled, concentrated, and fragmented with DNase I. Products were subsequently labeled, denatured, and hybridized overnight to the respective arrays. Arrays were washed using the Affymetrix 450 fluidic array station and scanned using the GeneChip scanner 3000 7G. We generated CEL files using the Affymetrix GeneChip Command Console software (AGCC) 3.0. The tissues and reference 103 genomic DNA were processed in a same batch and hybridized using the ProfileXpert platform. CGH and genotyping data have been deposited in Gene Expression Omnibus under the accession number GSE 22615.

Copy Number Alterations (CNA) Analysis

Affymetrix CEL files were extracted using the Genotyping Console software version 3.0 (Affymetrix). For SNP genotyping, we used the Birdseed (v2.2) analysis algorithm. Accuracy of genotyping was checked by performing a concordance test between the processed reference 103 and a pre-processed reference 103 (Affymetrix). The test of concordance showed a 99.79% homology between the two genotypes indicating a good performance of the platform. Moreover, samples showing a call rate >96% and a median of the absolute values of all pairwise differences (MAPD) metric <4 were considered in further analysis. CNA analysis was performed using Partek Genomics Suite version 6.4 (Partek, St Louis, MO) following normalization by invariant set normalization procedure and computed signal intensities using perfect match and mismatch (PM/MM) model-based expression. Raw copy number data was computed using a batch of 270 normal external controls samples from the International HapMap project and used as reference. To remove alterations not associated with tumor phenotype, copy number variation was also analyzed on a pool of normal pituitary samples processed simultaneously in the same batch as tumor samples and compared to the references. Inferred copy numbers were predicted using genomic segmentation algorithm. Only copy number alterations with cut-offs of >2.7 copies for gain and <1.3 for loss were considered.

RESULTS

Clinical and Pathological Features of the Analyzed Cohort of Lactotroph Tumors

In order to explore the genes and mechanisms related to estrogen signaling in the sex-associated aggressiveness of lactotroph tumors, we selected a cohort of 30 tumors from 20 male and 10 female patients. Tumors were classified into five grades, ranging from benign (grades 1a-1b), invasive (grade 2a), suspected of malignancy (grade 2b), to malignant with metastasis (grade 3). Detailed clinical features of the selected tumors are summarized in **Table 1**. Interestingly, while the number of patients is rather limited, with an overrepresentation of tumors from men, the sex-related clinicopathological differences previously reported are obvious (4). Tumors in men were significantly larger, mostly invasive, and negative for ERα. Proliferation markers and tumor grades were also higher in men although this was not statistically significant. Taken together, these observations indicate that our cohort of 30 lactotroph tumors present consistent sex-related differences that should facilitate the identification of sex-associated candidate genes.

Transcriptomic Analyses Reveal Sex-Specific Gene Expression Differences Between Lactotroph Tumors From Men and Women

Having validated the sexual dimorphism of our cohort, we next performed a gene expression analysis. Transcriptomic profiling was achieved through the use of a CodeLink Uniset Human Whole Genome Bioarray. Comparative exploration of male and female expression profiles revealed that 140 genes showed a significant deregulation of at least 2-fold between lactotroph tumors from men and women (**Table S1**), with an overrepresentation of genes with increased expression. Indeed, while 120 genes were increased, only 20 showed a reduced expression. Interestingly, we found that nearly 10% (11/120) of the genes showing an increased expression in men were located on the Y chromosome (*DDX3Y, EIF1AY, KDM5D, NLGN4Y, PRKY, RPS4Y1, RPS4Y2, TTTY14, TXLNGY, USP9Y, ZFY*). Surprisingly, analysis of the Y chromosome-located *TMSB4Y* tumor suppressor did not reveal any altered expression between lactotroph tumors from men and women. Similarly, our analysis revealed that almost 6% (7/120) of the genes overexpressed in male tumors were located on the X chromosome (*FGF13, VEGFD*, *CTAG2*, *SLC6A8, DDX3P1,*

TABLE 1 | Sex-related comparison of clinical, biological, and pathological characteristics in 30 patients with lactotroph tumors.

	Women ($n = 10$)	Men ($n = 20$)
Age (years)	35 ± 3	51 ± 2
MRI DATA		
• Tumor size, (mm)	11 ± 1	27 ± 3
-<10 mm, *n*	3	1
–10–40 mm, *n*	7	13
->40mm, *n*	0	6
• Invasive tumors, *n* (%)	3 (30)	15 (75)
TUMOR CHARACTERISTICS		
•ERα expression (IR score)	7 ± 1	3 ± 1
•Proliferative markers		
-Mitotic count	1 ± 1	4 ± 1
-Ki-67 (%)	0.8 ± 0.5	2.5 ± 0.7
-p53 (%)	0.3 ± 0.1	0.6 ± 0.2
•Prognostic classification		
-Grade 1a, *n*	6	4
-Grade 1b, *n*	1	1
-Grade 2a, *n*	1	8
-Grade 2b (–>3*), *n*	2	7 (2)

**Two of the seven male tumors were classified grade 3 based on metastasis during the follow-up. For continuous variables, results are presented as the mean ± SE (median).*

TABLE 2 | Correlation between CTAG2 and markers of aggressiveness in lactotroph tumors.

Genes	Major functions	Tumors in women		Tumors in men	
		Pearson correlation	*p*-value	Pearson correlation	*p*-value
ADAMTS6	Development	0.32	$1.9.10^{-01}$	0.47	$1.9.10^{-02}$
AURKB	Cell cycle	0.24	$2.6.10^{-01}$	0.93	$1.2.10^{-09}$
CCNB1	Cell cycle	0.19	$3.0.10^{-01}$	0.87	$3.0.10^{-07}$
CENPE	Cell cycle	−0.02	$5.2.10^{-01}$	0.78	$2.9.10^{-05}$
PTTG1	Cell cycle	−0.15	$6.6.10^{-01}$	0.8	$1.3.10^{-05}$

FRMPD4, TMEM35A). Out of these candidates, we found that *FGF13* was already expressed at higher levels in normal male pituitaries compared to female ones, whereas *VEGFD*, *CTAG2,* and *SLC6A8* showed comparable expression between the sexes in normal pituitary tissues. Interestingly, *FGF13* and *VEGFD* are both involved in mechanisms such as angiogenesis, cell growth/proliferation, and control of cellular movement/morphology. *VEGFD* is further involved in cell cycle control (12, 13), supporting the overall importance of this candidate in the sex-linked aggressiveness of lactotroph tumors. Besides *FGF13* and *VEGFD,* the candidate *CTAG2* is involved in cellular movement and has previously been associated with invasion in breast cancer (6). As shown in **Table 2**, correlative analysis revealed that, in men, *CTAG2* expression was strongly correlated with known lactotroph tumor aggressiveness markers implicated in the cell cycle (*CENPE, AURKB, CCNB1, ADAMTS6*) (11). Finally, it is interesting to note that the overexpression of the phosphocreatine transporter gene *SLC6A8* suggests the existence of metabolic advantages in male tumors.

Chromosomic Alterations in Lactotroph Tumors Define a Sex-Specific Gene Landscape

Following the identification of a sex-specific gene expression, we further determined whether exploration of chromosomic alterations could pinpoint a genetic origin of the sexual dimorphism that exists in lactotroph tumors. Taking advantage of a CGH array we previously performed on 13 lactotroph tumors (14), of which 12 are included in the transcriptomic study, we investigated whether the observed chromosomal alterations were sex-linked. Clinical details and sex (seven men, six females) of those 13 tumors are provided in **Table 3**. Through this work, we confirmed the sex-independent association of several abnormalities of chromosome 1 (gain & loss) and chromosome 11 (deletion) in aggressive tumors grade 2b (10). We further found that chromosomes 3, 5, and 14 were frequently affected without any sex- or tumor grade-specific correlations. Interestingly, we observed that chromosomic abnormalities were more numerous in aggressive than in non-aggressive tumors and that a specific gain of chromosome 19p was found in three aggressive lactotroph tumors from men (**Table 3** and **Figure 1**). Comparative analysis of CGH and transcriptomic data was subsequently carried out using the average number of known genes for each chromosome to calculate the chromosomic distribution of deregulated genes between lactotroph tumors from men and women. As summarized in **Table 4**, we found that chromosomes 19, 3, 2, and 5 represented the top four chromosomes with the highest percentage of deregulated genes (0.8, 0.77, 0.75, and 0.73%, respectively) that stand furthest from the median (0.53%). Having revealed chromosome 19 to be the sole chromosome subjected to sex-specific rearrangement, we wished to identify the candidate genes located within the concerned regions. We subsequently identified four genes (*CRB3*, *FAM138F*, *MATK,* and *STAP2*) that presented a minimum of a 2-fold statistically significantly increased expression in male lactotroph tumors (**Table S1**).

Identification of Sex-Associated Candidate Genes Through a Functional Signature Analysis

We next proceeded with gene stratification using an Ingenuity pathway analysis combined with an in-depth exploration of the scientific literature to further understand the function of the identified genes (**Table S1**). Using such an approach, we reviewed the 140 identified candidate genes with a focused interest in biological function relating to cancer biology, tumor progression, and aggressiveness. In this way, we found that several genes had been reported to contribute to angiogenesis

TABLE 3 | Pathological and genetic data from patients with lactotroph tumors.

Tumor number	Sex	Clinical behavior	Pathological group	Chromosome gains	Chromosome losses
1	M	Recurrence, death	2b	**3p**, **5**, 8, **14q**, **19p**	**11p**
2	M	Recurrences, metastasis, death	2b->3	**1q**, **3p**, 8q, 9, **14q**, **19p**	**1q, 11**
3	M	Recurrences, metastasis, death	2b->3	**1q, 5,** 15q, **19p#**	**11**, 17p
4	F	Recurrence	2b	4q	**1p**, **11p**
5*	F	Recurrences, metastasis, death	2b->3	**1q**, 8q, 15q	**1**, 4, **5q**, **11**, 13q, 15, 16
6	F	Recurrence	2b	–	–
7	M	Persistence	2a	Y	–
8	M	Persistence	2a	–	15q, 2p
9	M	Remission	1a	7, 9	–
10	M	Remission	1a	8, Y	–
11	F	Remission	1a	9	–
12	F	Remission	1a	7p, 20	13q
13	F	Remission	1a	9	—

Not included in transcriptomic analysis. #In the publication Wierinckx et al. (14), an error occurred in case 3 of this table; it was reported to have an insertion of 19q, while the insertion is 19p as indicated here. In bold the chromosomes presented on* ***figure 1**.*

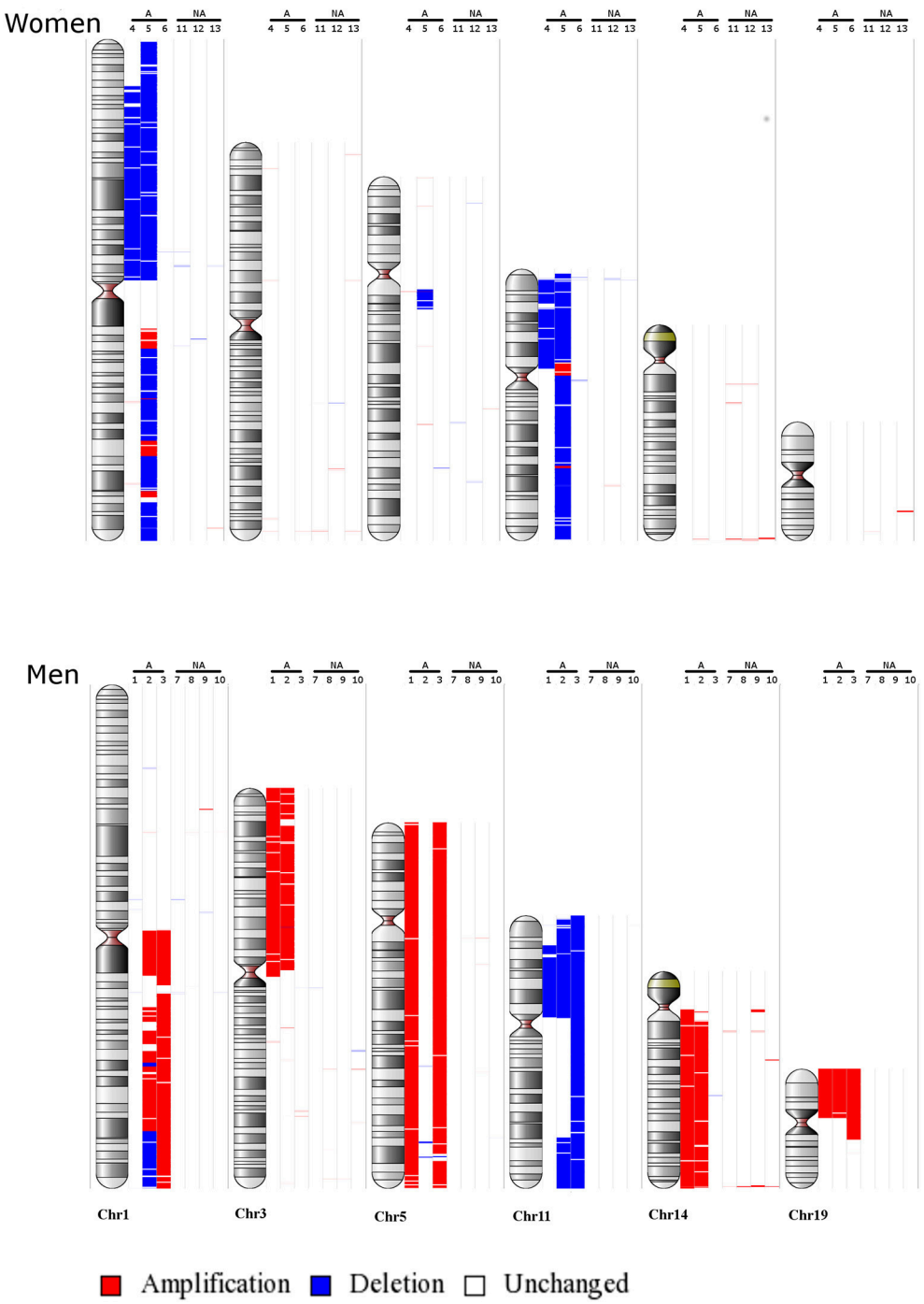

FIGURE 1 | Main chromosomic abnormalities in lactotroph tumors from seven men and six women. Gains are indicated by red bars and losses by blue bars. NA, non-aggressive lactotroph tumors; A, aggressive lactotroph tumors. Genomic DNA reference was cont103 (Affymetrix).

(10 genes), cell growth and proliferation (29 genes), cell death and survival (6 genes), control of cell morphology (12 genes), control of cellular movement (32 genes), and development (35 genes) (**Table S1**). In parallel, we further categorized genes involved in normal and pathological pituitary functions and found a substantial number of the identified genes to be related to the endocrine system (10 genes), estrogen signaling (25 genes), pituitary tumors (10 genes), or to be involved in sexual dimorphism (11 genes) (**Table S1**). Following this classification, we cross-analyzed the two lists (*i.e* oncology processes vs. normal/pathological pituitary functions) of genes and isolated a subset of 32 candidates that were the most representative

TABLE 4 | Chromosomic deregulated genes between men and women in lactotroph tumors.

Localization	Deregulated genes (*n*)	Δ Genes represented (%)
chr19	**12**	0.80
chr3	**10**	0.77
chr2	**12**	0.75
chr5	**8**	0.73
chr13	**3**	0.60
chr9	**6**	0.60
chr8	**5**	0.59
chr16	**6**	0.59
chr7	**7**	0.58
chr1	**13**	0.57
chr11	8	0.53*
chr4	5	0.53*
chr6	6	0.44
chr14	4	0.42
chr21	1	0.33
chr18	1	0.29
chr20	2	0.29
chr17	3	0.22
chr12	2	0.17
chr22	1	0.15
chr15	1	0.13
chr10	1	0.10

Median, in bold number of genes above the median

$$\Delta\text{Genes represented by the chromosome } \lambda = \left[\frac{\text{number of genes deregulated chromosome } \lambda}{\text{number of deregulated genes}}\right] - \left[\frac{\text{number of genes on chromosome } \lambda}{\text{number of total genes}}\right]$$

genes linked to the potent sex specificity of lactotroph tumors (**Table 5**).

Genes Involved in Estrogen Signaling and Sexual Dimorphism

Having previously reported the contribution of the estrogen signaling pathway in the sex specificity of lactotroph tumors through the identification of a low expression level of ERα in male tumors (4), we first confirmed that the expression of the estrogen receptor 1 gene (*ESR1)* found in our analysis strongly correlated (pearson correlation = 0.817, $p = 1.767\text{e-}08$) with the protein expression of ERα addressed by immunohistochemistry in our previous work (**Figure 2**) (4). Despite this observation, analysis of both *ESR1* and *AR* genes, coding for ERα and the andogen receptor, respectively, did not reveal significant different expression levels between lactotroph tumors from men and women. In contrats to protein expression of ERα addressed by immunohistochemistry, expression of the *ESR1* mRNA between men and women lactotroph tumors was not significantly reduced ($FC = -1.5$; $p = 0.13$), but in the aggressive tumors in women, the level of *ESR1* mRNA is very low. Then, if we removed these two samples from our statistical analysis, we observed that *ESR1* mRNA expression was significantly lower in men ($n = 20$) than in women ($n = 8$) ($FC = -1.9$, $p = 0.0016$) lactotroph tumors. Comparing only the non-aggressive lactotroph tumors between men and women, the expression level of *ESR1* mRNA remained significantly lower in men compared to women ($FC = -1.6$; $p = 0.031$) and in normal pituitary, although not representative of the normal prolactin cells, the level of *ESR1* mRNA expression was lower in men than in women ($FC = -2.41$). Next, we assessed whether a subset of estrogen signaling-related genes could be found within our list of candidates (**Table S1**). Out of the 140 genes differentially expressed between male and female lactotroph tumors, we found that 25 genes related to estrogen signaling (**Table S1**). Out of these, 22 were also associated with oncologic processes (**Table 5**) and 9 were related to sex differences (**Table S1** and **Table 5**). From these analyses, a series of appealing candidate genes were identified. Among them we found *ERBIN,* previously shown to be expressed in hepatocellular carcinoma and to promote tumorigenesis (15), and *FOXA1*, which significantly negatively correlated with *ESR1* expression (Pearson Correlation $= -0.45$; $p = 0.014$) and is known to regulate *ISL1* and *PPP1R14C, two* other identified estrogen-related genes. Finally, *SLC6A8* also attracted our interest based on its significant 2.6-fold overexpression in male lactotroph tumors ($p = 0.00231$) and its capacity to be inhibited by estrogens and stimulated by testosterone (16).

DISCUSSION

We have previously reported that lactotroph tumors that develop in men are of a higher grade and are resistant to treatment, and men have an overall worse prognosis compared to women (4). Despite this evident sexual dimorphism, there have been few studies carried out to compare gene expression between the sexes. Here, we used a comparative set of analyses involving transcriptomic and CGH experimental data obtained from lactotroph tumors from 20 men and 10 women to undertake such an analysis. We paid particular attention to the importance of the estrogen signaling pathway in sex-specific behavior due to our previous identification of a reduced ERα protein expression in male lactotroph tumors (4) and the well-established correlation between the grade of malignancy and low ERα protein expression that exists in breast tissues and bladder tumors (17–19).

Here, we confirm the importance of estrogen signaling in defining the sex specificity of aggressive lactotroph tumors. While our work demonstrates that a very strong correlation exists between the expression of ERα and the product of its gene *ESR1*, our analysis further reveals that 18% of the genes differentially expressed between male and female lactotroph tumors are involved in estrogen signaling (**Table S1**). Whereas, a low level of ERα expression correlated with aggressiveness for all tumors from men, out of ten tumors from women, this observation only occurred in the two tumors that were classified as aggressive (tumor grade 2b). The low *ESR1* mRNA level

TABLE 5 | Major functions of genes deregulated by a factor of two between male and female lactotroph tumors.

Symbol	Expr fold change	Expr *p*-value	Description	Chromosome	Angiogenesis	Cell growth and proliferation	Cell death and survival	Cell morphology	Cellular movement	Development	Endocrine system	Estrogen signaling	Pituitary tumors	Sexual dimorphism	Symbol
BHLHE41	2.077	0.00365	Basic helix-loop-helix family member e41	12					x	x		x			BHLHE41
CDK8	2.599	$5.59\ 10^{-5}$	Cyclin dependent kinase 8	13		x						x			CDK8
CHL1	3.117	0.0296	Cell adhesion molecule L1 like	3		x		x	x	x			x		CHL1
CTAG2	2.332	0.0242	Cancer/testis antigen 2	X					x			x			CTAG2
ENC1	2.023	0.0336	Ectodermal-neural cortex 1	5		x		x	x				x		ENC1
ERBIN	2.008	0.0191	Erbb2 interacting protein	5		x		x		x		x		x	ERBIN
ETS2	2.366	$5.76\ 10^{-4}$	ETS proto-oncogene 2, transcription factor	21			x			x		x	x		ETS2
EXT1	2.181	0.00196	Exostosin glycosyltransferase 1	8		x			x	x		x			EXT1
EZR	−2.199	0.0187	Ezrin	6		x		x	x	x			x		EZR
FGF13	3.419	0.0067	Fibroblast growth factor 13	X		x	x	x	x	x		x			FGF13
FOXA1	2.35	0.0338	Forkhead box A1	14		x		x	x	x	x	x		x	FOXA1
FOXQ1	5.758	0.0393	Forkhead box Q1	6					x	x		x			FOXQ1
GADD45G	−2.656	0.0281	Growth arrest and DNA damage inducible gamma	9		x							x		GADD45G
ISL1	2.163	0.0338	ISL LIM homeobox 1	5	x	x	x		x	x	x				ISL1
KDM5D	18.032	$4.12\ 10^{-10}$	Lysine demethylase 5d	Y		x								x	KDM5D
LTBP1	2.246	0.0367	Latent transforming growth factor beta binding protein 1	2	x	x	x			x		x	x	x	LTBP1
MYH7	−4.706	0.00688	Myosin heavy chain 7	14						x		x			MYH7
NMU	3.336	0.00721	Neuromedin u	4					x			x			NMU
OBSCN	2.596	0.0158	Obscurin, cytoskeletal calmodulin and titin-interacting rhogef	1			x					x			OBSCN
PITX1	2.459	0.00579	Paired like homeodomain 1	5						x	x	x	x		PITX1
PPID	2.261	0.0369	Peptidylprolyl isomerase d	4					x					x	PPID
PTGS1	2.554	0.0263	Prostaglandin-endoperoxide synthase 1	9	x					x	x	x			PTGS1
PTPRZ1	2.393	0.0496	Protein tyrosine phosphatase, receptor type z1	7	x	x		x	x	x		x			PTPRZ1
ROBO1	2.033	0.0144	Roundabout guidance receptor 1	3	x	x		x	x	x		x			ROBO1
SLC12A4	3.348	0.00534	Solute carrier family 12 member 4	16						x			x		SLC12A4
SLC2A11	2.342	0.0131	Solute carrier family 2 member 11	22		x					x		x		SLC2A11
SLC6A8	2.577	0.00231	Solute carrier family 6 member 8	X			x					x		x	SLC6A8
SNCB	2.022	0.013	Synuclein beta	5				x		x		x			SNCB
SOSTDC1	6.814	0.0103	Sclerostin domain containing 1	7						x		x			SOSTDC1
STAP2	2.122	0.00363	Signal transducing adaptor family member 2	19					x			x			STAP2
TSPAN8	3.232	0.0371	Tetraspanin 8	12					x			x			TSPAN8
VEGFD	2.27	0.0363	vascular endothelial growth factor d	X	x	x		x	x	x			x		VEGFD

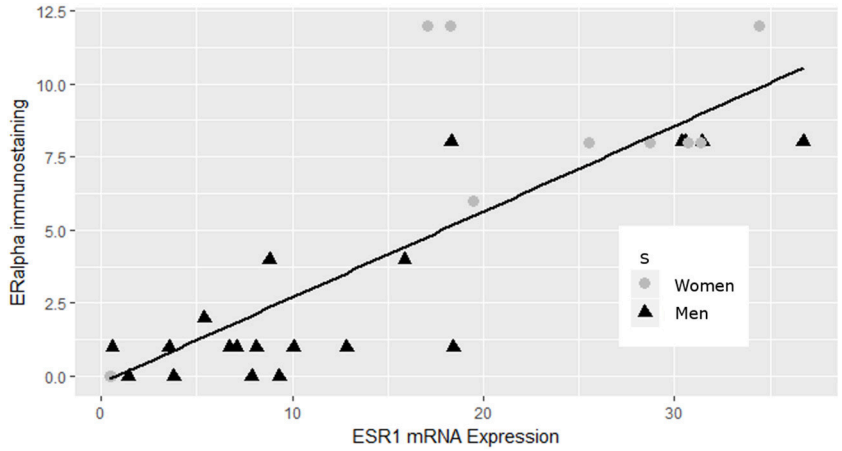

FIGURE 2 | Correlation between ERα and *ESR1* mRNA expression in lactotroph tumors. ERα data from immunoblotting (4) strongly correlated (pearson correlation = 0.817, $p = 1.767e\text{-}08$) with the expression of the *ESR1* gene.

observed in aggressive female lactotroh tumors, may explain the non-significant differential expression of *ESR1* mRNA, between men and women. When the expression data of this gene from the two aggressive women tumors were removed, the differential expression of *ESR1* mRNA became significantly different between men and women lactotroph tumors. We therefore hypothesized that a high level of ERα expression may result in a protective effect against aggressiveness in lactotroph tumors in women. In contrast, the low expression level of ERα found in male tumors may explain the higher risk of more aggressive tumor behavior, recurrence, and resistance to treatment. As the *ESR1* mRNA level was already lower in the normal pituitaries of men compared to women, we suggested that early divergence of the ERα level and sex-associated regulation of estrogen signaling may have a major influence on vascularization, tumor growth, and chromosomic alteration (**Figure 3**).

Among all the estrogen signaling-associated genes we identified, *STAP2* appears to be one of the most interesting candidates to explore. Indeed, *STAP2* is regulated by estrogen and increases during menopause in women, when the estrogen level decreases (20). Thus, the higher *STAP2* mRNA level in lactotroph tumors from men compared to women may be related to the lower level of ERα. *STAP2* is known to increase cell growth and tumor progression in breast and prostate cancer by interacting with the Brk and STAT pathways (21–23). In male lactotroph tumors, while we found *STAP2* to be increased at all tumor grades, we noted that *STAT3* and *STAT5* were higher in male grade 2b/3 than in female grade 2b tumors (**Figure S1**). More interestingly, the unphosphorylated form of STAT has been shown to participate in DNA damage protection through the stabilization of the heterochromatin protein 1 (24). Taken together, such observations suggest that the low level of ERα could increase the level of *STAP2* mRNA, therefore contributing to the aggressiveness of male lactotroph tumors through a reduced genome integrity mediated by STAT signaling. Consistent with this hypothesis, we found chromosome abnormalities to be more numerous in both tumors from men and aggressive tumors (14). Even if the following observations as to be confirmed on a larger number of lactotroph tumors, the additional gain of chromosome 19p which was observed only in the 3 aggressive or malignant tumors in man may suggest that specific gains of chromosome 19p could have an influence on tumors aggressiveness. These findings suggest that the sexual dimorphism of lactotroph tumors and their more aggressive behavior in men than in women may be related to increased chromosomic abnormalities in men compared to women.

Besides confirming the importance of estrogen signaling in the sex-related aggressiveness of lactotroph tumors, our work sheds light on the potent role of a series of sex chromosome-related candidates. Indeed, our analysis highlights several X chromosome-located genes that are overexpressed in male lactotroph tumors, especially the cancer-testis antigen (*CTAG2*), the creatine-transporter (*SLC6A8*), and two growth factors (*FGF13* and *VEGFD*). *CTAG2*, normally only expressed in the testis, is involved in the invasive behavior of breast cancer (6) and is highly expressed in gastrointestinal and breast carcinomas (25). Moreover, the cancer-testis antigens are implicated in repressing estrogen signaling (26). In our study, *CTAG2* is specifically upregulated and correlated with markers of aggressiveness *ADAMTS6, AURKB, CCNB1, CENPE,* and *PTTG1* (11, 27) only in male lactotroph tumors. SLC6A8, a transporter that imports extracellular phosphocreatine into the cell inhibited by estrogens, was shown to induce sex differences in creatine metabolism (16). As in lactotroph tumors in men, *FGF13* is upregulated in cancer cells (28, 29). This growth factor is not a cancer driver but serves to enhance survival of cancer cells (28, 29). Indeed, the higher expression of *SLC6A8* and *FGF13* genes may contribute to increased cell survival in lactotroph tumors in men. Not only *VEGFD,* but also an adaptor protein involved in VEGF signaling, *SH2D2A*, and five other genes *LTBP1, ISL1, PTGS1, PTPRZ1,* and *ROBO1* (30–34), known to promote angiogenesis,

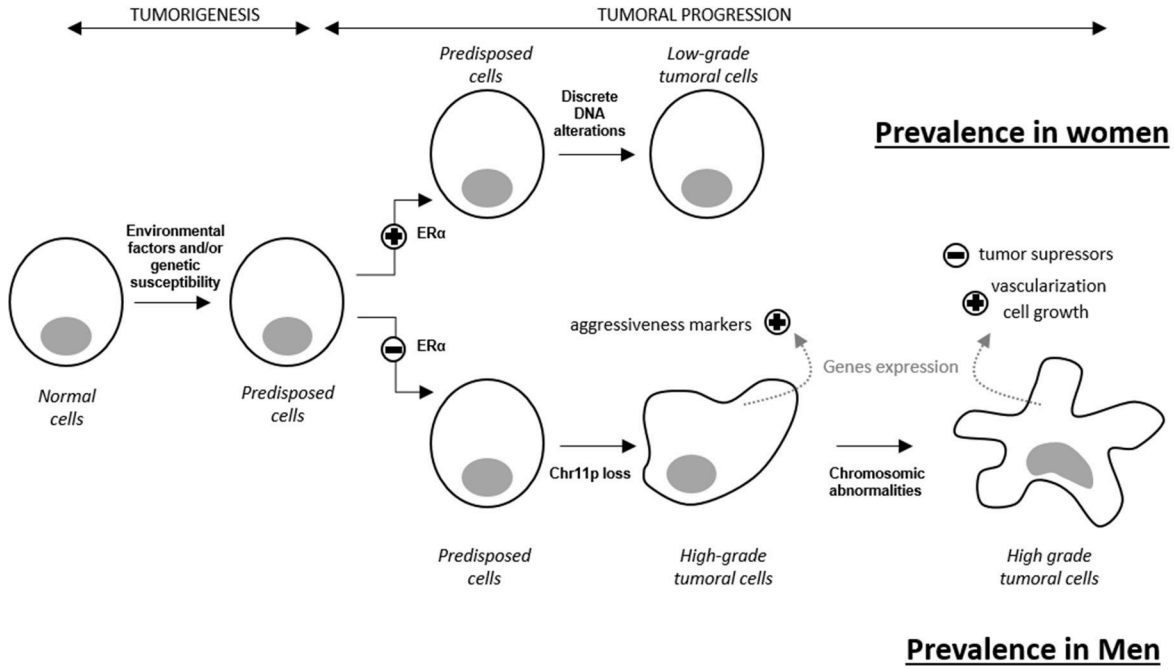

Correlations between tumor characteristics and protein/gene expression					
Parameters	**ERα/ESR1 mRNA**	**Chromosomic alterations**	**Genes implicated in angiogenesis**	**Genes implicated in proliferation**	**Sex prevalence**
Level	low	numerous	high	high	**Men**
Tumor characteristics	*aggressive*	*high grade*	*much vascularized*	*large and proliferative*	
Level	high	few	low	low	**Women**
Tumor characteristics	*non aggressive*	*low grade*	*no much vascularized*	*small and benign*	

FIGURE 3 | Hypothetical model of lactotroph tumor progression explaining the higher prevalence of aggressive tumors in men compared to women. ERα level influences tumor incidence and progression. A high level of ERα induces the development of lactotroph tumors and protects against worse progression. In contrast, a low level of ERα reduces incidence but promotes tumor evolution to higher grade by inducing cell proliferation and vascularization. Discrete and sparse alterations lead to a non-aggressive phenotype. These data highlight the impact of the ERα expression level on genetic instability, cell growth, and vascularization, therefore explaining the prevalence of high-grade tumors and a predisposition to treatment resistance in men compared to women.

were overexpressed in men. A high expression of VEGF was observed by immunohistochemistry in 60.7% of the lactotroph tumors (35). Its expression was higher in pituitary carcinomas compared to benign adenomas (36), as was microvascular density (37). One case of our series (case 3) illustrates the importance of VEGF in lactotroph tumors. This malignant lactotroph tumor from a man had abnormalities in chromosome 1, chromosome 11, chromosome 19, a neoangiogenesis (38), and showed endothelial cell expression of endocan, another angiogenic factor which is controlled by VEGF and FGF2 (39). This overexpression of VEGF in lactotroph tumors could be of therapeutic interest. Indeed, it has been also reported that an anti-VEGF (bevacizumab) treatment stabilized the progression of a pituitary carcinoma and induced extensive perivascular fibrosis (40). Finally, despite the fact that lactotroph tumors are less responsive to dopamine agonists in men than in women, we did not find a sex-related difference in the expression of the dopamine agonist receptor D2 itself. However, the growth inhibiting action of dopamine on lactotroph cells is partly mediated by the transforming growth factor (TGF)- β1 system (41). The availability of TGFβ1 is modulated by latent TGFβ-binding proteins (LTBP) and bone morphogenetic protein 1 (BMP1) is one of the activators of latent TGFβ1. Estradiol has been shown to inhibit pituitary LTBP1 expression (42) and we observe in our series a significantly increased LTBP1 expression among males. Sclerostin domain-containing 1 (SOSTDC1), a BMP antagonist, is inhibited by estrogens (43) and appears here to be highly upregulated in males lactotroph tumors. Thus, we can speculate that the lack of ERα observed in men could result in an inhibition of TGFβ1 and thus in an impairment of the control of lactotroph proliferation by dopamine.

This study, based on a combined series of analysis ranging from transcriptomics and CGH array to a detailed literature review, demonstrates that the prevalence of aggressive lactotroph tumors in men is not linked to a single factor. Our data further suggest that among the many factors differentially expressed between lactotroph tumors from men and women, an important subset belongs to the estrogen signaling pathway, while androgen or testosterone signaling molecules are not differently impacted. To that extent, this study enriches our model of lactotroph tumor progression by highlighting that a low expression of ERα is an early factor favoring higher aggressiveness of lactotroph tumor cells in men compared to women. Besides this important observation, our work sheds light on a novel series of mechanisms, identifying a sex-specific gene expression in lactotroph tumors in men that relates to a genetic instability and to the increased expression of several candidate genes promoting angiogenesis, cell proliferation, and survival of lactotroph tumor cells.

AUTHOR CONTRIBUTIONS

AW, ED, JT, and GR designed research studies. AW conducted experiments and acquired data. AW and ED analyzed data. AW, ED, PB, JL, JT, and GR discussed results. PF, EJ, and PC provided human material and biopsies. AW and ED wrote the manuscript.

FUNDING

This work was supported by Institut National de la Santé et de la Recherche Médicale (INSERM) and by the University of Lyon. This work was supported by the Ligue Contre le Cancer (comités Puy de Dôme and Rhône-Alpes). This work was supported by the Région RhôneAlpes (France). This work was supported by the Programme Hospitalier de Recherche Clinique National (Hypopronos no.2743).

ACKNOWLEDGMENTS

We thank Louise Ball from The English Edition for help with the English translation.

SUPPLEMENTARY MATERIAL

The Supplementary Material for this article can be found online at: https://www.frontiersin.org/articles/10.3389/fendo.2018.00706/full#supplementary-material

Figure S1 | STAT3 and STAT5B mRNA expression in aggressive lactotroph tumors. Gray bar were the average relative mRNA expression measured in the 2 aggressive lactotroph tumors in woman classified as 2b. Dark bar were the average relative mRNA expression measured in the 7 aggressive lactotroph tumors in men classified as 2b or 3.

Table S1 | Genes differentially deregulated between Men and Women lactotroph tumors.

REFERENCES

1. Carter JN, Tyson JE, Tolis G, Van Vliet S, Faiman C, Friesen HG. Prolactin-screening tumors and hypogonadism in 22 men. *N Engl J Med.* (1978) 299:847–52. doi: 10.1056/NEJM197810192991602
2. Delgrange E, Trouillas J, Maiter D, Donckier J, Tourniaire J. Sex-related difference in the growth of prolactinomas: a clinical and proliferation marker study. *J Clin Endocrinol Metab.* (1997) 82:2102–7. doi: 10.1210/jc.82.7.2102
3. Calle-Rodrigue RD, Giannini C, Scheithauer BW, Lloyd RV, Wollan PC, Kovacs KT, et al. Prolactinomas in male and female patients: a comparative clinicopathologic study. *Mayo Clin Proc.* (1998) 73:1046–52. doi: 10.4065/73.11.1046
4. Delgrange E, Vasiljevic A, Wierinckx A, Francois P, Jouanneau E, Raverot G, Trouillas J. Expression of estrogen receptor alpha is associated with prolactin pituitary tumor prognosis and supports the sex-related difference in tumor growth. *Eur J Endocrinol.* (2015) 172:791–801. doi: 10.1530/EJE-14-0990
5. Liu R, Kain M, Wang L. Inactivation of X-linked tumor suppressor genes in human cancer. *Future Oncol.* (2012) 8:463–81. doi: 10.2217/fon.12.26
6. Maine EA, Westcott JM, Prechtl AM, Dang TT, Whitehurst AW, Pearson GW. The cancer-testis antigens SPANX-A/C/D and CTAG2 promote breast cancer invasion. *Oncotarget* (2016) 7:14708–26. doi: 10.18632/oncotarget.7408
7. Wong HY, Wang GM, Croessmann S, Zabransky DJ, Chu D, Garay JP, et al. TMSB4Y is a candidate tumor suppressor on the Y chromosome and is deleted in male breast cancer. *Oncotarget* (2015) 6:44927–40. doi: 10.18632/oncotarget.6743
8. Forsberg LA, Rasi C, Malmqvist N, Davies H, Pasupulati S, Pakalapati G, et al. Mosaic loss of chromosome Y in peripheral blood is associated with shorter survival and higher risk of cancer. *Nat Genet.* (2014) 46:624–8. doi: 10.1038/ng.2966
9. Kido T, Lau YF. Roles of the Y chromosome genes in human cancers. *Asian J Androl.* (2015) 17:373–80. doi: 10.4103/1008-682X.150842
10. Trouillas J, Roy P, Sturm N, Dantony E, Cortet-Rudelli C, Viennet G, et al. A new prognostic clinicopathological classification of pituitary adenomas: a multicentric case-control study of 410 patients with 8 years post-operative follow-up. *Acta Neuropathol.* (2013) 126:123–35. doi: 10.1007/s00401-013-1084-y
11. Wierinckx, Auger C, Devauchelle P, Reynaud A, Chevallier P, Jan M, et al. A diagnostic marker set for invasion, proliferation, and aggressiveness of prolactin pituitary tumors. *Endocr Relat Cancer* (2007) 14:887–900. doi: 10.1677/ERC-07-0062
12. Kimura, Honda R, Okai H, Okabe M. Vascular endothelial growth factor promotes cell-cycle transition from G0 to G1 phase in subcultured endothelial cells of diabetic rat thoracic aorta. *Jpn J Pharmacol.* (2000) 83:47–55. doi: 10.1254/jjp.83.47
13. Orlandini M, Marconcini L, Ferruzzi R, Oliviero S. Identification of a c-fos-induced gene that is related to the platelet-derived growth factor/vascular endothelial growth factor family. *Proc Natl Acad Sci USA.* (1996) 93:11675–80. doi: 10.1073/pnas.93.21.11675
14. Wierinckx, Roche M, Raverot G, Legras-Lachuer C, Croze S, Nazaret N, et al. Integrated genomic profiling identifies loss of chromosome 11p impacting transcriptomic activity in aggressive pituitary PRL tumors. *Brain Pathol.* (2011) 21:533–43. doi: 10.1111/j.1750-3639.2011.00476.x
15. Wu H, Yao S, Zhang S, Wang JR, Guo PD, Li XM, et al. Elevated expression of Erbin destabilizes ERalpha protein and promotes tumorigenesis in hepatocellular carcinoma. *J Hepatol.* (2017) 66:1193–204. doi: 10.1016/j.jhep.2017.01.030
16. Joncquel-Chevalier Curt M, Cheillan D, Briand G, Salomons GS, Mention-Mulliez K, Dobbelaere D, et al. Creatine and guanidinoacetate reference values in a French population. *Mol Genet Metab.* (2013) 110:263–7. doi: 10.1016/j.ymgme.2013.09.005
17. Krol MB, Galicki M, Gresner P, Wieczorek E, Jablonska E, Reszka E, et al. The ESR1 and GPX1 gene expression level in human malignant

and non-malignant breast tissues. *Acta Biochim Pol.* (2018) 65:51–7. doi: 10.18388/abp.2016_1425
18. Ide H, Inoue S, Miyamoto H. Histopathological and prognostic significance of the expression of sex hormone receptors in bladder cancer: a meta-analysis of immunohistochemical studies. *PLoS ONE* (2017) 12:e0174746. doi: 10.1371/journal.pone.0174746
19. Miyamoto H, Yao JL, Chaux A, Zheng Y, Hsu I, Izumi K, et al. Expression of androgen and oestrogen receptors and its prognostic significance in urothelial neoplasm of the urinary bladder. *BJU Int.* (2012) 109:1716–26. doi: 10.1111/j.1464-410X.2011.10706.x
20. Moon YJ, Bai SW, Jung CY, Kim CH. Estrogen-related genome-based expression profiling study of uterosacral ligaments in women with pelvic organ prolapse. *Int Urogynecol J.* (2013) 24:1961–7. doi: 10.1007/s00192-013-2124-9
21. Ikeda O, Mizushima A, Sekine Y, Yamamoto C, Muromoto R, Nanbo A, et al. Involvement of STAP-2 in Brk-mediated phosphorylation and activation of STAT5 in breast cancer cells. *Cancer Sci.* (2011) 102:756–61. doi: 10.1111/j.1349-7006.2010.01842.x
22. Ikeda O, Sekine Y, Mizushima A, Nakasuji M, Miyasaka Y, Yamamoto C, et al. Interactions of STAP-2 with Brk and STAT3 participate in cell growth of human breast cancer cells. *J Biol Chem.* (2010) 285:38093–103. doi: 10.1074/jbc.M110.162388
23. Kitai Y, Iwakami M, Saitoh K, Togi S, Isayama S, Sekine Y, et al. STAP-2 protein promotes prostate cancer growth by enhancing epidermal growth factor receptor stabilization. *J Biol Chem.* (2017) 292:19392–9. doi: 10.1074/jbc.M117.802884
24. Yan SJ, Lim SJ, Shi S, Dutta P, Li WX. Unphosphorylated STAT and heterochromatin protect genome stability. *FASEB J.* (2011) 25:232–41. doi: 10.1096/fj.10-169367
25. Mashino, Sadanaga N, Tanaka F, Yamaguchi H, Nagashima H, Inoue H, et al. Expression of multiple cancer-testis antigen genes in gastrointestinal and breast carcinomas. *Br J Cancer* (2001) 85:713–20. doi: 10.1054/bjoc.2001.1974
26. Chen L, Zhou WB, Zhao Y, Liu XA, Ding Q, Zha XM, et al. Cancer/testis antigen SSX2 enhances invasiveness in MCF-7 cells by repressing ERalpha signaling. *Int J Oncol.* (2012) 40:1986-94. doi: 10.3892/ijo.2012.1369
27. Raverot G, Wierinckx A, Dantony E, Auger C, Chapas G, Villeneuve L, et al. Prognostic factors in prolactin pituitary tumors: clinical, histological, and molecular data from a series of 94 patients with a long postoperative follow-up. *J Clin Endocrinol Metab.* (2010) 95:1708–16. doi: 10.1210/jc.2009-1191
28. Bublik DR, Bursac S, Sheffer M, Orsolic I, Shalit T, Tarcic O, et al. Regulatory module involving FGF13, miR-504, and p53 regulates ribosomal biogenesis and supports cancer cell survival. *Proc Natl Acad Sci USA.* (2017) 114:E496–505. doi: 10.1073/pnas.1614876114
29. Yu L, Toriseva M, Tuomala M, Seikkula H, Elo T, Tuomela J, et al. Increased expression of fibroblast growth factor 13 in prostate cancer is associated with shortened time to biochemical recurrence after radical prostatectomy. *Int J Cancer* (2016) 139:140–52. doi: 10.1002/ijc.30048
30. Li, Sun F, Chen X, Zhang M. ISL1 is upregulated in breast cancer and promotes cell proliferation, invasion, and angiogenesis. *Onco Targets Ther.* (2018) 11:781–9. doi: 10.2147/OTT.S144241
31. Niu X, Zhang K. Dysregulated expression of inflammation-related genes in psoriatic dermis mesenchymal stem cells. *Acta Biochim Biophys Sin.* (2016) 48:587–8. doi: 10.1093/abbs/gmw036
32. Ribot J, Caliaperoumal G, Paquet J, Boisson-Vidal C, Petite H, Anagnostou F. Type 2 diabetes alters mesenchymal stem cell secretome composition and angiogenic properties. *J Cell Mol Med.* (2017) 21:349–63. doi: 10.1111/jcmm.12969
33. Ulbricht U, Brockmann MA, Aigner A, Eckerich C, Muller S, Fillbrandt R, et al. Expression and function of the receptor protein tyrosine phosphatase zeta and its ligand pleiotrophin in human astrocytomas. *J Neuropathol Exp Neurol.* (2003) 62:1265–75. doi: 10.1093/jnen/62.12.1265
34. Zhang X, Dong J, He Y, Zhao M, Liu Z, Wang N, et al. miR-218 inhibited tumor angiogenesis by targeting ROBO1 in gastric cancer. *Gene* (2017) 615:42–9. doi: 10.1016/j.gene.2017.03.022
35. Wang Y, Li J, Tohti M, Hu Y, Wang S, Li W, et al. The expression profile of Dopamine D2 receptor, MGMT and VEGF in different histological subtypes of pituitary adenomas: a study of 197 cases and indications for the medical therapy. *J Exp Clin Cancer Res* (2014) 33:56. doi: 10.1186/s13046-014-0056-y
36. Lloyd RV, Scheithauer BW, Kuroki T, Vidal S, Kovacs K, Stefaneanu L. Vascular Endothelial Growth Factor (VEGF) expression in human pituitary adenomas and carcinomas. *Endocr Pathol.* (1999) 10:229–35. doi: 10.1007/BF02738884
37. Vidal S, Kovacs K, Horvath E, Scheithauer BW, Kuroki T, Lloyd RV. Microvessel density in pituitary adenomas and carcinomas. *Virchows Arch.* (2001) 438:595–602. doi: 10.1007/s004280000373
38. Zemmoura, Wierinckx A, Vasiljevic A, Jan M, Trouillas J, Francois P. Aggressive and malignant prolactin pituitary tumors: pathological diagnosis and patient management. *Pituitary* (2013) 16:515–22. doi: 10.1007/s11102-012-0448-y
39. Cornelius, Cortet-Rudelli C, Assaker R, Kerdraon O, Gevaert MH, Prevot V, et al. Endothelial expression of endocan is strongly associated with tumor progression in pituitary adenoma. *Brain Pathol.* (2012) 22:757–64. doi: 10.1111/j.1750-3639.2012.00578.x
40. Ortiz LD, Syro LV, Scheithauer BW, Ersen A, Uribe H, Fadul CE, et al. Anti-VEGF therapy in pituitary carcinoma. *Pituitary* (2012) 15:445–9. doi: 10.1007/s11102-011-0346-8
41. Sarkar DK, Chaturvedi K, Oomizu S, Boyadjieva NI, Chen CP. Dopamine, dopamine D2 receptor short isoform, transforming growth factor (TGF)-beta1, and TGF-beta type II receptor interact to inhibit the growth of pituitary lactotropes. *Endocrinology* (2005) 146:4179–88. doi: 10.1210/en.2005-0430
42. Recouvreux MV, Lapyckyj L, Camilletti MA, Guida MC, Ornstein A, Rifkin DB, et al. Sex differences in the pituitary transforming growth factor-beta1 system: studies in a model of resistant prolactinomas. *Endocrinology* (2013) 154:4192–205. doi: 10.1210/en.2013-1433
43. Fujita K, Roforth MM, Demaray S, McGregor U, Kirmani S, McCready LK, et al. Effects of estrogen on bone mRNA levels of sclerostin and other genes relevant to bone metabolism in postmenopausal women. *J Clin Endocrinol Metab.* (2014) 99:E81–8. doi: 10.1210/jc.2013-3249

Conflict of Interest Statement: The authors declare that the research was conducted in the absence of any commercial or financial relationships that could be construed as a potential conflict of interest.

frontiers in Endocrinology

REVIEW
published: 17 January 2019
doi: 10.3389/fendo.2018.00814

Metabolomics—A Promising Approach to Pituitary Adenomas

Oana Pînzariu[1], *Bogdan Georgescu*[2] *and Carmen E. Georgescu*[1,3]*

[1] 6th Department of Medical Sciences, Department of Endocrinology, Iuliu Hatieganu University of Medicine and Pharmacy, Cluj-Napoca, Romania, [2] Department of Ecology, Environmental Protection and Zoology, University of Agricultural Sciences and Veterinary Medicine Cluj-Napoca, Cluj-Napoca, Romania, [3] Endocrinology Clinic, Cluj County Emergency Clinical Hospital, Cluj-Napoca, Romania

Background: Metabolomics—the novel science that evaluates the multitude of low-molecular-weight metabolites in a biological system, provides new data on pathogenic mechanisms of diseases, including endocrine tumors. Although development of metabolomic profiling in pituitary disorders is at an early stage, it seems to be a promising approach in the near future in identifying specific disease biomarkers and understanding cellular signaling networks.

Objectives: To review the metabolomic profile and the contributions of metabolomics in pituitary adenomas (PA).

Methods: A systematic review was conducted via PubMed, Web of Science Core Collection and Scopus databases, summarizing studies that have described metabolomic aspects of PA.

Results: Liquid chromatography tandem mass spectrometry (LC-MS/MS) and nuclear magnetic resonance (NMR) spectrometry, which are traditional techniques employed in metabolomics, suggest amino acids metabolism appears to be primarily altered in PA. N-acetyl aspartate, choline-containing compounds and creatine appear as highly effective in differentiating PA from healthy tissue. Deoxycholic and 4-pyridoxic acids, 3-methyladipate, short chain fatty acids and glucose-6-phosphate unveil metabolite biomarkers in patients with Cushing's disease. Phosphoethanolamine, N-acetyl aspartate and myo-inositol are down regulated in prolactinoma, whereas aspartate, glutamate and glutamine are up regulated. Phosphoethanolamine, taurine, alanine, choline-containing compounds, homocysteine, and methionine were up regulated in unclassified PA across studies. Intraoperative use of ultra high mass resolution matrix-assisted laser desorption/ionization mass spectrometry imaging (MALDI-MSI), which allows localization and delineation between functional PA and healthy pituitary tissue, may contribute to achievement of complete tumor resection in addition to preservation of pituitary cell lines and vasopressin secretory cells, thus avoiding postoperative diabetes insipidus.

Conclusion: Implementation of ultra high performance metabolomics analysis techniques in the study of PA will significantly improve diagnosis and, potentially, the therapeutic approach, by identifying highly specific disease biomarkers in addition to novel molecular pathogenic mechanisms. Ultra high mass resolution MALDI-MSI

OPEN ACCESS

Edited by:
Xianquan Zhan,
Central South University, China

Reviewed by:
Leila Warszawski,
Instituto Estadual de Diabetes e Endocrinologia Luiz Capriglione, Brazil
Na Li,
Central South University, China

***Correspondence:**
Carmen E. Georgescu
cgeorgescu@umfcluj.ro

Specialty section:
This article was submitted to Pituitary Endocrinology, a section of the journal Frontiers in Endocrinology

Received: *03 September 2018*
Accepted: *27 December 2018*
Published: *17 January 2019*

Citation:
Pînzariu O, Georgescu B and Georgescu CE (2019) Metabolomics—A Promising Approach to Pituitary Adenomas. Front. Endocrinol. 9:814. doi: 10.3389/fendo.2018.00814

emerges as a helpful clinical tool in the neurosurgical treatment of pituitary tumors. Therefore, metabolomics appears to be a science with a promising prospect in the sphere of PA, and a starting point in pituitary care.

Keywords: pituitary adenoma, metabolomics, metabolite, mass spectrometry (MS), nuclear magnetic resonance (NMR), MALDI-MS, magnetic resonance spectroscopy (MRS)

INTRODUCTION

Metabolomics, one of the newest "omics" sciences, assesses small molecules with molecular mass below 1,500 Da (1) within various bio-fluids (e.g., serum, plasma, cerebrospinal fluid, urine, saliva etc.) or tissues, to potentially set correlates to physiological or pathological status of an organism. Given its contribution to the understanding of cellular signaling mechanisms, in addition to identification and quantification of novel biomarkers in various clinical conditions, metabolomics is underpinning the development of personalized medicine.

Metabolites include carbohydrates, amino acids, nucleic acids, lipids, vitamins, organic acids, polyphenols, alkaloids, and inorganic species. A range of analytical techniques is applied, with either nuclear magnetic resonance (NMR), also known as magnetic resonance spectroscopy (MRS), or, more frequently, mass spectrometry (MS)-based platforms being routinely employed in assessing the metabolic fingerprint, the later method as a combination with other analysis techniques (i.e., gas-chromatography-mass spectrometry (GC-MS), liquid chromatography-mass spectrometry (LC-MS) (2, 3), ultra-performance liquid-chromatography tandem mass spectrometry (UPLC–MS/MS) (4, 5), ultra-high performance liquid chromatography-quadrupole time-of-flight mass spectrometry (UHPLC/Q-TOF-MS) (6, 7), capillary electrophoresis (CE-MS) (8, 9) or matrix-assisted laser desorption/ionization mass spectrometry (MALDI-MS) (10, 11) etc.) to overcome the limitations of MS, such as erroneous interpretation of the metabolomic analysis in presence of impurities or modest reproducibility of the method (12, 13). Further, complex informatics tools (e.g., principal component analysis, Mascot search etc.) that significantly improve identification of metabolomic panels by multivariate statistical analysis are integrated into most types of equipment.

Ionization of atoms and molecules followed by their separation according to the mass/charge ratio is a key principle of MS-based techniques; the methods most commonly used being electrospray ionization and electron impact ionization, followed by atmospheric pressure photoionization and atmospheric pressure chemical ionization (14).

Although sensitivity of MS is clearly superior to NMR spectrometry, the later is increasingly employed because the method is fast, highly reproducible and does not require additional steps of biological samples preparation, including separation and derivatization (15). In addition, NMR spectrometry can identify unknown compounds with identical masses, even those with different isotopic distribution.

The basic principle of NMR spectrometry consists of the spinning of atomic nuclei. The most common nuclei used in this technique are ^{1}H (proton), ^{13}P (phosphorus), ^{15}N (nitrogen) and ^{13}C (carbon), the highest sensitivity being attributed to ^{1}H (16). With the time, MRS has proven to be a highly used and non-invasive technique in cerebral tumors, particularly *in vivo* MRS, using brain MRI images (17). The technique allows identification of various metabolites by obtaining signals from a cerebral region of interest (ROI), more exactly a three-dimensional volume of this region measuring at least 1 cm^3 or the so-called *voxel* (18). However, a considerable disadvantage using this technique is the identification of a limited number of metabolites, those with extremely high concentrations (17).

Matrix-assisted laser desorption/ionization mass spectrometry imaging (MALDI-MSI) profiles as a valuable method that is able to identify peptides and proteins with a mass of up to 50,000 Da (19–21). In view of this aspect, MALDI-MSI appears to be useful in approaching pituitary gland disorders, since most of the pituitary hormones are proteins or peptides. The underlying principle of MALDI-MSI is to use a matrix that absorbs the energy emitted from an ultraviolet or infrared laser beam, followed by desorption and ionization of the analyzed metabolite, similarly to electrospray ionization (19). The method is fast and highly sensitive (22). Implementation of MALDI-MSI has made it possible to shift from assessing the metabolic fingerprint in biological products such as plasma, serum or urine directly to tissue sections.

A major advantage of the development of this technique is the correlation of MALDI-MSI results with the tumor histopathology, thus the demarcation of the tumor contour can be established. Further, MALDI-MSI is able to identify new biomarkers in an *in situ* context (i.e., paraphin embedded tissue or fixed tissue sections), while the combination of MALDI-MSI with computed tomography (CT), magnetic resonance imaging (MRI) or positron emission tomography (PET) imaging aims to improve the future approach to research (22).

Whichever technique is used, *untargeted* metabolomic analysis allows rapid and global description of a large number of metabolites (e.g., lipids, amino acids etc.), termed metabolomic fingerprint in a single sample that subsequently is subjected to interpretation and validation to define differences between physiological and pathological conditions (15, 23–25); while, *targeted* metabolomic analysis consists of the qualitative and quantitative assessment of a small number of preselected well known metabolites that are specific to a particular metabolic pathway (15).

The future prospects for improving the identification and quantification of metabolites are the combination of NMR spectrometry (MRS) and MS (26).

In past years, metabolomics has considerably developed in the field of endocrinology, including diabetes mellitus (27–30), obesity (27, 31, 32), polycystic ovary syndrome (33–37), thyroid cancer (38–41), osteoporosis (42, 43) and particularly adrenal diseases, i.e., adrenal cancer, Cushing's syndrome (44, 45), primary aldosteronism (46, 47) and pheochromocytoma (48) and resulted in description of novel cellular and molecular signaling mechanisms and characterization of complex panels of biomarkers of risk.

Metabolomics in pituitary disorders is currently at an early stage. In 2014, Höybye et al. (49) conducted a pilot study comparing serum metabolites in adult patients with growth hormone deficiency (GHD) to a healthy control group. The endpoint was to identify potential biomarkers for the diagnosis of GHD, concomitantly aiming to draw up a metabolomics-based individualized recombinant human GH (rhGH) replacement treatment protocol among affected subjects. Metabolomics analysis performed by GC-MS identified a number of 285 untargeted metabolites, 13 of them differentiating between patients with GHD and controls. Among these, lower levels of threonic acid, cystine, cysteine and palmitoleic acid and higher levels of glutamic acid, glyceric acid, aspartic acid, uridine and hypoxanthine-like were reported in adult GHD. Furthermore, rhGH treatment caused a decrease in levels of glutamic and glyceric acid and an increase in levels of hexadecanoic and palmitoleic acid.

Recently, Zhan and Desiderio (50) described the remarkable contribution that "omics" sciences, including metabolomics, will play in understanding the heterogeneity of pituitary adenomas (PA). The present review will focus on the contribution that metabolomics analysis techniques might provide to improve the diagnosis of PA, aiming to shed light on some molecular mechanisms underlying their tumor development.

MATERIALS AND METHODS

Search Strategy and Eligibility Criteria

A systematic review of the literature was conducted independently by two of the authors via PubMed, Web of Science Core Collection and Scopus databases until 11th December 2018, using following keywords: *metabolomics pituitary adenoma/tumor*, *metabolomic biomarker pituitary adenoma/tumor*, *metabolomic analysis pituitary adenoma/tumor*, *metabolomic profile pituitary adenoma/tumor*, *metabolites pituitary adenoma, LC-MS pituitary adenoma/tumor*, *GC-MS pituitary adenoma/tumor*, *NMR spectrometry pituitary adenoma/tumor*, *MALDI pituitary adenoma/tumor, deoxycholic acid pituitary adenomas, 4-pyridoxic acid pituitary adenomas, phosphoethanolamine pituitary adenomas, alanine pituitary adenomas, N-acetyl aspartate pituitary adenomas, myo-inositol pituitary adenomas, 3-methyladipate pituitary adenomas, glutamate pituitary adenomas, glutamine pituitary adenomas, taurine pituitary adenomas*. Search keywords included specific metabolites to optimize data selection. The endpoint was to perform an overview of metabolomic aspects relevant to the approach of PA and potentially provide a source of detection and treatment targets for pituitary tumors. Inclusion criteria were represented by (1) studies that have evaluated the metabolomic profile or metabolomic biomarkers associated with PA or the contribution of NMR spectrometry and MS-based techniques in PA, (2) studies written in English, and (3) studies on human subjects. Exclusion criteria included (1) absence of PA group, (2) evaluation of other types of pituitary tumors, (3) studies that provide insufficient data on metabolomics in PA, (4) studies including overlapping groups of patients, (5) studies written in languages other than English, (6) proteomics studies, (7) high molecular weight compounds studies, and (8) reviews. According to the flowchart (**Figure 1**), 1,107 articles were included for analysis by searching electronic databases. Additionally, an article has been added to our research through hand searching (51). Duplicate ($n = 389$) and irrelevant ($n = 692$) articles were excluded. An article was excluded due to insufficient data on metabolomics in PA (52). Three articles studied the same group of patients with PA (53–55), so only the last one (55) was included in our review, the other two being excluded (53, 54). An article was excluded because it was not written in English (56). Two articles were excluded because they provided proteomics data (57, 58) and another article was excluded, evaluating compounds with a molecular weight greater than 1,500 Da (59). A study that evaluated other types of pituitary tumors (60) and a review (61) were also excluded. Finally, 18 studies enrolling 241 patients with PA were eligible for our review (**Table 1**). Of these, 8 articles described *in vivo* MRS approach in PA, providing specific metabolites measurements.

TABLE 1 | Clinical cases of pituitary adenomas (PA) included for metabolomics analysis.

No. of cases	Pituitary adenoma type	No.	Percentage (%)
241 patients	ACTH-secreting pituitary adenoma	26	10.78
	GH-secreting pituitary adenoma	8	3.31
	PRL-secreting pituitary adenoma	36	14.93
	GH and PRL-secreting pituitary adenoma	4	1.65
	FSH-secreting pituitary adenoma	2	0.82
	FSH and LH-secreting pituitary adenoma	8	3.31
	Clinically non-functional pituitary adenoma	28	11.61
	Pituitary adenoma (functional and non-functional)	129	53.52

Study Quality Assessment

Assessment of the quality of included studies was performed using the QUADAS2 tool (62) following four domains: patient selection, index test, reference standard and flow and timing.

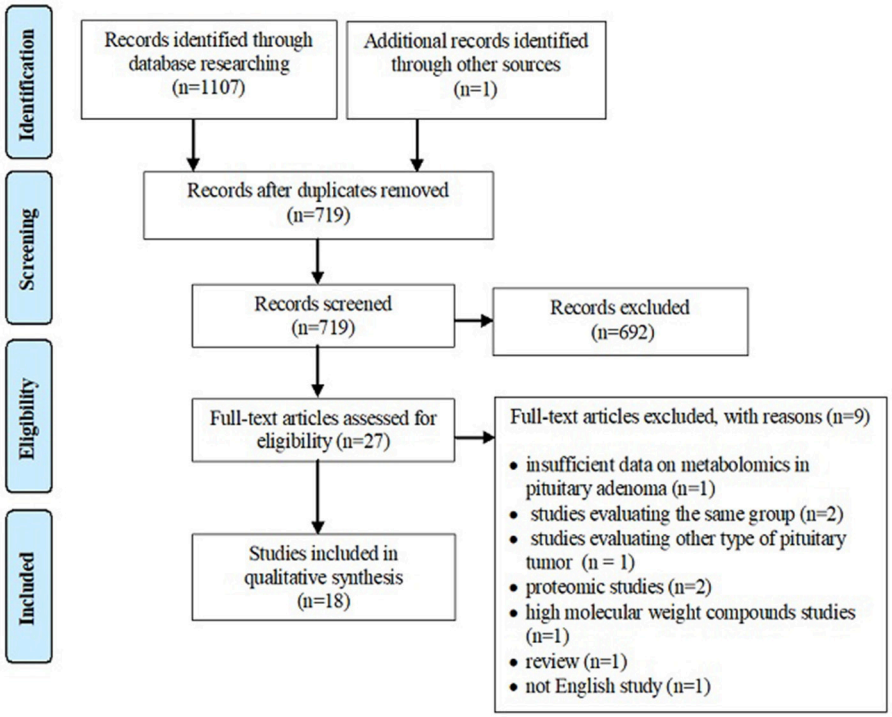

FIGURE 1 | PRISMA style flowchart of the selected studies.

The index test was represented by metabolomic analysis. Histopatological examination was the reference standard for PA diagnosis. We evaluated the risk of bias using all four domains of QUADAS2 tool. We also used the first three domains for the concern regarding applicability.

RESULTS

Metabolomics vs. Immunohistochemistry in Functional PA

Calligaris et al. (63) demonstrated the specific endocrine functionality of both non-pathological pituitary tissue (6 samples) and pituitary tumors (45 samples), using MALDI-MSI. The purpose of this study was to locate functional PA and to identify the delineation between them and healthy pituitary tissue, an aspect of potentially key relevance, especially during surgery, on one hand facilitating total adenoma resection and on the other hand preserving vasopressin secretory cells within the neurohypophysis and pituitary stalk, thus avoiding central diabetes insipidus, the most common postoperative complication. In a first step, using positive-mode MALDI-MS, the metabolic fingerprint of non-pathological pituitary tissue was assessed, to confirm presence of vasopressin and neurophysin 2 in the neurohypophyseal tissue in addition to GH, α-melanocytic stimulation hormone (MSH), adrenocorticotrophic hormone (ACTH), β-endorphin, joining peptide, γ-lipotrophin (LPH), and β-LPH in the anterior pituitary (**Table 2**). Afterwards, using matrix sublimation/recrystallization, prolactin (PRL) was identified in the lactotrophic area of the anterior lobe, in addition to detection of neurophysin 1 in the posterior pituitary. The distribution of these metabolites, reported by this study, highly corresponds to the immunohistochemical distribution of hormones within the pituitary gland (79).

GH, ACTH and neurophysin 2 were identified by Mascot searches. In addition, secretion of these peptides was confirmed by MALDI in-source decay (ISD) fragmentation, by identification of c-series ion fragments of GH (c13), ACTH (c10) and neurophysin 2 (c16) in the anterior and posterior pituitary gland. Moreover, the identification of b- and y-series ions of vasopressin was possible using MALDI time-of-flight/time-of-flight mass spectrometry (MALDI TOF/TOF).

In his study, Calligaris et al. (63) included ACTH- (n = 6), GH- (n = 7), PRL- (n = 6), GH- and PRL- (n = 4), FSH- (n = 2), FSH- and LH-secreting PA (n = 5) and clinically non-functional PA (n = 15). In the majority of cases, metabolomics analysis confirmed hormonal hypersecretion within pituitary tumor cells in agreement to clinical and biochemical suspicion. Metabolomics data correlated with histopathological findings, including haematoxylin-eosin and reticulin staining, respectively. Therefore, identification of intact GH and the c13 ion fragment, corroborated with a disruption of reticulin fiber network diagnosed GH-secreting PA. In the same manner, identification of intact ACTH and the c10 ion fragment, corroborated with a disruption of reticulin fiber network diagnosed ACTH-secreting PA.

TABLE 2 | Metabolomic aspects in pituitary adenomas (PA).

No.	Reference	Biological sample	Analytical Technique	Results
1.	Calligaris et al. (63)	45 PA vs. 6 healthy pituitary glands	MALDI-MSI	**Non-pathological pituitary tissue** ► presence of vasopressin, neurophysin 2 and neurophysin 1 in the neurohypophysis ► identification of GH, α-MSH, ACTH, β-endorphin, joining peptide, γ-LPH, β-LPH and PRL in the anterior lobe ► identification of b- and y-series ions of vasopressin and c-series ion fragments of GH (c13), ACTH (c10) and neurophysin 2 (c16) in the posterior and anterior pituitary gland, respectively **Pituitary adenomas** ► elevated levels of GH, PRL and ACTH have been identified within GH-secreting PA, PRL-secreting PA and ACTH-secreting PA, respectively ► identification of the demarcation between PA and healthy pituitary tissue
2.	Oklu et al. (64)	16 central blood samples (plasma) from 7 patients with ACTH-secreting PA, who underwent bilateral IPSS vs. 9 control samples	LC-MS/MS	**Metabolites:** ► deoxycholic acid, 3-methyladipate, pyridoxate **Pathways:** ► alanine, aspartate and glutamate metabolism (the most affected), ► vitamin B metabolism, ► lysine biosynthesis, ► purine metabolism, ► amino sugar and nucleotide sugar metabolism, ► glycolysis and gluconeogenesis, ► aminoacetyl-tRNA biosynthesis, ► starch and sucrose metabolism
3.	Feng et al. (65)	brain tissue samples from 6 PA with ACTH-secreting PA vs. 7 healthy brain samples	GC-MS	**Metabolites:** up-regulation of short chain fatty acids (heptanoic acid, octanoic acid, nonanoic acid, hexanoic acid and capric acid), down-regulation of glucose-6-phosphate **Pathways:** ► fatty acids metabolism, ► glycolysis/gluconeogenesis
4.	Ijare et al. (51)	post-surgery tumor tissue samples from 3 gonadotropin-secreting PA and 3 PRL-secreting PA	NMR spectrometry	**Metabolites:** ► phosphoethanolamine, glutamate, glutamine, N-acetyl aspartate, aspartate and myo-inositol - significantly altered in both types of adenomas ► down regulation of phosphoethanolamine, N-acetyl aspartate and myo-inositol and up regulation of aspartate, glutamate and glutamine in PRL-secreting PA compared to gonadotropin-secreting PA
5.	Lee et al. (66)	urine samples from 27 PRL-secreting PA *vs*. 31 healthy group	GC-MS	**Metabolites:** up regulation of estrogen metabolites and 17-ketosteroids, high level of c5 beta/5 alpha-hydrogensteroids and delta 5/delta 4-steroids ratio
6.	Kinoshita et al. (55)	2 surgically excised samples of PA vs. 4 non-tumorous brain samples	^{1}H-MRS	**Metabolites:** up regulation of phosphoethanolamine, taurine and alanine
7.	Jarmusch et al. (67)	brain tissue sample from 14 PA *vs*. normal brain parenchyma and other brain tumors (gliomas, meningiomas)	DESI-MS	**Metabolites:** lipids
8.	Bicíková et al. (68)	brain tissue sample from 25 patients with PA vs. meningioma, glioma and glioblastoma	GC/FID	**Metabolites**: up-regulation of homocysteine and methionine
9.	Usenius et al. (69)	brain tissue sample from 6 PA vs. normal brain tissue	^{1}H-MRS	**Metabolites:** down-regulation of N-acetyl aspartate and creatine and up regulation of choline-containing compounds
10.	Solivera et al. (70)	brain tissue sample from 3 PA vs. 3 health brain tissue	^{31}P-MRS	**Metabolites:** up regulation of phosphatidylinositol and phosphatidylcholine, down regulation of phosphatidylserine and sphingomyelin

(Continued)

TABLE 2 | Continued

No.	Reference	Biological sample	Analytical Technique	Results
11.	Einstein et al. (71)	brain MRI sequences from 28 PA	^{1}H-MRS	**Metabolites:** down-regulation of N-acetyl aspartate and creatine and up regulation of choline-containing compounds
12.	Chernov et al. (72)	brain MRI sequences from 19 PA	^{1}H-MRS	**Metabolites:** down-regulation of N-acetyl aspartate and creatine and up regulation of choline-containing compounds
13.	Faghih Jouibari et al. (73)	brain MRI sequences from 10 non-functional PA	^{1}H-MRS	**Metabolites:** up regulation of choline
14.	Isobe et al. (74)	brain MRI sequence from 5 PA vs. 7 healthy volunteers	^{1}H-MRS	**Metabolites:** up regulation of choline, lack of N-acetyl aspartate and total creatine
15.	Sutton et al. (75)	brain MRI sequences from 3 non-functional PA *vs*. 17 healthy individuals	^{1}H-MRS	**Metabolites:** up regulation of choline
16.	Stadlbauer et al. (76)	MRI sequences from 27 functional and non-functional PA	^{1}H-MRS	**Metabolites:** up regulation of choline
17.	Kozić et al. (77)	brain MRI sequences from 1 GH-secreting PA	^{1}H-MRS	**Metabolites:** up regulation of choline
18.	Khiat et al. (78)	brain MRI sequences from 7 ACTH-secreting PA vs. 40 healthy individuals	^{1}H-MRS	**Metabolites:** down regulation of choline

PA, pituitary adenoma; MALDI-MSI, matrix-assisted laser desorption/ionization mass spectrometry imaging; LC-MS/MS, liquid chromatography tandem mass spectrometry; GC-MS, gas chromatography-mass spectrometry; ^{1}H-MRS, proton magnetic resonance spectroscopy; NMR, nuclear magnetic resonance; DESI-MS, desorption electrospray ionization-mass spectrometry; GC/FID, gas chromatography with flame ionization detection; ^{31}P-MRS, ^{31}P-magnetic resonance spectroscopy.

Besides the ability to confirm pituitary hypersecretion, MALDI-MSI seems to be a good approach in differentiating pituitary tumor tissue from intact pituitary tissue with an overall specificity (Sp) of 93% and a sensitivity (Se) of 83%. To be emphasized, sensitivity was highly variable among various types of PA, reaching 100% in ACTH-secreting PA but only 50% in prolactinomas and 82% in GH-secreting PA. On the contrary, specificity was high, irrespective of the type of PA (i.e., 93% in ACTH-secreting PA and 100% in PRL- and GH-secreting PA, respectively).

Metabolomic Pathways in ACTH-Secreting PA

In a metabolomics research, Oklu et al. (64) evaluated 8 patients with suspicion of Cushing's disease in whom clinical features of hypercorticism were present (i.e., weight gain, hypertension, osteoporosis, easy bruising, moon face, fatigue, diabetes mellitus, and hirsutism), nonetheless with indeterminate pituitary imaging.

To confirm diagnosis, all patients underwent bilateral inferior petrosal sinus sampling (IPSS). ACTH-secreting PA was confirmed in 7 patients, while in one patient the diagnosis was excluded. The metabolic profile was determined in plasma samples from the ipsilateral IPS of patients (7 samples) and compared to contralateral samples plus two samples from the patient in whom ACTH hypersecretion failed to be confirmed (9 samples).

Postoperative follow-up showed improvement of symptomatology in 4 patients and disease remission in the remaining three.

Using LC-MS/MS, 12 distinct metabolites were reported in patients with ACTH-secreting PA in comparison to the control group, specifically 2-hydroxybutyric acid, aminoadipic acid, L-aspartic acid, 3-hydroxyphenylacetic acid, hypoxanthine, 4-pyridoxic acid, quinolinic acid, sucrose, xanthine, glucose 6-phosphate, deoxycholic acid, and 3-methyladipate. After Bonferroni adjustment, however, only deoxycholic and 4-pyridoxic acids and 3-methyladipate remained statistically significant (**Table 2**).

Using Kyoto Encyclopedia of Genes and Genomes (KEGG) pathway database, 8 main pathways affected in Cushing's disease were identified (64) that involved: (1) Alanine, aspartate and glutamate metabolism, which appeared to be the most affected metabolic pathway, (2) Vitamin B metabolism, (3) Lysine biosynthesis, (4) Purine metabolism, (5) Amino sugar and nucleotide sugar metabolic pathways, (6) Glycolysis and gluconeogenesis pathways, (7) Aminoacetyl-tRNA biosynthesis, and (8) Starch and sucrose metabolism (**Table 2**).

Recently, Feng et al. (65) conducted a metabolomic (via GC-MS) and proteomic study in a group of patients with ACTH-secreting PA. For metabolomic analysis, the author included brain tumor samples from 6 patients with ACTH-secreting PA vs. healthy brain tissue from 7 control subjects. It was found that short chain fatty acids (heptanoic acid, octanoic acid, nonanoic acid, hexanoic acid and capric acid) were up regulated, while glucose-6-phosphate was down regulated. Thus the metabolomic pathways involved in PA were the metabolism of fatty acids and glycolysis/gluconeogenesis (**Table 2**).

Metabolomics Studies in Gonadotropin- and PRL-Secreting PA

In 2017, Ijare et al. (51) used *ex vivo* NMR spectrometry to assess the metabolomic profile of postoperative pituitary

tissue sampled from patients with gonadotropin- and PRL-secreting PA, respectively, with the main finding that both types of PA contain central nervous system metabolites such as phosphoethanolamine, glutamate, glutamine, N-acetyl aspartate, aspartate, and myo-inositol.

When comparing these two types of PA, it was found that phosphoethanolamine, N-acetyl aspartate and myo-inositol are down regulated in prolactinoma, whereas aspartate, glutamate and glutamine are up regulated (**Table 2**). Ijare's study is currently underway, so a larger number of patients could provide additional insights into the evaluation of the metabolomic fingerprint in these types of pituitary tumors. However, a true control group was apparently not considered, a major limitation of this study.

Lee et al. (66) conducted a study of 26 women with PRL-secreting PA compared to 31 healthy controls, analyzing their urine using GC-MS. A high level of all estrogen metabolites and 17-ketosteroids in the urine of these patients was shown. In addition, high c5 beta/5 alpha-hydrogensteroids and delta 5/delta 4-steroids ratios were identified (**Table 2**).

Metabolites of PA Compared to Other Brain Tumors

In 2015, Jarmusch et al. (67) performed a study of 58 brain tumors, including 14 patients with PA, the rest of the tumors being gliomas, astrocytomas and meningiomas. Analyzing brain tissue samples through desorption electrospray ionization (DESI)-MS, the author identified lipid peaks, which allow differentiation of PA from normal brain parenchyma and other brain tumors (gliomas, meningioma), respectively (**Table 2**). Moreover, the discriminant model of brain tumors using DESI-MS shows an overall Sp of 99.7% and Se of 99.4%. The metabolomic profile was explicitly described in the case of gliomas, indicating a decrease in N-acetyl aspartate and 2-hydroxyglutaric acid, while this was not very well achieved in PA.

Bicíková et al. (68) analyzed tumoral brain tissue samples from 25 patients with PA within a series of brain tumors, using GC with flame ionization detection (GC/FID). Patients with PA presented a marked increase in homocysteine. Homocysteine was also increased in patients with glioblastoma. At the opposite pole, meningiomas and gliomas were characterized by low level of homocysteine. Likewise, PA were characterized by an increased level of methionine, while gliomas exhibited low levels of this amino acid (**Table 2**).

A large body of evidence resulted from MRS-based studies (55, 69, 70) to show alterations of phospholipid metabolism in PA tumor samples as evidenced by high levels of phosphoetanolamine (55), phosphatidylcholine (69, 70) and phosphatidylinositol (70) concentrations (**Table 2**). The pattern is not specific, as phosphoetanolamine and choline-containing compounds were abundantly present in meningioma (55), medulloblastoma (80), glioblastoma (81) and malignant lymphoma tumor samples (70). Cerebral metastases from hepatocellular carcinoma presented high concentrations of choline-containing compounds, while craniopharyngiomas showed decreased levels of these (55). Elevated alanine but low N-acetyl-aspartate concentrations were reported in PA, nonetheless, a similar pattern was apparent in meningioma and gliomas (55, 69). Additionally, a high level of taurine was observed in PA, medulloblastoma and cerebral metastases with kidney starting point (55, 80) (**Table 2**). Ependymoma presented an increased level of myo-inositol, whereas pilocytic astrocytoma exhibited increased levels of fatty acids (80).

An increased concentration of glycine was linked to neuroectodermal tumors (81), while neurinomas, glioblastomas (55) and ependymomas (80) showed a high peak of myo-inositol.

PA Metabolites by *in vivo* Proton MRS

A series of studies performed single vortex proton (^{1}H)-MRS on patients with various suprasellar tumors that included cases of PA. Across 3 studies including a total of 57 patients with both functional (29/57) and non-functional (28/57) PA, markedly decreased N-acetyl aspartate levels were demonstrated by single vortex ^{1}H MRS, in addition to absent or low levels of creatine and moderately elevated levels of choline-containing compounds (71–73) (**Table 2**). Moreover, in up to 50% of cases, including 2 cases of pituitary apoplexy, the concentration of N-acetyl aspartate remained unidentified. No significant differences between the two types of PA were observed (71, 72). Nonetheless, a similar metabolomic pattern was found in suprasellar gliomas and chordomas while craniopharyngiomas presented low levels of all evaluated metabolites (71, 72). Further, it was found that in diagnosis of suprasellar tumors the overall efficacy of proton MRS in association with MRI (87%) was greater than MRI alone (69.6%), but this difference was not statistically significant (73). Referring to other types of suprasellar tumors, the authors reported low levels of N-acetyl aspartate and creatine and high levels of choline-containing compounds in the case of gliomas. Chordomas showed low levels of N-acetyl aspartate and creatine, but high levels of lipids and choline-containing compounds. Craniopharyngiomas showed low levels of all evaluated metabolites (71, 72).

Likewise, in a series of brain tumors from 57 patients, including 5 PA vs. 7 healthy volunteers, Isobe et al. (74) identified an increased peak of choline and a lack of N-acetyl aspartate and total creatine. The choline peak was confirmed in a small series of 3 children with non-functional PA (75) (**Table 2**).

Stadlbauer et al. (76) evaluated 27/37 patients with large functional and non-functional PA and a volume $\geq$4 cm^3. Of the 27, 11 PA presented hemorrhagic areas, while 16 were non-hemorrhagic. Non-hemorrhagic PA group revealed a peak of choline (**Table 2**). The concentration of this metabolite was strongly correlated with the MIB-1 index on the immunohistochemical examination of these 16 patients.

Kozić et al. (77) described the case of a 41-year-old patient with an ectopic 53/40 mm pituitary macroadenoma. Preoperatively, the patient was examined using *in vivo* single vortex ^{1}H-MRS, and a high peak of choline was noticed (**Table 2**). Due to disease persistence, after surgery the patient required treatment with somatostatin analogs (lanreotide 120 mg/4 weeks). Approximately 1 year later marked adenoma

shrinkage and the lack of choline peak in the tumor were demonstrated along with a favorable clinical outcome.

Khiat et al. (78) evaluated a series of 13 patients including 7 patients with ACTH-secreting PA and 6 patients with ACTH-independent Cushing's syndrome vs. 40 healthy individuals. The objective of the study was the characterization of cerebral metabolites in the thalamic, temporal and frontal region by analyzing the brain MRI sequences. Irrespective of the etiology of Cushing's syndrome, choline/creatine ratio showed a marked decrease in the thalamus and frontal area (**Table 2**).

Quality Assessment of Studies

The risk of bias and the concern regarding applicability in included studies is illustrated in **Figures 2**, **3**. Patient selection in studies was low in 16.66% of cases. Regarding the index test, 88.88% of studies accurately described the metabolomic analysis. The reference standard for PA diagnosis was histopatological examination that was described in 66.66% of cases. The flow of patients through the study and timing of reference standard and the index test were low in 27.77% of cases.

DISCUSSION

The approach of metabolomics techniques in neuroendocrinology and neurosurgery has grown in recent years, providing additional information to genomics and proteomics. As from the metabolomic perspective, glioblastoma, the most common and severe type of brain cancer in adults (82), has begun to be studied years ago when elevated concentration of phosphocholine was reported and found to be even higher in primary glioblastoma compared to recurrent disease (81). Recently, MALDI-MSI has been successfully implemented in differentiation of brain tumor vs. healthy brain tissue on a murine model of high-grade glioblastoma (83).

Metabolomic analysis has already proven its potential with regard to brain tumors, as in the classification of both meningioma and astrocytoma, depending on their aggressiveness. High-grade meningioma presents decreased levels of alanine and creatine in comparison to low-grade meningioma (84). Also, N-acetyl aspartate, myo-inositol, lactate, creatine and glycine show statistically significant differences depending on tumor aggression in astrocytoma (85).

The present review, conducted in a systematic manner, identified a series of metabolites to be altered in PA as illustrated in **Figure 4**.

Summarizing data, we observed that N-acetyl aspartate, choline-containing compounds and creatine were main metabolites highly effective in differentiating PA from healthy tissue. The most obvious pattern consisted of decreased N-acetyl aspartate and creatine and increased choline-containing compounds levels.

N-acetyl aspartate is a derivative of aspartic acid abundantly found in the human brain. Except for Canavan disease, a genetic disorder characterized by toxic accumulation of N-acetyl aspartate caused by aspartoacylase inactivation (86), down regulation of this metabolite seems to be constant in

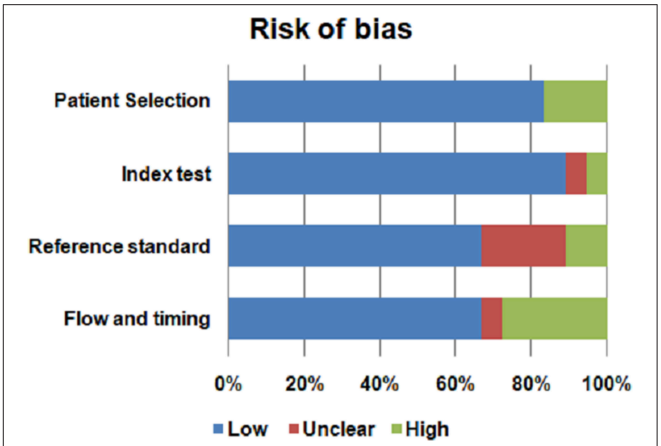

FIGURE 2 | Risk of bias of the included studies.

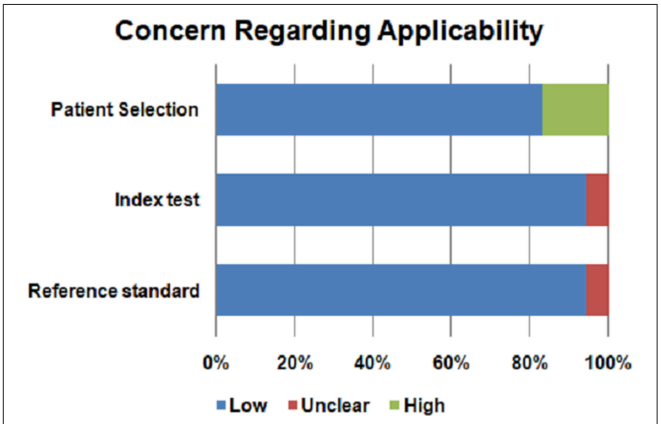

FIGURE 3 | Concern regarding applicability of the included studies.

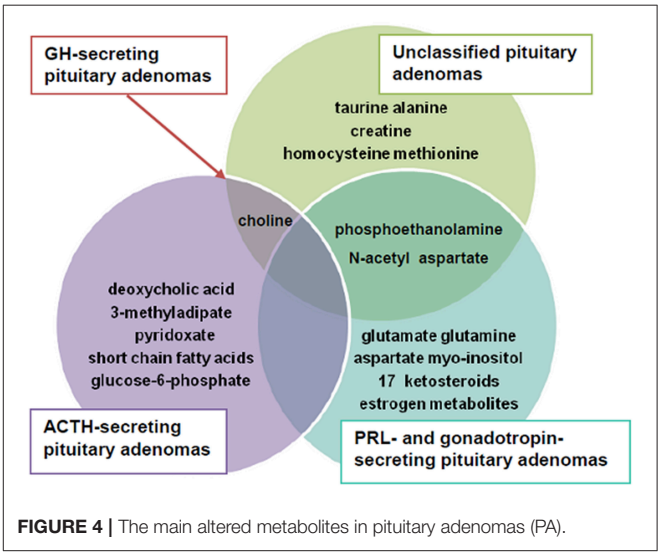

FIGURE 4 | The main altered metabolites in pituitary adenomas (PA).

clinical conditions that associate neuronal dysfunction, including epilepsy (87–89), multiple sclerosis (90), Alzheimer's disease (91, 92), schizophrenia (93, 94), stroke (95), brain injury (96, 97) and brain tumors (98, 99).

Choline-containing compounds (choline, phosphatidylcholine etc.) are involved in the synthesis and degradation of the cell membrane. Thus, a high concentration of these compounds is suggestive of accelerated cell membrane turnover in PA (100). In addition, the high level of choline correlates with tumor proliferation (71). Decreased creatine availability may suggest a disruption of energy metabolism in PA, given that this metabolite plays an important role in the ATP/ADP cycle (71).

Phosphoethanolamine, which appeared to be the key metabolite found in pituitary tumor tissue vs. non-tumoral pituitaries, is a precursor of phosphatidylcholine and phosphatidylethanolamine, both of which are components of cell membranes. It seems that phosphoethanolamine down regulation is involved in tumor genesis, given that pharmacologic administration of phosphoethanolamine suppressed tumor growth both *in vivo* and *in vitro* studies performed in mice bearing melanoma (101). In line with that, Ferreira et al. (102) reported that synthetic phosphoethanolamine reduces tumor growth and has an inhibitory action on clonal metastases in an acute promyelocytic leukemia model.

Another observation of our review included the alteration of myo-inositol, aspartate, glutamate and glutamine in gonadotropin- and PRL-secreting PA. More than that, phosphoethanolamine, myo-inositol and N-acetyl aspartate were down regulated in prolactinoma, whereas aspartate, glutamate and glutamine were up regulated.

Myo-inositol, a component of many phospholipids that is found in considerable amounts in the brain functions as a second messenger in multiple intracellular signaling pathways. The low concentration of myo-inositol is linked to an imbalance in osmolyte function of malignant cells (103, 104). Myo-inositol is responsible for cell cycle control, apoptosis, inhibition of the PI3K/Akt pathway and NF-kB activity (105). Moreover, it exerts antioxidant, anti-inflammatory and anti-tumoral effects, through insulin modulation (104). Its potential role has been described in breast and colon cancer (106, 107). Accordingly, Kesler et al. (106) reported an increased level of prefrontal myo-inositol in a group of 19 breast cancer survivors after chemotherapy. Moreover, Derbal-Wolfrom et al. (107) postulated that myo-inositol trispyrophosphate treatment increased the oxygen load to result in inhibition of colon tumor growth and stimulation of homeobox gene Cdx2 expression within the intestinal wall.

As in the research conducted by Oklu et al. (64), Ijare et al. (51) also identified that the aspartate and glutamate metabolism is affected in PRL-secreting PA. Glutamine is another abundant free amino acid with roles in protein synthesis. Thus, it plays important roles in the growth of normal and cancerous cells and many studies have demonstrated these cells are dependent on glutamine concentration (108, 109), while glutamine deprivation on cell cultures is associated with malignant cells death (110, 111). The down regulation of this metabolite, which is particularly emphasized in PRL-secreting PA, seems to be involved in tumor genesis. At the opposite pole, the up-regulation of phosphoethanolamine in unclassified PA may suggest an activation of phosphatidylethanolamine metabolism, which is involved in membrane shape changes in tumor cells (55).

Alterations of the amino acids metabolism in PA, especially involving alanine, glutamate and aspartate represents another feature that deserves to be taken into account. Alanine, a non-essential amino acid, is an end product of glutamate oxidation, which is a major source of respiratory energy in the tumor cell. In addition, alanine exerts proliferative effects on malignant cells (112, 113).

A similar effect is attributed to glutamate (114); its actions are mediated through two main receptors predominantly expressed in the brain: ionotropic glutamate receptors (iGluRs) and metabotropic glutamate receptors (mGluRs) (114). Recent studies have described these receptors in peripheral organs and implicitly in a wide range of cancers such as lung, thyroid, digestive tract, breast and ovarian cancer (115–120).

Aspartate is a metabolite of the urea cycle, involved in gluconeogenesis, being derived from asparaginase. The concentration of this metabolite is decreased in malignant cells, being synthesized from oxaloacetate by aminotransferase activity (121). In 2015, Xie et al. (122) noticed a decreased level of aspartate in the plasma of 35 patients with breast cancer. In addition, Dornfeld et al. (123) demonstrated improved cell mitochondrial function and reduction of doxorubicin toxicity in breast cancer samples.

Up-regulation of homocysteine in PA may be responsible for citotoxicity (68) and oxidative stress. Increased levels of homocysteine have also been reported in anxiety disorders, Alzheimer's disease, dementia, breast cancer and thyropathies (68). Moreover, the alteration of methionine metabolism leads to neurological dysfunction (68).

The identification of estrogen metabolites and 17-ketosteroids in the urine of patients with PRL-secreting adenomas is most likely to be due to decreased activity of 3 beta-hydroxysteroid dehydrogenase and 5α-reductase that occurs among these patients (66).

Another important finding is the identification of deoxycholic acid, 4-pyridoxic acid, 3-methyladipate, short chain fatty acids and glucose-6-phosphate as potential metabolomic biomarkers in patients with Cushing's disease (64, 65).

Deoxycholic acid is a bile acid that acts as a fat emulsifier, improving intestinal absorption. Moreover, it induces deoxyribonucleic acid (DNA) damage by increasing intracellular production of oxidative stress (124, 125). Up to now, increased levels of deoxycholic acid have been demonstrated in digestive (126, 127) and breast cancers (128), but its involvement in the appearance of pituitary tumors has not yet been documented.

4-pyridoxic acid is a urinary catabolite of vitamin B6, being a biomarker of vitamin B6 status. Thus, deficiency of 4-pyridoxic acid is correlated with a deficiency in vitamin B6 that has been shown to be involved in tumor development and its progression by following mechanisms: cell cycle alteration, angiogenesis, chromosomal instability, inflammation and increased oxidative stress (129–131).

13-methyladipate is a catabolic product of phytanic acid, being a saturated fatty acid obtained by eating dairy products and ruminant meat. Recent studies have shown that the intake of phytanic acid is associated with an enhanced risk of non-Hodgkin lymphoma (132) and prostate cancer (133, 134).

Metabolic pathway analysis has shown that amino acid metabolism is the most altered one among patients with Cushing's disease. The same aspect has been highlighted in other endocrine tumors, such as thyroid cancer, where an elevated concentration of methionine, glutamine, glycine, tyrosine and taurine was reported (39, 103, 104, 135–139). This high level of amino acids is linked to cell proliferation and energy substrate. The main sources of amino acids are represented by the combination between the increase of protein catabolism, *de novo* amino acids synthesis and augmented extracellular matrix degradation (140–142). On the other hand, by using ^{1}H-NMR, a down-regulation of leucine, lysine, valine, serine, alanine and tyrosine was observed in plasma and serum of patients with thyroid cancer (138, 139). Also, alterations in amino acid metabolism have been observed in ovarian (143), breast (144) and prostate cancer (145)

Another important aspect was the involvement of short chain fatty acids metabolism in the pathogenesis of ACTH-secreting PA. This dysregulation is likely correlated with the increased cell turnover and lipids demand in membrane biosynthesis needed for cell proliferation (146).

Likewise, the decreased level of glucose-6-phosphate, which is a glycolic metabolite, along with pyruvate, represents a first step in demonstrating the involvement of glycolysis/gluconeogenesis pathway in ACTH-secreting PA.

The contribution of MALDI-MSI technique in the diagnosis of functional PA appears to be a major one, due to its high sensitivity and specificity in identifying pituitary hormones and fragments in addition to the possibility of delineating pituitary tumor tissue, making this method the most pertinent metabolomic assessment to be employed in the investigation of pituitary tumors.

The present review shows several limitations. Although conducted in a systematic fashion, only few articles could be included. Further, the limited number of patients/samples included in studies, the different types of biological samples analyzed (plasma, post-surgical tumor tissue, urine), differences in analytical techniques and a lack of homogeneity of PA may explain the heterogeneous results. Sensitivity and specificity of the metabolomic techniques was described in few studies. Moreover, the use of single voxel ^{1}H-MRS in some studies was able to identify only a limited number of metabolites by analyzing the brain MRI sequences. Furthermore, the sensitivity of these methods in the detection of PA needs to be considerably improved, perhaps the best approach in the future would imply the combination of NMR and MS-based techniques, the implementation of MALDI-MSI on an increased group of patients or the combination of MALDI-MSI with CT, MRI or PET imaging.

Future Perspectives

Although an emerging science, metabolomics has a huge potential compared to genomics, transcriptomics or proteomics, given its ability to characterize the molecular phenotype (147). This aspect makes it possible to significantly improve clinical approach to pituitary disorders in a personalized manner, for example in the diagnosis of MRI negative ACTH-secreting PA or gonadotropin-secreting PA. Likewise, identification of new metabolomic biomarkers in GH-secreting PA would considerably alleviate the prognosis of acromegaly and, potentially, predict therapeutic response. Characterization of specific metabolic pathways underlying PA including their functional alteration would bring new data into understanding their pathogenesis, thus making it possible to identify new therapeutic targets.

Metabolomics seems to be a promising tool in the future in neurosurgery, given that LC/MS and nanostructure imaging mass spectrometry (NIMS) have been able to identify brain region mapping on the animal model (148) and that first steps toward clinical application of MALDI MSI were initiated (63). Nonetheless, further studies are warranted to confirm preliminary results and deepen knowledge in the field.

CONCLUSION

Implementation of ultra high performance metabolomics analysis techniques in the study of PA will significantly improve diagnosis and, potentially, the therapeutic approach, by identifying highly specific disease biomarkers in addition to novel molecular pathogenic mechanisms. Ultra high mass resolution MALDI-MSI emerges as a helpful clinical tool in the neurosurgical treatment of pituitary tumors. Therefore, metabolomics appears to be a science with a promising prospect in the sphere of PA, and a starting point in pituitary care.

AUTHOR CONTRIBUTIONS

OP collected data, drafted the manuscript and wrote the review. BG contributed to the data collection. CG conceived the study design and wrote the review.

FUNDING

This work was supported by Iuliu Hatieganu University of Medicine and Pharmacy Cluj-Napoca, Romania, Ph.D. research grant no. 1300/50/13.01.2017.

REFERENCES

1. Xiao JF, Zhou B, Ressom HW. Metabolite identification and quantitation in LC-MS/MS-based metabolomics. *Trends Analyt Chem.* (2012) 32:1–14. doi: 10.1016/j.trac.2011.08.009
2. Zhang T, Wu X, Ke C, Yin M, Li Z, Fan L, et al. Identification of potential biomarkers for ovarian cancer by urinary metabolomic

profiling. *J Proteome Res.* (2003) 12:505–12. doi: 10.1021/pr3009572
3. Chen J, Zhou L, Zhang X, Lu X, Cao R, Xu CJ, et al. Urinary hydrophilic and hydrophobic metabolic profiling based on liquid chromatography–mass spectrometry methods: differential metabolite discovery specific to ovarian cancer. *Electrophoresis* (2012) 33:3361–9. doi: 10.1002/elps.201200140
4. Hampel D, York ER, Allen LH. Ultra-performance liquid chromatography tandem mass-spectrometry (UPLC–MS/MS) for the rapid, simultaneous analysis of thiamin, riboflavin, flavin adenine dinucleotide, nicotinamide and pyridoxal in human milk. *J Chromatogr B Analyt Technol Biomed Life Sci.* (2012) 903:7–13. doi: 10.1016/j.jchromb.2012.06.024
5. De Brouwer V, Storozhenko S, Stove CP, Van Daele J, Van der Straeten D, Lambert WE. Ultra-performance liquid chromatography-tandem mass spectrometry (UPLC-MS/MS) for the sensitive determination of folates in rice. *J Chromatogr B Analyt Technol Biomed Life Sci.* (2010) 878:509–13. doi: 10.1016/j.jchromb.2009.12.032
6. Zhang L, Shen H, Xu J, Xu JD, Li ZL, Wu J, et al. UPLC-QTOF-MS/MS-guided isolation and purification of sulfur-containing derivatives from sulfur-fumigated edible herbs, a case study on ginseng. *Food Chem.* (2018) 246:202–10. doi: 10.1016/j.foodchem.2017.10.151
7. Ibáñez M, Borova V, Boix C, Aalizadeh R, Bade R, Thomaidis NS, et al. UHPLC-QTOF MS screening of pharmaceuticals and their metabolites in treated wastewater samples from Athens. *J Hazard Mater.* (2017) 323(Pt A):26–35. doi: 10.1016/j.jhazmat.2016.03.078
8. Zhang W, Hankemeier T, Ramautar R. Next-generation capillary electrophoresis–mass spectrometry approaches in metabolomics. *Curr Opin Biotechnol.* (2017) 43:1–7.doi: 10.1016/j.copbio.2016.07.002
9. Mischak H, Coon JJ, Novak J, Weissinger EM, Schanstra JP, Dominicza AF. Capillary electrophoresis–mass spectrometry as a powerful tool in biomarker discovery and clinical diagnosis: an update of recent developments. *Mass Spectrom Rev.* (2009) 28:703–24. doi: 10.1002/mas.20205
10. Fujimura Y, Miura D. MALDI mass spectrometry imaging for visualizing *in situ* metabolism of endogenous metabolites and dietary phytochemicals. *Metabolites* (2014) 4:319–46. doi: 10.3390/metabo4020319
11. Miura D, Fujimura Y, Wariishi H. *In situ* metabolomic mass spectrometry imaging: Recent advances and difficulties. *J Proteomics* (2012) 75:5052–60. doi: 10.1016/j.jprot.2012.02.011
12. Aretz I, Meierhofer D. Advantages and pitfalls of mass spectrometry based metabolome profiling in systems biology. *Int J Mol Sci.* (2016) 17:632. doi: 10.3390/ijms17050632
13. Lei Z, Huhman DV, Sumner LW. Mass spectrometry strategies in metabolomics. *J Biol Chem.* (2011) 286:25435–42. doi: 10.1074/jbc.R111.238691
14. Gowda GA, Djukovic D. Overview of mass spectrometry-based metabolomics: opportunities and challenges. *Methods Mol Biol.* (2014) 1198:3–12. doi: 10.1007/978-1-4939-1258-2_1
15. Emwas AH. The strengths and weaknesses of NMR spectroscopy and mass spectrometry with particular focus on metabolomics research. *Methods Mol Biol.* (2015) 1277:161–93. doi: 10.1007/978-1-4939-2377-9_13
16. Markley JL, Brüschweiler R, Edison AS, Eghbalnia HR, Powers R, Raftery D, et al. The future of NMR-based metabolomics. *Curr Opin Biotechnol* (2017) 43:34–40. doi: 10.1016/j.copbio.2016.08.001
17. van der Graaf M. *In vivo* magnetic resonance spectroscopy: basic methodology and clinical applications. *Eur Biophys J.* (2010) 39:527–40. doi: 10.1007/s00249-009-0517-y
18. Quadrelli S, Mountford C, Ramadan S. Hitchhiker's guide to voxel segmentation for partial volume correction of in vivo magnetic resonance spectroscopy. *Magn Reson Insights* (2016) 27:1–8. doi: 10.4137/MRI.S32903
19. Walch A, Rauser S, Deininger SO, Höfler H. MALDI imaging mass spectrometry for direct tissue analysis: a new frontier for molecular histology. *Histochem Cell Biol.* (2008) 130:421–34. doi: 10.1007/s00418-008-0469-9
20. Murphy RC, Hankin JA, Barkley RM. Imaging of lipid species by MALDI mass spectrometry. *J Lipid Res.* (2009) 50:S317–22. doi: 10.1194/jlr.R800051-JLR200
21. DeKeyser SS, Kutz-Naber KK, Schmidt JJ, Barrett-Wilt GA, Li L. Mass spectral imaging of neuropeptides in decapod crustacean neronal tissues. *J Proteome Res.* (2007) 6:1782–91. doi: 10.1021/pr060603v
22. Franck J, Arafah K, Elayed M, Bonnel D, Vergara D, Jacquet A, et al. MALDI imaging mass spectrometry: state of the art technology in clinical proteomics. *Mol Cell Proteomics* (2009) 8:2023–33. doi: 10.1074/mcp.R800016-MCP200
23. Nicholson JK, Lindon JC. Systems biology: metabonomics. *Nature* (2008) 455:1054–6. doi: 10.1038/4551054a
24. Want EJ, Nordström A, Morita H, Siuzdak G. From exogenous to endogenous: the inevitable imprint of mass spectrometry in metabolomics. *J Proteome Res.* (2007) 6:45. doi: 10.1021/pr060505
25. Kind T, Wohlgemuth G, Lee DY, Lu Y, Palazoglu M, Shahbaz S, et al. Fiehnlib: mass spectral and retention index libraries for metabolomics based on quadrupole and time-of-flight gas chromatography/mass spectrometry. *Anal Chem.* (2009) 81:10038–48. doi: 10.1021/ac9019522
26. Bingol K, Brüschweiler R. Two elephants in the room: new hybrid nuclear magnetic resonance and mass spectrometry approaches for metabolomics. *Curr Opin Clin Nutr Metab Care* (2015) 18:471–7. doi: 10.1097/MCO.0000000000000206
27. Abu Bakar MH, Sarmidi MR, Cheng KK, Ali Khan A, Suan CL, Zaman Huri H, et al. Metabolomics - the complementary field in systems biology: a review on obesity and type 2 diabetes. *Mol Biosyst.* (2015) 11:1742–74. doi: 10.1039/c5mb00158g
28. Guasch-Ferré M, HrubyA, Toledo E, Clish CB, Martínez-González MA, Salas-Salvadó J, et al. Metabolomics in prediabetes and diabetes: a systematic review and meta-analysis. *Diabetes Care* (2016) 39:833–46. doi: 10.2337/dc15-2251
29. Sas KM, Karnovsky A, Michailidis G, Pennathur S. Metabolomics and diabetes: analytical and computational approaches. *Diabetes* (2015) 64:718–32. doi: 10.2337/db14-0509
30. Liu X, Gao J, Chen J, Wang Z, Shi Q, Man H, et al. Identification of metabolic biomarkers in patients with type 2 diabetic coronary heart diseases based on metabolomic approach. *Sci Rep.* (2016) 6:30785. doi: 10.1038/srep30785
31. Rauschert S, Uhl O, Koletzko B, Hellmuth C. Metabolomic biomarkers for obesity in humans: a short review. *Ann Nutr Metab.* (2014) 64:314–24. doi: 10.1159/000365040
32. Bagheri M, Farzadfar F, Qi L, Yekaninejad MS, Chamari M, Zeleznik OA, et al. Obesity-related metabolomic profiles and discrimination of metabolically unhealthy obesity. *J Proteome Res.* (2018) 17:1452–62. doi: 10.1021/acs.jproteome.7b00802
33. Murri M, Insenser M, Escobar-Morreale HF. Metabolomics in polycystic ovary syndrome. *Clin Chim Acta* (2014) 429:181–8. doi: 10.1016/j.cca.2013.12.018
34. Dong F, Deng D, Chen H, Cheng W, Li Q, Luo R, et al. Serum metabolomics study of polycystic ovary syndrome based on UPLC-QTOF-MS coupled with a pattern recognition approach. *Anal Bioanal Chem.* (2015) 407:4683–95. doi: 10.1007/s00216-015-8670-x
35. Georgescu CE, Moraru I, Ilie I, Vonica C, Pinzariu O, Socaciu C. Metabolomics, a novel approach to polycystic ovary syndrome. *Acta Endo.* (2017) 13(Suppl. 1):9.
36. Zou Y, Zhu FF, Fang CY, Xiong XY, Li HY. Identification of potential biomarkers for urine metabolomics of polycystic ovary syndrome based on gas chromatography-mass spectrometry. *Chin Med J.* (2018) 131:945–9. doi: 10.4103/0366-6999.229899
37. Omabe M, Elom S, Omabe KN. Emerging metabolomics biomarkers of polycystic ovarian syndrome; targeting the master metabolic disrupters for diagnosis and treatment. *Endocr Metab Immune Disord Drug Targets* (2018) 18:221–9. doi: 10.2174/1871530318666180122165415
38. Shang X, Zhong X, Tian X. Metabolomics of papillary thyroid carcinoma tissues: potential biomarkers for diagnosis and promising targets for therapy. *Tumour Biol.* (2016) 37:11163–75. doi: 10.1007/s13277-016-4996-z
39. Li Y, Chen M, Liu C, Xia Y, Xu B, Hu Y, et al. Metabolic changes associated with papillary thyroid carcinoma: a nuclear magnetic resonance-based metabolomics study. *Int J Mol Med.* (2018) 41:3006–14. doi: 10.3892/ijmm.2018.3494
40. Wojakowska A, Chekan M, Widlak P, Pietrowska M. Application of metabolomics in thyroid cancer research. *Int J Endocrinol.* (2015) 2015:1–13. doi: 10.1155/2015/258763
41. Ryoo I, Kwon H, Kim SC, Jung SC, Yeom JA, Shin HS, et al. Metabolomic analysis of percutaneous fine-needle aspiration specimens of thyroid

nodules: potential application for the preoperative diagnosis of thyroid cancer. *Sci Rep.* (2016) 6:30075. doi: 10.1038/srep30075
42. Moayyeri A, Cheung CL, Tan KC, Morris JA, Cerani A, Mohney RP, et al. Metabolomic pathways to osteoporosis in middle-aged women: a genome-metabolome-wide mendelian randomization study. *J Bone Miner Res.* (2018) 33:643–50. doi: 10.1002/jbmr.3358
43. Lv H, Jiang F, Guan D, Lu C, Guo B, Chan C, et al. Metabolomics and its application in the development of discovering biomarkers for osteoporosis research. *Int J Mol Sci.* (2016) 17:2018. doi: 10.3390/ijms17122018
44. Kotłowska A, Puzyn T, Sworczak K, Stepnowski P, Szefer P. Metabolomic biomarkers in urine of cushing's syndrome patients. *Int J Mol Sci.* (2017) 18:294. doi: 10.3390/ijms18020294
45. Eisenhofer G, Masjkur J, Peitzsch M, Di Dalmazi G, Bidlingmaier M, Grüber M, et al. Plasma steroid metabolome profiling for diagnosis and subtyping patients with cushing syndrome. *Clin Chem.* (2018) 64:586–96. doi: 10.1373/clinchem.2017.282582
46. Arlt W, Lang K, Sitch AJ, Dietz AS, Rhayem Y, Bancos I, et al. Steroid metabolome analysis reveals prevalent glucocorticoid excess in primary aldosteronism. *JCI Insight* (2017) 2:93136. doi: 10.1172/jci.insight.93136
47. Lang K, Beuschlein F, Biehl M, Dietz A, Riester A, Hughes BA, et al. Urine steroid metabolomics as a diagnostic tool in primary aldosteronism. *Endocr Abstracts* (2015) 38:OC1.6. doi: 10.1530/endoabs.38.OC1.6
48. Imperiale A, Moussallieh FM, Roche P, Battini S, Cicek AE, Sebag F, et al. Metabolome profiling by HRMAS NMR spectroscopy of pheochromocytomas and paragangliomas detects SDH deficiency: clinical and pathophysiological implications. *Neoplasia* (2015) 17:55–65. doi: 10.1016/j.neo.2014.10.010
49. Höybye C, Wahlström E, Tollet-Egnell P, Norstedt G. Metabolomics: a tool for the diagnosis of GH deficiency and for monitoring GH replacement? *Endocr Connect* (2014) 3:200–6. doi: 10.1530/EC-14-0098
50. Zhan X, Desiderio DM. Editorial: systems biological aspects of pituitary tumors. *Front Endocrinol.* (2016) 7:86. doi: 10.3389/fendo.2016.00086
51. Ijare O, Baskin DS, Pichumani K. Characterization of metabolism of pituitary tumors by NMR spectroscopy. *Neuro-Oncology* (2017) 19(Suppl. 6):145. doi: 10.1093/neuonc/nox168.592
52. Szigety SK, Allen PS, Huyser-wierenga D, Urtasun RC. The effect of radiation on normal human CNS as detected by NMR spectroscopy. *Int J Radiat Oncol Biol Phys.* (1993) 25:695–701 doi: 10.1016/0360-3016(93)90018-Q
53. Kinoshita Y, Yokota A, Koga Y. Phosphorylethanolamine content of human brain tumors. *Neurol Med Chir.* (1994) 34:803–652. doi: 10.2176/nmc.34.803
54. Kinoshita Y, Kajiwara H, Yokota A, Koga Y. Proton magnetic resonance spectroscopy of brain tumors: an *in vitro* study. *Neurosurgery* (1994) 35:606–13 doi: 10.1227/00006123-199410000-00005
55. Kinoshita Y, Yokota A. Absolute concentrations of metabolites in human brain tumors using *in vitro* proton magnetic resonance spectroscopy. *NMR Biomed.* (1997) 10:2–12.
56. Yoshida Y, Yoshioka Y. [Utility of proton magnetic resonance spectroscopy in the diagnosis of human brain tumors]. *No Shinkei Geka* (1991) 19:421–7.
57. Kertesz V, Calligaris D, Feldman DR, Changelian A, Laws ER, Santagata S, et al. Profiling of adrenocorticotropic hormone and arginine vasopressin in human pituitary gland and tumor thin tissue sections using droplet-based liquid-microjunction surface-sampling-HPLC-ESI-MS-MS. *Anal Bioanal Chem.* (2015) 407:5989–98. doi: 10.1007/s00216-015-8803-2
58. Zhan X, Desiderio DM. Nitroproteins from a human pituitary adenoma tissue discovered with a nitrotyrosine affinity column and tandem mass spectrometry. *Anal Biochem.* (2006) 354:279–89. doi: 10.1016/j.ab.2006.05.024
59. Kríz L, Bicíková M, Mohapl M, Hill M, Cerný I, Hampl R. Steroid sulfatase and sulfuryl transferase activities in human brain tumors. *J Steroid Biochem Mol Biol.* (2008) 109:31–9. doi: 10.1016/j.jsbmb.2007.12.004
60. Feng J, Zhang Q, Li C, Zhou Y, Zhao S, Hong L, et al. Enhancement of mitochondrial biogenesis and paradoxical inhibition of lactate dehydrogenase mediated by 14-3-3η in oncocytomas. *J Pathol.* (2018) 245:361–72. doi: 10.1002/path.5090
61. Kaibara T, Tyson RL, Sutherland GR. Human cerebral neoplasms studied using MR spectroscopy: a review. *Biochem Cell Biol.* (1998) 76:477–86 doi: 10.1139/o98-048
62. Whiting PF, Rutjes AW, Westwood ME, Mallett S, Deeks JJ, Reitsma JB, et al. QUADAS-2: a revised tool for the quality assessment of diagnostic accuracy studies. *Ann Intern Med.* (2011) 155:529–36. doi: 10.7326/0003-4819-155-8-201110180-00009
63. Calligaris D, Feldman DR, Norton I, Olubiyi O, Changelian AN, Machaidze R, et al. MALDI mass spectrometry imaging analysis of pituitary adenomas for near-real-time tumor delineation. *Proc Natl Acad Sci USA.* (2015) 112:9978–83. doi: 10.1073/pnas.1423101112
64. Oklu R, Deipolyi AR, Wicky S, Ergul E, Deik AA, Chen JW, et al. Identification of small compound biomarkers of pituitary adenoma: a bilateral inferior petrosal sinus sampling study. *Neuro Intervent Surg.* (2014) 6:541–6. doi: 10.1136/neurintsurg-2013-010821
65. Jie Feng, Qi Zhang, Yang Zhou, Shenyuan Yu, Lichuan Hong, Sida Zhao et al. Integration of proteomics and metabolomics revealed metabolite-protein networks in ACTH- pituitary adenoma. *Front Endocrinol.* (2018) 9:678. doi: 10.3389/fendo.2018.00678
66. Lee SH, Nam SY, Chung BC. Altered profile of endogenous steroids in the urine of patients with prolactinoma. *Clin Biochem.* (1998) 31:529–35 doi: 10.1016/S0009-9120(98)00063-0
67. Jarmusch AK, Pirro V, Baird Z, Hattab EM, Cohen-Gadol AA, Cooks RG. Lipid and metabolite profiles of human brain tumors by desorption electrospray ionization-MS. *Proc Natl Acad Sci USA.* (2016) 113:1486–91. doi: 10.1073/pnas.1523306113
68. Bicíková M, Kríz L, Mohapl M, Burkonová D, Tallová J, Husek P. Aminothiols in human brain tumors. *Clin Chem Lab Med.* (2006) 44:978–82. doi: 10.1515/CCLM.2006.170
69. Usenius JP, Kauppinen RA, Vainio PA, Hernesniemi JA, Vapalahti MP, Paljärvi LA, et al. Quantitative metabolite patterns of human brain tumors: detection by 1H NMR spectroscopy *in vivo* and *in vitro*. *J Comput Assist Tomogr* (1994) 18:705–13.
70. Solivera J, Cerdán S, Pascual JM, Barrios L, Roda JM. Assessment of 31P-NMR analysis of phospholipid profiles for potential differential diagnosis of human cerebral tumors. *NMR Biomed.* (2009) 22:663–74.
71. Einstein A, Virani RA. Clinical relevance of single-voxel 1H Mrs metabolites in discriminating suprasellar tumors. *J Clin Diagn Res* (2016) 10:TC01–TC04.
72. Chernov MF, Kawamata T, Amano K, Ono Y, Suzuki T, Nakamura R, et al. Possible role of single-voxel (1)H-MRS in differential diagnosis of suprasellar tumors. *J Neurooncol.* (2009) 91:191–8. doi: 10.1007/s11060-008-9698-y
73. Faghih Jouibari M, Ghodsi SM, Akhlaghpoor S, Mehrazin M, Saadat S, Khoshnevisan A, et al. Complementary effect of H MRS in diagnosis of suprasellar tumors. *Clin Imaging* (2012) 36:810–5. doi: 10.1016/j.clinimag.2012.01.021
74. Isobe T, Yamamoto T, Akutsu H, Shiigai M, Shibata Y, Takada K, et al. Preliminary study for differential diagnosis of intracranial tumors using in vivo quantitative proton MR spectroscopy with correction for T2 relaxation time. *Radiography* (2015) 21:42–6. doi: 10.1016/j.radi.2014.06.002
75. Sutton LN, Wang ZJ, Wehrli SL, Marwaha S, Molloy P, Phillips PC, et al. Proton spectroscopy of suprasellar tumors in pediatric patients. *Neurosurgery* (1997) 41:388–94. discussion: 394–5 doi: 10.1097/00006123-199708000-00009
76. Stadlbauer A, Buchfelder M, Nimsky C, Saeger W, Salomonowitz E, Pinker K, et al. Proton magnetic resonance spectroscopy in pituitary macroadenomas: preliminary results. *J Neurosurg.* (2008) 109:306–12. doi: 10.3171/JNS/2008/109/8/0306
77. Kozic D, Medic-Stojanoska M, Ostojic J, Popovic L, Vuckovic N. Application of MR spectroscopy and treatment approaches in a patient with extrapituitary growth hormone secreting macroadenoma. *Neuro Endocrinol Lett.* (2007) 28:560–4.
78. Khiat A, Bard C, Lacroix A, Rousseau J, Boulanger Y. Brain metabolic alterations in Cushing's syndrome as monitored by proton magnetic resonance spectroscopy. *NMR Biomed.* (1999) 12:357–63. doi: 10.1002/(SICI)1099-1492(199910)12:6<357::AID-NBM584>3.0.CO;2-U
79. Larkin S, Ansorge O. Development and microscopic anatomy of the pituitary gland. In: De Groot LJ, Chrousos G, Dungan K, Feingold KR, Grossman A, Hershman JM, Koch C, Korbonits M, McLachlan R, New M, Purnell J, Rebar R, Singer F, Vinik A, editors. *Endotext*. South Dartmouth, MA: MDText.com, Inc. (2000). (Accessed February, 15 2017).

80. Cuellar-Baena S, Morales JM, Martinetto H, Calvar J, Sevlever G, Castellano G, et al. Comparative metabolic profiling of paediatric ependymoma, medulloblastoma and pilocytic astrocytoma. *Int J Mol Med* (2010) 26:941–8. doi: 10.3892/ijmm_00000546
81. Vettukattil R, Gulati M, Sjøbakk TE, Jakola AS, Kvernmo NA, Torp SH, et al. Differentiating diffuse World Health Organization grade II and IV astrocytomas with *ex vivo* magnetic resonance spectroscopy. *Neurosurgery* (2013) 72:186–95. doi: 10.1227/NEU.0b013e31827b9c57
82. Davis ME. Glioblastoma: overview of disease and treatment. *Clin J Oncol Nurs.* (2016) 20:S2–8. doi: 10.1188/16.CJON.S1.2-8
83. Dilillo M, Ait-Belkacem R, Esteve C, Pellegrini D, Nicolardi S, Costa M, et al. Ultra-high mass resolution MALDI imaging mass spectrometry of proteins and metabolites in a mouse model of glioblastoma. *Sci Rep.* (2017) 7:603. doi: 10.1038/s41598-017-00703-w
84. Pfisterer WK, Nieman RA, Scheck AC, Coons SW, Spetzler RF, Preul MC. Using *ex vivo* proton magnetic resonance spectroscopy to reveal associations between biochemical and biological features of meningiomas. *Neurosurg Focus* (2010) 28:E12. doi: 10.3171/2009.11.FOCUS09216
85. Chen W, Lou H, Zhang H, Nie X, Lan W, Yang Y, et al. Grade classification of neuroepithelial tumors using high-resolution magic-angle spinning proton nuclear magnetic resonance spectroscopy and pattern recognition. *Sci China Life Sci.* (2011) 54:606–16. doi: 10.1007/s11427-011-4193-7
86. Namboodiri AM, Peethambaran A, Mathew R, Sambhu PA, Hershfield J, Moffett JR, et al. Canavan disease and the role of N-acetylaspartate in myelin synthesis. *Mol Cell Endocrinol.* (2006) 252:216–23. doi: 10.1016/j.mce.2006.03.016
87. Garcia PA, Laxer KD, van der Grond J, Hugg JW, Matson GB, Weiner MW. Correlation of seizure frequency with N-acetyl-aspartate levels determined by 1H magnetic resonance spectroscopic imaging. *Magn Reson Imaging* (1997) 15:475–8 doi: 10.1016/S0730-725X(96)00327-X
88. Vielhaber S, Kudin AP, Kudina TA, Stiller D, Scheich H, Schoenfeld A, et al. Hippocampal N-acetyl aspartate levels do not mirror neuronal cell densities in creatine-supplemented epileptic rats. *Eur J Neurosci.* (2003) 18:2292–300 doi: 10.1046/j.1460-9568.2003.02954.x
89. Vielhaber S, Niessen HG, Debska-Vielhaber G, Kudin AP, Wellmer J, Kaufmann J, et al. Subfield-specific loss of hippocampal N-acetyl aspartate in temporal lobe epilepsy. *Epilepsia* (2008) 49:40–50. doi: 10.1111/j.1528-1167.2007.01280.x
90. Enzinger C, Ropele S, Strasser-Fuchs S, Kapeller P, Schmidt H, Poltrum B, et al. Lower levels of N-acetylaspartate in multiple sclerosis patients with the apolipoprotein E epsilon4 allele. *Arch Neurol.* (2003) 60:65–70 doi: 10.1001/archneur.60.1.65
91. Chen JG, Charles HC, Barboriak DP, Doraiswamy PM. Magnetic resonance spectroscopy in Alzheimer's disease: focus on N-acetylaspartate. *Acta Neurol Scand Suppl.* (2000) 176:20–6 doi: 10.1034/j.1600-0404.2000.00303.x
92. Nitta A, Noike H, Sumi K, Miyanishi H, Tanaka T, Takaoka K, et al. Shati/Nat8l and N-acetylaspartate (NAA) have important roles in regulating nicotinic acetylcholine receptors in neuronal and psychiatric diseases in animal models and humans. In: Akaike A, Shimohama S, Misu Y, editors. *Nicotinic Acetylcholine Receptor Signaling in Neuroprotection*. Singapore: Springer (2018). p. 89–111.
93. Stanley AJ, Vemulapalli M, Nutche J, Montrose DM, Sweeney JA, Pettegrew JW, et al. Reduced n-acetyl-aspartate levels in schizophrenia patients with a younger onset age: a single-voxel 1h spectroscopy study. *Schizophr Res.* (2007) 93:23–32. doi: 10.1016/j.schres.2007.03.028
94. Mondino M, Brunelin J, Saoud M. N-acetyl-aspartate level is decreased in the prefrontal cortex in subjects at-risk for schizophrenia. *Front Psychiatry* (2013) 4:99.doi: 10.3389/fpsyt.2013.00099
95. Igarashi H, Suzuki Y, Huber VJ, Ida M, Nakada T. N-acetylaspartate decrease in acute stage of ischemic stroke: a perspective from experimental and clinical studies. *Magn Reson Med Sci.* (2015) 14:13–24. doi: 10.2463/mrms.2014-0039
96. Moffett JR, Arun P, Ariyannur PS, Namboodiri AMA. N-Acetylaspartate reductions in brain injury: impact on post-injury neuroenergetics, lipid synthesis, and protein acetylation. *Front Neuroenergetics* (2013) 5:11. doi: 10.3389/fnene.2013.00011
97. Shannon RJ, van der Heide S, Carter EL, Jalloh I, Menon DK, Hutchinson PJ, et al. Extracellular N-acetylaspartate in human traumatic brain injury. *J Neurotrauma* (2016) 33:319–29.doi: 10.1089/neu.2015.3950
98. Rigotti DJ, Inglese M, Gonen O. Whole-brain N-acetylaspartate as a surrogate marker of neuronal damage in diffuse neurologic disorders. *AJNR Am J Neuroradiol.* (2007) 28:1843–9. doi: 10.3174/ajnr.A0774
99. Long PM, Moffett JR, Namboodiri AMA, Viapiano MS, Lawler SE, Jaworski DM. N-Acetylaspartate (NAA) and N-Acetylaspartylglutamate (NAAG) promote growth and inhibit differentiation of glioma stem-like cells. *J Biol Chem.* (2013) 288:26188–200. doi: 10.1074/jbc.M113.487553
100. Horská A, Barker PB. Imaging of brain tumors: MR spectroscopy and metabolic imaging. *Neuroimaging Clin N Am.* (2010) 20:293–310. doi: 10.1016/j.nic.2010.04.003
101. Ferreira AK, Meneguelo R, Marques FL, Radin A, Filho OM, Neto SC, et al. Synthetic phosphoethanolamine a precursor of membrane phospholipids reduce tumor growth in mice bearing melanoma B16-F10 and *in vitro* induce apoptosis and arrest in G2/M phase. *Biomed Pharmacother.* (2012) 66:541–8. doi: 10.1016/j.biopha.2012.04.008
102. Ferreira AK, Santana-Lemos BA, Rego EM, Filho OM, Chierice GO, Maria DA. Synthetic phosphoethanolamine has *in vitro* and *in vivo* anti-leukemia effects. *Br J Cancer* (2013) 109:2819–28. doi: 10.1038/bjc.2013.510
103. Torregrossa L, Shintu L, Nambiath Chandran J, Tintaru A, Ugolini C, Magalhães A, et al. Toward the reliable diagnosis of indeterminate thyroid lesions: a HRMAS NMR-based metabolomics case of study. *J Proteome Res.* (2012) 11:3317–25. doi: 10.1021/pr300105e
104. Deja S, Dawiskiba T, Balcerzak W, Orczyk-Pawiłowicz M, Głód M, Pawełka D, et al. Follicular adenomas exhibit a unique metabolic profile. ^{1}H NMR studies of thyroid lesions. *PLoS ONE* (2013) 8:e84637. doi: 10.1371/journal.pone.0084637
105. Bizzarri M, Dinicola S, Bevilacqua A, Cucina A. Broad spectrum anticancer activity of myo-inositol and inositol hexakisphosphate. *Int J Endocrinol.* (2016) 2016:5616807. doi: 10.1155/2016/5616807
106. Kesler SR, Watson C, Koovakkattu D, Lee C, O'Hara R, Mahaffey ML, et al. Elevated prefrontal myo-inositol and choline following breast cancer chemotherapy. *Brain Imagin Behav.* (2013) 7:501–10. doi: 10.1007/s11682-013-9228-1
107. Derbal-Wolfrom L, Pencreach E, Saandi T, Aprahamian M, Martin E, Greferath R, et al. Increasing the oxygen load by treatment with myo-inositol trispyrophosphate reduces growth of colon cancer and modulates the intestine homeobox gene Cdx2. *Oncogene* (2013) 32:4313–18. doi: 10.1038/onc.2012.445
108. Medina MA. Glutamine and cancer. *J Nutr.* (2001) 131(Suppl. 9):2539S−42S. doi: 10.1093/jn/131.9.2539S
109. Wise DR, Thompson CB. Glutamine addiction: a new therapeut target in cancer. *Trends Biochem Sci.* (2010) 35:427–33. doi: 10.1016/j.tibs.2010.05.003
110. Eagle H. Nutrition needs of mammalian cells in tissue culture. *Science* (1955) 122:501–14 doi: 10.1126/science.122.3168.501
111. Mathews EH, Liebenberg L. Cancer control via glucose and glutamine deprivation. *J Intern Med.* (2013) 274:492. doi: 10.1111/joim.12068
112. Costello LC, Franklin RB. 'Why do tumour cells glycolyse?': from glycolysis through citrate to lipogenesis. *Mol Cell Biochem.* (2005) 280:1–8. doi: 10.1007/s11010-005-8841-8
113. Gu Y, Chen T, Fu S. Perioperative dynamics and significance of amino acid profiles in patients with cancer. *J Transl Med.* (2015) 13:35. doi: 10.1186/s12967-015-0408-1
114. Stepulak A, Rola R, Polberg K, Ikonomidou C. Glutamate and its receptors in cancer. *J Neural Transm.* (2014) 121:933–44. doi: 10.1007/s00702-014-1182-6
115. North WG, Gao G, Jensen A, Memoli VA, Du J. NMDA receptors are expressed by small-cell lung cancer and are potential targets for effective treatment. *Clin Pharmacol.* (2010) 2:31–40. doi: 10.2147/CPAA.S6262
116. Stepulak A, Luksch H, Gebhardt C, Uckermann O, Marzahn J, Sifringer M, et al. Expression of glutamate receptor subunits in human cancers. *Histochem Cell Biol.* (2009) 132:435–45. doi: 10.1007/s00418-009-0613-1

117. Liu JW, Kim MS, Nagpal J, Yamashita K, Poeta L, Chang X, et al. Quantitative hypermethylation of NMDAR2B in human gastric cancer. *Int J Cancer* (2007) 121:1994–2000 doi: 10.1002/ijc.22934
118. Li S, Qian J, Yang Y, Zhao W, Dai J, Bei JX, et al. GWAS identifies novel susceptibility loci on 6p21.32 and 21q21.3 for hepatocellular carcinoma in chronic hepatitis B virus carriers. *PLoS Genet* (2012) 8:e1002791. doi: 10.1371/journal.pgen.1002791
119. North WG, Gao G, Memoli VA, Pang RH, Lynch L. Breast cancer expresses functional NMDA receptors. *Breast Cancer Res Treat* (2010) 122:307–14. doi: 10.1007/s10549-009-0556-1
120. Choi CH, Choi JJ, Park YA, Lee YY, Song SY, Sung CO, et al. Identification of differentially expressed genes according to chemosensitivity in advanced ovarian serous adenocarcinomas: expression of GRIA2 predicts better survival. *Br J Cancer* (2012) 107:91–9. doi: 10.1038/bjc.2012.217
121. Allen EL, Ulanet DB, Pirman D, Mahoney CE, Coco J, Si Y, et al. Differential aspartate usage identifies a subset of cancer cells particularly dependent on OGDH. *Cell Rep.* (2016) 17:876–90. doi: 10.1016/j.celrep.2016.09.052
122. Xie G, Zhou B, Zhao A, Qiu Y, Zhao X, Garmire L, et al. Lowered circulating aspartate is a metabolic feature of human breast cancer. *Oncotarget* (2015) 6: 33369–81. doi: 10.18632/oncotarget.5409
123. Dornfeld K, Madden M, Skildum A, Wallace KB. Aspartate facilitates mitochondrial function, growth arrest and survival during doxorubicin exposure. *Cell Cycle* (2015) 14:3282–91. doi: 10.1080/15384101.2015.1087619
124. Ajouz H, Mukherji D, Shamseddine A. Secondary bile acids: an underrecognized cause of colon cancer. *World J Surg Oncol.* (2014) 12:164. doi: 10.1186/1477-7819-12-164
125. Bernstein H, Bernstein C, Payne CM, Dvorakova K, Garewal H. Bile acids as carcinogens in human gastrointestinal cancers. *Mutat Res.* (2005) 589:47–65 doi: 10.1016/j.mrrev.2004.08.001
126. Milovic V, Teller IC, Murphy GM, Caspary WF, Stein J. Deoxycholic acid stimulates migration in colon cancer cells. *Eur J Gastroenterol Hepatol.* (2001) 13:945–9 doi: 10.1097/00042737-200108000-00012
127. Abdel-Latif MM, Inoue H, Reynolds JV. Opposing effects of bile acids deoxycholic acid and ursodeoxycholic acid on signal transduction pathways in oesophageal cancer cells. *Eur J Cancer Prev.* (2016) 25:368–79. doi: 10.1097/CEJ.0000000000000198
128. Costarelli V, Sanders TAB. Plasma deoxycholic acid concentration is elevated in postmenopausal women with newly diagnosed breast cancer. *Eur J Clin Nutr.* (2002) 56:925–7. doi: 10.1038/sj.ejcn.1601396
129. Galluzzi L, Vacchelli E, Michels J, Garcia P, Kepp O, Senovilla L, et al. Effects of vitamin B6 metabolism on oncogenesis, tumor progression and therapeutic responses. *Oncogene* (2013) 32:4995–5004. doi: 10.1038/onc.2012.623
130. Ames BN, Wakimoto P. Are vitamin and mineral deficiencies a major cancer risk? *Nat Rev Cancer* (2002) 2:694–704 doi: 10.1038/nrc886
131. Wondrak GT, Jacobson EL. Vitamin B6: beyond coenzyme functions. *Subcell Biochem.* (2012) 56:291–300. doi: 10.1007/978-94-007-2199-9_15
132. Ollberding NJ, Aschebrook-Kilfoy B, Caces DB, Wright ME, Weisenburger DD, Smith SM, et al. Phytanic acid and the risk of non-Hodgkin lymphoma. *Carcinogenesis* (2013) 34:170–5. doi: 10.1093/carcin/bgs315
133. Wright EM, Albanes D, Moser AB, Weinstein SJ, Snyder K, Männistö S, et al. Serum phytanic and pristanic acid levels and prostate cancer risk in Finnish smokers. *Cancer Med.* (2014) 3:1562–9. doi: 10.1002/cam4.319
134. Wright ME, Bowen P, Virtamo J, Albanes D, Gann PH. Estimated phytanic acid intake and prostate cancer risk: a prospective cohort study. *Int J Cancer* (2012) 131:1396–406. doi: 10.1002/ijc.27372
135. Chen M, Shen M, Li Y, Liu C, Zhou K, Hu W, et al. GC-MS-based metabolomic analysis of human papillary thyroid carcinoma tissue. *Int J Mol Med.* (2015) 36:1607–14. doi: 10.3892/ijmm.2015.2368
136. Tian Y, Nie X, Xu S, Li Y, Huang T, Tang H, et al. Integrative metabonomics as potential method for diagnosis of thyroid malignancy. *Sci Rep.* (2015) 5:14869. doi: 10.1038/srep14869
137. Xu Y, Zheng X, Qiu Y, Jia W, Wang J, Yin S. Distinct metabolomic profiles of papillary thyroid carcinoma and benign thyroid adenoma. *J Proteome Res.* (2015)14:3315–21. doi: 10.1021/acs.jproteome.5b00351
138. Wojtowicz W, Zabek A, Deja S, Dawiskiba T, Pawelka D, Glod M, et al. Serum and urine ^{1}H NMR-based metabolomics in the diagnosis of selected thyroid diseases. *Sci Rep.* (2017) 7:9108. doi: 10.1038/s41598-017-09203-3
139. Lu J, Hu S, Miccoli P, Zeng Q, Liu S, Ran L, et al. Non-invasive diagnosis of papillary thyroid microcarcinoma: a NMR-based metabolomics approach. *Oncotarget* (2016) 7:81768–77. doi: 10.18632/oncotarget.13178
140. Cheng Y, Yang X, Deng X, Zhang X, Li P, Tao J, et al. Metabolomics in bladder cancer: a systematic review. *Int J Clin Exp Med.* (2015) 8:11052–63.
141. Hirayama A, Kami K, Sugimoto M, Sugawara M, Toki N, Onozuka H, et al. Quan-titative metabolome profiling of colon and stomach cancer microenvironment by capil-lary electrophoresis time-of-flight mass spec-trometry. *Cancer Res.* (2009) 69:4918–25. doi: 10.1158/0008-5472.CAN-08-4806
142. Argilés JM, Azcón-Bieto J. The metabolic environment of cancer. *Mol Cell Biochem.* (1988) 81:3–17.
143. Plewa S, Horała A, Derezinski P, Klupczynska A, Nowak-Markwitz E, Matysiak J, et al. Usefulness of amino acid profiling in ovarian cancer screening with special emphasis on their role in cancerogenesis. *Int J Mol Sci.* (2017) 18:2727. doi: 10.3390/ijms18122727
144. Possemato R, Marks KM, Shaul YD, Pacold ME, Kim D, Birsoy K, et al. Functional genomics reveal that the serine synthesis pathway is essential in breast cancer. *Nature* (2011) 476:346–50. doi: 10.1038/nature10350
145. Kelly RS, Vander Heiden MG, Giovannucci EL, Mucci LA. Metabolomic biomarkers of prostate cancer: prediction, diagnosis, progression, prognosis and recurrence. *Cancer Epidemiol Biomarkers Prev.* (2016) 25:887–906. doi: 10.1158/1055-9965.EPI-15-1223
146. Chen Y, Li P. Fatty acid metabolism and cancer development. *Sci Bull.* (2016) 61:1473–9. doi: 10.1007/s11434-016-1129-4
147. Clish CB. Metabolomics: an emerging but powerful tool for precision medicine. *Cold Spring Harb Mol Case Stud.* (2015) 1:a000588. doi: 10.1101/mcs.a000588
148. Ivanisevic J, Epstein A, Kurczy ME, Benton HP, Uritboonthai W, Fox HS, et al. Brain region mapping using global metabolomics. *Chem Biol.* (2014) 21:1575–84. doi: 10.1016/j.chembiol.2014.09.016

Conflict of Interest Statement: The authors declare that the research was conducted in the absence of any commercial or financial relationships that could be construed as a potential conflict of interest.

frontiers in Endocrinology

REVIEW
published: 22 January 2019
doi: 10.3389/fendo.2018.00768

The Mechanism and Pathways of Dopamine and Dopamine Agonists in Prolactinomas

Xiaoshuang Liu[1†], *Chao Tang*[2†], *Guodao Wen*[3], *Chunyu Zhong*[4], *Jin Yang*[4], *Junhao Zhu*[4] *and Chiyuan Ma*[2*]

[1] The State Key Laboratory of Pharmaceutical Biotechnology and Jiangsu Engineering Research Center for MicroRNA Biology and Biotechnology, School of Life Science, NJU Advanced Institute for Life Sciences, Nanjing University, Nanjing, China, [2] Department of Neurosurgery, School of Medicine, Jinling Hospital, Nanjing University, Nanjing, China, [3] Tungwah Hospital of Sun Yat-Sen University, Dongguan, China, [4] School of Medicine, Nanjing Medical University, Nanjing, China

Dopamine agonists such as bromocriptine and cabergoline are the predominant treatment drugs for prolactinoma by inhibiting prolactin secretion and shrinking tumor size. However, the pathways of either dopamine or its agonists that lead to the death of cells are incompletely understood and some are even conflicting conclusions. The main aim of this paper is to review the different pathways of dopamine and its agonists in prolactinomas to help to gain a better understanding of their functions and drug resistance mechanisms.

Keywords: dopamine agonists, bromocriptine, cabergoline, programmed cell death, prolactinomas

OPEN ACCESS

Edited by:
Carmen E. Georgescu, Iuliu Haţieganu University of Medicine and Pharmacy, Romania

Reviewed by:
Hiroshi Nishioka, Toranomon Hospital, Japan
Sergio P. A. Toledo, Federal University of São Paulo, Brazil

***Correspondence:**
Chiyuan Ma
machiyuan_nju@126.com

[†]*These authors share Co-first authorship*

Specialty section:
This article was submitted to Pituitary Endocrinology, a section of the journal Frontiers in Endocrinology

Received: *31 August 2018*
Accepted: *06 December 2018*
Published: *22 January 2019*

Citation:
Liu X, Tang C, Wen G, Zhong C, Yang J, Zhu J and Ma C (2019) The Mechanism and Pathways of Dopamine and Dopamine Agonists in Prolactinomas. Front. Endocrinol. 9:768. doi: 10.3389/fendo.2018.00768

INTRODUCTION

Pituitary adenomas (PAs) are common intracranial neoplasms. Typically, PAs are classified as either clinically non-functioning PAs or functioning PAs with characteristic clinical and endocrine symptoms, such as acromegaly and hyperprolactinemia or Cushing disease (1, 2).

Prolactinomas are the most common type of functioning PAs, which can cause headache, visual dysfunction, hypopituitarism, and hyperprolactinemia (3). The clinical features of hyperprolactinemia include impotence in males and oligo/amenorrhea in females (4, 5). The normalization of serum prolactin (PRL) levels and shrinkage of tumors are among the major goals of treatment in patients with prolactinomas (6). Dopamine agonists (DAs), such as bromocriptine (BRC) and cabergoline (CAB) are the first-line drugs for the treatment of patients with idiopathic hyperprolactinemia and prolactinomas (3, 7). The lactotroph adenoma cells express dopamine receptors, and DAs effectively suppress prolactin secretion and shrink the tumor by binding the cell-surface dopamine receptors in most patients (7, 8). This suggests that a "gene-network" may exist to regulate the activation of dopamine receptors, and may be involved in the mechanism of action of DAs for the treatment prolactinomas.

Although, two main DAs, namely BRC and CAB, have been approved as first-line drugs for the treatment of patients with hyperprolactinemia, a minority of patients with prolactinoma were resistant or intolerant to BRC, but responded adequately to CAB (9, 10). Currently, a better understanding of the pathophysiology of prolactinomas and the precise mechanisms of action of DAs in prolactinomas is greatly needed, especially considering that different pharmacological compounds act on lactotroph cells through different intracellular molecular pathways.

In this review, we summarize the current research advances on different pathways and mechanisms of dopamine and DAs effects on prolactinoma cells to help accelerate future research in this field (**Figure 1**).

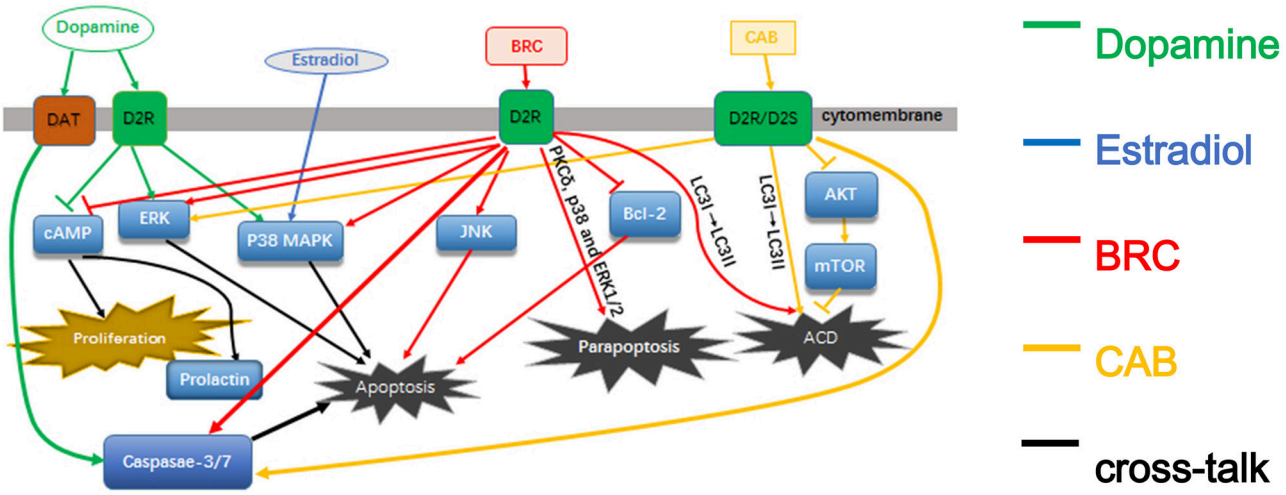

FIGURE 1 | The pathways of dopamine and dopamine agonists in prolactinomas.

DOPAMINE AND DOPAMINE RECEPTORS

Multiple *in vitro* and *in vivo* studies have demonstrated that dopamine is an effective inhibitor of PRL secretion (11, 12), PRL gene expression and lactotroph cell proliferation (13). It can also induces the apoptosis of lactotroph cells (14).

Based on the functions of the dopamine receptors, they can be divided into D1-like receptors, such as D1 and D5, and D2-like receptors including D2, D3, and D4. The two DA receptor families play different roles. For example, D1-like receptors can induce the production of cyclic adenosine monophosphate (cAMP) and activate cAMP-dependent protein kinase (PKA) (15). Conversely, D2-like receptors (D2, D3, and D4) can reduce the accumulation of cAMP through interaction with Gi/G0 proteins (16). The activation of D2 receptors can also inhibit PRL secretion by decreasing the cell calcium levels through the G13 protein (17), but the activation of D1 receptors instead stimulates PRL secretion by stimulating vasoactive intestinal peptide (VIP) secretion (18, 19).

There are two isoforms of D2R produced by alternative splicing, namely the short and long isoforms (D2S and D2L) (13), which differ by only 29 amino acids derived from an additional exon in D2L, encoding the third intracellular loop of the receptor (20). D2S and D2L receptors are hypothesized to have distinct functions in the mitogen-activated protein kinase (MAPK) pathways (21). The pituitary size and PRL levels were found to be reduced in mice overexpressing D2S compared to wild type (WT) or D2L overexpressing mice (22). These observations suggest that dopamine effects on lactotrophs are mediated through the D2S receptor isoform and is an estrogen-dependent process. The decrease of D2S expression may play a part in D2R agonist resistant prolactinomas (21). In the pituitary gland, the expression level of D2L is much lower than that of D2S (20).

Most researchers use rodent or murine tumor cell lines to study dopamine functions in the pituitary and PAs (22, 23). In particular, studies on the rodent GH3 pituitary cell line have contributed significantly to the understanding of mechanisms of dopamine-induced apoptosis (23, 24). The receptors for VIP, thyroid-stimulating hormone (TRH) were found in GH3 cells, but no dopamine receptors (25). Many studies have demonstrated that GH3 cells do not express functional D2 receptors (26, 27). Indeed, some studies suggested that dopamine-induced apoptosis could not occur in the GH3 cell line unless it was transfected with a functional D2R (26).

DOPAMINE REDUCE PRL AND INDUCE APOPTOSIS OF PITUITARY ADENOMA CELLS

In cells expressing either transfected or endogenous D2R receptors, the p38 MAPK or extracellular-signal-regulated kinase (ERK) were shown to be involved in the process of dopamine-induced apoptosis (22, 26). However, it should be noted that there are many conflicting reports about the regulation of the ERK pathway by the D2S receptor and it could be a cell type-dependent process. Previous research found that in non-neuronal cells, dopamine-D2 receptors stimulate ERK activity and cell proliferation (28). However, in neuroendocrine cells, such as GH4-rD2S, the phosphorylation of ERK was inhibited by D2S receptors (29). Another study found that in normal rat pituitary cells, ERK was inhibited by D2R (30). There is another hypothesis suggesting that the regulation of the ERK pathway by dopamine is a dynamic process, whereby the activated ERK may be reduced by dopamine to antagonize the stimulation thus leading to changes in gene expression and cell growth (30).

Different from these findings, another study demonstrated that the apoptosis induced by dopamine is promoted through the dopamine transporter (DAT) instead of D2R (23). In contrast, based on this assumption, in a co-culture experiments with a specific DAT inhibitor and dopamine, the apoptotic response was not attenuated, thus indicating that dopamine-induced apoptosis is not mediated through the DAT (31). Nevertheless, in GH3 cells which do not express D2R, an increase in apoptosis was observed with increasing time and concentration of dopamine (23, 31). Although no activation of any of the analyzed MAPKs was observed within 0.25–24 h, including p38-kinase, JNK, and ERK which is different from BRC challenged cells (23, 31). These observations indicate that dopamine may also induce apoptosis through other receptors and pathways.

Some studies indicated that the apoptosis of lactotrophs induced by dopamine is also an estrogen-dependent process (21). Studies on PRL cells found that it is not sufficient for D2S to induce apoptosis by dopamine, and estradiol-dependent activity is also needed. Estradiol can also increase the phosphorylation of p38 MAPK induced by dopamine. Despite this, the phosphorylation of p38 is induced by D2S activation regardless of the presence or absence of estradiol (21). Based on these findings, estradiol seems to be necessary but not sufficient for p38 MAPK phosphorylation to induce apoptosis in lactotrophs. The expression of p53 was also found to be increased by estradiol in anterior pituitary cells (32). As p53 is a target of p38 MAPK, the estradiol on anterior pituitary cells may induce p53 activation by increasing p38 MAPK phosphorylation (33).

DOPAMINE AGONISTS

BRC and CAB are the two main DAs used as first-line treatment for prolactinomas, including microprolactinomas, macroprolactinomas, and giant prolactinomas. They can inhibit PRL secretion and shrink tumors effectively.

BRC was the first dopamine agonist used in clinical practice. It is a D2 receptor agonist, as well as D1 receptors antagonist. BRC is a semi-synthetic ergot derivative which binds to the D2R of anterior pituitary cells, especially on lactotrophs. The secretion of PRL is decreased by BRC through the stimulation of Na^+, K^+-ATPase activity and/or cytosolic Ca^{2+} elevation, which further inhibit the production of cAMP (34).

CAB has a higher affinity and selectivity for D2 receptors compared with BRC. In most people, CAB is more effective and has a longer half-life than BRC. It is also better-tolerated and has fewer side effects. For patients who are resistant or not very responsive to BRC, CAB has been proven to be effective (10). Besides prolactinomas, CAB is also effective for other types of PAs, such as acromegalic and ACTH-secreting adenomas (35). Accordingly, it is a valuable medicine for PAs.

The effect of CAB on reducing the size of prolactinomas is also mediated through the activation of the D2R (D2S) of anterior pituitary cells and is estrogen-dependent. Studies have found that ERK and phosphatidylinositol 3-kinase (PI3K) signaling is oppositely regulated by D2S and D2L, with D2L inhibiting both pathways, and D2S stimulating both pathways once activated by CAB (36).

DAs Induced Pituitary Adenoma Cell Death

According to different criteria, such as morphological appearance, immunological characteristics, enzymological property and functions (37), programmed cell death (PCD) can be classified into three main types (38). Type 1 is known as apoptosis, in which cells display obvious morphological appearance, such as cytoplasmic, nuclear shrinkage, and chromosomal DNA fragmentation. The activation of caspases is a central mechanism of apoptosis (39). Type 2 corresponds to autophagic cell death (ACD), in which cells show regular degradation and recycling of cellular components (40). Mammalian target of rapamycin (mTOR) and PI3K pathways are considered as primary autophagy regulatory pathways (41). Microtubule-associated protein 1A/1B-light chain 3 (LC3) is also associated with autophagy activation. A cytosolic form of LC3 (LC3-I) is converted to an LC3-phosphatidylethanolamine conjugate (LC3-II), which is associated with autophagic vesicles (42). Type 3 is called paraptosis, which is a non-lysosomal vacuolated degeneration (43, 44). The features of paraptosis are cytoplasmic vacuoles, lack of apoptotic morphology and independence of caspase activation and inhibition (45).

BRC Induces Apoptosis

During treatment with BRC, typical apoptotic features were found in GH3 and AtT-20 cell lines, such as fragmented nuclei and condensed chromatin, which are indicative of apoptosis (46). The proportion of tumor cells undergoing apoptosis also increased with time (46). As an initial anti-apoptotic regulator, which protect cells from apoptosis (47), the suppression of bcl-2 was also observed in BRC-treated GH3 cells and AtT-20 cells (46).

Studies in GH3 cells revealed that apoptosis induced by BRC is regulated through the activation of certain MAPK pathway members, such as p38-MAPK, JNK, and ERK (24, 31). P38 MAPK was found to be more closely associated with BRC-induced apoptosis. However, inhibition of p38 MAPK did not reduce the apoptotic effect of BRC (31). Accordingly, there may be other mechanisms mediating the apoptotic response to BRC and they should be studied to understand such a complex regulatory process involving numerous factors (24, 46).

Additional studies in GH3 cells show that dopamine and BRC utilize distinct intracellular pathways. BRC-induced apoptosis is sensitive to the inhibition of JNK, whereas dopamine-induced apoptosis is not. However, subsequently caspase-3/7 can be activated by both of them (31). The activation of JNK precedes cytochrome c release (31). In dopamine-treated cells the release of mitochondrial cytochrome c was also observed but it was preceded by an increase in reactive oxygen species (ROS) (23, 31). Through engagement and co-activation of these pathways BRC and dopamine ultimately synergistically induce cell death (31). These findings have motivated us to study the effects of these drugs in co-incubation experiments (31).

CAB Induces Apoptosis

The CAB-induced apoptosis observed in PRL-D2S cells involved the p38 MAPK pathways and could be reverted by a p38 MAPK inhibitor (21). Another study in MMQ cells, a prolactin-secreting clonal cell line that is responsive to dopamine, demonstrated that CAB increased the expression of apoptotic related proteins, such as PARP and cleaved caspase-3, indicating that the apoptosis is caspase-dependent (42). However, in CAB-treated GH3 cells, the PARP protein was not involved in the process of cell death (42).

DA-Regulated Paraptosis and ACD

Some studies have demonstrated that CAB and BRC not only induce apoptosis but also non-apoptotic cell death (42, 48). The autophagic degradation of organelles which precedes nuclear destruction is an important characteristic of ACD (49). The JNK pathway may also participate in ACD (50). Cytoplasmic vacuolization in mitochondria and endoplasmic reticulum is one of the morphological features of paraptosis, and do not involve the lysosomal system (48). Paraptotic cells lack apoptotic morphology (48). For apoptosis, an explicit mechanism is the activation of caspases (39), but it is not involved in parapoptosis. ERK1/2 has also been shown to promote cell death by paraptosis in 293T cells and Hepa1c1c7 cells (45).

BRC Induces Parapoptosis and ACD

Protein kinase C δ (PKCδ) is also involved in tumor progression of various tumor types and plays an important role in the PCD of prolactinomas cells. A study in GH3B6 tumor somatolactotrophic cells found that PKCδ may also contribute to the apoptotic process (51). Also, a study on male rats found that BRC caused mainly paraptosis instead of apoptosis with the involvement of PKCδ, p38, and the ERK1/2 pathways. As indicated by the absence of morphological features of apoptosis, such as internucleosomal fragmentation and the production of an unspecific smear compatible with necrosis, as well as the failure to detect the active fragment of caspase 3 in the experiment (48).

It has also been reported that BRC may induce cell death by ACD, as indicated by a higher conversion ratio of LC3-I to LC3-II found in MMQ and GH3 cells compared with the controls (52). BRC could also regulate the cell cycle as more cells were arrested in the G_0-G_1 phase and there were much fewer cells in the S phase compared with the controls. However, the precise mechanism still remains to be elucidated (52). Several cell cycle regulators may be important for such study, such as cyclin E/D1, p16/21/27, etc. (5).

CAB Induces ACD

Several studies have demonstrated that autophagic and apoptotic cell death may coexist in CAB-mediated tumor shrinkage, as a result of the release of lysosomal enzymes (42, 53).

In MMQ and GH3 cells treated with CAB, a time-dependent decrease in mTOR and AKT phosphorylation was found, indicating that ACD is involved in CAB-treated cells through the inhibition of the mTOR or AKT pathways (42). In addition, it has been found that the AKT and mTOR pathways can regulate cell survival and death by integrating signals from various stresses and growth factors (54). mTOR has also been identified as a negative regulator of ACD (55). The conversion of LC3-I to LC3-II was also detected in GH3 and MMQ cells at early stages of CAB treatment (42). By knocking-down certain proteins, such Becn1 and ATG5/7, which are essential for autophagy, it was confirmed that CAB can induce ACD (42).

DISCUSSION

Prolactinomas are the most common pituitary tumors and DAs have been shown to be highly effective in most cases. Nevertheless, many patients, who do not respond satisfactorily to DAs, are considered to be drug resistant (56, 57). The potential mechanisms involved in such resistance are not completely understood. Some studies found that less D2R mRNA was expressed in prolactinomas patients who are resistant to DAs compared to responsive patients (58). As another key receptor in prolactinomas, the estrogen receptor also plays important roles in tumorigenesis, metastasis and therapy (59), which should be studied further. Some studies have found that DA-induced apoptosis in lactotrophs is an estrogen and D2R dependent process. Furthermore, in DA-resistant prolactinoma patients, the D2L/D2S expression ratio has been found to be reduced (60), which is contradictory to other studies (21, 61, 62). Noteworthy, some studies found that the expression of D2S mRNA was significantly different for invasive and non-invasive tumors (62), thus researchers should pay more attention to the patients/cell lines in the studies. Since D2L and D2S receptors have distinct functions in MAPK pathways, more studies should be focused on them, especially in cell lines transfected with D2R. Reduced TGFβ1 activity is a common feature in the development of prolactinoma, studies also found that the recovery of TGFβ1 activity emerges as a novel therapeutic target for the treatment of DA-resistant patients (6). According to some studies, in diabetic patients with different types of tumors, metformin showed a survival benefit (63). There were two clinical cases showing that the combination of BRC and metformin might be a new effective therapy for DA-resistant prolactinomas patients (64). Ultimately, there is a great need to explore the molecular mechanisms of dopamine and DAs effects on prolactinomas in order to find a better treatment.

It has been confirmed by many studies that apoptosis induced by DAs is mediated through D2S, involve the activation of the MAPK pathway and is an estrogen-dependent process. However, studies in cell lines without dopamine receptors, such as GH3, indicate that DAs can also induce apoptosis without the activation of any of the MAPKs, suggesting that other receptors may participate in the process. In BRC-treated GH3 cells, which do not have the D2R, apoptosis is induced and is closely associated with the activation of p38 MAPK. However, the inhibition of p38 MAPK has no impact on the apoptotic response, so other mechanisms may contribute to the apoptotic process, which need to be explored.

Although some studies have demonstrated the involvement of paraptosis or autophagic mode of cell death in BRC and CAB treated cells, more evidence is still needed. Also, even though CAB and BRC are both dopamine agonists, the signal transduction pathways activated by the two drugs seem to be different. It has been found that the inhibition of p38 MAPK

can revert CAB-induced apoptosis, which is different from BRC. Autophagy and apoptosis are also considered to coexist in CAB-treated cells. Autophagy, paraptosis and apoptosis are different cell death modes that share some regulators, thus further studies should be concentrated on the detailed regulation of DAs in prolactinoma. Finally, dopamine-induced oxidative stress has been proposed as a potential mechanism of apoptosis and neurotoxicity (65). Since it has been reported that dopamine neurotoxicity can induce the death of neurons (66), more attention should be paid to the cytotoxic mechanisms of dopamine in pituitary adenoma cells.

AUTHOR CONTRIBUTIONS

GW, CZ, JY, and JZ carried out the literature search. CT and XL drafted the manuscript. CT and CM performed manuscript review.

ACKNOWLEDGMENTS

This study was supported by Grants from the Social Development Project of Jiangsu Province (No. BE2015684).

REFERENCES

1. Daly AF, Tichomirowa MA, Beckers A. The epidemiology and genetics of pituitary adenomas. *Best Pract Res Clin Endocrinol Metab.* (2009) 23:543–54. doi: 10.1016/j.beem.2009.05.008
2. Lleva RR, Inzucchi SE. Diagnosis and management of pituitary adenomas. *Curr Opin Oncol.* (2011) 23:53–60. doi: 10.1097/CCO.0b013e328341000f
3. Casanueva FF, Molitch ME, Schlechte JA, Abs R, Bonert V, Bronstein MD, et al. Guidelines of the Pituitary Society for the diagnosis and management of prolactinomas. *Clin Endocrinol.* (2006) 65:265–73. doi: 10.1111/j.1365-2265.2006.02562.x
4. Gillam MP, Molitch ME, Lombardi G, Colao A. Advances in the treatment of prolactinomas. *Endocr Rev.* (2006) 27:485–534. doi: 10.1210/er.2005-9998
5. Melmed S. Pathogenesis of pituitary tumors. *Endocrinol Metab Clin North Am.* (1999) 28:1–12. doi: 10.1016/S0889-8529(05)70055-4
6. Recouvreux MV, Camilletti MA, Rifkin DB, Díaz-Torga G. The pituitary TGFbeta1 system as a novel target for the treatment of resistant prolactinomas. *J Endocrinol.* (2016) 228:R73–83. doi: 10.1530/joe-15-0451
7. Melmed S, Casanueva FF, Hoffman AR, Kleinberg DL, Montori VM, Schlechte JA, et al. Diagnosis and treatment of hyperprolactinemia: an Endocrine Society clinical practice guideline. *J Clin Endocrinol Metab.* (2011) 96:273–88. doi: 10.1210/jc.2010-1692
8. Romijn JA. Hyperprolactinemia and prolactinoma. *Handb Clin Neurol.* (2014) 124:185–95. doi: 10.1016/B978-0-444-59602-4.00013-7
9. Delgrange E, Maiter D, Donckier J. Effects of the dopamine agonist cabergoline in patients with prolactinoma intolerant or resistant to bromocriptine. *Eur J Endocrinol.* (1996) 134:454–6. doi: 10.1530/eje.0.1340454
10. Colao A, Di Sarno A, Sarnacchiaro F, Ferone D, Di Renzo G, Merola B, et al. Prolactinomas resistant to standard dopamine agonists respond to chronic cabergoline treatment. *J Clin Endocrinol Metab.* (1997) 82:876–83. doi: 10.1210/jcem.82.3.3822
11. MacLeod RM. Influence of norepinephrine and catecholamine-depleting agents on the synthesis and release of prolactin and growth hormone. *Endocrinology* (1969) 85:916–23. doi: 10.1210/endo-85-5-916
12. MacLeod RM, Fontham EH, Lehmeyer JE. Prolactin and growth hormone production as influenced by catecholamines and agents that affect brain catecholamines. *Neuroendocrinology* (1970) 6:283–94. doi: 10.1159/000121933
13. Ben-Jonathan N, Hnasko R. Dopamine as a prolactin (PRL) inhibitor. *Endocr Rev.* (2001) 22:724–63. doi: 10.1210/edrv.22.6.0451
14. Radl DB, Zárate S, Jaita G, Ferraris J, Zaldivar V, Eijo G, et al. Apoptosis of lactotrophs induced by D2 receptor activation is estrogen dependent. *Neuroendocrinology* (2008) 88:43–52. doi: 10.1159/000116117
15. Beninger RJ, Miller R. Dopamine D1-like receptors and reward-related incentive learning. *Neurosci Biobehav Rev.* (1998) 22:335–45. doi: 10.1016/S0149-7634(97)00019-5
16. Missale C, Nash SR, Robinson SW, Jaber M, Caron MG. Dopamine receptors: from structure to function. *Physiol Rev.* (1998) 78:189–225. doi: 10.1152/physrev.1998.78.1.189
17. Lincoln GA, Clarke IJ. Noradrenaline and dopamine regulation of prolactin secretion in sheep: role in prolactin homeostasis but not photoperiodism. *J Neuroendocrinol.* (2002) 14:36–44. doi: 10.1046/j.0007-1331.2001.00734.x
18. Schnell SA, You S, El Halawani ME. D1 and D2 dopamine receptor messenger ribonucleic acid in brain and pituitary during the reproductive cycle of the turkey hen. *Biol Reprod.* (1999) 60:1378–83. doi: 10.1095/biolreprod60.6.1378
19. Ben-Jonathan N, Hugo E. Prolactin (PRL) in adipose tissue: regulation and functions. *Adv Exp Med Biol.* (2015) 846:1–35. doi: 10.1007/978-3-319-12114-7_1
20. Usiello A, Baik JH, Rougé-Pont F, Picetti R, Dierich A, LeMeur M, et al. Distinct functions of the two isoforms of dopamine D2 receptors. *Nature* (2000) 408:199–203. doi: 10.1038/35041572
21. Radl DB, Ferraris J, Boti V, Seilicovich A, Sarkar DK, Pisera D. Dopamine-induced apoptosis of lactotropes is mediated by the short isoform of D2 receptor. *PLoS ONE* (2011) 6:e18097. doi: 10.1371/journal.pone.0018097
22. Iaccarino C, Samad TA, Mathis C, Kercret H, Picetti R, Borrelli E. Control of lactotrop proliferation by dopamine: essential role of signaling through D2 receptors and ERKs. *Proc Natl Acad Sci USA.* (2002) 99:14530–5. doi: 10.1073/pnas.222319599
23. Jaubert A, Ichas F, Bresson-Bepoldin L. Signaling pathway involved in the pro-apoptotic effect of dopamine in the GH3 pituitary cell line. *Neuroendocrinology* (2006) 83:77–88. doi: 10.1159/000094044
24. Kanasaki H, Fukunaga K, Takahashi K, Miyazaki K, Miyamoto E. Involvement of p38 mitogen-activated protein kinase activation in bromocriptine-induced apoptosis in rat pituitary GH3 cells. *Biol Reprod.* (2000) 62:1486–94. doi: 10.1095/biolreprod62.6.1486
25. Stojilkovic SS, Tabak J, Bertram R. Ion channels and signaling in the pituitary gland. *Endocr Rev.* (2010) 31:845–915. doi: 10.1210/er.2010-0005
26. An JJ, Cho SR, Jeong DW, Park KW, Ahn YS, Baik JH. Anti-proliferative effects and cell death mediated by two isoforms of dopamine D2 receptors in pituitary tumor cells. *Mol Cell Endocrinol.* (2003) 206:49–62. doi: 10.1016/S0303-7207(03)00236-3
27. Cronin MJ, Faure N, Martial JA, Weiner RI. Absence of high affinity dopamine receptor in GH3 cells: a prolactin-secreting clone resistant to the inhibitory action of dopamine. *Endocrinology* (1980) 106:718–23. doi: 10.1210/endo-106-3-718
28. Albert PR, Robillard L. G protein specificity: traffic direction required. *Cell Signal.* (2002) 14:407–18. doi: 10.1016/S0898-6568(01)00259-5
29. Banihashemi B, Albert PR. Dopamine-D2S receptor inhibition of calcium influx, adenylyl cyclase, and mitogen-activated protein kinase in pituitary cells: distinct Galpha and Gbetagamma requirements. *Mol Endocrinol.* (2002) 16:2393–404. doi: 10.1210/me.2001-0220
30. Liu JC, Baker RE, Sun C, Sundmark VC, Elsholtz HP. Activation of Go-coupled dopamine D2 receptors inhibits ERK1/ERK2 in pituitary cells. A key step in the transcriptional suppression of the prolactin gene. *J Biol Chem.* (2002) 277:35819–25. doi: 10.1074/jbc.M202920200
31. Rowther FB, Richardson A, Clayton RN, Farrell WE. Bromocriptine and dopamine mediate independent and synergistic apoptotic pathways in pituitary cells. *Neuroendocrinology* (2010) 91:256–67. doi: 10.1159/000279753
32. Ying C. Potential involvement of tumor suppressor gene expression in the formation of estrogen-inducible pituitary tumors in rats. *Endocr J.* (2000) 47:1–5. doi: 10.1507/endocrj.47.1
33. Wu GS. The functional interactions between the p53 and MAPK signaling pathways. *Cancer Biol Ther.* (2004) 3:156–61. doi: 10.4161/cbt.3.2.614

34. Hussain T, Abdul-Wahab R, Lokhandwala MF. Bromocriptine stimulates Na^+, K^+-ATPase in renal proximal tubules via the cAMP pathway. *Eur J Pharmacol.* (1997) 321:259–63. doi: 10.1016/S0014-2999(97)00039-3
35. Colao A, Lombardi G, Annunziato L. Cabergoline. *Expert Opin Pharmacother.* (2000) 1:555–74. doi: 10.1517/14656566.1.3.555
36. Roof AK, Jirawatnotai S, Trudeau T, Kuzyk C, Wierman ME, Kiyokawa H, et al. The balance of PI3K and ERK signaling is dysregulated in prolactinoma and modulated by dopamine. *Endocrinology* (2018) 159:2421–34. doi: 10.1210/en.2017-03135
37. Galluzzi L, Vitale I, Aaronson SA, Abrams JM, Adam D, Agostinis P, et al. Molecular mechanisms of cell death: recommendations of the Nomenclature Committee on Cell Death 2018. *Cell Death Differ.* (2018) 25:486–541. doi: 10.1038/s41418-017-0012-4
38. Clarke PG. Developmental cell death: morphological diversity and multiple mechanisms. *Anat Embryol.* (1990) 181:195–213. doi: 10.1007/BF00174615
39. Okada H, Mak TW. Pathways of apoptotic and non-apoptotic death in tumour cells. *Nat Rev Cancer* (2004) 4:592–603. doi: 10.1038/nrc1412
40. Mizushima N, Komatsu M. Autophagy: renovation of cells and tissues. *Cell* (2011) 147:728–41. doi: 10.1016/j.cell.2011.10.026
41. Yang Z, Klionsky DJ. Mammalian autophagy: core molecular machinery and signaling regulation. *Curr Opin Cell Biol.* (2010) 22:124–31. doi: 10.1016/j.ceb.2009.11.014
42. Lin SJ, Leng ZG, Guo YH, Cai L, Cai Y, Li N, et al. Suppression of mTOR pathway and induction of autophagy-dependent cell death by cabergoline. *Oncotarget* (2015) 6:39329–41. doi: 10.18632/oncotarget.5744
43. Pagnussat AS, Faccioni-Heuser MC, Netto CA, Achaval M. An ultrastructural study of cell death in the CA1 pyramidal field of the hippocapmus in rats submitted to transient global ischemia followed by reperfusion. *J Anat.* (2007) 211:589–99. doi: 10.1111/j.1469-7580.2007.00802.x
44. Sperandio S, de Belle I, Bredesen DE. An alternative, nonapoptotic form of programmed cell death. *Proc Natl Acad Sci USA.* (2000) 97:14376–81. doi: 10.1073/pnas.97.26.14376
45. Asare N, Landvik NE, Lagadic-Gossmann D, Rissel M, Tekpli X, Ask K, et al. 1-Nitropyrene (1-NP) induces apoptosis and apparently a non-apoptotic programmed cell death (paraptosis) in Hepa1c1c7 cells. *Toxicol Appl Pharmacol.* (2008) 230:175–86. doi: 10.1016/j.taap.2008.02.015
46. Yin D, Tamaki N, Kokunai T, Yasuo K, Yonezawa K. Bromocriptine-induced apoptosis in pituitary adenoma cells: relationship to p53 and bcl-2 expression. *J Clin Neurosci.* (1999) 6:326–31. doi: 10.1016/S0967-5868(99)90057-7
47. Hockenbery D, Nuñez G, Milliman C, Schreiber RD, Korsmeyer SJ. Bcl-2 is an inner mitochondrial membrane protein that blocks programmed cell death. *Nature* (1990) 348:334–6. doi: 10.1038/348334a0
48. Palmeri CM, Petiti JP, Sosa Ldel V, Gutiérrez S, De Paul AL, Mukdsi JH, et al. Bromocriptine induces parapoptosis as the main type of cell death responsible for experimental pituitary tumor shrinkage. *Toxicol Appl Pharmacol.* (2009) 240:55–65. doi: 10.1016/j.taap.2009.07.002
49. Bursch W. Multiple cell death programs: Charon's lifts to Hades. *FEMS Yeast Res.* (2004) 5:101–10. doi: 10.1016/j.femsyr.2004.07.006
50. Zhou YY, Li Y, Jiang WQ, Zhou LF. MAPK/JNK signalling: a potential autophagy regulation pathway. *Biosci Rep.* (2015) 35:e0019. doi: 10.1042/BSR20140141
51. Leverrier S, Vallentin A, Joubert D. Positive feedback of protein kinase C proteolytic activation during apoptosis. *Biochem J.* (2002) 368 (Pt. 3):905–13. doi: 10.1042/bj20021253
52. Geng X, Ma L, Li Z, Li Z, Li J, Li M, et al. Bromocriptine induces autophagy-dependent cell death in pituitary adenomas. *World Neurosurg.* (2017) 100:407–16. doi: 10.1016/j.wneu.2017.01.052
53. Bevan JS, Webster J, Burke CW, Scanlon MF. Dopamine agonists and pituitary tumor shrinkage. *Endocr Rev.* (1992) 13:220–40. doi: 10.1210/edrv-13-2-220
54. Kim YC, Guan KL. mTOR: a pharmacologic target for autophagy regulation. *J Clin Invest.* (2015) 125:25–32. doi: 10.1172/JCI73939
55. Yorimitsu T, Klionsky DJ. Autophagy: molecular machinery for self-eating. *Cell Death Differ.* (2005) 12 (Suppl. 2):1542–52. doi: 10.1038/sj.cdd.4401765
56. Molitch ME. Pharmacologic resistance in prolactinoma patients. *Pituitary* (2005) 8:43–52. doi: 10.1007/s11102-005-5085-2
57. Hamilton DK, Vance ML, Boulos PT, Laws ER. Surgical outcomes in hyporesponsive prolactinomas: analysis of patients with resistance or intolerance to dopamine agonists. *Pituitary* (2005) 8:53–60. doi: 10.1007/s11102-005-5086-1
58. Passos VQ, Fortes MA, Giannella-Neto D, Bronstein MD. Genes differentially expressed in prolactinomas responsive and resistant to dopamine agonists. *Neuroendocrinology* (2009) 89:163–70. doi: 10.1159/000156116
59. Wang W, Knosp E, Tai G, Zhao Y, Liang Q, Guo Y. Differential effects of estrogen and estrogen receptor antagonist, ICI 182 780, on the expression of calbindin-D9k in rat pituitary prolactinoma GH cells. *Int J Clin Exp Pathol.* (2014) 7:8498–505.
60. Shimazu S, Shimatsu A, Yamada S, Inoshita N, Nagamura Y, Usui T, et al. Resistance to dopamine agonists in prolactinoma is correlated with reduction of dopamine D2 receptor long isoform mRNA levels. *Eur J Endocrinol.* (2012) 166:383–90. doi: 10.1530/EJE-11-0656
61. Caccavelli L, Feron F, Morange I, Rouer E, Benarous R, Dewailly D, et al. Decreased expression of the two D2 dopamine receptor isoforms in bromocriptine-resistant prolactinomas. *Neuroendocrinology* (1994) 60:314–22.
62. Wu ZB, Zheng WM, Su ZP, Chen Y, Wu JS, Wang CD, et al. Expression of D2RmRNA isoforms and ERmRNA isoforms in prolactinomas: correlation with the response to bromocriptine and with tumor biological behavior. *J Neurooncol.* (2010) 99:25–32. doi: 10.1007/s11060-009-0107-y
63. Bowker SL, Majumdar SR, Veugelers P, Johnson JA. Increased cancer-related mortality for patients with type 2 diabetes who use sulfonylureas or insulin. *Diabetes Care* (2006) 29:254–8. doi: 10.2337/diacare.29.02.06.dc05-1558
64. Liu X, Liu Y, Gao J, Feng M, Bao X, Deng K, et al. Combination treatment with bromocriptine and metformin in patients with bromocriptine-resistant prolactinomas: pilot study. *World Neurosurg.* (2018) 115:94–8. doi: 10.1016/j.wneu.2018.02.188
65. Gabby M, Tauber M, Porat S, Simantov R. Selective role of glutathione in protecting human neuronal cells from dopamine-induced apoptosis. *Neuropharmacology* (1996) 35:571–8. doi: 10.1016/0028-3908(96)84626-0
66. Coronas V, Féron F, Hen R, Sicard G, Jourdan F, Moyse E. *In vitro* induction of apoptosis or differentiation by dopamine in an immortalized olfactory neuronal cell line. *J Neurochem.* (1997) 69:1870–81.

Conflict of Interest Statement: The authors declare that the research was conducted in the absence of any commercial or financial relationships that could be construed as a potential conflict of interest.

frontiers in Endocrinology

REVIEW
published: 24 January 2019
doi: 10.3389/fendo.2019.00007

Molecular Network Basis of Invasive Pituitary Adenoma: A Review

*Qi Yang and Xuejun Li**

Department of Neurosurgery, Xiangya Hospital, Central South University, Changsha, China

Cases with pituitary adenoma comprise 10–25% of intracranial neoplasm, being the third most common intracranial tumor, most of the adenomas are considered to be benign. About 35% of pituitary adenomas are invasive. This review summarized the known molecular basis of the invasiveness of pituitary adenomas. The study pointed out that hypoxia-inducible factor-1α, pituitary tumor transforming gene, vascular endothelial growth factor, fibroblast growth factor-2, and matrix metalloproteinases (MMPs, mainly MMP-2, and MMP-9) are core molecules responsible for the invasiveness of pituitary adenomas. The reason is that these molecules have the ability to directly or indirectly induce cell proliferation, epithelial-to-mesenchymal transition, angiogenesis, degradation, and remodeling of extracellular matrix. HIF-1α induced by hypoxia or apoplexy inside the adenoma might be the initiating factor of invasive transformation, followed with angiogenesis for overexpressed VEGF, EMT for overexpressed PTTG, degradation of ECM for overexpressed MMPs, creating a suitable microenvironment within the tumor. Together, they form a complex interactive network. More investigations are required to further elucidate the mechanisms underlying the invasiveness of pituitary adenomas.

Keywords: angiogenesis, endocrinology, invasiveness, molecular network, pituitary adenoma

OPEN ACCESS

Edited by:
Adam Mamelak, Cedars-Sinai Medical Center, United States

Reviewed by:
Manuel Dos Santos Faria, Universidade Federal do Maranhão, Brazil
Murat Aydin Sav, Yeditepe University, Turkey

****Correspondence:***
Xuejun Li
lxjneuro@csu.edu.cn

Specialty section:
This article was submitted to Pituitary Endocrinology, a section of the journal Frontiers in Endocrinology

Received: *28 August 2018*
Accepted: *09 January 2019*
Published: *24 January 2019*

Citation:
Yang Q and Li X (2019) Molecular Network Basis of Invasive Pituitary Adenoma: A Review. Front. Endocrinol. 10:7. doi: 10.3389/fendo.2019.00007

INTRODUCTION

Cases with pituitary adenoma comprise 10–25% of intracranial neoplasm (1) and has a prevalence rate of about 17% in the general population (2). Most of the adenomas are considered to be benign. The symptoms of pituitary adenomas contain two major aspects, endocrine related and tumor occupying symptoms, the former differs according to the various hormones that get involved, the later one includes vision loss and headache. Some adenomas found accidentally on an MRI scan also show no clinical symptoms at all. The diagnosis of pituitary adenoma requires both imaging evidence and serum hormone level. About 35% of pituitary adenomas are invasive (3), which are defined and graded by the extent of tumor invading the adjacent sphenoid sinus and cavernous sinus. Invasive pituitary adenomas not only are more difficult to achieve total resection, but also have a higher recurrent rate after standard surgery compared to benign ones.

A few classification systems are available for evaluating invasive pituitary adenomas to aid surgical planning, including Hardy classification, Wilson–Hardy classification, and Knosp classification. Invasive pituitary adenomas are more difficult to surgically remove, and most of the time, they require surgical resection for the relatively more severe symptoms. An invasive pituitary adenoma was considered synonymous with an aggressive adenoma in a number of studies, moreover, aggressive ones are usually macroadenoma (4). However, some scholars (4, 5) preferred to regard an aggressive adenoma as a separated type that displays more aggressive clinical progression despite of the tumor size and should be diagnosed based on the elevated

immunoreactivity of Ki-67 and P53 over more "benign" types of pituitary adenoma using tissue immunohistochemistry. Ki-67 is a biomarker widely used to evaluate cell proliferation. P53 is also a biomarker that indicates malignancy and invasiveness when found strongly positive on tumor tissue immunohistochemistry. The 4th edition of WHO classification of pituitary tumors has removed the term atypical pituitary adenoma (APA) for the difficulty and inconsistency in determining proper cutoff of the diagnostic criteria being used before (4, 6–9), in the previous 3rd version, APA is defined as tumors that display invasive growth, Ki-67 index >3%, extensive nuclear staining for p53 and elevated mitotic activity (10), which is vague. So the 4th edition of WHO classification of pituitary tumors has also suggested that the grading of aggressive pituitary adenoma should be evaluated on an individual case basis with criteria mentioned above (7). In some ways, aggressive, and invasive pituitary adenomas can be different in clinical behavior, but they largely share the same molecular basis in terms of malignancy and invasiveness. P53 protein and Ki-67 protein are common biomarkers shared between kinds of tumors, the difficulty (i.e., inconsistent criteria) of using them in grading of pituitary adenoma means that we need some more accurate biomarkers to better distinguish them from benign pituitary adenomas.

Compared with non-invasive pituitary adenomas, those with invasive behavior are difficult to tackle with. Therefore, it is necessary to identify their causes. This review summarized the known molecular basis of the invasiveness of invasive pituitary adenomas, providing insights for further exploration in this field.

VASCULAR ENDOTHELIAL GROWTH FACTOR AND RELATED FACTORS IN AN INVASIVE PITUITARY ADENOMA

Increased angiogenesis is found to be essential for the invasiveness and spread of many types of tumors including invasive pituitary adenoma. Invasive macroprolactinomas and non-functional adenomas were more vascular compared with non-invasive ones (11) on surgically removed human pituitary adenomas. As shown in **Figure 1**, angiogenesis in the tumor is a complex and dynamic process involving the endothelial matrix degradation, proliferation, and migration of endothelial cells, and remodeling of the vascular basement membrane. In general, whether pituitary adenomas are more vascular is still controversial (12–14), but when it comes to invasive or aggressive pituitary adenomas and carcinomas, it is safe to say that angiogenesis is essential (15).

Vascular Endothelial Growth Factor

Vascular endothelial growth factor (VEGF) is proved to be the key factor in angiogenesis in many human tumors. Overexpression of VEGF in clinical samples of invasive pituitary adenomas is observed by many scholars (16). Meaning that VEGF could also be used as an independent prognosis-predicting factor except for Ki-67 and P53. There is a significant relationship between the expression of VEGF and apoplexy of pituitary adenoma (17), which, from another point of view, is an indicator of rapid tumor vascular growth. VEGF secreted by tumor cells promotes neovascularization via downstream pathways including the MAPK signaling pathway (18), FAK pathway (19), PI3K/Akt pathway (20), and p38 MAP kinase pathway (21), directly stimulating tumor cell proliferation (22). The function and the role of IP3 signaling pathway, which is also a classic downstream pathway of VEGF, in the invasiveness of pituitary adenoma are not clear yet. This could be a new entry point for the investigation of VEGF and its peripheral signaling pathways. The activation of these pathways promotes angiogenesis in many ways, including vascular endothelial cell proliferation, migration, and increase in the permeability of newly formed vessels. The controversial results on the microvascular density of pituitary adenomas indicate that VEGF has a more direct and pivotal role in tumorigenesis and invasiveness rather than just in angiogenesis because VEGF-related pathways have been found to directly promote tumor cell proliferation in other cancers recently (23). The immune escape modulated by VEGF was reported (24) and left untested in pituitary adenomas.

Tumor Necrosis Factor α

Some other molecules involving angiogenesis have shown a regulatory effect on the expression of VEGF. Tumor necrosis factor- α (TNF-α) has been reported to upregulate the expression of VEGF and matrix metalloproteinase-9 (MMP-9) in rodent cell line MMQ. In human pituitary adenoma surgical specimens, higher expression levels of TNF-α, VEGF, and MMP-9 were found in hemorrhagic adenomas than in non-hemorrhagic ones. Also, the expression levels of both VEGF and MMP-9 were positively correlated with TNF-α (25). Pituitary apoplexy can cause secondary hypoxia of the tumor tissue, so the elevation of TNF-α and VEGF expression might just be the self-saving struggle under extreme conditions.

Hypoxia-Inducible Factor-1α

Hypoxia-inducible factor-1α (HIF-1α) is able to regulate VEGF in pituitary adenomas and other human tumors. More than a decade ago, the apoptotic protective function of HIF-1α in human pituitary adenoma cell line HP75 under hypoxic conditions via a knockdown experiment was observed (26). VEGF was then confirmed to be activated by HIF-1α (27), but the HIF-1α overexpression model of rodent MMQ cell culture showed a higher apoptotic rate compared with the control, which contradicted the results of knockdown experiments in the human cell line. RWD-containing sumoylation enhancer (RSUME), a stabilizer of HIF-1α under hypoxia (28), is reported to upregulate VEGF *in vitro*, substantiating the interaction between HIF-1α and VEGF (29). There is overexpression of RSUME, HIF-1α, and VEGF-A in invasive pituitary adenoma surgical specimens compared with non-invasive ones, confirming RSUME as an upstream regulator of expression after the HIF-1α knockdown. Furthermore, the RSUME knockdown rodent AtT-20 cell line demonstrated a more invasive behavior (30). All these experiments displayed the whole picture of an invasiveness-inducing pathway of RSUME–HIF-1α-VEGF.

Notably, the von Hippel-Lindau gene-related protein (pVHL) is a known negative regulator of HIF-1α. Its low expression with

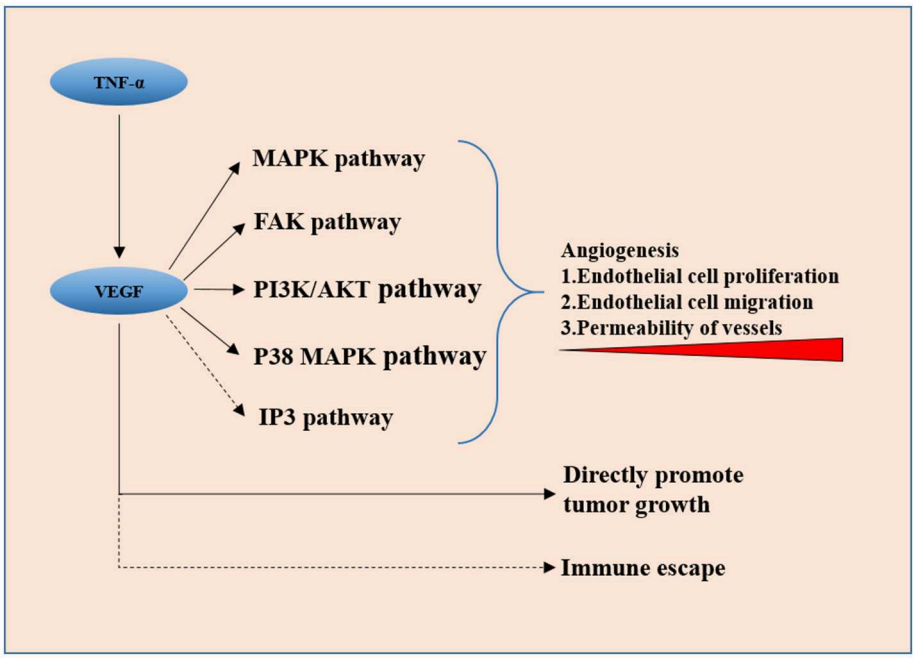

FIGURE 1 | VEGF secreted by tumor cells promotes neovascularization via downstream pathways including the MAPK signaling pathway, FAK pathway, PI3K/Akt pathway, and p38 MAP kinase pathway, it also directly promotes tumor cell proliferation. IP3 pathway and VEGF-induced immune escape might be involved in invasiveness of the pituitary adenoma.

a high expression level of VEGF leads to a higher recurrence rate and more aggressive behavior (31). A study reported an aggressive GH-PRL pituitary adenoma in a young patient with a VHL gene missense mutation (32). All these further confirm the importance of VEGF-related pathways in the invasiveness and aggressiveness of pituitary adenomas.

Fibroblast Growth Factor-2

It has been shown that fibroblast growth factor-2 (FGF-2), a growth factor, also promotes vascular endothelial cell proliferation and differentiation similar to VEGF. It is an upstream upregulator of VEGF in human vascular endothelial cells (33) and rodent GH3 pituitary cell line (34). However, FGF-2 had no significant modulatory effect on VEGF at the transcription level in human pituitary cell line HP75 (35). The overexpression of fibroblast growth factor receptor 1 (FGFR1), a receptor of FGF-2, is also closely related to the invasiveness of pituitary adenomas (36). Additionally, FGF-2 had significantly reduced expression levels in male and female prolactinoma patients (37), together with the study showing that FGF-2 had no regulatory effect on cell proliferation (38) and no significant modulating effect on VEGF at the transcription level in human gonadotrophic cell line HP75 (35), indicating FGF-2 might only be effective only in early stages of the development of pituitary adenoma, moreover, only in human prolactinoma.

Exploiting VEGF-Related Pathways in Treating Pituitary Adenoma

Advances in molecular biology have provided a better understanding of invasive pituitary adenomas, improving clinical prognosis. Many successful attempts had been made to exploit VEGF-related pathways in treating pituitary adenomas, from directly targeting VEGF (39–42) to its upstream pathways (43, 44), and to other related molecules (45).

PITUITARY TUMOR TRANSFORMING GENE

First cloned in 1997 (46), the pituitary tumor transforming gene (PTTG) is a known oncogene and upregulator of VEGF (47). The relationship between PTTG and VEGF was later elucidated with the findings that the PTTG upregulate and co-locate with VEGF, thus indirectly promoting angiogenesis in pituitary adenomas.

The PTTG1 is also called securin protein, which counters the function of separin. The degradation of PTTG1 triggers the anaphase of mitosis. Separin then promotes chromosome segregation (48). In human pituitary surgical specimens, invasive pituitary adenomas had the highest level of PTTG followed by non-invasive ones. And the PTTG doesn't express in a normal pituitary tissue (36, 49). Other researchers also reported PTTG as an indicator of both invasiveness and aggressiveness of pituitary adenomas in clinical studies (50–52). A meta-analysis on 15 cohorts of a total 752 patients with a pituitary adenoma further corroborated the relationship between PTTG and invasiveness in pituitary adenomas (53). The elevated PTTG expression level is expected to directly increase cell proliferation and chromosomal instability (54), implying enhanced tumor invasiveness.

Apart from the relationship with VEGF, the PTTG has a wide interaction spectrum with many genes and molecules related to survival, mitogenesis, tumor growth, and invasion. Estrogen receptor α (ERα), a nucleus-located receptor and the

mediator of estrogen, is positively related to the invasiveness of human pituitary adenomas (55, 56) and has a significantly higher expression in male patients with prolactinoma than in normal pituitary tissue (37). In the present study, male patients had much higher serum PRL level and much larger tumor volume compared with female patients. The expression of ERα was also elevated in female patients, but not significantly. Estrogen is the first discovered inducer of PTTG, the transcription and translation levels of the PTTG both increased within 48 h after estrogen administration in a "synced" fashion to the estrogen administration in a study using prolactinoma rat model, and under the administration of estrogen, PTTG, FGF-2, VEGF showed the same expression pattern, showing that estrogen is an inducer of PTTG. In the same study, microscopic observation of the pituitary tumor showed progressive neovascularization and remodeling of the extracellular matrix (ECM) (57). All these findings elucidated that PTTG, FGF-2, and VEGF might act in synergy from the early development to increase the invasiveness and angiogenesis of pituitary adenomas, especially prolactinoma (58) and growth hormone–secreting adenomas (59). Connexins (Cx) is a protein family forming the gap connections of cells, expression changes of which between tumor and normal tissue have been reported in many types of cancers (60). Among them, Cx43 is ubiquitously expressed in vertebrates and is considered a tumor suppressor, in most cancer types like testis cancer (61, 62), breast cancer (63, 64), and colorectal cancer (65) tumor cells tend to have lower expression of it, but that is not the case in prolactinoma. Experiments on rat prolactinoma model has shown us that estrogen can induce increasing of gap junctions and of course Cx43, and the silencing of Cx43 could attenuate estrogen-induced up-regulation of PTTG (66). Cx43 might play an import part in tumorigenesis of prolactinoma, the relationship between Cx43 and VEGF, HIF-1α in pituitary adenomas requires future investigation. It is worth mentioning that the PTTG can upregulate the expression and secretion of MMP-2 in HEK293 cells (67), MMP-2 is capable of inducing invasiveness in pituitary adenomas. It could be the same for the PTTG in pituitary adenomas. The clarification of this would be worthwhile because both PTTG and MMPs are potentially valuable therapeutic targets.

DEGRADATION AND REMODELING OF ECM BY MATRIX METALLOPROTEINASES FAMILY

Matrix metalloproteinases (MMPs) are a group of calcium-dependent zinc-containing endopeptidases with the ability to degrade basement membrane and ECM. Together with the tissue inhibitor of metalloproteinases (TIMPs), they are the essential elements in the stability and remodeling of ECM (11). A dynamic balance is maintained between MMPs and TIMPs. The major types of MMPs involved in pituitary adenoma invasion can be classified into collagenases (MMP-1), gelatinases (MMP-2 and MMP-9), stromelysins (MMP-3), and membrane type (MMP-14) according to their function and location. TIMPs (TIMP-1, TIMP-2, TIMP-3, and TIMP-4) and reversion-inducing cysteine-rich protein with Kazal motifs (RECK) act as inhibitors, and extracellular matrix metalloproteinase inducer (EMMPRIN) acts as the inducer of MMPs.

MMP-9 is the first matrix metalloproteinase found to have a significantly higher expression level in pituitary adenomas invaded to cavernous sinus (68). However, TIMP-1 was undetectable by immunochemistry staining in all samples (69). The correlation between MMP-9 overexpression and invasiveness of pituitary adenomas has been verified by many researchers in human pituitary adenoma specimens (70–75) as well as cell lines (76). Later studies showed that high expression levels of EMMPRIN (77, 78), MMP-2 (71, 75, 79), and MMP-14 (80, 81) and low expression levels of TIMP-2 (82, 83), TIMP-3 (82, 84), and RECK (85) were also correlated with invasiveness. There is a report that found TIMP-2 have higher expression in more patients of invasive prolactinomas then non-invasive ones (74), most of the aforementioned studies were performed on patients with prolactinoma or mixed patients of all secreting types, the contradicting results of TIMP-2 indicating that different types of pituitary adenoma might have distinct signaling pathways regarding to invasiveness. However, no statistical difference in the MMP-9 expression level between invasive and non-invasive non-functioning pituitary adenomas could be found (86).

MMP-9 plays an important role in promoting invasiveness in many type of pituitary adenomas. A transcriptome analysis on somatotroph pituitary adenomas (87) identified genes having a differential expression pattern between the two groups depending on the invasiveness. Hepatocellular carcinoma, downregulated 1 (HEPN1) was found to be less expressed in invasive somatotroph pituitary adenoma. First found to be downregulated in hepatocellular carcinoma. HEPN1 can induce apoptosis when overexpressed in HepG2 (88). In rodent cell lines GH3 and GT1-1, it inhibited the expression of MMP-2 and MMP-9, resulting in reduced invasiveness (87). A transcriptome and proteome analyses on pituitary null cell adenomas, a subtype of non-functioning pituitary adenomas, by the same research team (89), identified that upregulated IL-6R/JAK2/STAT3 promoted invasiveness via MMP-9.

MMPs not only promote invasiveness by the degradation of ECM and the consequential release of various ECM-anchored growth factors (90, 91), other functions are also observed. Interfering with the expression of MMP-14 using shRNA could result in the reduced expression of PTTG, VEGF, and TGFβ in rodent AtT-20 cells (80), implying that MMPs would also directly promote tumor growth and angiogenesis. IL-17 and IL-17 receptors were positively related to MMP-19 in terms of expression levels. The levels were all elevated in invasive pituitary adenomas compared with non-invasive ones (92).

More recent studies have demonstrated the difference in genotyping of patients with pituitary adenoma; polymorphisms of MMP-9 (93) and promoter of MMP-1 (94) could affect invasive phenotype. Other proteases were also demonstrated to promote the invasiveness of human pituitary adenomas, including a disintegrin and metalloproteinase 12 (ADAM12) (81) and serine proteases urokinase-type plasminogen activator (uPA) (83). Interestingly, the same research team reported the involvement of ADAM12 in invasiveness. They later demonstrated that

ADAM12 was also involved in epithelial-to-mesenchymal transition (EMT) (95).

Enhancer of zeste homolog 2 (EZH2) is widely involved in many cancers. It is a key catalytic component in polycomb repressive complex 2 (PRC2), which is responsible for the methylation modification of many development- and differentiation-related genes. It is therefore important in tumorigenesis of many human cancers (96). The overexpression of EZH2 in pituitary tumors was found to be related to invasiveness possibly via the upregulation of MMP-14 (97).

Potentials of MMP Inhibitors in Treating Pituitary Adenoma

Efforts were made to evaluate the potential of MMP inhibitor in treating invasive and chemotherapy-refractory pituitary adenomas. Batimastat showed inhibitory effect on the rat prolactinoma model (98) by reducing the cell proliferation rate and promoting the apoptosis.

EMT AND INVASIVE PITUITARY ADENOMA

EMT is a process that increases the invasiveness of tumor characterized by the loss of epithelial-cadherin (E-cadherin) and the enhanced expression of transcription factor snail family transcriptional repressor 1 (SNAI1) gene (also referred to as Snail), transcription factor snail family transcriptional repressor 2 (SNAI2) gene (also referred to as Slug), forkhead box C1 (FOXC1), twist-related protein 1(TWIST1), neural cadherin (N-cadherin), and Vimentin.

In an early study employing immunohistochemistry on 30 pituitary adenomas, the semi-quantified immunoreactivity of E-cadherin level was not correlated with cavernous sinus invasion (99). A follow-up study with larger sample size and better methodology, using quantitative real-time polymerase chain reaction on cadherin 13 (CDH13) and immunohistochemistry on E-cadherin and β-catenin, demonstrated the expected significantly lower expression levels of E-cadherin (100–102), CHD13 (101), and β-catenin (100, 102) in invasive pituitary adenomas, resulting from a more frequently methylated CDH13 and E-cadherin genes (101). Also, a study reported the nuclear accumulation and translocation of E-cadherin (103), suggesting another possible mechanism for the less expressed E-cadherin in invasive pituitary adenomas.

In a microarray analysis of human somatotroph adenomas, epithelial splicing regulatory protein 1(ESRP1) was differentially expressed in two groups with relatively low or high transcription levels of E-cadherin; the results were validated with RT-PCR and *in vivo* experiment in GH3 cells. A gene set comprising ESRP1, PKP2, TP53, PERP, IRF6, ROBO1, BICC1, SPINT1, and of course, CDH1 (E-cadherin) was also found to have reduced expression levels (104). With the same sample set, they demonstrated that it was possible to accurately discriminate invasive pituitary adenomas from non-invasive ones using the binary tree analysis on a group of genes including ESRP1, CDH1, and CTNNb1. Therefore, the potential EMT and invasiveness promoting function of genes in this set makes them valuable targets worth further investigation. Among them, the expression level of ESRP1 was confirmed related to the invasiveness of prolactinoma and GH-secreting adenoma later (105).

A number of miRNAs were reported to regulate EMT. The overexpressed miR-133 could upregulate the expression of E-cadherin and downregulate the expression of N-cadherin and Snail (106). The overexpression of miR-132, miR-15a, and miR-16 could downregulate the expression of N-cadherin and TWIST1 genes (107). The expression of Slug was positively correlated with ERα and invasiveness in clinical pituitary adenoma specimens (56), showing that the ERα-Slug–E-cadherin pathway was vital in the invasiveness of pituitary adenomas. The overexpression of miR-133 suppressed invasion by downregulating the expression of transcription factor forkhead box C1 (FOXC1) in HP75 cells (106), implying the involvement of miR-133 in EMT; FOXC1 is a known promoter of EMT (108).

PTTG-induced EMT is an important mechanism of tumor invasiveness and metastasis in lung cancer (109) and ovarian cancer (110). However, its involvement in pituitary adenomas has not been elucidated yet.

MiRNAs AND INVASIVE PITUITARY ADENOMA

Available evidence shows that the levels of miR-24, miR-34a, miR-93 (111), miR-148-3p, miR-152 (112), miR-132, miR-15a, and miR-16 (107) are significantly lower in invasive pituitary adenomas (111) compared with non-invasive ones. The overexpression of miR-148-3p and miR-152 suppressed invasion by downregulating activated leukocyte cell adhesion molecule (ALCAM) in rodent GH3 cells (112). Also, the overexpression of miR-132, miR-15a, and miR-16 suppressed invasion by downregulating sex-determining region Y-box protein 5 (Sox5) gene in rodent GH3 cells (107). Some miRNAs are reported to have elevated expression levels in invasive pituitary adenomas. MiR-93-5p was overexpressed in invasive (113) corticotroph pituitary adenomas. The expression of miR-106b-5p, miR-93-5p, miR-93-3p, and miR-25-3p, as a cluster, is also positively correlated with invasiveness. The enhanced expression of miR-106b can induce invasiveness via PI3K/PTEN/Akt pathway and sequential overexpression of MMP-9 in HP75 cells (114). Using a miRNA microarray, many differentially expressed miRNAs in non-functioning pituitary adenomas was identified in a single study. The expression levels of miR-181b-5p, miR-181d, miR-191-3p, and miR-598 were upregulated, and the expression levels of miR-3676-5p and miR-383 were downregulated (115). Caveolin-1 (Cav-1) was reported to promote invasiveness via the EGR1/KLF5 pathway in GH3 cells. Its knockdown resulted in a cytoplasmic enrichment of EGR1, which then induced miR-145, miR-124, and miR-183 targeting FSCN1, PTTG1IP, and EZR, respectively (116). MiRNAs are critical in prompting invasiveness in pituitary adenoma, many molecules and pathways are involved, miRNA sequencing would be a proper method comprehensively identifying differentiatly expressed miRNAs, after which targets of these miRNAs can be predicted with

bioinformatics tools, functions of them would then be validated with pertinence.

OTHER GENES INVOLVED IN THE INVASIVENESS OF PITUITARY ADENOMA

In a prospective study on 94 patients with prolactinoma, A Disintegrin And Metalloproteinase With Thrombospondin Motifs 6 (ADAMTS6) and Collapsin Response Mediator Protein 1 (CRMP1) were found to be positively related to invasiveness, while the overexpression of PTTG, Cyclin B1(CCNB1), Aurora Kinase B(AURKB), and Centromere Protein E(CENPE) indicated both invasive and aggressive behavior (51), these genes are all mitosis or development related, they might be the key biological processes that transduce invasiveness transformation. A causative CDH23 gene mutation was identified in a family of familial pituitary adenoma and sporadic patients with this mutation have non-invasive phenotype (117). Secreted frizzled-related protein 1(sFRP1) and Wnt inhibitory factor 1(WIF-1) genes were found to be less expressed in invasive non-functioning pituitary adenomas (118). Also, transforming growth factor, beta receptor II(TGFβII), is less expressed in invasive non-functioning pituitary adenomas (119).

Epidermal growth factor-like domain multiple 7(EGFL7) has a higher level of cytoplasmic expression in invasive growth hormone–secreting pituitary adenomas (120), and is positively correlated with Notch2 and Dll3 in knockdown experiments on GH3 cells. Later the invasiveness reduction phenomenon was reported after the knockdown of EGFL7 in GH3 and GT1-1 cells *in vitro* (121), confirming EGFL7 as a valuable therapeutic target.

Recent reports implied that long non-coding RNAs (lncRNAs) were involved in invasiveness. The expression of lncRNA C5orf66-AS1 was downregulated and inversely related to invasiveness in pituitary null cell adenoma compared with normal pituitary and non-invasive ones (122). However, lncRNA H19 was upregulated in invasive growth hormone–secreting pituitary adenomas (123).

Epigenetic modification of certain genes has been proved to induce invasiveness in pituitary adenomas including P16, DAPK, and Rb1 (124–129), these genes could be new targets of therapy (130). High throughput sequencing of methylation status (i.e., ChIP-sequencing) in the future will hopefully provide us with the global view of the epigenome of pituitary adenomas.

Next-generation sequencing (NGS) is a powerful tool discovering new disease-related genes at a relatively low cost, especially RNA sequencing and whole-exome sequencing. Using NGS on invasive pituitary adenomas and 6 non-invasive pituitary adenomas, 15 genes with pathogenic mutations were identified (131), including EGFL7, LRP1B, MGAM, MAST4, DSPP, PRDM2, PRDM8, ZNF717, LRRC50, TRIOBP, MX2, DPCR1, PRB3, SPANXN2, and KIAA0226. They also reported that CAT, CLU, CHGA, EZR, KRT8, LIMA1, SH3GLB2, and SLC2A1 were invasion-related genes in non-functioning pituitary adenomas (132). And data mining on existing pituitary adenoma RNA sequencing data from the National Center for Biotechnology Information Gene Expression Omnibus identified invasion-associated genes (133), including CLDN7, CNTNAP2, ITGA6, JAM3, PTPRC, and CTNNA1. All these genes could be the critical cause for invasiveness, which needs further exploration.

CONCLUSIONS AND PERSPECTIVE

Efforts were made to elucidate the molecular mechanisms of the invasiveness in pituitary adenomas, from the observation of possible biomarkers on tumor specimens to function verification experiments *in vitro*, and to recent application of multi-omics analysis. Yet, the whole picture is unclear because the molecular basis of invasiveness is highly complex involving multiple genes, proteins, and pathways. What makes it even more difficult is the fact that subtypes of pituitary adenomas are different in many ways rather than just the hormone they secrete.

Luckily, studies in the last two decades provide some clues in this regard. The key nodes of the invasiveness molecular network are easily spotted out in the review of literature. As shown in **Figure 2**, HIF-1α, PTTG, VEGF, FGF-2, and MMPs (mainly MMP-2 and MMP-9) are core molecules responsible for invasiveness owing to their ability to directly or indirectly induce cell proliferation, EMT, angiogenesis, degradation, and remodeling of ECM. HIF-1α induced by hypoxia or apoplexy inside the adenoma might be the initiating factor of invasive transformation, followed with angiogenesis for overexpressed VEGF, EMT for overexpressed PTTG, degradation of ECM for overexpressed MMPs, creating a suitable microenvironment within the tumor. Next generation sequencing could be the

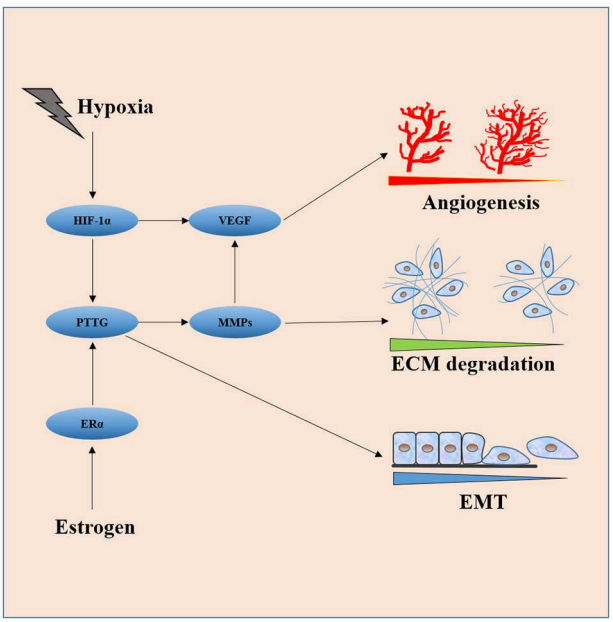

FIGURE 2 | Interaction of core molecules with each other and their relationship with EMT, angiogenesis, and ECM degradation. HIF-1α induced by hypoxia or apoplexy inside the adenoma might be the initiating factor of invasive transformation, followed with angiogenesis for overexpressed VEGF, EMT for overexpressed PTTG, degradation of ECM for overexpressed MMPs.

next point of breakthrough for the investigation of pituitary adenomas, high throughput genomic data on methylation status, expression, copy number variance $$et al. on bulk samples and single cell level would push our understanding of the invasive pituitary adenomas to a much higher level.

Many of the studies demonstrated interactions between these molecules both *in vivo* and *in vitro*. Most of them focusing on the invasiveness of pituitary adenomas finally came down to the conclusion that a molecule or part of the network was involved. This network is far from complete, and the factors inducing the aforementioned changes are still not known.

More systemic investigations are required to fully understand the mechanisms of the invasiveness of different subtypes of pituitary adenomas. Attempts can still be made targeting one or many molecules at a time, to the invention of new drugs or testing existing chemicals on certain molecules.

AUTHOR CONTRIBUTIONS

XL designed the study. QY performed the research and wrote the paper. All authors listed have made a substantial, direct and intellectual contribution to the work, and approved it for publication.

FUNDING

This study was supported by the National Natural Science Foundation of China (Grant No. 81770781).

REFERENCES

1. Landman RE, Horwith M, Peterson RE, Khandji AG, Wardlaw SL. Long-term survival with ACTH-secreting carcinoma of the pituitary: a case report and review of the literature. *J Clin Endocrinol Metab.* (2002) 87:3084–9. doi: 10.1210/jcem.87.7.8667
2. Ezzat S, Asa SL, Couldwell WT, Barr CE, Dodge WE, Vance ML, et al. The prevalence of pituitary adenomas: a systematic review. *Cancer* (2004) 101:613–9. doi: 10.1002/cncr.20412
3. Scheithauer BW, Kovacs KT, Laws ER Jr, Randall RV. Pathology of invasive pituitary tumors with special reference to functional classification. *J Neurosurg.* (1986) 65:733–44. doi: 10.3171/jns.1986.65.6.0733
4. Raverot G, Burman P, McCormack A, Heaney A, Petersenn S, Popovic V, et al. European society of endocrinology clinical practice guidelines for the management of aggressive pituitary tumours and carcinomas. *Eur J Endocrinol.* (2018) 178:G1–24. doi: 10.1530/EJE-17-0796
5. Di Ieva A, Rotondo F, Syro LV, Cusimano MD, Kovacs K. Aggressive pituitary adenomas–diagnosis and emerging treatments. *Nat Rev Endocrinol.* (2014) 10:423–35. doi: 10.1038/nrendo.2014.64
6. Miermeister CP, Petersenn S, Buchfelder M, Fahlbusch R, Ludecke DK, Holsken A, et al. Histological criteria for atypical pituitary adenomas - data from the German pituitary adenoma registry suggests modifications. *Acta Neuropathol Commun.* (2015) 3:50. doi: 10.1186/s40478-015-0229-8
7. Lopes MBS. The 2017 World Health Organization classification of tumors of the pituitary gland: a summary. *Acta Neuropathol.* (2017) 134:521–35. doi: 10.1007/s00401-017-1769-8
8. Mete O, Lopes MB. Overview of the 2017 WHO classification of pituitary tumors. *Endocr Pathol.* (2017) 28:228–43. doi: 10.1007/s12022-017-9498-z
9. Dworakowska D, Grossman AB. Aggressive and malignant pituitary tumours: state-of-the-art. *Endocr Relat Cancer* (2018) 25:R559–75. doi: 10.1530/ERC-18-0228
10. Al-Shraim M, Asa SL. The 2004 World Health Organization classification of pituitary tumors: what is new? *Acta Neuropathol.* (2006) 111:1–7. doi: 10.1007/s00401-005-1093-6
11. Turner HE, Nagy Z, Gatter KC, Esiri MM, Harris AL, Wass JA. Angiogenesis in pituitary adenomas-relationship to endocrine function, treatment and outcome. *J Endocrinol.* (2000) 165:475–81. doi: 10.1677/joe.0.1650475
12. Viacava P, Gasperi M, Acerbi G, Manetti L, Cecconi E, Bonadio AG, et al. Microvascular density and vascular endothelial growth factor expression in normal pituitary tissue and pituitary adenomas. *J Endocrinol Invest.* (2003) 26:23–8. doi: 10.1007/BF03345118
13. Takada K, Yamada S, Teramoto A. Correlation between tumor vascularity and clinical findings in patients with pituitary adenomas. *Endocr Pathol.* (2004) 15:131–9. doi: 10.1385/EP:15:2:131
14. Takano S, Akutsu H, Hara T, Yamamoto T, Matsumura A. Correlations of vascular architecture and angiogenesis with pituitary adenoma histotype. *Int J Endocrinol.* (2014) 2014:989574. doi: 10.1155/2014/989574
15. Cristina C, Luque GM, Demarchi G, Lopez Vicchi F, Zubeldia-Brenner L, Perez Millan MI, et al. Angiogenesis in pituitary adenomas: human studies and new mutant mouse models. *Int J Endocrinol.* (2014) 2014:608497. doi: 10.1155/2014/608497
16. Sanchez-Ortiga R, Sanchez-Tejada L, Moreno-Perez O, Riesgo P, Niveiro M, Pico Alfonso AM. Over-expression of vascular endothelial growth factor in pituitary adenomas is associated with extrasellar growth and recurrence. *Pituitary* (2013) 16:370–7. doi: 10.1007/s11102-012-0434-4
17. Jin Kim Y, Hyun Kim C, Hwan Cheong J, Min Kim J. Relationship between expression of vascular endothelial growth factor and intratumoral hemorrhage in human pituitary adenomas. *Tumori* (2011) 97:639–46. doi: 10.1177/030089161109700517
18. Zhan X, Desiderio DM. Signaling pathway networks mined from human pituitary adenoma proteomics data. *BMC Med Genomics* (2010) 3:13. doi: 10.1186/1755-8794-3-13
19. Wang F, Shu K, Lei T, Xue D. The expression of integrinbeta1 and FAK in pituitary adenomas and their correlation with invasiveness. *J Huazhong Univ Sci Technol Med Sci.* (2008) 28:572–5. doi: 10.1007/s11596-008-0518-6
20. Zhao C, Zhang M, Liu W, Wang C, Zhang Q, Li W. beta-Catenin knockdown inhibits pituitary adenoma cell proliferation and invasion via interfering with AKT and gelatinases expression. *Int J Oncol.* (2015) 46:1643–50. doi: 10.3892/ijo.2015.2862
21. Kanasaki H, Fukunaga K, Takahashi K, Miyazaki K, Miyamoto E. Involvement of p38 mitogen-activated protein kinase activation in bromocriptine-induced apoptosis in rat pituitary GH3 cells. *Biol Reprod.* (2000) 62:1486–94. doi: 10.1095/biolreprod62.6.1486
22. Onofri C, Theodoropoulou M, Losa M, Uhl E, Lange M, Arzt E, et al. Localization of vascular endothelial growth factor (VEGF) receptors in normal and adenomatous pituitaries: detection of a non-endothelial function of VEGF in pituitary tumours. *J Endocrinol.* (2006) 191:249–61. doi: 10.1677/joe.1.06992
23. Elaimy AL, Guru S, Chang C, Ou J, Amante JJ, Zhu LJ, et al. VEGF-neuropilin-2 signaling promotes stem-like traits in breast cancer cells by TAZ-mediated repression of the Rac GAP beta2-chimaerin. *Sci Signal.* (2018) 11:eaao6897. doi: 10.1126/scisignal.aao6897
24. Voron T, Colussi O, Marcheteau E, Pernot S, Nizard M, Pointet AL, et al. VEGF-A modulates expression of inhibitory checkpoints on CD8+ T cells in tumors. *J Exp Med.* (2015) 212:139–48. doi: 10.1084/jem.20140559
25. Xiao Z, Liu Q, Mao F, Wu J, Lei T. TNF-alpha-induced VEGF and MMP-9 expression promotes hemorrhagic transformation in pituitary adenomas. *Int J Mol Sci.* (2011) 12:4165–79. doi: 10.3390/ijms12064165
26. Yoshida D, Kim K, Noha M, Teramoto A. Anti-apoptotic action by hypoxia inducible factor 1-alpha in human pituitary adenoma cell line, HP-75 in hypoxic condition. *J Neurooncol.* (2006) 78:217–25. doi: 10.1007/s11060-005-9017-9
27. Xiao Z, Liu Q, Zhao B, Wu J, Lei T. Hypoxia induces hemorrhagic transformation in pituitary adenomas via the HIF-1alpha signaling pathway. *Oncol Rep.* (2011) 26:1457–64. doi: 10.3892/or.2011.1416
28. Carbia-Nagashima A, Gerez J, Perez-Castro C, Paez-Pereda M, Silberstein S, Stalla G, et al. RSUME, a small RWD-containing protein, enhances

SUMO conjugation and stabilizes HIF-1alpha during hypoxia. *Cell* (2007) 131:309–23. doi: 10.1016/j.cell.2007.07.044
29. Shan B, Gerez J, Haedo M, Fuertes M, Theodoropoulou M, Buchfelder M, et al. RSUME is implicated in HIF-1-induced VEGF-A production in pituitary tumour cells. *Endocr Relat Cancer* (2012) 19:13–27. doi: 10.1530/ERC-11-0211
30. He W, Huang L, Shen X, Yang Y, Wang D, Yang Y, et al. Relationship between RSUME and HIF-1alpha/VEGF-A with invasion of pituitary adenoma. *Gene* (2017) 603:54–60. doi: 10.1016/j.gene.2016.12.012
31. Shimoda Y, Ogawa Y, Watanabe M, Tominaga T. Clinicopathological investigation of vascular endothelial growth factor and von Hippel-Lindau gene-related protein expression in immunohistochemically negative pituitary adenoma–possible involvement in tumor aggressiveness. *Endocr Res.* (2013) 38:242–50. doi: 10.3109/07435800.2013.774411
32. Tudorancea A, Francois P, Trouillas J, Cottier JP, Girard JJ, Jan M, et al. Von Hippel-Lindau disease and aggressive GH-PRL pituitary adenoma in a young boy. *Ann Endocrinol.* (2012) 73:37–42. doi: 10.1016/j.ando.2011.12.001
33. Seghezzi G, Patel S, Ren CJ, Gualandris A, Pintucci G, Robbins ES, et al. Fibroblast growth factor-2 (FGF-2) induces vascular endothelial growth factor (VEGF) expression in the endothelial cells of forming capillaries: an autocrine mechanism contributing to angiogenesis. *J Cell Biol.* (1998) 141:1659–73. doi: 10.1083/jcb.141.7.1659
34. Lombardero M, Vidal S, Hurta R, Roman A, Kovacs K, Lloyd RV, et al. Modulation of VEGF/Flk-1 receptor expression in the rat pituitary GH3 cell line by growth factors. *Pituitary* (2006) 9:137–43. doi: 10.1007/s11102-006-9989-2
35. Horiguchi H, Jin L, Ruebel KH, Scheithauer BW, Lloyd RV. Regulation of VEGF-A, VEGFR-I, thrombospondin-1,−2, and−3 expression in a human pituitary cell line (HP75) by TGFbeta1, bFGF, and EGF. *Endocrine* (2004) 24:141–6. doi: 10.1385/ENDO:24:2:141
36. McCabe CJ, Khaira JS, Boelaert K, Heaney AP, Tannahill LA, Hussain S, et al. Expression of pituitary tumour transforming gene (PTTG) and fibroblast growth factor-2 (FGF-2) in human pituitary adenomas: relationships to clinical tumour behaviour. *Clin Endocrinol.* (2003) 58:141–50. doi: 10.1046/j.1365-2265.2003.01598.x
37. Lv H, Li C, Gui S, Zhang Y. Expression of estrogen receptor alpha and growth factors in human prolactinoma and its correlation with clinical features and gender. *J Endocrinol Invest.* (2012) 35:174–80. doi: 10.3275/7607
38. Atkin SL, Landolt AM, Jeffreys RV, Diver M, Radcliffe J, White MC. Basic fibroblastic growth factor stimulates prolactin secretion from human anterior pituitary adenomas without affecting adenoma cell proliferation. *J Clin Endocrinol Metab.* (1993) 77:831–7.
39. Onofri C, Carbia Nagashima A, Schaaf L, Feirer M, Lohrer P, Stummer W, et al. Estradiol stimulates vascular endothelial growth factor and interleukin-6 in human lactotroph and lactosomatotroph pituitary adenomas. *Exp Clin Endocrinol Diabetes* (2004) 112:18–23. doi: 10.1055/s-2004-815722
40. Schaaf C, Shan B, Onofri C, Stalla GK, Arzt E, Schilling T, et al. Curcumin inhibits the growth, induces apoptosis and modulates the function of pituitary folliculostellate cells. *Neuroendocrinology* (2010) 91:200–10. doi: 10.1159/000287236
41. Luque GM, Perez-Millan MI, Ornstein AM, Cristina C, Becu-Villalobos D. Inhibitory effects of antivascular endothelial growth factor strategies in experimental dopamine-resistant prolactinomas. *J Pharmacol Exp Ther.* (2011) 337:766–74. doi: 10.1124/jpet.110.177790
42. Gagliano T, Filieri C, Minoia M, Buratto M, Tagliati F, Ambrosio MR, et al. Cabergoline reduces cell viability in non-functioning pituitary adenomas by inhibiting vascular endothelial growth factor secretion. *Pituitary* (2013) 16:91–100. doi: 10.1007/s11102-012-0380-1
43. Shan B, Schaaf C, Schmidt A, Lucia K, Buchfelder M, Losa M, et al. Curcumin suppresses HIF1A synthesis and VEGFA release in pituitary adenomas. *J Endocrinol.* (2012) 214:389–98. doi: 10.1530/JOE-12-0207
44. Kun Z, Yuling Y, Dongchun W, Bingbing X, Xiaoli L, Bin X. HIF-1alpha inhibition sensitized pituitary adenoma cells to temozolomide by regulating presenilin 1 expression and autophagy. *Technol Cancer Res Treat* (2016) 15:NP95–104. doi: 10.1177/1533034615618834
45. Zhao Y, Xiao Z, Chen W, Yang J, Li T, Fan B. Disulfiram sensitizes pituitary adenoma cells to temozolomide by regulating O6-methylguanine-DNA methyltransferase expression. *Mol Med Rep.* (2015) 12:2313–22. doi: 10.3892/mmr.2015.3664
46. Pei L, Melmed S. Isolation and characterization of a pituitary tumor-transforming gene (PTTG). *Mol Endocrinol.* (1997) 11:433–41. doi: 10.1210/mend.11.4.9911
47. McCabe CJ, Boelaert K, Tannahill LA, Heaney AP, Stratford AL, Khaira JS, et al. Vascular endothelial growth factor, its receptor KDR/Flk-1, and pituitary tumor transforming gene in pituitary tumors. *J Clin Endocrinol Metab.* (2002) 87:4238–44. doi: 10.1210/jc.2002-020309
48. Zou H, McGarry TJ, Bernal T, Kirschner MW. Identification of a vertebrate sister-chromatid separation inhibitor involved in transformation and tumorigenesis. *Science* (1999) 285:418–22. doi: 10.1126/science.285.5426.418
49. Zhang X, Horwitz GA, Heaney AP, Nakashima M, Prezant TR, Bronstein MD, et al. Pituitary tumor transforming gene (PTTG) expression in pituitary adenomas. *J Clin Endocrinol Metab.* (1999) 84:761–7. doi: 10.1210/jcem.84.2.5432
50. Filippella M, Galland F, Kujas M, Young J, Faggiano A, Lombardi G, et al. Pituitary tumour transforming gene (PTTG) expression correlates with the proliferative activity and recurrence status of pituitary adenomas: a clinical and immunohistochemical study. *Clin Endocrinol.* (2006) 65:536–43. doi: 10.1111/j.1365-2265.2006.02630.x
51. Raverot G, Wierinckx A, Dantony E, Auger C, Chapas G, Villeneuve L, et al. Prognostic factors in prolactin pituitary tumors: clinical, histological, and molecular data from a series of 94 patients with a long postoperative follow-up. *J Clin Endocrinol Metab.* (2010) 95:1708–16. doi: 10.1210/jc.2009-1191
52. Robertson AM, Heaney AP. Molecular markers in pituitary tumors. *Curr Opin Endocrinol Diabetes Obes.* (2016) 23:324–30. doi: 10.1097/MED.0000000000000266
53. Li Y, Zhou LP, Ma P, Sui CG, Meng FD, Tian X, et al. Relationship of PTTG expression with tumor invasiveness and microvessel density of pituitary adenomas: a meta-analysis. *Genet Test Mol Biomarkers* (2014) 18:279–85. doi: 10.1089/gtmb.2013.0447
54. Chesnokova V, Melmed S. Pituitary senescence: the evolving role of Pttg. *Mol Cell Endocrinol.* (2010) 326:55–9. doi: 10.1016/j.mce.2010.02.012
55. Pereira-Lima JF, Marroni CP, Pizarro CB, Barbosa-Coutinho LM, Ferreira NP, Oliveira MC. Immunohistochemical detection of estrogen receptor alpha in pituitary adenomas and its correlation with cellular replication. *Neuroendocrinology* (2004) 79:119–24. doi: 10.1159/000077269
56. Zhou W, Song Y, Xu H, Zhou K, Zhang W, Chen J, et al. In non-functional pituitary adenomas, estrogen receptors and slug contribute to development of invasiveness. *J Clin Endocrinol Metab.* (2011) 96:E1237–45. doi: 10.1210/jc.2010-3040
57. Heaney AP, Horwitz GA, Wang Z, Singson R, Melmed S. Early involvement of estrogen-induced pituitary tumor transforming gene and fibroblast growth factor expression in prolactinoma pathogenesis. *Nat Med.* (1999) 5:1317–21. doi: 10.1038/15275
58. Heaney AP, Fernando M, Melmed S. Functional role of estrogen in pituitary tumor pathogenesis. *J Clin Invest.* (2002) 109:277–83. doi: 10.1172/JCI0214264
59. Ozkaya HM, Comunoglu N, Keskin FE, Oz B, Haliloglu OA, Tanriover N, et al. Locally produced estrogen through aromatization might enhance tissue expression of pituitary tumor transforming gene and fibroblast growth factor 2 in growth hormone-secreting adenomas. *Endocrine* (2016) 52:632–40. doi: 10.1007/s12020-015-0802-8
60. Kandouz M, Batist G. Gap junctions and connexins as therapeutic targets in cancer. *Expert Opin Ther Targets* (2010) 14:681–92. doi: 10.1517/14728222.2010.487866
61. Chevallier D, Carette D, Gilleron J, Segretain D, Pointis G. The emerging role of connexin 43 in testis pathogenesis. *Curr Mol Med.* (2013) 13:1331–44. doi: 10.2174/15665240113139990066
62. Chevallier D, Carette D, Segretain D, Gilleron J, Pointis G. Connexin 43 a check-point component of cell proliferation implicated in a wide range of human testis diseases. *Cell Mol Life Sci.* (2013) 70:1207–20. doi: 10.1007/s00018-012-1121-3

63. McLachlan E, Shao Q, Laird DW. Connexins and gap junctions in mammary gland development and breast cancer progression. *J Membr Biol.* (2007) 218:107–21. doi: 10.1007/s00232-007-9052-x
64. Grek CL, Rhett JM, Bruce JS, Ghatnekar GS, Yeh ES. Connexin 43, breast cancer tumor suppressor: missed connections? *Cancer Lett.* (2016) 374:117–26. doi: 10.1016/j.canlet.2016.02.008
65. Kanczuga-Koda L, Koda M, Sulkowski S, Wincewicz A, Zalewski B, Sulkowska M. Gradual loss of functional gap junction within progression of colorectal cancer – a shift from membranous CX32 and CX43 expression to cytoplasmic pattern during colorectal carcinogenesis. *In Vivo* (2010) 24:101–7. Available online at: http://iv.iiarjournals.org/content/24/1/101.long
66. Wang H, Zhang Y, Zhou A, Zhang R, Meng Q. Effects of silencing connexin43 on expression of pituitary tumor-transforming gene in prolactinomas. *Neurol Res.* (2015) 37:153–8. doi: 10.1179/1743132814Y.0000000419
67. Malik MT, Kakar SS. Regulation of angiogenesis and invasion by human Pituitary tumor transforming gene (PTTG) through increased expression and secretion of matrix metalloproteinase-2 (MMP-2). *Mol Cancer* (2006) 5:61. doi: 10.1186/1476-4598-5-61
68. Kawamoto H, Uozumi T, Kawamoto K, Arita K, Yano T, Hirohata T. Type IV collagenase activity and cavernous sinus invasion in human pituitary adenomas. *Acta Neurochir* (1996) 138:390–5. doi: 10.1007/BF01420300
69. Kawamoto H, Kawamoto K, Mizoue T, Uozumi T, Arita K, Kurisu K. Matrix metalloproteinase-9 secretion by human pituitary adenomas detected by cell immunoblot analysis. *Acta Neurochir* (1996) 138:1442–8. doi: 10.1007/BF01411124
70. Turner HE, Nagy Z, Esiri MM, Harris AL, Wass JA. Role of matrix metalloproteinase 9 in pituitary tumor behavior. *J Clin Endocrinol Metab.* (2000) 85:2931–5. doi: 10.1210/jcem.85.8.6754
71. Liu W, Matsumoto Y, Okada M, Miyake K, Kunishio K, Kawai N, et al. Matrix metalloproteinase 2 and 9 expression correlated with cavernous sinus invasion of pituitary adenomas. *J Med Invest.* (2005) 52:151–8. doi: 10.2152/jmi.52.151
72. Pan LX, Chen ZP, Liu YS, Zhao JH. Magnetic resonance imaging and biological markers in pituitary adenomas with invasion of the cavernous sinus space. *J Neurooncol.* (2005) 74:71–6. doi: 10.1007/s11060-004-6150-9
73. Gong J, Zhao Y, Abdel-Fattah R, Amos S, Xiao A, Lopes MB, et al. Matrix metalloproteinase-9, a potential biological marker in invasive pituitary adenomas. *Pituitary* (2008) 11:37–48. doi: 10.1007/s11102-007-0066-2
74. Gultekin GD, Cabuk B, Vural C, Ceylan S. Matrix metalloproteinase-9 and tissue inhibitor of matrix metalloproteinase-2: prognostic biological markers in invasive prolactinomas. *J Clin Neurosci.* (2015) 22:1282–7. doi: 10.1016/j.jocn.2015.02.021
75. Liu HY, Gu WJ, Wang CZ, Ji XJ, Mu YM. Matrix metalloproteinase-9 and−2 and tissue inhibitor of matrix metalloproteinase-2 in invasive pituitary adenomas: a systematic review and meta-analysis of case-control trials. *Medicine* (2016) 95:e3904. doi: 10.1097/MD.0000000000003904
76. Hussaini IM, Trotter C, Zhao Y, Abdel-Fattah R, Amos S, Xiao A, et al. Matrix metalloproteinase-9 is differentially expressed in non-functioning invasive and non-invasive pituitary adenomas and increases invasion in human pituitary adenoma cell line. *Am J Pathol.* (2007) 170:356–65. doi: 10.2353/ajpath.2007.060736
77. Qu X, Yang W, Jiang M, Han T, Han L, Qu Y, et al. CD147 expression in pituitary adenomas and its significance for clinical outcome. *Hum Pathol.* (2010) 41:1165–71. doi: 10.1016/j.humpath.2009.10.023
78. Zhang Y, He N, Zhou J, Chen Y. The relationship between MRI invasive features and expression of EMMPRIN, galectin-3, and microvessel density in pituitary adenoma. *Clin Imaging* (2011) 35:165–73. doi: 10.1016/j.clinimag.2010.06.002
79. Liu W, Kunishio K, Matsumoto Y, Okada M, Nagao S. Matrix metalloproteinase-2 expression correlates with cavernous sinus invasion in pituitary adenomas. *J Clin Neurosci.* (2005) 12:791–4. doi: 10.1016/j.jocn.2005.03.010
80. Hui P, Xu X, Xu L, Hui G, Wu S, Lan Q. Expression of MMP14 in invasive pituitary adenomas: relationship to invasion and angiogenesis. *Int J Clin Exp Pathol.* (2015) 8:3556–67.
81. Wang J, Voellger B, Benzel J, Schlomann U, Nimsky C, Bartsch JW, et al. Metalloproteinases ADAM12 and MMP-14 are associated with cavernous sinus invasion in pituitary adenomas. *Int J Cancer* (2016) 139:1327–39. doi: 10.1002/ijc.30173
82. Beaulieu E, Kachra Z, Mousseau N, Delbecchi L, Hardy J, Beliveau R. Matrix metalloproteinases and their inhibitors in human pituitary tumors. *Neurosurgery* (1999) 45:1432–40; discussion 1440–31. doi: 10.1097/00006123-199912000-00033
83. Knappe UJ, Hagel C, Lisboa BW, Wilczak W, Ludecke DK. Expression of serine proteases and metalloproteinases in human pituitary adenomas and anterior pituitary lobe tissue. *Acta Neuropathol.* (2003) 106:471–8. doi: 10.1007/s00401-003-0747-5
84. Sun B, Liu X, Yang Y, Dai C, Li Y, Jiao Y, et al. The clinical utility of TIMP3 expression in ACTH-secreting pituitary tumor. *J Mol Neurosci.* (2016) 58:137–44. doi: 10.1007/s12031-015-0698-z
85. Yoshida D, Nomura R, Teramoto A. Regulation of cell invasion and signalling pathways in the pituitary adenoma cell line, HP-75, by reversion-inducing cysteine-rich protein with kazal motifs (RECK). *J Neurooncol.* (2008) 89:141–50. doi: 10.1007/s11060-008-9606-5
86. Yokoyama S, Hirano H, Moroki K, Goto M, Imamura S, Kuratsu JI. Are non-functioning pituitary adenomas extending into the cavernous sinus aggressive and/or invasive? *Neurosurgery* (2001) 49:857–62; discussion 862–53. doi: 10.1097/00006123-200110000-00014
87. Peng H, Fan J, Wu J, Lang J, Wang J, Liu H, et al. Silencing of HEPN1 is responsible for the aggressive biological behavior of pituitary somatotroph adenomas. *Cell Physiol Biochem.* (2013) 31:379–88. doi: 10.1159/000343375
88. Moh MC, Lee LH, Yang X, Shen S. HEPN1, a novel gene that is frequently down-regulated in hepatocellular carcinoma, suppresses cell growth and induces apoptosis in HepG2 cells. *J Hepatol.* (2003) 39:580–6. doi: 10.1016/S0168-8278(03)00359-3
89. Feng J, Yu SY, Li CZ, Li ZY, Zhang YZ. Integrative proteomics and transcriptomics revealed that activation of the IL-6R/JAK2/STAT3/MMP9 signaling pathway is correlated with invasion of pituitary null cell adenomas. *Mol Cell Endocrinol.* (2016) 436:195–203. doi: 10.1016/j.mce.2016.07.025
90. Whitelock JM, Murdoch AD, Iozzo RV, Underwood PA. The degradation of human endothelial cell-derived perlecan and release of bound basic fibroblast growth factor by stromelysin, collagenase, plasmin, and heparanases. *J Biol Chem.* (1996) 271:10079–86. doi: 10.1074/jbc.271.17.10079
91. Paez Pereda M, Ledda MF, Goldberg V, Chervin A, Carrizo G, Molina H, et al. High levels of matrix metalloproteinases regulate proliferation and hormone secretion in pituitary cells. *J Clin Endocrinol Metab.* (2000) 85:263–9. doi: 10.1210/jc.85.1.263
92. Qiu L, He D, Fan X, Li Z, Liao C, Zhu Y, et al. The expression of interleukin (IL)-17 and IL-17 receptor and MMP-9 in human pituitary adenomas. *Pituitary* (2011) 14:266–75. doi: 10.1007/s11102-011-0292-5
93. Glebauskiene B, Liutkeviciene R, Vilkeviciute A, Kriauciuniene L, Jakstiene S, Zlatkute E, et al. Does MMP-9 gene polymorphism play a role in pituitary adenoma development? *Dis Markers* (2017) 2017:5839528. doi: 10.1155/2017/5839528
94. Altas M, Bayrak OF, Ayan E, Bolukbasi F, Silav G, Coskun KK, et al. The effect of polymorphisms in the promoter region of the MMP-1 gene on the occurrence and invasiveness of hypophyseal adenoma. *Acta Neurochir* (2010) 152:1611–7; discussion 1617. doi: 10.1007/s00701-010-0671-0
95. Wang J, Zhang Z, Li R, Mao F, Sun W, Chen J, et al. ADAM12 induces EMT and promotes cell migration, invasion and proliferation in pituitary adenomas via EGFR/ERK signaling pathway. *Biomed Pharmacother.* (2018) 97:1066–77. doi: 10.1016/j.biopha.2017.11.034
96. Volkel P, Dupret B, Le Bourhis X, Angrand PO. Diverse involvement of EZH2 in cancer epigenetics. *Am J Transl Res.* (2015) 7:175–93.
97. Liu B, Pang B, Wang Q, Yang S, Gao T, Ding Q, et al. EZH2 upregulation correlates with tumor invasiveness, proliferation, and angiogenesis in human pituitary adenomas. *Hum Pathol.* (2017) 66:101–7. doi: 10.1016/j.humpath.2017.03.028
98. Mucha SA, Melen-Mucha G, Godlewski A, Stepien H. Inhibition of estrogen-induced pituitary tumor growth and angiogenesis in Fischer 344 rats by the matrix metalloproteinase inhibitor batimastat. *Virchows Arch.* (2007) 450:335–41. doi: 10.1007/s00428-006-0351-x
99. Kawamoto H, Mizoue T, Arita K, Tominaga A, Eguchi K, Kurisu K. Expression of epithelial cadherin and cavernous sinus invasion

in human pituitary adenomas. *J Neurooncol.* (1997) 34:105–9. doi: 10.1023/A:1005709014239
100. Qian ZR, Li CC, Yamasaki H, Mizusawa N, Yoshimoto K, Yamada S, et al. Role of E-cadherin, alpha-, beta-, and gamma-catenins, and p120 (cell adhesion molecules) in prolactinoma behavior. *Mod Pathol.* (2002) 15:1357–65. doi: 10.1097/01.MP.0000039572.75188.1A
101. Qian ZR, Sano T, Yoshimoto K, Asa SL, Yamada S, Mizusawa N, et al. Tumor-specific downregulation and methylation of the CDH13 (H-cadherin) and CDH1 (E-cadherin) genes correlate with aggressiveness of human pituitary adenomas. *Mod Pathol.* (2007) 20:1269–77. doi: 10.1038/modpathol.3800965
102. Zhou K, Jin H, Luo Y. Expression and significance of E-cadherin and beta-catenins in pituitary adenoma. *Int J Surg Pathol.* (2013) 21:363–7. doi: 10.1177/1066896912471850
103. Elston MS, Gill AJ, Conaglen JV, Clarkson A, Cook RJ, Little NS, et al. Nuclear accumulation of e-cadherin correlates with loss of cytoplasmic membrane staining and invasion in pituitary adenomas. *J Clin Endocrinol Metab.* (2009) 94:1436–42. doi: 10.1210/jc.2008-2075
104. Lekva T, Berg JP, Fougner SL, Olstad OK, Ueland T, Bollerslev J. Gene expression profiling identifies ESRP1 as a potential regulator of epithelial mesenchymal transition in somatotroph adenomas from a large cohort of patients with acromegaly. *J Clin Endocrinol Metab.* (2012) 97:E1506–14. doi: 10.1210/jc.2012-1760
105. Chauvet N, Romano N, Meunier AC, Galibert E, Fontanaud P, Mathieu MN, et al. Combining cadherin expression with molecular markers discriminates invasiveness in growth hormone and prolactin pituitary adenomas. *J Neuroendocrinol.* (2016) 28:12352. doi: 10.1111/jne.12352
106. Wang DS, Zhang HQ, Zhang B, Yuan ZB, Yu ZK, Yang T, et al. miR-133 inhibits pituitary tumor cell migration and invasion via down-regulating FOXC1 expression. *Genet Mol Res.* (2016) 15:gmr7453. doi: 10.4238/gmr.15017453
107. Renjie W, Haiqian L. MiR-132, miR-15a and miR-16 synergistically inhibit pituitary tumor cell proliferation, invasion and migration by targeting Sox5. *Cancer Lett.* (2015) 356:568–78. doi: 10.1016/j.canlet.2014.10.003
108. Yu M, Bardia A, Wittner BS, Stott SL, Smas ME, Ting DT, et al. Circulating breast tumor cells exhibit dynamic changes in epithelial and mesenchymal composition. *Science* (2013) 339:580–4. doi: 10.1126/science.1228522
109. Shah PP, Fong MY, Kakar SS. PTTG induces EMT through integrin alphaVbeta3-focal adhesion kinase signaling in lung cancer cells. *Oncogene* (2012) 31:3124–35. doi: 10.1038/onc.2011.488
110. Shah PP, Kakar SS. Pituitary tumor transforming gene induces epithelial to mesenchymal transition by regulation of Twist, Snail, Slug, and E-cadherin. *Cancer Lett.* (2011) 311:66–76. doi: 10.1016/j.canlet.2011.06.033
111. Yu G, Wang H, Yu S, Li C, Bai J, Gui S, et al. Study on miRNAs' expression for the invasion of pituitary adenomas. *Turk Neurosurg.* (2017) 28:530–7. doi: 10.5137/1019-5149.JTN.20760-17.1
112. He W, Huang L, Li M, Yang Y, Chen Z, Shen X. MiR-148b, MiR-152/ALCAM axis regulates the proliferation and invasion of pituitary adenomas cells. *Cell Physiol Biochem.* (2017) 44:792–803. doi: 10.1159/000485342
113. Garbicz F, Mehlich D, Rak B, Sajjad E, Maksymowicz M, Paskal W, et al. Increased expression of the microRNA 106b∼25 cluster and its host gene MCM7 in corticotroph pituitary adenomas is associated with tumor invasion and Crooke's cell morphology. *Pituitary* (2017) 20:450–63. doi: 10.1007/s11102-017-0805-y
114. Zheng Z, Zhang Y, Zhang Z, Yang Y, Song T. Effect of miR-106b on invasiveness of pituitary adenoma via PTEN-PI3K/AKT. *Med Sci Monit.* (2017) 23:1277–85. doi: 10.12659/MSM.900092
115. Wu S, Gu Y, Huang Y, Wong T, Ding H, Liu T, et al. Novel biomarkers for non-functioning invasive pituitary adenomas were identified by using analysis of microRNAs expression profile. *Biochem Genet.* (2017) 55:253–67. doi: 10.1007/s10528-017-9794-9
116. Yang W, Xu T, Qiu P, Xu G. Caveolin-1 promotes pituitary adenoma cells migration and invasion by regulating the interaction between EGR1 and KLF5. *Exp Cell Res.* (2018) 367:7–14. doi: 10.1016/j.yexcr.2018.01.008
117. Zhang Q, Peng C, Song J, Zhang Y, Chen J, Song Z, et al. Germline mutations in CDH23, encoding cadherin-related 23, are associated with both familial and sporadic pituitary adenomas. *Am J Hum Genet.* (2017) 100:817–23. doi: 10.1016/j.ajhg.2017.03.011
118. Song W, Qian L, Jing G, Jie F, Xiaosong S, Chunhui L, et al. Aberrant expression of the sFRP and WIF1 genes in invasive non-functioning pituitary adenomas. *Mol Cell Endocrinol.* (2018) 474:168–75. doi: 10.1016/j.mce.2018.03.005
119. Gu YH, Feng YG. Down-regulation of TGF-beta RII expression is correlated with tumor growth and invasion in non-functioning pituitary adenomas. *J Clin Neurosci.* (2018) 47:264–8. doi: 10.1016/j.jocn.2017.07.033
120. Wang J, Liu Q, Gao H, Wan D, Li C, Li Z, et al. EGFL7 participates in regulating biological behavior of growth hormone-secreting pituitary adenomas via Notch2/DLL3 signaling pathway. *Tumour Biol.* (2017) 39:1010428317706203. doi: 10.1177/1010428317706203
121. Liu Q, Wang J, Yang H, Gao H, Li C, Lan X, et al. Attenuation of EGFL7 expression inhibits growth hormone-producing pituitary adenomas growth and invasion. *Hum Gene Ther.* (2018) 29:1396–406. doi: 10.1089/hum.2017.200
122. Yu G, Li C, Xie W, Wang Z, Gao H, Cao L, et al. Long non-coding RNA C5orf66-AS1 is downregulated in pituitary null cell adenomas and is associated with their invasiveness. *Oncol Rep.* (2017) 38:1140–8. doi: 10.3892/or.2017.5739
123. Lu T, Yu C, Ni H, Liang W, Yan H, Jin W. Expression of the long non-coding RNA H19 and MALAT-1 in growth hormone-secreting pituitary adenomas and its relationship to tumor behavior. *Int J Dev Neurosci.* (2018) 67:46–50. doi: 10.1016/j.ijdevneu.2018.03.009
124. Woloschak M, Yu A, Post KD. Frequent inactivation of the p16 gene in human pituitary tumors by gene methylation. *Mol Carcinog.* (1997) 19:221–4. doi: 10.1002/(SICI)1098-2744(199708)19:4<221::AID-MC1>;3.0.CO;2-F
125. Jaffrain-Rea ML, Ferretti E, Toniato E, Cannita K, Santoro A, Di Stefano D, et al. p16 (INK4a, MTS-1) gene polymorphism and methylation status in human pituitary tumours. *Clin Endocrinol.* (1999) 51:317–25. doi: 10.1046/j.1365-2265.1999.00774.x
126. Simpson DJ, Bicknell JE, McNicol AM, Clayton RN, Farrell WE. Hypermethylation of the p16/CDKN2A/MTSI gene and loss of protein expression is associated with non-functional pituitary adenomas but not somatotrophinomas. *Genes Chromosomes Cancer* (1999) 24:328–36. doi: 10.1002/(SICI)1098-2264(199904)24:4<328::AID-GCC6>;3.0.CO;2-P
127. Seemann N, Kuhn D, Wrocklage C, Keyvani K, Hackl W, Buchfelder M, et al. CDKN2A/p16 inactivation is related to pituitary adenoma type and size. *J Pathol.* (2001) 193:491–7. doi: 10.1002/path.833
128. Ogino A, Yoshino A, Katayama Y, Watanabe T, Ota T, Komine C, et al. The p15(INK4b)/p16(INK4a)/RB1 pathway is frequently deregulated in human pituitary adenomas. *J Neuropathol Exp Neurol.* (2005) 64:398–403. doi: 10.1093/jnen/64.5.398
129. Pease M, Ling C, Mack WJ, Wang K, Zada G. The role of epigenetic modification in tumorigenesis and progression of pituitary adenomas: a systematic review of the literature. *PLoS ONE* (2013) 8:e82619. doi: 10.1371/journal.pone.0082619
130. Yacqub-Usman K, Richardson A, Duong CV, Clayton RN, Farrell WE. The pituitary tumour epigenome: aberrations and prospects for targeted therapy. *Nat Rev Endocrinol.* (2012) 8:486–94. doi: 10.1038/nrendo.2012.54
131. Lan X, Gao H, Wang F, Feng J, Bai J, Zhao P, et al. Whole-exome sequencing identifies variants in invasive pituitary adenomas. *Oncol Lett.* (2016) 12:2319–28. doi: 10.3892/ol.2016.5029
132. Chen Y, Chuan HL, Yu SY, Li CZ, Wu ZB, Li GL, et al. A novel invasive-related biomarker in three subtypes of non-functioning pituitary adenomas. *World Neurosurg.* (2017) 100:514–21. doi: 10.1016/j.wneu.2017.01.010
133. Cao C, Wang W, Ma C, Jiang P. Computational analysis identifies invasion-associated genes in pituitary adenomas. *Mol Med Rep.* (2015) 12:1977–82. doi: 10.3892/mmr.2015.3564

Conflict of Interest Statement: The authors declare that the research was conducted in the absence of any commercial or financial relationships that could be construed as a potential conflict of interest.

frontiers in Endocrinology

CORRECTION
published: 24 September 2019
doi: 10.3389/fendo.2019.00657

Corrigendum: Molecular Network Basis of Invasive Pituitary Adenoma: A Review

*Qi Yang and Xuejun Li**

Department of Neurosurgery, Xiangya Hospital, Central South University, Changsha, China

Keywords: angiogenesis, endocrinology, invasiveness, molecular network, pituitary adenoma

A Corrigendum on

Molecular Network Basis of Invasive Pituitary Adenoma: A Review
by Yang, Q., and Li, X. (2019). Front. Endocrinol. 10:7. doi: 10.3389/fendo.2019.00007

In the original article, there was an error. In Gültekin's article, Matrix metalloproteinase-9 and tissue inhibitor of matrix metalloproteinase-2: Prognostic biological markers in invasive prolactinomas, he found that TIMP-2 is lowly expressed in more clinical samples from invasive pituitary adenoma, which was incorrectly cited by us to prove the opposite.

A correction has been made to the section ***Degradation and Remodeling of ECM by Matrix Metalloproteinases Family***, paragraph two:

"MMP-9 is the first matrix metalloproteinase found to have a significantly higher expression level in pituitary adenomas invaded to cavernous sinus (68). However, TIMP-1 was undetectable by immunochemistry staining in all samples (69). The correlation between MMP-9 overexpression and invasiveness of pituitary adenomas has been verified by many researchers in human pituitary adenoma specimens (70–75) as well as cell lines (76). Later studies showed that high expression levels of EMMPRIN (77, 78), MMP-2 (71, 75, 79), and MMP-14 (80, 81) and low expression levels of TIMP-2 (82, 83), TIMP-3 (82, 84), and RECK (85) were also correlated with invasiveness. There is a report that found TIMP-2 have higher expression in more patients of invasive prolactinomas then non-invasive ones (74), most of the aforementioned studies were performed on patients with prolactinoma or mixed patients of all secreting types, the contradicting results of TIMP-2 indicating that different types of pituitary adenoma might have distinct signaling pathways regarding to invasiveness. However, no statistical difference in the MMP-9 expression level between invasive and non-invasive non-functioning pituitary adenomas could be found (86)."

The authors apologize for this error and state that this does not change the scientific conclusions of the article in any way. The original article has been updated.

OPEN ACCESS

Edited and reviewed by:
Adam Mamelak, Cedars-Sinai Medical Center, United States

****Correspondence:***
Xuejun Li
lxjneuro@csu.edu.cn

Specialty section:
This article was submitted to Pituitary Endocrinology, a section of the journal Frontiers in Endocrinology

Received: *28 June 2019*
Accepted: *11 September 2019*
Published: *24 September 2019*

Citation:
Yang Q and Li X (2019) Corrigendum: Molecular Network Basis of Invasive Pituitary Adenoma: A Review. Front. Endocrinol. 10:657. doi: 10.3389/fendo.2019.00657

frontiers in Endocrinology

MINI REVIEW
published: 19 March 2019
doi: 10.3389/fendo.2019.00141

Phosphodiesterases and cAMP Pathway in Pituitary Diseases

Mariana Ferreira Bizzi[1†], *Graeme B. Bolger*[2,3†‡], *Márta Korbonits*[4†] and *Antonio Ribeiro-Oliveira Jr.*[1*†]

[1] Department of Internal Medicine, Federal University of Minas Gerais, Belo Horizonte, Brazil, [2] Department of Medicine, University of Alabama at Birmingham, Birmingham, AL, United States, [3] Department of Pharmacology, University of Alabama at Birmingham, Birmingham, AL, United States, [4] Center for Endocrinology, Barts and The London School of Medicine, William Harvey Research Institute, Queen Mary University of London, London, United Kingdom

OPEN ACCESS

Edited by:
Xianquan Zhan,
Central South University, China

Reviewed by:
Kjetil Taskén,
Oslo University Hospital, Norway
Josanne Vassallo,
University of Malta, Malta

***Correspondence:**
Antonio Ribeiro-Oliveira Jr.
antoniorojr@gmail.com

[†]These authors have contributed equally to this work

‡Present Address:
Graeme B. Bolger,
BZI Pharma LLC, Birmingham, AL, United States

Specialty section:
This article was submitted to Pituitary Endocrinology, a section of the journal Frontiers in Endocrinology

Received: 02 October 2018
Accepted: 15 February 2019
Published: 19 March 2019

Citation:
Bizzi MF, Bolger GB, Korbonits M and Ribeiro-Oliveira A Jr (2019) Phosphodiesterases and cAMP Pathway in Pituitary Diseases. Front. Endocrinol. 10:141. doi: 10.3389/fendo.2019.00141

Human phosphodiesterases (PDEs) comprise a complex superfamily of enzymes derived from 24 genes separated into 11 PDE gene families (PDEs 1–11), expressed in different tissues and cells, including heart and brain. The isoforms PDE4, PDE7, and PDE8 are specific for the second messenger cAMP, which is responsible for mediating diverse physiological actions involving different hormones and neurotransmitters. The cAMP pathway plays an important role in the development and function of endocrine tissues while phosphodiesterases are responsible for ensuring the appropriate intensity of the actions of this pathway by hydrolyzing cAMP to its inactive form 5'-AMP. PDE1, PDE2, PDE4, and PDE11A are highly expressed in the pituitary, and overexpression of some PDE4 isoforms have been demonstrated in different pituitary adenoma subtypes. This observed over-expression in pituitary adenomas, although of unknown etiology, has been considered a compensatory response to tumorigenesis. PDE4A4/5 has a unique interaction with the co-chaperone aryl hydrocarbon receptor-interacting protein (AIP), a protein implicated in somatotroph tumorigenesis via germline loss-of-function mutations. Based on the association of low PDE4A4 expression with germline *AIP*-mutation-positive samples, the available data suggest that lack of AIP hinders the upregulation of PDE4A4 protein seen in sporadic somatotrophinomas. This unique disturbance of the cAMP-PDE pathway observed in the majority of *AIP*-mutation positive adenomas could contribute to their well-described poor response to somatostatin analogs and may support a role in tumorigenesis.

Keywords: phosphodiesterases, cAMP pathway, pituitary, AIP (Aryl hydrocarbon receptor interacting protein), acromegaly, gigantism

INTRODUCTION

Human phosphodiesterases (PDEs) comprise a complex superfamily of enzymes classified into 11 families, encoded by 24 genes representing over 100 different proteins. Many of these genes express several different mRNAs, and the resulting proteins vary widely in their distribution in various tissues and in various intracellular compartments (1).

PDE isoforms differ in their kinetics, distribution, and susceptibility to pharmacological inhibition, as well as selectivity for their different substrates, 3',5' cyclic monophosphate (cAMP) and 3',5' cyclic guanosine monophosphate (cGMP) (1). PDEs share some common structural characteristics: all PDE isoforms have a conserved catalytic domain of ∼300 amino acids, located in the C-terminal portion of the protein, and most PDE isoforms contain family-specific regulatory regions in their N-terminal portions (2).

The catalytic regions of each family member differ in amino acid sequence and tertiary structure, which accounts for their specificity for substrate (cAMP and/or cGMP) and their ability to be inhibited by family- and isoform-specific inhibitors. PDE 4, 7, and 8 selectively hydrolyze cAMP, PDE 5, 6, and 9 are selective for cGMP, while PDEs 1, 2, 3, 10, and 11 hydrolyze both, although the specificity is variable (1, 3, 4).

The expression pattern of PDE isoforms varies between tissues and reflects their proliferative state and hormonal stimuli. In this mini review we aim to highlight the important role of these enzymes in pituitary diseases, especially the PDE4A4/5 isoform, encoded by the PDE4A gene, which has been implicated in GH-secreting adenomas due to its selective interaction with aryl hydrocarbon receptor-interacting protein (AIP), a known tumor suppressor gene (5).

PDEs AND cAMP PATHWAYS IN THE NORMAL PITUITARY GLAND

The pituitary gland is a target of different neuroendocrine hormones, which play a crucial role in the control of cell differentiation and proliferation, in addition to hormone secretion, through specific interactions with members of the superfamily of G protein-coupled receptors (GPCRs) (6, 7) (**Figure 1**). The regulatory, usually hypothalamic, hormone couples to the G protein-coupled receptor in the cell of interest and a conformational change results in activation of the G protein complex. In the case of GHRH, the Gsα subunit is released from the αβγ G protein complex and binds to adenylyl cyclase, which then catalyzes the conversion of ATP into the second messenger cAMP. cAMP activates a cascade of other enzymes, thus amplifying the cellular reaction (3). Following GHRH activation of somatotrophs cAMP binds the regulatory subunit of protein kinase A (PKA) (3, 6). The activated catalytic subunit of PKA then phosphorylate a series of targets that regulate effector enzymes, ion channels, and activate the transcription of specific genes that mediate cell growth and differentiation. Additional effectors of cAMP include the exchange factor regulated by cAMP (EPAC) protein, cyclic nucleotide-gated ion channels, Popeye proteins, and possibly additional targets that are still under investigation (1, 8).

PDEs act as regulators of the cAMP pathway, as they are capable of hydrolyzing cAMP to its inactive 5'-AMP form, which is the main pathway for inactivation of cAMP (3, 6). As a consequence, cAMP can either suppress cell proliferation and the mitogenic action of growth factors in some cell types, or conversely, promote the transition from cell cycle G0 to G1 and stimulate cell growth in others (9, 10). It is unclear, for example, why cAMP has a proliferative role in the somatotroph cells while an anti-proliferative role in gonadotroph cells (6, 9, 10). cAMP signaling is temporally, spatially, and functionally regulated by

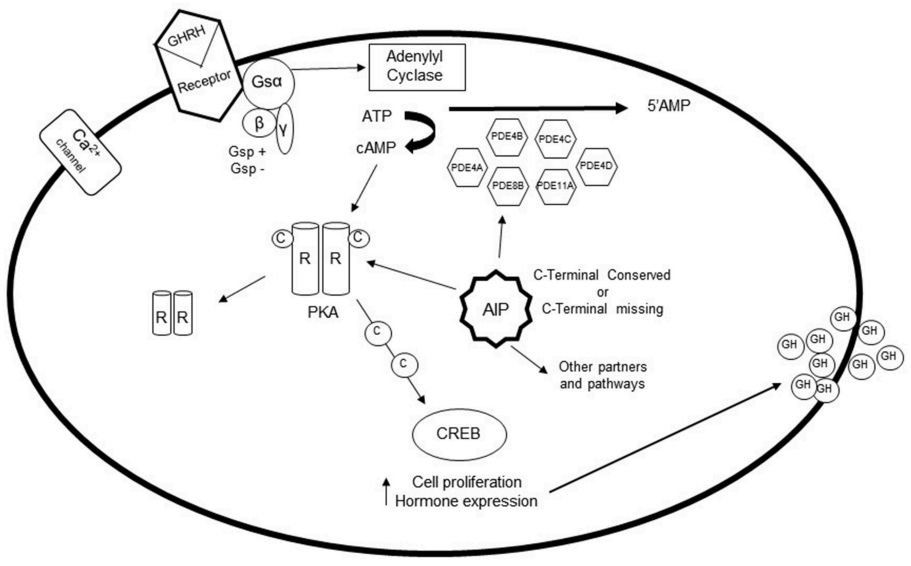

FIGURE 1 | The role of phosphodiesterases (PDEs) in the pituitary gland: After stimulation of somatotroph cells via GHRH, the G protein coupled receptor is activated, which causes a conformational change of the receptor. The Gsα subunit detaches from the complex, and binds to adenylyl cyclase, which catalyzes the conversion of ATP to cAMP. Elevation of intracellular cAMP leads to dissociation of the catalytic subunit and the regulatory subunit of protein kinase A (PKA). Activation of protein kinase A can then phosphorylate a number of targets that regulate effector enzymes and ion channels as well as activates gene transcription that play a role in cell growth and differentiation. PDEs are fundamental in regulating this pathway, since they are the only enzymes capable of hydrolyzing cAMP to its inactive 5'-AMP form. PDE4A, PDE4B, PDE4C, PDE4D, PDE8B, and PDE11A are increased in GH-secreting adenomas, possibly as a compensatory mechanism. However, *gsp* and *AIP* mutations interfere with the expression of these PDEs.

compartmentalization and influenced by a complex network of cell- and tissue-specific downstream effectors and regulators (11). In the pituitary, cAMP acts as a key signaling molecule that controls responsiveness to mitogens and secretagogues, such as hypothalamic hormones, neurotransmitters, and other peripheral factors (7) and a dysregulated cAMP-pathway is involved in the pathogenesis and response to therapy of pituitary adenomas (11).

PDEs are directly implicated in various endocrine disorders affecting the pituitary, adrenals, thyroid, testes, and ovaries (3). Little is known about the expression of PDE isoforms in the pituitary gland, especially in humans, since the vast majority of studies on the association between PDEs and endocrine functions have been performed *in vitro* or in animals. mRNA studies have implicated PDE1, PDE2, PDE4, and PDE11A as being the most highly expressed PDEs in the pituitary (3, 12–14). Interestingly, PDE4 is the only selective PDE for cAMP. The discovery of the physiological role of PDEs in the human pituitary has been hindered due to the lack of availability of specific antibodies. In addition, mRNA does not always reflect the protein amount or function due to variations in translation, protein stability, or posttranslational modifications.

PDE4 isoforms in mammals are encoded by four different genes (PDE4A, PDE4B, PDE4C, and PDE4D) and each of these genes encodes multiple isoforms, through the use of specific promoters for each isoform and alternative messenger RNA processing (15–17). PDE4s differ from the other PDE families by their specific catalytic regions (15–17), as well as by the presence of two "signature" regions called upstream conserved regions (UCRs), which are located in the N-terminal third of the proteins and referred to as UCR1 and UCR2 (18). The various isoforms encoded by each of the PDE4A, PDE4B, PDE4C, and PDE4D genes are divided into three groups: 'long' isoforms that contain both UCR1 and UCR2, "short" isoforms that do not have UCR1 but include UCR2, and "super short" isoforms that do not have UCR1 and contain a truncated UCR2 (18).

PDE4A8 is a long isoform of the PDE4A family with an N-terminal region distinct from the other PDE4A long isoforms PDE4A4, PDE4A10, and PDE4A11 (19–22). It is expressed at significant levels in various regions of the brain, especially in regions involved in coordination, sensation and higher cognitive functions (12, 20). It is also expressed in the pituitary gland (23).

PDE4A4, the human analog of rodent PDE4A5, is an isoform expressed in a wide variety of tissues, including lung and various brain regions (18–20, 24, 25). This isoform has UCR1 and UCR2 as well as a unique N-terminal region, which is highly conserved in mammals and has 88% similarity to the N-terminal region of rat PDE4A5 (20). This high degree of conservation between species suggests that the unique amino-terminal region of the PDE4A4 isoform has specific functions (26). The truncation of the PDE4A4 N-terminal region alters its enzymatic activities, its intracellular targeting, and its interaction with other proteins (27, 28). PDE4A5 interacts with AIP and has a reduced expression in *AIP*-mutation-positive adenomas (5, 26, 29, 30). PDE4A4 is expressed in the human pituitary (23). Furthermore, reduced AIP levels were shown to disproportionally enhance the PKA pathway activity under PDE4-specific inhibition in pituitary somatotrophs, pointing out to a link with the disease process involved in Carney complex (31).

By semi quantitative RT-PCR, PDE4C, and PDE4D were also shown to be expressed in the normal pituitary while no expression was detected for PDE8B (14).

PHOSPHODIESTERASES IN PITUITARY TUMORS

Both PDE4A4 and PDE4A8 expression is increased in GH-, PRL-, ACTH- and FSH-secreting adenoma cells compared to their respective normal pituitary cells (23). Interestingly, the augmentation of PDEs observed in pituitary adenomas reflects a consequent increase in PKA activating transcription of cell growth promoting genes, suggesting that these phosphodiesterases might be increased as a possible adaptation or compensation to tumorigenesis, in an attempt to suppress the proliferative drive (23).

Protein-protein interaction between AIP and PDE2A (PDE2A1, PDE2A2, and PDE2A3) has been described (32). Although PDE2As has cGMP as their preferred substrate it may also hydrolyze cAMP (33).

PDE11A has higher expression in GH-secreting adenomas when compared with normal GH-cells (13), which is also described as a phenotype modifier in patients with Carney complex due to *PRKAR1A* mutations (34). The presence and role of PDE11A expression and variants were studied in somatotroph adenomas. Although nonsense and missense PDE11A variants were found in 20% of patients with acromegaly, there was no significant difference in variant frequency compared with controls, suggesting that these variants are unlikely to contribute to the pathogenesis of GH-secreting adenomas since the conservation of the wild-type allele of PDE11A remains in the majority of tumor samples and no significant clinical phenotype could be observed in patients with variant PDE11A (13).

Interestingly, although PDE8B was not detected in normal pituitary, this isoform was shown to be overexpressed in all GH-secreting adenomas, especially higher levels were observed in *gsp*-positive tumors (14). This study also showed that while PDE4C and 4D RNA expression is not increased in *gsp*-mutation negative GH-secreting adenomas compared to normal pituitary, *gsp*-positive samples had seven times higher expression (14). As cAMP-responsive element-binding protein represents the main endpoint of the cAMP pathway, the observed enhanced phosphodiesterase activities may significantly impact the phenotypic expression of *gsp* mutations in somatotrophinomas (14).

PDE4A FAMILY AND AIP

Compared to other PDE isoforms, human PDE4A4 is specifically associated with AIP (also called XAP2 or ARA9), a co-chaperone of HSP90 and HSC70 (26, 35). AIP has several partners, including the aryl hydrocarbon receptor (AhR), PDE4A5, PDE2A, survivin, Tom20, hepatitis B virus protein X, thyroid hormone receptor 1 (TRβ1), Epstein-Barr virus encoded nuclear antigen 3 and

TABLE 1 | Summary of data for variants tested in in the PDE4A4/5—AIP interaction assays.

Mutation (DNA level [protein level])	Type	More than 1 patient	Youngest known age of onset	Youngest known age of diagnosis	Macro	Adenoma type	Giant	Gnomad MAF	LOH	Frutify rescued (suggesting not pathogenic) (43)	PDE4A5 binding (5, 23, 29)	PDE4A4 and/or PDE4A8 staining (30)	Half-life (35, 44)	HSP90 co-IP (35)	Proliferation/ cAMP generation (5, 45, 46)	Annotation	Pathogenic[$]	References
c.26G>A (p.R9Q)	M	YES	21	N/A	YES	GH, ACTH, PRL	YES	0,000238	N/A	N/A	N/A	N/A	Normal	N/A	Inc/Inc	Polyphen: benign; SIFT: tolerated	Unlikely	(47–50)
c.38T>A (p.I13N)	M	NO	N/A	N/A	YES	GH	YES	0,00000825	YES	NO	N/A	N/A	N/A	N/A	N/A	Polyphen: possibly _damaging; SIFT: deleterious	Yes	(43, 51)
c.47G>A (p.R16H)	M	YES	N/A	15	YES	GH, PRL	YES	0,00196	NO	YES	<30%	N/A	Normal	N/A	Inc/Inc	Polyphen: possibly _damaging; SIFT: deleterious	No	(48, 52–63)
c.66_71delAGGAGA (p.G23_E24del)	D	YES	N/A	20	YES	GH	Unknown	Not present	N/A	N/A	high	N/A	N/A	N/A	N/A	–	Yes	(53)
c.145G>A (V49M)	M	NO	N/A	N/A	N/A	GH	YES	0,0002745	NO	N/A	>30%	N/A	Short	N/A	Inc/Inc	Polyphen: benign; SIFT: deleterious	Unlikely	(64)
c.208C>A (p.L70M)	M	YES	N/A	22	YES	GH & PRL, PRL	Unknown	Not present	N/A	N/A	<30%	N/A	N/A	N/A	N/A	Polyphen: probably _damaging; SIFT: deleterious	Likely	(65)
c.241C>T (p.R81*)	N	YES	3	4	YES	GH	YES	Not present	YES	N/A	<30%	N/A	N/A	N/A	N/A	Loss-of-Function: High-confidence	Yes	(5, 66–69)
c.308A>G (p.K103R)	M	NO	N/A	6	YES	ACTH	NO	0,0000041	N/A	N/A	>30%	N/A	Normal	N/A	no change/no change	Polyphen: benign; SIFT: tolerated	VUS	(46, 70)
c.490C>T (p.Q164*)	N	YES	15	23	YES	GH	YES	Not present	N/A	N/A	<30%	low	N/A	N/A	N/A	Loss-of-Function: High-confidence	Yes	(29)
c.562C>T (R188W)	M	NO	10	12	YES	GH & PRL	YES	0,000032	N/A	N/A	N/A	N/A	Very short	N/A	N/A	Polyphen: benign; SIFT: deleterious	Likely	(35)
c.649C>T (p.Q217*)	N	YES	N/A	17	YES	GH, GH & PRL	Unknown	Not present	N/A	N/A	<30%	N/A	N/A	N/A	N/A	Loss-of-Function: High-confidence	Yes	(55, 71)
c.662dupC (p.E222*)	F	NO	22	24	YES	GH	YES	Not present	N/A	N/A	<30%	low	N/A	N/A	N/A	Loss-of-Function: High-confidence	Yes	(29)
c.713G>A (p.C238Y)	M	YES	18	19	YES	GH	NO	0,000004025	YES	NO	<30%	N/A	Very short	N/A	Inc / N/A	Polyphen: possibly _damaging; SIFT: deleterious	Yes	(5, 23, 35)
c.721A>G (p.K241E)	M	YES	N/A	40	YES	PRL, NFPA	NO	0,00003622	N/A	N/A	<30%	N/A	Short	N/A	N/A	Polyphen: possibly _damaging; SIFT: tolerated	Likely	(55)

(Continued)

TABLE 1 | Continued

Mutation (DNA level [protein level])	Type	More than 1 patient	Youngest known age of onset	Youngest known age of diagnosis	Macro	Adenoma type	Giant	Gnomad MAF	LOH	Frutifly rescued (suggesting not pathogenic) (43)	PDE4A5 binding (5, 23, 29)	PDE4A4 and/or PDE4A8 staining (30)	Half-life (35, 44)	HSP90 co-IP (35)	Proliferation/ cAMP generation (5, 45, 46)	Annotation	Pathogenic$	References
c.742_744delTAC (p.Y248del)	D	NO	N/A	19	YES	GH	YES	Not present	YES	N/A	<30%	N/A	N/A	N/A	N/A	Loss-of-Function: High confidence	Yes	(72)
c.760T>C (p.C254R)	M	YES	14	33	YES	GH	YES	Not present	N/A	N/A	N/A	N/A	Very short	N/A	N/A	Polyphen: possibly _damaging; SIFT: tolerated	Likely	(35)
c.769A>G (p.I257V)	M	NO	N/A	39	YES	TSH	NO	Not present	N/A	N/A	<30%	N/A	Short	lost	N/A	Polyphen: benign; SIFT: tolerated	Likely	(73)
c.805_825dup (F269_H275dup)	I	YES	9	13	YES	GH, GH & PRL	YES	Not present	N/A	N/A	N/A	low	Very short	N/A	N/A	Loss-of-Function: High-confidence	Yes	(5, 44)
c.811C>T (p.R271W)	M	NO	15	16	YES	GH & PRL, GH, PRL	YES	Not present	N/A	N/A	<30%	N/A	Very short	N/A	N/A	Polyphen: probably _damaging; SIFT: deleterious	Yes	(5, 29, 55, 59, 68, 69, 74, 75)
c.815G>A (p.G272D)	M	YES	38	43	YES	GH	YES	0,00000409	N/A	NO	<30%	N/A	N/A	lost	N/A	Polyphen: possibly _damaging; SIFT: deleterious	Likely	(76–78)
c.871G>A (p.V291M)	M	NO	N/A	30	N/A	GH & PRL	NO	Not present	NO	N/A	<30%	N/A	Very short	N/A	N/A	Polyphen: probably _damaging; SIFT: deleterious	Likely	(48)
c.910C>T (p.R304*)	N	YES	6	6	YES	GH, PRL, GH & PRL	YES	0,00001436	YES	N/A	<30%	low	Very short	N/A	N/A	Loss-of-Function: High-confidence	Yes	(5, 29, 37, 48, 54, 55, 59, 79–84)
c.911G>A (p.R304Q)	M	YES	17	18	YES	GH, PRL, GH & PRL, ACTH	YES	0,00000842	NO	YES	<30%	N/A	Normal	N/A	N/A	Polyphen: possibly _damaging; SIFT: tolerated	VUS	(5, 29, 48, 53, 54, 59, 81, 85–88)
c.911C>T (p.R304*)	N	YES	6	6	YES	GH, GH & PRL	YES	0.00001436	YES	N/A	N/A	low N/A	Very short	lost	N/A	Loss-of-Function: High-confidence	Yes	(37 and many others)
c.940C>T (p.R314W)	M	NO	18	N/A	YES	GH	YES	0,00001445	YES	YES	N/A	N/A	N/A	N/A	N/A	Polyphen: probably _damaging; SIFT: deleterious	VUS	(60)
c.991T>C (p.*331R)	M	NO	11	15	YES	GH	YES	Not present	YES	N/A	N/A	N/A	N/A	N/A	N/A	Loss of stop codon	Likely	(89)

M, missense; N, nonsense; D, deletion; N/A, not available; LOH, loss of heterozygosity; $ Pathogenicity is based on authors' judgement following the American College of Medical Genetics and Genomics principles (90); F, frameshift; I, insertion; MAF, minor allele frequency; Inc, increased; VUS, variant of unknown significance.

peroxisome proliferator-activated receptor—PPARα (36). This gene is described as a tumor suppressor gene in the pituitary (37, 38). Loss-of-function germline mutations predispose to pituitary adenomas, while reduced expression could be lead to altered epigenetic regulation via microRNAs alterations (39, 40).

AIP is expressed in GH- and PRL-cells and electron microscopy studies have identified AIP in the secretory vesicles (5). AIP is abundant in NFPAs (non-functioning pituitary adenomas), and has been shown in corticotrophinomas, although not in the secretory vesicles. However, no AIP expression has been detected in normal gonadotroph and corticotroph cells. Interestingly, it has been demonstrated that the overexpression of wild-type AIP reduces the cell proliferation in three different types of cell lines: GH3 cells, HEK293 cells, and TIG3 fibroblasts (5). These data confirmed that AIP has tumor suppressor gene properties (37, 41). Loss of interaction between AIP and PDE4A5 was seen in a β-galactosidase quantitative two-hybrid assay for pathogenic *AIP* mutations (R81*, Q164*, K103R, Q217*, C238Y, Y248del, R271W, V291M, and R304* (5, 23). For the K241E and R304Q variants, a borderline statistical significance was found for this interaction. For the R16H, V49M, I257V, and A229V variants, there were no clear reduction in their binding (23, 29). Many of the changes disrupting PDE4A5—AIP interaction are known to be important to the stability of the TPR structure of the AIP (42). Clinical data suggest that the R16H, V49M, and A229V may be polymorphisms while the I257V variant affects the TPR structure and clinical data would support a functional impact (29). We summarized data from variants tested in the PDE4A4/5—AIP interaction assay or with PDE4A4 or PDE4A8 immunostaining (**Table 1**), gathering clinical, frequency, prediction, and experimental data. We note that few variants were tested with more than one functional assay.

There are different PDE4A4 and PDE4A8 expression patterns in somatotroph adenomas from patients with *AIP* mutations compared to patients with wild-type *AIP* (**Table 2**). It has been previously shown that the C-terminal part of AIP is a key for its functional effects. Mutations affecting the C-terminal end lead either to nonsense-mediated decay of the abnormal RNA (probably relevant for p.E222*), create a protein with significantly shortened half-life [as shown for p.F269_H275dup (44) and p.R304* (35)], or lose interaction with protein partners (91). *AIP* mutation-positive samples had significantly decreased PDE4A4 expression compared to sporadic somatotroph adenomas, suggesting that *AIP* mutation-positive somatotroph cells are unable to upregulate PDE4A4 expression (30).

For PDE4A8, although no interaction with AIP has been shown due to the fact that this protein cannot be produced *in vitro* for the two-hybrid assay, a reduced protein expression was observed in *AIP* mutation-positive samples (30). These differences in PDE4A8 protein expression suggest that, similarly to PDE4A4/5, AIP may support expression or stability of PDE4A8, leading to closely regulated cAMP pathway activity (30).

PHOSPHODIESTERASE INHIBITION

The use of PDEs inhibitors, either selective or nonselective, represents an effective targeted strategy for the treatment of many human diseases, such as respiratory disorders, erectile dysfunction, prostate cancer and inflammatory diseases (92–95).

The inhibitory effect of heterologously expressed *AIP* on cAMP levels has not been altered by the general inhibition of phosphodiesterases (by IBMX) or the PDE4-specific inhibitor

TABLE 2 | Phosphodiesterases (PDE) isoforms and their respective protein/RNA expression in different pituitary cells types.

	Normal pituitary	Sporadic GH-secreting Adenomas	Sporadic PRL-secreting adenomas	Sporadic ACTH-secreting Adenomas	Sporadic Non-functioning adenomas (FSH+)	GH-secreting adenoma AIP mutation
PDE4A (14)	Presence of RNA in GH cells	Gsp+ RNA ↑ Gsp– RNA =	NA	NA	NA	NA
PDE4A4 (23, 30)	Presence of the protein in GH/PRL/ACTH/FSH cells	↑	↑	↑	↑	F269_H275dup = R304* = E222* =
PDE4A8 (23, 30)	Presence of the protein in GH/PRL/ACTH/FSH cells	↑	↑	↑	↑	F269_H275dup ↓ R304* = Q164* ↓
PDE4B (14)	Presence of RNA in GH cells	Gsp+ RNA ↑ Gsp- RNA ↑	NA	NA	NA	NA
PDE4C (14)	Presence of RNA in GH cells	Gsp+ RNA ↑ Gsp- RNA =	NA	NA	NA	NA
PDE4D (14)	Presence of RNA in GH cells	Gsp+ RNA ↑ Gsp- RNA =	NA	NA	NA	NA
PDE8B (14)	Absent GH cells	Gsp+ RNA ↑ Gsp- RNA ↑	NA	NA	NA	NA
PDE11A (13)	Presence of the protein GH cells	Protein ↑	NA	NA	NA	NA

All comparisons are in relation to the respective normal cell. ↑ increase ↓ decrease = equal.

rolipram. Furthermore, the GH secretion was not altered by the use of these inhibitors (45). However, it has been shown that in rat somatotrophinoma GH3 cells, AIP regulates cAMP signaling and GH secretion independently of the AIP–PDE interaction. In the rat somatotrophinoma GH3 cells treated with forskolin, a drug that increases the cAMP levels, it was shown that the *AIP* overexpression could attenuate the cAMP response to the drug, even in the absence of PDE activity, while *AIP* knockdown activates the cAMP pathway. Although these effects are not observed in untreated cells, these results suggest that AIP may itself act as a tumor suppressor by reducing cAMP signaling (38, 45). However, GH-secreting adenomas with positive *AIP* mutation show reduced phosphorylation of the mitogen-activated protein kinases (MAPKs) 3 and 1 as well as reduction of phosphorylation of the cAMP response element binding protein (CREB). Also, AIP knockout causes reduced CREB phosphorylation in mouse embryonic fibroblasts although AIP knockdown rat somatotrophinoma GH3 cells do not show any of these changes on cAMP effectors (38, 96). To this point, the binding between PDE4A5-AIP does not seem to be the only regulator of this pathway.

In rat corticotroph cells, cAMP levels are related to selective activity of PDE1 (PDE1A or PDE1C) or PDE4, depending on the type and intensity of stress conditions (97). On the other hand, mouse corticotroph cell line AtT-20 with forskolin-induced elevated cAMP levels showed no response to IBMX with or without rolipram (98). Further studies are needed to clarify the possible therapeutic role of PDE manipulation in pituitary adenomas.

SUMMARY

The cAMP pathway plays a key role in somatotroph tumorigenesis, as suggested by altered cAMP pathway in *GNAS*, *PRKAR1A, AIP,* and *GPR101* mutated samples. Targeted therapies influencing this pathway may have a key role in the medical treatment of these currently often treatment-resistant conditions.

AUTHOR CONTRIBUTIONS

All authors listed have made a substantial, direct and intellectual contribution to the work, and approved it for publication.

ACKNOWLEDGMENTS

We are grateful for the support by Fundação de Amparo à Pesquisa de Minas Gerais—Fapemig (AR-O), Conselho Nacional de Desenvolvimento Científico e Tecnológico—CNPq (AR-O, MB) and the Medical Research Council UK (MK), and the NIH, USA (GB).

REFERENCES

1. Francis SH, Blount MA, Corbin JD. Mammalian cyclic nucleotide phosphodiesterases: molecular mechanisms and physiological functions. *Physiol Rev.* (2011) 91:651–90. doi: 10.1152/physrev.00030.2010
2. Conti M, Beavo J. Biochemistry and physiology of cyclic nucleotide phosphodiesterases: essential components in cyclic nucleotide signaling. *Annu Rev Biochem.* (2007) 76:481–511. doi: 10.1146/annurev.biochem.76.060305.150444
3. Vezzosi D, Bertherat J. Phosphodiesterases in endocrine physiology and disease. *Eur J Endocrinol.* (2011) 165:177–88. doi: 10.1530/EJE-10-1123
4. Tian Y, Cui W, Huang M, Robinson H, Wan Y, Wang Y, et al. Dual specificity and novel structural folding of yeast phosphodiesterase-1 for hydrolysis of second messengers cyclic adenosine and guanosine 3',5'-monophosphate. *Biochemistry*. (2014) 53:4938–45. doi: 10.1021/bi500406h
5. Leontiou CA, Gueorguiev M, van der Spuy J, Quinton R, Lolli F, Hassan S, et al. The role of the aryl hydrocarbon receptor-interacting protein gene in familial and sporadic pituitary adenomas. *J Clin Endocrinol Metab.* (2008) 93:2390–401. doi: 10.1210/jc.2007-2611
6. Lania A, Mantovani G, Spada A. cAMP pathway and pituitary tumorigenesis. *Ann Endocrinol.* (2012) 73:73–5. doi: 10.1016/j.ando.2012.03.027
7. Peverelli E, Mantovani G, Lania AG, Spada A. cAMP in the pituitary: an old messenger for multiple signals. *J Mol Endocrinol.* (2014) 52:R67–77. doi: 10.1530/JME-13-0172
8. Maurice DH, Ke H, Ahmad F, Wang Y, Chung J, Manganiello VC. Advances in targeting cyclic nucleotide phosphodiesterases. *Nat Rev Drug Discov.* (2014) 13:290–314. doi: 10.1038/nrd4228
9. Mantovani G, Bondioni S, Ferrero S, Gamba B, Ferrante E, Peverelli E, et al. Effect of cyclic adenosine 3',5'-monophosphate/protein kinase a pathway on markers of cell proliferation in nonfunctioning pituitary adenomas. *J Clin Endocrinol Metab.* (2005) 90:6721–4. doi: 10.1210/jc.2005-0977
10. Pertuit M, Barlier A, Enjalbert A, Gérard C. Signalling pathway alterations in pituitary adenomas: involvement of Gsalpha, cAMP and mitogen-activated protein kinases. *J Neuroendocrinol.* (2009) 21:869–77. doi: 10.1111/j.1365-2826.2009.01910.x
11. Hernández-Ramírez LC, Trivellin G, Stratakis CA. Cyclic 3',5'-adenosine monophosphate (cAMP) signaling in the anterior pituitary gland in health and disease. *Mol Cell Endocrinol.* (2017) 463:72–86. doi: 10.1016/j.mce.2017.08.006
12. Mackenzie KF, Topping EC, Bugaj-Gaweda B, Deng C, Cheung YF, Olsen AE, et al. Human PDE4A8, a novel brain-expressed PDE4 cAMP-specific phosphodiesterase that has undergone rapid evolutionary change. *Biochem J.* (2008) 411:361–9. doi: 10.1042/BJ20071251
13. Peverelli E, Ermetici F, Filopanti M, Elli FM, Ronchi CL, Mantovani G, et al. Analysis of genetic variants of phosphodiesterase 11A in acromegalic patients. *Eur J Endocrinol.* (2009) 161:687–94. doi: 10.1530/EJE-09-0677
14. Persani L, Borgato S, Lania A, Filopanti M, Mantovani G, Conti M, et al. Relevant cAMP-specific phosphodiesterase isoforms in human pituitary: effect of Gs(alpha) mutations. *J Clin Endocrinol Metab.* (2001) 86:3795–800. doi: 10.1210/jcem.86.8.7779
15. Conti M, Richter W, Mehats C, Livera G, Park JY, Jin C. Cyclic AMP-specific PDE4 phosphodiesterases as critical components of cyclic AMP signaling. *J Biol Chem.* (2003) 278:5493–6. doi: 10.1074/jbc.R200029200
16. Houslay MD, Sullivan M, Bolger GB. The multienzyme PDE4 cyclic adenosine monophosphate-specific phosphodiesterase family: intracellular targeting, regulation, and selective inhibition by compounds exerting anti-inflammatory and antidepressant actions. *Adv Pharmacol.* (1998) 44:225–342. doi: 10.1016/S1054-3589(08)60128-3
17. Houslay MD, Adams DR. PDE4 cAMP phosphodiesterases: modular enzymes that orchestrate signalling cross-talk, desensitization and compartmentalization. *Biochem J.* (2003) 370:1–18. doi: 10.1042/bj20021698
18. Beard MB, Olsen AE, Jones RE, Erdogan S, Houslay MD, Bolger GB. UCR1 and UCR2 domains unique to the cAMP-specific phosphodiesterase family form a discrete module via electrostatic interactions. *J Biol Chem.* (2000) 275:10349–58. doi: 10.1074/jbc.275.14.10349
19. Bolger GB, McPhee I, Houslay MD. Alternative splicing of cAMP-specific phosphodiesterase mRNA transcripts. Characterization of a novel

tissue-specific isoform, RNPDE4A8. *J Biol Chem.* (1996) 271:1065–71. doi: 10.1074/jbc.271.2.1065
20. Bolger GB, Rodgers L, Riggs M. Differential CNS expression of alternative mRNA isoforms of the mammalian genes encoding cAMP-specific phosphodiesterases. *Gene*. (1994) 149:237–44. doi: 10.1016/0378-1119(94)90155-4
21. Rena G, Begg F, Ross A, MacKenzie C, McPhee I, Campbell L, et al. Molecular cloning, genomic positioning, promoter identification, and characterization of the novel cyclic AMP-specific phosphodiesterase PDE4A10. *Mol Pharmacol.* (2001) 59:996–1011. doi: 10.1124/mol.59.5.996
22. Wallace DA, Johnston LA, Huston E, MacMaster D, Houslay TM, Cheung YF, et al. Identification and characterization of PDE4A11, a novel, widely expressed long isoform encoded by the human PDE4A cAMP phosphodiesterase gene. *Mol Pharmacol.* (2005) 67:1920–34. doi: 10.1124/mol.104.009423
23. Bolger GB, Bizzi MF, Pinheiro SV, Trivellin G, Smoot L, Accavitti MA, et al. cAMP-specific PDE4 phosphodiesterases and AIP in the pathogenesis of pituitary tumors. *Endocr Relat Cancer*. (2016) 23:419–31. doi: 10.1530/ERC-15-0205
24. McPhee I, Cochran S, Houslay MD. The novel long PDE4A10 cyclic AMP phosphodiesterase shows a pattern of expression within brain that is distinct from the long PDE4A5 and short PDE4A1 isoforms. *Cell Signal.* (2001) 13:911–8. doi: 10.1016/S0898-6568(01)00217-0
25. Bolger G, Michaeli T, Martins T, St John T, Steiner B, Rodgers L, et al. A family of human phosphodiesterases homologous to the dunce learning and memory gene product of Drosophila melanogaster are potential targets for antidepressant drugs. *Mol Cell Biol.* (1993) 13:6558–71. doi: 10.1128/MCB.13.10.6558
26. Bolger GB, Peden AH, Steele MR, MacKenzie C, McEwan DG, Wallace DA, et al. Attenuation of the activity of the cAMP-specific phosphodiesterase PDE4A5 by interaction with the immunophilin XAP2. *J Biol Chem.* (2003) 278:33351–63. doi: 10.1074/jbc.M303269200
27. Huston E, Beard M, McCallum F, Pyne NJ, Vandenabeele P, Scotland G, et al. The cAMP-specific phosphodiesterase PDE4A5 is cleaved downstream of its SH3 interaction domain by caspase-3. Consequences for altered intracellular distribution. *J Biol Chem.* (2000) 275:28063–74. doi: 10.1074/jbc.M906144199
28. Beard MB, Huston E, Campbell L, Gall I, McPhee I, Yarwood S, et al. In addition to the SH3 binding region, multiple regions within the N-terminal noncatalytic portion of the cAMP-specific phosphodiesterase, PDE4A5, contribute to its intracellular targeting. *Cell Signal.* (2002) 14:453–65. doi: 10.1016/S0898-6568(01)00264-9
29. Igreja S, Chahal HS, King P, Bolger GB, Srirangalingam U, Guasti L, et al. Characterization of aryl hydrocarbon receptor interacting protein (AIP) mutations in familial isolated pituitary adenoma families. *Hum Mutat.* (2010) 31:950–60. doi: 10.1002/humu.21292
30. Bizzi MF, Pinheiro SVB, Bolger GB, Schweizer JROL, Giannetti AV, Dang MN, et al. Reduced protein expression of the phosphodiesterases PDE4A4 and PDE4A8 in AIP mutation positive somatotroph adenomas. *Mol Cell Endocrinol.* (2018) 476:103–9. doi: 10.1016/j.mce.2018.04.014
31. Schernthaner-Reiter MH, Trivellin G, Stratakis CA. Interaction of AIP with protein kinase A (cAMP-dependent protein kinase). *Hum Mol Genet.* (2018). doi: 10.1093/hmg/ddy166
32. de Oliveira SK, Hoffmeister M, Gambaryan S, Müller-Esterl W, Guimaraes JA, Smolenski AP. Phosphodiesterase 2A forms a complex with the co-chaperone XAP2 and regulates nuclear translocation of the aryl hydrocarbon receptor. *J Biol Chem.* (2007) 282:13656–63. doi: 10.1074/jbc.M610942200
33. Martinez SE, Wu AY, Glavas NA, Tang XB, Turley S, Hol WG, et al. The two GAF domains in phosphodiesterase 2A have distinct roles in dimerization and in cGMP binding. *Proc Natl Acad Sci USA*. (2002) 99:13260–5. doi: 10.1073/pnas.192374899
34. Libé R, Horvath A, Vezzosi D, Fratticci A, Coste J, Perlemoine K, et al. Frequent phosphodiesterase 11A gene (PDE11A) defects in patients with Carney complex (CNC) caused by PRKAR1A mutations: PDE11A may contribute to adrenal and testicular tumors in CNC as a modifier of the phenotype. *J Clin Endocrinol Metab.* (2011) 96:E208–14. doi: 10.1210/jc.2010-1704
35. Hernández-Ramírez LC, Martucci F, Morgan RM, Trivellin G, Tilley D, Ramos-Guajardo N, et al. Rapid proteasomal degradation of mutant proteins is the primary mechanism leading to tumorigenesis in patients with missense AIP mutations. *J Clin Endocrinol Metab.* (2016) 101:3144–54. doi: 10.1210/jc.2016-1307
36. Trivellin G, Korbonits M. AIP and its interacting partners. *J Endocrinol.* (2011) 210:137–55. doi: 10.1530/JOE-11-0054
37. Vierimaa O, Georgitsi M, Lehtonen R, Vahteristo P, Kokko A, Raitila A, et al. Pituitary adenoma predisposition caused by germline mutations in the AIP gene. *Science*. (2006) 312:1228–30. doi: 10.1126/science.1126100
38. Hernández-Ramírez LC, Trivellin G, Stratakis CA. Role of phosphodiesterases on the function of Aryl Hydrocarbon Receptor-Interacting Protein (AIP) in the pituitary gland and on the evaluation of AIP gene variants. *Horm Metab Res*. (2017) 49:286–95. doi: 10.1055/s-0043-104700
39. Dénes J, Kasuki L, Trivellin G, Colli LM, Takiya CM, Stiles CE, et al. Regulation of aryl hydrocarbon receptor interacting protein (AIP) protein expression by MiR-34a in sporadic somatotropinomas. *PLoS ONE*. (2015) 10:e0117107. doi: 10.1371/journal.pone.0117107
40. Trivellin G, Butz H, Delhove J, Igreja S, Chahal HS, Zivkovic V, et al. MicroRNA miR-107 is overexpressed in pituitary adenomas and inhibits the expression of aryl hydrocarbon receptor-interacting protein *in vitro*. *Am J Physiol Endocrinol Metab*. (2012) 303:E708–19. doi: 10.1152/ajpendo.00546.2011
41. Gadelha MR, Prezant TR, Une KN, Glick RP, Moskal SF, Vaisman M, et al. Loss of heterozygosity on chromosome 11q13 in two families with acromegaly/gigantism is independent of mutations of the multiple endocrine neoplasia type I gene. *J Clin Endocrinol Metab.* (1999) 84:249–56.
42. Morgan RM, Hernández-Ramírez LC, Trivellin G, Zhou L, Roe SM, Korbonits M, et al. Structure of the TPR domain of AIP: lack of client protein interaction with the C-terminal α-7 helix of the TPR domain of AIP is sufficient for pituitary adenoma predisposition. *PLoS ONE*. (2012) 7:e53339. doi: 10.1371/journal.pone.0053339
43. Aflorei ED, Klapholz B, Chen C, Radian S, Dragu AN, Moderau N, et al. *In vivo* bioassay to test the pathogenicity of missense human AIP variants. *J Med Genet.* (2018) 55:522–9. doi: 10.1136/jmedgenet-2017-105191
44. Salvatori R, Radian S, Diekmann Y, Iacovazzo D, David A, Gabrovska P, et al. In-frame seven amino-acid duplication in AIP arose over the last 3000 years, disrupts protein interaction and stability and is associated with gigantism. *Eur J Endocrinol*. (2017) 177:257–66. doi: 10.1530/EJE-17-0293
45. Formosa R, Xuereb-Anastasi A, Vassallo J. Aip regulates cAMP signalling and GH secretion in GH3 cells. *Endocr Relat Cancer*. (2013) 20:495–505. doi: 10.1530/ERC-13-0043
46. Formosa R, Vassallo J. Aryl Hydrocarbon Receptor-Interacting Protein (AIP) N-terminus gene mutations identified in pituitary adenoma patients alter protein stability and function. *Horm Cancer*. (2017) 8:174–84. doi: 10.1007/s12672-017-0288-3
47. Formosa R, Farruga C, Xuereb-Anastasi A, Korbonits M, Vassallo J. Aryl hydrocarbon receptor- interacting protein: mutational analysis and functional validation in primary pituitary cell cultures. *Endocr Abstr.* (2010) 22:P436.
48. Cazabat L, Bouligand J, Salenave S, Bernier M, Gaillard S, Parker F, et al. Germline AIP mutations in apparently sporadic pituitary adenomas: prevalence in a prospective single-center cohort of 443 patients. *J Clin Endocrinol Metab.* (2012) 97:E663–70. doi: 10.1210/jc.2011-2291
49. Farrugia DJ, Agarwal MK, Pankratz VS, Deffenbaugh AM, Pruss D, Frye C, et al. Functional assays for classification of BRCA2 variants of uncertain significance. *Cancer Res.* (2008) 68:3523–31. doi: 10.1158/0008-5472.CAN-07-1587
50. Oriola J, Lucas T, Halperin I, Mora M, Perales MJ, Alvarez-Escolá C, et al. Germline mutations of AIP gene in somatotropinomas resistant to somatostatin analogues. *Eur J Endocrinol*. (2013) 168:9–13. doi: 10.1530/EJE-12-0457
51. Salvatori R, Daly AF, Quinones-Hinojosa A, Thiry A, Beckers A. A clinically novel AIP mutation in a patient with a very large, apparently sporadic somatotrope adenoma. *Endocrinol Diabetes Metab Case Rep.* (2014) 2014:140048. doi: 10.1530/EDM-14-0048
52. Georgitsi M, Karhu A, Winqvist R, Visakorpi T, Waltering K, Vahteristo P, et al. Mutation analysis of aryl hydrocarbon receptor interacting protein (AIP) gene in colorectal, breast, and prostate cancers. *Br J Cancer*. (2007) 96:352–6. doi: 10.1038/sj.bjc.6603573

53. Georgitsi M, Raitila A, Karhu A, Tuppurainen K, Mäkinen MJ, Vierimaa O, et al. Molecular diagnosis of pituitary adenoma predisposition caused by aryl hydrocarbon receptor-interacting protein gene mutations. *Proc Natl Acad Sci USA*. (2007) 104:4101–5. doi: 10.1073/pnas.0700004104
54. Cazabat L, Libè R, Perlemoine K, René-Corail F, Burnichon N, Gimenez-Roqueplo AP, et al. Germline inactivating mutations of the aryl hydrocarbon receptor-interacting protein gene in a large cohort of sporadic acromegaly: mutations are found in a subset of young patients with macroadenomas. *Eur J Endocrinol*. (2007) 157:1–8. doi: 10.1530/EJE-07-0181
55. Daly AF, Vanbellinghen JF, Khoo SK, Jaffrain-Rea ML, Naves LA, Guitelman MA, et al. Aryl hydrocarbon receptor-interacting protein gene mutations in familial isolated pituitary adenomas: analysis in 73 families. *J Clin Endocrinol Metab*. (2007) 92:1891–6. doi: 10.1210/jc.2006-2513
56. Buchbinder S, Bierhaus A, Zorn M, Nawroth PP, Humpert P, Schilling T. Aryl hydrocarbon receptor interacting protein gene (AIP) mutations are rare in patients with hormone secreting or non-secreting pituitary adenomas. *Exp Clin Endocrinol Diabetes*. (2008) 116:625–8. doi: 10.1055/s-2008-1065366
57. Guaraldi F, Salvatori R. Familial isolated pituitary adenomas: from genetics to therapy. *Clin Transl Sci*. (2011) 4:55–62. doi: 10.1111/j.1752-8062.2010.00254.x
58. Raitila A, Georgitsi M, Bonora E, Vargiolu M, Tuppurainen K, Mäkinen MJ, et al. Aryl hydrocarbon receptor interacting protein mutations seem not to associate with familial non-medullary thyroid cancer. *J Endocrinol Invest*. (2009) 32:426–9. doi: 10.1007/BF03346480
59. Tichomirowa MA, Barlier A, Daly AF, Jaffrain-Rea ML, Ronchi C, Yaneva M, et al. High prevalence of AIP gene mutations following focused screening in young patients with sporadic pituitary macroadenomas. *Eur J Endocrinol*. (2011) 165:509–15. doi: 10.1530/EJE-11-0304
60. Baciu I, Capatana C, Aflorei D, Botusan I, Coculescu M, Radian S. Screening of AIP mutations in young Romanian patients with sporadic pituitary adenomas. In: *15th International Congress of Endocrinology* (Florence) (2012). p. P786.
61. Baciu I, Radian S, Capatina C, Botusan I, Aflorei D, Stancu C, et al. The P.R16H (C.47G > A) AIP gene variant in a case with invasive non-functioning pituitary macroadenoma and screening of a control cohort. *Acta Endocrinol Bucharest*. (2013) 9:97–108. doi: 10.4183/aeb.2013.97
62. Zatelli MC, Torre ML, Rossi R, Ragonese M, Trimarchi F, degli Uberti E, et al. Should aip gene screening be recommended in family members of FIPA patients with R16H variant? *Pituitary*. (2013) 16:238–44. doi: 10.1007/s11102-012-0409-5
63. Dinesen PT, Dal J, Gabrovska P, Gaustadnes M, Gravholt CH, Stals K, et al. An unusual case of an ACTH-secreting macroadenoma with a germline variant in the aryl hydrocarbon receptor-interacting protein (AIP) gene. *Endocrinol Diabetes Metab Case Rep*. (2015) 2015:140105. doi: 10.1530/EDM-14-0105
64. Iwata T, Yamada S, Mizusawa N, Golam HM, Sano T, Yoshimoto K. The aryl hydrocarbon receptor-interacting protein gene is rarely mutated in sporadic GH-secreting adenomas. *Clin Endocrinol*. (2007) 66:499–502. doi: 10.1111/j.1365-2265.2007.02758.x
65. Beckers A, Aaltonen LA, Daly AF, Karhu A. Familial isolated pituitary adenomas (FIPA) and the pituitary adenoma predisposition due to mutations in the aryl hydrocarbon receptor interacting protein (AIP) gene. *Endocr Rev*. (2013) 34:239–77. doi: 10.1210/er.2012-1013
66. Toledo RA, Sekiya T, Longuini VC, Coutinho FL, Lourenço DM, Toledo SP. Narrowing the gap of personalized medicine in emerging countries: the case of multiple endocrine neoplasias in Brazil. *Clinics*. (2012) 67 (Suppl. 1):3–6. doi: 10.6061/clinics/2012(Sup01)02
67. Guaraldi F, Corazzini V, Gallia GL, Grottoli S, Stals K, Dalantaeva N, et al. Genetic analysis in a patient presenting with meningioma and familial isolated pituitary adenoma (FIPA) reveals selective involvement of the R81X mutation of the AIP gene in the pathogenesis of the pituitary tumor. *Pituitary*. (2012) 15 (Suppl. 1):S61–7. doi: 10.1007/s11102-012-0391-y
68. Hernández-Ramírez LC, Gabrovska P, Dénes J, Stals K, Trivellin G, Tilley D, et al. Landscape of familial isolated and young-onset pituitary adenomas: prospective diagnosis in AIP mutation carriers. *J Clin Endocrinol Metab*. (2015) 100:E1242–54. doi: 10.1210/jc.2015-1869
69. Caimari F, Hernández-Ramírez LC, Dang MN, Gabrovska P, Iacovazzo D, Stals K, et al. Risk category system to identify pituitary adenoma patients with. *J Med Genet*. (2018) 55:254–60. doi: 10.1136/jmedgenet-2017-104957
70. Stratakis CA, Tichomirowa MA, Boikos S, Azevedo MF, Lodish M, Martari M, et al. The role of germline AIP, MEN1, PRKAR1A, CDKN1B and CDKN2C mutations in causing pituitary adenomas in a large cohort of children, adolescents, and patients with genetic syndromes. *Clin Genet*. (2010) 78:457–63. doi: 10.1111/j.1399-0004.2010.01406.x
71. Cai F, Zhang YD, Zhao X, Yang YK, Ma SH, Dai CX, et al. Screening for AIP gene mutations in a Han Chinese pituitary adenoma cohort followed by LOH analysis. *Eur J Endocrinol*. (2013) 169:867–84. doi: 10.1530/EJE-13-0442
72. Georgitsi M, De Menis E, Cannavò S, Mäkinen MJ, Tuppurainen K, Pauletto P, et al. Aryl hydrocarbon receptor interacting protein (AIP) gene mutation analysis in children and adolescents with sporadic pituitary adenomas. *Clin Endocrinol*. (2008) 69:621–7. doi: 10.1111/j.1365-2265.2008.03266.x
73. Daly AF, Tichomirowa MA, Petrossians P, Heliövaara E, Jaffrain-Rea ML, Barlier A, et al. Clinical characteristics and therapeutic responses in patients with germ-line AIP mutations and pituitary adenomas: an international collaborative study. *J Clin Endocrinol Metab*. (2010) 95:E373–83. doi: 10.1210/jc.2009-2556
74. Jennings JE, Georgitsi M, Holdaway I, Daly AF, Tichomirowa M, Beckers A, et al. Aggressive pituitary adenomas occurring in young patients in a large Polynesian kindred with a germline R271W mutation in the AIP gene. *Eur J Endocrinol*. (2009) 161:799–804. doi: 10.1530/EJE-09-0406
75. De Sousa SM, McCabe MJ, Wu K, Roscioli T, Gayevskiy V, Brook K, et al. Germline variants in familial pituitary tumour syndrome genes are common in young patients and families with additional endocrine tumours. *Eur J Endocrinol*. (2017) 176:635–44. doi: 10.1530/EJE-16-0944
76. Karaca Z, Taheri S, Tanriverdi F, Unluhizarci K, Kelestimur F. Prevalence of AIP mutations in a series of Turkish acromegalic patients: are synonymous AIP mutations relevant? *Pituitary*. (2015) 18:831–7. doi: 10.1007/s11102-015-0659-0
77. Radian S, Diekmann Y, Gabrovska P, Holland B, Bradley L, Wallace H, et al. Increased population risk of AIP-related acromegaly and gigantism in Ireland. *Hum Mutat*. (2017) 38:78–85. doi: 10.1002/humu.23121
78. Bell DR, Poland A. Binding of Aryl Hydrocarbon Receptor (AhR) to AhR-interacting protein. *J Biol Chem*. (2000) 275:36407–14. doi: 10.1074/jbc.M004236200
79. Occhi G, Jaffrain-Rea ML, Trivellin G, Albiger N, Ceccato F, De Menis E, et al. The R304X mutation of the aryl hydrocarbon receptor interacting protein gene in familial isolated pituitary adenomas: mutational hot-spot or founder effect? *J Endocrinol Invest*. (2010) 33:800–5. doi: 10.1007/BF03350345
80. Chahal HS, Stals K, Unterländer M, Balding DJ, Thomas MG, Kumar AV, et al. AIP mutation in pituitary adenomas in the 18th century and today. *N Engl J Med*. (2011) 364:43–50. doi: 10.1056/NEJMoa1008020
81. Cuny T, Pertuit M, Sahnoun-Fathallah M, Daly A, Occhi G, Odou MF, et al. Genetic analysis in young patients with sporadic pituitary macroadenomas: besides AIP don't forget MEN1 genetic analysis. *Eur J Endocrinol*. (2013) 168:533–41. doi: 10.1530/EJE-12-0763
82. de Lima DS, Martins CS, Paixao BM, Amaral FC, Colli LM, Saggioro FP, et al. SAGE analysis highlights the putative role of underexpression of ribosomal proteins in GH-secreting pituitary adenomas. *Eur J Endocrinol*. (2012) 167:759–68. doi: 10.1530/EJE-12-0760
83. Niyazoglu M, Sayitoglu M, Firtina S, Hatipoglu E, Gazioglu N, Kadioglu P. Familial acromegaly due to aryl hydrocarbon receptor-interacting protein (AIP) gene mutation in a Turkish cohort. *Pituitary*. (2014) 17:220–6. doi: 10.1007/s11102-013-0493-1
84. Williams F, Hunter S, Bradley L, Chahal HS, Storr HL, Akker SA, et al. Clinical experience in the screening and management of a large kindred with familial isolated pituitary adenoma due to an aryl hydrocarbon receptor interacting protein (AIP) mutation. *J Clin Endocrinol Metab*. (2014) 99:1122–31. doi: 10.1210/jc.2013-2868
85. Pardi E, Marcocci C, Borsari S, Saponaro F, Torregrossa L, Tancredi M, et al. Aryl hydrocarbon receptor interacting protein (AIP) mutations occur rarely in sporadic parathyroid adenomas. *J Clin Endocrinol Metab*. (2013) 98:2800–10. doi: 10.1210/jc.2012-4029
86. Occhi G, Trivellin G, Ceccato F, De Lazzari P, Giorgi G, Dematté S, et al. Prevalence of AIP mutations in a large series of sporadic Italian acromegalic patients and evaluation of CDKN1B status in acromegalic

patients with multiple endocrine neoplasia. *Eur J Endocrinol*. (2010) 163:369–76. doi: 10.1530/EJE-10-0327
87. Vargiolu M, Fusco D, Kurelac I, Dirnberger D, Baumeister R, Morra I, et al. The tyrosine kinase receptor RET interacts *in vivo* with aryl hydrocarbon receptor-interacting protein to alter survivin availability. *J Clin Endocrinol Metab*. (2009) 94:2571–8. doi: 10.1210/jc.2008-1980
88. Mothojakan N, Ferrau F, Dang M, Barlier A, Chanson P, Occhi G. Polymorphism or mutation? - the role of the R304Q missense AIP mutation in the predisposition to pituitary adenoma. *Endocr Abstr Biosci*. (2016) 44:P167. doi: 10.1530/endoabs.44.P167
89. Imran SA, Aldahmani KA, Penney L, Croul SE, Clarke DB, Collier DM, et al. Unusual AIP mutation and phenocopy in the family of a young patient with acromegalic gigantism. *Endocrinology Diabetes Metab Case Rep*. (2018) 2018:17-0092. doi: 10.1530/EDM-17-0092
90. Richards S, Aziz N, Bale S, Bick D, Das S, Gastier-Foster J, et al. Standards and guidelines for the interpretation of sequence variants: a joint consensus recommendation of the American college of medical genetics and genomics and the association for molecular pathology. *Genet Med*. (2015) 17:405–24. doi: 10.1038/gim.2015.30
91. Kazlauskas A, Poellinger L, Pongratz I. Two distinct regions of the immunophilin-like protein XAP2 regulate dioxin receptor function and interaction with hsp90. *J Biol Chem*. (2002) 277:11795–801. doi: 10.1074/jbc.M200053200
92. Bolger GB. The PDE4 cAMP-specific phosphodiesterases: targets for drugs with antidepressant and memory-enhancing action. *Adv Neurobiol*. (2017) 17:63–102. doi: 10.1007/978-3-319-58811-7_4
93. Mokra D, Mokry J, Matasova K. Phosphodiesterase inhibitors: potential role in the respiratory distress of neonates. *Pediatr Pulmonol*. (2018) 53:1318–25. doi: 10.1002/ppul.24082
94. Moustafa F, Feldman SR. A review of phosphodiesterase-inhibition and the potential role for phosphodiesterase 4-inhibitors in clinical dermatology. *Dermatol Online J*. (2014) 20:22608. Available online at: https://escholarship.org/uc/item/2hx1m6kv
95. Hamilton TK, Hu N, Kolomitro K, Bell EN, Maurice DH, Graham CH, et al. Potential therapeutic applications of phosphodiesterase inhibition in prostate cancer. *World J Urol*. (2013) 31:325–30. doi: 10.1007/s00345-012-0848-7
96. Tuominen I, Heliövaara E, Raitila A, Rautiainen MR, Mehine M, Katainen R, et al. AIP inactivation leads to pituitary tumorigenesis through defective Gαi-cAMP signaling. *Oncogene*. (2015) 34:1174–84. doi: 10.1038/onc.2014.50
97. Ang KL, Antoni FA. Functional plasticity of cyclic AMP hydrolysis in rat adenohypophysial corticotroph cells. *Cell Signal*. (2002) 14:445–52. doi: 10.1016/S0898-6568(01)00267-4
98. Nikodemova M, Kasckow J, Liu H, Manganiello V, Aguilera G. Cyclic adenosine 3',5'-monophosphate regulation of corticotropin-releasing hormone promoter activity in AtT-20 cells and in a transformed hypothalamic cell line. *Endocrinology*. (2003) 144:1292–300. doi: 10.1210/en.2002-220990

Conflict of Interest Statement: The authors declare that the research was conducted in the absence of any commercial or financial relationships that could be construed as a potential conflict of interest.

frontiers in Endocrinology

REVIEW
published: 14 May 2019
doi: 10.3389/fendo.2019.00290

The Epigenomics of Pituitary Adenoma

Blake M. Hauser[1], *Ashley Lau*[1], *Saksham Gupta*[1], *Wenya Linda Bi*[1]* *and Ian F. Dunn*[2]*

[1] *Center for Skull Base and Pituitary Surgery, Department of Neurosurgery, Brigham and Women's Hospital and Harvard Medical School, Boston, MA, United States,* [2] *Department of Neurosurgery, University of Oklahoma Health Sciences Center, Oklahoma City, OK, United States*

Background: The vast majority of pituitary tumors are benign and behave accordingly; however, a fraction are invasive and are more aggressive, with a very small fraction being frankly malignant. The cellular pathways that drive transformation in pituitary neoplasms are poorly characterized, and current classification methods are not reliable correlates of clinical behavior. Novel techniques in epigenetics, the study of alterations in gene expression without changes to the genetic code, provide a new dimension to characterize tumors, and may hold implications for prognostication and management.

Methods: We conducted a review of primary epigenetic studies of pituitary tumors with a focus on histone modification, DNA methylation, and transcript modification.

Results: High levels of methylation have been identified in invasive and large pituitary tumors. DNA methyltransferase overexpression has been detected in pituitary tumors, especially in macroadenomas. Methylation differences at CpG sites in promoter regions may distinguish several types of tumors from normal pituitary tissue. Histone modifications have been linked to increased p53 expression and longer progression-free survival in pituitary tumors; sirtuins are expressed at higher values in GH-expressing compared to nonfunctional adenomas and correlate inversely with size in somatotrophs. Upregulation in citrullinating enzymes may be an early pathogenic marker of prolactinomas. Numerous genes involved with cell growth and signaling show altered methylation status for pituitary tumors, including cell cycle regulators, components of signal transduction pathways, apoptotic regulators, and pituitary developmental signals.

Conclusions: The limited clinical predictive capacity of the current pituitary tumor classification system suggests that tumor subclasses likely remain to be discovered. Ongoing epigenetic studies could provide a basis for adding methylation and/or acetylation screening to standard pituitary tumor workups. Identifying robust correlations between tumor epigenetics and corresponding histological, radiographic, and clinical course information could ultimately inform clinical decision-making.

Keywords: pituitary tumor, pituitary adenoma, epigenetics, precision medicine, endocrine surgery, epigenome

OPEN ACCESS

Edited by:
Xianquan Zhan, Xiangya Hospital, Central South University, China

Reviewed by:
Yona Greenman, Tel Aviv Sourasky Medical Center, Israel
Jacqueline Trouillas, Université Claude Bernard Lyon 1, France

***Correspondence:**
Wenya Linda Bi
wbi@bwh.harvard.edu
Ian F. Dunn
ian-dunn@ouhsc.edu

Specialty section:
This article was submitted to Pituitary Endocrinology, a section of the journal Frontiers in Endocrinology

Received: *15 December 2018*
Accepted: *23 April 2019*
Published: *14 May 2019*

Citation:
Hauser BM, Lau A, Gupta S, Bi WL and Dunn IF (2019) The Epigenomics of Pituitary Adenoma. Front. Endocrinol. 10:290. doi: 10.3389/fendo.2019.00290

INTRODUCTION

Pituitary tumors constitute at least 15% of intracranial neoplasms (1–4). The anterior pituitary is composed of several hormone-producing cell types, including corticotrophs, somatotrophs, lactotrophs, mammosomatotrophs, thyrotrophs, and gonadotrophs, all of which can give rise to tumors, leading to the heterogeneous group of neoplasms encompassed by the diagnosis of pituitary adenomas (5, 6). Recent work suggests that the term "pituitary tumor" may be more appropriate than "pituitary adenoma," but "adenoma" has been used in this review in some instances to accurately reflect findings reported in the literature (7). These tumors can be functional—producing hormones that reflect their lineage with concordant systemic effects—or nonfunctional, producing systemic sequelae through compromised pituitary function. Each general group can produce symptoms by offending any of a number of adjacent anatomical structures. These groups and individual tumors can have a wide range of clinical behaviors, from benign to highly invasive. Their long-term behavior and response to therapy are not reliably predicted by current classification methods.

The biological underpinnings of pituitary tumors have been investigated to predict and manage them with more precision. The accumulation of genetic mutations confers downstream oncogenic changes such as sustained proliferation, invasion, angiogenesis, growth suppression evasion, and cell death resistance (8). These mutations can consist of changes to the DNA sequence, as well as chromosomal alterations and copy number changes (**Figure 1**; **Table 1**). Large scale genomic sequencing has revealed several mutations in subtypes of pituitary adenomas (9–18). However, on the whole, mutations that drive oncogenesis are sparse across pituitary tumors. Consequently, non-mutational sources of gene expression alteration in pituitary tumors are undergoing investigation.

Epigenetics—the study of alterations in gene expression without changes to DNA sequence—provides an alternative avenue of tumorigenesis and disease characterization (**Figure 1**). DNA methylation by DNA methyltransferases (DMNTs), amongst other enzymes, typically silences gene expression by reducing the access of transcriptional machinery to methylated segments of DNA (**Table 1**). Changes to histone placement can also affect DNA transcription. Histone deacetylases (HDACs) and sirtuins modulate histone acetylation, which generally improves transcriptional access to surrounding DNA, while histone methyltransferases like RIZI alter methylation, which either improves or restricts transcriptional access depending on the methylation site (**Table 1**). Histone citrullination can also affect chromatin expression, and it can be mediated by peptidylarginine deaminase (PAD) enzymes (**Table 1**).

Epigenetic changes can also alter mRNA transcript levels, resulting in either upregulation or downregulation of gene expression. Changes in messenger RNA (mRNA) transcript levels can occur as part of oncogenic transformation (**Figure 1**; **Table 1**). Alterations in mRNA expression can modulate downstream changes in protein expression levels, which in turn drive cellular function. Additionally, differential expression of long non-coding RNA (lncRNA) and microRNA (miRNA) can result in or accompany oncogenesis (**Table 1**).

Incorporating epigenetics into tumor classification schemes for other types of cancer has improved clinical reliability. In breast cancer, DNA hypermethylation of promoter CpG islands corresponds to the presence of certain hormonal receptors as well as clinical tumor progression (19). Similarly, promoter methylation in glioblastoma correlates with response to therapy (20), and DNA methylation-based classification schemes have shown utility in tumor subclassification and prognosis in meningioma (21). For pituitary tumors, subclassification is a more complicated problem given that the multiple cell types present in the pituitary can give rise to tumors with varied secretory properties. Additionally, with the exception of metastasis, criteria for pituitary tumor malignancy remain unclear. Recent studies profiling epigenetic changes in pituitary tumors have shed new insights into the classification of pituitary tumors and may possibly augment prediction of clinical behavior.

CURRENT CLASSIFICATION SCHEMES

The World Health Organization (WHO) classification draws upon pituitary adenohypophyseal cell lineage to categorize tumors into acidophilic, corticotroph, and gonadotroph subtypes based on transcription factor and hormone expression (22, 23). The absence of hormones and transcription factors defines a null cell adenoma. Subtypes with a propensity to exhibit invasiveness, rapid growth, recurrence, and resistance are categorized as clinically aggressive. Terms such as "aggressive," "invasive," and "large" are sometimes used interchangeably in the literature, even though these terms refer to distinct features of pituitary tumors. This review maintains the same terminology accompanying the discussed finding from the cited literature. Clinically aggressive tumors often have high mitotic activity and Ki-67 expression but are not defined by a single biomarker (24). Invasive tumors are loosely defined by a combination of clinical, radiological, and histopathological findings, and do not necessarily imply clinical aggressiveness in terms of disease control or recurrence risk (24). Aggressive tumors are defined by clinical characteristics, and primarily reflect a tumor's rate of recurrence (25). Invasion of the dura can be seen in up to 45.5% of pituitary adenomas (26). Combining multiple modes of information to classify tumors likely provides more accurate prognostic information (27). Novel biomarkers may facilitate the division of pituitary tumors into more clinically useful categories.

GENOMIC ALTERATIONS

Large-scale genomic studies to identify molecular alterations have been thorough, but pituitary tumors display relatively few genetic aberrations compared to other tumor types and cancers. As a result, pituitary tumor genetic information has limited potential to inform the course of treatment for the numerous pituitary tumors without these identified genetic aberrations. Genome-wide association studies (GWAS) have been used

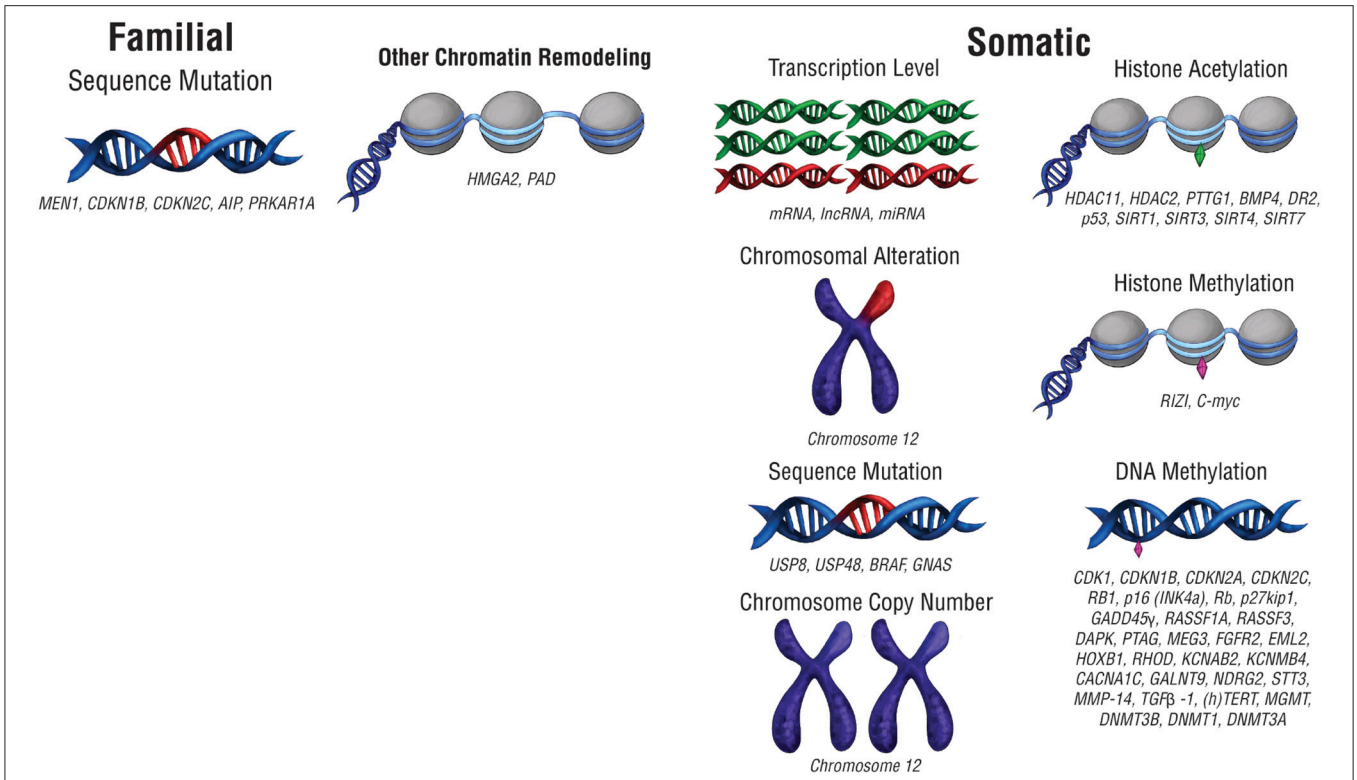

FIGURE 1 | Pre-translational modifications that affect gene expression. Modifications that affect gene expression can occur at any point along the path from packaged DNA to protein expression. Alterations to chromosome structure or changes in chromosome copy number can affect expression at a chromosomal level. Epigenetic chromatin modifications, including histone acetylation and histone methylation, can also alter gene expression levels. At the DNA level, mutations in DNA sequence or DNA methylation can change the nature of the genes expressed as well as their level of expression. RNA transcript copy number also affects protein expression.

TABLE 1 | Genetic, regulatory, and epigenetic mutations.

Genetic	RNA interference	Epigenetic
Sequence mutation	Long non-coding RNA (lncRNA)	DNA methylation
Chromosome alteration	microRNA (miRNA)	Histone acetylation
Chromosome copy number change		Histone methylation Histone citrullination

Changes in gene expression can result from changes in DNA sequence, RNA expression as mediated by RNA interference, or epigenetic regulation. The changes in each of these categories discussed in this review are outlined below.

to identify genetic markers associated with pituitary tumor development. GWAS has revealed common variants (10p12.31, 10q21.1, and 13q12.13) that are associated with sporadic pituitary tumors (17).

Recurrent genetic mutations have been identified in small subsets of pituitary tumors. The first category of tumors with recurrent genetic mutations are those that arise due to familial syndromes (**Table 2**) which include McCune-Albright syndrome, multiple endocrine neoplasia types 1 and 4 (MEN1 and MEN4), familial isolated pituitary adenomas (FIPA), and Carney complex (28). Interestingly, only a small percentage of sporadic pituitary tumors harbor mutations in the genes implicated in familial pituitary tumor disorders [*MEN1*, Cyclin Dependent Kinase Inhibitor 1B *(CDKN1B),* Cyclin Dependent Kinase Inhibitor 2C *(CDKN2C)*, Aryl-Hydrocarbon Receptor Interacting Protein (*AIP)*, and Protein Kinase cAMP-Dependent Type 1 Regulatory Subunit Alpha *(PRKAR1A)* (9–11)]. Select somatic genetic alterations have been identified in several subtypes of adenomas, including high mobility group A 2 (*HMGA2*) amplification via focal amplification or abnormalities of chromosome 12 in prolactinomas (12), Ubiquitin Specific Peptidase 8 (*USP8),* Ubiquitin Specific Peptidase 48 *(USP48),* and *BRAF* in corticotroph adenomas (13, 15, 29), and activating mutations in *GNAS* in GH-secreting pituitary adenomas (14, 16). Chromosome arm-level copy-number alterations also recur within a subset of pituitary tumors, the majority of which are functional macroadenomas (18). In some cases, familial mutations and chromosome abnormalities have been associated with larger tumor size. Genetic associations offer limited utility beyond distinguishing tumor subtype, which may indicate that epigenetic regulation plays a role in the clinical course of pituitary tumors.

TRANSCRIPTIONAL PROFILING

The distinct gene expression profiles of pituitary tumors correlate to some extent with hormone expression status. Additionally,

TABLE 2 | Familial and somatic mutations associated with pituitary tumors.

Familial syndrome	**Gene affected (Germline)**
Multiple endocrine neoplasia type 1	*MEN1, CDKN1B, CDKN2C*
Multiple endocrine neoplasia type 4	*CDKN1B*
Familial isolated pituitary adenomas	*AIP*
Carney complex	*PRKAR1A*
McCune-Albright	*GNAS*
Tumor subtype	**Gene affected**
Prolactinoma	*HMGA2* (a)
Corticotroph	*USP8, USP48, BRAF*
GH-secreting	*GNAS*

Familial syndromes are listed in the top part of the table, and subtype-specific somatic alterations and their mechanisms are listed in the bottom portion of the table. a, amplification; all other genes are mutated.

gene expression profiles may have some predictive value with respect to clinical aggressiveness (18). Tumor classification systems with a molecular basis often yield more insight into tumor origin, tumor behavior, and probable clinical outcomes than purely histological approaches (21, 30, 31). The idea that gene expression signatures may provide insights about tumor behavior and outcome has motivated transcriptomic studies in pituitary tumors to gain a better understanding of how signatures correlate with tumor properties and patient outcomes. These studies also permit the evaluation of the effect of genetic mutations on a protein level, which can improve the clinical utility of tumor genetic information.

Subtypes of pituitary tumors express distinct transcriptional profiles from each other and from normal pituitary gland tissue as assessed by gene microarrays and RNA-Seq. Given that transcription profile differences correlate with tumor presence and subtype, it is possible that they also offer a molecular approach to improving classification schemes. Relative to normal pituitary tissue, pituitary tumors have differentially expressed mRNA transcripts (32–37), lncRNA transcripts (36, 38), and miRNA transcripts (39–42). Notably, investigations have found that two miRNAs (miR196a-2 and miR-212) which target HMGA transcripts can be deregulated in all tumor types (43–47). Changes in expression profile also manifest in different subclasses of tumors (48–50). In particular, deregulation of miR-183 in prolactinomas has been associated with clinical aggressiveness (51).

However, large-scale transcriptome analyses often produce gene expression results that conflict with the findings in other studies. Heterogeneity within tumor samples, a small patient sample that fails to capture a representative selection of tumor samples, and different experimental conditions may contribute to divergent study results. Furthermore, one potential shortcoming of transcriptome studies is the use of predetermined histological or radiographic categories to partition gene expression results. This approach can identify gene expression differences representative of each tumor type or subclass but precludes identification of novel classes within the tumor population that are independent of histological characteristics. The disparate clinical trajectories of pituitary tumor subtypes suggest that there are likely to be subclasses with varying degrees of invasiveness and aggressiveness that remain to be discovered. However, no system for classifying pituitary tumors accurately correlates genetic markers with clinical outcomes, so tumor genetic information still has limited clinical utility.

EPIGENETIC MODIFICATIONS

Given the centrality of gene expression changes and the relative dearth of genetic abnormalities in pituitary tumors, epigenetic modifications have received considerable attention.

DNA methylation was examined (**Figure 2**), particularly at CpG islands in gene promoters, where methylation often correlates with gene silencing (52). Approximately two-thirds of reference epigenomes have been found to contain quiescent signatures, whereas only 5% of genomes contain promoter and enhancer signatures (53). The "histone code" hypothesis, which states that certain patterns of post-translational modifications on histone tails can function as signals in gene regulatory processes (54) (**Figure 2**), has also led to a small number of studies that assay histone modifications in pituitary tumors.

DNA Methylation

Methylation of gene promoters is frequently deregulated in tumors (55), and appears to be a common mechanism for gene inactivation in pituitary tumors. Given the simplicity of detecting DNA methylation at targeted locations within the genome, clinically meaningful epigenetic findings could be implemented rapidly to guide treatment plan development.

DNA methyltransferase (DNMT) enzymes catalyze methylation at CpG dinucleotides, with DNMT3A and DNMT3B serving as the *de novo* methyltransferases, and DNMT1 as the maintenance methyltransferase. Ten-eleven translocation (TET) enzymes may also participate in regulating methylation as removers of methylation modifications (56). Early observations that classic oncogene and tumor suppressor mutations were absent in pituitary tumors led to the realization that promoter methylation changes constituted an alternative mechanism by which causative genes could be deregulated. Numerous genes involved with cell growth and signaling show altered methylation status, including cell cycle regulators [Cyclin Dependent Kinase 1 (*CDK1)* (57), *CDKN1B* (58), Cyclin Dependent Kinase Inhibitor 2A *(CDKN2A)* (59), *CDKN2C* (59, 60), Retinoblastoma Transcriptional Corepressor 1 *(RB1)* (58, 61), CDKN2A protein ($p16^{INK4a}$) (58), Retinoblastoma (*Rb)* (62), CDKN1B protein (p27kip1) (63), Growth Arrest and DNA Damage 45γ *(GADD45γ)* (64, 65)]; components of signal transduction pathways [Ras Associated Domain Family Member 1A (*RASSF1A)* (66) and Ras Associated Domain Family Member 3 *(RASSF3)*]; apoptotic regulators [Death-Associated Protein Kinase (*DAPK)* (67) and Pituitary Tumor Apoptosis Gene *(PTAG)* (68)]; developmental gene Maternally Expressed 3 *(MEG3)* (69); and the growth factor signaling component Fibroblast Growth Factor Receptor 2 *(FGFR2)* (70).

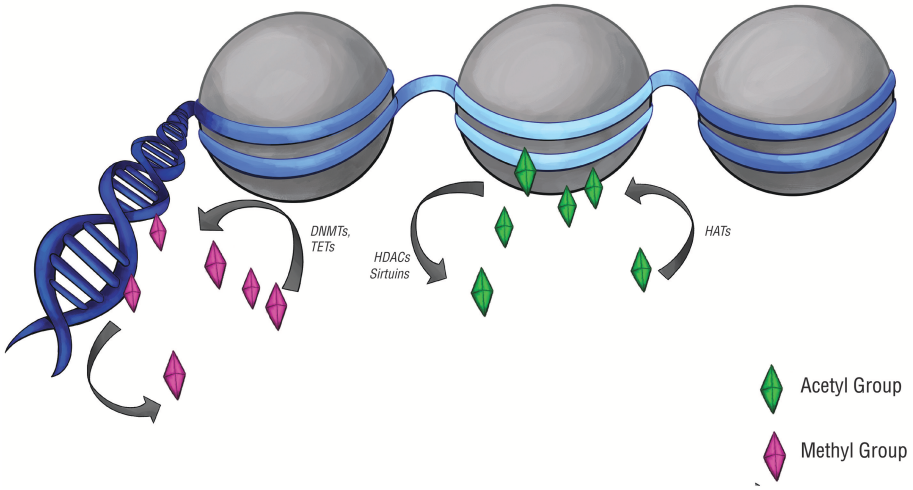

FIGURE 2 | Epigenetic modifications and regulators. Epigenetic modifications are carried out by a set of specialized enzymes that act directly on DNA or on the histones around which chromatin is wrapped. Histone acetyltransferases (HATs) place acetyl groups on chromatin, while histone deacetylases (HDACs) and sirtuins do the opposite. Acetylation of histones typically upregulates gene expression, denoted here by the light blue region of DNA. DNA methyltransferases (DNMTs) and ten-eleven translocation enzymes (TETs) can alter the level of DNA or histone methylation, which typically downregulates gene expression. This is denoted by the navy-blue regions of DNA.

TABLE 3 | Altered regulation of epigenetic modifiers in aggressive, invasive, or large, and functional tumors.

	Pituitary tumor	Functional	Aggressive, invasive, or large
Upregulated	DNMT3B (71), HDAC11 (72)	HDAC2 (73), RIZI (74), PAD (75), *SIRT1* (76), *SIRT3* (76), *SIRT4* (76), *SIRT7* (76)	DNMT1 (77), DNMT3A (77)
Downregulated	*HMGA2* (78)		*SIRT1* (76), *SIRT3* (76)

DNA modifiers (in red) and histone modifiers (in blue) shown. (Gene names italicized, protein names non-italicized).

DNA Methylation Enzymes

High levels of methylation may be associated with clinically aggressive behavior in pituitary tumors (**Table 3**). DNMT1 and DNMT3A overexpression has been detected in pituitary tumors (77). Both were significantly associated with more aggressive tumors, with DNMT1 levels also significantly higher in macroadenomas. Relatively higher levels of expression of DNMT3B has also been found in pituitary tumors in comparison to normal tissue with no difference in DNMT1 and DNMT3A expression (71). It is possible that the transfer of methyl groups will also result in regions of DNA being hypomethylated and therefore expressed at a higher level. As DNA hypomethylation has also shown some association with cancerous behavior, high levels of DNMT expression could theoretically increase the risk of malignancy through hypomethylation mechanism as well (79).

CpG Methylation

Genome-wide methylome studies have found methylation differences at promoter region CpG sites to distinguish several types of adenomas from normal pituitary tissue (80). A subset of genes are hypermethylated in nonfunctional adenomas as well as growth hormone (GH) and prolactin (PRL) secreting adenomas. However, only Echinoderm Microtubule Associated Protein Like 2 *(EML2)*, Homeobox B1 *(HOXB1)*, and Rho-Related GTP-Binding Protein *(RHOD)*, also demonstrate a corresponding decrease in expression, suggesting that the degree of promoter methylation may not always translate to actual changes in gene expression. *HOXB1* has been identified as a tumor suppressor gene in glioma (81), and *RHOD* may affect cytoskeletal reorganization and transportation (82).

Variations in methylation may also exist at CpG sites across the genome, including intergenic sites and gene body regions (83, 84). Nonfunctional tumors have displayed global hypermethylation relative to hormonally active tumors (84), particularly GH (83). Genes involved in ion channel signaling, including Voltage-Gated Potassium Channel Subunit Beta-2 *(KCNAB2)*, Calcium-Activated Potassium Channel Subunit Beta-4 *(KCNMB4)*, and Calcium Voltage-Gated Channel Subunit Alpha1 C *(CACNA1C)*, can be hypermethylated in nonfunctional tumors (83). However, expression does not consistently correlate with methylation at promoter CpG sites, so it is unclear to what extent such epigenetic changes affect phenotype. Hypomethylated CpGs are significantly more common in invasive NF pituitary adenomas than hypermethylated CpGs (84). One differentially methylated site was associated with Polypeptide N-acetylgalactosaminyltransferase 9 *(GALNT9)*, and its expression was downregulated significantly in the invasive tumors. A number of other differentially methylated sites correspond to genes involved in cell adhesion, indicating a possible mechanism by which methylation changes influence tumor phenotype. Characteristic methylation patterns can also be associated with GH-secreting, ACTH-secreting and NF pituitary

tumor subtypes, but further investigation is required to better elucidate the extent to which differential methylation exists across subtypes of pituitary tumors (85).

Promoter Methylation

The lack of correlation between hypermethylation and gene expression implies that additional regulatory mechanisms beyond methylation remain to be discovered. Methylation and expression levels of the N-myc Downstream-Regulated Gene 2 *(NDRG2)* and Signal Transducer and Activator of Transcription 3 *(STAT3)* promoters are also uncorrelated, along with a lack of correlation with clinical factors (86, 87). Methylation of the Matrix Metallopeptidase 14 *(MMP-14)* and Transforming Growth Factor Beta 1 *(TGFβ-1)* promoters was also not associated with tumor functionality or recurrence (88). Hypermethylation of the Human Telomerase Reverse Transcriptase *(hTERT*) promoter, which can contribute to cellular immortalization and tumorigenesis, has also been noted across different pituitary tumor subtypes but has not been associated with significant differences in tumor parameters, tumor subtype, or prognosis (89). However, differential methylation of *TERT* promoters has not been consistently observed (90). Larger patient sample sizes are required to better understand the clinical impact of specific epigenetic changes in pituitary tumors.

Methylation at the O^6-Methylguanine-DNA Methyltransferase *(MGMT)* promoter is of particular interest given its utility epigenetic modification in determining response to temozolomide (TMZ) in glioblastoma (20). Temozolomide has been used for aggressive pituitary adenomas, with mixed results (91, 92). Thus far, *MGMT* expression, rather than promoter methylation, appears to better correlate with TMZ response in pituitary adenomas; however, a limited number of studies have examined this relationship, and TMZ is still administered, particularly in the context of aggressive pituitary tumors, regardless of *MGMT* status (24, 93). MGMT promoter methylation has also been associated with tumor regrowth in pituitary adenoma (94). Even though *MGMT* methylation does not offer as much predictive value for pituitary tumors as glioblastoma, finding clinically informative methylation markers remains the goal.

Histone Modifications

Acetylation of histone tails, particularly H3 and H4, is generally seen as a mark of active regions of the genome, whereas methylation of histone tails, particularly lysine 9 on H3 (H3K9), is associated with inactive heterochromatin (95). Epigenetic markers can be dynamically modified by chromatin regulators including the histone acetyltransferases (HATs) and histone deacetylases (HDACs).

Histone Acetylation Regulators

Multiple chromatin regulators are differentially regulated in pituitary tumors, including *HMGA2* and HDAC2 (73, 78), suggesting that pituitary tumors likely have altered patterns of histone modifications (**Table 3**). HDAC11 has been shown to interfere with p53 expression in pituitary tumor cells (72). Global acetylation resulted in an increase in Pituitary Tumor-Transforming Gene 1 *(PTTG1),* Bone Morphogenic Protein 4 *(BMP4),* and Dopamine Receptor 2 *(DR2)* expression in pituitary tumor cells, suggesting that global alterations in epigenetic modifications may result in gene expression changes (96, 97). Given the nonspecific effects of global acetylation modification, it is unclear how relevant global acetylation findings are to pituitary tumor pathogenesis and therapeutic applications.

The differential expression of some members of the sirtuin family (*SIRT*) of HDACs has been observed in somatotropinomas as compared to NF pituitary adenomas (76). *SIRT1* was overexpressed in somatotropinomas, while *SIRT3*, *SIRT4*, and *SIRT7* were under-expressed in NF pituitary adenomas. *SIRT1* overexpression correlated with smaller tumor size, while *SIRT3* under-expression correlated with larger tumor size. There was no association between sirtuin levels and invasiveness or Ki-67 proliferative index.

Histone Methylation Regulators

Non-invasive pituitary adenomas express significantly higher levels of RIZI, which acts as a tumor-suppressor as well as a possible histone methyltransferase, and lower levels of C-myc, as compared to invasive pituitary adenomas (74). Increased RIZI expression also correlates with significant differences in methylation at four CpG sites, reduced H3K4/H3K9 methylation, and enhanced H3K27 methylation, as well as significantly longer progression-free survival (74). Additionally, p53 mis-expression correlates with H3K9 methylation (98). Specific examples of correlations between epigenetic modifications and gene expression further affirm the possibility that histone modifications may alter gene expression in pituitary tumors.

Histone Citrullination Regulators

Peptidylarginine deaminase (PAD) enzymes facilitate histone citrullination, which can modulate chromatin expression (**Table 3**). Increased PAD prevalence in prolactinomas and somatoprolactinomas has been associated with increased mRNA targeting of oncogenes *HMGA*, Insulin-like Growth Factor 1 *(IGF-1)*, and Neuroblastoma MYC Oncogene *(N-MYC)* by miRNAs, which may yield insight into the etiology of the affected tumor subtypes (75).

CURRENT LIMITATIONS AND FUTURE DIRECTIONS

The limited ability of existing pituitary tumor classification systems to predict clinical behavior motivates investigation into a molecular taxonomy with clinical implications. Though epigenetic signatures are not yet incorporated into clinical decision making for pituitary tumors, the importance of methylation and epigenetic signatures is increasingly appreciated across brain tumors with clinical implications (20, 21). Given the absence of recurrent oncogenic mutations and copy number alterations in many pituitary tumors, epigenetic mechanisms present an intriguing biological avenue for further exploration.

Further elucidation of the mechanisms underlying gene deregulation is needed before viable therapeutic strategies can be developed. Several compounds that inhibit epigenetic modifications are FDA approved, though it remains to be determined whether compounds that globally affect DNA methylation and histone modifications can provide specificity and efficacy in targeting the genetic pathways deregulated in pituitary tumors. More targeted strategies for modulating epigenetic modifications, though currently still in early development, may hold promise for treatment of pituitary tumors (99). Ultimately, an integrated classification of epigenetic, genetic, and histopathologic features may augment the collective predictive power of molecular taxonomy in translating to clinical practice.

AUTHOR CONTRIBUTIONS

BH, AL, and SG contributed to the review of the literature and the drafting of the manuscript. WB and ID conceived of the project and provided guidance throughout the writing process.

ACKNOWLEDGMENTS

The authors acknowledge Natalie Charewicz for contributing the original illustrations shown in **Figures 1**, **2**. BH was supported by award Number T32GM007753 from the National Institute of General Medical Sciences. The content is solely the responsibility of the authors and does not necessarily represent the official views of the National Institute of General Medical Sciences or the National Institutes of Health.

REFERENCES

1. Gittleman H, Ostrom QT, Farah PD, Ondracek A, Chen Y, Wolinsky Y, et al. Descriptive epidemiology of pituitary tumors in the United States, 2004-2009. *J Neurosurg.* (2014) 121:527–35. doi: 10.3171/2014.5.JNS131819
2. Fernandez A, Karavitaki N, Wass JA. Prevalence of pituitary adenomas: a community-based, cross-sectional study in Banbury (Oxfordshire, UK). *Clin Endocrinol.* (2010) 72:377–82. doi: 10.1111/j.1365-2265.2009.03667.x
3. Daly AF, Rixhon M, Adam C, Dempegioti A, Tichomirowa MA, Beckers A. High prevalence of pituitary adenomas: a cross-sectional study in the province of Liege, Belgium. *J Clin Endocrinol Metab.* (2006) 91:4769–75. doi: 10.1210/jc.2006-1668
4. Raappana A, Koivukangas J, Ebeling T, Pirila T. Incidence of pituitary adenomas in Northern Finland in 1992-2007. *J Clin Endocrinol Metab.* (2010) 95:4268–75. doi: 10.1210/jc.2010-0537
5. Melmed S. Pathogenesis of pituitary tumors. *Nat Rev Endocrinol.* (2011) 7:257–66. doi: 10.1038/nrendo.2011.40
6. Asa SL, Ezzat S. The pathogenesis of pituitary tumours. *Nat Rev Cancer.* (2002) 2:836–49. doi: 10.1038/nrc926
7. Asa SL, Casar-Borota O, Chanson P, Delgrange E, Earls P, Ezzat S, et al. From pituitary adenoma to pituitary neuroendocrine tumor (PitNET): an International Pituitary Pathology Club proposal. *Endocr Relat Cancer.* (2017) 24:C5–8. doi: 10.1530/ERC-17-0004
8. Hanahan D, Weinberg RA. Hallmarks of cancer: the next generation. *Cell.* (2011) 144:646–74. doi: 10.1016/j.cell.2011.02.013
9. Lecoq AL, Kamenicky P, Guiochon-Mantel A, Chanson P. Genetic mutations in sporadic pituitary adenomas–what to screen for? *Nat Rev Endocrinol.* (2015) 11:43–54. doi: 10.1038/nrendo.2014.181
10. Wenbin C, Asai A, Teramoto A, Sanno N, Kirino T. Mutations of the MEN1 tumor suppressor gene in sporadic pituitary tumors. *Cancer Lett.* (1999) 142:43–7. doi: 10.1016/S0304-3835(99)00111-1
11. Vierimaa O, Georgitsi M, Lehtonen R, Vahteristo P, Kokko A, Raitila A, et al. Pituitary adenoma predisposition caused by germline mutations in the AIP gene. *Science.* (2006) 312:1228–30. doi: 10.1126/science.1126100
12. Finelli P, Pierantoni GM, Giardino D, Losa M, Rodeschini O, Fedele M, et al. The High Mobility Group A2 gene is amplified and overexpressed in human prolactinomas. *Cancer Res.* (2002) 62:2398–405.
13. Ma ZY, Song ZJ, Chen JH, Wang YF, Li SQ, Zhou LF, et al. Recurrent gain-of-function USP8 mutations in Cushing's disease. *Cell Res.* (2015) 25:306–17. doi: 10.1038/cr.2015.20
14. Ronchi CL, Peverelli E, Herterich S, Weigand I, Mantovani G, Schwarzmayr T, et al. Landscape of somatic mutations in sporadic GH-secreting pituitary adenomas. *Eur J Endocrinol.* (2016) 174:363–72. doi: 10.1530/EJE-15-1064
15. Reincke M, Sbiera S, Hayakawa A, Theodoropoulou M, Osswald A, Beuschlein F, et al. Mutations in the deubiquitinase gene USP8 cause Cushing's disease. *Nat Genet.* (2015) 47:31–8. doi: 10.1038/ng.3166
16. Landis CA, Masters SB, Spada A, Pace AM, Bourne HR, Vallar L. GTPase inhibiting mutations activate the alpha chain of Gs and stimulate adenylyl cyclase in human pituitary tumours. *Nature.* (1989) 340:692–6. doi: 10.1038/340692a0
17. Ye Z, Li Z, Wang Y, Mao Y, Shen M, Zhang Q, et al. Common variants at 10p12.31, 10q21.1 and 13q12.13 are associated with sporadic pituitary adenoma. *Nat Genet.* (2015) 47:793–7. doi: 10.1038/ng.3322
18. Bi WL, Horowitz P, Greenwald NF, Abedalthagafi M, Agarwalla PK, Gibson WJ, et al. Landscape of genomic alterations in pituitary adenomas. *Clin Cancer Res.* (2017) 23:1841–51. doi: 10.1158/1078-0432.CCR-16-0790
19. Wu Y, Sarkissyan M, Vadgama JV. Epigenetics in breast and prostate cancer. *Methods Mol Biol.* (2015) 1238:425–66. doi: 10.1007/978-1-4939-1804-1_23
20. Hegi ME, Diserens AC, Gorlia T, Hamou MF, de Tribolet N, Weller M, et al. MGMT gene silencing and benefit from temozolomide in glioblastoma. *N Engl J Med.* (2005) 352:997–1003. doi: 10.1056/NEJMoa043331
21. Sahm F, Schrimpf D, Stichel D, Jones DTW, Hielscher T, Schefzyk S, et al. DNA methylation-based classification and grading system for meningioma: a multicentre, retrospective analysis. *Lancet Oncol.* (2017) 18:682–94. doi: 10.1016/S1470-2045(17)30155-9
22. Lopes MBS. The 2017 World Health Organization classification of tumors of the pituitary gland: a summary. *Acta Neuropathol.* (2017) 134:521–35. doi: 10.1007/s00401-017-1769-8
23. Mete O, Lopes MB. Overview of the 2017 WHO classification of pituitary tumors. *Endocr Pathol.* (2017) 28:228–43. doi: 10.1007/s12022-017-9498-z
24. Di Ieva A, Rotondo F, Syro LV, Cusimano MD, Kovacs K. Aggressive pituitary adenomas–diagnosis and emerging treatments. *Nat Rev Endocrinol.* (2014) 10:423–35. doi: 10.1038/nrendo.2014.64
25. Raverot G, Burman P, McCormack A, Heaney A, Petersenn S, Popovic V, et al. European Society of Endocrinology Clinical Practice Guidelines for the management of aggressive pituitary tumours and carcinomas. *Eur J Endocrinol.* (2018) 178:G1–24. doi: 10.1530/EJE-17-0796
26. Meij BP, Lopes MB, Ellegala DB, Alden TD, Laws ER Jr. The long-term significance of microscopic dural invasion in 354 patients with pituitary adenomas treated with transsphenoidal surgery. *J Neurosurg.* (2002) 96:195–208. doi: 10.3171/jns.2002.96.2.0195
27. Trouillas J, Roy P, Sturm N, Dantony E, Cortet-Rudelli C, Viennet G, et al. A new prognostic clinicopathological classification of pituitary adenomas: a multicentric case-control study of 410 patients with 8 years post-operative follow-up. *Acta Neuropathol.* (2013) 126:123–35. doi: 10.1007/s00401-013-1084-y
28. Bi WL, Larsen AG, Dunn IF. Genomic alterations in sporadic pituitary tumors. *Curr Neurol Neurosci Rep.* (2018) 18:4. doi: 10.1007/s11910-018-0811-0
29. Chen J, Jian X, Deng S, Ma Z, Shou X, Shen Y, et al. Identification of recurrent USP48 and BRAF mutations in Cushing's disease. *Nat Commun.* (2018) 9:3171. doi: 10.1038/s41467-018-05275-5

30. Pajtler KW, Witt H, Sill M, Jones DT, Hovestadt V, Kratochwil F, et al. Molecular classification of ependymal tumors across all CNS compartments, histopathological grades, and age groups. *Cancer Cell.* (2015) 27:728–43. doi: 10.1016/j.ccell.2015.04.002
31. Capper D, Jones DTW, Sill M, Hovestadt V, Schrimpf D, Sturm D, et al. DNA methylation-based classification of central nervous system tumours. *Nature.* (2018) 555:469–74. doi: 10.1038/nature26000
32. Evans CO, Moreno CS, Zhan X, McCabe MT, Vertino PM, Desiderio DM, et al. Molecular pathogenesis of human prolactinomas identified by gene expression profiling, RT-qPCR, and proteomic analyses. *Pituitary.* (2008) 11:231–45. doi: 10.1007/s11102-007-0082-2
33. Evans CO, Young AN, Brown MR, Brat DJ, Parks JS, Neish AS, et al. Novel patterns of gene expression in pituitary adenomas identified by complementary deoxyribonucleic acid microarrays and quantitative reverse transcription-polymerase chain reaction. *J Clin Endocrinol Metab.* (2001) 86:3097–107. doi: 10.1210/jcem.86.7.7616
34. Moreno CS, Evans CO, Zhan X, Okor M, Desiderio DM, Oyesiku NM. Novel molecular signaling and classification of human clinically nonfunctional pituitary adenomas identified by gene expression profiling and proteomic analyses. *Cancer Res.* (2005) 65:10214–22. doi: 10.1158/0008-5472.CAN-05-0884
35. Morris DG, Musat M, Czirjak S, Hanzely Z, Lillington DM, Korbonits M, et al. Differential gene expression in pituitary adenomas by oligonucleotide array analysis. *Eur J Endocrinol.* (2005) 153:143–51. doi: 10.1530/eje.1.01937
36. Li J, Li C, Wang J, Song G, Zhao Z, Wang H, et al. Genome-wide analysis of differentially expressed lncRNAs and mRNAs in primary gonadotrophin adenomas by RNA-seq. *Oncotarget.* (2017) 8:4585–606. doi: 10.18632/oncotarget.13948
37. Ibanez-Costa A, Gahete MD, Rivero-Cortes E, Rincon-Fernandez D, Nelson R, Beltran M, et al. In1-ghrelin splicing variant is overexpressed in pituitary adenomas and increases their aggressive features. *Sci Rep.* (2015) 5:8714. doi: 10.1038/srep08714
38. Yu G, Li C, Xie W, Wang Z, Gao H, Cao L, et al. Long non-coding RNA C5orf66-AS1 is downregulated in pituitary null cell adenomas and is associated with their invasiveness. *Oncol Rep.* (2017) 38:1140–8. doi: 10.3892/or.2017.5739
39. Stilling G, Sun Z, Zhang S, Jin L, Righi A, Kovacs G, et al. MicroRNA expression in ACTH-producing pituitary tumors: up-regulation of microRNA-122 and−493 in pituitary carcinomas. *Endocrine.* (2010) 38:67–75. doi: 10.1007/s12020-010-9346-0
40. He W, Huang L, Li M, Yang Y, Chen Z, Shen X. MiR-148b, MiR-152/ALCAM axis regulates the proliferation and invasion of pituitary adenomas cells. *Cell Physiol Biochem.* (2017) 44:792–803. doi: 10.1159/000485342
41. Zhen W, Qiu D, Zhiyong C, Xin W, Mengyao J, Dimin Z, et al. MicroRNA-524-5p functions as a tumor suppressor in a human pituitary tumor-derived cell line. *Horm Metab Res.* (2017) 49:550–7. doi: 10.1055/s-0043-106437
42. Seltzer J, Ashton CE, Scotton TC, Pangal D, Carmichael JD, Zada G. Gene and protein expression in pituitary corticotroph adenomas: a systematic review of the literature. *Neurosurg Focus.* (2015) 38:E17. doi: 10.3171/2014.10.FOCUS14683
43. Bottoni A, Zatelli MC, Ferracin M, Tagliati F, Piccin D, Vignali C, et al. Identification of differentially expressed microRNAs by microarray: a possible role for microRNA genes in pituitary adenomas. *J Cell Physiol.* (2007) 210:370–7. doi: 10.1002/jcp.20832
44. Palmieri D, D'Angelo D, Valentino T, De Martino I, Ferraro A, Wierinckx A, et al. Downregulation of HMGA-targeting microRNAs has a critical role in human pituitary tumorigenesis. *Oncogene.* (2012) 31:3857–65. doi: 10.1038/onc.2011.557
45. Kitchen MO, Yacqub-Usman K, Emes RD, Richardson A, Clayton RN, Farrell WE. Epidrug mediated re-expression of miRNA targeting the HMGA transcripts in pituitary cells. *Pituitary.* (2015) 18:674–84. doi: 10.1007/s11102-014-0630-5
46. Esposito F, De Martino M, D'Angelo D, Mussnich P, Raverot G, Jaffrain-Rea ML, et al. HMGA1-pseudogene expression is induced in human pituitary tumors. *Cell Cycle.* (2015) 14:1471–5. doi: 10.1080/15384101.2015.1021520
47. Wierinckx A, Roche M, Legras-Lachuer C, Trouillas J, Raverot G, Lachuer J. MicroRNAs in pituitary tumors. *Mol Cell Endocrinol.* (2017) 456:51–61. doi: 10.1016/j.mce.2017.01.021
48. Ruebel KH, Leontovich AA, Jin L, Stilling GA, Zhang H, Qian X, et al. Patterns of gene expression in pituitary carcinomas and adenomas analyzed by high-density oligonucleotide arrays, reverse transcriptase-quantitative PCR, and protein expression. *Endocrine.* (2006) 29:435–44. doi: 10.1385/ENDO:29:3:435
49. Hussaini IM, Trotter C, Zhao Y, Abdel-Fattah R, Amos S, Xiao A, et al. Matrix metalloproteinase-9 is differentially expressed in nonfunctioning invasive and noninvasive pituitary adenomas and increases invasion in human pituitary adenoma cell line. *Am J Pathol.* (2007) 170:356–65. doi: 10.2353/ajpath.2007.060736
50. Galland F, Lacroix L, Saulnier P, Dessen P, Meduri G, Bernier M, et al. Differential gene expression profiles of invasive and non-invasive non-functioning pituitary adenomas based on microarray analysis. *Endocr Relat Cancer.* (2010) 17:361–71. doi: 10.1677/ERC-10-0018
51. Roche M, Wierinckx A, Croze S, Rey C, Legras-Lachuer C, Morel AP, et al. Deregulation of miR-183 and KIAA0101 in aggressive and malignant pituitary tumors. *Front Med.* (2015) 2:54. doi: 10.3389/fmed.2015.00054
52. Bird A. DNA methylation patterns and epigenetic memory. *Genes Dev.* (2002) 16:6–21. doi: 10.1101/gad.947102
53. Roadmap Epigenomics Consortium, Kundaje A, Meuleman W, Ernst J, Bilenky M, Yen A, et al. Integrative analysis of 111 reference human epigenomes. *Nature.* (2015) 518:317–30. doi: 10.1038/nature14248
54. Strahl BD, Allis CD. The language of covalent histone modifications. *Nature.* (2000) 403:41–5. doi: 10.1038/47412
55. Baylin SB, Jones PA. A decade of exploring the cancer epigenome - biological and translational implications. *Nat Rev Cancer.* (2011) 11:726–34. doi: 10.1038/nrc3130
56. Jones PA. Functions of DNA methylation: islands, start sites, gene bodies and beyond. *Nat Rev Genet.* (2012) 13:484–92. doi: 10.1038/nrg3230
57. Lidhar K, Korbonits M, Jordan S, Khalimova Z, Kaltsas G, Lu X, et al. Low expression of the cell cycle inhibitor p27Kip1 in normal corticotroph cells, corticotroph tumors, and malignant pituitary tumors. *J Clin Endocrinol Metab.* (1999) 84:3823–30. doi: 10.1210/jcem.84.10.6066
58. Yoshino A, Katayama Y, Ogino A, Watanabe T, Yachi K, Ohta T, et al. Promoter hypermethylation profile of cell cycle regulator genes in pituitary adenomas. *J Neurooncol.* (2007) 83:153–62. doi: 10.1007/s11060-006-9316-9
59. Kirsch M, Morz M, Pinzer T, Schackert HK, Schackert G. Frequent loss of the CDKN2C (p18INK4c) gene product in pituitary adenomas. *Genes Chromosomes Cancer.* (2009) 48:143–54. doi: 10.1002/gcc.20621
60. Hossain MG, Iwata T, Mizusawa N, Qian ZR, Shima SW, Okutsu T, et al. Expression of p18(INK4C) is down-regulated in human pituitary adenomas. *Endocr Pathol.* (2009) 20:114–21. doi: 10.1007/s12022-009-9076-0
61. Simpson DJ, Hibberts NA, McNicol AM, Clayton RN, Farrell WE. Loss of pRb expression in pituitary adenomas is associated with methylation of the RB1 CpG island. *Cancer Res.* (2000) 60:1211–6.
62. Tateno T, Nakano-Tateno T, Ezzat S, Asa SL. NG2 targets tumorigenic Rb inactivation in Pit1-lineage pituitary cells. *Endocr Relat Cancer.* (2016) 23:445–56. doi: 10.1530/ERC-16-0013
63. Nakayama K, Ishida N, Shirane M, Inomata A, Inoue T, Shishido N, et al. Mice lacking p27(Kip1) display increased body size, multiple organ hyperplasia, retinal dysplasia, and pituitary tumors. *Cell.* (1996) 85:707–20. doi: 10.1016/S0092-8674(00)81237-4
64. Zhang X, Sun H, Danila DC, Johnson SR, Zhou Y, Swearingen B, et al. Loss of expression of GADD45 gamma, a growth inhibitory gene, in human pituitary adenomas: implications for tumorigenesis. *J Clin Endocrinol Metab.* (2002) 87:1262–7. doi: 10.1210/jcem.87.3.8315
65. Bahar A, Bicknell JE, Simpson DJ, Clayton RN, Farrell WE. Loss of expression of the growth inhibitory gene GADD45gamma, in human pituitary adenomas, is associated with CpG island methylation. *Oncogene.* (2004) 23:936–44. doi: 10.1038/sj.onc.1207193
66. Qian ZR, Sano T, Yoshimoto K, Yamada S, Ishizuka A, Mizusawa N, et al. Inactivation of RASSF1A tumor suppressor gene by aberrant promoter hypermethylation in human pituitary adenomas. *Lab Invest.* (2005) 85:464–73. doi: 10.1038/labinvest.3700248
67. Simpson DJ, Clayton RN, Farrell WE. Preferential loss of Death Associated Protein kinase expression in invasive pituitary tumours is associated with either CpG island methylation or homozygous deletion. *Oncogene.* (2002) 21:1217–24. doi: 10.1038/sj.onc.1205195

68. Bahar A, Simpson DJ, Cutty SJ, Bicknell JE, Hoban PR, Holley S, et al. Isolation and characterization of a novel pituitary tumor apoptosis gene. *Mol Endocrinol.* (2004) 18:1827–39. doi: 10.1210/me.2004-0087
69. Zhao J, Dahle D, Zhou Y, Zhang X, Klibanski A. Hypermethylation of the promoter region is associated with the loss of MEG3 gene expression in human pituitary tumors. *J Clin Endocrinol Metab.* (2005) 90:2179–86. doi: 10.1210/jc.2004-1848
70. Zhu X, Lee K, Asa SL, Ezzat S. Epigenetic silencing through DNA and histone methylation of fibroblast growth factor receptor 2 in neoplastic pituitary cells. *Am J Pathol.* (2007) 170:1618–28. doi: 10.2353/ajpath.2007.061111
71. Zhu X, Mao X, Hurren R, Schimmer AD, Ezzat S, Asa SL. Deoxyribonucleic acid methyltransferase 3B promotes epigenetic silencing through histone 3 chromatin modifications in pituitary cells. *J Clin Endocrinol Metab.* (2008) 93:3610–7. doi: 10.1210/jc.2008-0578
72. Wang W, Fu L, Li S, Xu Z, Li X. Histone deacetylase 11 suppresses p53 expression in pituitary tumor cells. *Cell Biol Int.* (2017) 41:1290–5. doi: 10.1002/cbin.10834
73. Bilodeau S, Vallette-Kasic S, Gauthier Y, Figarella-Branger D, Brue T, Berthelet F, et al. Role of Brg1 and HDAC2 in GR trans-repression of the pituitary POMC gene and misexpression in Cushing disease. *Genes Dev.* (2006) 20:2871–86. doi: 10.1101/gad.1444606
74. Xue Y, Chen R, Du W, Yang F, Wei X. RIZ1 and histone methylation status in pituitary adenomas. *Tumour Biol.* (2017) 39:1010428317711794. doi: 10.1177/1010428317711794
75. DeVore SB, Young CH, Li G, Sundararajan A, Ramaraj T, Mudge J, et al. Histone citrullination represses miRNA expression resulting in increased oncogene mRNAs in somatolactotrope cells. *Mol Cell Biol.* (2018) 38:e00084-18. doi: 10.1128/MCB.00084-18
76. Grande IPP, Amorim P, Freire A, Jallad RS, Musolino NR, Cescato VA, et al. Differential gene expression of sirtuins between somatotropinomas and nonfunctioning pituitary adenomas. *Pituitary.* (2018) 21:355–61. doi: 10.1007/s11102-018-0881-7
77. Ma HS, Wang EL, Xu WF, Yamada S, Yoshimoto K, Qian ZR, et al. Overexpression of DNA (Cytosine-5)-methyltransferase 1 (DNMT1) and DNA (Cytosine-5)-methyltransferase 3A (DNMT3A) is associated with aggressive behavior and hypermethylation of tumor suppressor genes in human pituitary adenomas. *Med Sci Monit.* (2018) 24:4841–50. doi: 10.12659/MSM.910608
78. D'Angelo D, Esposito F, Fusco A. Epigenetic mechanisms leading to overexpression of HMGA proteins in human pituitary adenomas. *Front Med.* (2015) 2:39. doi: 10.3389/fmed.2015.00039
79. Ehrlich M. DNA hypomethylation in cancer cells. *Epigenomics.* (2009) 1:239–59. doi: 10.2217/epi.09.33
80. Duong CV, Emes RD, Wessely F, Yacqub-Usman K, Clayton RN, Farrell WE. Quantitative, genome-wide analysis of the DNA methylome in sporadic pituitary adenomas. *Endocr Relat Cancer.* (2012) 19:805–16. doi: 10.1530/ERC-12-0251
81. Han L, Liu D, Li Z, Tian N, Han Z, Wang G, et al. HOXB1 is a tumor suppressor gene regulated by miR-3175 in glioma. *PLoS ONE.* (2015) 10:e0142387. doi: 10.1371/journal.pone.0142387
82. Gad AK, Nehru V, Ruusala A, Aspenstrom P. RhoD regulates cytoskeletal dynamics via the actin nucleation-promoting factor WASp homologue associated with actin Golgi membranes and microtubules. *Mol Biol Cell.* (2012) 23:4807–19. doi: 10.1091/mbc.e12-07-0555
83. Ling C, Pease M, Shi L, Punj V, Shiroishi MS, Commins D, et al. A pilot genome-scale profiling of DNA methylation in sporadic pituitary macroadenomas: association with tumor invasion and histopathological subtype. *PLoS ONE.* (2014) 9:e96178. doi: 10.1371/journal.pone.0096178
84. Gu Y, Zhou X, Hu F, Yu Y, Xie T, Huang Y, et al. Differential DNA methylome profiling of nonfunctioning pituitary adenomas suggesting tumour invasion is correlated with cell adhesion. *J Neurooncol.* (2016) 129:23–31. doi: 10.1007/s11060-016-2139-4
85. Salomon MP, Wang X, Marzese D, Hsu SC, Nelson N, Zhang X, et al. The epigenomic landscape of pituitary adenomas reveals specific alterations and differentiates among acromegaly, Cushing's disease and endocrine-inactive subtypes. *Clin Cancer Res.* (2018) 24:4126–36. doi: 10.1158/1078-0432.CCR-17-2206
86. Vaitkiene P, Valiulyte I, Glebauskiene B, Liutkeviciene R. N-myc downstream-regulated gene 2 (NDRG2) promoter methylation and expression in pituitary adenoma. *Diagn Pathol.* (2017) 12:33. doi: 10.1186/s13000-017-0622-7
87. Valiulyte I, Steponaitis G, Skiriute D, Tamasauskas A, Vaitkiene P. Signal transducer and activator of transcription 3 (STAT3) promoter methylation and expression in pituitary adenoma. *BMC Med Genet.* (2017) 18:72. doi: 10.1186/s12881-017-0434-3
88. Ruskyte K, Liutkeviciene R, Vilkeviciute A, Vaitkiene P, Valiulyte I, Glebauskiene B, et al. MMP-14 and TGFbeta-1 methylation in pituitary adenomas. *Oncol Lett.* (2016) 12:3013–7. doi: 10.3892/ol.2016.4919
89. Kochling M, Ewelt C, Furtjes G, Peetz-Dienhart S, Koos B, Hasselblatt M, et al. hTERT promoter methylation in pituitary adenomas. *Brain Tumor Pathol.* (2016) 33:27–34. doi: 10.1007/s10014-015-0230-8
90. Boresowicz J, Kober P, Rusetska N, Maksymowicz M, Goryca K, Kunicki J, et al. Telomere length and TERT abnormalities in pituitary adenomas. *Neuro Endocrinol Lett.* (2018) 39:49–55.
91. McCormack A, Dekkers OM, Petersenn S, Popovic V, Trouillas J, Raverot G, et al. Treatment of aggressive pituitary tumours and carcinomas: results of a European Society of Endocrinology (ESE) survey 2016. *Eur J Endocrinol.* (2018) 178:265–76. doi: 10.1530/endoabs.49.OC12.2
92. Syro LV, Rotondo F, Camargo M, Ortiz LD, Serna CA, Kovacs K. Temozolomide and pituitary tumors: current understanding, unresolved issues, and future directions. *Front Endocrinol.* (2018) 9:318. doi: 10.3389/fendo.2018.00318
93. Salehi F, Scheithauer BW, Kros JM, Lau Q, Fealey M, Erickson D, et al. MGMT promoter methylation and immunoexpression in aggressive pituitary adenomas and carcinomas. *J Neurooncol.* (2011) 104:647–57. doi: 10.1007/s11060-011-0532-6
94. Arya S, Majaid MA, Shwetha SD, Sravani K, Arivazhagan A, Sampath S, et al. Implications of MGMT methylation status in pituitary adenoma. *Pathol Res Pract.* (2014) 210:407–11. doi: 10.1016/j.prp.2014.02.010
95. Jenuwein T, Allis CD. Translating the histone code. *Science.* (2001) 293:1074–80. doi: 10.1126/science.1063127
96. Yacqub-Usman K, Duong CV, Clayton RN, Farrell WE. Preincubation of pituitary tumor cells with the epidrugs zebularine and trichostatin A are permissive for retinoic acid-augmented expression of the BMP-4 and D2R genes. *Endocrinology.* (2013) 154:1711–21. doi: 10.1210/en.2013-1061
97. Li T, Huang H, Huang B, Huang B, Lu J. Histone acetyltransferase p300 regulates the expression of human pituitary tumor transforming gene (hPTTG). *J Genet Genomics.* (2009) 36:335–42. doi: 10.1016/S1673-8527(08)60122-8
98. Ebrahimi A, Schittenhelm J, Honegger J, Schluesener HJ. Histone acetylation patterns of typical and atypical pituitary adenomas indicate epigenetic shift of these tumours. *J Neuroendocrinol.* (2011) 23:525–30. doi: 10.1111/j.1365-2826.2011.02129.x
99. Dawson MA, Kouzarides T, Huntly BJ. Targeting epigenetic readers in cancer. *N Engl J Med.* (2012) 367:647–57. doi: 10.1056/NEJMra1112635

Conflict of Interest Statement: The authors declare that the research was conducted in the absence of any commercial or financial relationships that could be construed as a potential conflict of interest.

frontiers in Endocrinology

ORIGINAL RESEARCH
published: 22 May 2019
doi: 10.3389/fendo.2019.00328

Quantitative Analysis of Ubiquitinated Proteins in Human Pituitary and Pituitary Adenoma Tissues

Shehua Qian[1,2,3], *Xiaohan Zhan*[1,2,3], *Miaolong Lu*[1,2,3], *Na Li*[1,2,3], *Ying Long*[1,2,3], *Xuejun Li*[4], *Dominic M. Desiderio*[5] *and Xianquan Zhan*[1,2,3,6]*

[1] *Key Laboratory of Cancer Proteomics of Chinese Ministry of Health, Xiangya Hospital, Central South University, Changsha, China,* [2] *Hunan Engineering Laboratory for Structural Biology and Drug Design, Xiangya Hospital, Central South University, Changsha, China,* [3] *State Local Joint Engineering Laboratory for Anticancer Drugs, Xiangya Hospital, Central South University, Changsha, China,* [4] *Department of Neurosurgery, Xiangya Hospital, Central South University, Changsha, China,* [5] *The Charles B. Stout Neuroscience Mass Spectrometry Laboratory, Department of Neurology, College of Medicine, University of Tennessee Health Science Center, Memphis, TN, United States,* [6] *National Clinical Research Center for Geriatric Disorders, Xiangya Hospital, Central South University, Changsha, China*

OPEN ACCESS

Edited by:
Hidenori Fukuoka,
Kobe University, Japan

Reviewed by:
Ken Fujiwara,
Jichi Medical University, Japan
Tomoaki Tanaka,
Chiba University, Japan

***Correspondence:**
Xianquan Zhan
yjzhan2011@gmail.com

Specialty section:
This article was submitted to Pituitary Endocrinology, a section of the journal Frontiers in Endocrinology

Received: *08 January 2019*
Accepted: *07 May 2019*
Published: *22 May 2019*

Citation:
Qian S, Zhan X, Lu M, Li N, Long Y, Li X, Desiderio DM and Zhan X (2019) Quantitative Analysis of Ubiquitinated Proteins in Human Pituitary and Pituitary Adenoma Tissues. Front. Endocrinol. 10:328. doi: 10.3389/fendo.2019.00328

Protein ubiquitination is an important post-translational modification that is associated with multiple diseases, including pituitary adenomas (PAs). Protein ubiquitination profiling in human pituitary and PAs remains unknown. Here, we performed the first ubiquitination analysis with an anti-ubiquitin antibody (specific to K-ε-GG)-based label-free quantitative proteomics method and bioinformatics to investigate protein ubiquitination profiling between PA and control tissues. A total of 158 ubiquitinated sites and 142 ubiquitinated peptides in 108 proteins were identified, and five ubiquitination motifs were found. KEGG pathway network analysis of 108 ubiquitinated proteins identified four statistically significant signaling pathways, including PI3K-AKT signaling pathway, hippo signaling pathway, ribosome, and nucleotide excision repair. R software Gene Ontology (GO) analysis of 108 ubiquitinated proteins revealed that protein ubiquitination was involved in multiple biological processes, cellular components, and molecule functions. The randomly selected ubiquitinated 14-3-3 zeta/delta protein was further analyzed with Western blot, and it was found that upregulated 14-3-3 zeta/delta protein in nonfunctional PAs might be derived from the significantly decreased level of its ubiquitination compared to control pituitaries, which indicated a contribution of 14-3-3 zeta/delta protein to pituitary tumorigenesis. These findings provided the first ubiquitinated proteomic profiling and ubiquitination-involved signaling pathway networks in human PAs. This study offers new scientific evidence and basic data to elucidate the biological functions of ubiquitination in PAs, insights into its novel molecular mechanisms of pituitary tumorigenesis, and discovery of novel biomarkers and therapeutic targets for effective treatment of PAs.

Keywords: pituitary adenoma, ubiquitination, quantitative proteomics, mass spectrometry, bioinformatics

INTRODUCTION

Pituitary adenomas (PAs) are a common type of intracranial tumor (1) that accounts for about 10% of intracranial tumors (2). Clinical manifestations include abnormalities of hormone secretion, pituitary apoplexy, compressing syndromes of tumor that surrounds the pituitary gland, and other anterior pituitary dysfunctions. PAs are divided into functional PAs (FPAs) and nonfunctional PAs (NFPAs) according to their hormone-secreting functions (3). FPAs display hormone hypersecretion. Because an FPA has its secondary symptoms and signs of excessive secretion of tumor hormones, it is easily diagnosed and treated at an earlier stage. NFPAs do not have any hormone hypersecretion and are more difficult to diagnosis (4). An NFPA usually has a larger volume at the time of diagnosis, and is often characterized by hypophysis dysfunction, visual field defect, and headache (5). Although a PA is commonly a benign tumor (6), secondary symptoms are caused by a large number of hormones produced by FPA and compression of surrounding tissues—causing vision loss, headaches, and so on by NFPA (7). Therefore, it is necessary to in-depth understand its molecular mechanisms of PAs and to discover novel biomarkers and therapeutic targets for effective treatment of PAs.

Protein ubiquitination is an important post-translational modification (PTM), which plays important roles in maintenance of the balance between protein synthesis and degradation, and in cell signaling, and associates with multiples diseases, including cancers (8, 9). For example, Luo et al. (10) found that TRAF6 regulates melanoma invasion and metastasis through ubiquitination of Basigin. Ubiquitin is a highly conserved small protein that consists of 76 amino acids, and is a heat-stable protein. In structure, ubiquitin is a polypeptide of 8.5 kDa (9, 11, 12). The full length of the ubiquitin molecule contains seven lysine sites (K6, K11, K27, K29, K33, K48, and K63), a methionine site at the N-terminus, and one glycine site at the C-terminus (13, 14). Ubiquitin can be covalently bound to the target protein under catalysis of a series of enzymes. This process is called ubiquitination. Ubiquitination is a process that modulates the PTMs of multiple cells and modifies protein function, stability, and localization (15–19). The ubiquitination process involves the synergy of three enzymes: ubiquitin-activating enzyme E1, ubiquitin-coupled enzyme E2, and ubiquitin ligase E3 (20–22). First, E1 utilizes the energy provided by ATP to form a high-energy thioester bond between the carboxyl group on the lysine C-terminal Lys residue and the thiol group on its own cysteine residue to activate the ubiquitin molecule. The activated ubiquitin is re-bound to the Cys residue of E2 through the thioester bond. Finally, the activated ubiquitin is either directly linked to the protein substrate via E2, or the ubiquitin is transferred to the ubiquitin to form an amino isopeptide bond between the carboxyl terminal of ubiquitin and the amino group of the Lys residue of the target protein under the action of E3 (9, 11). In this series of enzymatic cascades, E3 plays the most-important role in the specific recognition of target proteins and the regulation of ubiquitination system activity (20, 23), because E3 ligase recognizes substrates through specific protein-protein interactions (21). E1, E2, and E3 can form several different ubiquitination substrates. Some substrate proteins are only monoubiquitinated, and some have multiple lysine residues. Under appropriate conditions, multiple sites are monoubiquitinated, and some proteins form polyubiquitin chains at a single lysine site.

NFPAs are more common than FPAs in the population of PA patients. However, it is difficult for NFPA patients to obtain an early accurate diagnosis. The treatment of PA patients is generally surgery, radiotherapy, and chemotherapy; however, it is often difficult to achieve a complete cure. It is necessary to investigate new molecular mechanisms of pituitary tumorigenesis and biomarkers for treatment of PAs. Protein ubiquitination is one of PTMs that contribute to the generation of proteoforms. It is well-known that an important function of protein ubiquitination is in the degradation of proteins to maintain the balance of synthesis and degradation of proteins in human body. Furthermore, studies found that the ubiquitin proteasome system changes in pituitary adenomas (24), and that ubiquitination is involved in pituitary tumorigenesis (25). Our previous study also identified ubiquitin-proteasome, and that its proteasome subunit alpha type 2 was nitrated in pituitary adenomas, which affected the function of the proteasome that is a multicatalytic proteinase complex in the cytoplasmic and nuclear regions and is involved in an intracellular, ATP/ubiquitin-dependent, nonlysosomal proteolytic pathway (26). In addition, in our previous series of studies on PA comparative proteomics, an interesting phenomenon is that the number of down-regulated proteins is much more than the number of up-regulated proteins in PAs (27–30), the mRNA expression of ubiquitin-conjugating enzymes E2 and E3 was significantly increased in NFPAs (28), the mRNA expression of ubiquitin specific protease 34 was significantly decreased in PAs (29), ubiquitin carboxyl-terminal hydrolase isozyme L1 was identified in NFPAs (27), and the protein ubiquitination pathway was changed in NFPAs (30). Therefore, it is hypothesized that ubiquitination plays important roles in this interesting phenomenon to discover the key protein ubquitinations for in-depth insights into molecular mechanisms of NFPAs, and to discover reliable biomarkers and effective therapeutic targets. It is important to investigate protein ubiquitinations in human NFPAs.

Anti-ubiquitin antibody-based label-free quantitative proteomics is an effective method to globally detect, identify, and quantify protein ubiquination in a given condition, such as tumors vs. controls (31–43). Briefly, the total proteins extracted from tumor and control tissues were digested with trypsin, respectively. The ubiquitinated tryptic peptides in the tryptic peptide mixture were isolated and enriched with an anti-ubiquitin antibody specific to a K-ε-GG group. Isolated ubiquitinated peptides were analyzed with liquid

Abbreviations: BP, biological process; CC, cellular component; DTT, dithiothreitol; FPA, functional pituitary adenoma; GO, gene ontology; HCD, higher-energy collisional dissociation; HPLC, high performance liquid chromatography; IAP, immunoaffinity purification; LAMC2, lamnin subunit gamma 2; LC, liquid chromatography; MF, molecular function; MS/MS, tandem mass spectrometry; NER, nucleotide excision repair; NFPA, nonfunctional pituitary adenoma; PA, pituitary adenoma; PI3K, phosphatidylinostiol 3-kinase; PTMs, post-translational modifications; TFA, trifluoroacetate.

chromatography-tandem mass spectrometry (LC-MS/MS). The MS/MS data were used to search protein database to identify proteins and determine ubiquitinated sites, and the level of protein ubiquitination was determined with MaxQuant algorithms. MaxQuant is the leading qualitative and quantitative algorithm for label-free quantitative proteomics.

Trypsin digestion, anti-ubiquitin antibody-based enrichment, and label-free quantitative proteomics are addressed here. The ubiquitin molecule is made up of 76 amino acids, and the C-terminal glycine is conjugated via its carboxy group to the amino group of a lysine side-chain or to the N-terminus. Trypsin digestion of ubiquitinated proteins cleaves off all but the two C-terminal glycine residues of ubiquitin from the modified protein. These two C-terminal glycine (GG) residues remain linked to the ε-amino group of the modified lysine residue in the tryptic peptide derived from digestion of the substrate protein. The presence of the GG on the side chain of that lysine prevents cleavage by trypsin at that site, to result in an internal modified lysine residue in a formerly ubiquitinated peptide. The K-ε-GG group is recognized and enriched with an antibody specific to K-ε-GG (37). For the ubiquitinated K (Ub-K) residue at the C-terminus, N-terminus, or the middle in a peptide, it mainly results from steric bulk hindrance, which does not affect the MS identification (42). The distinct mass shift (114.04 Da) caused by the GG remnant enables identification and precise localization of ubiquitylation sites based on peptide fragments (41). The identified ubiquitinated peptides were quantified with MaxQuant algorithms (43).

This study used anti-ubiquitin antibody-based label-free quantitative proteomics to identify ubiquitinated proteins and sites, and to quantify the level of ubiquitination. Pathway network analysis was used to investigate any molecular network alteration that protein ubiquitination is involved in. Selected ubiquitinated proteins were further analyzed to reveal the roles of ubiquitinated proteins in PAs. These findings will help to elucidate the molecular mechanisms, and discover biomarkers and therapeutic targets for PAs.

MATERIALS AND METHODS

Tissue Samples

Eight PA tissues were obtained from the Department of Neurosurgery of Xiangya Hospital, China, as approved by the Xiangya Hospital Medical Ethics Committee of Central South University. Post-mortem control pituitary tissues were obtained from the Memphis Regional Medical Center ($n = 5$), as approved by the University of Tennessee Health Science Center Internal Review Board. Written informed consent was obtained from

TABLE 1 | Clinical characteristic of NFPA and control tissue samples.

Group	Sex	Age	Clinical information	Immunohistochemistry	Experiments
Control	Female	40	White, Multiple toxic compounds. Blood: HepB (+), HepC (+), HIV(–).	DNT	Proteomics; Western blot
	Male	45	White, Drowning. Blood alcohol = 3.1 g/L; no other drugs detected. Blood: HepB (+), HepC (+), HIV (–).	DNT	Western blot
	Male	36	White, Multiple toxic materials. Blood alcohol = 0.5 g/L. Blood: HepB (+), HepC (–), HIV (–).	DNT	Proteomics; Western blot
	Female	34	Black, Gunshot wound to chest. Blood alcohol = 0.3 g/L; no drugs. Blood: HepB (+), HepC (–), HIV (–).	DNT	Proteomics
	Female		White, 15 h gunshot wound to head. No drugs or alcohol. Blood: HepB (–), HepC (–), HIV (–).	DNT	Proteomics
NFPA	Female	43	NFPA in sellar region. Sellar floor bone thinning, enriched blood supply in tumor, and tumor size: 4 × 3 × 3 cm^3	ACTH (–), hGH (–), PRL (–), FSH (+), LH (–), TSH (–)	Proteomics
	Male	53	NFPA in sellar region. Sellar floor bone thinning, and tumor size: 3 × 3 × 2.5 cm^3	ACTH (–), hGH (–), PRL (–), FSH (–), LH (–), TSH (–)	Proteomics
	Female	43	NFPA in sellar region. Adhesion of surrounding tissues, and tumor size: 4.5 × 4 × 6 cm^3	ACTH (–), hGH (–), PRL (–), FSH (+), LH (–), TSH (–)	Proteomics; Western blot
	Male	58	NFPA in sellar region. Sellar floor bone destruction, enriched blood supply in tumor, and tumor size: 4.5 × 3 × 3 cm^3	ACTH (–), hGH (–), PRL (–), FSH (–), LH (–), TSH (–)	Proteomics; Western blot
	Male	40	NFPA in sellar region. Recurrent tumor, old blooding in tumor, and tumor size 2 × 2 × 1.8 cm^3.	ACTH(–), hGH(–), PRL(–), FSH(+), LH(–), TSH(–)	Western blot
	Male	59	NFPA in sellar region. Sellar floor bone thinning, and enriched blood supply in tumor, and tumor size 2.1 × 1.8 × 2 cm^3.	ACTH(–), hGH(–), PRL(–), FSH(+), LH(–), TSH(–)	Western blot
	Male	49	NFPA in sellar region. Sellar floor bone thinning, old blooding in tumor, and tumor size 2 × 4 × 3 cm^3.	ACTH(–), hGH(–), PRL(–), FSH(–), LH(–), TSH(–)	Western blot
	Female	53	NFPA in sellar region. Sellar floor bone thinning, enriched blood supply, and tumor size 3 × 3.5 × 2.5 cm^3.	ACTH(–), hGH(–), PRL(–), FSH(–), LH(–), TSH(–)	Western blot

DNT, do not test.

each patient or the family of each control pituitary subject (post-mortem tissues) after full explanation of the purpose and nature of all experimental procedures. The detailed information of PA and control pituitary tissue samples are collected in **Table 1**. Quantitative ubiquitination proteomics was performed between the four mixed NFPA samples and the four mixed control samples. Western blot experiments were performed between the six mixed NFPA samples and the three mixed control samples.

Cleavage and Quantification of Proteins

A volume (1 ml) of urea pyrolysis solution [20 mM 2-hydroxyethyl (HEPES), 9 M urea, 2.5 mM sodium pyrophosphate, 1 mM sodium orthovanadate, and 1 mM β-glycerophosphate, pH 8.0] was added to each tissue sample (100 mg) for an ice-bath ultrasonic treatment (100 W, 10 s, interval 10 s, 10 times). The solution was centrifuged (18,000 × g, 30 min, 4°C). The supernatant was the protein extraction, and its protein content was determined with a Bradford Protein Quantification Kit (YEASEN, Cat# 20202ES76).

Enzymatic Hydrolysis of Proteins

Four NFPA protein samples (1.5 mg/each sample) were equally mixed as tumor protein sample (6 mg), and four control protein samples (1.5 mg/each sample) were equally mixed as control protein sample (6 mg). Each mixed sample (tumor; control) was equally divided into three parts (2 mg/part) for proteomics experiment. A volume of 1 M dithiothreitol (DTT) was added to each sample part (tumor: $n = 3$; control: $n = 3$) to produce a final concentration of 10 mM; the mixture was incubated (37°C for 2.5 h), and cooled to room temperature. A volume of 1 M iodoacetamide was added to the mixture to achieve a final concentration of 50 mM, and the mixture was incubated in the dark for 30 min. Five volumes of water were added to dilute the urea concentration to 1.5 M. Trypsin (2 μg/μL) was added at 1:50 (v:v) and the mixture was digested (37°C for 18 h). The tryptic peptide mixture was desalted and lyophilized with an SPE C18 column (Waters WAT051910).

Enrichment of Ubiquitinated Peptides

Each lyophilized tryptic peptide sample (tumor; control) was reconstituted in 1.4 mL of pre-cooled immunoaffinity purification (IAP) buffer. The pretreated anti-K-ε-GG antibody beads [PTMScan ubiquitin remnant motif (K-ε-GG) kit, Cell Signal Technology] were added. The mixture was incubated (1.5 h at 4°C) and centrifuged (2,000 × g, 30 s, 4°C). The supernatant was discarded (44). The pretreated anti-K-ε-GG antibody beads with peptides were washed three times with 1 mL of pre-cooled IAP buffer, and washed three times with 1 mL of pre-chilled water. After washing the anti-K-ε-GG antibody beads with peptides, 40 μL of 0.15% trifluoroacetate (TFA) was added. The mixture was incubated at room temperature for 10 min and centrifuged (30 s at 2,000 × g). The above incubation with 0.15% TFA and centrifugation steps (2,000 × g, 30 s) was performed three times. The supernatant that contained ubiquitinated peptides was desalted with C18 STAGE Tips (45).

LC-MS/MS Analysis of Enriched Ubiquitinated Peptides

The enriched ubiquitinated peptides from PA and control tissues were analyzed with LC-MS/MS. Peptides of each sample were separated with a high performance liquid chromatography (HPLC) system EASY-nLC1000 at nanoliter flow rate. The solution A was 0.1% formic acid and 2% acetonitrile aqueous solution. The solution B was 0.1% formic acid and 84% acetonitrile aqueous solution. The chromatographic column was equilibrated with 100% solution A. The enriched ubiquitinated peptide sample was loaded with an autosampler onto a sample-spindle Thermo Scientific EASY column (2 cm*100 μm 5 μm-C18), and peptides were separated with an analytical column of 75 μm × 250 mm 3 μm-C18 at a flow rate of 250 nL/min. The HPLC liquid-phase gradients were as follows: solution B linear gradient from 0 to 55% during 0–220 min, solution B linear gradient from 55 to 100% during 220–228 min, and solution B maintained at 100% during 228–240 min. The enriched peptide products were separated with capillary HPLC according to the HPLC liquid-phase gradients within 240 min, and analyzed with a Q-Exactive mass spectrometer (Thermo Finnigan). The mass spectrometry (MS) detection was in the positive-ion mode. The scan range of the precursor ion was *m/z* 350–1800. The most-intense 20 ions in each MS spectrum were selected for higher-energy collisional dissociation (HCD) fragmentation for MS/MS analysis. The MS resolution was 70,000 at *m/z* 200, and the resolution of MS/MS was 17,500 at *m/z* 200. The enriched ubiquitinated peptide products from PAs or controls were analyzed three times with LC-MS/MS.

Label-Free Analysis With MaxQuant

Six LC-MS/MS original files (tumor: $n = 3$; Control: $n = 3$) were imported into MaxQuant software (version 1.3.0.5) for database review, protein identification, ubiquitination-site determination, and quantification of ubiquitination level. The protein database was uniprot_human_154578_20160815.fasta (list of 154,578 entries, downloaded on 15 August 2016). The main search parameters were: main search ppm was 6, missed cleavage was 4, MS/MS tolerance ppm was 20, de-isotopic was TRUE, enzyme was trypsin, database was uniprot_human_154578_20160815.fasta, fixed modification was carbamidomethyl (C), variable modification was oxidation (M), acetyl (protein N-term), and GlyGly (K), decoy database pattern was reverse, iBAQ was TRUE, match between analyses was 2 min, peptide false discovery rate (FDR) was 0.01, and protein FDR was 0.01. Thus, the protein was characterized, ubiquitination site was determined with amino acid sequence analysis, and its ubiquitination level was quantified with MaxQuant algorithms.

Statistical and Bioinformatics Analysis

The checksum files obtained by MaxQuant were analyzed with Perseus software (version 1.3.0.4). The DAVID database was used to perform KEGG signaling pathway-enrichment analysis of the ubiquitinated proteins. Gene ontology (GO) was used to annotate proteome with R software, and these ubiquitinated proteins were classified with GO annotation based on three

TABLE 2 | Ubiquitinated proteins identified in nonfunctional pituitary adenomas relative to controls.

Accession No.	Gene name	Protein name	Modified peptides	Peptide length	Modified positions	Modified probabilities	Modified level (N)	Modified level (T)	Ratio (T/N)	*t*-test *p*-value
A0A0A6YY96	IREB2	Iron-responsive element-binding protein 2	GFQIAAEK*QK*	10	483;485	1; 1	3.59E+07	1.62E+08	4.52	4.55E-06
P16104	H2AFX	Histone H2AX	K*TSATVGPK	9	120	1	3.50E+07	1.43E+09	40.96	1.39E-05
P48200	IREB2	Iron-responsive element-binding protein 2	GFQIAAEK*QK*	10	483;485	1; 1	3.46E+07	1.63E+08	4.71	3.31E-05
B2RDW1	RPS30A	Epididymis luminal protein 112	TLTGK*TITLEVEPSDTIENVK	21	11	1	1.70E+08	1.26E+09	7.40	3.64E-05
			TLSDYNIQK*ESTLHLVLR	18	63	1	3.71E+07	1.64E+08	4.43	6.07E-03
			LIFAGK*QLEDGR	12	48	1	2.91E+09	7.32E+09	2.52	6.88E-03
			IQDK*EGIPPDQQR	13	33	1	2.68E+06	3.68E+07	13.74	9.55E-03
			TITLEVEPSDTIENVK*AK	18	27	0.956		1.95E+07		
			MQIFVK*TLTGK	11	6	0.923				
			TITLEVEPSDTIENVKAK*	18	29	0.594				
			VDENGK*ISR	9	113	1				
P62979	RPS27A	Ubiquitin-40S ribosomal protein S27a	TLTGK*TITLEVEPSDTIENVK	21	11	1	1.72E+08	1.27E+09	7.37	3.78E-05
			TLSDYNIQK*ESTLHLVLR	18	63	1	3.71E+07	1.96E+08	5.27	6.89E-04
P68871	HBB	Hemoglobin subunit beta	FFESFGDLSTPDAVMGNPK*VK*	21	60;62	0.5; 0.5	1.69E+06	2.01E+07	11.87	3.71E-04
			GTFATLSELHCDK*LHVDPENFR	22	96	1	1.89E+07	9.13E+07	4.83	1.23E-02
			K*VLGAFSDGLAHLDNLK	17	67	1	2.07E+06	1.02E+07	4.92	1.22E-01
L7N2F9		Uncharacterized protein	VNVDK*VLER	9	52	1	1.04E+07	1.23E+08	11.86	8.99E-04
			ADALQAGASQFETSAAK*LK	19	83	0.876		2.01E+07		
			ADALQAGASQFETSAAKLK*	19	85	0.539		4.61E+07		
			DQK*LSELDDR	10	59	1	6.10E+06	5.24E+07	8.60	2.47E-03
D9YZU5	HBB	Beta-globin	FFESFGDLSTPDAVMGNPK*VK*	21	60;62	0.5; 0.5	2.48E+06	2.02E+07	8.14	1.14E-03
			K*VLGAFSDGLAHLDNLK	17	67	1	1.79E+06	1.02E+07	5.69	4.65E-02
P62979	RPS27A	Ubiquitin-40S ribosomal protein S27a	IQDK*EGIPPDQQR	13	33	1	3.34E+06	5.10E+07	15.27	1.16E-03
			LIFAGK*QLEDGR	12	48	1	2.90E+09	7.33E+09	2.53	6.90E-03
F5H5D3	TUBA1C	Tubulin alpha-1C chain1	VGINYQPPTVVPGGDLAK*VQR	21	370	1	2.27E+07	3.78E+07	1.67	1.38E-03
			DVNAAIATIK*TK*	12	336;338	0.679;0.57		2.98E+06		
Q9HCC9	ZFYVE28	Lateral signaling target protein 2	DFCVK*FPEEIR	11	87	1	7.36E+06	2.31E+07	3.14	1.50E-03
A0A024R017	HIST1H2AC	Histone H2A	NDEELNK*LLGR	11	96	1		3.45E+06		
			VTIAQGGVLPNIQAVLLPK*K*	20	119;120	0.5; 0.5	6.31E+07	1.13E+08	1.80	1.52E-03
P69905	HBA1	Hemoglobin subunit alpha	AAWGK*VGAHAGEYGAEALER	20	17	1		7.09E+06		
			TYFPHFDLSHGSAQVK*	16	57	1	1.94E+06	2.06E+08	106.34	5.10E-03
P08670	VIM	Vimentin	K*LLEGEESR	9	402	1	1.70E+06	5.54E+06	3.26	5.62E-03
			EK*LQEEMLQR	10	188	1	1.40E+07	2.02E+07	1.44	2.44E-01
			QVDQLTNDK*AR	11	168	1	1.99E+06	2.97E+06	1.49	2.74E-01
			K*LLEGEESR	9	393	1		5.54E+06		
C8C504	HBB	Beta-globin	GTFATLSELHCDK*LHVDPENFR	22	96	1	2.04E+07	8.43E+07	4.14	5.79E-03

(Continued)

TABLE 2 | Continued

Accession No.	Gene name	Protein name	Modified peptides	Peptide length	Modified positions	Modified probabilities	Modified level (N)	Modified level (T)	Ratio (T/N)	*t*-test *p*-value
Q96T46	HBA2	Hemoglobin alpha 2	TYFPHFDLSHGSAQVK*	16	33	1	1.94E+06	2.03E+08	104.44	6.08E-03
Q9H582	ZNF644	Zinc finger protein 644	RSFLQQDVNK*	10	11	1	9.99E+06	4.56E+07	4.56	6.13E-03
Q9H3H9	TCEAL2	Transcription elongation factor A protein-like 2	QYK*EAIHDMNFSNEDMIR	18	154	1	3.49E+06	1.77E+07	5.07	6.49E-03
E9PL57	NEDD8-MDP1	Protein NEDD8-MDP1	TLTGK*EIEIDIEPTDKVER	19	11	1	3.50E+06	1.20E+07	3.43	6.76E-03
Q59EJ3		Heat shock 70kDa protein 1A variant	MVQEAEK*YK	9	592	0.891	9.34E+05	9.36E+06	10.02	1.11E-02
D6R956	UCHL1	Ubiquitin carboxyl-terminal hydrolase	CFEK*NEAIQAAHDAVAQEGQCR	22	135	1		5.86E+06		
			MQLK*PMEINPEMLNK	15	4	1	2.77E+06	8.80E+06	3.17	1.61E-02
P14735	IDE	Insulin-degrading enzyme	EVNAVDSEHEK*NVMNDAWR	19	192	1	2.05E+06	7.47E+06	3.65	1.94E-02
Q6ZUF2		cDNA FLJ43763 fis, clone TESTI2048603	FFSPPNMSVTHK*EAHERK	18	19	0.977	1.39E+08	2.50E+08	1.80	5.15E-02
P61088	UBE2N	Ubiquitin-conjugating enzyme E2 N	ICLDILKDK*	9	94	0.962	1.74E+07	2.27E+07	1.30	7.06E-02
D1MGQ2	HBA2	Alpha-2 globin chain	AAWGK*VGAHAGEYGAEALER	20	17	1		7.09E+06		
			TYFPHFDLSHGSAQVK*	16	57	1	2.22E+06	1.26E+08	56.71	1.21E-01
P02042	HBD	Hemoglobin subunit delta	GTFSQLSELHCDK*LHVDPENFR	22	96	1	1.57E+07	2.01E+07	1.28	1.43E-01
D3DQ48	TMEM59	Transmembrane protein 59, isoform CRA_e	TEDHEEAGPLPTK*VNLAHSEI	21	316	1	3.64E+06	1.31E+07	3.61	1.63E-01
K7EPI4	GFAP	Glial fibrillary acidic protein	GGK*STK*DGENHK*	12	10;13;19	1;1;1	2.32E+06	2.06E+07	8.87	2.34E-01
A0A024R5H9	PLEKHB1	Pleckstrin homology domain containing, family B (Evectins) member 1, isoform CRA_a	LHLCAETK*DDALAWK	15	113	0.999	6.23E+06	0.00E+00	0.00	1.39E-01
B7WPA5	PLEKHB2	Pleckstrin homology domain-containing family B member 2	QNIEDK*VHMPMDCINIR	17	46	1	1.30E+07	7.08E+06	0.54	3.41E-01
Q3BBV0	NBPF1	Neuroblastoma breakpoint family member 1	VGWALDMDEIEK*	12	950	1	8.76E+06	5.34E+06	0.61	4.18E-01
A4UGR9	XIRP2	Xin actin-binding repeat-containing protein 2	WLFETQPMESLYEK*	14	934	1	1.82E+07	2.61E+07	1.44	5.39E-01
B7ZMF0	CEP192	CEP192 protein	IVSPK*NSDLK	10	556	0.908	1.14E+07	1.96E+07	1.71	6.03E-01
A0N071	HBD	Delta globin	GTFSQLSELHCDK*LHVDPENFR	22	96	1	2.08E+07	2.20E+07	1.05	8.73E-01
A0A024QZP6	H2AFY2	Core histone macro-H2A	IHPELLAK*K*	9	116;117	0.705; 0.585				
A0A024R466	ITM2C	Integral membrane protein 2C, isoform CRA_a	ISFQPAVAGIK*GDK	14	14	0.855		1.33E+07		
A0A024R6B3	TMEM63C	Transmembrane protein 63C, isoform CRA_a	DIEDPELIIK*HFHEAYPGSVVTR	23	239	1		3.89E+06		
A0A024R7G8	RAD23A	RAD23 homolog A (*S. cerevisiae*), isoform CRA_a	LIYAGK*ILSDDVPIR	15	53	1		1.24E+07		
A0A024RDB0	UBE1L2	Ubiquitin-activating enzyme E1-like 2, isoform CRA_a	IDAHLNK*VCPTTETIYNDEFYTK	23	544	1		4.66E+06		
A0A087WZE4	SPTA1	Spectrin alpha chain, erythrocytic 1	VNILTDK*SYEDPTNIQGK	18	79	1		6.34E+06		
A0A0K0KMI2	POU5F1	POU class 5 homeobox 1 transcript variant OCT4B4	K*LGGQLGR	8	1	1		7.82E+06		
A0A0U1RRH7		Histone H2A	NDEELNK*LLGK	11	96	0.996				
A0A140VJZ1		Testicular tissue protein Li 218	LEK*IFQNAPTDPTQDFSTQVAK	22	360	1				
A0AVT1	UBA6	Ubiquitin-like modifier-activating enzyme 6	IDAHLNK*VCPTTETIYNDEFYTK	23	544	1		4.54E+06		

(Continued)

TABLE 2 | Continued

Accession No.	Gene name	Protein name	Modified peptides	Peptide length	Modified positions	Modified probabilities	Modified level (N)	Modified level (T)	Ratio (T/N)	*t*-test *p*-value
A4D2P6	GRID2IP	Delphilin	GK*MGTVSK*SR	10	570;576	1; 1				
A6NNT2	C16orf96	Uncharacterized protein C16orf96	SALAGK*ASR	9	819	1				
A6ZKI3	FAM127A	Protein FAM127A	K*ESPLLNDYR	10	86	1		1.64E+07		
A8K6M4		cDNA FLJ75725, highly similar to Homo sapiens vesicle transport through interaction with t-SNAREs homolog 1B (yeast) (VTI1B), mRNA	ASSAASSEHFEK*LHEIFR	18	13	1		9.09E+06		
B1A4G6	GH1	Growth hormone 1 isoform 1	EETQQK*SNLELLR	13	96	1	5.87E+06			
B4DPP6		cDNA FLJ54371, highly similar to Serum albumin	K*LVAASQAALGL	12	607	1				
			K*QTALVELVK	10	558	1				
B4DR52		Histone H2B	HAVSEGTK*AVTK	12	117	1		4.70E+07		
B4E1J8		cDNA FLJ56285, highly similar to ADP-ribosylation factor-like protein 8B	DLPNALDEK*QLIEK	14	193	1				
B9EGU6	RC3H1	Ring finger and CCCH-type zinc finger domains 1	KEIMAQLEERK*	11	769	0.999		7.15E+06		
C9JLQ8	AEBP1	Adipocyte enhancer-binding protein 1	MPPEKTK*DK*	9	7;9	0.985;1				
E7EX29	YWHAZ	14-3-3 protein zeta/delta	MDKNELVQKAK*	11	11	0.537	2.35E+06			
K7EPF9	APOC1	Apolipoprotein C-I	EFGNTLEDK*AR	11	47	1		7.55E+06		
M1VKI3	SDC4-ROS1_S4;R32	Tyrosine-protein kinase receptor	AGSGSQVPTEPKK*	13	105	0.554		1.53E+07		
P01241	GH1	Somatotropin	EETQQK*SNLELLR	13	96	1	4.23E+06			
P02671	FGA	Fibrinogen alpha chain	EK*VTSGSTTTTR	12	448	1		4.06E+06		
			TVIGPDGHK*EVTK	13	476	0.86				
P02768	ALB	Serum albumin	K*LVAASQAALGL	12	598	1				
			K*QTALVELVK	10	549	1				
P04908	HIST1H2AB	Histone H2A type 1-B/E	NDEELNK*LLGR	11	96	1		3.45E+06		
P09960	LTA4H	Leukotriene A-4 hydrolase	FSYK*SITTDDWK	12	418	1		4.10E+06		
P19021	PAM	Peptidyl-glycine alpha-amidating monooxygenase	AFGDSEHK*LETSSGR	15	901	1				
P23396	RPS3	40S ribosomal protein S3	KPLPDHVSIVEPK*DEILPTTPISEQK	26	214	1		2.84E+07		
P31946	YWHAB	14-3-3 protein beta/alpha	SELVQKAK*	8	13	0.672				
P35212	GJA4	Gap junction alpha-4 protein	ALPAK*DPQVER	11	119	1		2.26E+06		
P35251	RFC1	Replication factor C	KLVSETVK*	8	22	1				
P45974	USP5	Ubiquitin carboxyl-terminal hydrolase 5	LEK*IFQNAPTDPTQDFSTQVAK	22	360	1		9.83E+06		
P54725	RAD23A	UV excision repair protein RAD23 homolog A	LIYAGK*ILSDDVPIR	15	53	1		1.39E+07		
			LIYAGK*ILNDDTALK	15	51	0.993				

(Continued)

TABLE 2 | Continued

Accession No.	Gene name	Protein name	Modified peptides	Peptide length	Modified positions	Modified probabilities	Modified level (N)	Modified level (T)	Ratio (T/N)	*t*-test *p*-value
P54727	RAD23B	UV excision repair protein RAD23 homolog B	LIYAGK*ILNDDTALK	15	51	0.993				
P55072	VCP	Transitional endoplasmic reticulum ATPase	ASGADSK*GDDLSTAILK	17	8	1		7.91E+06		
P60709	ACTB	Actin, cytoplasmic 1	DSYVGDEAQSK*R	12	61	1		2.05E+06		
P60866	RPS20	40S ribosomal protein S20	DTGK*TPVEPEVAIHR	15	8	1		9.48E+06		
P61981	YWHAG	14-3-3 protein gamma	EQLVQK*AR	8	10	1				
P62979	RPS27A	Ubiquitin-40S ribosomal protein S27a	TITLEVEPSDTIENVK*AK	18	27	0.956		1.72E+07		
			MQIFVK*TLTGK	11	6	0.923				
			TITLEVEPSDTIENVKAK*	18	29	0.594				
			VDENGK*ISR	9	113	1				
P83916	CBX1	Chromobox protein homolog 1	KEESEK*PR	8	109	1				
Q0VDD8	DNAH14	Dynein heavy chain 14, axonemal	SLLSNVSQWDTFK*	13	2919	1				
Q13753	LAMC2	Laminin subunit gamma-2	ITSTFHQDVDGWK*	13	219	1		1.99E+07		
Q15149	PLEC	Plectin	SELELTLGK*LEQVR	14	1210	1		2.72E+06		
Q4LE39	ARID4B	AT-rich interactive domain-containing protein 4B	K*ENIK*PSLGSK*	11	462;466;472	1;1;1		2.05E+07		
Q59EQ3		Nudix-type motif 6 isoform a variant	LDAAAFQK*GLQGK*	13	84;89	1;1		5.22E+06		
Q5I0G2	PRL	Growth hormone A1	AVEIEEQTK*R	10	153	1		5.21E+06		
Q5JWF2	GNAS	Guanine nucleotide-binding protein G(s) subunit alpha isoforms XLas	IDVIK*QADYVPSDQDLLR	18	829	1				
Q5VXU3	CHIC1	Cysteine-rich hydrophobic domain-containing protein 1	SIQK*LIEWENNR	12	176	1				
Q92625	ANKS1A	Ankyrin repeat and SAM domain-containing protein 1A	GK*EQELLEAAR	11	3	1		8.07E+06		
Q93045	STMN2	Stathmin-2	DLSLEEIQKK*	10	87	0.569		2.05E+06		
			DLSLEEIQK*K	10	86	0.5				
Q93100	PHKB	Phosphorylase b kinase regulatory subunit beta	AYLQLGINEK*	10	546	1	2.91E+07			
Q96AP7	ESAM	Endothelial cell-selective adhesion molecule	ALEEPANDIK*EDAIAPR	17	286	1				
Q96EI5	TCEAL4	Transcription elongation factor A protein-like 4	EYK*EAIHDMNFSNEDMIR	18	142	1		8.59E+06		
Q96N64	PWWP2A	PWWP domain-containing protein 2A	TGLEK*MRSGK*	10	496;501	1; 1	1.06E+07			
Q9BT67	NDFIP1	NEDD4 family-interacting protein 1	TK*AEATIPLVPGR	13	83	1				
Q9BUL8	PDCD10	Programmed cell death protein 10	QILSK*IPDEINDR	13	116	1		2.54E+07		
Q9BWQ8	FAIM2	Protein lifeguard 2	APGTEGQQQVHGEK*K	15	25	0.822		2.50E+06		
Q9H3Z4	DNAJC5	DnaJ homolog subfamily C member 5	FK*EINNAHAILTDATK	16	58	1		4.81E+06		
Q9H598	SLC32A1	Vesicular inhibitory amino acid transporter	DQVGGGGEFGGHDK*PK	16	113	0.832		9.03E+06		
Q9NQX7	ITM2C	Integral membrane protein 2C	ISFQPAVAGIK*GDK	14	14	0.855		1.33E+07		
Q9NV96	TMEM30A	Cell cycle control protein 50A	DEVDGGPPCAPGGTAK*TR	18	24	1		3.72E+06		

(Continued)

TABLE 2 | Continued

Accession No.	Gene name	Protein name	Modified peptides	Peptide length	Modified positions	Modified probabilities	Modified level (N)	Modified level (T)	Ratio (T/N)	*t*-test *p*-value
Q9NX12		cDNA FLJ20496 fis, clone KAT08729	SGEEALIIPPDAVAVDCK*DPDDVVPVGQR	29	39	1		6.69E+06		
			VTFNSALAQK*EAK	13	13	0.733				
Q9P0M6	H2AFY2	Core histone macro-H2A.2	IHPELLAK*K*	9	116;117	0.705; 0.585				
Q9P1W3	TMEM63C	Calcium permeable stress-gated cation channel 1	DIEDPELIIK*HFHEAYPGSVVTR	23	239	1		5.57E+06		
Q9UBB4	ATXN10	Ataxin-10	ITSDEPLTK*DDIPVFLR	17	262	1		1.14E+07		
Q9UEU0	VTI1B	Vesicle transport through interaction with t-SNAREs homolog 1B	ASSAASSEHFEK*LHEIFR	18	13	1		9.35E+06		
Q9UF11	PLEKHB1	Pleckstrin homology domain-containing family B member 1	LHLCAETK*DDALAWK	15	113	0.999	6.23E+06			
Q9UKJ5	CHIC2	Cysteine-rich hydrophobic domain-containing protein 2	SIEK*LLEWENNR	12	117	1		4.92E+06		
Q9UQB3	CTNND2	Catenin delta-2	SPSIDSIQK*DPR	12	540	1		3.06E+06		
Q9Y287	ITM2B	Integral membrane protein 2B	SGEEALIIPPDAVAVDCK*DPDDVVPVGQR	29	39	1		6.69E+06		
			VTFNSALAQK*EAK	13	13	0.733				
S4R435	RPS10-NUDT3	Protein RPS10-NUDT3	SAVPPGADKK*	10	139	0.574		5.99E+07		
			SAVPPGADK*K	10	138	0.846		6.91E+07		
U6FSN9	Mprip-Ntrk1 fusion gene	Tyrosine-protein kinase receptor	GWLTK*QYEDGQWK	13	396	1				

Ratio (T/N), Ration of tumors (B) to controls(A). K, Ubiquitinated lysine residue.*

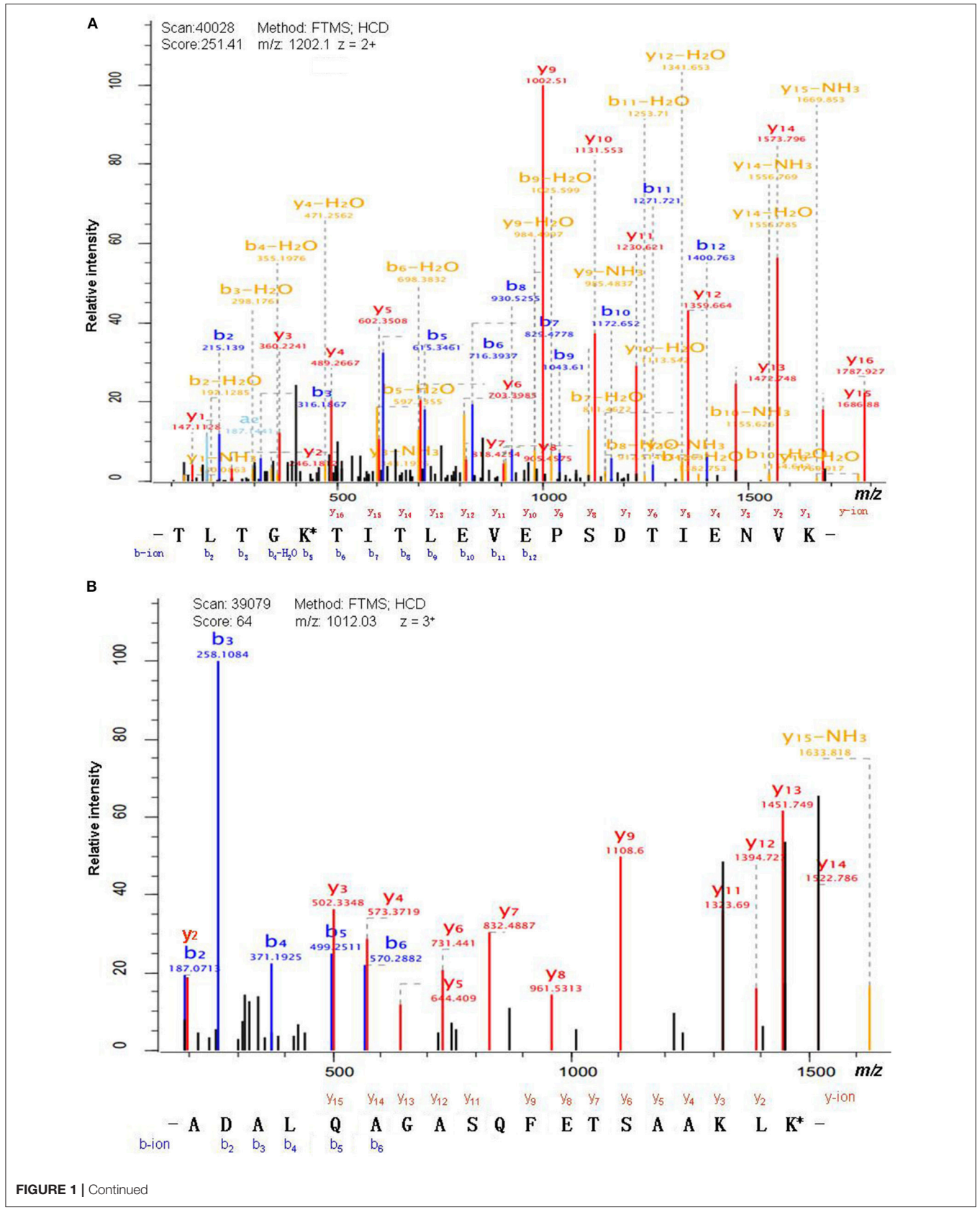

FIGURE 1 | Continued

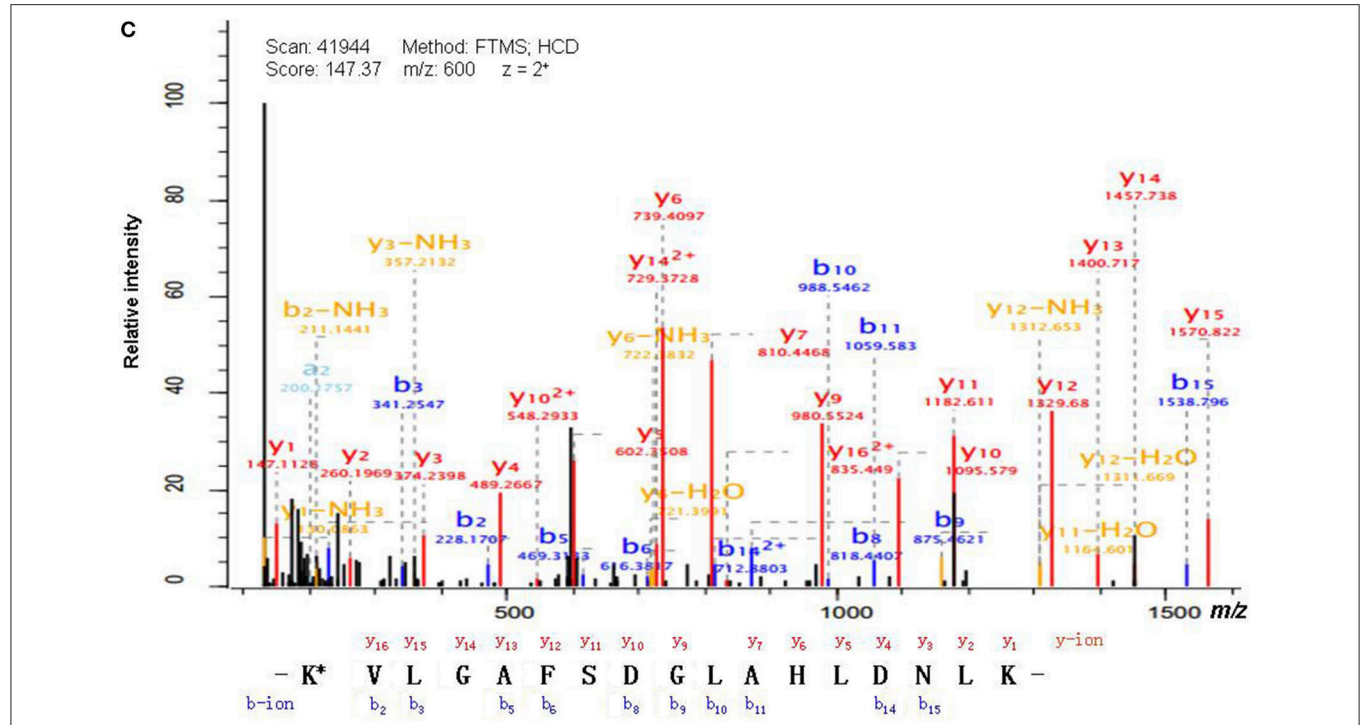

FIGURE 1 | MS/MS spectrum of the tryptic peptide. **(A)** The tryptic peptide TLTGK*TITLEVEPSDTIENVK from epididymis luminal protein 112 (B2RDW1) or ubiquitin-40S ribosomal protein S27a (P62979). **(B)** The tryptic peptide ADALQAGASQFETSAAKLK* from uncharacterized protein (L7N2F9). **(C)** The tryptic peptide K*VLGAFSDGLAHLDNLK from hemoglobin subunit beta (P68871) or beta-globin (D9YZU5). The observed b- and y-ions were labeled in each MS/MS spectrum. K* = ubiquitinated lysine residue.

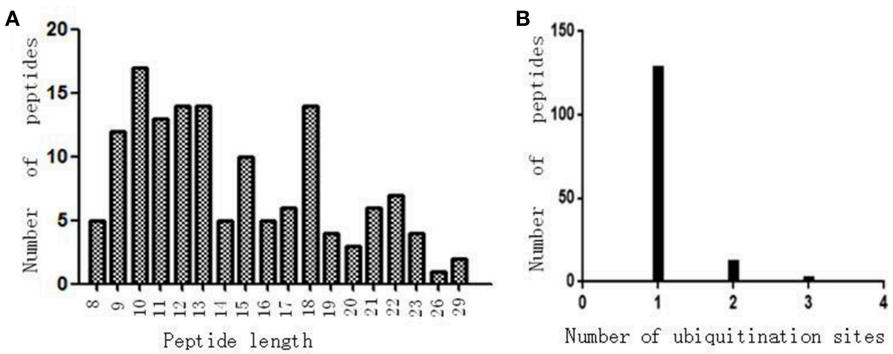

FIGURE 2 | The ubiquitination profile in normal pituitaries and pituitary tumors. **(A)** Peptide length distribution of all ubiquitinated peptides. **(B)** Distribution of ubiquitinated peptides based on number of ubiquitination sites.

categories: cellular components (CC), biological processes (BP), and molecular functions (MF). Motif-X software (http://motif-x.med.harvard.edu/motif-x.html) was used to analyze the model of ubiquitinated peptide sequences in specific positions of ubiquityl-31-mers (15 amino acid upstream and 15 amino acid downstream at the ubiquitination site) in all protein sequences. The International Protein Index (IPI) human proteome was used as the background database; setting parameters were width = 15, occurrences = 20, significance = 0.005; other parameters were set to default values.

Western Blot Analysis of 14-3-3 Zeta/Delta Protein

Six NFPA protein samples were equally mixed as the tumor protein sample, and three control protein samples were equally mixed as the control protein sample (**Table 1**); the equal-load amount (tumor: 22 μg; control: 22 μg) of mixed samples were used for Western blot experiment. Based on the enriched signaling pathways, which include the PI3K-AKT signaling pathway and the Hippo signaling pathway, protein 14-3-3 zeta/delta was the key molecule, and was ubiquitinated in

theses pathways; therefore, protein 14-3-3 zeta/delta was selected for Western blot (WB) analysis, and detailed experimental steps for protein extraction was described previously (46). The anti-protein 14-3-3 zeta/delta antibody (Cusabio, China) was diluted with Tris-buffered saline tween (TBST) (v1: v2 = 1:1000). The secondary antibody (Signalway Antibody, U.S.A.) was diluted with TBST (v1: v2 = 1:5000). The detailed experimental steps for WB were described previously (47–49). Briefly, proteins from PA and control samples were separated with 10% SDS-PAGE gel, transferred to a polyvinylidene fluoride (PVDF) membrane, incubated with anti-protein 14-3-3 zeta/delta antibody, incubated with secondary antibody, and visualized.

RESULTS

Protein Ubiquitination in Control Pituitaries and Pituitary Adenomas

Antibody enrichment-based label-free quantitative proteomics identified 158 ubiquitinated sites and 142 ubiquitinated peptides from 108 proteins in PAs and control pituitaries (**Table 2**). A representative MS/MS spectrum was from ubiquitinated peptides ^{7}TLTGK*TITLEVEPSDTIENVK^{27} ($[M + 2H]^{2+}$, m/z = 1202.14; K* = ubiquitinated lysine residue) of epididymis luminal protein 112 (B2RDW1) or ubiquitin-40S ribosomal protein S27a (P62979) (**Figure 1A**), with a high-quality MS/MS spectrum, excellent signal-to-noise (S/N) ratio, and extensive product-ion b-ion and y-ion series (b_2, b_3, b_4-H_2O, b_5, b_6, b_7, b_8, b_9, b_{10}, b_{11}, and b_{12}; y_1, y_2, y_3, y_4, y_5, y_6, y_7, y_8, y_9, y_{10}, y_{11}, y_{12}, y_{13}, y_{14}, y_{15}, and y_{16}). The ubiquitination site was localized to amino acid residue K^*_{11}, and the ubiquitination level was significantly increased in PAs compared to controls (**Table 2**). Another representative MS/MS spectrum was from ubiquitinated peptide ^{67}ADALQAGASQFETSAAKLK*^{85} of uncharacterized protein (L7N2F9) (**Figure 1B**), which localized the ubiquitination sites at K residue in the peptide C-terminal, with a high-quality MS/MS spectrum, excellent S/N ratio, and extensive product-ion b-ion and y-ion series (b_2, b_3, b_4, b_5, and b_6; y_2, y_3, y_4, y_5, y_6, y_7, y_8, y_9, y_{11}, y_{12}, y_{13}, y_{14}, and y_{15}). The ubiquitination site was localized to amino acid residue K^*_{85}, and the protein

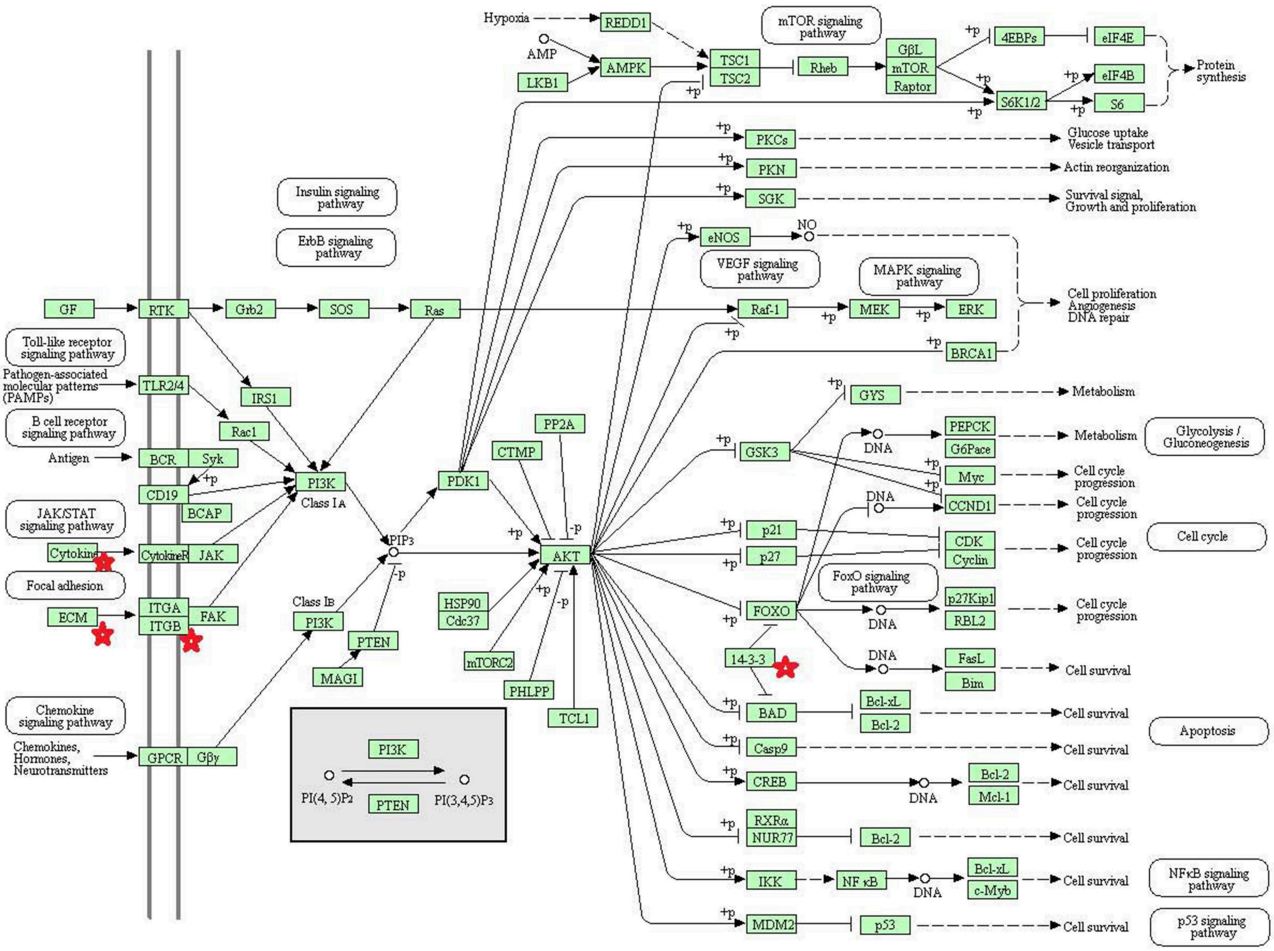

FIGURE 3 | The PI3K-AKT signaling pathway which was achieved by DAVID pathway analysis. The ubiquitinated proteins are shown by red stars.

was ubiquitinated in PAs but not in controls (**Table 2**). The third representative MS/MS spectrum was from ubiquitinated peptide ^{67}K*VLGAFSDGLAHLDNLK^{83} of hemoglobin subunit beta (P68871) or beta-globin (D9YZU5) (**Figure 1C**), which localized the ubiquitination site at K residue in the peptide N-terminal, with a high-quality MS/MS spectrum, excellent S/N ratio, and extensive product-ion b-ion and y-ion series (b_2, b_3, b_5, b_6, b_8, b_9, b_{10}, b_{11}, b_{14}, and b_{15}; y_1, y_2, y_3, y_4, y_5, y_6, y_7, y_9, y_{10}, y_{11}, y_{12}, y_{13}, y_{14}, y_{15}, and y_{16}). The ubiquitination site was localized to amino acid residue K^*_{67}, and the ubiquitination level was significantly increased in PAs compared to controls (**Table 2**). With the same method, each ubiquitinated peptide and ubiquitination site was identified with MS/MS data, and quantified. Among the 142 ubiquitinated peptides that were identified, 45 ubiquitinated peptides were quantified in PA and control tissues, including 30 statistically significantly differentially ubiquitinated peptides in PAs compared to controls ($p < 0.05$). A total of 56 ubiquitinated peptides were quantified in PAs, but not in control pituitaries, and six ubiquitinated peptides were quantified in control pituitaries, but not in PAs. A total of 35 ubiquitinated peptides were identified but not quantified in PAs and controls. Moreover, most ubiquitinated peptides were 8–22 amino acids long (**Figure 2A**). Among 142 ubiquitinated peptides 90.1% (128/142) peptides contained only one ubiquitinated site, 8.5% peptides contained two ubiquitinated sites, 7.8% peptides contained three ubiquitinated sites, and 1.4% peptides contained over three ubiquitinated sites (**Figure 2B**).

Signaling Pathways Involved in Ubiquitinated Proteins

Eight statistically significant KEGG signaling pathways ($p < 0.05$) were identified with DAVID KEGG pathway-enrichment analysis from 108 ubiquitinated proteins, including PI3K-AKT signaling pathway, Hippo signaling pathway, ribosome, nucleotide excision repair, alcoholism, systemic lupus erythematosus, African trypanosomiasis, and malaria. Among them, PI3K-AKT signaling pathway (**Figure 3**) is activated by many types of cellular stimulation and toxic damage, and regulates essential cellular functions such as transcription, translation, proliferation,

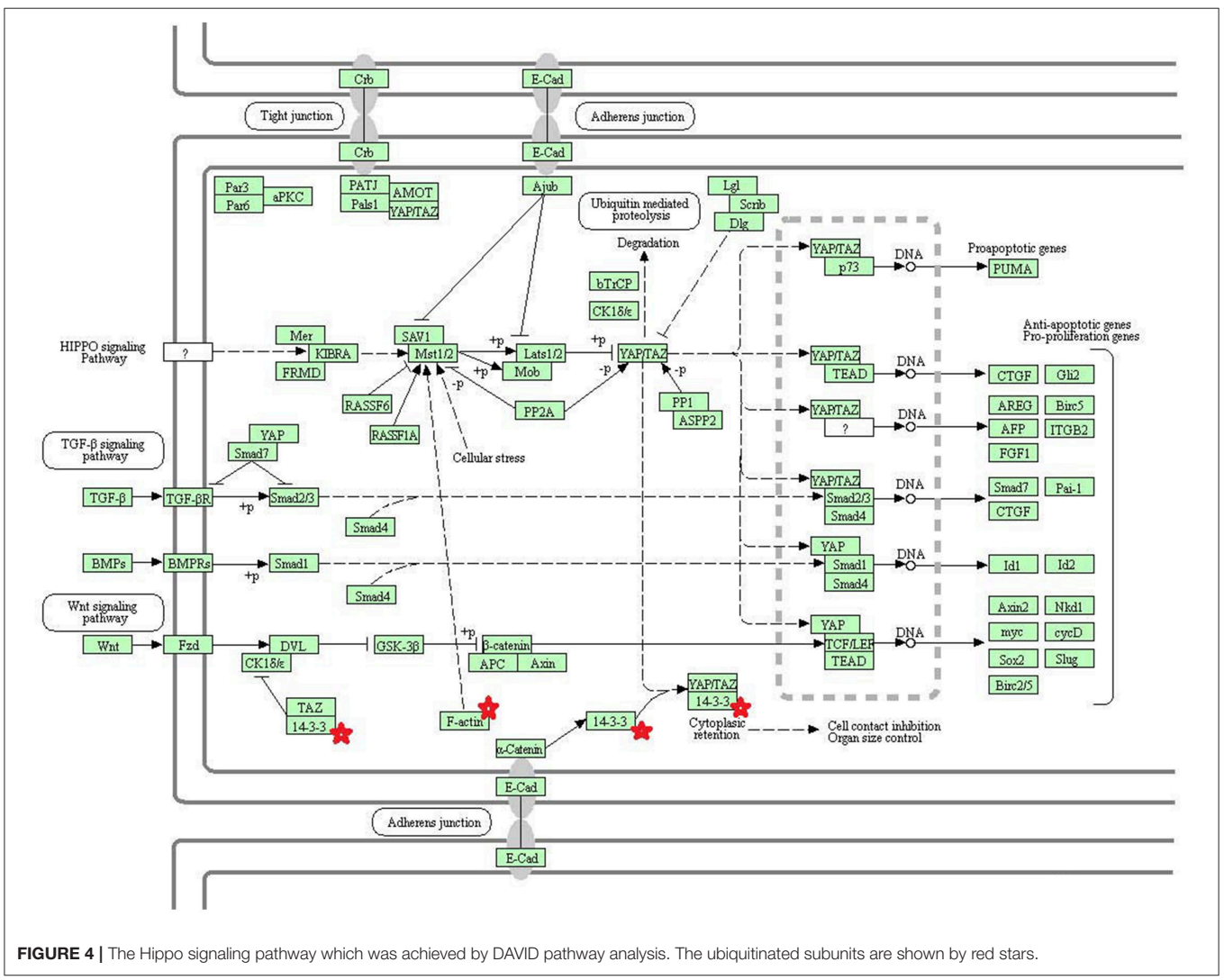

FIGURE 4 | The Hippo signaling pathway which was achieved by DAVID pathway analysis. The ubiquitinated subunits are shown by red stars.

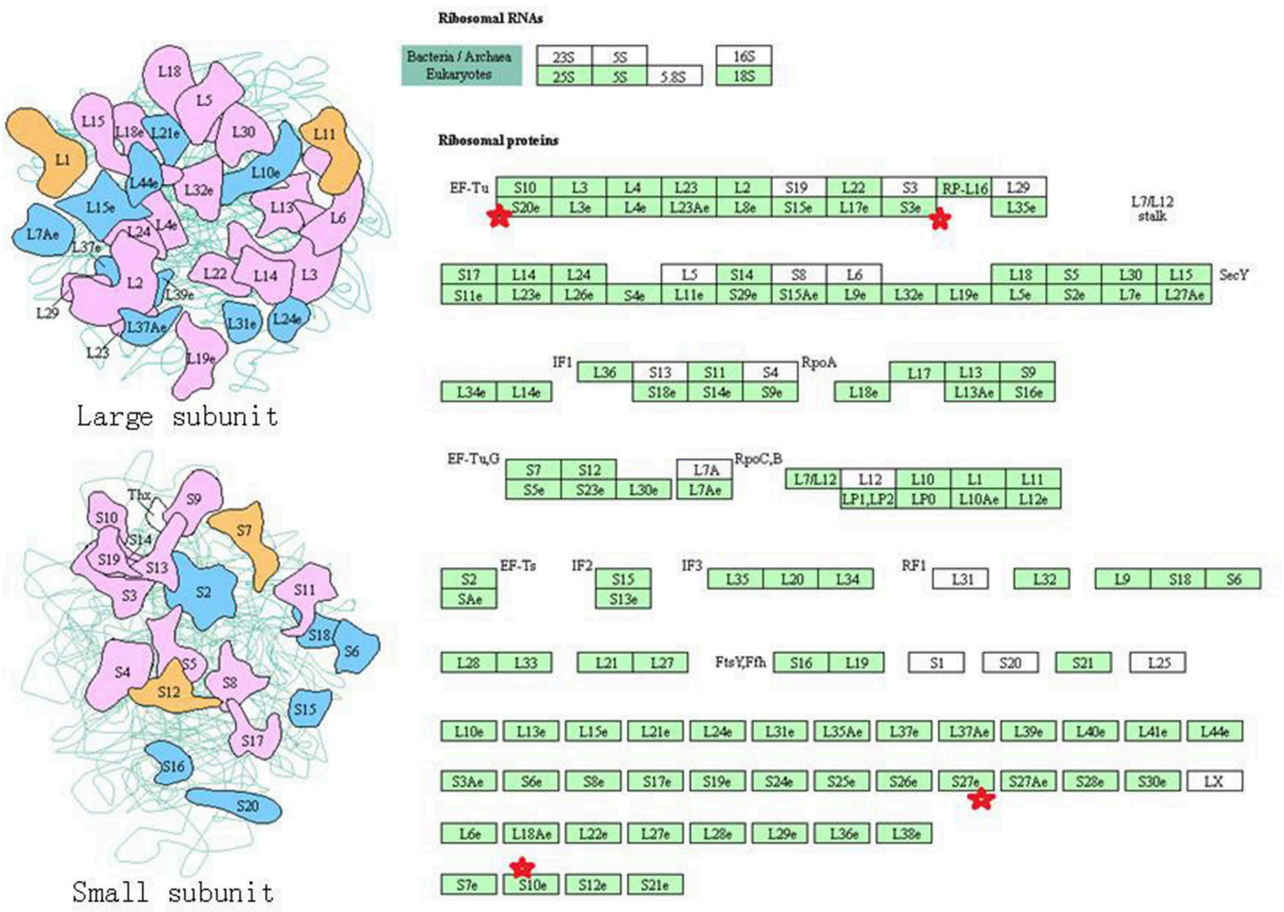

FIGURE 5 | The ribosome signaling pathway which was achieved by DAVID pathway analysis. The ubiquitinated subunits are shown by red stars.

survival, and growth. Hippo signaling pathway (**Figure 4**) is an evolutionarily conserved signaling pathway that controls the size of organs from flies to humans. For human and mouse, Hippo signaling pathway consists of MST1 and MST2 kinases, their cofactors Salvador, LATS1, and LATS2. In response to high cell density, activated LATS1/2 phosphorylates the transcriptional coactivators YAP and TAZ to promote their cytoplasmic localization, leads to apoptosis, and limits organ-size overgrowth. When the Hippo signaling pathway is inactivated at low cell densities, YAP/TAZ translocate into the nucleus to bind to the transcriptional factor enhancer (TEAD/TEF) family to promote cell growth and proliferation. YAP/TAZ also interact with other transcriptional factors or signaling molecules to allow Hippo pathway-mediated processes interact with other key signaling cascade processes, such as TGF-β and Wnt signaling pathways. Because the function of ribosomes is to translate the genetic code (nucleotide sequence) on the mRNA into the amino acid sequence on the polypeptide chain, the ribosome is closely related to protein synthesis. Ribosome signaling pathway (**Figure 5**) was enriched, and indicated that certain ubiquitinated proteins are closely related to this signaling pathway to thus affect protein synthesis. Nucleotide Excision repair (NER) (**Figure 6**) is a mechanism to recognize and repair large amounts of DNA damage caused by compounds, environmental carcinogens, and ultraviolet radiation. Protein ubiquitination might be involved in the nucleotide excision repair process to affect protein synthesis and the corresponding biological functions in PAs. Therefore, protein ubiquitination participated in multiple signaling pathway systems and biological processes in human PAs.

Functional Characteristics of Ubiquitinated Proteins

In order to further understand the biological function of the ubiquitinated proteins in the development of PAs, GO enrichment analysis of identified ubiquitinated proteins revealed multiple CCs, BPs, and MFs. For CC analysis (**Table 3**), 33 ubiquitinated proteins were assigned to different CCs. A large number of ubiquitinated proteins were located on ribosome and vesicle. It is well-known that ribosomes are complexes composed of rRNA and proteins, and are important sites for protein synthesis. In addition, vesicles and ribosomal subunits also play an important role in protein synthesis. Ubiquitinated proteins can be degraded by the proteasome

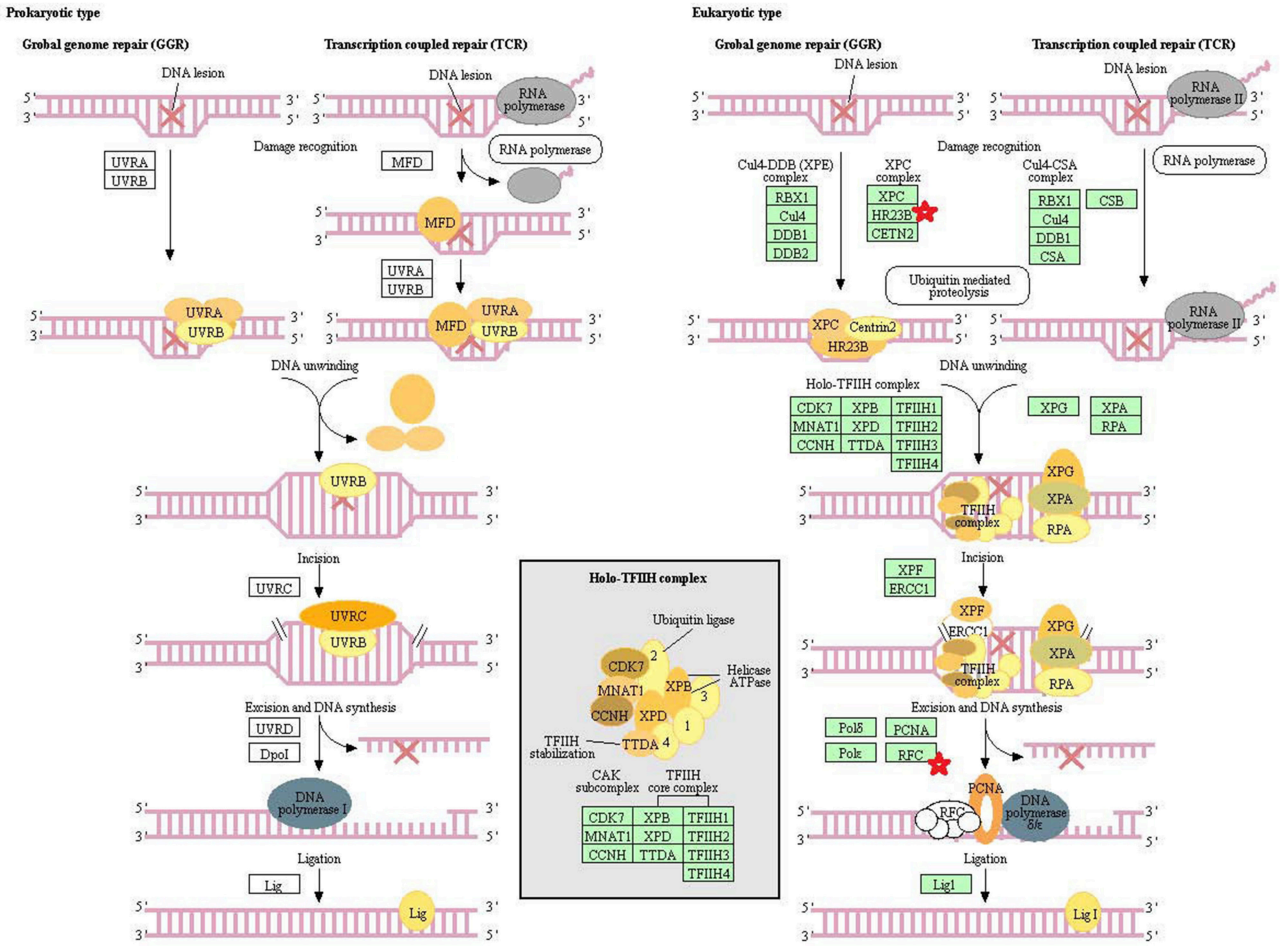

FIGURE 6 | The nucleotide excision repair which was achieved by DAVID pathway analysis. The ubiquitinated subunits are shown by red stars.

pathway (8). When the protein on ribosome or vesicle is usually ubiquitinated, the protein might degrade and affect the synthesis and secretion of other proteins, affect the normal physiological function of the body, and lead to PAs. For BP analysis (**Table 4**), most ubiquitinated proteins were associated with some important biological processes such as cellular responses to certain substances, self-regulation of cells, DNA repair, etc. Abnormal DNA repair was involved in the occurrence and development of tumors (50). When the proteins involved in DNA repair were ubiquitinated, abnormal DNA repair might occur and lead to PAs. In PA patients, the primary treatment was surgery; however, prolactinomas were usually treated with dopamine agonists (51, 52). The ubiquitinated proteins were associated with drug transport, which might make it difficult for drugs in PA patients to get to the target and thus allow development of tumors. For MF analysis (**Table 5**), 31 ubiquitinated proteins were significantly enriched in different MFs. The molecular functions of enriched ubiquitinated proteins were mainly combined with other substances, such as oxygen, organic acids, cofactors, etc. An important tumor marker was the infinite proliferation of tumor cells and angiogenesis (53). The proliferation of cells and the production of new blood vessels were inseparable from oxygen and nutrients. Ubiquitinated proteins could bind to oxygen, which might affect the transport of oxygen and nutrients, to thus affect the occurrence and development of PAs.

Characterization of Ubiquitinated Peptides

Some studies showed that conservative ubiquitination motifs might not exist in humans (34, 40, 54). To elucidate regulation of ubiquitination in human PAs, ubiquitination motif analysis was carried out by examining the sequences from −15 to +15 amino acid residues in the ubiquitination sites of the 142 ubiquitinated peptides with Motif-X software. Five significantly distinguished motifs were identified (**Figures 7A,B**), including K*-$X_{(2)}$-E, D-$X_{(4)}$-K*, K-$X_{(4)}$-K*, K-$X_{(3)}$-K*, and K*A, which refers to 42, 22, 29, 26, and 23 unique ubiquitinated peptides, respectively (K* = the ubiquitinated lysine residue; X = any amino acid residue). Those ubiquitinated peptides had different abundances, which together accounted for 99.3% of the identified ubiquitinated peptides (**Figure 7C**). Although Zhang et al. studied the ubiquitination modification of wheat (55),

TABLE 3 | Statistically significant GO cellular components (CC) derived from ubiquitinated proteins in human pituitary adenomas.

ID	Cellular components	GeneRatio	BgRatio	*P*-value	*P*.adjust	*Q*-value	GeneID	Count
GO:0022627	Cytosolic small ribosomal subunit	4/33	45/19659	9.34E-07	1.33E-04	8.26E-05	RPS3/RPS20/HBA1/HBA2	4
GO:0015935	Small ribosomal subunit	4/33	73/19659	6.60E-06	4.68E-04	2.92E-04	RPS3/RPS20/HBA1/HBA2	4
GO:0022626	Cytosolic ribosome	4/33	115/19659	3.99E-05	1.89E-03	1.18E-03	RPS3/RPS20/HBA1/HBA2	4
GO:0044445	Cytosolic part	5/33	250/19659	5.67E-05	2.01E-03	1.25E-03	IDE/RPS3/RPS20/HBA1/HBA2	5
GO:0072562	Blood microparticle	4/33	147/19659	1.04E-04	2.95E-03	1.83E-03	FGA/ALB/HBA1/HBA2	4
GO:0031838	Haptoglobin-hemoglobin complex	2/33	11/19659	1.49E-04	3.17E-03	1.97E-03	HBA1/HBA2	2
GO:0005833	Hemoglobin complex	2/33	12/19659	1.78E-04	3.17E-03	1.97E-03	HBA1/HBA2	2
GO:0060198	Clathrin-sculpted vesicle	2/33	12/19659	1.78E-04	3.17E-03	1.97E-03	DNAJC5/SLC32A1	2
GO:0044391	Ribosomal subunit	4/33	191/19659	2.83E-04	4.47E-03	2.78E-03	RPS3/RPS20/HBA1/HBA2	4
GO:0071682	Endocytic vesicle lumen	2/33	19/19659	4.59E-04	6.52E-03	4.06E-03	HBA1/HBA2	2
GO:0005840	Ribosome	4/33	276/19659	1.13E-03	1.46E-02	9.07E-03	RPS3/RPS20/HBA1/HBA2	4
GO:0060205	Cytoplasmic vesicle lumen	4/33	338/19659	2.37E-03	2.62E-02	1.63E-02	FGA/ALB/HBA1/HBA2	4
GO:0031983	Vesicle lumen	4/33	339/19659	2.40E-03	2.62E-02	1.63E-02	FGA/ALB/HBA1/HBA2	4
GO:0098563	Intrinsic component of synaptic vesicle membrane	2/33	46/19659	2.70E-03	2.74E-02	1.71E-02	DNAJC5/SLC32A1	2
GO:0035577	Azurophil granule membrane	2/33	58/19659	4.26E-03	4.03E-02	2.51E-02	DNAJC5/TMEM30A	2
GO:0030658	Transport vesicle membrane	3/33	204/19659	4.78E-03	4.24E-02	2.64E-02	DNAJC5/SLC32A1/TMEM30A	3
GO:0031093	Platelet alpha granule lumen	2/33	67/19659	5.64E-03	4.71E-02	2.94E-02	FGA/ALB	2
GO:0031300	Intrinsic component of organelle membrane	3/33	226/19659	6.34E-03	4.98E-02	3.10E-02	DNAJC5/SLC32A1/ITM2B	3
GO:0005844	Polysome	2/33	73/19659	6.67E-03	4.98E-02	3.10E-02	VIM/RPS3	2

GeneRatio = The ratio of the number of genes enriched by the CC to the total number of genes enriched. BgRatio = The ratio of the number of genes contained in the CC to the number of genes in the BP database.

the ubiquitination motifs of wheat are completely different from the human ubiquitination motif. This result might reveal differences in ubiquitination motifs among different species. The ubiquitination motifs of human proteins obtained in this study might provide ubiquitin-binding loci for future research. However, one must realize that because this study incorporated a small number of ubiquitinated peptides, the characterized human protein ubiquitination motifs still need to be validated from a large number of ubiquitinated peptide sequences.

Further Analysis of Ubiquitinated Proteins in Pituitary Adenomas

After comprehensive analysis of ubiquitination data, KEGG pathways, and GO enrichment data, eight statistically significant KEGG signaling pathways ($p < 0.05$) were identified. Only four of these enriched signaling pathways were associated with tumors, and the protein 14-3-3 zeta/delta was an important molecule in the PI3K-AKT signaling pathway and the Hippo signaling pathway. Also, the peptide from protein 14-3-3 zeta/delta underwent ubiquitination in control pituitary tissues, but not in NFPA tissues (**Table 2**). Therefore, the ubiquitinated protein 14-3-3 zeta/delta was chosen for further analysis with Western immunoaffinity blot. The result showed that protein 14-3-3 zeta/delta was significantly upregulated in NFPAs compared to controls. Quantitative ubiquitinated proteomics showed that the peptide from protein 14-3-3 zeta/delta was ubiquitinated in controls but not in NFPAs (**Figure 8**; **Table 2**). The decreased ubiquitination level of protein 14-3-3 zeta/delta in NFPAs might inhibit degradation of this protein and change the signaling transduction of this protein in PAs.

DISCUSSION

The Functions of Protein Ubiquitination

Ubiquitination in a protein is under a wide range of functions, and regulates a variety of basic cellular processes, including gene transcription, DNA repair and replication, protein degradation, viral particle sprouting, and intracellular trafficking (56). Monoubiquitination is involved in the regulation of lysosome targeting, endocytosis, and chromatin remodeling and meiosis. Polyubiquitination involves DNA damage and repair, targets modified proteins to proteasomal degradation, and includes immune signal transduction (17). Chen et al. suggest that ubiquitination has become a key regulator of the immune system involved in transduction of intracellular signals, control of T cell differentiation, and induction of immune tolerance (57). The ubiquitination regulatory pattern recognizes receptor signaling, initiates adaptive immune responses, and maturates dendritic cells required to mediate innate immune responses. For T cells, ubiquitination regulates their development, activation, and differentiation to thereby maintain immune tolerance to their own tissues and an effective adaptive immune response to pathogens (20). The role of ubiquitination in immune regulation was first discovered in studies of antigen presentation and transcription factor nuclear factor NFκB family (58). The transcription factor nuclear factor NF-κB controls basic functions of many cells, including cell proliferation, immune responses, and apoptosis (59). Excessive apoptosis can result in anemia, neurodegenerative diseases, and graft rejection. A reduction of apoptosis can lead to autoimmune diseases and cancer.

TABLE 4 | Statistically significant GO biological processes (BP) derived from ubiquitinated proteins in human pituitary adenomas.

ID	Biological process	GeneRatio	BgRatio	*P*-value	*P*.adjust	*Q*-value	GeneID	Count
GO:0097237	Cellular response to toxic substance	5/30	235/18493	3.49E-05	1.66E-02	1.27E-02	ALB/RPS3/HBA1/HBA2/PDCD10	5
GO:0042542	Response to hydrogen peroxide	4/30	141/18493	7.61E-05	1.66E-02	1.27E-02	RPS3/HBA1/HBA2/PDCD10	4
GO:0045739	Positive regulation of DNA repair	3/30	61/18493	1.30E-04	1.66E-02	1.27E-02	H2AFX/RPS3/UBE2N	3
GO:0042983	Amyloid precursor protein biosynthetic process	2/30	11/18493	1.39E-04	1.66E-02	1.27E-02	ITM2C/ITM2B	2
GO:0042984	Regulation of amyloid precursor protein biosynthetic process	2/30	11/18493	1.39E-04	1.66E-02	1.27E-02	ITM2C/ITM2B	2
GO:0046677	Response to antibiotic	5/30	323/18493	1.57E-04	1.66E-02	1.27E-02	RPS3/HBA1/PRL/HBA2/PDCD10	5
GO:0010561	Negative regulation of glycoprotein biosynthetic process	2/30	12/18493	1.66E-04	1.66E-02	1.27E-02	ITM2C/ITM2B	2
GO:0031581	Hemidesmosome assembly	2/30	12/18493	1.66E-04	1.66E-02	1.27E-02	LAMC2/PLEC	2
GO:0015671	Oxygen transport	2/30	15/18493	2.64E-04	2.11E-02	1.62E-02	HBA1/HBA2	2
GO:1903019	Negative regulation of glycoprotein metabolic process	2/30	15/18493	2.64E-04	2.11E-02	1.62E-02	ITM2C/ITM2B	2
GO:0015893	Drug transport	4/30	217/18493	3.98E-04	2.56E-02	1.96E-02	HBA1/HBA2/SLC32A1/TMEM30A	4
GO:0015669	Gas transport	2/30	19/18493	4.28E-04	2.56E-02	1.96E-02	HBA1/HBA2	2
GO:2001022	Positive regulation of response to DNA damage stimulus	3/30	92/18493	4.39E-04	2.56E-02	1.96E-02	H2AFX/RPS3/UBE2N	3
GO:0000302	Response to reactive oxygen species	4/30	224/18493	4.48E-04	2.56E-02	1.96E-02	RPS3/HBA1/HBA2/PDCD10	4
GO:0098869	Cellular oxidant detoxification	3/30	101/18493	5.77E-04	3.08E-02	2.36E-02	ALB/HBA1/HBA2	3
GO:1990748	Cellular detoxification	3/30	105/18493	6.46E-04	3.23E-02	2.47E-02	ALB/HBA1/HBA2	3
GO:0006282	Regulation of DNA repair	3/30	115/18493	8.41E-04	3.96E-02	3.03E-02	H2AFX/RPS3/UBE2N	3
GO:0031112	Positive regulation of microtubule polymerization or depolymerization	2/30	29/18493	1.01E-03	4.30E-02	3.30E-02	RPS3/STMN2	2
GO:0098754	Detoxification	3/30	123/18493	1.02E-03	4.30E-02	3.30E-02	ALB/HBA1/HBA2	3
GO:0042744	Hydrogen peroxide catabolic process	2/30	32/18493	1.22E-03	4.77E-02	3.66E-02	HBA1/HBA2	2
GO:0051291	Protein heterooligomerization	3/30	132/18493	1.25E-03	4.77E-02	3.66E-02	IDE/HBA1/HBA2	3

GeneRatio = The ratio of the number of genes enriched by the BP to the total number of genes enriched. BgRatio = The ratio of the number of genes contained in the BP to the number of genes in the BP database.

Therefore, moderate apoptosis is of great importance to the body. Ubiquitination of apoptotic proteins is a key component of the apoptosis signaling cascade (60). The ubiquitination mentioned above has an effect on DNA damage and repair. Improper response of DNA damage might accelerate the aging process, cause genomic instability, and eventually lead to various human diseases, including neurodegenerative diseases and cancer (61). Ubiquitination plays an important role to regulate the tumor suppressor function of Beclin1 (62). Thus, ubiquitination might play a crucial part in cancer. Some publications have described that ubiquitination disorders affect the occurrence, development, and metastasis of cancer (22, 63, 64).

Ubiquitinated Proteins Regulated Diverse Biological Process

This study found the mainly GO biological processes were related to synthesis and metabolism of proteins, which included glycoprotein, amyloid precursor protein, regulation of proteasomal ubiquitin-dependent protein, etc. This result suggests that ubiquitinated proteins might be involved in the synthesis and metabolism of certain proteins. Our long-term proteomics studies found that the number of down-regulated proteins was much more than up-regulated proteins in different subtypes of NFPAs compared to control pituitaries (28), mRNA expressions of ubiquitin-conjugating enzymes E2 and E3 were significantly increased in NFPAs (28), mRNA expression of ubiquitin specific protease 34 was significantly decreased in PAs (29), proteasome subunit alpha type 2 was nitrated in PAs (26), and the protein ubiquitination pathway was changed in NFPAs (30). It is well-known that synthesis and degradation of proteins in humans maintain in a dynamic balance. The increased number of down-regulated proteins in PAs might mean a disrupted balance between synthesis and degradation of proteins compared to control pituitaries. This study clearly found that ubiquitinated proteins in PAs were related to the synthesis and metabolism of proteins. The ubiquitinated proteasome system is one of the main pathways for intracellular protein degradation (8, 65, 66). Ubiquitination can achieve protein degradation by ubiquitinating the proteasome. Therefore, the increased number of these downregulated proteins in human NFPAs might undergo ubiquitination to result in more degradation of the proteins relative to normal pituitaries.

TABLE 5 | Statistically significant GO molecular functions (MF) derived from ubiquitinated proteins in human pituitary adenomas.

ID	Molecular functions	GeneRatio	BgRatio	*P*-value	*P*.adjust	*Q*-value	GeneID	Count
GO:0019825	Oxygen binding	3/31	36/17632	3.38E-05	4.97E-03	3.48E-03	ALB/HBA1/HBA2	3
GO:0031720	Haptoglobin binding	2/31	10/17632	1.33E-04	8.10E-03	5.68E-03	HBA1/HBA2	2
GO:0001540	Amyloid-beta binding	3/31	61/17632	1.65E-04	8.10E-03	5.68E-03	IDE/ITM2C/ITM2B	3
GO:0005344	Oxygen carrier activity	2/31	14/17632	2.69E-04	9.87E-03	6.93E-03	HBA1/HBA2	2
GO:0043177	Organic acid binding	4/31	204/17632	4.29E-04	1.12E-02	7.84E-03	ALB/PAM/HBA1/HBA2	4
GO:0016209	Antioxidant activity	3/31	86/17632	4.56E-04	1.12E-02	7.84E-03	ALB/HBA1/HBA2	3
GO:0050699	WW domain binding	2/31	31/17632	1.35E-03	2.83E-02	1.99E-02	NDFIP1/TCEAL2	2
GO:0048037	Cofactor binding	5/31	495/17632	1.59E-03	2.92E-02	2.05E-02	ALB/PAM/RPS3/HBA1/HBA2	5
GO:0140104	Molecular carrier activity	2/31	43/17632	2.58E-03	4.22E-02	2.96E-02	HBA1/HBA2	2

GeneRatio = The ratio of the number of genes enriched by the MF to the total number of genes enriched. BgRatio = The ratio of the number of genes contained in the MF to the number of genes in the BP database.

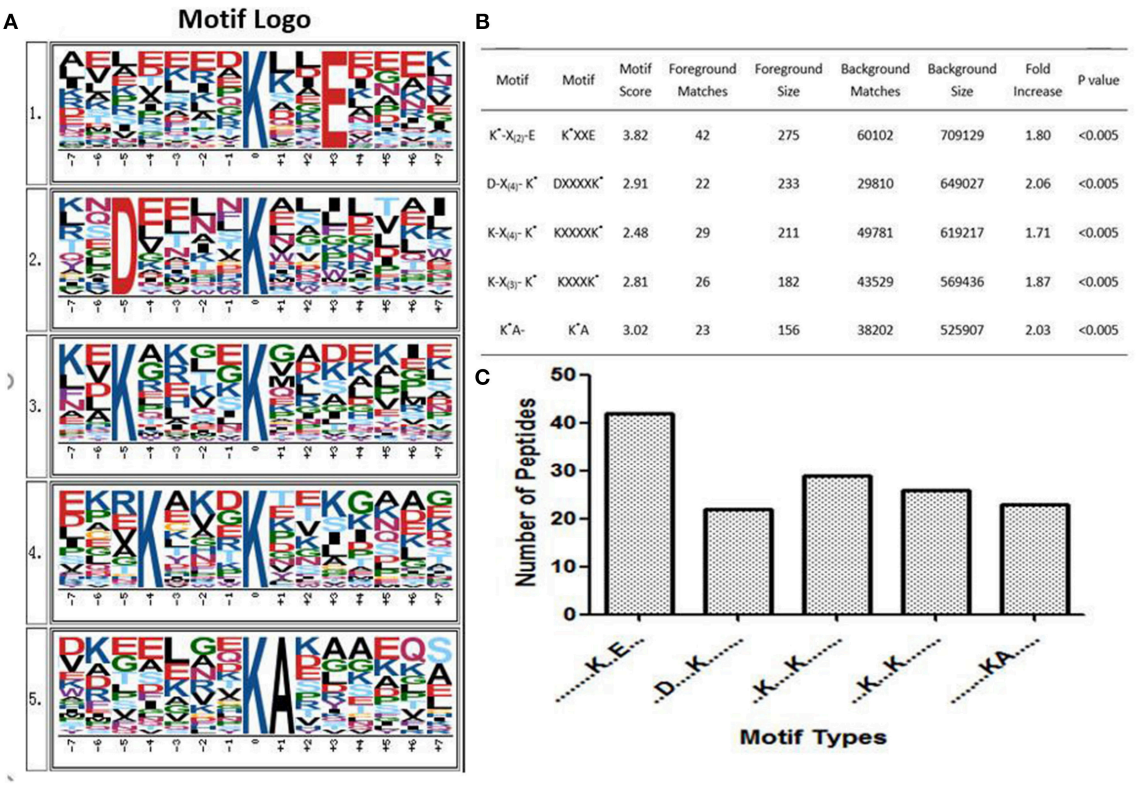

FIGURE 7 | Ubiquitinated protein motifs in human. **(A)** Ubiquitination motifs and the conservation of ubiquitination sites. The central K stands for the ubiquitinated protein. The size of each letter is related to the frequency of amino acid residues occurring at that position. **(B)** Taking the ubiquitinated peptide sequence as a foreground, the sequence window of the ubiquitinated related protein non-ubiquitinated lysine was used as a background control. **(C)** The number of identified ubiquitinated peptides in each motif. K* = ubiquitinated lysine residue. X = any amino acid residue.

The phosphatidylinositol 3-kinase (PI3K)-AKT signaling pathway is activated by many types of cellular and toxic damage and regulates basic cellular functions such as transcription, translation, proliferation, growth, and survival. Binding of growth factors to their receptor tyrosine kinase or G protein-coupled receptor stimulates the Ia and Ib PI3K subtypes, respectively. PI3K catalyzes the production of phosphatidylinositol-3, 4, 5-triphosphate on the cell membrane. PIP3 in turn acts as a second messenger to activate AKT. The activated AKT can control key cellular processes through phosphorylation involved in apoptosis, protein synthesis, metabolism, and cell cycle substrates. The PI3K-AKT signaling pathway is an important signaling pathway in cells, and its main function is to inhibit apoptosis and promote proliferation. In various malignant tumors, the PI3K-AKT signaling pathway is abnormally regulated to promote formation of new blood

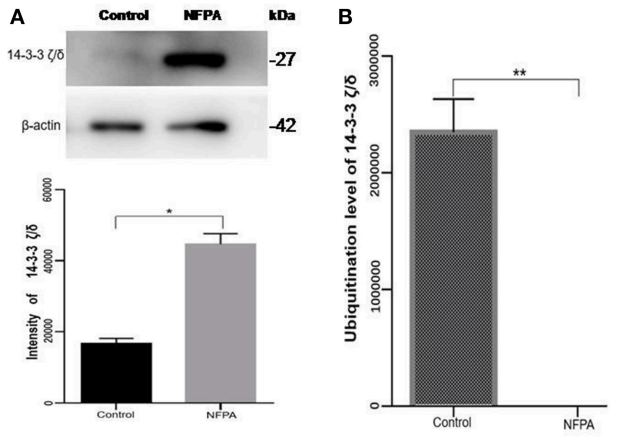

FIGURE 8 | The protein expression level and its ubiquitinated level of protein 14-3-3 zeta/delta in NFPAs compared to controls. **(A)** Western blot analysis of the protein expression level of protein 14-3-3 zeta/delta in NFPAs compared to controls. **(B)** The ubiquitination level of protein 14-3-3 zeta/delta in NFPAs compared to controls. $^{*}p < 0.05$. $^{**}p < 0.01$. NFPA, nonfunctional pituitary adenomas; Control, control pituitaries.

vessels, proliferation of tumor cells, and inhibition of apoptosis, and is closely related to tumor metastasis and invasion. The HVP90 inhibitor NVPAUY922 and the PI3K-mTOR inhibitor NVP-BEZ235, alone or in combination, have a significant effect on the apoptosis of cholangiocarcinoma cells; and these inhibitors act on the rat model of cholangiocarcinoma to decrease the tumor (67). These results indirectly indicate that activation of PI3K-AKT signaling pathway contributes to the proliferation of cholangiocarcinoma cells. Study also found that the P110α subunit of PI3K is a regulator of angiogenesis, and the inactivation of P110α leads to non-functional angiogenesis, which in turn prevents tumor growth (68). In the PI3K-AKT signaling pathway, the key molecules are cytokine, ECM, ITGB, and 14-3-3. Lamnin subunit gamma2 (LAMC2), which is a molecule in ECM, has been reported to be involved in the development and progression of various tumors (69). Smith et al. (70) found that LAMC2 was associated with bladder cancer metastasis, and its expression level increased with an increase of human tumor stage. In colorectal cancer, stable overexpressed LAMC2 promotes proliferation, migration, and invasion of cancer cells (71). The grade of LAMC2 expression was significantly associated with the pattern and depth of invasion of oral squamous cell carcinoma (72). This study found that LAMC2 was ubiquitinated at position 219. PAs are generally benign tumors, and do not metastasize; however, they do proliferate and invade of tumor cells.

The core components of the Hippo signaling pathway include upstream and downstream regulatory factors, core kinase cassettes, and downstream oncogenes. The core kinase cassette includes Lats1/2, Mst2, SAV1, and Mob. Activation of the Lats1/2 phosphorylation of the transcriptional coactivators YAP and TAZ ultimately leads to apoptosis, limits organ size overgrowth, or promotes cell growth and proliferation (73). Therefore, the Hippo signaling pathway prevents tissue growth and tumorigenesis (74). However, the abnormality of this pathway usually leads to the occurrence of tumors (75). For example, when Lats1 is ubiquitinated, the kinase activity of Lats1 is reduced and subsequently inhibited by Hippo signaling only promotes cell proliferation, but also inhibits cell apoptosis and attenuates tumor suppressor function (76). NEDD4, an E3 ubiquitin ligase, can directly interact with Lats1 to lead to its ubiquitination and decreased levels of Lats to thereby increase the localization of nuclear YAP, and activate proliferative and anti-apoptotic genes (77). Lignitto et al. (78) found that the ubiquitination-proteasome system can degrade Mob to attenuate the Hippo cascade and maintain the growth of glioblastoma cells *in vivo*. So what is the impact of ubiquitination on the Hippo signaling pathway? Toloczko et al. (73) found that USP9X, a deubiquitinating protease, can enhance LATS kinase to inhibit tumor growth. Therefore, the Hippo signaling pathway is closely related to tumorigenesis, and the ubiquitination and deubiquitination of the core kinase cassette in the Hippo signaling pathway have a great influence on tumor growth. Therefore, ubiquitination and deubiquitination of the core kinase cassette are worthy of further study, and might lead to the development of new treatments for tumors. In addition, some key molecules in the Hippo signaling pathway are 14-3-3 protein and F-actin. The 14-3-3 protein in the Hippo signaling pathway is closely related to tumors.

The Ubiquitination of 14-3-3 Proteins in Pituitary Adenomas

Humans 14-3-3 proteins have many subtypes, including 14-3-3 protein beta/alpha, 14-3-3 protein gamma, 14-3-3 protein theta, etc. 14-3-3 subtypes are considered to play nocogenic roles in a variety of tumors (79). Raungrut et al. (80) found that 14-3-3 gamma is involved in the metastasis of lung cancer cells, and found that knockdown of 14-3-3 gamma could inhibit lung cancer metastasis. The 14-3-3 beta protein has been shown to possess carcinogenic potential, and its increased expression has been detected in many types of cancers. Tang et al. (81) found that 14-3-3 beta promotes migration and invasion of human hepatocellular carcinoma cells by modulating expression of MMP2 and MMP9 through the PI3K/Akt/NF-κB pathway. Also, 14-3-3 τ can promote breast cancer invasion and metastasis by inhibiting RhoGDI (82). However, few studies are involved in the relationship of 14-3-3 zeta/delta proteins and tumorigenesis. This study found the 14-3-3 zeta/delta protein was ubiquitinated in pituitary control tissues but not in PA tissues. However, Western blot analysis found that 14-3-3 zeta/delta protein was highly expressed in NFPAs compared to control tissues. The ubiquitinated proteasome system is one of the major pathways for intracellular protein degradation (8, 65, 66). Ubiquitination can achieve protein degradation by ubiquitination of the proteasome. Thus, it is hypothesized that proteins can be degraded by ubiquitination modification to result in lower protein levels in tumors than control tissues. Therefore, up-regulated expression of 14-3-3 zeta/delta protein in NFPAs might be due to the decreased ubiquitination level, and contribute to pituitary tumorigenesis. These findings might

provide a better basis for biomarker discovery and the early treatment of PA patients.

Strengths and Limitations of This Study

This study, for the first time, used anti-ubiquitin antibody (specific to K-ε-GG)-based label-free quantitative proteomics to identify protein ubiquitination profiling between NFPAs and control pituitaries. A total of 158 ubiquitinated sites in 108 ubiquitinated proteins was identified and quantified, which is the first ubiquitinome profile in NFPAs compared to controls. Further, pathway network analysis revealed alterations of multiple ubiquitination-involved signaling pathway systems in NFPAs to offer novel insights into molecular mechanisms of NFPAs and to provide a new source to discover new biomarkers for NFPAs. However, one must realize that a ubiquitinome is dynamic, and varies with different conditions and pathophysiological status. PAs are highly heterogeneous among tumor individuals, different subtype of NFPAs, and different subtypes of FPAs. In order to further in-depth insight into functional significance of each ubiquitination in PA pathogenesis, one must significantly expand the number of human tissue samples studied to validate and quantify each ubiquitination among individuals and different PA subtypes; also, biological functions of each ubiquitination should be examined in the cell model and animal model. For this current study, due to the very limited, precious pituitary adenoma and control tissue samples, only very limited amount of proteins were used for trypsin digestion, anti-ubiquitin antibody-based enrichment, and LC-MS/MS analysis. The number of ubiquitinated sites and ubiquitinated proteins might be significantly increased with an increased amount of proteins in future ubiquitinomics analysis among PA individuals and among different PA subtypes, to significantly expand the ubiquitinome database of PAs, which will offer the increased opportunity to in-depth explore biological roles of protein ubiquitination in PAs.

CONCLUSION

Ant-ubiquitin antibody-based label-free quantitative proteomics effectively identified and quantified protein lysine ubiquitination in human PAs compared to controls. This study provides the first protein ubiquitination profiling of human PAs and control pituitaries to understand ubiquitination-mediated multiple cellular functions and biological processes. This study expanded the range of physiological processes regulated by ubiquitination, and serves as a valuable reference for biological functions of protein ubiquitination in human PAs.

ETHICS STATEMENT

PA tissues were obtained from the Department of Neurosurgery of Xiangya Hospital, China, as approved by the Xiangya Hospital Medical Ethics Committee of Central South University. Control pituitary tissues were obtained from the Memphis Regional Medical Center ($n = 5$), as approved by University of Tennessee Health Science Center Internal Review Board. The consent was attained from each patient or the family of each control pituitary subject (post-mortem tissues) after full explanation of the purpose and nature of all experimental procedures.

AUTHOR CONTRIBUTIONS

SQ analyzed data, carried out Western blot experiment, prepared figures and tables, designed and wrote the manuscript. XhZ participated in the analysis, and revised the manuscript. ML and NL participated in partial data analysis. YL prepared the protein samples. XL collected tissue samples and performed clinical diagnosis. DD provided the control tissues, and critically evaluated and revised the manuscript. XqZ conceived the concept, designed experiments and manuscript, instructed experiments, analyzed data, obtained the ubiquitinated proteomic data, supervised results, coordinated, wrote and critically revised manuscript, and was responsible for its financial supports and the corresponding works. All authors approved the final manuscript.

FUNDING

This work was supported by the grants from the China 863 Plan Project (Grant No. 2014AA020610-1 to XqZ), National Natural Science Foundation of China (Grant No. 81572278, 81272798, and 81770781), the Hunan Provincial Hundred Talent Plan (to XqZ), the Xiangya Hospital Funds for Talent Introduction (to XqZ), and the Hunan Provincial Natural Science Foundation of China (Grant No. 14JJ7008 to XqZ).

REFERENCES

1. Zhan X, Wang X, Cheng T. Human pituitary adenoma proteomics: new progresses and perspectives. *Front Endocrinol.* (2016) 7:54. doi: 10.3389/fendo.2016.00054
2. Levy A. Molecular and trophic mechanisms of tumorigenesis. *Endocrinol Metab Clin North Am.* (2008) 37:23–50. doi: 10.1016/j.ecl.2007.10.009
3. Jaffe CA. Clinically non-functioning pituitary adenoma. *Pituitary.* (2006) 9:317–21. doi: 10.1007/s11102-006-0412-9
4. Andela CD, Lobatto DJ, Pereira AM, van Furth WR, Biermasz NR. How non-functioning pituitary adenomas can affect health-related quality of life: a conceptual model and literature review. *Pituitary.* (2018) 21:208–16. doi: 10.1007/s11102-017-0860-4
5. Greenman Y, Stern N. Non-functioning pituitary adenomas. *Best Pract Res Clin Endocrinol Metab.* (2009) 23:625–38. doi: 10.1016/j.beem.2009.05.005
6. Tampourlou M, Fountas A, Ntali G, Karavitaki N. Mortality in patients with non-functioning pituitary adenoma. *Pituitary.* (2018) 21:203–7. doi: 10.1007/s11102-018-0863-9
7. Penn DL, Burke WT, Laws ER. Management of non-functioning pituitary adenomas: surgery. *Pituitary.* (2018) 21:145–53. doi: 10.1007/s11102-017-0854-2
8. Mettouchi A, Lemichez E. Ubiquitylation of active Rac1 by the E3 ubiquitin-ligase HACE1. *Small GTPases.* (2012) 3:102–6. doi: 10.4161/sgtp.19221
9. Popovic D, Vucic D, Dikic I. Ubiquitination in disease pathogenesis and treatment. *Nat Med.* (2014) 20:1242–53. doi: 10.1038/nm.3739

10. Luo Z, Zhang X, Zeng W, Su J, Yang K, Lu L, et al. TRAF6 regulates melanoma invasion and metastasis through ubiquitination of Basigin. *Oncotarget.* (2016) 7:7179–92. doi: 10.18632/oncotarget.6886
11. Lin AW, Man HY. Ubiquitination of neurotransmitter receptors and postsynaptic scaffolding proteins. *Neural Plast.* (2013) 2013:432057. doi: 10.1155/2013/432057
12. Gao C, Huang W, Kanasaki K, Xu Y. The role of ubiquitination and sumoylation in diabetic nephropathy. *Biomed Res Int.* (2014) 2014:160692. doi: 10.1155/2014/160692
13. Xiao Z, Zhang P, Ma L. The role of deubiquitinases in breast cancer. *Cancer Metastasis Rev.* (2016) 35:589–600. doi: 10.1007/s10555-016-9640-2
14. Hock AK, Vousden KH. The role of ubiquitin modification in the regulation of p53. *Biochim Biophys Acta.* (2014) 1843:137–49. doi: 10.1016/j.bbamcr.2013.05.022
15. Ding F, Yin Z, Wang HR. Ubiquitination in rho signaling. *Curr Top Med Chem.* (2011) 11:2879–87 doi: 10.2174/156802611798281357
16. Fulda S, Rajalingam K, Dikic I. Ubiquitylation in immune disorders and cancer: from molecular mechanisms to therapeutic implications. *EMBO Mol Med.* (2012) 4:545–56. doi: 10.1002/emmm.201100707
17. Zhou MJ, Chen FZ, Chen HC. Ubiquitination involved enzymes and cancer. *Med Oncol.* (2014) 31:93. doi: 10.1007/s12032-014-0093-6
18. Vadasz I, Weiss CH, Sznajder JI. Ubiquitination and proteolysis in acute lung injury. *Chest.* (2012) 141:763–71. doi: 10.1378/chest.11-1660
19. Ebner P, Versteeg GA, Ikeda F. Ubiquitin enzymes in the regulation of immune responses. *Crit Rev Biochem Mol Biol.* (2017) 52:425–60. doi: 10.1080/10409238.2017.1325829
20. Hu H, Sun SC. Ubiquitin signaling in immune responses. *Cell Res.* (2016) 26:457–83. doi: 10.1038/cr.2016.40
21. Kawabe H, Brose N. The role of ubiquitylation in nerve cell development. *Nat Rev Neurosci.* (2011) 12:251–68. doi: 10.1038/nrn3009
22. Morrow JK, Lin HK, Sun SC, Zhang S. Targeting ubiquitination for cancer therapies. *Future Med Chem.* (2015) 7:2333–50. doi: 10.4155/fmc.15.148
23. Zheng N, Shabek N. Ubiquitin ligases: structure, function, and regulation. *Annu Rev Biochem.* (2017) 86:129–57. doi: 10.1146/annurev-biochem-060815-014922
24. Lehman NL. The ubiquitin proteasome system in neuropathology. *Acta Neuropathol.* (2009) 118:329–47. doi: 10.1007/s00401-009-0560-x
25. Xu M, Knox AJ, Michaelis KA, Kiseljak-Vassiliades K, Kleinschmidt-DeMasters BK, Lillehei KO, et al. Reprimo (RPRM) is a novel tumor suppressor in pituitary tumors and regulates survival, proliferation, and tumorigenicity. *Endocrinology.* (2012) 153:2963–73. doi: 10.1210/en.2011-2021
26. Zhan X, Desiderio DM. Nitroproteins from a human pituitary adenoma tissue discovered with a nitrotyrosine affinity column and tandem mass spectrometry. *Anal Biochem.* (2006) 354:279–89. doi: 10.1016/j.ab.2006.05.024
27. Zhan X, Desiderio DM. A reference map of a human pituitary adenoma proteome. *Proteomics.* (2003) 3:699–713. doi: 10.1002/pmic.200300408
28. Moreno CS, Evans CO, Zhan X, Okor M, Desiderio DM, Oyesiku NM. Novel molecular signaling and classification of human clinically nonfunctional pituitary adenomas identified by gene expression profiling and proteomic analyses. *Cancer Res.* (2005) 65:10214–22. doi: 10.1158/0008-5472.CAN-05-0884
29. Evans CO, Moreno CS, Zhan X, McCabe MT, Vertino PM, Desiderio DM, et al. Molecular pathogenesis of human prolactinomas identified by gene expression profiling, RT-qPCR, and proteomic analyses. *Pituitary.* (2008) 11:231–45. doi: 10.1007/s11102-007-0082-2
30. Zhan X, Wang X, Long Y, Desiderio DM. Heterogeneity analysis of the proteomes in clinically nonfunctional pituitary adenomas. *BMC Med Genomics.* (2014) 7:69. doi: 10.1186/s12920-014-0069-6
31. Zhang H, Fang L, Zhu X, Wang D, Xiao S. Global analysis of ubiquitome in PRRSV-infected pulmonary alveolar macrophages. *J Proteomics.* (2018) 184:16–24. doi: 10.1016/j.jprot.2018.06.010
32. Chen XL, Xie X, Wu L, Liu C, Zeng L, Zhou X, et al. Proteomic analysis of ubiquitinated proteins in rice (*Oryza sativa*) after treatment with pathogen-associated molecular pattern (PAMP) elicitors. *Front Plant Sci.* (2018) 9:1064. doi: 10.3389/fpls.2018.01064
33. Lee KA, Hammerle LP, Andrews PS, Stokes MP, Mustelin T, Silva JC, et al. Ubiquitin ligase substrate identification through quantitative proteomics at both the protein and peptide levels. *J Biol Chem.* (2011) 286:41530–8. doi: 10.1074/jbc.M111.248856
34. Kim W, Bennett EJ, Huttlin EL, Guo A, Li J, Possemato A, et al. Systematic and quantitative assessment of the ubiquitin-modified proteome. *Mol Cell.* (2011) 44:325–40. doi: 10.1016/j.molcel.2011.08.025
35. Liu B, Jiang S, Li M, Xiong X, Zhu M, Li D, et al. Proteome-wide analysis of USP14 substrates revealed its role in hepatosteatosis via stabilization of FASN. *Nat Commun.* (2018) 9:4770. doi: 10.1038/s41467-018-07185-y
36. Aguilar-Hernandez V, Kim DY, Stankey RJ, Scalf M, Smith LM, Vierstra RD. Mass spectrometric analyses reveal a central role for ubiquitylation in remodeling the arabidopsis proteome during photomorphogenesis. *Mol Plant.* (2017) 10:846–65. doi: 10.1016/j.molp.2017.04.008
37. Udeshi ND, Mertins P, Svinkina T, Carr SA. Large-scale identification of ubiquitination sites by mass spectrometry. *Nat Protoc.* (2013) 8:1950–60. doi: 10.1038/nprot.2013.120
38. Yu K, Phu L, Varfolomeev E, Bustos D, Vucic D, Kirkpatrick DS. Immunoaffinity enrichment coupled to quantitative mass spectrometry reveals ubiquitin-mediated signaling events. *J Mol Biol.* (2015) 427:2121–34. doi: 10.1016/j.jmb.2015.03.018
39. Xu G, Paige JS, Jaffrey SR. Global analysis of lysine ubiquitination by ubiquitin remnant immunoaffinity profiling. *Nat Biotechnol.* (2010) 28:868–73. doi: 10.1038/nbt.1654
40. Kim DY, Scalf M, Smith LM, Vierstra RD. Advanced proteomic analyses yield a deep catalog of ubiquitylation targets in Arabidopsis. *Plant Cell.* (2013) 25:1523–40. doi: 10.1105/tpc.112.108613
41. Wagner SA, Beli P, Weinert BT, Nielsen ML, Cox J, Mann M, et al. A proteome-wide, quantitative survey of *in vivo* ubiquitylation sites reveals widespread regulatory roles. *Mol Cell Proteomics.* (2011) 10:M111.013284. doi: 10.1074/mcp.M111.013284
42. Beaudette P, Popp O, Dittmar G. Proteomic techniques to probe the ubiquitin landscape. *Proteomics.* (2016) 16:273–87. doi: 10.1002/pmic.201500290
43. Li XM, Chao DY, Wu Y, Huang X, Chen K, Cui LG, et al. Natural alleles of a proteasome alpha2 subunit gene contribute to thermotolerance and adaptation of African rice. *Nat Genet.* (2015) 47:827–33. doi: 10.1038/ng.3305
44. Thompson JW, Nagel J, Hoving S, Gerrits B, Bauer A, Thomas JR, et al. Quantitative Lys–Gly-Gly (diGly) proteomics coupled with inducible RNAi reveals ubiquitin-mediated proteolysis of DNA damage-inducible transcript 4 (DDIT4) by the E3 ligase HUWE1. *J Biol Chem.* (2014) 289:28942–55. doi: 10.1074/jbc.M114.573352
45. Rappsilber J, Mann M, Ishihama Y. Protocol for micro-purification, enrichment, pre-fractionation and storage of peptides for proteomics using StageTips. *Nat Protoc.* (2007) 2:1896–906. doi: 10.1038/nprot.2007.261
46. Qian S, Yang Y, Li N, Cheng T, Wang X, Liu J, et al. Prolactin variants in human pituitaries and pituitary adenomas identified with two-dimensional gel electrophoresis and mass spectrometry. *Front Endocrinol.* (2018) 9:468. doi: 10.3389/fendo.2018.00468
47. Bi W, He CN, Li XX, Zhou LY, Liu RJ, Zhang S, et al. Ginnalin A from Kujin tea (*Acer tataricum* subsp. ginnala) exhibits a colorectal cancer chemoprevention effect via activation of the Nrf2/HO-1 signaling pathway. *Food Funct.* (2018) 9:2809–19. doi: 10.1039/C8FO00054A
48. Guo AY, Liang XJ, Liu RJ, Li XX, Bi W, Zhou LY, et al. Flotilin-1 promotes the tumorigenicity and progression of malignant phenotype in human lung adenocarcinoma. *Cancer Biol Ther.* (2017) 18:715–22. doi: 10.1080/15384047.2017.1360445
49. Yang S, Xing Z, Liu T, Zhou J, Liang Q, Tang T, et al. Synovial tissue quantitative proteomics analysis reveals paeoniflorin decreases LIFR and ASPN proteins in experimental rheumatoid arthritis. *Drug Des Devel Ther.* (2018) 12:463–73. doi: 10.2147/DDDTS153927
50. Loriot Y, Meynard G, Klajer E, Bolognini C, Gassian N, Thiery-Vuillemin A. [DNA damage repair: an emerging strategy in metastatic prostate cancer]. *Bull Cancer.* (2018) 105:944–54. doi: 10.1016/j.bulcan.2018.05.017
51. Maldaner N, Serra C, Tschopp O, Schmid C, Bozinov O, Regli L. [Modern management of pituitary adenomas - current state of diagnosis, treatment and follow-up]. *Praxis.* (2018) 107:825–35. doi: 10.1024/1661-8157/a003035
52. Zatelli MC, Ambrosio MR, Bondanelli M, Uberti EC. Control of pituitary adenoma cell proliferation by somatostatin analogs, dopamine agonists and

novel chimeric compounds. *Eur J Endocrinol.* (2007) 156(Suppl. 1):S29–35. doi: 10.1530/eje.1.02352
53. Hanahan D, Weinberg RA. Hallmarks of cancer: the next generation. *Cell.* (2011) 144:646–74. doi: 10.1016/j.cell.2011.02.013
54. Danielsen JM, Sylvestersen KB, Bekker-Jensen S, Szklarczyk D, Poulsen JW, Horn H, et al. Mass spectrometric analysis of lysine ubiquitylation reveals promiscuity at site level. *Mol Cell Proteomics.* (2011) 10:M110.003590. doi: 10.1074/mcp.M110.003590
55. Zhang N, Zhang L, Shi C, Tian Q, Lv G, Wang Y, et al. Comprehensive profiling of lysine ubiquitome reveals diverse functions of lysine ubiquitination in common wheat. *Sci Rep.* (2017) 7:13601. doi: 10.1038/s41598-017-13992-y
56. Chen Z, Zhou Y, Zhang Z, Song J. Towards more accurate prediction of ubiquitination sites: a comprehensive review of current methods, tools and features. *Brief Bioinform.* (2015) 16:640–57. doi: 10.1093/bib/bbu031
57. Chen Z, Luo X, Lu Y, Zhu T, Wang J, Tsun A, et al. Ubiquitination signals critical to regulatory T cell development and function. *Int Immunopharmacol.* (2013) 16:348–52. doi: 10.1016/j.intimp.2013.01.023
58. Jiang X, Chen ZJ. The role of ubiquitylation in immune defence and pathogen evasion. *Nat Rev Immunol.* (2011) 12:35–48. doi: 10.1038/nri3111
59. Won M, Byun HS, Park KA, Hur GM. Post-translational control of NF-kappaB signaling by ubiquitination. *Arch Pharm Res.* (2016) 39:1075–84. doi: 10.1007/s12272-016-0772-2
60. Vucic D, Dixit VM, Wertz IE. Ubiquitylation in apoptosis: a post-translational modification at the edge of life and death. *Nat Rev Mol Cell Biol.* (2011) 12:439–52. doi: 10.1038/nrm3143
61. Wang Z, Zhu WG, Xu X. Ubiquitin-like modifications in the DNA damage response. *Mutat Res.* (2017) 803–805:56–75. doi: 10.1016/j.mrfmmm.2017.07.001
62. Abrahamsen H, Stenmark H, Platta HW. Ubiquitination and phosphorylation of beclin 1 and its binding partners: tuning class III phosphatidylinositol 3-kinase activity and tumor suppression. *FEBS Lett.* (2012) 586:1584–91. doi: 10.1016/j.febslet.2012.04.046
63. Chen Z, Lu W. Roles of ubiquitination and SUMOylation on prostate cancer: mechanisms and clinical implications. *Int J Mol Sci.* (2015) 16:4560–80. doi: 10.3390/ijms16034560
64. Gallo LH, Ko J, Donoghue DJ. The importance of regulatory ubiquitination in cancer and metastasis. *Cell Cycle.* (2017) 16:634–48. doi: 10.1080/15384101.2017.1288326
65. Portney BA, Khatri R, Meltzer WA, Mariano JM, Zalzman M. ZSCAN4 is negatively regulated by the ubiquitin-proteasome system and the E3 ubiquitin ligase RNF20. *Biochem Biophys Res Commun.* (2018) 498:72–8. doi: 10.1016/j.bbrc.2018.02.155
66. Nguyen LK, Kolch W, Kholodenko BN. When ubiquitination meets phosphorylation: a systems biology perspective of EGFR/MAPK signalling. *Cell Commun Signal.* (2013) 11:52. doi: 10.1186/1478-811X-11-52
67. Chen MH, Chiang KC, Cheng CT, Huang SC, Chen YY, Chen TW, et al. Antitumor activity of the combination of an HSP90 inhibitor and a PI3K/mTOR dual inhibitor against cholangiocarcinoma. *Oncotarget.* (2014) 5:2372–89. doi: 10.18632/oncotarget.1706
68. Soler A, Serra H, Pearce W, Angulo A, Guillermet-Guibert J, Friedman LS, et al. Inhibition of the p110alpha isoform of PI 3-kinase stimulates nonfunctional tumor angiogenesis. *J Exp Med.* (2013) 210:1937–45. doi: 10.1084/jem.20121571
69. Garg M, Braunstein G, Koeffler HP. LAMC2 as a therapeutic target for cancers. *Expert Opin Ther Targets.* (2014) 18:979–82. doi: 10.1517/14728222.2014.934814
70. Smith SC, Nicholson B, Nitz M, Frierson HF Jr., Smolkin M, Hampton G, et al. Profiling bladder cancer organ site-specific metastasis identifies LAMC2 as a novel biomarker of hematogenous dissemination. *Am J Pathol.* (2009) 174:371–9. doi: 10.2353/ajpath.2009.080538
71. Huang D, Du C, Ji D, Xi J, Gu J. Overexpression of LAMC2 predicts poor prognosis in colorectal cancer patients and promotes cancer cell proliferation, migration, and invasion. *Tumour Biol.* (2017) 39:1010428317705849. doi: 10.1177/1010428317705849
72. Nguyen CT, Okamura T, Morita KI, Yamaguchi S, Harada H, Miki Y, et al. LAMC2 is a predictive marker for the malignant progression of leukoplakia. *J Oral Pathol Med.* (2017) 46:223–31. doi: 10.1111/jop.12485
73. Toloczko A, Guo F, Yuen HF, Wen Q, Wood SA, Ong YS, et al. Deubiquitinating enzyme USP9X suppresses tumor growth via LATS kinase and core components of the hippo pathway. *Cancer Res.* (2017) 77:4921–33. doi: 10.1158/0008-5472.CAN-16-3413
74. Bao Y, Hata Y, Ikeda M, Withanage K. Mammalian hippo pathway: from development to cancer and beyond. *J Biochem.* (2011) 149:361–79. doi: 10.1093/jb/mvr021
75. Tremblay AM, Camargo FD. Hippo signaling in mammalian stem cells. *Semin Cell Dev Biol.* (2012) 23:818–26. doi: 10.1016/j.semcdb.2012.08.001
76. Mei L, Yuan L, Shi W, Fan S, Tang C, Fan X, et al. SUMOylation of large tumor suppressor 1 at Lys751 attenuates its kinase activity and tumor-suppressor functions. *Cancer Lett.* (2017) 386:1–11. doi: 10.1016/j.canlet.2016.11.009
77. Salah Z, Cohen S, Itzhaki E, Aqeilan RI. NEDD4 E3 ligase inhibits the activity of the Hippo pathway by targeting LATS1 for degradation. *Cell Cycle.* (2013) 12:3817–23. doi: 10.4161/cc.26672
78. Lignitto L, Arcella A, Sepe M, Rinaldi L, Delle Donne R, Gallo A, et al. Proteolysis of MOB1 by the ubiquitin ligase praja2 attenuates Hippo signalling and supports glioblastoma growth. *Nat Commun.* (2013) 4:1822. doi: 10.1038/ncomms2791
79. Tzivion G, Gupta VS, Kaplun L, Balan V. 14-3-3 proteins as potential oncogenes. *Semin Cancer Biol.* (2006) 16:203–13. doi: 10.1016/j.semcancer.2006.03.004
80. Raungrut P, Wongkotsila A, Champoochana N, Lirdprapamongkol K, Svasti J, Thongsuksai P. Knockdown of 14-3-3gamma suppresses epithelial-mesenchymal transition and reduces metastatic potential of human non-small cell lung cancer cells. *Anticancer Res.* (2018) 38:3507–14. doi: 10.21873/anticanres.12622
81. Tang Y, Lv P, Sun Z, Han L, Zhou W. 14-3-3beta promotes migration and invasion of human hepatocellular carcinoma cells by modulating expression of MMP2 and MMP9 through PI3K/Akt/NF-kappaB pathway. *PLoS ONE.* (2016) 11:e0146070. doi: 10.1371/journal.pone.0146070
82. Xiao Y, Lin VY, Ke S, Lin GE, Lin FT, Lin WC. 14-3-3tau promotes breast cancer invasion and metastasis by inhibiting RhoGDIalpha. *Mol Cell Biol.* (2014) 34:2635–49. doi: 10.1128/MCB.00076-14

Conflict of Interest Statement: The authors declare that the research was conducted in the absence of any commercial or financial relationships that could be construed as a potential conflict of interest.

frontiers in Endocrinology

REVIEW
published: 22 May 2019
doi: 10.3389/fendo.2019.00330

The MAPK Pathway-Based Drug Therapeutic Targets in Pituitary Adenomas

Miaolong Lu[1,2,3], *Ya Wang*[1,2,3] *and Xianquan Zhan*[1,2,3,4]*

[1] Key Laboratory of Cancer Proteomics of Chinese Ministry of Health, Xiangya Hospital, Central South University, Changsha, China, [2] Hunan Engineering Laboratory for Structural Biology and Drug Design, Xiangya Hospital, Central South University, Changsha, China, [3] State Local Joint Engineering Laboratory for Anticancer Drugs, Xiangya Hospital, Central South University, Changsha, China, [4] National Clinical Research Center for Geriatric Disorders, Xiangya Hospital, Central South University, Changsha, China

Mitogen-activated protein kinases (MAPKs) include ERK, p38, and JNK MAPK subfamilies, which are crucial regulators of cellular physiology, cell pathology, and many diseases including cancers. For the MAPK signaling system in pituitary adenomas (PAs), the activation of ERK signaling is generally thought to promote cell proliferation and growth; whereas the activations of p38 and JNK signaling are generally thought to promote cell apoptosis. The role of MAPK in treatment of PAs is demonstrated through the effects of currently used medications such as somatostatin analogs such as SOM230 and OCT, dopamine agonists such as cabergoline and bromocriptine, and retinoic acid which inhibit the MAPK pathway. Further, there are potential novel therapies based on putative molecular targets of the MAPK pathway, including 18beta-glycyrrhetinic acid (GA), dopamine-somatostatin chimeric compound (BIM-23A760), ursolic acid (UA), fulvestrant, Raf kinase inhibitory protein (RKIP), epidermal growth factor pathway substrate number 8 (Eps8), transmembrane protein with EGF-like and two follistatin-like domains (TMEFF2), cold inducible RNA-binding protein (CIRP), miR-16, and mammaliansterile-20-like kinase (MST4). The combined use of ERK inhibitor (e.g., SOM230, OCT, or dopamine) plus p38 activator (e.g., cabergoline, bromocriptine, and fulvestrant) and/or JNK activator (e.g., UA), or the development of single drug (e.g., BIM-23A760) to target both ERK and p38 or JNK pathways, might produce better anti-tumor effects on PAs. This article reviews the advances in understanding the role of MAPK signaling in pituitary tumorigenesis, and the MAPK pathway-based potential therapeutic drugs for PAs.

Keywords: MAPK, ERK, p38, JNK, signaling pathway, pituitary tumor, biomarker, therapeutic drug

OPEN ACCESS

Edited by:
Hidenori Fukuoka, Kobe University, Japan

Reviewed by:
Odelia Cooper, Cedars-Sinai Medical Center, United States
Sergei I. Bannykh, Cedars-Sinai Medical Center, United States
Zhousheng Xiao, The University of Tennessee Health Science Center, United States

***Correspondence:**
Xianquan Zhan
yjzhan2011@gmail.com.

Specialty section:
This article was submitted to Pituitary Endocrinology, a section of the journal Frontiers in Endocrinology

Received: *08 January 2019*
Accepted: *07 May 2019*
Published: *22 May 2019*

Citation:
Lu M, Wang Y and Zhan X (2019) The MAPK Pathway-Based Drug Therapeutic Targets in Pituitary Adenomas. Front. Endocrinol. 10:330. doi: 10.3389/fendo.2019.00330

INTRODUCTION

Pituitary adenomas (PAs) are commonly benign tumors, accounting for about ten percent of intracranial tumors (1, 2), and are clinically divided into functioning PAs (FPAs) and non-functioning PAs (NFPAs) (3, 4). It can cause significant morbidity and mortality (5). The molecular mechanisms in tumorigenesis and functional regulation of PAs have been extensively studied. This review article focuses on the roles of mitogen-activated protein kinase (MAPK) in PA tumorigenesis and the MAPK pathway-based potential therapeutic targets for PAs. MAPKs mainly include three

subfamilies based on the conserved Thr-Xaa-Tyr motif signature: ERK1/2, p38, and JNK (Jun N-terminal kinase) (6), which are activated by multiple factors such as growth factors and stress. The activation of ERK promotes cell proliferation; whereas, the activations of p38 and JNK promote cell apoptosis. Studies demonstrate that MAPKs are involved in multiple cellular processes, such as cell differentiation, proliferation, apoptosis, inflammation, stress responses, and immune defense (7–9).

The MAPK signaling pathways play important roles in cell dissemination, survival, and drug resistance of human cancers including PAs (2, 10–12). With the in-depth studies of the MAPK signaling pathway network, MAPK pathways-based target-specific drugs have been developed, and some drugs has been used for clinical trials; and the relevance of MAPK in response and resistance to antitumor drugs has also been recognized (**Figure 1** and **Table 1**). Because of the important roles of MAPK signaling pathways in tumorigenesis, the use of the MAPK signaling pathways as therapeutic targets has continuously been considered as a promising strategy for cancer therapy. This review highlights new advances in the role of MAPK signaling in pituitary tumorigenesis and development, the key molecules in this pathway network, and anti-pituitary tumor drugs targeting MAPK signaling pathway.

THE ERK PATHWAY IN PAs

The ERK/MAPK pathway delivers signals from cellular surface receptors via ERK pathway. Briefly, different cellular surface receptors such as EGFR, GPCR, and RKT are activated by the corresponding extracellular factors (e.g., growth factors, hormones, and stresses) to activate Ras and small GTPase. The activated Ras-small GTPase complex recruits Raf kinase to the cell membrane and activates it. Then, Raf activates MEK (MAPK and ERK kinase) through phosphorylation. The phosphorylated MEK subsequently activates ERK through phosphorylation (35) (**Figure 1**). Rafs include Raf-1, A-Raf, and B-Raf. Raf-1 can bind to the pro-apoptotic kinases, such as mammalian sterile-twenty-like-2 (MST2) and apoptosis signal-regulating kinase (ASK1), to involve in cell apoptosis (36). Raf-1 also exerts scaffolding function in regulation of the Rho pathway (37). Typically, cytokines and growth factors binding to TKR activate ERK1/2, which transduces the signals into its upstream Ras/Raf/MEK pathway. In PAs, H-Ras mutations have been identified in two cases of prolactinomas, which indicates that Ras/ERK takes part in regulation of PAs (38, 39). Overexpression of B-Raf is predominantly observed in NFPAs (40). The downstream kinases of B-Raf in ERK MAPK pathway are also over-activated in NFPAs, growth hormone (GH)-secreting PAs, ACTH-secreting PAs, and prolactinomas. The phosphorylation levels at pSer217/221 of MEK 1/2 and pThr183 of ERK1/2 are significantly increased in these PAs compared to controls (41), which indicates that Raf/MEK/ERK pathway acts as a pro-proliferative role in PAs.

Abbreviations: ACTH, Adrenocorticotropin; CIRP, Cold inducible RNA binding protein; CRH, Corticotropin-releasing hormone; CSAIDs, Cytokine-suppressive anti-inflammatory drugs; Eps8, Epidermal growth factor pathway substrate number 8; ERK, Extracellular signal-related kinase; GA, 18beta-glycyrrhetinic acid; GH, Growth hormone; GnRH, gonadotropin-releaseing hormone; GPCR, G protein-coupled receptor; IGF1, Insulin-like growth factor 1; JNK, Jun N-terminal kinase; LPS, Lipopolysaccharide; MAPKs, Mitogen-activated protein kinases; MKK, MAPK kinases; MKKK, MAPK kinase kinases; MKPs, MAPK phosphatases; MST4, Mammalian sterile-20-like kinase; PRL, Prolactin; RA, Retinoic acid; RKIP, Raf kinase inhibitory protein; RTK, Receptor tyrosine kinase; SAPKs, Stress-activated protein kinases; SSTs, Somatostatin analogs; SST, Somatostatin; TSH, Thyroid-stimulating hormone.

The Effects of ERK MAPK on Different-Origin PAs

The effect of ERK signaling on PAs depends on the PA subtypes. (i) In lactotroph cells, the ERK signaling exerts different effect on cell proliferation based on the exposure time. Short-time activation of the ERK (24–96 h) leads to increased proliferation in rat pituitary lactotroph or somatolactotroph cell lines *in vitro* (42, 43). However, long-time activation of ERK (over 6 days) promotes somatolactotroph cell differentiation into a lactotroph cell phenotype, and then decreases proliferation and tumorigenicity with time (44). Thus, persistent activation of ERK signaling produces anti-proliferative and anti-tumorigenic effects in somatolactotroph cells. (ii) In somatotroph cells, ERK signaling produces pro-proliferative effects. Protein kinase A (PKA) and C (PKC) pathways regulate ERK signaling. PKA pathway activates ERK signaling, and leads to improved proliferation in GH-secreting cells. PKC stimulates ERK signaling and increases cell proliferation through regulating GH-releasing hormone (GHRH) (45). ERK pathway is necessary for somatotrophs to produce GH. In somatotroph PAs, GH-releasing hormone (GHRH) can promote cell proliferation through activating ERK signaling (46). In addition to regulation of cell proliferation, ERK signaling also contributes to GH secretion by somatotrophs (47). Somatostatin (SST) analogs are used in clinical treatment of GH-secreting PAs due to its anti-proliferative effect on somatotroph cells. SST treatment results in a reduction of pERK1/2 expression and a significant increase in p27 protein expression. In addition, cell proliferation is driven by cell cycle which is regulated by a series of cyclins and cyclin dependent kinases (CDKs). A cyclin-dependent kinase (CDK) inhibitor has a negative effect on cell-cycle progression which has a synergistic effect with SST analogs (13). (iii) In gonadotroph cells, gonadotropin-releasing hormone (GnRH) can activate ERK, p38, and JNK signaling in the LβT2 gonadotroph cell lines to contribute to production of luteinizing hormone (LH), and GnRH phosphorylated ERK via PKC-dependent pathways (48). Most of NFPAs originate from gonadotroph cells where B-Raf is upregulated and ERK is over-activated relative to control pituitary tissues (40, 49). (iv) In thyrotroph cells, ERK cascade has anti-proliferative effects. The ERK pathway is activated to cause growth arrest after thyrotroph adenomas are treated with thyroid hormone (50). And (v) In corticotroph cells, ERK signaling is activated to produce pro-proliferative effects (51).

ERK MAPK Pathway-Targeted Pharmacological Treatments of PAs

Somatostatin (SST) Analogs Treatment

SST inhibits cell growth, through G protein-coupled receptors to inhibit the release of growth factors and angiogenesis, and increases apoptosis. The majority of NFPAs express SST receptors on cell membranes. An appropriate concentration of

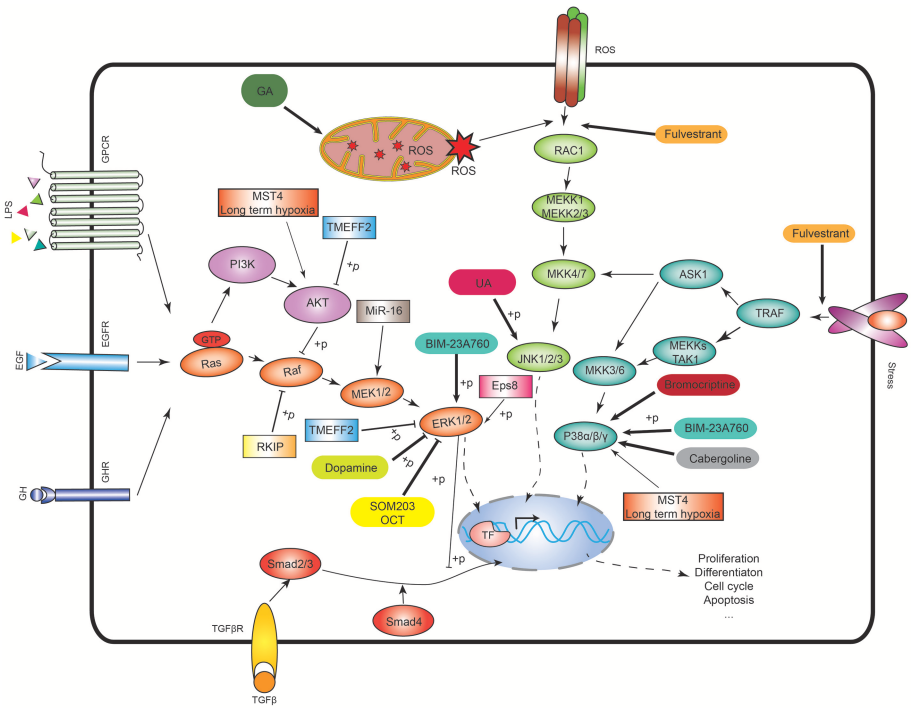

FIGURE 1 | MAPK signaling pathways and the potential therapeutic targets. In the ERK signaling, Ras activates the serine/threonine protein kinase Raf to activate MEK1/2, then MEK1/2 phosphorylates the ERK1/2. In p38 signaling, TNF receptor-associated factor (TRAF) activates ASK1, TAK1, or MEKK1, which activates MKK3/6, and then MKK3/6 phosphorylates p38 isoforms. In JNK signaling, RAC1 activates MEKK1 or MEKK2/3 to activate MKK4/7, and then MKK4/7 phosphorylates JNK1/2/3. The ASK1 in the p38 signaling also activates MKK4/7 to crosstalk with JNK signaling. ROS means reactive oxygen species. GA means 18beta-glycyrrhetinic acid. BIM-23A760 is a dopamine–somatostatin chimeric compound. OCT means octreotide. SOM230 and OCT are somatostatin analogs. Rectangle means the potential drug targets.

SST analogs (octreotide or SOM230) can inhibit the release of GH, prolactin (PRL), and their α-subunit in GH-secreting PAs, PRL-secreting PAs, ACTH-secreting PAs, and NFPAs, respectively (14–18). Their anti-tumor effects are in that SST analogs can inactivate ERK signaling pathways; for example, octreotide acts on both ERK and PI3K/Akt signaling pathways, and SOM230 acts on ERK signaling pathway (13, 52). Octreotide can bind to and activate SST receptor subtype-2 (SSTR2) and SSTR5, while pasireotide (SOM230) can activate SSTR1, 2, 3, and 5 (53, 54). A study shows that octreotide or SOM230 reduces cell proliferation and pERK1/2 expression in rat somatotroph cell line GH3 (13). Octreotide also blocks the transient G0/G1 cell cycle to produce a cytostatic effect on GH3 cell proliferation (55). SST analogs (octreotide and pasireotide) also decrease secretion of LH induced by GnRH in LβT2 cells (19), and inhibit NFPA cell viability *in vitro* (56–59). The SST analogs are the primary medical therapy to treat acromegaly for maintenance of GH homeostasis and shrinkage of tumor size (60–62). Moreover, octreotide and lanreotide bind with high affinity to SSTR2, and with low affinity to SSTR3 and SSTR5. The decreased expression of SSTR2 in tumor is associated with lack of response to SST analogs (63, 64). Some studies demonstrate that SST analogs exert their anti-proliferative effects on somatotroph cells through inhibition of ERK signaling (13).

Dopamine and Dopamine Agonists Treatment

Hypothalamic dopamine suppresses the production of pituitary PRL (65). Dopamine acts via the D2 receptor to inhibit cAMP/PKA and MAPK signaling pathways to control PRL-secretion and lactotroph proliferation (20). Dopamine agonists such as bromocriptine (BRC) and cabergoline (CAB) are primary medical therapy drugs for prolactinomas and idiopathic hyperprolactinemia and prolactinomas (66). Dopamine agonists target the dopamine D2 receptor (D2R) subtype to exert its anti-tumor effects. D2R-activated ERK signaling cascades inhibit the synthesis and release of PRL in the pituitary. D2R includes D2L and D2S isoforms. Overexpression of D2L elevates PRL, and overexpression of D2S reduces PRL. The ratio of D2L to D2S affects PRL-secretion of lactotroph cells (67). A study shows that when pituitary tumor cells are treated with dopamine, D2S activation stimulates ERK signaling to inhibit lactotroph cell proliferation (68).

TGFβ Treatment

TGFβ is widely considered to be a tumor suppressor (69). However, TGFβ1 produces weak growth inhibitory effect on pituitary tumor cells. TGFβ mainly uses Smad signaling pathway to convey signals from cytosol to nucleus to regulate expression of genes that control cell cycle progression (70). In addition, TGFβ

TABLE 1 | Drugs or molecules involved in MAPK signaling pathway in PAs.

Drugs or molecules involved in MAPK signaling pathway			Tumor subtype	Molecular mechanism	Biological effect	Research models	References
Therapeutic drugs	Somatostatin analogs (SSTs)	SOM230 (FDA approved)	GH-secreting PAs	SOM230 combines with somatostatin receptor subtype 2 (SSTR2) and inhibits ERK pathway	Inhibits GH release and proliferation of tumor cells	Primary GH-secreting adenoma cells, and rat pituitary cell line (GH3)	(13–15)
			PRL-secreting PAs	SOM230 combines with SSTR5 and inhibits ERK pathway	Inhibits PRL release and proliferation of tumor cells	Primary PRL-secreting adenoma cells, and rat pituitary cell line (GH3)	(13–15)
			Corticotropin-secreting PAs	SOM230 binds to SSTR5 not SSTR2 to inhibit ERK pathway	Suppresses CRH-induced ACTH release and decreases urinary free cortisol (UFC), and serum cortisol	AtT20/D16V mouse tumor cells, and pituitary dependent Cushing's disease patients	(16–18)
			Gonadotroph PAs	Suppresses the phosphorylation of ERK	Reduces GnRH-induced LH secretion	Mouse gonadotroph LβT2 cells	(19)
		Octreotide (OCT) (FDA approved)	GH-secreting PAs	OCT combines with SSTR2 and inhibits ERK pathway	Inhibits GH-release and proliferation of tumor cells	Primary GH-secreting adenoma cells, and rat pituitary cell line (GH3)	(13–15)
			Gonadotroph PAs	Suppresses the phosphorylation of ERK	Reduces GnRH-induced LH secretion	Mouse gonadotroph LβT2 cells	(19)
	Dopamine and Dopamine agonists	Dopamine	PRL-secreting PAs	Suppresses the phosphorylation of ERK1/2	Reduces PRL secretion	PRL-secreting cells (GH4ZR7), and primary pituitary cells	(20)
		Bromocriptine (BRC) (FDA approved)	PRL secreting pituitary adenoma	Activates p38 MAPK	Increases GH3 cell apoptosis	Rat pituitary cell line (GH3)	(21)
		Cabergoline (CAB) (FDA approved)	PRL secreting pituitary adenoma	Activates p38 MAPK	Increases GH3 cell apoptosis	PRL-D2S cells	(22)
	TGFβ		Lactosomatotroph PAs	Cross-talks with ERK pathway	Decreases the cell proliferation	Rat lactosomatotroph pituitary adenoma cells (GH3B6)	(23)
	18beta-glycyrrhetinic acid (GA)		GH-secreting PAs	Activates mitochondria-mediated ROS, JNK and P38 pathways	G0/G1 phase arrest and increases apoptosis rate	Rat pituitary adenoma-derived MMQ and GH3 cells	(24)
			PRL-secreting PAs				
	The dopamine–somatostatin chimeric compound	BIM-23A760	NFPAs	Activates ERK1/2 and p38 pathways	Inhibits cell proliferation and induces apoptosis	Primary NFPA cells	(25)
	Ursolic Acid (UA)		ACTH-secreting PAs	Upregulates JNK phosphorylation and increases the degradation of Bcl-2	Induces apoptosis of AtT20 cells and decreases ACTH secretion	AtT20 pituitary corticotroph cell line	(26)
	Fulvestrant		GH-secreting PAs	Activates PTEN/MAPK signaling pathways	Increases apoptotic cell death	Rat pituitary cell line (GH3)	(27)
			PRL-secreting PAs				
Potential targets	Raf kinase inhibitory protein (RKIP)		Somatotroph PAs	Non-phosphorylated RKIP binds to and inhibits Raf1 kinase and attenuates MAPK signaling	Low levels of RKIP correlate to poor clinical response to SSTs	Patients with active acromegaly	(28)

(Continued)

TABLE 1 | Continued

Drugs or molecules involved in MAPK signaling pathway	Tumor subtype	Molecular mechanism	Biological effect	Research models	References
Epidermal growth factor pathway substrate number 8 (Eps8)	Gonadotroph PAs	Increases phosphorylated ERK	Promotes proliferation and cell survival	Mouse gonadotroph LβT2 cells	(29, 30)
TMEFF2 (transmembrane protein with EGF-like and two follistatin-likedomains)	Corticotroph PAs	Inhibits phosphorylation of AKT and ERK1/2	Decreases proliferation of corticotrope cells and reduces secretion of ACTH	AtT20 pituitary corticotrope tumor cells GH3 pituitary lactosomatotroph tumor cells	(31)
Cold inducible RNA-binding protein (CIRP)	Corticotroph PAs	Induces cyclinD1 and decreases p27 expression via Erk1/2 signaling pathway	Promotes cells proliferation and tumor recurrence	AtT20 pituitary corticotroph cell line	(32)
MiR-16	Non-functional PAs	Inhibits ERK/MAPK pathway activty via the suppression of MEK1 expression	Inhibits cell proliferation and induces apoptosis and cell-cycle arrest	Human HP75 tumor cells	(33)
Mammalian sterile-20-like kinase (MST4)	Gonadotroph PAs	Activates p38 MAPK and AKT during long-term hypoxia	Increases colony formation and accelerates cell proliferation	Mouse gonadotroph LβT2 cells	(34)

PAs, pituitary adenomas. NFPAs, Non-functional pituitary adenomas.

can also use non-Smad signaling pathway to convey signals, such as MAPK pathway (71). TGFβ1 treatment decreases pituitary tumor cell proliferation, and this inhibitory effect is amplified by MEK inhibitors, because TGFβ1/Smad pathway cross-talks with MEK/ERK1/2 pathway (23). It clearly demonstrates that inhibition of MEK/ERK1/2 pathway synergizes with TGFβ1 to inhibit pituitary tumor cell proliferation.

Potential Targets Related to ERK MAPK Signaling Pathway for PA Treatment

Components and regulators of the ERK MAPK pathway are all potential targets for treating pituitary tumors. (i) Raf kinase inhibitory protein (RKIP). RKIP is a modulator of MAPK signaling, which inhibits Raf-1 phosphorylation to inhibit Ras/Raf-1/MEK/ERK signaling pathway (72–74). RKIP interferes with Raf-1 in several mechanisms. One is that Raf-1 binding to RKIP causes the conformational change of Raf-1 (75). Another is that RKIP inhibits phosphorylation of MAPK-MEK-1 to interfere with the interaction between two kinases (76). Moreover, protein kinase C (PKC) can negatively regulate the roles of RKIP because PKC phosphorylates RKIP to cause the separation of RKIP from Raf-1 (73). Studies demonstrate that the low expression level of RKIP in GH-secreting adenomas is correlated with less GH and IGF-1 reduction with SST analog therapy because RKIP can inhibit the phosphorylation of Raf1 kinase to attenuate the activity of MAPK signaling pathway (28).

(ii) Epidermal growth factor pathway substrate number 8 (Eps8). Over-expression of Eps8 and over-activation of Raf, MEK, and ERK in the ERK signaling pathway promote cell proliferation and survival in PAs (41). Also, Eps8 is a substrate of receptor tyrosine kinases (RTKs) in the ERK signaling pathway (**Figure 1**), which can enhance EGF-dependent mitogenic signaling (29). Eps8 expression is significantly higher in human gonadotroph adenomas relative to controls. Upregulation of EGFR protein and phosphorylation of ERK are demonstrated in Eps8-overexpressing LβT2 cells. EGF ligand stimulation leads to increased proliferation in Eps8-overexpressing LβT2 cells. MAPK kinase inhibitor (PD98059) can abrogate the proliferative effects. Silence of Eps8 also inhibits cell proliferation, which suggests that Eps8 promotes pituitary tumor cell proliferation through enhancing the Raf/MEK/ERK signaling (30). Therefore, Eps8 is a potential drug target for PA treatment.

(iii) Retinoic acid (RA). RA has antiproliferative effect in corticotroph cell, and long-term treatment with RA has some clinical efficacy in patients with Cushing's disease (77). The mechanism of RA anti-tumor effects is shown with the expression of TMEFF2 (transmembrane protein with EGF-like and two follistatin-likedomains) that inhibits phosphorylation of AKT and ERK1/2 (31). TMEFF2 is significantly downregulated in corticotropinomas relative to control tissues, which suggests that TMEFF2 might be a tumor suppressor. Silence of TMEFF2 in pituitary corticotroph cell line AtT20 promotes cell proliferation, while over-expression of TMEFF2 inhibits cell proliferation (31). Thus, TMEFF2 is a potential therapeutic target for ACTH-secreting adenomas.

(iv) Cold inducible RNA binding protein (CIRP). The underlying mechanism of cold-shock protein (CIRP) in its role in tumorigenesis is through its induction of cyclinD1 which decreases p27 expression via ERK1/2 signaling (32, 78). CIRP is significantly upregulated at the mRNA and protein levels in multiple cancers (79, 80), including human corticotroph adenomas relative to normal pituitary tissues. CIRP over-expression is associated with recurrence of corticotroph adenomas in murine models (32). CIRP-overexpressing AtT20 cells have increased cell proliferative abilities. Tumor xenografts generated by CIRP-overexpressed AtT20 cells are significantly larger than AtT20 cells with normal level of CIRP expression.

THE P38 PATHWAY IN PAs

The p38 MAPK includes isoforms p38α, p38β, p38γ, and p38δ, with ∼60% of sequence similarity among four isoforms (81). Of these, p38α (MAPK14) and p38β (MAPK11) are highly expressed in various tissues, p38γ (MAPK12/ERK6) in muscle, and p38δ (MAPK13/SAPK4) in lung and kidney (34, 82). The p38 MAPK plays vital roles in cell responses to stimulators, including proinflammatory cytokines and environmental stresses such as ultraviolet irradiation and heat shock; and is involved in cellular differentiation, cell migration, and inflammation. Activation of p38 kinases are due to phosphorylations at Thr180 and Tyr182 within Thr-Gly-Try motif (83). This canonical phosphorylation is regulated by MKK3 and MKK6, which are highly selective for p38 MAPKs (84–86) (**Figure 1**). There exist a large body of substrates of p38 MAPKs both in cytoplasm and nucleus, such as transcription factors (p53, MEF2, CHOP, and ATF2), and other protein kinases (MNK1/MNK2, and MSK1/MSK2) which in turn phosphorylate other important proteins (Hsp27, and eIF-4E) (81). In PAs, p38 MAPK plays an important role in immune escape. Tumor immune escape means that tumor cells escape from the body's immune system recognition and attacking to survive and proliferate in the body. When tumor cells appear in the healthy body, the body's immune surveillance system can recognize and specifically remove these "non-self" tumor cells through natural and acquired immunity to prevent the development of tumors (87). However, in some cases, malignant cells can escape the immune surveillance of the body through various mechanisms to rapidly proliferate and form tumors. Studies demonstrate that phosphorylated p38 stimulates the expression of matrix metalloproteinase 9 (MMP9), which is involved in accelerating the process of tumor immune escape (88). In addition, studies based on murine gonadotroph cells LβT2 reveal that mammalian sterile-20-like kinase (MST4) is upregulated in the levels of mRNA and protein to promote cell proliferation by activating p38 MAPK and AKT during long-term hypoxia (89).

PA Treatment Related to p38 MAPK Signaling

Previous studies demonstrate that p38 MAPK is associated with apoptosis, and drugs that activate this pathway can thereby induce apoptosis in pituitary tumor cells. A study found that dopamine agonists such as BRC and CAB activate p38 pathway to induce cell apoptosis; for example, when BRC is used to treat rat lactosomatotroph GH3 cells, BRC activates p38 MAPK and promotes cell apoptosis. Moreover, p38 MAPK inhibitors (SB202190, SB203580) completely inhibit BRC-induced p38 MAPK activation and cell apoptosis (21). Similarly, CAB also activates p38 MAPK and induces apoptosis in PRL-D2S cells (22). In addition to dopamine agonists, the natural compound 18beta-glycyrrhetinic acid (GA) extracted from liquorice can induce several types of tumor cell apoptosis (24, 90). In rat PA cells MMQ and GH3, GA can induce cellular damage, decrease cell viability, and cause G0/G1 phase arrest to contribute to cell apoptosis (91). GA can enhance the phosphorylation of JNK and p38, and these effects are abrogated through pretreatment with JNK inhibitor (SP60125) or p38 inhibitor (SB203580). Furthermore, the fact that ROS inhibitor (NAC) abolished the activation of JNK and P38 suggests that GA exerts the anti-PA effects by activating ROS/MAPKs (JNK and P38)-dependent pathway (91). BIM-23A760, a dopamine-somatostatin chimeric compound, by activating p38 and ERK1/2, inhibits cell proliferation and demonstrates cytotoxic effects in primary culture of NFPAs (25).

Potential Targets Related to p38 MAPK Signaling Pathway for PA Treatment

In recent years, with the development of next-generation sequencing (NGS), a large number of non-coding RNAs have been identified (92, 93). Non-coding RNAs not only deepen our understanding of tumorigenesis and development, but also provide new directions for the diagnosis and treatment of tumors. Studies demonstrate that microRNA-16 (miR-16) is significantly downregulated in PAs compared to the healthy controls, and overexpression of miR-16 reduces the protein expressions of phosphorylated p38, VEGFR2, MMP-9, and NF-kB in HP75 cells, which suggests that miR-16 is involved in PA cell proliferation and angiogenesis via VEGFR2/p38/NF-κB pathway (94). Studies show that miR-16 suppresses MEK1 expressions thereby inhibiting ERK/MAPK pathway activity, leading to inhibition of cell proliferation, cell-cycle arrest, and apoptosis in PAs (33). Therefore, miR-16, as a regulator of p38 MAPK, might be a diagnostic biomarker and a target of PAs. In addition, based on miR-6-related studies, miR-6-protein and/or miR-6-lncRNA interactions are also worth further exploring for discovery of potential therapeutic targets. Further, MST4 promotes cell proliferation by activating p38 MAPK under long-term hypoxia. Therefore, MST4 might be a target for PA treatment (34).

THE JNK MAPK PATHWAY IN PAs

The JNK MAPK pathway is mainly activated by various stress stimuli, including oxidative stress, UV irradiation, osmotic shock, heat shock, and proinflammatory cytokines (95), and plays vital roles in controlling proliferation, cell growth, apoptosis, inflammatory, and immune responses (96–98). JNK includes three isoforms: JNK1 and JNK2 are extensively distributed in different tissues, and JNK3 is mainly expressed in testis, heart, and brain (99, 100). JNK is activated by a cascade reaction: stress signals are delivered by small GTPases (Rac, Rho, and cdc42)

to a series of kinase cascades, and eventually MKK4/7 activates JNKs (101). In addition, MKK4/7 can also be activated by a member of the germinal center kinase (GCK) family to activate JNKs (95). Moreover, MKK4 might also activate p38 MAPKs (p38α and p38δ), which lets JNK pathway cross-talk with p38 MAPK pathway (34). The activated JNKs are translocated from cytoplasm to nucleus where it can regulate the activity of multiple transcription factors (ATF-2, Elk-1, Smad4, p53, NFAT4, and Stat3) (102).

JNK pathway has been reported to be involved in many kinds of cancers, including retinoblastoma, melanoma, colorectal cancer, breast cancer, and ovarian cancer; and these cancers exhibit the elevated JNK activities (103–107). While there are limited studies on the role of the JNK pathway in the initiation and progression of pituitary tumors, several studies have demonstrated that alteration of JNK in the pituitary gland could be associated with pituitary tumoregensis. For instance, mice with a conditionally inactivated JNK1 in nestin-expressed cells ($JNK1^{\Delta NES}$) are used to study the effects of JNK1 signaling on glucose metabolism. Unexpectedly, the decreased somatic growth and increased thyroid axis activities are observed in $JNK1^{\Delta NES}$ mice with decreased levels of circulating GH and IGF1 (108). Another study shows that ablation of Jnk genes in anterior pituitary gland of mice leads to increased energy expenditure, and decreased obesity compared to control mice; and pituitary thyroid-stimulating hormone (TSH) and blood thyroid hormone (T4) are increased (109). Thus, JNK signaling might be involved in pituitary tumorigenesis (110).

JNK MAPK Pathway-Targeted Pharmacological Treatments of PAs

The first one is ursolic acid (UA), a triterpenoid compound found in food, medical herbs, and other plants (111), which has antitumor effects in a number of tumors such as hepatocellular carcinoma, melanoma, breast cancer, colorectal cancer, bladder cancer, and prostate cancer (112–117). In the treatment of PAs, UA decreases cell viability and induces apoptosis in AtT20 cells by upregulating JNK phosphorylation. JNK signaling can also cross-talk with UA-induced mitochondrial apoptotic signaling transduction through phosphorylation and degradation of Bcl-2 (26). Moreover, GA, as described above, can induce cellular cytotoxicity and apoptosis by enhancing the phosphorylation of JNK. With further research progress, it is strongly believed that more drugs will be developed to target JNK MAPK pathway.

THE MAPK PATHWAY NETWORK IN PAs

ERK, p38, and JNK signaling pathways both independently and concordantly contribute to pituitary tumorigenesis. Thus, some chemotherapeutic drugs for PAs may target several subfamilies of the MAPK signaling pathway at the same time. For example, fulvestrant is an estrogen receptor antagonist without agonist effects (118), which is approved in the EU and USA to treat post-menopausal women who have hormone-sensitive advanced breast cancer, after prior antiestrogen therapy (119). In the treatment of PAs, recent studies reveal that fulvestrant significantly suppresses the cell viability and invasion of rat PA GH3 cells by simultaneous regulation of ERK1/2, JNK1/2, and p38 signaling pathways (27). GA exerts anti-tumor effects against PAs through enhancing the activations of JNK and p38 MAPK signaling pathways (91). BIM-23A76 that is a dopamine-somatostatin chimeric compound demonstrates the function of inhibiting cell proliferative and cytotoxic effects by activating p38 and ERK1/2 (25).

The comprehensive pathway-network analysis of multiple sets of proteomic data in PAs (120–124) reveals that MAPK signaling abnormalities, including ERK-MAPK signaling pathway, are significantly associated with PAs (125), and that some important molecules such as ERK, p38, JNK, Ras, Akt, NF-kB, TNF, and TGFb1 in MAPK signaling pathway network are identified in human PAs. In addition, the regulatory effect of MAPK cascades on cell differentiation, proliferation, survival and apoptosis interact with other transduction pathways (126). For instance, both PI3K-Akt and Raf/MEK/ERK pathways synergistically promote cell proliferation at the initial stage of PAs (127). Another study demonstrates the critical role of ERK1/2 and cAMP in determination of tumoural phenotype in PAs (128). Thus, a combination of drugs that target pathways which cross-talk with MAPK signaling may produce a more effective treatment for PAs.

In the MAPK network system in PAs, the activation of ERK is generally thought to promote cell proliferation and growth; whereas the activations of p38 and JNK are generally thought to promote cell apoptosis. The MAPK signaling pathway can be targeted by several mechanisms. Two types of combination strategies can be used: (i) A single drug to target ERK pathway and p38 or JNK pathway. For example, BIM-23A76 inhibits cell proliferation through targeting ERK1/2 pathway, and promotes cytotoxic effects through targeting p38 pathway (25). And (ii) multiple drugs to target different ERK and p38 or JNK pathways, such as ERK inhibitor (e.g., SOM230, OCT, or dopamine) plus p38 activator (e.g., cabergoline, bromocriptine, and fulvestrant) and/or JNK activator (e.g., UA). Also, fulvestrant can target both p38 and JNK pathways to promote the cell apoptosis for cell cytotoxic effects. These MAPK pathway-based combination therapies might produce better anti-cancer effects on PAs.

CONCLUSION

This review summarized the studies of MAPK signaling in pituitary tumorigenesis. We discussed some important molecules involving in MAPK signaling pathway and potential drugs targeting the MAPK signaling (**Figure 1** and **Table 1**). The ERK-MAPK signaling, p38-MAPK signaling, and JNK signaling all play important roles in PAs. Some therapeutic drugs exert anti-tumor effects by targeting one of these pathways or all these three pathways at the same time. MAPK signaling is a very complex network, and always interacts with other pathways such as PI3K and cAMP pathway to affect tumor progression. The latest development of MAPK signaling in PAs and the related anti-tumor drugs targeting MAPK signaling pathways would provide

new insights on PA pathogenic mechanisms and pre-clinical data for treatment.

AUTHOR CONTRIBUTIONS

ML and YW collected and analyzed literature, prepared figures and tables, and wrote and revised manuscript. XZ conceived the concept, designed, coordinated, wrote and critically revised manuscript, and was responsible for its financial supports and the corresponding works. All authors approved the final manuscript.

FUNDING

This work was supported by the grants from the China 863 plan Project (Grant No. 2014AA020610-1 to XZ), National Natural Science Foundation of China (Grant No. 81572278 and 81272798 to XZ), the Hunan Provincial Hundred Talent Plan (to XZ), the Xiangya Hospital Funds for Talent Introduction (to XZ), and the Hunan Provincial Natural Science Foundation of China (Grant No. 14JJ7008 to XZ).

REFERENCES

1. Asa SL, Ezzat S. The pathogenesis of pituitary tumours. *Nat Rev Cancer.* (2002) 2:836–49. doi: 10.1038/nrc926
2. Zhan X, Wang X, Cheng T. Human pituitary adenoma proteomics: new progresses and perspectives. *Front Endocrinol.* (2016) 7:54. doi: 10.3389/fendo.2016.00054
3. Asa SL, Kovacs K. Clinically non-functioning human pituitary adenomas. *Can J Neurol Sci.* (1992) 19:228–35.
4. Zhan X, Desiderio DM, Wang X, Zhan X, Guo T, Li M, et al. Identification of the proteomic variations of invasive relative to non-invasive non-functional pituitary adenomas. *Electrophoresis.* (2014) 35:2184–94. doi: 10.1002/elps.201300590
5. Herman V, Fagin J, Gonsky R, Kovacs K, Melmed S. Clonal origin of pituitary adenomas. *J Clin Endocrinol Metab.* (1990) 71:1427–33. doi: 10.1210/jcem-71-6-1427
6. Su B, Karin M. Mitogen-activated protein kinase cascades and regulation of gene expression. *Curr Opin Immunol.* (1996) 8:402–11. doi: 10.1016/S0952-7915(96)80131-2
7. Boutros T, Chevet E, Metrakos P. Mitogen-activated protein (MAP) kinase/MAP kinase phosphatase regulation: roles in cell growth, death, and cancer. *Pharmacol Rev.* (2008) 60:261–310. doi: 10.1124/pr.107.00106
8. Duan W, Wong WS. Targeting mitogen-activated protein kinases for asthma. *Curr Drug Targets.* (2006) 7:691–8. doi: 10.2174/138945006777435353
9. Jeffrey KL, Camps M, Rommel C, Mackay CR. Targeting dual-specificity phosphatases: manipulating MAP kinase signalling and immune responses. *Nat Rev Drug Discov.* (2007) 6:391–403. doi: 10.1038/nrd2289
10. De Luca A, Maiello MR, D'Alessio A, Pergameno M, Normanno N. The RAS/RAF/MEK/ERK and the PI3K/AKT signalling pathways: role in cancer pathogenesis and implications for therapeutic approaches. *Expert Opin Ther Targets.* (2012) 16(Suppl. 2):S17–27. doi: 10.1517/14728222.2011.639361
11. Zhan X, Wang X, Long Y, Desiderio DM. Heterogeneity analysis of the proteomes in clinically nonfunctional pituitary adenomas. *BMC Med Genomics.* (2014) 7:69. doi: 10.1186/s12920-014-0069-6
12. Zhan X, Long Y. Exploration of Molecular network variations in different subtypes of human non-functional pituitary adenomas. *Front Endocrinol.* (2016) 7:13. doi: 10.3389/fendo.2016.00013
13. Hubina E, Nanzer AM, Hanson MR, Ciccarelli E, Losa M, Gaia D, et al. Somatostatin analogues stimulate p27 expression and inhibit the MAP kinase pathway in pituitary tumours. *Eur J Endocrinol.* (2006) 155:371–9. doi: 10.1530/eje.1.02213
14. Murray RD, Kim K, Ren SG, Lewis I, Weckbecker G, Bruns C, et al. The novel somatostatin ligand (SOM230) regulates human and rat anterior pituitary hormone secretion. *J Clin Endocrinol Metab.* (2004) 89:3027–32. doi: 10.1210/jc.2003-031319
15. Hofland LJ, van der Hoek J, van Koetsveld PM, de Herder WW, Waaijers M, Sprij-Mooij D, et al. The novel somatostatin analog SOM230 is a potent inhibitor of hormone release by growth hormone- and prolactin-secreting pituitary adenomas *in vitro*. *J Clin Endocrinol Metab.* (2004) 89:1577–85. doi: 10.1210/jc.2003-031344
16. van der Hoek J, Waaijers M, van Koetsveld PM, Sprij-Mooij D, Feelders RA, Schmid HA, et al. Distinct functional properties of native somatostatin receptor subtype 5 compared with subtype 2 in the regulation of ACTH release by corticotroph tumor cells. *Am J Physiol Endocrinol Metab.* (2005) 289:E278–87. doi: 10.1152/ajpendo.00004.2005
17. Colao A, Petersenn S, Newell-Price J, Findling JW, Gu F, Maldonado M, et al. A 12-month phase 3 study of pasireotide in Cushing's disease. *N Engl J Med.* (2012) 366:914–24. doi: 10.1056/NEJMoa1105743
18. Boscaro M, Ludlam WH, Atkinson B, Glusman JE, Petersenn S, Reincke M, et al. Treatment of pituitary-dependent Cushing's disease with the multireceptor ligand somatostatin analog pasireotide (SOM230): a multicenter, phase II trial. *J Clin Endocrinol Metab.* (2009) 94:115–22. doi: 10.1016/S0084-3741(09)79383-7
19. Toma K, Otsuka F, Oguni K, Terasaka T, Komatsubara M, Tsukamoto-Yamauchi N, et al. BMP-6 modulates somatostatin effects on luteinizing hormone production by gonadrotrope cells. *Peptides.* (2016) 76:96–101. doi: 10.1016/j.peptides.2016.01.011
20. Liu JC, Baker RE, Sun C, Sundmark VC, Elsholtz HP. Activation of Go-coupled dopamine D2 receptors inhibits ERK1/ERK2 in pituitary cells. A key step in the transcriptional suppression of the prolactin gene. *J Biol Chem.* (2002) 277:35819–25. doi: 10.1074/jbc.M202920200
21. Kanasaki H, Fukunaga K, Takahashi K, Miyazaki K, Miyamoto E. Involvement of p38 mitogen-activated protein kinase activation in bromocriptine-induced apoptosis in rat pituitary GH3 cells. *Biol Reprod.* (2000) 62:1486–94. doi: 10.1095/biolreprod62.6.1486
22. Radl DB, Ferraris J, Boti V, Seilicovich A, Sarkar DK, Pisera D. Dopamine-induced apoptosis of lactotropes is mediated by the short isoform of D2 receptor. *PLoS ONE.* (2011) 6:e18097. doi: 10.1371/journal.pone.0018097
23. Petiti JP, Sosa Ldel V, Sabatino ME, Vaca AM, Gutierrez S, De Paul AL, et al. Involvement of MEK/ERK1/2 and PI3K/Akt pathways in the refractory behavior of GH3B6 pituitary tumor cells to the inhibitory effect of TGFbeta1. *Endocrinology.* (2015) 156:534–47. doi: 10.1210/en.2014-1070
24. Lee CS, Yang JC, Kim YJ, Jang ER, Kim W, Myung SC. 18beta-Glycyrrhetinic acid potentiates apoptotic effect of trichostatin A on human epithelial ovarian carcinoma cell lines. *Eur J Pharmacol.* (2010) 649:354–61. doi: 10.1016/j.ejphar.2010.09.047
25. Peverelli E, Olgiati L, Locatelli M, Magni P, Fustini MF, Frank G, et al. The dopamine–somatostatin chimeric compound BIM-23A760 exerts antiproliferative and cytotoxic effects in human non-functioning pituitary tumors by activating ERK1/2 and p38 pathways. *Cancer Lett.* (2010) 288:170–6. doi: 10.1016/j.canlet.2009.06.034
26. Gong YY, Liu YY, Yu S, Zhu XN, Cao XP, Xiao HP. Ursolic acid suppresses growth and adrenocorticotrophic hormone secretion in AtT20 cells as a potential agent targeting adrenocorticotrophic hormone-producing pituitary adenoma. *Mol Med Rep.* (2014) 9:2533–9. doi: 10.3892/mmr.2014.2078
27. Gao H, Xue Y, Cao L, Liu Q, Liu C, Shan X, et al. ESR1 and its antagonist fulvestrant in pituitary adenomas. *Mol Cell Endocrinol.* (2017) 443:32–41. doi: 10.1016/j.mce.2016.12.029
28. Fougner SL, Bollerslev J, Latif F, Hald JK, Lund T, Ramm-Pettersen J, et al. Low levels of raf kinase inhibitory protein in growth hormone-secreting pituitary adenomas correlate with poor response to octreotide treatment. *J Clin Endocrinol Metab.* (2008) 93:1211–6. doi: 10.1210/jc.2007-2272

29. Fazioli F, Minichiello L, Matoska V, Castagnino P, Miki T, Wong WT, et al. Eps8, a substrate for the epidermal growth factor receptor kinase, enhances EGF-dependent mitogenic signals. *EMBO J.* (1993) 12:3799–808. doi: 10.1002/j.1460-2075.1993.tb06058.x
30. Xu M, Shorts-Cary L, Knox AJ, Kleinsmidt-DeMasters B, Lillehei K, Wierman ME. Epidermal growth factor receptor pathway substrate 8 is overexpressed in human pituitary tumors: role in proliferation and survival. *Endocrinology.* (2009) 150:2064–71. doi: 10.1210/en.2008-1265
31. Labeur M, Wolfel B, Stalla J, Stalla GK. TMEFF2 is an endogenous inhibitor of the CRH signal transduction pathway. *J Mol Endocrinol.* (2015) 54:51–63. doi: 10.1530/JME-14-0225
32. Jian F, Chen Y, Ning G, Fu W, Tang H, Chen X, et al. Cold inducible RNA binding protein upregulation in pituitary corticotroph adenoma induces corticotroph cell proliferation via Erk signaling pathway. *Oncotarget.* (2016) 7:9175–87. doi: 10.18632/oncotarget.7037
33. Wang DW, Wang YQ, Shu HS. MiR-16 inhibits pituitary adenoma cell proliferation via the suppression of ERK/MAPK signal pathway. *Eur Rev Med Pharmacol Sci.* (2018) 22:1241–8.
34. Jiang Y, Gram H, Zhao M, New L, Gu J, Feng L, et al. Characterization of the structure and function of the fourth member of p38 group mitogen-activated protein kinases, p38delta. *J Biol Chem.* (1997) 272:30122–8. doi: 10.1074/jbc.272.48.30122
35. Kolch W. Coordinating ERK/MAPK signalling through scaffolds and inhibitors. *Nat Rev Mol Cell Biol.* (2005) 6:827–37. doi: 10.1038/nrm1743
36. O'Neill E, Rushworth L, Baccarini M, Kolch W. Role of the kinase MST2 in suppression of apoptosis by the proto-oncogene product Raf-1. *Science.* (2004) 306:2267–70. doi: 10.1126/science.1103233
37. Ehrenreiter K, Piazzolla D, Velamoor V, Sobczak I, Small JV, Takeda J, et al. Raf-1 regulates Rho signaling and cell migration. *J Cell Biol.* (2005) 168:955–64. doi: 10.1083/jcb.200409162
38. Karga HJ, Alexander JM, Hedley-Whyte ET, Klibanski A, Jameson JL. Ras mutations in human pituitary tumors. *J Clin Endocrinol Metab.* (1992) 74:914–9. doi: 10.1210/jc.74.4.914
39. Cai WY, Alexander JM, Hedley-Whyte ET, Scheithauer BW, Jameson JL, Zervas NT, et al. ras mutations in human prolactinomas and pituitary carcinomas. *J Clin Endocrinol Metab.* (1994) 78:89–93. doi: 10.1210/jcem.78.1.8288721
40. Ewing I, Pedder-Smith S, Franchi G, Ruscica M, Emery M, Vax V, et al. A mutation and expression analysis of the oncogene BRAF in pituitary adenomas. *Clin Endocrinol.* (2007) 66:348–52. doi: 10.1111/j.1365-2265.2006.02735.x
41. Dworakowska D, Wlodek E, Leontiou CA, Igreja S, Cakir M, Teng M, et al. Activation of RAF/MEK/ERK and PI3K/AKT/mTOR pathways in pituitary adenomas and their effects on downstream effectors. *Endocr Relat Cancer.* (2009) 16:1329–38. doi: 10.1677/ERC-09-0101
42. Chaturvedi K, Sarkar DK. Mediation of basic fibroblast growth factor-induced lactotropic cell proliferation by Src-Ras-mitogen-activated protein kinase p44/42 signaling. *Endocrinology.* (2005) 146:1948–55. doi: 10.1210/en.2004-1448
43. Oomizu S, Chaturvedi K, Sarkar DK. Folliculostellate cells determine the susceptibility of lactotropes to estradiol's mitogenic action. *Endocrinology.* (2004) 145:1473–80. doi: 10.1210/en.2003-0965
44. Booth A, Trudeau T, Gomez C, Lucia MS, Gutierrez-Hartmann A. Persistent ERK/MAPK activation promotes lactotrope differentiation and diminishes tumorigenic phenotype. *Mol Endocrinol.* (2014) 28:1999–2011. doi: 10.1210/me.2014-1168
45. Lania A, Filopanti M, Corbetta S, Losa M, Ballare E, Beck-Peccoz P, et al. Effects of hypothalamic neuropeptides on extracellular signal-regulated kinase (ERK1 and ERK2) cascade in human tumoral pituitary cells. *J Clin Endocrinol Metab.* (2003) 88:1692–6. doi: 10.1210/jc.2002-021207
46. Pombo CM, Zalvide J, Gaylinn BD, Dieguez C. Growth hormone-releasing hormone stimulates mitogen-activated protein kinase. *Endocrinology.* (2000) 141:2113–9. doi: 10.1210/endo.141.6.7513
47. Cuny T, Gerard C, Saveanu A, Barlier A, Enjalbert A. Physiopathology of somatolactotroph cells: from transduction mechanisms to cotargeting therapy. *Ann N Y Acad Sci.* (2011) 1220:60–70. doi: 10.1111/j.1749-6632.2010.05924.x
48. Liu F, Austin DA, Mellon PL, Olefsky JM, Webster NJ. GnRH activates ERK1/2 leading to the induction of c-fos and LHbeta protein expression in LbetaT2 cells. *Mol Endocrinol.* (2002) 16:419–34. doi: 10.1210/mend.16.3.0791
49. Rubinfeld H, Shimon I. PI3K/Akt/mTOR and Raf/MEK/ERK signaling pathways perturbations in non-functioning pituitary adenomas. *Endocrine.* (2012) 42:285–91. doi: 10.1007/s12020-012-9682-3
50. Woodmansee WW, Kerr JM, Tucker EA, Mitchell JR, Haakinson DJ, Gordon DF, et al. The proliferative status of thyrotropes is dependent on modulation of specific cell cycle regulators by thyroid hormone. *Endocrinology.* (2006) 147:272–82. doi: 10.1210/en.2005-1013
51. Zhang D, Bergsneider M, Wang MB, Heaney AP. Targeting the ERK pathway for the treatment of Cushing's disease. *Oncotarget.* (2016) 7:69149–58. doi: 10.18632/oncotarget.12381
52. Theodoropoulou M, Zhang J, Laupheimer S, Paez-Pereda M, Erneux C, Florio T, et al. Octreotide, a somatostatin analogue, mediates its antiproliferative action in pituitary tumor cells by altering phosphatidylinositol 3-kinase signaling and inducing Zac1 expression. *Cancer Res.* (2006) 66:1576–82. doi: 10.1158/0008-5472.CAN-05-1189
53. Bruns C, Lewis I, Briner U, Meno-Tetang G, Weckbecker G. SOM230: a novel somatostatin peptidomimetic with broad somatotropin release inhibiting factor (SRIF) receptor binding and a unique antisecretory profile. *Eur J Endocrinol.* (2002) 146:707–16. doi: 10.1530/eje.0.1460707
54. Weckbecker G, Briner U, Lewis I, Bruns C. SOM230: a new somatostatin peptidomimetic with potent inhibitory effects on the growth hormone/insulin-like growth factor-I axis in rats, primates, and dogs. *Endocrinology.* (2002) 143:4123–30. doi: 10.1210/en.2002-220219
55. Cheung NW, Boyages SC. Somatostatin-14 and its analog octreotide exert a cytostatic effect on GH3 rat pituitary tumor cell proliferation via a transient G0/G1 cell cycle block. *Endocrinology.* (1995) 136:4174–81. doi: 10.1210/en.136.10.4174
56. Florio T, Thellung S, Arena S, Corsaro A, Spaziante R, Gussoni G, et al. Somatostatin and its analog lanreotide inhibit the proliferation of dispersed human non-functioning pituitary adenoma cells *in vitro*. *Eur J Endocrinol.* (1999) 141:396–408. doi: 10.1530/eje.0.1410396
57. Padova H, Rubinfeld H, Hadani M, Cohen ZR, Nass D, Taylor JE, et al. Effects of selective somatostatin analogs and cortistatin on cell viability in cultured human non-functioning pituitary adenomas. *Mol Cell Endocrinol.* (2008) 286:214–8. doi: 10.1016/j.mce.2007.12.011
58. Zatelli MC, Piccin D, Vignali C, Tagliati F, Ambrosio MR, Bondanelli M, et al. Pasireotide, a multiple somatostatin receptor subtypes ligand, reduces cell viability in non-functioning pituitary adenomas by inhibiting vascular endothelial growth factor secretion. *Endocr Relat Cancer.* (2007) 14:91–102. doi: 10.1677/ERC-06-0026
59. Colao A, Di Somma C, Pivonello R, Faggiano A, Lombardi G, Savastano S. Medical therapy for clinically non-functioning pituitary adenomas. *Endocr Relat Cancer.* (2008) 15:905–15. doi: 10.1677/ERC-08-0181
60. Kauppinen-Makelin R, Sane T, Reunanen A, Valimaki MJ, Niskanen L, Markkanen H, et al. A nationwide survey of mortality in acromegaly. *J Clin Endocrinol Metab.* (2005) 90:4081–6. doi: 10.1210/jc.2004-1381
61. Bates PR, Carson MN, Trainer PJ, Wass JA, Group UKNARS. Wide variation in surgical outcomes for acromegaly in the UK. *Clin Endocrinol.* (2008) 68:136–42. doi: 10.1111/j.1365-2265.2007.03012.x
62. Melmed S, Sternberg R, Cook D, Klibanski A, Chanson P, Bonert V, et al. A critical analysis of pituitary tumor shrinkage during primary medical therapy in acromegaly. *J Clin Endocrinol Metab.* (2005) 90:4405–10. doi: 10.1210/jc.2004-2466
63. Fougner SL, Borota OC, Berg JP, Hald JK, Ramm-Pettersen J, Bollerslev J. The clinical response to somatostatin analogues in acromegaly correlates to the somatostatin receptor subtype 2a protein expression of the adenoma. *Clin Endocrinol.* (2008) 68:458–65. doi: 10.1111/j.1365-2265.2007.03065.x
64. Hubina E, Ruscica M, Nanzer AM, Czirjak S, Goth MI, Grossman AB, et al. Novel molecular aspects of pituitary adenomas. *J Endocrinol Invest.* (2005) 28(11 Suppl. International):87–92.
65. Stack J, Surprenant A. Dopamine actions on calcium currents, potassium currents and hormone release in rat melanotrophs. *J Physiol.* (1991) 439:37–58. doi: 10.1113/jphysiol.1991.sp018655

66. Melmed S, Casanueva FF, Hoffman AR, Kleinberg DL, Montori VM, Schlechte JA, et al. Diagnosis and treatment of hyperprolactinemia: an Endocrine Society clinical practice guideline. *J Clin Endocrinol Metab.* (2011) 96:273–88. doi: 10.1210/jc.2010-1692
67. Iaccarino C, Samad TA, Mathis C, Kercret H, Picetti R, Borrelli E. Control of lactotrop proliferation by dopamine: essential role of signaling through D2 receptors and ERKs. *Proc Natl Acad Sci USA.* (2002) 99:14530–5. doi: 10.1073/pnas.222319599
68. Radl D, De Mei C, Chen E, Lee H, Borrelli E. Each individual isoform of the dopamine D2 receptor protects from lactotroph hyperplasia. *Mol Endocrinol.* (2013) 27:953–65. doi: 10.1210/me.2013-1008
69. Derynck R, Akhurst RJ, Balmain A. TGF-beta signaling in tumor suppression and cancer progression. *Nat Genet.* (2001) 29:117–29. doi: 10.1038/ng1001-117
70. Kang JS, Liu C, Derynck R. New regulatory mechanisms of TGF-beta receptor function. *Trends Cell Biol.* (2009) 19:385–94. doi: 10.1016/j.tcb.2009.05.008
71. Mu Y, Gudey SK, Landstrom M. Non-Smad signaling pathways. *Cell Tissue Res.* (2012) 347:11–20. doi: 10.1007/s00441-011-1201-y
72. Trakul N, Rosner MR. Modulation of the MAP kinase signaling cascade by Raf kinase inhibitory protein. *Cell Res.* (2005) 15:19–23. doi: 10.1038/sj.cr.7290258
73. Trakul N, Menard RE, Schade GR, Qian Z, Rosner MR. Raf kinase inhibitory protein regulates Raf-1 but not B-Raf kinase activation. *J Biol Chem.* (2005) 280:24931–40. doi: 10.1074/jbc.M413929200
74. Yeung K, Seitz T, Li S, Janosch P, McFerran B, Kaiser C, et al. Suppression of Raf-1 kinase activity and MAP kinase signalling by RKIP. *Nature.* (1999) 401:173–7. doi: 10.1038/43686
75. Eves EM, Shapiro P, Naik K, Klein UR, Trakul N, Rosner MR. Raf kinase inhibitory protein regulates aurora B kinase and the spindle checkpoint. *Mol Cell.* (2006) 23:561–74. doi: 10.1016/j.molcel.2006.07.015
76. Lee SJ, Lee SH, Yoon MH, Park BJ. A new p53 target gene, RKIP, is essential for DNA damage-induced cellular senescence and suppression of ERK activation. *Neoplasia.* (2013) 15:727–37. doi: 10.1593/neo.121862
77. Pecori Giraldi F, Ambrogio AG, Andrioli M, Sanguin F, Karamouzis I, Corsello SM, et al. Potential role for retinoic acid in patients with Cushing's disease. *J Clin Endocrinol Metab.* (2012) 97:3577–83. doi: 10.1210/jc.2012-2328
78. Nishiyama H, Itoh K, Kaneko Y, Kishishita M, Yoshida O, Fujita J. A glycine-rich RNA-binding protein mediating cold-inducible suppression of mammalian cell growth. *J Cell Biol.* (1997) 137:899–908. doi: 10.1083/jcb.137.4.899
79. Artero-Castro A, Callejas FB, Castellvi J, Kondoh H, Carnero A, Fernandez-Marcos PJ, et al. Cold-inducible RNA-binding protein bypasses replicative senescence in primary cells through extracellular signal-regulated kinase 1 and 2 activation. *Mol Cell Biol.* (2009) 29:1855–68. doi: 10.1128/MCB.01386-08
80. Guo X, Wu Y, Hartley RS. Cold-inducible RNA-binding protein contributes to human antigen R and cyclin E1 deregulation in breast cancer. *Mol Carcinog.* (2010) 49:130–40. doi: 10.1002/mc.20582
81. Zarubin T, Jiahuai H. Activation and signaling of the p38 MAP kinase pathway. *Cell Res.* (2005) 15:11–8. doi: 10.1038/sj.cr.7290257
82. Wang XS, Diener K, Manthey CL, Wang S, Rosenzweig B, Bray J, et al. Molecular cloning and characterization of a novel p38 mitogen-activated protein kinase. *J Biol Chem.* (1997) 272:23668–74. doi: 10.1074/jbc.272.38.23668
83. Raingeaud J, Gupta S, Rogers JS, Dickens M, Han J, Ulevitch RJ, et al. Pro-inflammatory cytokines and environmental stress cause p38 mitogen-activated protein kinase activation by dual phosphorylation on tyrosine and threonine. *J Biol Chem.* (1995) 270:7420–6. doi: 10.1074/jbc.270.13.7420
84. Derijard B, Raingeaud J, Barrett T, Wu IH, Han J, Ulevitch RJ, et al. Independent human MAP-kinase signal transduction pathways defined by MEK and MKK isoforms. *Science.* (1995) 267:682–5. doi: 10.1126/science.7839144
85. Lin A, Minden A, Martinetto H, Claret FX, Lange-Carter C, Mercurio F, et al. Identification of a dual specificity kinase that activates the Jun kinases and p38-Mpk2. *Science.* (1995) 268:286–90. doi: 10.1126/science.7716521
86. Raingeaud J, Whitmarsh AJ, Barrett T, Derijard B, Davis RJ. MKK3- and MKK6-regulated gene expression is mediated by the p38 mitogen-activated protein kinase signal transduction pathway. *Mol Cell Biol.* (1996) 16:1247–55. doi: 10.1128/MCB.16.3.1247
87. Liu Y, Cao X. Immunosuppressive cells in tumor immune escape and metastasis. *J Mol Med.* (2016) 94:509–22. doi: 10.1007/s00109-015-1376-x
88. Han X, Geng X, Li Z, Chen Z, Liu Y, Liu P, et al. The relationship between phospho-p38, MMP-9, and MICA expression in pituitary adenomas demonstrates a new mechanism of pituitary adenoma immune escape. *World* Neurosurg. (2018) 123:e116–24. doi: 10.1016/j.wneu.2018.11.077
89. Xiong W, Knox AJ, Xu M, Kiseljak-Vassiliades K, Colgan SP, Brodsky KS, et al. Mammalian Ste20-like kinase 4 promotes pituitary cell proliferation and survival under hypoxia. *Mol Endocrinol.* (2015) 29:460–72. doi: 10.1210/me.2014-1332
90. Sharma G, Kar S, Palit S, Das PK. 18beta-glycyrrhetinic acid induces apoptosis through modulation of Akt/FOXO3a/Bim pathway in human breast cancer MCF-7 cells. *J Cell Physiol.* (2012) 227:1923–31. doi: 10.1002/jcp.22920
91. Wang D, Wong HK, Feng YB, Zhang ZJ. 18beta-glycyrrhetinic acid induces apoptosis in pituitary adenoma cells via ROS/MAPKs-mediated pathway. *J Neuro Oncol.* (2014) 116:221–30. doi: 10.1007/s11060-013-1292-2
92. Lu M, Zhan X. The crucial role of multiomic approach in cancer research and clinically relevant outcomes. *EPMA J.* (2018) 9:77–102. doi: 10.1007/s13167-018-0128-8
93. Cheng T, Zhan X. Pattern recognition for predictive, preventive, and personalized medicine in cancer. *EPMA J.* (2017) 8:51–60. doi: 10.1007/s13167-017-0083-9
94. Lu B, Liu GL, Yu F, Li WJ, Xiang XX, Xiao HZ. MicroRNA16/VEGFR2/p38/NFkappaB signaling pathway regulates cell growth of human pituitary neoplasms. *Oncol Rep.* (2018) 39:1235–44. doi: 10.3892/or.2018.6227
95. Bogoyevitch MA, Ngoei KR, Zhao TT, Yeap YY, Ng DC. c-Jun N-terminal kinase (JNK) signaling: recent advances and challenges. *Biochim Biophys Acta.* (2010) 1804:463–75. doi: 10.1016/j.bbapap.2009.11.002
96. Karin M. Mitogen-activated protein kinase cascades as regulators of stress responses. *Ann N Y Acad Sci.* (1998) 851:139–46. doi: 10.1111/j.1749-6632.1998.tb08987.x
97. Weston CR, Davis RJ. The JNK signal transduction pathway. *Curr Opin Cell Biol.* (2007) 19:142–9. doi: 10.1016/j.ceb.2007.02.001
98. Barr RK, Bogoyevitch MA. The c-Jun N-terminal protein kinase family of mitogen-activated protein kinases (JNK MAPKs). *Int J Biochem Cell Biol.* (2001) 33:1047–63. doi: 10.1016/S1357-2725(01)00093-0
99. Gupta S, Barrett T, Whitmarsh AJ, Cavanagh J, Sluss HK, Derijard B, et al. Selective interaction of JNK protein kinase isoforms with transcription factors. *EMBO J.* (1996) 15:2760–70. doi: 10.1002/j.1460-2075.1996.tb00636.x
100. Davis RJ. Signal transduction by the JNK group of MAP kinases. *Cell.* (2000) 103:239–52. doi: 10.1016/S0092-8674(00)00116-1
101. Haeusgen W, Herdegen T, Waetzig V. The bottleneck of JNK signaling: molecular and functional characteristics of MKK4 and MKK7. *Eur J Cell Biol.* (2011) 90:536–44. doi: 10.1016/j.ejcb.2010.11.008
102. Mizukami Y, Yoshioka K, Morimoto S, Yoshida K. A novel mechanism of JNK1 activation. Nuclear translocation and activation of JNK1 during ischemia and reperfusion. *J Biol Chem.* (1997) 272:16657–62. doi: 10.1074/jbc.272.26.16657
103. Gulmann C, Sheehan KM, Conroy RM, Wulfkuhle JD, Espina V, Mullarkey MJ, et al. Quantitative cell signalling analysis reveals down-regulation of MAPK pathway activation in colorectal cancer. *J Pathol.* (2009) 218:514–9. doi: 10.1002/path.2561
104. Chen Z, Yang A, Xu C, Xing Y, Gong W, Li J. c-Jun N-terminal kinase is involved in the regulation of proliferation and apoptosis by integrin-linked kinase in human retinoblastoma cells. *Graefes Arch Clin Exp Ophthalmol.* (2011) 249:1399–407. doi: 10.1007/s00417-010-1607-3
105. Jorgensen K, Davidson B, Florenes VA. Activation of c-jun N-terminal kinase is associated with cell proliferation and shorter relapse-free period

in superficial spreading malignant melanoma. *Mod Pathol.* (2006) 19:1446–55. doi: 10.1038/modpathol.3800662
106. Wang X, Chao L, Li X, Ma G, Chen L, Zang Y, et al. Elevated expression of phosphorylated c-Jun NH2-terminal kinase in basal-like and "triple-negative" breast cancers. *Hum Pathol.* (2010) 41:401–6. doi: 10.1016/j.humpath.2009.08.018
107. Odegaard E, Staff AC, Abeler VM, Kopolovic J, Onsrud M, Lazarovici P, et al. The activated nerve growth factor receptor p-TrkA is selectively expressed in advanced-stage ovarian carcinoma. *Hum Pathol.* (2007) 38:140–6. doi: 10.1016/j.humpath.2006.06.027
108. Belgardt BF, Mauer J, Wunderlich FT, Ernst MB, Pal M, Spohn G, et al. Hypothalamic and pituitary c-Jun N-terminal kinase 1 signaling coordinately regulates glucose metabolism. *Proc Natl Acad Sci USA.* (2010) 107:6028–33. doi: 10.1073/pnas.1001796107
109. Vernia S, Cavanagh-Kyros J, Barrett T, Jung DY, Kim JK, Davis RJ. Diet-induced obesity mediated by the JNK/DIO2 signal transduction pathway. *Genes Dev.* (2013) 27:2345–55. doi: 10.1101/gad.223800.113
110. Chen XH, Ling XM, Shi S. microRNA-106a induces the proliferation and apoptosis of glioma cells through regulating JNK/MAPK pathway. *Eur Rev Med Pharmacol Sci.* (2015) 19:3412–7.
111. Liu J. Pharmacology of oleanolic acid and ursolic acid. *J Ethnopharmacol.* (1995) 49:57–68. doi: 10.1016/0378-8741(95)90032-2
112. Shyu MH, Kao TC, Yen GC. Oleanolic acid and ursolic acid induce apoptosis in HuH7 human hepatocellular carcinoma cells through a mitochondrial-dependent pathway and downregulation of XIAP. *J Agric Food Chem.* (2010) 58:6110–8. doi: 10.1021/jf100574j
113. Harmand PO, Duval R, Delage C, Simon A. Ursolic acid induces apoptosis through mitochondrial intrinsic pathway and caspase-3 activation in M4Beu melanoma cells. *Int J Cancer.* (2005) 114:1–11. doi: 10.1002/ijc.20588
114. De Angel RE, Smith SM, Glickman RD, Perkins SN, Hursting SD. Antitumor effects of ursolic acid in a mouse model of postmenopausal breast cancer. *Nutr Cancer.* (2010) 62:1074–86. doi: 10.1080/01635581.2010.492092
115. Prasad S, Yadav VR, Sung B, Reuter S, Kannappan R, Deorukhkar A, et al. Ursolic acid inhibits growth and metastasis of human colorectal cancer in an orthotopic nude mouse model by targeting multiple cell signaling pathways: chemosensitization with capecitabine. *Clin Cancer Res.* (2012) 18:4942–53. doi: 10.1158/1078-0432.CCR-11-2805
116. Zheng QY, Jin FS, Yao C, Zhang T, Zhang GH, Ai X. Ursolic acid-induced AMP-activated protein kinase (AMPK) activation contributes to growth inhibition and apoptosis in human bladder cancer T24 cells. *Biochem Biophys Res Commun.* (2012) 419:741–7. doi: 10.1016/j.bbrc.2012.02.093
117. Kassi E, Papoutsi Z, Pratsinis H, Aligiannis N, Manoussakis M, Moutsatsou P. Ursolic acid, a naturally occurring triterpenoid, demonstrates anticancer activity on human prostate cancer cells. *J Cancer Res Clin Oncol.* (2007) 133:493–500. doi: 10.1007/s00432-007-0193-1
118. Vergote I, Abram P. Fulvestrant, a new treatment option for advanced breast cancer: tolerability versus existing agents. *Ann Oncol.* (2006) 17:200–4. doi: 10.1093/annonc/mdj047
119. McCormack P, Sapunar F. Pharmacokinetic profile of the fulvestrant loading dose regimen in postmenopausal women withhormone receptor-positive advanced breast cancer. *Clin Breast Cancer.* (2008) 8:347–51. doi: 10.3816/CBC.2008.n.040
120. Zhan X, Desiderio DM. A reference map of a human pituitary adenoma proteome. *Proteomics.* (2003) 3:699–713. doi: 10.1002/pmic.200300408
121. Moreno CS, Evans CO, Zhan X, Okor M, Desiderio DM, Oyesiku NM. Novel molecular signaling and classification of human clinically nonfunctional pituitary adenomas identified by gene expression profiling and proteomic analyses. *Cancer Res.* (2005) 65:10214–22. doi: 10.1158/0008-5472.CAN-05-0884
122. Evans CO, Moreno CS, Zhan X, McCabe MT, Vertino PM, Desiderio DM, et al. Molecular pathogenesis of human prolactinomas identified by gene expression profiling, RT-qPCR, and proteomic analyses. *Pituitary.* (2008) 11:231–45. doi: 10.1007/s11102-007-0082-2
123. Zhan X, Desiderio DM. Nitroproteins from a human pituitary adenoma tissue discovered with a nitrotyrosine affinity column and tandem mass spectrometry. *Anal. Biochem.* (2006) 354:279–89. doi: 10.1016/j.ab.2006.05.024
124. Zhan X, Desiderio DM. The human pituitary nitroproteome: detection of nitrotyrosyl-proteins with two-dimensional Western blotting, and amino acid sequence determination with mass spectrometry. *Biochem Biophys Res Commun.* (2004) 325:1180–6. doi: 10.1016/j.bbrc.2004.10.169
125. Zhan X, Desiderio DM. Signaling pathway networks mined from human pituitary adenoma proteomics data. *BMC Med Genomics.* (2010) 3:13. doi: 10.1186/1755-8794-3-13
126. Goldsmith ZG, Dhanasekaran DN. G protein regulation of MAPK networks. *Oncogene.* (2007) 26:3122–42. doi: 10.1038/sj.onc.1210407
127. Cakir M, Grossman AB. Targeting MAPK (Ras/ERK) and PI3K/Akt pathways in pituitary tumorigenesis. *Expert Opin Ther Targets.* (2009) 13:1121–34. doi: 10.1517/14728220903170675
128. Fernández M, Sanchez-Franco F, Palacios N, Sanchez I, Cacicedo L. IGF-I and vasoactive intestinal peptide (VIP) regulate cAMP-response element-binding protein (CREB)-dependent transcription via the mitogen-activated protein kinase (MAPK) pathway in pituitary cells: requirement of Rap1. *J Mol Endocrinol.* (2005) 34:699–712. doi: 10.1677/jme.1.01703

Conflict of Interest Statement: The authors declare that the research was conducted in the absence of any commercial or financial relationships that could be construed as a potential conflict of interest.

frontiers in Endocrinology

REVIEW
published: 09 October 2019
doi: 10.3389/fendo.2019.00690

Mitochondrial Dysfunction Pathway Networks and Mitochondrial Dynamics in the Pathogenesis of Pituitary Adenomas

Na Li [1,2,3] *and Xianquan Zhan* [1,2,3,4,5]*

[1] Key Laboratory of Cancer Proteomics of Chinese Ministry of Health, Xiangya Hospital, Central South University, Changsha, China, [2] Hunan Engineering Laboratory for Structural Biology and Drug Design, Xiangya Hospital, Central South University, Changsha, China, [3] State Local Joint Engineering Laboratory for Anticancer Drugs, Xiangya Hospital, Central South University, Changsha, China, [4] National Clinical Research Center for Geriatric Disorders, Xiangya Hospital, Central South University, Changsha, China, [5] Department of Oncology, Xiangya Hospital, Central South University, Changsha, China

Mitochondrion is a multi-functional organelle, which is associated with various signaling pathway networks, including energy metabolism, oxidative stress, cell apoptosis, cell cycles, autophagy, and immunity process. Mitochondrial proteins have been discovered to modulate these signaling pathway networks, and multiple biological behaviors to adapt to various internal environments or signaling events of human pathogenesis. Accordingly, mitochondrial dysfunction that alters the bioenergetic and biosynthetic state might contribute to multiple diseases, including cell transformation and tumor. Multiomics studies have revealed that mitochondrial dysfunction, oxidative stress, and cell cycle dysregulation signaling pathways operate in human pituitary adenomas, which suggest mitochondria play critical roles in pituitary adenomas. Some drugs targeting mitochondria are found as a therapeutic strategy for pituitary adenomas, including melatonin, melatonin inhibitors, temozolomide, pyrimethamine, 18 beta-glycyrrhetinic acid, gossypol acetate, Yougui pill, T-2 toxin, grifolic acid, cyclosporine A, dopamine agonists, and paeoniflorin. This article reviews the latest experimental evidence and potential biological roles of mitochondrial dysfunction and mitochondrial dynamics in pituitary adenoma progression, potential molecular mechanisms between mitochondria and pituitary adenoma progression, and current status and perspectives of mitochondria-based biomarkers and targeted drugs for effective management of pituitary adenomas.

Keywords: mitochondrial dysfunction, mitochondrial dynamics, pituitary adenomas, omics, systems biology

OPEN ACCESS

Edited by:
Corin Badiu, Carol Davila University of Medicine and Pharmacy, Romania

Reviewed by:
Leila Warszawski, Instituto Estadual de Diabetes e Endocrinologia Luiz Capriglione, Brazil
Cristiana Tanase, Victor Babes National Institute of Pathology, Romania

***Correspondence:**
Xianquan Zhan
yjzhan2011@gmail.com

Specialty section:
This article was submitted to Pituitary Endocrinology, a section of the journal Frontiers in Endocrinology

Received: *28 September 2018*
Accepted: *23 September 2019*
Published: *09 October 2019*

Citation:
Li N and Zhan X (2019) Mitochondrial Dysfunction Pathway Networks and Mitochondrial Dynamics in the Pathogenesis of Pituitary Adenomas. Front. Endocrinol. 10:690. doi: 10.3389/fendo.2019.00690

INTRODUCTION

Pituitary adenomas are intracranial tumors that develop in the pituitary gland, and account for 10 to 25% of all intracranial neoplasms. Most pituitary adenomas are benign, nearly 35% sufferers present invasiveness and just 0.1–0.2% are diagnosed as carcinomas (1). Pituitary adenomas are commonly divided into functional pituitary adenomas, and non-functional pituitary adenomas according to the clinical level of hormone secretion (2). Functional pituitary adenomas are hormone-secreting

pituitary adenomas that could cause hyperpituitarism, such as Cushing's syndrome, acromegaly, and hyperprolactinaemia; and non-functional pituitary adenomas are non-hormone-secreting pituitary adenomas (3). Pituitary adenomas are also divided into microadenomas (<10 mm) and macroadenomas (≥10 mm) according to tumor size (4). The clinically chief complaints of pituitary adenomas are visual field defects, headache, and increased intracranial pressure, which are usually derived from a compression of the neighboring tissues and structures. Another type of clinical problem is an inappropriate hormone secretion in hormone-secreting pituitary adenomas (5).

Currently, high-throughput omic technologies have been extensively used to study pituitary adenomas (6) from a multi-parameter systematic biology angle to overcome the irrationality that use a single molecule as biomarker for accurate predictive, preventive, and personalized medicine (PPPM) practice, because numerous molecules alter at the different levels of DNAs (genome), RNAs (transcriptome), proteins (proteome), and metabolites (metabolome), and are involved in different pathway network systems for tumorigenesis (7). Among the field of multiomics, transcriptomics, and proteomics are two important ways to systematically study the functions of genes (8, 9). Thousands of differentially expressed genes have been identified in human pituitary adenomas (10–12), which have addressed at a certain degree the functions of genes. However, transcriptiomics study cannot fully reveal the functions of genes, because proteins are the final performer of the corresponding genes, there are lots of regulations and modifications occurred in the process from mRNA to proteins. The number of proteins is much more than the number of transcripts, and the correlation coefficient only reaches 0.4 between proteomics and transcriptomics (13, 14). Therefore, proteomics is a more important way to address the functions of genes, especially subcellular proteomics such as mitochondrial proteomics is an effective method to reveal the specialized functions of a organelle to associate with a given diseases such as cancer (15). Currently mitochondrial proteomics has become a research hotpot because mitochondria are ubiquitously subcellular organelles responsible for providing energy to eukaryotic cells, and are the key links of metabolism, oxidative stress, cell apoptosis, cell cycles, autophagy, and immunity process (16), which are involved in a wide range of diseases including cancers (17). This review article will mainly focus on the mitochondrial dysfunction pathway alterations in pituitary adenomas from a systematic viewpoint.

Pituitary adenoma proteomics-based molecular network study have revealed that mitochondrial dysfunction, oxidative stress, cell cycle dysregulation, and MAPK signaling abnormality are significantly associated with the pathogenesis of pituitary adenomas (18–21). Mitochondria are actually center of oxidative stress, which clearly demonstrate that mitochondrial dysfunction pathway plays important roles in pituitary adenomas. Furthermore, electron microscopy morphology study demonstrates that mitochondria are abundantly filled in cytoplasm of pituitary oncocytoma cells (22–24). Some studies demonstrate that the volume of mitochondria is different among different subtypes in pituitary adenomas; for example, the volume of mitochondria of prolactinoma is larger than acromegaly (25). More important are that some drugs targeting mitochondria have been reported as a therapeutic strategy for pituitary adenomas (**Table 1**) (26–39), including melatonin, melatonin inhibits, temozolomide and pyrimethamine, 18 beta-glycyrrhetinic acid, gossypol acetate, Yougui pill, T-2 toxin, grifolic acid, and paeoniflorin. Those evidences clearly demonstrate the important roles of mitochondrial biological functions and dynamic shift in pituitary adenoma pathogenesis, however, their molecular mechanisms remain unclear yet (2, 40). Mitochondria-based study might provide new insights into molecular mechanisms of pituitary adenomas, discover new biomarkers and molecular targets for effective management of pituitary adenomas. This review article discusses observations in the context of how mitochondrial dysfunction can influence the biological status in pituitary adenoma, including energy metabolism, oxidative stress, cell apoptosis, autophagy, and immunity (**Figure 1**; **Table 2**).

Abbreviations: ACTH, Adrenocorticotrophic hormone; AIF, Apoptosis-inducing factor mitochondria-associated 1; AMPK, Protein kinase AMP-activated catalytic subunit alpha 1; APAF-1, Apoptotic protease-activating factor-1; ATP, Adenosine triphosphate; Bcl-2, Apoptosis regulator; BNIP3L, BCL2 interacting protein 3 like; CAF, Cancer-associated fibroblasts; CAPN2, Calpain 2; CK, Choline kinase alpha; CTLs, Certain cytotoxic T cells; DNA, Deoxyribonucleic acid; Drp1, Dynamin-related protein 1; ER, Endoplasmic reticulum; ESI-MS, Electro-spray ionization-mass spectrometry; FADH2, Flavin adenine dinucleotide reduced; Fis1, Mitochondrial fission factor fission-1; FUNDC1, FUN14 domain containing 1; GH, Growth hormone; HNE, 4-hydroxynonenal; HTRA2/OMI, HtrA serine peptidase 2; IDH1, Isocitrate dehydrogenase 1; IL-18, Interleukin-18; IL-1β, Interleukin 1β; ITPR1, Inositol 1,4,5-trisphosphate receptor type 1; KIi-67, Nuclcar-associated antigen; LDHA, Lactate dehydrogenase A; LKB1, Serine/threonine kinase 11; MAVS, Mitochondrial antiviral signaling; MDSCs, Myeloid-derived suppressor cells; MFF, Mitochondrial fission proteins; Mfn1, Mitochondrial fusion proteins mitofusin 1; MHC-I, Major histocompatibility complex, class I; MMP-9, Matrix metallopeptidase 9; MT/ND1, Mitochondrially encoded NADH dehydrogenase 1; mtNOS, Mitochondrial nitric oxide synthase; mtROS, Mitochondrial ROS; NADH, Nicotinamide adenine dinucleotide; NF-κB/IRF, Nuclear factor kappa B subunit 1/tripartite motif containing 63; NK, Natural killer; NLRP3, NLR family pyrin domain containing 3; NO, Nitric oxide; Nrf2, Nuclear factor erythroid 2 like 2; OPA1, Optic atrophy 1; OPTN, Optineurin; OXPHOS, Oxidative phosphorylation; PD-L1, Programmed cell death 1 ligand 1; PD-L2, Programmed cell death 1 ligand 2; PGAM5, PGAM family member 5; PI3K, Phosphatidylinositol-4,5-bisphosphate 3-kinase catalytic subunit beta; PINK1, PTEN-induced putative kinase protein 1; PITX2, Paired like homeodomain 2; PPP3CA, Protein phosphatase 3 catalytic subunit alpha; PPPM, Predictive, preventive, and personalized Medicine; PRKCA, Protein kinase C alpha; PTEN, Phosphatase and tensin homolog; Ras, RAS proto-oncogene GTPase; Rheb, Ras homolog mTORC1 binding; RIG-I, Retinoic acid-inducible gene I; RNA, Ribonucleic acid; RNS, Reactive nitrogen species; ROS, Reactive oxygen species; SDH, Succinate dehydrogenase; SIRT3, Programmed cell death 1PD-1, sirtuin 3; SMAC/DIABL, Diablo IAP-binding mitochondrial protein; TBK1, TANK binding kinase 1; TCA, Tricarboxylic acid cycle; TFF3, ENDOG trefoil factor 3; TLR2, Toll-like receptor 2; TNF, Tumor necrosis factor; Tregs, Regulatory T cells; TSC1/2, TSC complex subunit ½.

MITOCHONDRIAL DYSFUNCTION-MEDIATED REPROGRAMMING ENERGY METABOLISM

Energy metabolism alterations are an emerging hallmark in tumor, which are still an unresolved issue that how energy

TABLE 1 | Some drugs targeting mitochondria as a therapeutic strategy for pituitary adenomas.

References	Drug	Testing index	Mechanisms	Species
Yang et al. (26)	Melatonin	Caspase-3 activity, Bax mRNA expression, cytochrome c protein expression, Bcl-2 mRNA expression, and mitochondrial membrane potential.	Inhibits cell growth and increases cell apoptosis	Rat
Wang et al. (27)	Melatonin inhibitor	The activities of mitochondrial respiratory complexes, and the production of ATP.	Induces apoptosis	Rat
Dai et al. (28)	Temozolomide and pyrimethamine	Cell cycle arrest, DNA damage, cytochrome c release from mitochondria into cytosol, the expression of cathepsin B and Bax, decreased expressions of Bcl-2, MMP-2 and MMP-9, cleaved PARP, and phosphorylated histone H2AX as well as caspase3/7, 8, and 9 activities.	Inhibit proliferation, invasion and induce apoptosis of pituitary adenoma cell lines	Rat/mouse
Wang et al. (29)	18beta-glycyrrhetinic acid	Cell damage, cell viability, lactate dehydrogenase release, reactive oxygen species (ROS) and Ca(2+) concentration, G0/G1 phase arrest, apoptosis rate, mitochondrial membrane potential, a ratio of B cell lymphoma 2 (Bcl-2) and Bax, calcium/calmodulin-dependent protein kinase II (CaMKII), c-Jun N-terminal kinase (JNK), and P38.	Inhibits proliferation, and induces apoptosis	Rat
Tang et al. (30)	Gossypol acetate	Expressions of Bcl-2 and miR-15a.	Inhibits cell growth	Rat
Ji and Geng (31)	Yougui pill	The number of apoptotic cells, mRNA expressions of cytochrome c, caspase-3, caspase-9, and Bcl-2.	Mitochondria-mediated apoptosis pathway	Rat
Zhou et al. (32)	T-2 toxin	Intracellular NO and antioxidant enzyme activity, DeltaPsim, morphometric changes of mitochondria, the caspase pathway, and inflammatory factors.	Induces cell apoptosis	Rat
Zhao et al. (33)	Grifolic acid	Cellular ATP levels and the intracellular NAD/NADH ratio.	Induces cell death	Rat
Zhang et al. (34)	T-2 toxin	Reactive oxygen species (ROS), mitochondrial membrane potential, percentage of apoptotic cells, expression of p53, the activation of caspase-3, G1 cell population, mRNA and protein expressions of p16 and p21, cyclin D1, CDK4.	Induces cell apoptosis	Rat
Wei et al. (35)	Paeoniflorin	Protein expressions of cleave caspase-9, caspase-3, Bax, and Bcl-2, and phosphorylated p53.	Inhibits cell proliferation, and induces cell apoptosis	Rat
Deyu et al. (36)	T-2 toxin	Reactive oxygen species (ROS), DNA damage, the mitochondrial membrane potential, the superoxide dismutase (SOD) activity, expressions of glutathione peroxidase 1 (GPx-1), catalase (CAT), mitochondria-specific SOD-2, mitochondrial uncoupling protein-1, -2, and -3 (UCP-1, 2, and 3), adenosine triphosphate (ATP) levels, mitochondrial complex I activity, and the expressions of most of mitochondrial electron transport chain subunits, the expressions of mitophagy-specific proteins NIP-like protein X (NIX), PTEN-induced putative kinase protein 1 (PINK1), and E3 ubiquitin ligase Parkin.	Causes cell apoptosis	Rat
Kim et al. (37)	Cyclosporine A (CsA)	CsA induced a dose-dependent increase in expression of the autophagy markers LC3-I and LC3-II. Cell viability decreased significantly with increasing CsA concentrations largely due to an increase in apoptosis, with the changing level of Bcl-2 and Bax.	Induction of apoptotic or autophagic cell death i	Rat
Leng et al. (38)	Dopamine agonists	Dopamine receptor D5 activation increased production of reactive oxygen species (ROS), inhibited the MTOR pathway, induced macroautophagy/autophagy, and led to autophagic cell death (ACD) *in vitro* and *in vivo*.	Induced macroautophagy/autophagy	Human pituitary tumor cell
Wang et al. (39)	Bromocriptine (BRC) and artesunate (ART)	Low-dose ART combined with BRC synergistically inhibited the growth of GH3 and MMQ cell lines, caused cell death, attenuated cell migration and invasion, and suppressed the expression of extracellular prolactin. The induction of apoptosis after co-treatment was confirmed by immunofluorescent staining, assessment of caspase-3 protein expression, and flow cytometry.	Induction of apoptosis	Rat

metabolism system plays in formation and progression of tumors or metastases. Tumor cell energy metabolism has mainly focused on glucose metabolism and lipid metabolism. The metabolism of glucose to lactic acid in the presence of oxygen have been recognized in cancer cells, commonly called the Warburg effect (63). Further, the reverse Warburg effect put forward in 2009 provides complementary mechanisms for cancer energy metabolism (64). In addition, novel evidence is shedding light

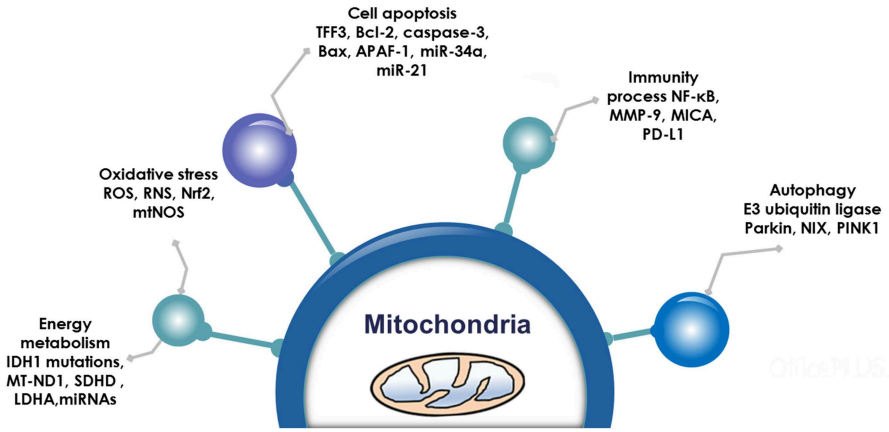

FIGURE 1 | Mitochondrial functions. Emerging data show that mitochondria are associated with energy metabolism, oxidative stress, cell apoptosis autophagy, and immunity process in pituitary adenomas.

on alterations in lipid metabolism-associated pathways that have been discussed for past years. A gene expression study find that the upregulated lipogenesis pathways are associated with poor survival outcomes (65), and the elevated levels of lipid droplets are associated with cancer aggressiveness, which has been proposed to predict prognosis of cancer (66). More interesting is that lipids could be transferred from adipocytes to cancer cells by co-culture condition to promote cancer cell growth (67). It clearly indicates that lipid metabolism disorder is closely associated with tumorigenesis, whose study would be significantly enhanced with the development of lipidomics based on electrospray ionization/mass spectrometry (ESI-MS) (68).

The citric acid cycle, oxidative phosphorylation (OXPHOS), and fatty acid beta-oxidation occur in the matrix of the mitochondrion in eukaryotic cells. Mitochondrial dysfunction is closely associated with energy metabolism reprogramming to associate cancer formation or progression (69). In the Warburg and reverse Warburg effects, cancer cells have metabolic symbiosis with mesenchymal cells, especially cancer-associated fibroblasts (CAFs), namely cancer cells produce reactive oxygen species (ROS) to induce oxidative stress and aerobic glycolysis of CAFs; in turn, CAFs produce lots of nourishments (especially lactate and pyruvate) to feed the adjacent cancer cells to produce more ATPs (64). The reverse Warburg effect shows metabolic interplay between high glycolytic cells and mitochondrial OXPHOS activates cells via lactate shuttle. Important enzymes involved in mitochondrial OXPHOS include the enzymes in the citric acid cycle and electron transport chain. The citric acid cycle is a series of enzymatic reactions to release energy through the oxidation of acetyl-CoA into ATP and carbon dioxide. The citric acid cycle is undergoing 10 steps to complete ATP production with a series of enzymatic reactions, including citrate synthase, aconitase, isocitrate dehydrogenase, α-ketoglutarate dehydrogenase, succinyl-CoA synthetase, succinate dehydrogenase, fumarase, and malate dehydrogenase. OXPHOS is the metabolic pathway in which cells use enzymes to oxidize nutrients for releasing energy to produce ATP. The eukaryotic electron transport chain contains NADH-coenzyme Q oxidoreductase (complex I), succinate-Q oxidoreductase (complex II), Q-cytochrome c oxidoreductase (complex III), cytochrome coxidase (complex IV), and ATP synthase (complex V). Furthermore, fatty acid molecules are broken down in the eukaryotic mitochondria to transform into acetyl-CoA to enter the citric acid cycle, and generate NADH and FADH2 that are co-enzymes used in the electron transport chain (**Figure 2**).

Mitochondria are the main location of energy metabolism pathways (citric acid cycle, OXPHOS, and fatty acid beta-oxidation). Some mitochondria-associated proteins have been reported to play a critical role in pituitary adenomas. For example, overexpression of lactate dehydrogenase A significantly promotes proliferation and invasion of pituitary adenomas, and positively correlates with higher Ki-67 index (41). Mutant succinate dehydrogenase in the citric acid cycle occurs in the pituitary adenomas (42). In addition, DNA sequencing-based genotypic studies demonstrate identical IDH1 mutations (c.394 C > T) in pituitary adenomas tissues (43). The high frequency of respiratory complex I mutations are found in mitochondrial DNA in a large panel of oncocytic pituitaries, which indicates dysfunction of respiratory complex I to cause instability of HIF1alpha in pituitary adenomas. Briefly, mutations in the mitochondria-coded MT-ND1 gene, an important composition of respiratory complex I, is closely associated with energy metabolic impairment to influence balance of succinate and alpha-ketoglutarate, which leads to the abnormal citric acid cycle metabolites (succinate and alpha-ketoglutarate) to be responsible for HIF1alpha stabilization in pituitary adenomas (44). The multifunctional succinate dehydrogenase (SDH) is located in the inner membrane of mitochondria, and serves as a critical step in Krebs cycle and a crucial member of the respiratory chain. SDH subunit D (SDHD) mutation is found in an aggressive GH-secreting pituitary adenoma, indicating SDHD mutation might link to the progression of pituitary adenomas (45). The study on SDH subunit B (SDHB) (+/–) mice finds that SDHx-deficiency is a main initiator to result

TABLE 2 | Mitochondrial dysfunction pathway in the pathogenesis of pituitary adenomas.

References	Biological process	The related molecules	Function mechanism	Species
An et al. (41)	Energy metabolism	Lactate dehydrogenase A (LDHA)	LDHA suppresses glucose uptake, lactate secretion, invasion and proliferation.	GH3 cells
Casar-Borota et al. (42)	Energy metabolism	Isocitrate dehydrogenase (IDH) 1 and 2	Mutant IDH1 and IDH2.	Human tissue specimen
Hao et al. (43)	Energy metabolism	Isocitrate dehydrogenase 1 (IDH1)	Somatic IDH1 mutation.	Human tissue specimen
Porcelli et al. (44)	Energy metabolism	Hypoxia inducible factor 1 subunit alpha(HIF1A)	A high frequency of homoplasmic disruptive mutations implicates disassembly of respiratory complex I *in vivo* which in turn contributes to the inability of oncocytic tumors to stabilize HIF1alpha.	Human tissue specimen and cell
Xekouki and Stratakis (45)	Energy metabolism	Succinate dehydrogenase (SDHx)	Loss of heterozygosity at the SDHD locus.	Human tissue specimen
Xekouki et al. (46)	Energy metabolism	Succinate dehydrogenase (SDH)	SDHD mutation.	Human tissue specimen and rats
Wu et al. (47)	Energy metabolism	Hsa-mir-181a-5p	Prolactin signaling pathway, and mitochondria related calcium reabsorption.	Human tissue specimen
Feng et al. (48)	Energy metabolism	14-3-3η protein	14-3-3η is exclusively overexpressed in oncocytomas, and 14-3-3η is capable of inhibiting glycolysis, leading to mitochondrial biogenesis in the presence of rotenone. In particular, 14-3-3η inhibits LDHA by direct interaction in the setting of complex I dysfunction.	Human tissue specimen and cell
Wang et al. (29)	Oxidative stress	Reactive oxygen species (ROS) and Ca^{2+} concentration	Activation of ROS/MAPKs-mediated pathway.	MMQ and GH3 cells
Pawlikowski et al. (49)	Oxidative stress	Nitric oxide synthase (NOS)	NOS immunoreactivity is also detectable in all but two human pituitary adenomas and seems to negatively correlate with microvascularization.	Human tissue specimen and rats
Sabatino et al. (50)	Oxidative stress	Nuclear factor, erythroid 2 like 2 (Nrf2)	The evidence of oxidative stress in pituitary cells, accompanies by bigger and round mitochondria during tumor development, associates with augmented biogenesis and an increased fusion process.	Rats
Jaubert et al. (51)	Oxidative stress	Dopamine (DA)	(i) loss of mitochondrial potential; (ii) relocation of Bax to the mitochondria; (iii) cytochrome c release; (iv) caspase-3 activation, and (v) nuclear fragmentation, resulting in apoptosis.	GH3 cells
Onishi et al. (52)	Oxidative stress	The inducible NOS (iNOS)	Invasive adenomas have higher iNOS immunoreactivity, and this correlates with the MIB-1 labeling index.	Human tissue specimen
Huang et al. (53)	Oxidative stress	Nitric oxide (NO)	Nitric oxide mediates Nivalenol (NIV)-induced oxidative stress. Additionally, NIV induces caspase-dependent apoptosis, decrease in mitochondrial membrane potential and mitochondrial ultrastructural changes.	GH3 cells
Babula et al. (54)	Oxidative stress	Nitric oxide (NO) metabolites level in serum	The decrease of NO level after pituitary adenoma resection indicates the relationship between NO synthesis and pituitary adenoma occurrence.	Human
Guzzo et al. (55)	Apoptosis	Bcl-2 family	The intrinsic pathway (or mitochondrial) and extrinsic (or death-receptor pathway)	Rat pituitary cell lines, and human pituitaries tissue

(Continued)

TABLE 2 | Continued

References	Biological process	The related molecules	Function mechanism	Species
Gottardo et al. (56)	Apoptosis	Humanin (HN) and Rattin (HNr)	Intratumor injection of BV-shHNr to nude mice bearing s.c. GH3 tumors increases the number of apoptotic cells, delays tumor growth, and enhances survival rate, suggesting that endogenous HNr may be involved in pituitary tumor progression.	GH3 cells
Gao et al. (57)	Apoptosis	Trefoil factor 3 (TFF3)	TFF3 protein level in pituitary adenoma is about 3.61 ± 0.48 folds of that in normal tissues ($P < 0.01$). After transfecting with small interference RNA (siRNA) against TFF3, the apoptotic ration is significantly elevated.	Human pituitary adenoma cell HP75
Tanase et al. (58)	Apoptosis	Apoptotic protease-activating factor-1 (APAF-1)	A bidirectional-inverted relationship between APAF-1 and cathepsin B expressions may result in changes in pituitary adenoma behavior.	Human tissue specimen
Yang et al. (59)	Apoptosis	MicroRNA-34a	miR-34a expression is significantly lower in GH4C1 cells, whereas miR-34a overexpression significantly inhibits GH4C1 cell proliferation and promotes cell apoptosis though SRY-box 7 (SOX7).	Rats
Cui et al. (60)	Apoptosis	MicroRNA-21	MiR-21 targets 3'-UTR of PITX2 gene to inhibit its expression. The elevated miR-21 and/or silencing PITX2 significantly depress PITX2 expression in HP75 cells, potentiate caspase-3 activity, decrease cell proliferation, and facilitate apoptosis.	Human tissue specimen
Wang et al. (39)	Apoptosis	MicroRNA-200c	MicroRNA-200c expression was inversely associated with Pten expression and facilitated apoptosis.	GH3 cells
Gong et al. (61)	Apoptosis	Adrenocorticotrophic hormone	UA inhibits the viability, and induces apoptosis of AtT20 cells, and decreases ACTH secretion.	AtT20 cells
Deyu et al. (36)	Autophagy	T-2 toxin	T-2 toxin induces abnormal cell morphology, cytoplasm and nuclear shrinkage, nuclear fragmentation and formation of apoptotic bodies, and autophagosomes.	GH3 cells
Kim et al. (37)	Autophagy	Cyclosporine A	Bcl-2 levels showed drug dose-dependent augmentation in autophagy and were decreased in apoptosis.	GH3 cells
Leng et al. (38)	Autophagy	Dopamine agonists	The increasing Reactive oxygen species (ROS) inhibited the MTOR pathway, induced macroautophagy/autophagy, and led to autophagic cell death (ACD) *in vitro* and *in vivo*.	Human pituitary tumor cell
Tagliati et al. (62)	Tumor immune	Presequence translocase associated motor 16 (MAGMAS)	Mitochondria-associated protein is involved in granulocyte-macrophage colony-stimulating factor signal transduction.	Human tissue specimen and AtT-20 D16v-F2 cells

in the cascade of molecular events for the formation of pituitary adenomas (46). The whole-exome sequencing analysis of pituitary oncocytomas found mitochondrial DNA mutations, respiratory complex I dysfunction, and reductions of lactate and lactate dehydrogenase A (LDHA) (48). Besides glycometabolism change, lipid metabolism is also alerted in pituitary adenomas. The gene microarray analysis of miRNAs expression profile between invasive and non-invasive non-functional pituitary adenomas finds that fatty acid metabolism plays a prominent role in pituitary adenomas (47). Therefore, energy metabolism alteration plays important roles in pituitary adenomas with high metabolic demand, which also influences cell proliferation, growth, and angiogenesis. The development of new drugs targeted mitochondria might be an new approach to block

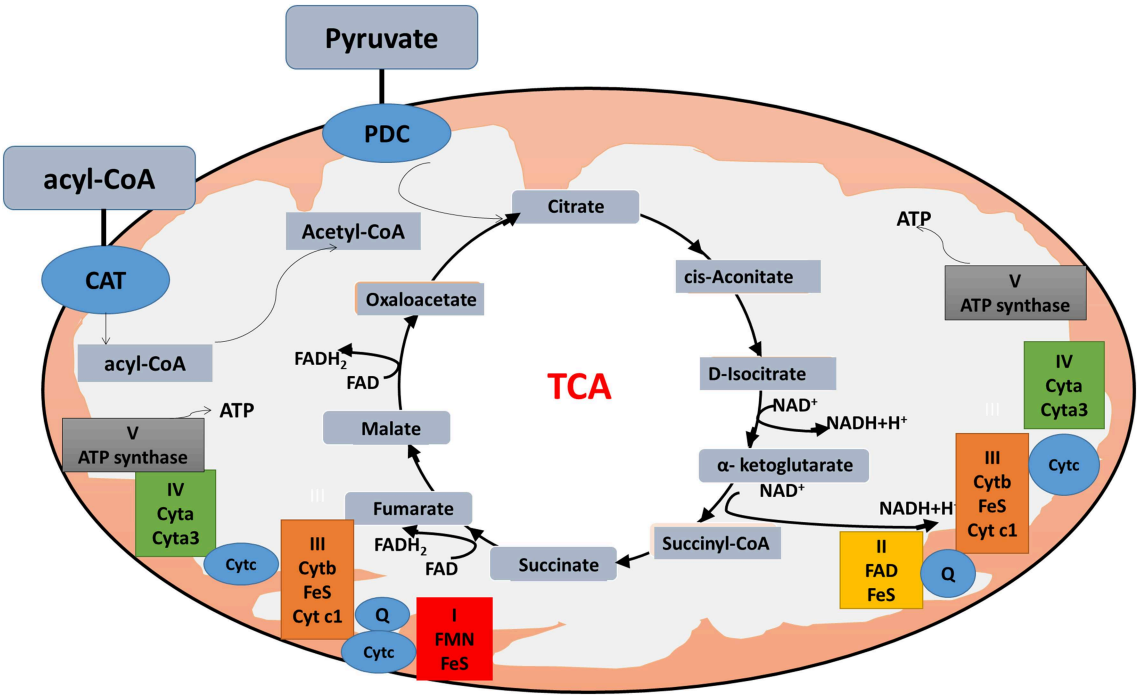

FIGURE 2 | Mitochondrial physiology. Acetyl-CoA enters the mitochondrion via pyruvate or fatty acids. Pyruvate is imported through the mitochondrial inner membrane by the pyruvate dehydrogenase complex (PDC), and is oxidatively decarboxylated to produce acetyl-CoA. Fatty acids form acyl-CoA in the cytosol, and are transported into mitochondrion through carnitine (CAT) for β-oxidation. Acyl-CoA enters the citric acid cycle, and generates NADH and FADH2 (co-enzymes used in the electron transport chain) to produce ATP.

energy metabolism pathways for effective treatment of pituitary adenomas (70).

MITOCHONDRIAL DYSFUNCTION-MEDIATED OXIDATIVE STRESS

Oxidative stress reflects an imbalance between free radical/reactive oxygen/nitrogen species (ROS/RNS) productions and endogenous antioxidant defense mechanisms in the cells and body, which results in damage to proteins, DNA, membrane, and cellular organelles so on (71). ROS/RNS can be beneficial because they take part in attacking and killing pathogens by the immune system (72). Short-term oxidative stress might also be meaningful in prevention from aging (73). However, oxidative stress is also involved in the development of various diseases including cancers (74–79). Severely oxidative stresses even cause cell death, apoptosis, necrosis, cell migration, fibrosis, and angiogenesis. The lipid peroxidation of fatty acids as a type of oxidative stress increased ROS/RNS to injury bilayer lipid membranes. The secondary products of lipid peroxides such as malondialdehyde, aldehydes, 4-hydroxynonenal (HNE), hexanal, or acrolein have very long and broad effects (80).

Elevated level of ROS was a key constituent in cancer survival and resistance to treatment. The mitochondrial OXPHOS system is the major sites where produce endogenous ROS, including OH and superoxide radicals ($O_2^{\cdot -}$) (81). Mitochondrial complexes I, II, and III play a crucial role in the generation of mitochondrial ROS. Electrons tend to be leaky at complexes I and III to cause the incomplete reduction of oxygen to generate a free radical such as superoxide (80). Mitochondrial dysfunction could result in the increased ROS in cancer cells to mediate tumor-related signaling pathways and activate pro-oncogenic signaling, which regulate cancer progression, angiogenesis, metastasis, and survival (**Figure 3**). Although increased ROS does not benefit the cancer cell survival, however, antioxidant substance system is also activated in cancer cells to help cancer cell death escape (82). Moreover, the presence of mitochondrial nitric oxide synthase (mtNOS) provided the opportunity to review complementary aspects of mitochondrial physiology. The mtNOS could cause the generation of a partial nitric oxide (NO) in mitochondria (83), besides large amounts of NO produced by inducible NOS (iNOS) in pathophysiological status (84). NO can react quickly with the superoxide radicals to generate more toxic peroxynitrite anion ($ONOO^-$) or hydroxyl radical ($\cdot OH$). Mitochondria, as generators and targets of NO, determine the steady-state of NO though modulating the rates of consumption and production at the subcellular levels. Thus, mtNOS plays a crucial role in this process, which was activated by calcium and transcriptional/translational regulation (85). Furthermore, NO production in mitochondria was still decided by subcellular localization of mtNOS due to post-translational modification or protein-protein interactions. Therefore, mitochondria could

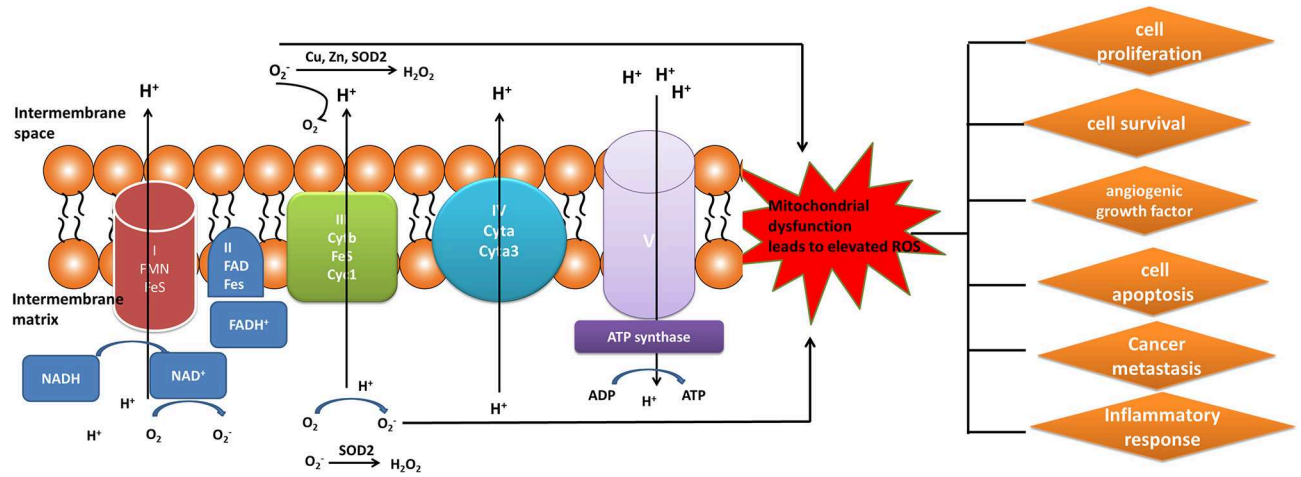

FIGURE 3 | Mitochondrial generation of ROS. Complexes I, II, and III (complexes located on electron transport chain) play a pivotal role in the generation of ROS during the process of oxidative phosphorylation. The increased ROS regulated cancer progression, angiogenesis, metastasis, and survival.

produce NO by temporospatial distribution of mtNOS, and receive NO signal to regulate mitochondrial events (86).

It needs further study for imbalance of ROS and RNS production resulted from mitochondria dysfunction in pituitary adenomas. Many studies found the presence of ROS/RNS in human pituitaries, and the increased activities of ROS/RNS in pituitary adenoma compared to control tissues (41, 49). Also, oxidative stress in pituitary adenoma cells is accompanied by mitochondria swelling during tumor development, and associated with an increased fusion process and augmented biogenesis. An activation of the nuclear factor erythroid 2 like 2 (Nrf2) pathway and the reduction of oxidative damage signals were also observed during tumor development, which might provide survival advantages to pituitary adenoma cells (50). ROS pathway tends to be a medium in human pituitary cells. The pro-apoptotic effects are regulated partly by the dopamine transporter in GH3 pituitary cell lines, and involve oxidative stress as well as ROS formation. The use of only dopamine to treat hypophysis cells found that intracellular ROS was increased rapidly, and antioxidant N-acetyl-L-cysteine effectively inhibited dopamine-induced ROS generation and apoptosis (51). These data clearly demonstrated that ROS formation was closely related to signaling pathways in pituitary adenomas to affect tumor biological behavior. Studies found that 18beta-glycyrrhetinic acid had significantly antitumor effects on pituitary adenomas because this drug activated mitochondria-mediated ROS-mitogen-activated protein kinase (MAPK) pathways to induce cell apoptosis in pituitary adenomas, and that these activating effects were attenuated in pituitary adenomas by pretreatment with N-acetyl-L-cysteine, a ROS inhibitor (29). Moreover, many studies found the presence of NOS in human pituitaries, and NOSs were markedly higher expressed in invasive relative to non-invasive pituitary adenomas (52). NO mediated oxidative stress in pituitary adenoma cell lines to induce caspase-dependent apoptosis (53). Another study found that serum NO concentration was significantly decreased after the surgery of patients with pituitary adenomas ($n = 21$), thus monitoring serum NO level after pituitary adenoma surgery might benefit the prediction of its occurrence (54).

Thereby, oxidative stress has been considered as one of essential factors to contribute in the pathogenesis of pituitary adenomas. However, its molecular mechanisms remain unclear. The previous studies have been provided clues to the mechanism; for example, "mitochondrial theory of aging" increased production of ROS with altered expression of caveolae (87). It is meaningful to explore the roles of oxidative stress-mediated apoptosis, ER stress, DNA damage, metabolism, autophagy, migration, and anticancer drugs. The in-depth understanding of the relationship between oxidative stress and mitochondrial dysfunction might benefit improvement of chemotherapeutic approaches based on ROS/RNS-modulating drugs in the treatments of pituitary adenomas.

MITOCHONDRIAL DYSFUNCTION-MEDIATED CELL APOPTOSIS DYSREGULATION

Apoptosis is a gene-controlled form of programmed cell death, and is closely related to cancer. Apoptosis activation mechanisms include extrinsic and intrinsic pathways (88). The extrinsic pathway including FAS path and TNF path is activated by receptor-ligand-mediated model. Extracellular ligands binding to membrane death receptors result in the formation of death-inducing signaling complex (89). The intrinsic pathway including mitochondrial apoptosis and endoplasmic reticulum apoptosis pathways is activated by intracellular signals. Internal mitochondrial apoptosis pathway could be activated by internal apoptosis stimulators, such as persistent DNA damage, cell hypoxia, and cell growth factor deletion (90), or by death ligands and caspase 12. The Bcl-2 family proteins decrease the mitochondrial membrane potential

promotion and increase mitochondrial outer membrane permeabilization, which leads to release pro-apoptotic factors such as AIF, cytochrome c, SMAC/DIABL, HTRA2/OMI, and ENDOG from the mitochondria into the cytosol (91). The increased mitochondrial outer membrane permeabilization is generally considered to activate the apoptotic pathway because the formation of apoptosome in the cytosol induces the caspase cascade (**Figure 4**) (92). Mitochondrial dysfunction occurred in a human pituitary tumor with mitochondrial morphological and functional changes, including large mitochondria, mitochondrial irregular swelling, and partly or fully disintegrated cristaes (16). Mitochondrial dysfunction caused change of mitochondrial membrane potential and internal apoptosis stimulator responses, which leads to mitochondria-mediated apoptosis signaling pathway alteration (93).

From the embryology angle, many apoptotic cells are formed in Rathke's pouch tissues from the roof of oral ectoderm at an early stage of pituitary gland formation. However, when adenohypophysis is formed in the distal part of the gland, the ratio of apoptotic cells was significantly lower than early stage. It means that an imbalance in apoptosis process might be the boundary between embryonic development and tumor progress. It is interested that pituitary adenoma cells undergo the imbalanced expressions of apoptosis-related genes/proteins to cause uncontrolled cell proliferation (55). Study found that targeting mitochondria could have an effective impact on the treatment of pituitary tumors through apoptosis pathway (56). For example, trefoil factor 3 (TFF3) is an apoptosis-related protein, and its knockout in human pituitary adenoma cell line decreased the levels of apoptosis-related proteins Bcl-2 and caspase-3, and increased the levels of Bax and cleaved caspase-3. It clearly demonstrated that TFF3 protein knockout can accelerate the apoptosis in human pituitary adenoma cells via mitochondrial apoptosis pathway (57). Moreover, apoptotic protease-activating factor-1 (APAF-1) is a pivotal functional protein to involve in the intrinsic mitochondrial apoptosis pathway. Low expression of APAF-1 was detected in most invasive pituitary adenomas, and was negatively correlated with the aggressive behavior of invasive pituitary adenoma, which suggested that shifting the balance of apoptosis mediators in cells could lead to changes of pituitary tumor behaviors (58). In addition, some microRNAs-target genes to mediate apoptosis pathway also have been found in pituitary adenomas. For example, tumor suppressor microR-34a overexpression significantly inhibited cell proliferation and promoted cell apoptosis in pituitary adenoma cells (59). miR-21 expression was lower in invasive relative to non-invasive pituitary adenoma tissues, and miR-21 targeted 3'-UTR of PITX2 gene to enhance caspase-3 activity, which inhibits cell proliferation and facilitates apoptosis in pituitary adenoma cells (60). Dysregulation of apoptosis-related proteins might be meaningful indicator of tumor progression because mitochondrial dysfunction pathway might facilitate tumorigenesis and tumor development (94).

The novel mechanisms in mitochondrial dysfunction-mediated cell apoptosis would facilitate the development of effective anti-cancer drugs. For example, the classical antitumor effect of paclitaxel is to target on tubulin in the cytoplasm. However, further study found that paclitaxel induced apoptosis by promoting the release of Cyt C after binding with Bcl-2 (95), which promoted one to accurately deliver paclitaxel though well-designed nanocarrier to improve its treatment performance (94). Furthermore, for adrenocorticotrophic hormone (ACTH)-producing pituitary adenomas (96), ursolic acid was found to be a potential agent targeting ACTH-producing AtT20 cells because ursolic acid inhibited cell proliferation, reduced ACTH secretion, and induced cell apoptosis in AtT20 cells with the decreased ratio of Bcl-2 to Bcl2-associated X protein to cause the release of mitochondrial cytochrome c from mitochondria to the cytosol, and activate subsequently caspase-9, -3/7, and -8. It indicates that ursolic acid may be a promising candidate drug for the treatment of ACTH-producing pituitary adenomas (61). Therefore, insights into mitochondria-mediated apoptosis might benefit the development of novel pro-apoptotic therapeutic drugs and discovery of biomarkers for early detection to treat a pituitary adenoma.

MITOCHONDRIAL DYSFUNCTION-MEDIATED AUTOPHAGY DYSREGULATION

Autophagy or autophagocytosis meaning "self-devouring" is the natural process and common cellular phenomenon, which is involved in the processes of phagocytosis and degradation of dysfunctional or unnecessary cell components, and also reusing of cellular components (97, 98). Briefly, the dysfunctional or unnecessary components are engulfed to form a double membrane called autophagosome, and then autophagosome is fused with the lysosome, followed by degradation of the contents into smaller constituents via acidic lysosomal hydrolase within lysosome (99). Autophagy takes part in various cellular functions, and particular attention has been paid to dual functions of autophagy in cancer—both protection cells against cancer and a potentially factor in cancer cell survival. Autophagy is regulated by many of the proteins, including oncogene and tumor suppressor proteins. Specifically, tumor suppressor proteins that negatively regulate mTOR pathway, such as LKB1, PTEN, TSC1/2, and AMPK, stimulate autophagy, while oncogenes that activate mTOR pathway, such as Ras, class I PI3K, AKT, and Rheb, inhibit autophagy, indicating the contribution of autophagy to cancer growth or tumor suppression. Moreover, the inhibition of autophagy induces genomic instability, oxidative stress, and tumorigenesis. Nevertheless, autophagy also functions as a protective factor under stress conditions, including nutrient starvation, and hypoxia that facilitates tumor cell survival and sensitivity and resistance to chemotherapy (100).

Mitophagy is the complex biological process that cells selectively eliminate mitochondria by autophagy. The engulfment of mitochondria forms a double-membrane-enclosed autophagosome and then fuses with lysosomes. The process emits high-energy substances to recycle cell compartment, including fatty acids and amino acids (**Figure 5**) (101). Defective mitochondria undergoing damage or stress tend to the induction of mitophagy. However, the occurrence of mitophagy is not only

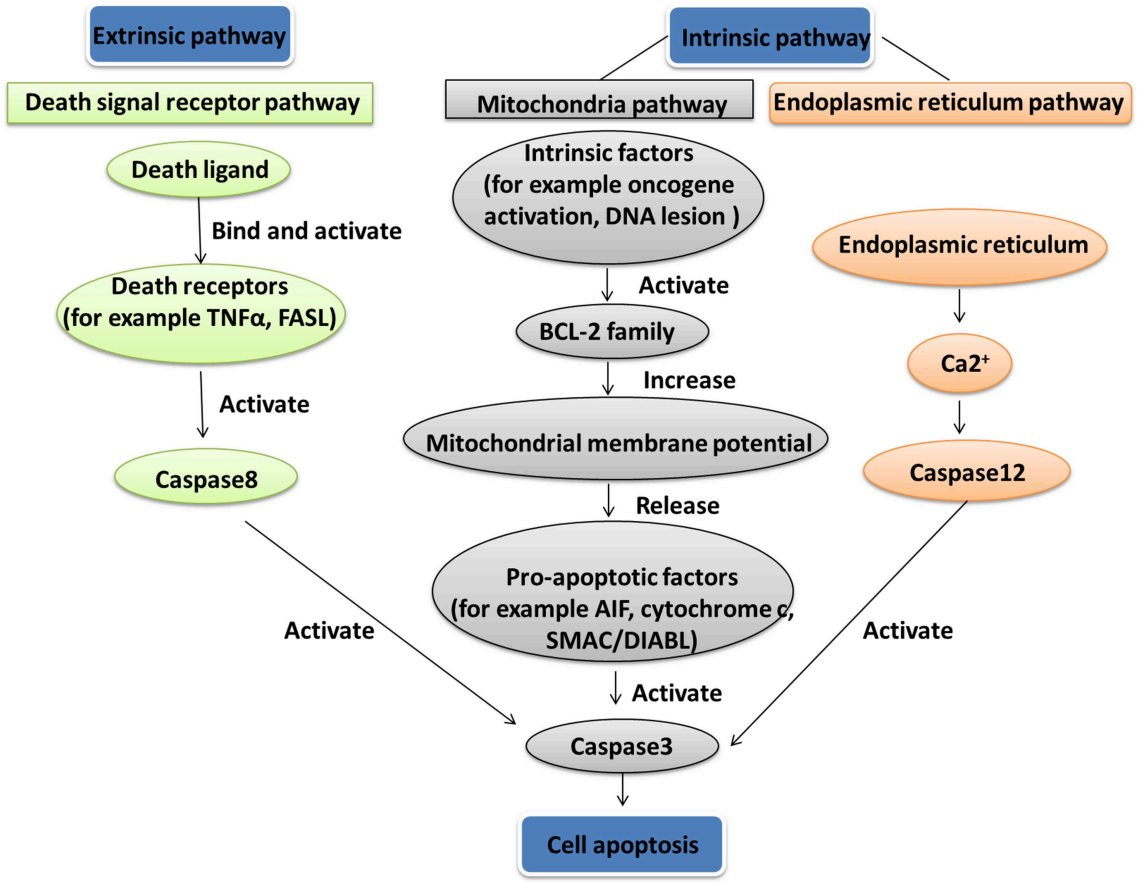

FIGURE 4 | Apoptosis pathway. Two apoptosis activation mechanisms are the extrinsic and intrinsic pathways. The extrinsic pathway, including Fas path and TNF path, is activated by receptor-ligand-mediated model. The intrinsic pathway, including the mitochondrial apoptosis pathway and endoplasmic reticulum apoptosis pathway, is activated by intracellular signals.

restricted to the defective mitochondria but also involves normal ones (102). Mitophagy promotes turnover and the selective degradation of mitochondria, and prevents accumulation of dysfunctional mitochondria, which can lead to keep steady-state mitochondrial turnover, cellular metabolic needs, and certain cellular developmental stages (102). In this process, mitophagy depends on the general autophagy mechanism, meanwhile, both "mitophagy adaptors" and regulatory molecules are involved, such as p62, FUNDC1, prohibitin2, BNIP3L (NIX), PGAM5, OPA1, TBK1, CK, OPTN, and Bcl2-L13 (103). Those autophagy-related proteins activate downstream mitophagy pathways by post-translational modifications (104). Two distinct principal mitophagy mechanisms had been proved in mammalian cells. Firstly, receptor-mediated mitophagy is activated, and then recruits Atg8-like proteins to mitochondria to increase combination. Secondly, the highly ubiquitylated mitochondrial outer membrane proteins recruit bifunctional adapter proteins, which in turn increases the binding of Atg8-like proteins (105). Atg8-like proteins prompts encapsulation of mitochondria into autophagosomes through the expansion of the phagophore membrane; and fusion with the lysosome results in the formation of autolysosomes facilitating degradation of selected dysfunctional mitochondria (106). Also, mitophagy receptors exist some complex regulation mechanisms. An unmodified receptor is phosphorylated by a kinase, activating or deactivating downstream mitophagy pathway by increasing or decreasing Atg8-like proteins binding. This effect can be reversed by phosphatases. For NIX (BNIP3L), BCL2L13, and BNIP3, only the activated phosphorylation and the modified residue mechanism are understood but the kinases or phosphatases have not been identified yet for FUNDC1, the activated and deactivated phosphorylation intracellular mechanisms, the modified residues and participated kinases or phosphatases are well-known (107).

Mitochondrial dysfunction might affect mitophagy that can be related to metabolic reprogramming, inflammatory signaling, cell fate determination and differentiation, DNA damage responses in response to stress, which in turn lead to human disease incidence and etiology, including malignant tumor (103). It is well-known that mitophagy and mitochondrial dysfunction are related to pituitary adenomas. The mitochondrial toxicity and protective mechanisms of T-2 toxin are not fully understood

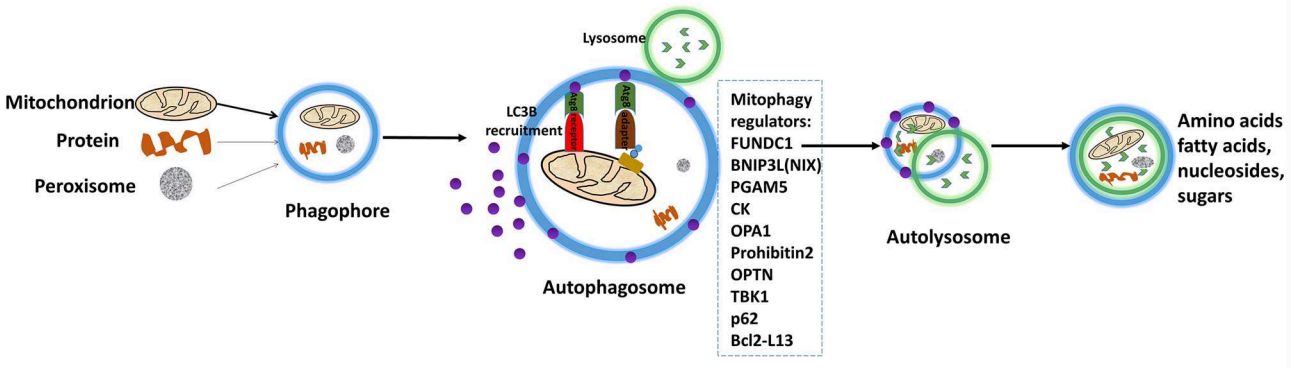

FIGURE 5 | Depiction of the process of mitophagy. The engulfment of mitochondria forms a double-membrane-enclosed autophagosome, and then fuses with lysosomes. The process emits high-energy substances to recycle cell compartment, for example fatty acids and amino acids. Modified from Li et al. (15), with permission from Bioscientifica Limt.

in mammalian cells (108). The investigation of the cellular and mitochondrial toxicity of T-2 toxin shows that T-2 toxin significantly increases mitophagic activity, ROS and DNA damage in rat pituitary GH3 cells. With the increased expression of mitophagy-specific proteins, including E3 ubiquitin ligase Parkin, NIP-like protein X (NIX), and PTEN-induced putative kinase protein 1 (PINK1), T-2 toxin can be increased (109). The regulating mechanism of mitophagy is also mediated by nuclear factor (erythroid-derived 2)-like 2 (Nrf2)/PINK1/Parkin pathway in pituitary GH3 cells. The relevant drug activates the protective protein kinase A signaling pathway, which activates the Nrf2/PINK1/Parkin pathway to mediate mitophagy. Taken together, increasing mitophagy and mitochondrial dysfunction might increase chemo-resistance in pituitary GH3 cells (36). Sometimes apoptosis and autophagy coexist. Dopamine agonists such as bromocriptine and cabergoline have been successfully used in the treatment of pituitary prolactinomas. DRD5 activation increases production of ROS, inhibits the MTOR pathway, induces macroautophagy/autophagy, and leads to autophagic cell death (ACD) in human pituitary tumor cells (38). In addition, when cyclosporine A (CsA) induces apoptotic and ACD in pituitary GH3 cells, Bcl-2 levels show dose-dependent augmentation in autophagy and are decreased in apoptosis (37).

Autophagy can promote survival of tumor cells in starvation mode, or degrade cell apoptotic mediators to maintain the tumor clone. In such cases, treated patients with the late stage of autophagy—blockers (such as chloroquine), on the cells that depend on autophagy to survive, may be one of viable therapeutic measurements in fighting cancer (110). Thus, the qualities of mitophagy can be used as a therapeutic method for cancer prevention. Mitophagy plays a role in tumor suppression and tumor cell survival. One strategy is to induce mitophagy and enhance the function of antitumor. The other strategy is to inhibit mitophagy and thus induce apoptosis (111). The first strategy has been tested by monitoring dose-response anti-tumor effects during autophagy-targeted therapies. These treatment effects have shown that autophagy has some dose-dependence in tumor suppression and tumor cell survival progression. The result supports the development of therapies through autophagy (112). In addition, inhibition of the protein related to autophagy pathways may also serve as an anticancer therapy (113). Autophagy is a protein degradation system to play a role in maintaining homeostasis and inducing apoptosis. Thus, sometimes inhibition of autophagy has on the probability of existential risk as it may lead to tumor development instead of the desired cell death (114).

MITOCHONDRIAL DYSFUNCTION-MEDIATED TUMOR IMMUNITY

Tumor immune escape is an important hallmark in cancer (115). Tumor-evading immune destruction is closely correlated with prognosis or survival in various tumors (116). A study found a number of tumor immunity-related inflammatory cells, for example, cytotoxic T cells (CTLs), regulatory T cells (Tregs), myeloid-derived suppressor cells (MDSCs), and natural killer (NK) cells (37). It also found a number of tumor immunity-related pathways, such as altered interleukin signaling (117), MHC-I pathway (118), type 1 cytokine-induced T-cell (119), interferon gamma signaling (120), type I interferon-mediated responses (121), and transcription factor nuclear factor-kappa B (122). Along with the advancement in tumor immunology, the immune-checkpoint blockade therapy has been an important aspect in the mode of combined therapy of tumor. One of the most important immune checkpoint pathways has been applied between the PD-1 receptor expressed on activated T cells and its ligands, programmed death-1 ligand (PD-L1) and PD-L2 (123).

Immunity process is interlinked with mitochondrial function. Mitochondria can regulate immunity in different ways (**Figure 6**): (i) Current literature shows that many changes of cancers occurred in substance metabolism pathways such as TCA cycle, oxidative phosphorylation, fatty acid oxidation, and amino acid metabolism. Mitochondria that induce transcriptional key enzymes or important molecule changes

can lead to completely different results in immune cells (116). Thus, mitochondria can regulate differentiation, activation, and survival of immune cells (124). (ii) Mitochondrial DNA (mtDNA) could translocate from the mitochondria to cytoplasm and activate the NLRP3 inflammasome to induce IL-1β and IL-18 release (125). (iii) Mitochondria can transmit signals through mtDNA or mitochondrial ROS (mtROS) to regulate gene expressions of immune cells (126). (iv) Mitophagy is crucial for degradation of the damaged mitochondria, and the decreased mitophagy causes ROS increasing which further makes the susceptibility to infections (127). (v) Immune functions are influenced by fission and fusion of mitochondria, which determines mitochondrial mobility and mass. (vi) When mitochondria are located near endoplasmic reticulum (ER), the mitochondria and ER junction signaling could be activated in immune cells to influence immune cell metabolism (128). (vii) The inflammatory response can be initiated by mitochondrial antiviral signaling (MAVS). Therefore, mitochondrial machinery is crucial for immune functions, such as metabolic pathways, mtDNA, mtROS, mitochondrial dynamics, and mitophagy.

Tumor immune microenvironment is gradually recognized as a critical contributor in tumor progression, development, and control. The increasing studies show that immune cells infiltrate in pituitary adenomas. Dysregulation of several genes in granulocyte-macrophage colony-stimulating factor signal transduction has been regarded as a possible alteration underlying the occurrence and development of pituitary tumors, such as mitochondria-associated protein Tim 16. High-expression of Tim 16 is identified in mouse and human ACTH-secreting pituitary adenomas compared to normal pituitary to protect pituitary cells from apoptosis (62). Also, more macrophages are identified in larger pituitary adenomas, and more T cells are detected in GH-secreting pituitary adenomas. A positive correlation is found between the numbers of CD68+ macrophages and tumor sizes and grades for pituitary adenoma invasiveness. The density of infiltrated CD4+ and CD8+ T-lymphocytes may be relatively insufficient in these pituitary adenomas, but CD4+ and CD8+ T lymphocytes are significantly more in GH-secreting adenomas than non-GH adenomas. Both densely and sparsely granulated GH-adenomas had significantly more CD4+ cells than ACTH-adenomas, and significantly more CD8+ cells than null cell adenomas. These results suggest an association of the enhanced T-lymphocytes infiltration and invasiveness in pituitary adenomas, and that adjuvant immunotherapy might block the tumor enlargement and invasiveness of pituitary adenomas (129). Furthermore, study shows that low expression levels of immune-related genes induce the occurrence of pituitary adenomas (130). Another study show reveals the association of NF-κB, MMP-9, and MICA in pituitary adenomas, the higher expressions of MICA, MMP-9, and NF-κB in mRNA and protein levels in pituitary adenomas relative to healthy tissues; which found that the upregulation of NF-κB can activate the expression of MICA and increase MMP-9 expression to hydrolyze MICA into sMICA to facilitate tumor immune escape (131). Although most pituitary adenomas are treated successfully, it remains challenging to treat invasive non-functional pituitary adenomas as well as functional pituitary adenomas unresponsive to traditional therapy. Immunotherapy might be a potential alternative therapy for pituitary tumors that are resistant to traditional therapy (132). The positive PD-L1 immunostaining is significantly more frequent in functional relative to non-functional pituitary adenomas ($p = 0.000$). The expression level of PD-L1 is more related to the increased blood levels of ACTH-, PRL-, GH-, and cortisol-secreting pituitary adenomas. PD-L1 expression is also associated with GH and PRL immunostaining density and higher Ki-67 index (133). Thereby, immunotherapy might be a promising therapy option of functional pituitary adenomas on the basis of in-depth understanding of mitochondria-mediated immunity in pituitary adenomas.

THE MITOCHONDRIAL DYNAMICS IN CANCER

Mitochondrion is a highly dynamic organelle under the coordination between fission and fusion cycles, which is referred as "mitochondrial dynamics." Fission-fusion cycles affect mitochondria shape, size, and distribution (134). Mitochondria transient and rapid morphological adaptations are crucial for various cellular processes such as apoptosis (135), energy metabolism (136), cell cycle (137), ROS (138), immunity (139), mitophagy (140), and mitochondrial quality control (**Figure 7**). Mutations of the key machinery components or defects of mitochondrial dynamics are associated with lots of human diseases, including cancer (141). These dynamic transitions are primarily regulated by large GTPases. Mitochondrial fission and fusion cycle is a multi-step process. Mitochondrial fission is controlled by recruitment of dynamin-related protein 1 (Drp1) by adaptors at ER- and actin-mediated mitochondrial constriction sites. Drp1 oligomerization results in mitochondrial constriction, which leads to dynamin 2 recruitment to terminate mitochondrial outer membrane scission. Inner mitochondrial membrane constriction is an independent process, and mediated by calcium influx. Mitochondrial fusion is driven by mitofusins 1 and 2 within the outer mitochondrial membrane, and mediated by optic atrophy 1 with inner membrane (142). Moreover, several members of membrane lipid composition could undergo post-translational modifications to regulate these processes (143). Therefore, it is crucial for one to in-depth understand molecular mechanisms of mitochondrial dynamics for further studying various cellular processes associated with human diseases.

Various cellular processes, such as apoptosis (135), energy metabolism (136), cell cycle (137), ROS (138), immunity (139), and mitophagy (140), are closely related to mitochondrial dynamics and mitochondrial dysfunction. The relationship study between cell apoptosis and mitochondrial fission found that IR-783 induces Drp1 translocation from cytoplasm to mitochondria, makes the expression of mitochondrial fission proteins (MFF) and mitochondrial fission factor fission-1 (Fis1) increased, and the expression of optic atrophy 1 (OPA1) and mitochondrial fusion proteins mitofusin1 (Mfn1) decreased. The process of mitochondrial translocation of Drp1 mediated mitochondrial fission and markedly induced apoptosis *in vivo*

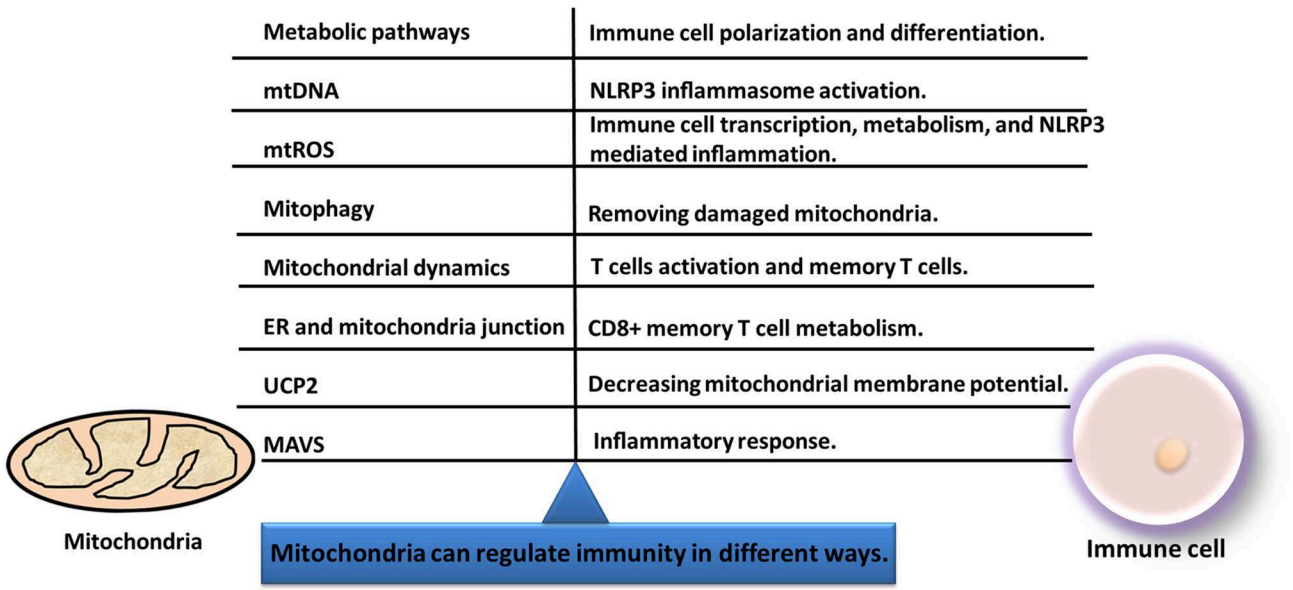

FIGURE 6 | Immunity and mitochondria are interlinked with each other. Mitochondria can regulate immunity in different ways, including metabolic pathways, mitochondrial dynamics, mtDNA, mitophagy, mtROS, MAVS, UCP2, and ER-mitochondria junction.

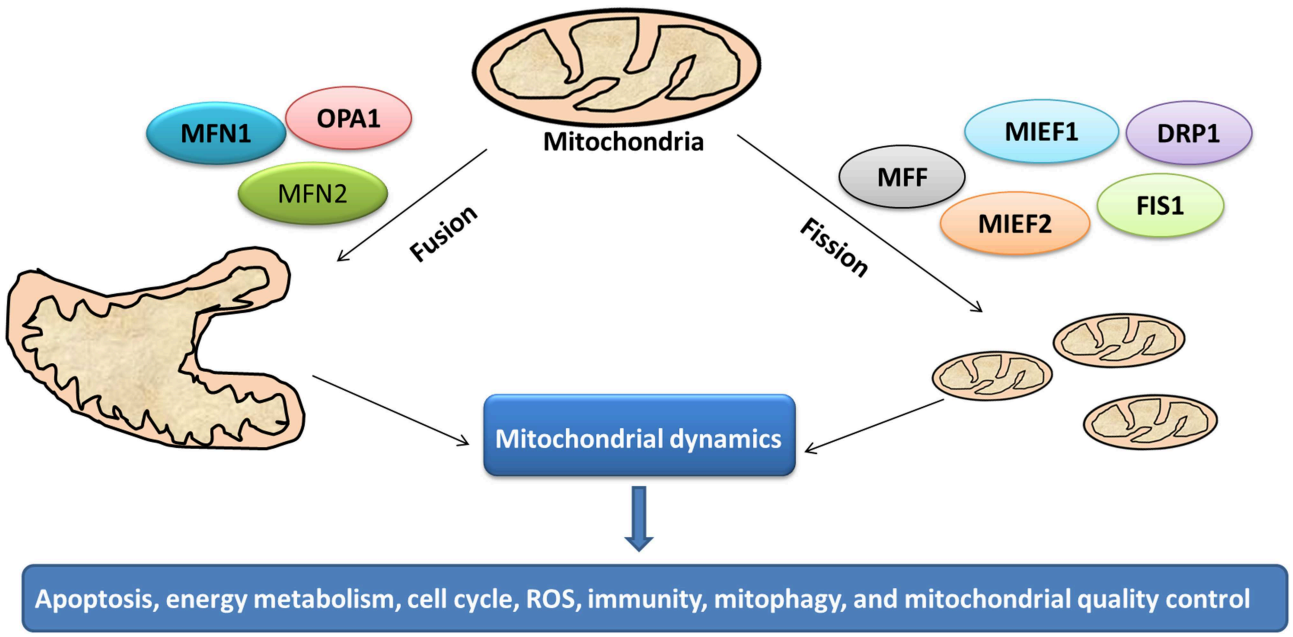

FIGURE 7 | Mitochondrial dynamics in cancer. Cycles of fission and fusion are crucial for various cellular processes such as apoptosis, energy metabolism, cell cycle, ROS, immunity, mitophagy, and mitochondrial quality control.

and xenograft model (144). The signaling pathways involved in mitochondrial dynamics regulation and their roles in maintaining energy metabolism has become an active area of research. Mitochondrial dynamic events, such as fusion, fission, and transport, affect the mitochondrial shape, size, function, and subcellular localization. Mitochondria dynamic changes play a crucial role in assisting metabolite transfer, biogenesis, and degradation to maintain energy homeostasis (136). Mitochondrial electron transport chain-derived ROS and mitochondrial fission/fusion rates influence this delicate balance between mitochondrial dynamics and mitochondria-derived ROS production, which plays main roles in malignant diseases (138). In addition, mitochondrial dynamics role in cancer growth connects with the immune system activity, especially

T cells. Although it has not been directly verified whether or not mitochondrial dynamics are associated with lymphocytes memory formation, Drp1-dependent mitochondrial fission has the potential contribution to regulate NK memory phase. It is indicated that mitochondrial dynamics is also possible to play role in the cytotoxic activity of these lymphocytes against cancer. Thereby, mitochondria can control local calcium influx to regulate the inner mitochondrial membrane constriction. It would be then interesting to see how mitochondrial dynamics to regulate the release of cytotoxic granules by T lymphocytes (139). The close interactions between mitochondrial dynamics and mitophagy become main players in the physiological cell processes in cancers. The new metabolic changes that mainly lead to mitochondrial functions and dysfunctions are strongly related to cancers, mitochondrial dynamics, and mitophagy (140). Study demonstrates that the BCL2/BCLXL inhibitor ABT737 mediates intrinsic apoptotic pathways and mitophagy through increasing levels of DRP1 in mitochondria and rates of mitochondrial fission (145).

CONCLUSION

In spite of considerable progresses in understanding mitochondrial dysfunction pathway networks and mitochondrial dynamics in the pathogenesis of pituitary adenomas, many key issues remain unclear. Several lines of evidence indicate that mitochondrial dysfunction emerge cross-links with various complex biological processes, including energy metabolism, oxidative stress, cell apoptosis, cell cycle, mitophagy, and immunity process. Moreover, mitochondrial dynamics is closely associated with mitochondrial dysfunction, and also plays a critical role in many biological processes. This review breaks new ground in the comprehensive understanding of potential mechanisms underlying between mitochondrial homeostasis and tumorigenesis in pituitary adenomas. The association of mitochondrial dysfunction, mitochondrial dynamics, and the complex biological processes helps to broaden the knowledge of mitochondrial functions in cancer and perspectives regarding tumor treatment. It offers the new promising to develop new candidate targets based on mitochondrial dysfunction pathway and mitochondrial dynamics, for effective therapy in pituitary adenomas.

AUTHOR CONTRIBUTIONS

NL collected and analyzed references, prepared figures and tables, and wrote the manuscript. XZ conceived the concept, designed, coordinated, critically revised/wrote manuscript, and was responsible for its financial supports and the corresponding works. All authors approved the final manuscript.

FUNDING

This work was supported by the grants from Hunan Provincial Hundred Talent Plan (to XZ), the China 863 Plan Project (Grant No. 2014AA020610-1 to XZ), National Natural Science Foundation of China (Grant No. 81572278 and 81272798), the Xiangya Hospital Funds for Talent Introduction (to XZ), and the Hunan Provincial Natural Science Foundation of China (Grant No. 14JJ7008 to XZ).

REFERENCES

1. Stalla GK, Ciato D, Dimopoulou C. "The adrenal gland: central relay in health and disease - Current challenges and perspectives 2018" - Cushing's disease. *Exp Clin Endocrinol Diabetes*. (2018) 127:147–55. doi: 10.1055/a-0664-7632
2. Zhan X, Wang X, Cheng T. Human pituitary adenoma proteomics: new progresses and perspectives. *Front Endocrinol*. (2016) 7:54. doi: 10.3389/fendo.2016.00054
3. Qian S, Yang Y, Li N, Cheng T, Wang X, Liu J, et al. Prolactin variants in human pituitaries and pituitary adenomas identified with two-dimensional gel electrophoresis and mass spectrometry. *Front Endocrinol*. (2018) 9:468. doi: 10.3389/fendo.2018.00468
4. Lopes MBS. The 2017 World Health Organization classification of tumors of the pituitary gland: a summary. *Acta Neuropathol*. (2017) 134:521–35. doi: 10.1007/s00401-017-1769-8
5. Reimondo G, Puglisi S, Pia A, Terzolo M. Autonomous hypercortisolism: definition and clinical implications. *Minerva Endocrinol*. (2018) 44:33–42. doi: 10.23736/s0391-1977.18.02884-5
6. Zhan X, Huang Y, Long Y. Two-dimensional gel electrophoresis coupled with mass spectrometry methods for an analysis of human pituitary adenoma tissue proteome. *J Vis Exp*. (2018) 134:e56739. doi: 10.3791/56739
7. Cheng T, Zhan X. Pattern recognition for predictive, preventive, and personalized medicine in cancer. *Epma J*. (2017) 8:51–60. doi: 10.1007/s13167-017-0083-9
8. Zhu H, Tamura T, Hamachi I. Chemical proteomics for subcellular proteome analysis. *Curr Opin Chem Biol*. (2018) 48:1–7. doi: 10.1016/j.cbpa.2018.08.001
9. Robin T, Bairoch A, Muller M, Lisacek F. Large-scale reanalysis of publicly available hela cell proteomics data in the context of the human proteome project. (2018) 17:4160–70. doi: 10.1021/acs.jproteome.8b00392
10. Moreno CS, Evans CO, Zhan X, Okor M, Desiderio DM, Oyesiku NM. Novel molecular signaling and classification of human clinically nonfunctional pituitary adenomas identified by gene expression profiling and proteomic analyses. *Cancer Res*. (2005) 65:10214–22. doi: 10.1158/0008-5472.can-05-0884
11. Evans CO, Moreno CS, Zhan X, McCabe MT, Vertino PM, Desiderio DM, et al. Molecular pathogenesis of human prolactinomas identified by gene expression profiling, RT-qPCR, and proteomic analyses. *Pituitary*. (2008) 11:231–245. doi: 10.1007/s11102-007-0082-2
12. Tanase C, Codrici E, Popescu ID, Cruceru ML, Enciu AM, Albulescu R, et al. Angiogenic markers: molecular targets for personalized medicine in pituitary adenoma. *Per Med*. (2013) 10:539–48. doi: 10.2217/pme.13.61
13. Gygi SP, Rochon Y, Franza BR, Aebersold R. Correlation between protein and mRNA abundance in yeast. *Mol Cell Biol*. (1999) 19:1720–30.
14. Anderson L, Seilhamer J. A comparison of selected mRNA and protein abundances in human liver. *Electrophoresis*. (1997) 18:533–7. doi: 10.1002/elps.1150180333
15. Li N, Li H, Cao L, Zhan X. Quantitative analysis of the mitochondrial proteome in human ovarian carcinomas. *Endocr Relat Cancer*. (2018) 25:909–31. doi: 10.1530/erc-18-0243
16. Wallace DC. Mitochondria and cancer. *Nat Rev Cancer*. (2012) 12:685–98. doi: 10.1038/nrc3365
17. Magalhaes J, Venditti P, Adhihetty PJ, Ramsey JJ, Ascensao A. Mitochondria in health and disease. *Oxid Med Cell Longev*. (2014) 2014:814042. doi: 10.1155/2014/814042

18. Zhan X, Desiderio DM. Signaling pathway networks mined from human pituitary adenoma proteomics data. *BMC Med Genomics*. (2010) 3:13. doi: 10.1186/1755-8794-3-13
19. Zhan X, Wang X, Long Y, Desiderio DM. Heterogeneity analysis of the proteomes in clinically nonfunctional pituitary adenomas. *BMC Med Genomics*. (2014) 7:69. doi: 10.1186/s12920-014-0069-6
20. Lu M, Wang Y, Zhan X. The MAPK pathway-based drug therapeutic targets in pituitary adenomas. *Front Endocrinol*. (2019) 10:330. doi: 10.3389/fendo.2019.00330
21. Tanase CP, Neagu M, Albulescu R. Key signaling molecules in pituitary tumors. *Expert Rev Mol Diagn*. (2009) 9:859–77. doi: 10.1586/erm.09.60
22. Fujisawa H, Tohma Y, Muramatsu N, Kida S, Kaizaki Y, Tamamura H. Spindle cell oncocytoma of the adenohypophysis with marked hypervascularity. Case report. *Neurol Med Chir*. (2012) 52:594–8. doi: 10.2176/nmc.52.594
23. Saeger W, Rubenach-Gerz K, Caselitz J, Ludecke DK. Electron microscopical morphometry of GH producing pituitary adenomas in comparison with normal GH cells. *Virchows Arch A Pathol Anat Histopathol*. (1987) 411:467–72.
24. Yamada S, Asa SL, Kovacs K. Oncocytomas and null cell adenomas of the human pituitary: morphometric and *in vitro* functional comparison. *Virchows Arch A Pathol Anat Histopathol*. (1988) 413:333–9.
25. Saeger W, Kant P, Caselitz J, Ludecke DK. Electron microscopical morphometry of pituitary adenomas. Comparison of tumours in acromegaly and hyperprolactinemia. *Pathol Res Pract*. (1988) 183:17–24.
26. Yang QH, Xu JN, Xu RK, Pang SF. Antiproliferative effects of melatonin on the growth of rat pituitary prolactin-secreting tumor cells *in vitro*. *J Pineal Res*. (2007) 42:172–9. doi: 10.1111/j.1600-079X.2006.00403.x
27. Wang BQ, Yang QH, Xu RK, Xu JN. Elevated levels of mitochonrial respiratory complexes activities and ATP production in 17-beta-estradiol-induced prolactin-secretory tumor cells in male rats are inhibited by melatonin *in vivo* and *in vitro*. *Chin Med J*. (2013) 126:4724–30. doi: 10.3760/cma.j.issn.0366-6999.20131965
28. Dai C, Zhang B, Liu X, Guo K, Ma S, Cai F, et al. Pyrimethamine sensitizes pituitary adenomas cells to temozolomide through cathepsin B-dependent and caspase-dependent apoptotic pathways. *Int J Cancer*. (2013) 133:1982–93. doi: 10.1002/ijc.28199
29. Wang D, Wong HK, Feng YB, Zhang ZJ. 18beta-glycyrrhetinic acid induces apoptosis in pituitary adenoma cells via ROS/MAPKs-mediated pathway. *J Neurooncol*. (2014) 116:221–30. doi: 10.1007/s11060-013-1292-2
30. Tang J, Wang Z, Chen L, Huang G, Hu X. Gossypol acetate induced apoptosis of pituitary tumor cells by targeting the BCL-2 via the upregulated microRNA miR-15a. *Int J Clin Exp Med*. (2015) 8:9079–85.
31. Ji YZ, Geng L. Chinese herbal medicine Yougui Pill reduces exogenous glucocorticoid-induced apoptosis in anterior pituitary cells. *Neural Regen Res*. (2016) 11:1962–8. doi: 10.4103/1673-5374.197138
32. Zhou HB, Wei HC, Chen HD, Liu X, Guo P, Liu A, et al. Nitric oxide (NO)-mediated mitochondrial damage plays a critical role in T-2 toxin-induced apoptosis and growth hormone deficiency in rat anterior pituitary GH3 cells. *Food Chem Toxicol*. (2017) 102:11–23. doi: 10.1016/j.fct.2017.01.017
33. Zhao Y, Zhang L, Yan A, Chen D, Xie R, Liu Y, et al. Grifolic acid induces GH3 adenoma cell death by inhibiting ATP production through a GPR120-independent mechanism. *BMC Pharmacol Toxicol*. (2018) 19:26. doi: 10.1186/s40360-018-0215-4
34. Zhang Q, Li C, Zhou Y, Zhao S, Hong L, Song Q, et al. The critical role of p16/Rb pathway in the inhibition of GH3 cell cycle induced by T-2 toxin. *Toxicology*. (2018) 400–1:28–39. doi: 10.1016/j.tox.2018.03.006.
35. Wei Y, Zhou X, Ren L, Wang C, Li Y. The prolactin-release inhibitor paeoniflorin suppresses proliferation and induces apoptosis in prolactinoma cells via the mitochondria-dependent pathway. *J Cell Biochem*. (2018) 119:5704–14. doi: 10.1002/jcb.26752
36. Deyu H, Luqing C, Xianglian L, Pu G, Qirong L, Xu W, et al. Protective mechanisms involving enhanced mitochondrial functions and mitophagy against T-2 toxin-induced toxicities in GH3 cells. *Toxicol Lett*. (2018) 295:41–53. doi: 10.1016/j.toxlet.2018.05.041
37. Kim HS, Choi SI, Jeung EB, Yoo YM. Cyclosporine A induces apoptotic and autophagic cell death in rat pituitary GH3 cells. *PLoS ONE*. (2014) 9:e108981. doi: 10.1371/journal.pone.0108981
38. Leng ZG, Lin SJ, Wu ZR, Guo YH, Cai L, Shang HB, et al. Activation of DRD5 (dopamine receptor D5) inhibits tumor growth by autophagic cell death. *Autophagy*. (2017) 13:1404–19. doi: 10.1080/15548627.2017.1328347
39. Wang X, Du Q, Mao Z, Fan X, Hu B, Wang Z, et al. Combined treatment with artesunate and bromocriptine has synergistic anticancer effects in pituitary adenoma cell lines. *Oncotarget*. (2017) 8:45874–87. doi: 10.18632/oncotarget.17437
40. Wang X, Guo T, Peng F, Long Y, Mu Y, Yang H, et al. Proteomic and functional profiles of a follicle-stimulating hormone positive human nonfunctional pituitary adenoma. *Electrophoresis*. (2015) 36:1289–304. doi: 10.1002/elps.201500006
41. An J, Zhang Y, He J, Zang Z, Zhou Z, Pei X, et al. Lactate dehydrogenase A promotes the invasion and proliferation of pituitary adenoma. *Sci Rep*. (2017) 7:4734. doi: 10.1038/s41598-017-04366-5
42. Casar-Borota O, Oystese KA, Sundstrom M, Melchior L, Popovic VA. high-throughput analysis of the IDH1(R132H) protein expression in pituitary adenomas. *Pituitary*. (2016) 19:407–14. doi: 10.1007/s11102-016-0720-7
43. Hao S, Hong CS, Feng J, Yang C, Chittiboina P, Zhang J, et al. Somatic IDH1 mutation in a pituitary adenoma of a patient with Maffucci syndrome. *J Neurosurg*. (2016) 124:1562–7. doi: 10.3171/2015.4.jns15191
44. Porcelli AM, Ghelli A, Ceccarelli C, Lang M, Cenacchi G, Capristo M, et al. The genetic and metabolic signature of oncocytic transformation implicates HIF1alpha destabilization. *Hum Mol Genet*. (2010) 19:1019–32. doi: 10.1093/hmg/ddp566
45. Xekouki P, Stratakis CA. Succinate dehydrogenase (SDHx) mutations in pituitary tumors: could this be a new role for mitochondrial complex II and/or Krebs cycle defects? *Endocr Relat Cancer*. (2012) 19:C33–40. doi: 10.1530/erc-12-0118
46. Xekouki P, Szarek E, Bullova P, Giubellino A, Quezado M, Mastroyannis SA, et al. Pituitary adenoma with paraganglioma/pheochromocytoma (3PAs) and succinate dehydrogenase defects in humans and mice. *J Clin Endocrinol Metab*. (2015) 100:E710–9. doi: 10.1210/jc.2014-4297
47. Wu S, Gu Y, Huang Y, Wong TC, Ding H, Liu T, et al. Novel biomarkers for non-functioning invasive pituitary adenomas were identified by using analysis of microRNAs expression profile. *Biochem Genet*. (2017) 55:253–67. doi: 10.1007/s10528-017-9794-9
48. Feng J, Zhang Q, Li C, Zhou Y, Zhao S, Hong L, et al. Enhancement of mitochondrial biogenesis and paradoxical inhibition of lactate dehydrogenase mediated by 14-3-3eta in oncocytomas. *J Pathol*. (2018) 245:361–72. doi: 10.1002/path.5090
49. Pawlikowski M, Winczyk K, Jaranowska M. Immunohistochemical demonstration of nitric oxide synthase (NOS) in the normal rat pituitary gland, estrogen-induced rat pituitary tumor and human pituitary adenomas. *Folia Histochem Cytobiol*. (2003) 41:87–90.
50. Sabatino ME, Grondona E, Sosa LDV, Mongi Bragato B, Carreno L, Juarez V, et al. Oxidative stress and mitochondrial adaptive shift during pituitary tumoral growth. *Free Radic Biol Med*. (2018) 120:41–55. doi: 10.1016/j.freeradbiomed.2018.03.019
51. Jaubert A, Ichas F, Bresson-Bepoldin L. Signaling pathway involved in the pro-apoptotic effect of dopamine in the GH3 pituitary cell line. *Neuroendocrinology*. (2006) 83:77–88. doi: 10.1159/000094044
52. Onishi K, Kamida T, Momii Y, Abe T, Fujiki M. The clinical and pathological significance of nitric oxide synthase in human pituitary adenomas: a comparison with MIB-1. *Endocrine*. (2014) 46:154–9. doi: 10.1007/s12020-013-0046-4
53. Huang D, Cui L, Guo P, Xue X, Wu Q, Hussain HI, et al. Nitric oxide mediates apoptosis and mitochondrial dysfunction and plays a role in growth hormone deficiency by nivalenol in GH3 cells. *Sci Rep*. (2017) 7:17079. doi: 10.1038/s41598-017-16908-y
54. Babula D, Horecka A, Luchowska-Kocot D, Kocot J, Kurzepa J. Decreased nitric oxide serum level after pituitary adenoma resection. *J Neurosurg Sci*. (2017). doi: 10.23736/s0390-5616.17.04083-8. [Epub ahead of print].
55. Guzzo MF, Carvalho LR, Bronstein MD. Apoptosis: its role in pituitary development and neoplastic pituitary tissue. *Pituitary*. (2014) 17:157–62. doi: 10.1007/s11102-013-0481-5

56. Gottardo MF, Pidre ML, Zuccato C, Asad AS, Imsen M, Jaita G, et al. Baculovirus-based gene silencing of Humanin for the treatment of pituitary tumors. *Apoptosis*. (2018) 23:143–51. doi: 10.1007/s10495-018-1444-0
57. Gao F, Pan S, Liu B, Zhang H. TFF3 knockout in human pituitary adenoma cell HP75 facilitates cell apoptosis via mitochondrial pathway. *Int J Clin Exp Pathol*. (2015) 8:14568–73.
58. Tanase C, Albulescu R, Codrici E, Calenic B, Popescu ID, Mihai S, et al. Decreased expression of APAF-1 and increased expression of cathepsin B in invasive pituitary adenoma. *Onco Targets Ther*. (2015) 8:81–90. doi: 10.2147/ott.s70886
59. Yang Z, Zhang T, Wang Q, Gao H. Overexpression of microRNA-34a attenuates proliferation and induces apoptosis in pituitary adenoma cells via SOX7. *Mol Ther Oncol*. (2018) 10:40–7. doi: 10.1016/j.omto.2018.07.001
60. Cui M, Zhang M, Liu HF, Wang JP. Effects of microRNA-21 targeting PITX2 on proliferation and apoptosis of pituitary tumor cells. *Eur Rev Med Pharmacol Sci*. (2017) 21:2995–3004.
61. Gong YY, Liu YY, Yu S, Zhu XN, Cao XP, Xiao HP. Ursolic acid suppresses growth and adrenocorticotrophic hormone secretion in AtT20 cells as a potential agent targeting adrenocorticotrophic hormone-producing pituitary adenoma. *Mol Med Rep*. (2014) 9:2533–9. doi: 10.3892/mmr.2014.2078
62. Tagliati F, Gentilin E, Buratto M, Mole D, degli Uberti EC, Zatelli MC. Magmas, a gene newly identified as overexpressed in human and mouse ACTH-secreting pituitary adenomas, protects pituitary cells from apoptotic stimuli. *Endocrinology*. (2010) 151:4635–42. doi: 10.1210/en.2010-0441
63. Warburg O. On the origin of cancer cells. *Science*. (1956) 123:309–14.
64. Pavlides S, Whitaker-Menezes D, Castello-Cros R, Flomenberg N, Witkiewicz AK, Frank PG, et al. The reverse Warburg effect: aerobic glycolysis in cancer associated fibroblasts and the tumor stroma. *Cell Cycle*. (2009) 8:3984–4001. doi: 10.4161/cc.8.23.10238
65. Vargas T, Moreno-Rubio J, Herranz J, Cejas P, Molina S, Gonzalez-Vallinas M, et al. ColoLipidGene: signature of lipid metabolism-related genes to predict prognosis in stage-II colon cancer patients. *Oncotarget*. (2015) 6:7348–63. doi: 10.18632/oncotarget.3130
66. Yue S, Li J, Lee SY, Lee HJ, Shao T, Song B, et al. Cholesteryl ester accumulation induced by PTEN loss and PI3K/AKT activation underlies human prostate cancer aggressiveness. *Cell Metab*. (2014) 19:393–406. doi: 10.1016/j.cmet.2014.01.019
67. Nieman KM, Kenny HA, Penicka CV, Ladanyi A, Buell-Gutbrod R, Zillhardt MR, et al. Adipocytes promote ovarian cancer metastasis and provide energy for rapid tumor growth. *Nat Med*. (2011) 17:1498–503. doi: 10.1038/nm.2492
68. Griffiths WJ, Wang Y. An update on oxysterol biochemistry: new discoveries in lipidomics. *Biochem Biophys Res Commun*. (2018) 504:617–22. doi: 10.1016/j.bbrc.2018.02.019
69. Wanet A, Arnould T, Najimi M, Renard P. Connecting mitochondria, metabolism, and stem cell fate. *Stem Cells Dev*. (2015) 24:1957–71. doi: 10.1089/scd.2015.0117
70. Oldfield EH, Merrill MJ. Apoplexy of pituitary adenomas: the perfect storm. *J Neurosurg*. (2015) 122: 1444–9. doi: 10.3171/2014.10.jns141720
71. Sinha N, Dabla PK. Oxidative stress and antioxidants in hypertension-a current review. *Curr Hypertens Rev*. (2015) 11:132–42. doi: 10.2174/1573402111666150529130922
72. Xu H, Wang X, Burchiel SW. Toxicity of environmentally-relevant concentrations of arsenic on developing T lymphocyte. *Environ Toxicol Pharmacol*. (2018) 62:107–13. doi: 10.1016/j.etap.2018.07.003
73. Kaarniranta K, Kajdanek J, Morawiec J, Pawlowska E, Blasiak J. PGC-1alpha protects RPE cells of the aging retina against oxidative stress-induced degeneration through the regulation of senescence and mitochondrial quality control. The significance for AMD pathogenesis. *Int J Mol Sci*. (2018) 19:E2317. doi: 10.3390/ijms19082317
74. Hassanzadeh K, Rahimmi A. Oxidative stress and neuroinflammation in the story of Parkinson's disease: could targeting these pathways write a good ending? *J Cell Physiol*. (2018) 234:23–32. doi: 10.1002/jcp.26865
75. Matsuzaki J, Ochiya T. Extracellular microRNAs and oxidative stress in liver injury: a systematic mini review. *J Clin Biochem Nutr*. (2018) 63:6–11. doi: 10.3164/jcbn.17-123
76. Siasos G, Tsigkou V, Kosmopoulos M, Theodosiadis D, Simantiris S, Tagkou NM, et al. Mitochondria and cardiovascular diseases-from pathophysiology to treatment. *J Cell Physiol*. (2018) 6:256. doi: 10.21037/atm.2018.06.21
77. van der Vliet A, Janssen-Heininger YMW, Anathy V. Oxidative stress in chronic lung disease: from mitochondrial dysfunction to dysregulated redox signaling. *Mol Aspects Med*. (2018). 63:59–69. doi: 10.1016/j.mam.2018.08.001
78. Tsuchiya T, Kijima A, Ishii Y, Takasu S, Yokoo Y, Nishikawa A, et al. Mechanisms of oxidative stress-induced *in vivo* mutagenicity by potassium bromate and nitrofurantoin. *J Toxicol Pathol*. (2018) 31:179–88. doi: 10.1293/tox.2018-0024
79. Rekha VR, Sunil S, Rathy R. Evaluation of oxidative stress markers in oral lichen planus. *J Oral Maxillofac Pathol*. (2017) 21:387–93. doi: 10.4103/jomfp.JOMFP_19_17
80. Kumari S, Badana AK, G MM, GS, Malla R. Reactive oxygen species: a key constituent in cancer survival. *Biomark Insights*. (2018) 13:1177271918755391. doi: 10.1177/1177271918755391
81. Fischer N, Seo EJ, Efferth T. Prevention from radiation damage by natural products. *Phytomedicine*. (2018) 47:192–200. doi: 10.1016/j.phymed.2017.11.005
82. Tang JY, Farooqi AA, Ou-Yang F, Hou MF, Huang HW, Wang HR, et al. Oxidative stress-modulating drugs have preferential anticancer effects - involving the regulation of apoptosis, DNA damage, endoplasmic reticulum stress, autophagy, metabolism, and migration. *Semin Cancer Biol*. (2018) 58:109–17. doi: 10.1016/j.semcancer.2018.08.010
83. Kato K, Giulivi C. Critical overview of mitochondrial nitric-oxide synthase. *Front Biosci*. (2006) 11:2725–38. doi: 10.2741/2002
84. Shvedova M, Anfinogenova Y, Popov SV, Atochin DN. Connexins and nitric oxide inside and outside mitochondria: significance for cardiac protection and adaptation. *Front Physiol*. (2018) 9:479. doi: 10.3389/fphys.2018.00479
85. Navarro A, Boveris A. Mitochondrial nitric oxide synthase, mitochondrial brain dysfunction in aging, and mitochondria-targeted antioxidants. *Adv Drug Deliv Rev*. (2008) 60:1534–44. doi: 10.1016/j.addr.2008.05.002
86. Zaobornyj T, Ghafourifar P. Strategic localization of heart mitochondrial NOS: a review of the evidence. *Am J Physiol Heart Circ Physiol*. (2012) 303:H1283–93. doi: 10.1152/ajpheart.00674.2011
87. Caravia L, Dudau M, Gherghiceanu M, Tanase C, Enciu AM. Could caveolae be acting as warnings of mitochondrial ageing? *Mech Ageing Dev*. (2015) 146–8:81–7. doi: 10.1016/j.mad.2015.04.003
88. Jin Y, Chen S, Li N, Liu Y, Cheng G, Zhang C, et al. Defect-related luminescent bur-like hydroxyapatite microspheres induced apoptosis of MC3T3-E1 cells by lysosomal and mitochondrial pathways. *Sci China Life Sci*. (2018) 61:464–75. doi: 10.1007/s11427-017-9258-3
89. Zakeri Z, Lockshin RA. Cell death: history and future. *Adv Exp Med Biol*. (2008) 615:1–11. doi: 10.1007/978-1-4020-6554-5_1
90. Visalli G, Baluce B, Bertuccio M, Picerno I, Di Pietro A. Mitochondrial-mediated apoptosis pathway in alveolar epithelial cells exposed to the metals in combustion-generated particulate matter. *J Toxicol Environ Health A*. (2015) 78:697–709. doi: 10.1080/15287394.2015.1024081
91. Hantusch A, Rehm M, Brunner T. Counting on Death - Quantitative aspects of Bcl-2 family regulation. *FEBS J*. (2018) 285:4124–38. doi: 10.1111/febs.14516
92. Pena-Blanco A, Garcia-Saez AJ. Bax, Bak and beyond - mitochondrial performance in apoptosis. *FEBS J*. (2018) 285:416–31. doi: 10.1111/febs.14186
93. Xiong S, Mu T, Wang G, Jiang X. Mitochondria-mediated apoptosis in mammals. *Protein Cell*. (2014) 5:737–49. doi: 10.1007/s13238-014-0089-1
94. Hou XS, Wang HS, Mugaka BP, Yang GJ, Ding Y. Mitochondria: promising organelle targets for cancer diagnosis and treatment. *Biomater Sci*. (2018) 6:2786–97. doi: 10.1039/c8bm00673c
95. Andre N, Braguer D, Brasseur G, Goncalves A, Lemesle-Meunier D, Guise S, et al. Paclitaxel induces release of cytochrome c from mitochondria isolated from human neuroblastoma cells'. *Cancer Res*. (2000) 60:5349–53.
96. Ogando-Rivas E, Alalade AF, Boatey J, Schwartz TH. Double pituitary adenomas are most commonly associated with GH- and ACTH-secreting tumors: systematic review of the literature. *Pituitary*. (2017) 20:702–8. doi: 10.1007/s11102-017-0826-6
97. Mizushima N, Komatsu M. Autophagy: renovation of cells and tissues. *Cell*. (2011) 147:728–41. doi: 10.1016/j.cell.2011.10.026

98. Dlugonska H. Autophagy as a universal intracellular process. A comment on the 2016 Nobel Prize in Physiology or Medicine. *Ann Parasitol*. (2017) 63:153–7. doi: 10.17420/ap6303.100
99. Klionsky DJ, Abdelmohsen K, Abe A, Abedin MJ, Abeliovich H, Acevedo Arozena A, et al. Guidelines for the use and interpretation of assays for monitoring autophagy (3rd edition). *Autophagy*. (2016) 12:1–222. doi: 10.1080/15548627.2015.1100356
100. Avalos Y, Canales J, Bravo-Sagua R. Tumor suppression and promotion by autophagy. *Biomed Res Int*. (2014) 2014:603980. doi: 10.1155/2014/603980
101. Martins WK, Santos NF, Rocha CS, Bacellar IOL, Tsubone TM, Viotto AC, et al. Parallel damage in mitochondria and lysosomes is an efficient way to photoinduce cell death. *Autophagy*. (2018) 15:259–79. doi: 10.1080/15548627.2018.1515609
102. Youle RJ, Narendra DP. Mechanisms of mitophagy. *Nat Rev Mol Cell Biol*. (2011) 12:9–14. doi: 10.1038/nrm3028
103. Drake LE, Springer MZ, Poole LP, Kim CJ, Macleod KF. Expanding perspectives on the significance of mitophagy in cancer. *Semin Cancer Biol*. (2017) 47:110–24. doi: 10.1016/j.semcancer.2017.04.008
104. Wu H, Wei H, Sehgal SA, Liu L, Chen Q. Mitophagy receptors sense stress signals and couple mitochondrial dynamic machinery for mitochondrial quality control. *Free Radic Biol Med*. (2016) 100:199–209. doi: 10.1016/j.freeradbiomed.2016.03.030
105. Zimmermann M, Reichert A S. How to get rid of mitochondria: crosstalk and regulation of multiple mitophagy pathways. *Biol Chem*. (2017) 399:29–45. doi: 10.1515/hsz-2017-0206
106. Boyle KB, Randow F. The role of 'eat-me' signals and autophagy cargo receptors in innate immunity. *Curr Opin Microbiol*. (2013) 16:339–48. doi: 10.1016/j.mib.2013.03.010
107. Zhang L, Qin Y, Chen M. Viral strategies for triggering and manipulating mitophagy. *Autophagy*. (2018) 14:1665–73. doi: 10.1080/15548627.2018.1466014
108. Yang L, Tu D, Zhao Z, Cui J. Cytotoxicity and apoptosis induced by mixed mycotoxins (T-2 and HT-2 toxin) on primary hepatocytes of broilers *in vitro*. *Toxicon*. (2017) 129:1–10. doi: 10.1016/j.toxicon.2017.01.001
109. Zhu CC, Zhang Y, Duan X, Han J, Sun SC. Toxic effects of HT-2 toxin on mouse oocytes and its possible mechanisms. *Arch Toxicol*. (2016) 90:1495–505. doi: 10.1007/s00204-015-1560-3
110. Vlahopoulos S, Critselis E, Voutsas IF, Perez SA, Moschovi M, Baxevanis CN, et al. New use for old drugs? Prospective targets of chloroquines in cancer therapy. *Curr Drug Targets*. (2014) 15:843–51. doi: 10.2174/1389450115666140714121514
111. Wu J, Li J, and Wang H. Mitochondrial-targeted penetrating peptide delivery for cancer therapy. *Expert Opin Drug Deliv*. (2018) 15:951–64. doi: 10.1080/17425247.2018.1517750
112. Desantis V, Saltarella I, Lamanuzzi A, Mariggio MA, Racanelli V, Vacca A, et al. Autophagy: a new mechanism of prosurvival and drug resistance in multiple myeloma. *Transl Oncol*. (2018) 11:1350–7. doi: 10.1016/j.tranon.2018.08.014
113. Rademacher BL, Meske LM, Matkowskyj KA, Hanlon BM, Carchman EH. Genetic inhibition of autophagy in a transgenic mouse model of anal cancer. *J Carcinog*. (2018) 17:3. doi: 10.4103/jcar.JCar_4_18
114. Bishop E, Bradshaw TD. Autophagy modulation: a prudent approach in cancer treatment? *Cancer Chemother Pharmacol*. (2018) 82:913–22. doi: 10.1007/s00280-018-3669-6
115. Leone K, Poggiana C, Zamarchi R. The interplay between circulating tumor cells and the immune system: from immune escape to cancer immunotherapy. *Diagnostics*. (2018) 8:E59. doi: 10.3390/diagnostics8030059
116. Sica A, Massarotti M. Myeloid suppressor cells in cancer and autoimmunity. *J Autoimmun*. (2017) 85:117–25. doi: 10.1016/j.jaut.2017.07.010
117. Watza D, Lusk CM, Dyson G, Purrington KS, Chen K, Wenzlaff AS, et al. Prognostic modeling of the immune-centric transcriptome reveals interleukin signaling candidates contributing to differential patient outcomes. *Carcinogenesis*. (2018) 39:1447–54. doi: 10.1093/carcin/bgy119
118. Going CC, Tailor D, Kumar V, Birk AM, Pandrala M, Rice MA, et al. Quantitative proteomic profiling reveals key pathways in the anti-cancer action of methoxychalcone derivatives in triple negative breast cancer. *J Proteome Res*. (2018). 17:3574–85. doi: 10.1021/acs.jproteome.8b00636
119. Ma W, Concha-Benavente F, Santegoets S, Welters MJP, Ehsan I, Ferris RL, et al. EGFR signaling suppresses type 1 cytokine-induced T-cell attracting chemokine secretion in head and neck cancer. *PLoS ONE*. (2018) 13:e0203402. doi: 10.1371/journal.pone.0203402
120. Bhat MY, Solanki HS, Advani J, Khan AA, Keshava Prasad TS, Gowda H, et al. Comprehensive network map of interferon gamma signaling. *J Cell Commun Signal*. (2018) 12:745–51. doi: 10.1007/s12079-018-0486-y
121. Budhwani M, Mazzieri R, Dolcetti R. Plasticity of type I interferon-mediated responses in cancer therapy: from anti-tumor immunity to resistance. *Front Oncol*. (2018) 8:322. doi: 10.3389/fonc.2018.00322
122. Giuliani C, Bucci I, Napolitano G. The role of the transcription factor nuclear factor-kappa B in thyroid autoimmunity and cancer. *Front Endocrinol*. (2018) 9:471. doi: 10.3389/fendo.2018.00471
123. Sui H, Ma N. Anti-PD-1/PD-L1 Therapy for non-small-cell lung cancer: toward personalized medicine and combination strategies. *J Immunol Res*. (2018) 2018:6984948. doi: 10.1155/2018/6984948
124. Angajala A, Lim S, Phillips JB, Kim JH, Yates C, You Z, et al. Diverse roles of mitochondria in immune responses: novel insights into immuno-metabolism. *Front Immunol*. (2018) 9:1605. doi: 10.3389/fimmu.2018.01605
125. Nakahira K, Haspel JA, Rathinam VA, Lee SJ, Dolinay T, Lam HC, et al. Autophagy proteins regulate innate immune responses by inhibiting the release of mitochondrial DNA mediated by the NALP3 inflammasome. *Nat Immunol*. (2011) 12:222–30. doi: 10.1038/ni.1980
126. Agod Z, Fekete T, Budai MM, Varga A, Szabo A, Moon H, et al. Regulation of type I interferon responses by mitochondria-derived reactive oxygen species in plasmacytoid dendritic cells. *Redox Biol*. (2017) 13:633–45. doi: 10.1016/j.redox.2017.07.016
127. Lawlor KE, Vince JE. Ambiguities in NLRP3 inflammasome regulation: is there a role for mitochondria? *Biochim Biophys Acta*. (2014) 1840:1433–40. doi: 10.1016/j.bbagen.2013.08.014
128. Misawa T, Takahama M, Saitoh T. Mitochondria-endoplasmic reticulum contact sites mediate innate immune responses. *Adv Exp Med Biol*. (2017) 997:187–97. doi: 10.1007/978-981-10-4567-7_14
129. Lu JQ, Adam B, Jack AS, Lam A, Broad RW, Chik CL. Immune cell infiltrates in pituitary adenomas: more macrophages in larger adenomas and more T cells in growth hormone adenomas. *Endocr Pathol*. (2015) 26:263–72. doi: 10.1007/s12022-015-9383-6
130. Wang W, Xu Z, Fu L, Liu W, Li X. Pathogenesis analysis of pituitary adenoma based on gene expression profiling. *Oncol Lett*. (2014) 8:2423–30. doi: 10.3892/ol.2014.2613
131. Chen Z, Li Z, Chang Y, Ma L, Xu W, Li M, et al. Relationship between NF-kappaB, MMP-9, and MICA expression in pituitary adenomas reveals a new mechanism of pituitary adenomas immune escape. *Neurosci Lett*. (2015) 597:77–83. doi: 10.1016/j.neulet.2015.04.025
132. Maghathe T, Miller WK, Mugge L, Mansour TR, Schroeder J. Immunotherapy and potential molecular targets for the treatment of pituitary adenomas resistant to standard therapy: a critical review of potential therapeutic targets and current developments. *J Neurosurg Sci*. (2018). doi: 10.23736/s0390-5616.18.04419-3. [Epub ahead of print].
133. Wang PF, Wang TJ, Yang YK, Yao K, Li Z, Li YM. The expression profile of PD-L1 and CD8(+) lymphocyte in pituitary adenomas indicating for immunotherapy. *J Neurooncol*. (2018) 139:89–95. doi: 10.1007/s11060-018-2844-2
134. Tilokani L, Nagashima S, Paupe V, Prudent J. Mitochondrial dynamics: overview of molecular mechanisms. *Essays Biochem*. (2018) 62:341–60. doi: 10.1042/ebc20170104
135. Cook SJ, Stuart K, Gilley R, Sale MJ. Control of cell death and mitochondrial fission by ERK1/2 MAP kinase signalling. *FEBS J*. (2017) 284:4177–95. doi: 10.1111/febs.14122
136. Yu SB, Pekkurnaz G. Mechanisms orchestrating mitochondrial dynamics for energy homeostasis. *J Mol Biol*. (2018) 430:3922–41. doi: 10.1016/j.jmb.2018.07.027
137. Rasmussen ML, Ortolano NA. Wnt signaling and its impact on mitochondrial and cell cycle dynamics in pluripotent stem cells. *Genes*. (2018) 9:E109. doi: 10.3390/genes9020109
138. Jezek J, Cooper KF, Strich R. Reactive oxygen species and mitochondrial dynamics: the Yin and Yang of mitochondrial dysfunction and cancer progression. *Antioxidants*. (2018) 7:E13. doi: 10.3390/antiox7010013

139. Simula L, Nazio F, Campello S. The mitochondrial dynamics in cancer and immune-surveillance. *Semin Cancer Biol*. (2017) 47:29–42. doi: 10.1016/j.semcancer.2017.06.007
140. Bordi M, Nazio F, Campello S. The close interconnection between mitochondrial dynamics and mitophagy in cancer. *Front Oncol*. (2017) 7:81. doi: 10.3389/fonc.2017.00081
141. van der Ende M, Grefte S, Plas R, Meijerink J, Witkamp R, Keijer J, et al. Mitochondrial dynamics in cancer-induced cachexia. *Biochim Biophys Acta*. (2018) 1870:137–50. doi: 10.1016/j.bbcan.2018.07.008
142. Lopez-Lluch G, Hernandez-Camacho JD, Fernandez-Ayala DJM, Navas P. Mitochondrial dysfunction in metabolism and ageing: shared mechanisms and outcomes? *Biogerontology*. (2018) 19:461–80. doi: 10.1007/s10522-018-9768-2
143. Kameoka S, Adachi Y, Okamoto K, Iijima M, Sesaki H. Phosphatidic acid and cardiolipin coordinate mitochondrial dynamics. *Trends Cell Biol*. (2018) 28:67–76. doi: 10.1016/j.tcb.2017.08.011
144. Tang Q, Liu W, Zhang Q, Huang J, Hu C, Liu Y, et al. Dynamin-related protein 1-mediated mitochondrial fission contributes to IR-783-induced apoptosis in human breast cancer cells. *J Cell Mol Med*. (2018) 22:4474–85. doi: 10.1111/jcmm.13749
145. Yu Y, Xu L, Qi L, Wang C, Xu N, Liu S, et al. ABT737 induces mitochondrial pathway apoptosis and mitophagy by regulating DRP1-dependent mitochondrial fission in human ovarian cancer cells. *Biomed Pharmacother*. (2017) 96:22–9. doi: 10.1016/j.biopha.2017.09.111

Conflict of Interest: The authors declare that the research was conducted in the absence of any commercial or financial relationships that could be construed as a potential conflict of interest.

frontiers in Endocrinology

ORIGINAL RESEARCH
published: 05 December 2019
doi: 10.3389/fendo.2019.00854

Quantitative Analysis of Proteome in Non-functional Pituitary Adenomas: Clinical Relevance and Potential Benefits for the Patients

Tingting Cheng[1,2,3], *Ya Wang*[1,2,3], *Miaolong Lu*[1,2,3], *Xiaohan Zhan*[1,2,3], *Tian Zhou*[1,2,3], *Biao Li*[1,2,3] *and Xianquan Zhan*[1,2,3,4,5]*

[1] Key Laboratory of Cancer Proteomics of Chinese Ministry of Health, Xiangya Hospital, Central South University, Changsha, China, [2] Hunan Engineering Laboratory for Structural Biology and Drug Design, Xiangya Hospital, Central South University, Changsha, China, [3] State Local Joint Engineering Laboratory for Anticancer Drugs, Xiangya Hospital, Central South University, Changsha, China, [4] Department of Oncology, Xiangya Hospital, Central South University, Changsha, China, [5] National Clinical Research Center for Geriatric Disorders, Xiangya Hospital, Central South University, Changsha, China

Background: Non-functional pituitary adenoma (NFPA) is a common tumor that occurs in the pituitary gland, and generally without any symptoms at its early stage and without clinical elevation of hormones, which is commonly diagnosed when it grows up to compress its surrounding tissues and organs. Currently, the pathogenesis of NFPA has not been clarified yet. It is necessary to investigate molecular alterations in NFPA, and identify reliable biomarkers and drug therapeutic targets for effective treatments.

Methods: Tandem mass tags (TMT)-based quantitative proteomics was used to identify and quantify proteins in NFPAs. GO and KEGG enrichment analyses were used to analyze the identified proteins. Differentially expressed genes (DEGs) between NFPA and control tissues were obtained from GEO datasets. These two sets of protein and gene data were analyzed to obtain overlapped molecules (genes; proteins), followed by further GO and KEGG pathway analyses of these overlapped molecules, and molecular network analysis to obtain the hub molecules with Cytoscape. Two hub molecules (SRC and AKT1) were verified with Western blotting.

Results: Totally 6076 proteins in NFPA tissues were identified, and 3598 DEGs between NFPA and control tissues were identified from GEO database. Overlapping analysis of 6076 proteins and 3598 DEGs obtained 1088 overlapped molecules (DEGs; proteins). KEGG pathway analysis of 6076 proteins obtained 114 statistically significant pathways, including endocytosis, and spliceosome signaling pathways. KEGG pathway analysis of 1088 overlapped molecules obtained 52 statistically significant pathways, including focal adhesion, cGMP-PKG pathway, and platelet activation signaling pathways. These pathways play important roles in cell energy supply, adhesion, and maintenance of the tumor microenvironment. According to the association degree in Cytoscape, ten hub molecules (DEGs; proteins) were identified, including GAPDH, ALB, ACACA, SRC, ENO2, CALM1, POTEE, HSPA8, DECR1, and AKT1. Western-blotting analysis confirmed the upregulated expressions of SRC and PTMScan experiment confirmed the increased levels of pAKT1, in NFPAs compared to controls.

OPEN ACCESS

Edited by:
Fabienne Langlois, Centre Hospitalier Universitaire de Sherbrooke, Canada

Reviewed by:
Cristiana Tanase, Victor Babes National Institute of Pathology, Romania
Olga Golubnitschaja, University of Bonn, Germany

***Correspondence:**
Xianquan Zhan
yjzhan2011@gmail.com

Specialty section:
This article was submitted to Pituitary Endocrinology, a section of the journal Frontiers in Endocrinology

Received: *01 October 2018*
Accepted: *21 November 2019*
Published: *05 December 2019*

Citation:
Cheng T, Wang Y, Lu M, Zhan X, Zhou T, Li B and Zhan X (2019) Quantitative Analysis of Proteome in Non-functional Pituitary Adenomas: Clinical Relevance and Potential Benefits for the Patients. Front. Endocrinol. 10:854. doi: 10.3389/fendo.2019.00854

Conclusions: This study established the large-scale quantitative protein profiling of NFPA tissue proteome. It offers a basis for subsequent in-depth proteomics analysis of NFPAs, and insight into the molecular mechanism of NFPAs. It also provided the basic data to discover reliable biomarkers and therapeutic targets for NFPA patients.

Keywords: non-functional pituitary adenomas, quantitative proteomics, molecular network, Transcriptomics, Integrative analysis of proteomics and transcriptomics, signaling pathway, predictive preventive personalized medicine, biomarker pattern

INTRODUCTION

Pituitary adenoma is an intracranial tumor, which is clinically classified as functional pituitary adenomas (FPAs) with the elevation of the corresponding hormone in blood and non-functional pituitary adenomas (NFPAs) without clinical elevation of hormones in the blood. NFPA has the prevalence of 7-22/100,000 (1, 2), the standardized incidence of 1.02/100,000 (3), and accounts for 15–37% of all pituitary adenomas, with a median age range from 51.5 to 65.5 years (1–3). Because NFPA does not have excessive hormone secretion, it is not easily diagnosed at its early stage, but is often recognized only when it grows up to compress its surrounding tissues and organs; and commonly 67–90% of diagnosed NFPAs have reached up to a quite large volume (1–3). The natural course of NFPA has not been fully understood. Most NFPAs are benign, only a very small number of NFPAs has the characteristics of invasiveness, aggressiveness, or malignancy. Conversely, the tumor volume of some NFPA patients is also gradually decreasing during its pathological process (4, 5). Currently, no early-stage-diagnosis biomarkers are used for NFPAs, and the classic oncogene mutations that occur in other tumors are not also found in NFPAs. However, studies show that the disrupted cell cycle control and growth factor signaling likely contribute to pathogenesis and natural history of NFPAs (6).

NFPA has a very complex pathogenesis process, involves multiple molecular systems (7), and has heterogeneity in origin of cells and in hormone expressions (8, 9). A study shows that Ki-67 is involved in the growth and reproduction of NFPA, just like other tumors, which is the most consistent marker to assess biological behavior in NFPAs (10). One proteomics analysis of 34 sera from NFPA patients and healthy controls with matched age and sex factors identified nine serum differentially expressed proteins (DEPs) (7 up-regulated and 2 down-regulated), which was able to discriminate NFPAs from normal controls with a good sensitivity (82.4%) and specificity (82.4%) (11). A two-dimensional gel electrophoresis (2DGE)-based mapping proteomic analysis of human FSH-positive NFPA tissues detected ∼1,200 protein spots, which identified 192 redundant proteins from 141 spots and revealed several important pathway-network changes (cell cycle dysregulation, oxidative stress, mitochondrial dysfunction, and MAPK signaling abnormality) (12). However, this 2DGE mapping proteomic study has a relative narrow throughput in identification of proteins, and does not get quantitative information of proteins. Therefore, it is necessary to obtain a high-throughput and large-scale proteomic profile for in-depth understanding of molecular mechanisms and discovery of effective biomarkers for NFPAs. Mass spectrometry (MS) is an essential technique to identify and quantify proteins and post-translational modifications (PTMs) in a proteome (12). 2DGE or two-dimensional difference in-gel electrophoresis (2D DIGE) coupled with MS was extensively used to study pituitary adenomas (8, 13). However, the previous 2DGE-based proteomics in human pituitary adenomas usually achieved the relative low throughput (dozens to several hundreds) in identification of proteins due to the conventional concept of 2DGE (14, 15). Tandem mass tags (TMT)-based two-dimensional liquid chromatography-tandem mass spectrometry (2DLC-MS/MS) can easily achieve several thousands of proteins to significantly increase the throughput in identification of proteins for more effectively mining proteomic components, which is an effective peptide-based protein identification method (13). Moreover, studies have demonstrated that non-coding RNAs, including microRNAs (miRNAs) and long non-coding RNAs (lncRNAs), are involved in the development of NFPAs (16). For example, miR-145-5p in NFPA samples is significantly reduced and negatively correlated with NFPA invasiveness, and overexpression of miR-145-5p can inhibit proliferation and invasiveness of NFPA cells and promote apoptosis (17). Another study shows that CXCR4 mRNA is expressed in 92% of growth hormone secretory pituitary adenomas (GHoma) and 81% NFPAs, whereas SDF1 is found in 63% of GHomas and 78% of NFPAs; and CXCR4 and SDF1 are the strong homogenous markers in all tumor cells of GHomas and NFPAs (18). Therefore, integrative analysis of protomics and transcriptomics has significantly scientific merit for NFPAs (19, 20).

This study used TMT-labeled 2DLC–MS/MS to identify and quantify protein expression profiles of NFPAs. The identified protein data were compared to differentially expressed genes (DEGs) that were obtained from the Gene Expression Omnibus (GEO) database to obtain the overlapped molecules (DEGs; proteins). The overlapped molecules were analyzed with gene ontology (GO) enrichment, KyotoEncyclopaedia Gene and Genome (KEGG) pathway, and protein-protein interactions. The hub molecules (DEGs; proteins) were obtained from KEGG pathway networks, and verified with Western blotting analysis. The resulting data established the large-scale database for NFPA proteome, and provided the scientific data to in-depth understand molecular mechanisms of NFPAs, and discover reliable biomarkers for NFPA treatment.

TABLE 1 | Clinical characteristics of NFPA and control tissue samples.

Group	Sex	Age (year)	Immunohistochemistry (IHC) or clinical information	Experiments
NFPAs	Male	49	ACTH(–), hGH(–), PRL(–), FSH(–), LH(–), TSH(–)	Proteomics
	Female	53	ACTH(–), hGH(–), PRL(–), FSH(–), LH(–), TSH(–)	Proteomics
	Male	40	ACTH(–), hGH(–), PRL(–), FSH(+), LH(–), TSH(–)	Proteomics
	Male	52	ACTH(–), hGH(–), PRL(–), FSH(+), LH(–), TSH(–)	Proteomics
	Female	43	ACTH(–), hGH(–), PRL(–), FSH(+), LH(–), TSH(–)	Proteomics; Western blot
	Male	58	ACTH(–), hGH(–), PRL(–), FSH(–), LH(–), TSH(–)	Proteomics; Western blot
	Female	44	ACTH(–), hGH(–), PRL(–), FSH(+), LH(–), TSH(–)	Western blot
	Male	53	ACTH(–), hGH(–), PRL(–), FSH(–), LH(–), TSH(–)	Western blot
Controls	Female	40	White, Multiple toxic compounds. Blood: HepB (+), HepC (+), HIV(–). IHC: do not test.	Western blot
	Male	36	White, Multiple toxic materials. Blood alcohol = 0.5 g/L. Blood: HepB (+), HepC (–), HIV (–). IHC: do not test.	Western blot
	Female	34	Black, Gunshot wound to chest. Blood alcohol = 0.3 g/L; no drugs. Blood: HepB (+), HepC (–), HIV (–). IHC: do not test.	Western blot
	Female	/	White, 15 h gunshot wound to head. No drugs or alcohol. Blood: HepB (–), HepC (–), HIV (–). IHC: do not test.	Western blot

MATERIALS AND METHODS

NFPA and Control Pituitary Tissues

The post-mortem control pituitary tissue samples used for Western blotting analysis were obtained from Memphis Regional Medical Center, with an approval of University of Tennessee Health Science Center Internal Review Board (UTHSC-IRB). The NFPA tissue samples used for proteomics and Western blotting analyses were obtained from Department of Neurosurgery, Xiangya Hospital, Central South University, with an approval of the Medical Ethics Committee of Xiangya Hospital of Central South University. The written consent information was obtained from the family of each control pituitary donor or each patient after the purpose and nature of all used procedures were fully explained. The detailed information was shown for these NFPA and control pituitary tissue samples (**Table 1**).

Protein Extraction

Each sample was grinded with liquid nitrogen. The grinded samples were collected into a 5-mL centrifuge tube, and a volume of lysis buffer was added that contained 8 M urea, 10 mM dithiothreitol (DTT), 2 mM ethylene diamine tetraacetic acid (EDTA), and 1% protease inhibitor cocktail III, followed by sonication (3x; ice), and centrifugation (20,000 g, 4°C, 10 min). The proteins in the supernatant were precipitated (2 h; −20°C) with a volume of 15% trichloroacetic acid (TCA), and centrifuged (4°C, 10 min) to discard the supernatant. The proteins in precipitate were washed with cold acetone (3x), and then redissolved in a volume of buffer that contained 8 M urea, and 150 μl 100 mM tetraethylammonium bromide (TEAB) at pH 8.0. The 2-D Quant kit was used to determine the protein concentration.

Trypsin Digestion

A volume of reducing solution including 10 mM DTT was added to the protein samples, incubated (37°C; 2 h) in water bath, and cooled at room temperature, followed by a quick addition of alkylating reagent (20 mM iodoacetamide) and incubation in the dark (room temperature; 45 min). The solution of 100 mM TEAB was added to each protein sample to dilute urea concentration to 2M or less. Finally, an amount of trypisn (trypsin/protein mass ratio = 1:50) was added to each tube for overnight hydrolysis, and then added trypsin (trypsin/protein mass ratio = 1: 100) to each tube for another 4 h digestion. The tryptic peptides (100 μg) of each sample were used for subsequent experiments.

TMT Labeling

Each tryptic peptide sample was desalted with Strata X C18 solid-phase extraction column (Phenomenex), and vacuum dried. Each desalted tryptic peptide sample was dissolved in the solution of 0.5 M TEAB, and labeled with 6-plex TMT reagent according to the manufacturer's procedure with a ratio of 1 unit of TMT reagent to 100 μg of tryptic peptides. Briefly, the tryptic peptide sample was incubated (room temperature; 2 h) with TMT reagent, mixed together (1:1), desalted, and lyophilized by vacuum centrifugation. Parallel replicates of the peptide fragments of two groups were performed to eliminate errors due to external confounding factors such as experimental procedures and instrument.

HPLC Fractionation

The desalted TMT-labeled tryptic peptide mixture was fractionated into 80 fractions over 80 min with high-pH reverse-phase high-performance liquid chromatography (HPLC). The Agilent 300 Extend C18 column (5 μm particles, 4.6 mm ID, and 250 mm length) was used to separate peptides with a 2–60% acetonitrile (ACN) plus 10% ammonium bicarbonate at pH 10. Finally, 80 fractions were grouped into 18 fractionated samples, and vacuum dried.

LC-MS/MS

For 18 fractionated peptide samples, each fractionated peptide sample was added with a volume of 0.1% trifluoroacetic acid (TFA), mixed well, and loaded onto the Acclaim PepMap 100

reverse-phase precolumn (Thermo Scientific) to online enter the Acclaim PepMap RSLC reverse-phase analytical column (Thermo Scientific). The LC gradient was set as a 5–25% increase of solvent B (0.1% TFA plus 98% ACN) over 60 min, a 25–35% increase of solvent B in 12 min, and an increase to 80% of solvent B in 4 min, then remained in 80% of solvent B for the last 4 min, with a constant flow-rate (320 nl/min) on an EASY-nLC 1000 UPLC system. MS/MS spectra were obtained on an OrbiTrap Fusion^{TM} MS instrument (ThermoFisher Scientific). Its detection resolution was set as 70,000 for precursor ions in the MS spectrum. Product ion information in the MS/MS spectrum was obtained with high energy collision dissociation (HCD) cleavage for fragmentation of precursor ion, with the collision energy of 38. The resolution of product ions was set as 15,000. The electrospray voltage was set as 2.0 kV. With the automatic gain control (AGC) function, the pre-scan before each sample scan automatically balanced the number of ion implants to prevent charge overload in the analyzer. Cumulative 5E4 intensity ions in the MS spectra were analyzed for MS/MS. The primary MS scan range was set as m/z 400–1,600, the starting point of the secondary MS scan range was fixed at m/z 100.

Database Search of MS/MS Data and Functional Characteristics of Identified Proteins

Mascot search engine (v.2.3.0) was used to search proteins with MS/MS data against UniProt human database (https://www.uniprot.org). UniProt is the most informative and resource-rich protein database. Its data are mainly the subsequent protein sequences, which are derived from the completion of the genome sequencing. It contains a wealth of information on the biological functions of proteins from the literature. The R-software cluster profile was used to reveal gene ontology (GO) characteristics of identified proteins: cellular components (CCs), biological processes (BPs), and molecular functions (MFs). KEGG pathway enrichments were performed for the identified proteins. Benjamini-Hochberg-based adjusted $p < 0.05$ was used as statistical significance. PANTHER (http://www.pantherdb.org/) and Cytoscape software were also used to enrich CCs.

GEO Gene Data of NFPAs

The GEO database is a high-throughput gene expression database submitted by research institutions around the world, which is created in 2000 and maintained by the National Center for Biotechnology Information (NCBI). This study obtained microarray gene data GSE51618 profile datasets of human pituitary adenomas from the public GEO database (http://www.ncbi.nlm.nih.gov/geo/), which were derived from the analysis of 11 tissue samples (3 control pituitaries, 4 non-invasive NFPAs, and 4 invasive NFPAs) with a gene chip human genome platform (Agilent-014850 Whole Human Genome Microarray 4x44K G4112F) in other laboratory. The R-software was used to analyze these NFPA vs. control GEO gene data. False discovery rate (FDR) < 0.05 and fold-changes (FC) ≥ 2 were used to determine each DEG. DEGs were obtained between non-invasive NFPAs and controls, and between invasive NFPAs and controls. Because non-invasive and invasive NFPAs were all NFPAs, thus two sets of DEG data were combined to become one set of DEG data between NFPA and control tissues, which were overlapped with the identified proteins in NFPAs.

Overlapping Analysis of Protein Data and DEG Data

The gene name corresponding to each identified protein was obtained in UniProt human database. Thus, overlapping analysis was performed between the gene names of identified proteins in NFPAs and DEG data between NFPA and control tissues, to obtain the overlapped molecules (DEGs; proteins) for further bioinformatics and functional analysis.

GO and KEGG Pathway Enrichments of Overlapped Molecules

The Database for Annotation, Visualization, and Integrated Discovery (DAVID) provides the comprehensive functional annotation tools for investigators to understand biological meaning behind a large list of genes. DAVID-based GO and KEGG pathway enrichments were used to analyze those overlapped molecules (DEGs; proteins). The parameters ($p < 0.05$ and gene count > 5) were considered as statistical significance. Furthermore, each p-value was corrected with FDR for multiple testing.

Prediction of Protein–Protein Interaction

STRING 10.0 (http://string-db.org/cgi/input.pl) was used to construct the protein-protein interaction (PPI) network of those overlapped molecules (DEGs; proteins) with a high confidence (>0.700). Then Cytoscape software (3.6.1) was used to get hub molecules (genes; proteins) based on degrees (Pearson's correlation coefficient >0.50, $P < 0.05$).

Western Blotting

The 10% sodium dodecyl sulfate-polyacrylamide gel electrophoresis (SDS-PAGE) gel was used to separate proteins (NFPAs; controls). The separated proteins were transferred onto a polyvinylidene fluoride (PVDF) membrane. The proteins on PVDF membrane were incubated (4°C; overnight) with mouse anti-human SRC antibody (1:1000), AKT1 antibody (1:1000), and β-actin antibody (1:2000), followed by incubation (2 h; room temperature) with secondary antibody (horseradish peroxidase-conjugated goat anti-mouse antibody; 1:5000). The Western blotting experiments of each protein between NFPAs and controls were repeated (≥ 3). Student's t-test was used to calculate the p-value, with a statistical significance level of $p < 0.05$.

RESULTS

Proteomic Profiling of NFPAs and Its Functional Characteristics

TMT-based quantitative proteomics identified 6076 proteins in NFPAs (**Supplemental Table 1**), including 4666 proteins with quantitative information. Peptide sequence match (PSM) was set as ≥ 1 for identification of each protein. The analysis of 6076

proteins revealed that more than 94% of identified proteins were distributed in the range of 7–200 kDa and pH 4–10. The top 11 abundance proteins (**Supplemental Table 1**) were SNRPB (small nuclear ribonucleoprotein-associated proteins B), TECR (very-long-chain enoyl-CoA reductase), TMEM263 (transmembrane protein 263), MARC1 (mitochondrial amidoxime-reducing component 1), APMAP (adipocyte plasma membrane-associated protein), CSNK1A1 (casein kinase I isoform alpha), APOC3 (apolipoprotein C-III), CSTB (cystatin-B), TTR (transthyretin), IGHA1 (immunoglobulin heavy constant alpha 1), and GET4 (Golgi to ER traffic protein 4 homolog). However, it is worth noting that many lower abundance proteins might play more important roles in the molecular networks (12).

Moreover, GO and KEGG pathway enrichment analyses were used to reveal the potential functions of those 6076 proteins. GO-based CC, BP, and MF enrichment analyses revealed the overall functional characteristics of 6076 proteins. Those proteins were mainly distributed in cell part (38 %), organelle (26 %), macromolecular complex (17 %), and membrane (13%) (**Figure 1**). KEGG pathway enrichment analysis ($P < 0.05$) of 6076 proteins identified 114 statistically significant signaling pathways (**Supplemental Table 2**). Based on the number of matched proteins in each pathway and the p-value, 12 important pathways were identified (**Figure 2**), including endocytosis, protein processing in endoplasmic reticulum, spliceosome, ribosome, carbon metabolism, platelet activation, valine, leucine and isoleucine degradation, fatty acid metabolism, proteasome, fatty acid degradation, pyruvate metabolism, and SNARE interactions in vesicular transport. These pathways were involved in cellular energy metabolism, protein synthesis and processing, which played important roles in tumorigenesis and progression.

DEG Profiling in NFPAs and Its Functional Characteristics

Microarray transcritpomic data of NFPAs were obtained from GEO database. A total of 1789 DEGs was obtained between non-invasive NFPAs and controls, including 900 (50.31%) upregulated and 889 (49.69%) downregulated DEGs (**Figure 3A**, **Supplemental Table 3**). A total of 2751 DEGs was identified between invasive NFPAs and controls, including 1274 (46.31%) upregulated and 1477 (53.69%) downregulated DEGs (**Figure 3B**, **Supplemental Table 4**). Because NFPAs include invasive and non-invasive NFPAs, these two sets of DEG data ($n = 1,798$ in non-invasive NFPAs; and $n = 2,751$ in invasive NFPAs) were combined into one set of DEG data ($n = 3,598$) between NFPAs and controls after removal of the repeated DEGs between invasive and non-invasive NFPAs, including 1761 upregulated DEGs, 1764 downregulated DEGs, and 73 genes that were inconsistent in two sets (non-invasive vs. invasive) of DEG data (**Supplemental Table 5**).

Overlapped Molecules Between 3598 DEGs and 6076 Proteins, and Their Functional Characteristics

Overlapped molecules (DEGs; proteins): An overlapping analysis was performed between 3598 DEG data and 6076 proteins, which obtained 1088 overlapped molecules (DEGs; proteins)

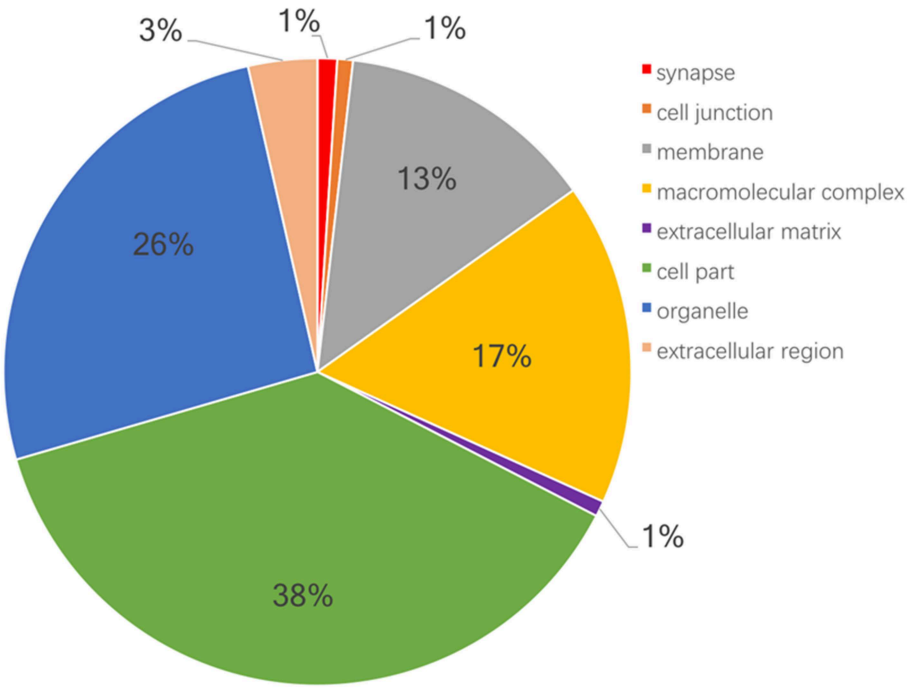

FIGURE 1 | Classification of 6076 proteins according to the cell components with PANTHER.

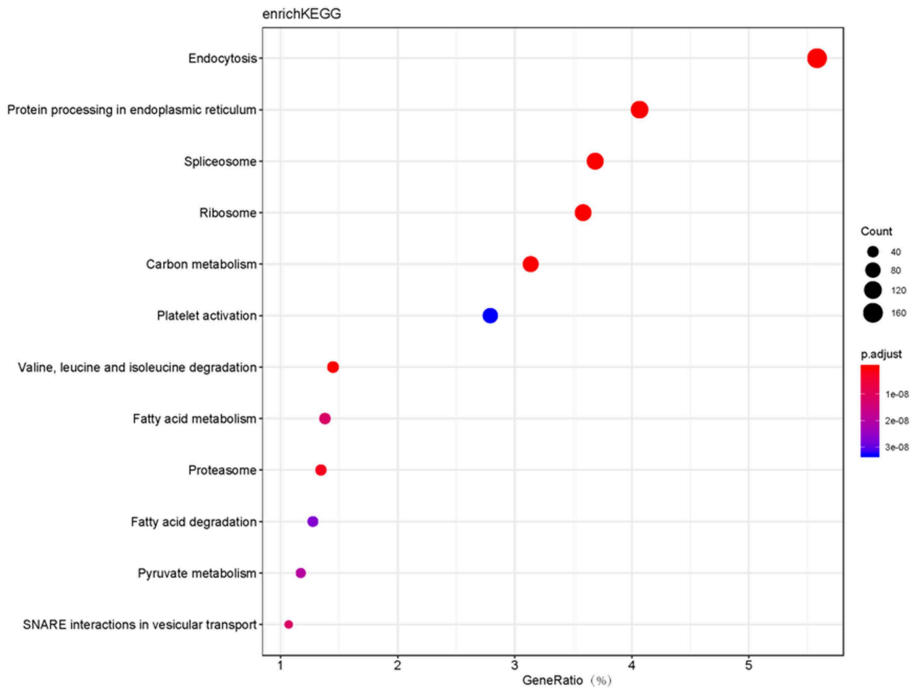

FIGURE 2 | The bubble plot of top 12 KEGG pathway enrichments with 6076 proteins ($P < 0.05$). The bubble color scaled the enrichment score. Red color means more significant enrichment. The size of the bubble scaled the count of the enriched genes. X-axis is equal to gene ratio, which means the percentage of enriched target genes among total 6076 genes. Y-axis is the name of the KEGG pathway.

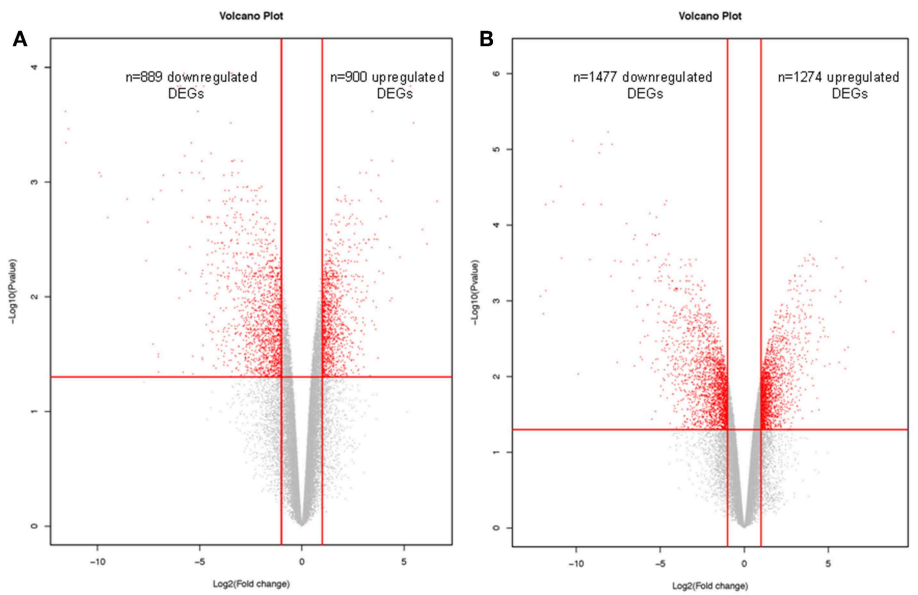

FIGURE 3 | Volcano plots of differentially expressed genes (DEGs) that were derived from microarray analysis of non-invasive NFPAs **(A)** and invasive NFPAs **(B)** compared to control tissues. The native $\log_{10}$ [false discovery rate (FDR) adjusted p-values] in the y-axis was plotted against the average $\log_2$(fold changes in expression) in the x axis. DEGs were determined using Limma followed by FDR correction. Horizontal dashed line indicated the threshold for significance (FDR adjusted $p < 0.05$) and vertical dashed line indicated the upregulated (right side) and downregulated (left side) probes.

(**Figure 4**), including 644 upregulated DEGs, 426 downregulated DEGs, and 18 genes that were inconsistent in two sets (non-invasive vs. invasive) of DEG data (**Supplemental Table 6**).

GO Enrichment Analysis

Those 1088 overlapped molecules (DEGs; proteins) were grouped according to BP, CC, and MF with Cytoscape software

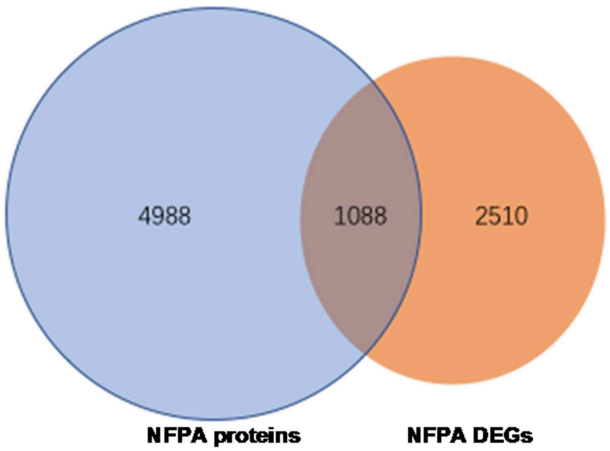

FIGURE 4 | The 1088 overlapped molecules (DEGs; proteins) between 6076 identified proteins and 3598 DEGs obtained from GEO database.

(**Figure 5**). For BP enrichment, the overlapped molecules (DEGs; proteins) were mainly enriched in neutrophil degranulation, neutrophil activation, neutrophil-mediated immunity, regulation of vesicle-mediated transport, small molecule catabolic process, signal release, organic hydroxy compound metabolic process, coenzyme metabolic process, organic acid biosynthetic process, and carboxylic acid biosynthetic process. For CC enrichment, the overlapped molecules (DEGs; proteins) were mainly enriched in cell-substrate junction, focal adhesion, cell-substrate adhesion junction, myelin sheath, cytoplasmic vesicle lumen, vesicle lumen, secretory granule lumen, ruffle membrane, postsynapse, and ruffle. For MF enrichment, the overlapped molecules (DEGs; proteins) were mainly involved in cell adhesion molecule binding, actin binding, cadherin binding, tubulin binding, coenzyme binding, guanyl ribonucleotide binding, guanyl nucleotide binding, ATPase activity coupled, and microtubule binding.

KEGG Pathways

KEGG pathway analysis of those 1088 overlapped molecules (DEGs; proteins) revealed 52 statistically significant pathways (adjusted p-value < 0.05, count>5) (**Figure 6**; **Supplemental Figure 1**). The overlapped molecules (DEGs; proteins) were mainly enriched in the following pathways: focal adhesion, cGMP-PKG signaling pathway, platelet activation, carbon metabolism, dopaminergic synapse, human cytomegalovirus infection, proteoglycans in cancer, regulation of actin cytoskeleton, retrograde endocannabinoid signaling, and biosynthesis of amino acids.

Construction of PPI Network to Select Hub Molecules

A hub molecule is a molecule that plays a vital role in biological processes, and regulates other molecules in a pathway network. The PPI network of 1088 overlapped molecules (DEGs; proteins) was constructed and the most significant module was obtained with Cytoscape (**Figure 7**). According to degree levels, the top 10 hub molecules (nodes: DEGs; proteins) were glyceraldehyde-3-phosphate dehydrogenase (GAPDH; degree = 148), serum albumin (ALB; degree = 143), acetyl-CoA carboxylase 1 (ACACA; degree = 137), proto-oncogene tyrosine-protein kinase (SRC; degree = 115), RAC-alpha serine/threonine-protein kinase (AKT1; degree = 114), calmodulin (CALM1; degree = 109), POTE ankyrin domain family member E (POTEE; degree = 108), heat shock cognate 71 kDa protein (HSPA8; degree = 92), mitochondrial 2,4-dienoyl-CoA reductase (DECR1; degree = 82), and gamma-enolase (ENO2; degree = 75). The degree of the vertice is the most basic structure of the graph, which refers to the number of edges associated with it. Molecular Complex Detection (MCODE) detects the densely connected regions in large protein-protein interaction networks that may represent molecular complexes (21). A significant module was subsequently constructed with 57 nodes and 347 edges, which gained the highest MCODE score (**Figure 8**).

Western Blotting Validation of Overlapped Molecules (DEGs; Proteins)

To validate the hub molecules, which were also overlapped molecules (DEGs; proteins) in NFPAs, western blotting was used to analyze the randomly selected hub molecules (SRC and AKT1). The results showed the fold-change of 1.31 for SRC and 1.01 for AKT (**Figure 9**). For SRC, western blotting analysis confirmed SRC was an unregulated DEG and its proteomic result. For AKT1, western blotting results demonstrated that AKT1 protein was expressed in NFPAs, but did not have significant difference between NFPAs and controls.

DISCUSSION

NFPA is a type of pituitary adenomas without specific clinical symptoms of hormone hypersecretion in its early stages (22). However, NFPA gradually grows up to compress its surrounding tissues, which results in visual defects and may progress to hypopituitarism. Thus, it is not easily diagnosed at its early stage, but often diagnosed at its middle or late stages. It is critically important to clarify molecular mechanisms of NFPAs for identification and development of more effective diagnostic and therapeutic strategies. The NFPA is a complex disease, and involves a series of molecular changes at the levels of genome, transcriptome, proteome, and metabolome. Multi-omics strategy is an effective approach to achieve those molecular changes in NFPAs (19, 20). This study integrated TMT-based quantitative proteomics and the public GEO transcriptomic data in NFPAs.

TMT-based quantitative proteomics identified a total of 6076 proteins in NFPA tissues. A total of 114 statistically significant KEGG pathways were enriched with those 6076 proteins, including endocytosis and spliceosome pathways. KEGG pathway analysis found that 162 proteins among 6076 proteins were involved in endocytosis (**Figure 10**, **Supplemental Table 7**). Endocytosis was the basic process of all eukaryotic cells, including extracellular nutrient uptake, processing and presentation of antigens, apoptotic cell clearance, and cell surface protein regulation such as adhesion proteins, channel proteins, and receptors. Endocytosis and endocytic

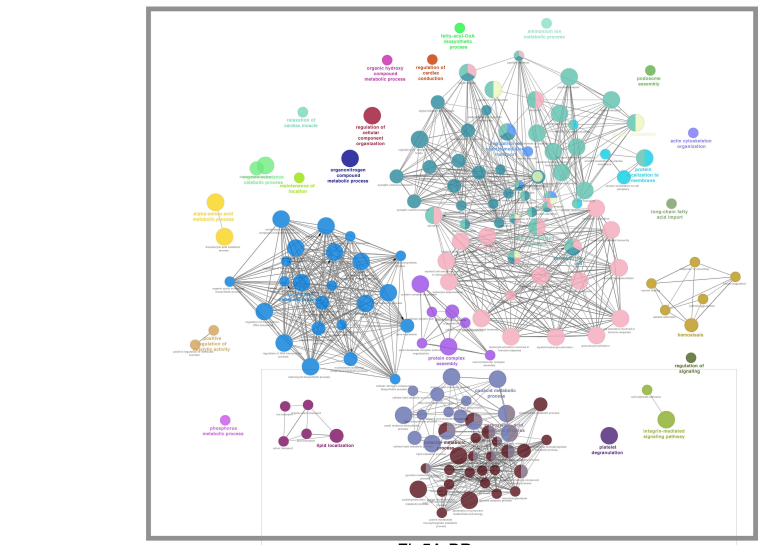

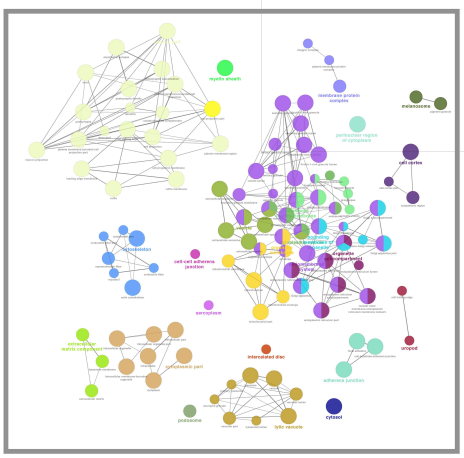

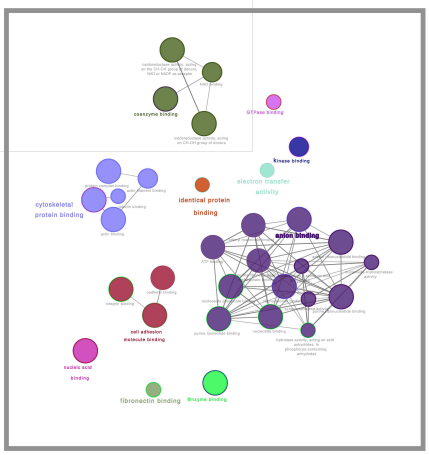

FIGURE 5 | The functional characteristics of 1088 overlapped molecules (DEGs; proteins) according to the biological process (BP), cellular component (CC), and molecular function (MF). The less p-value and more significant enrichments were shown with the greater node size. The same color indicated the same function group. Among the groups, a representative of the most significant term and lag highlighted was chosen. The larger node means less p-values and more significant enrichments. The same color represents the same functional group.

proteins regulated multiple biological processes, including cell apoptosis, cell cycle, and mitosis in cancer cells (23, 24). It is worth noting that 107 proteins among 6076 proteins were distributed in the spliceosome pathway (**Figure 11**, **Supplemental Table 8**). Spliceosome was an important way to regulate alternative splicing in cancer because spliceosomes made different transcripts for the same one gene in cancer cells, which was a driving factor for cancer progression (25). These pathways were involved in cellular energy metabolism, protein synthesis, and protein processing, which might significantly contribute to the pathogenesis of NFPAs.

Microarray and high throughput sequencing were widely used to detect and quantify the transcriptomic profile of the human genome, which is useful in the identification of target genes of interest for diagnosing or treating NFPAs (26). A total of 3598 DEGs was identified in NFPAs compared to controls with the public GEO transcriptomic data. An overlapping analysis was performed between 3598 DEG data and 6076 protein data, which obtained 1088 overlapped molecules (DEGs; proteins). It also means that these 1088 DEGs at the level of transcriptome, through transcriptional regulation and translation, ultimately functioned in the form of proteins in the body. The KEGG pathway analysis of those 1088 overlapped molecules (DEGs; proteins) revealed 52 statistically significantly KEGG pathways, including focal adhesion, cGMP/PKG, and platelet activation pathways.

The pathway with distribution of the most overlapped molecules (DEGs; proteins) was the focal adhesion pathway (**Figure 12**, **Supplemental Table 9**). Focal adhesion pathway consisted of many pro-survival signaling molecules such as

FIGURE 6 | The bubble plot of KEGG pathway enrichments of 1088 overlapped molecules (DEGs; proteins) ($P < 0.05$). The bubble color scaled the enrichment score. Red color means more significant enrichment. The size of the bubble scaled the count of the enriched genes. X-axis is equal to gene ratio, which means the percentage of enriched target genes among total 1088 molecules (DEGs; proteins). Y-axis is the name of the KEGG pathway.

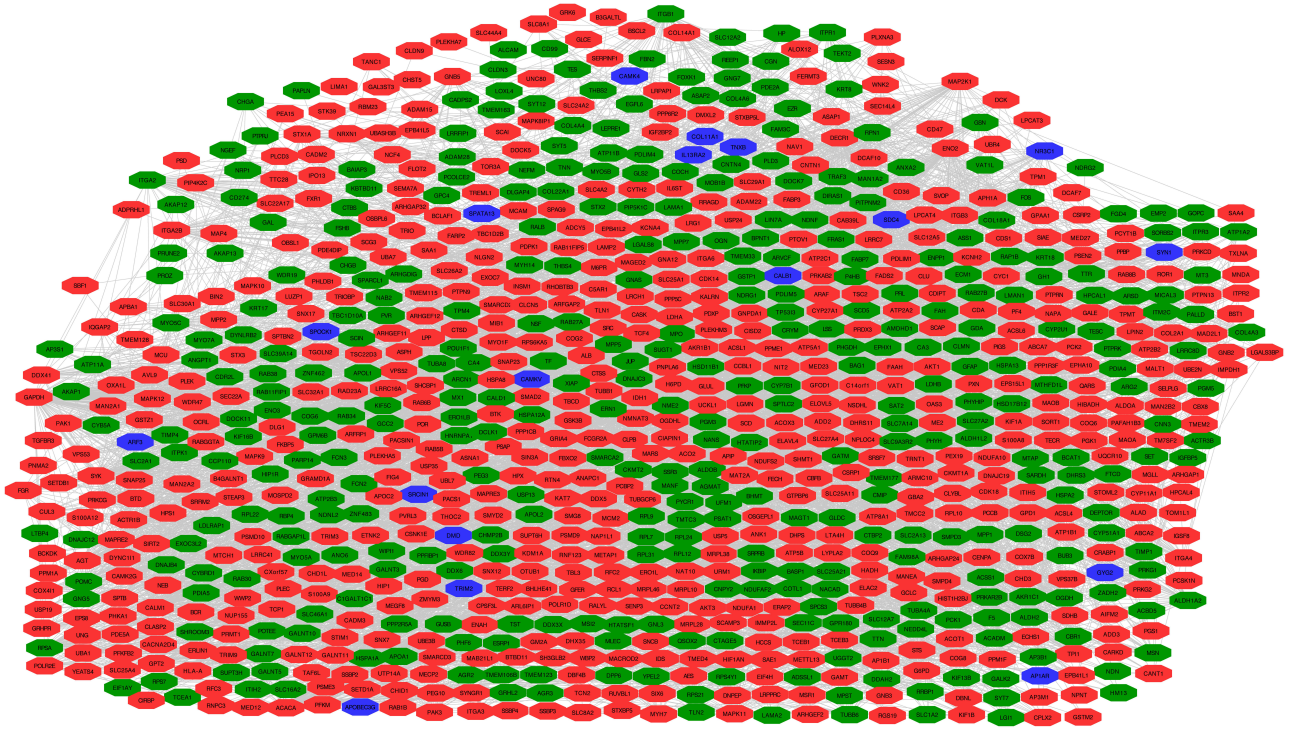

FIGURE 7 | Protein-protein interaction (PPI) network of 1088 overlapped molecules (DEGs; proteins). Pearson's correlation coefficient >0.50, and $P < 0.05$. Green indicates the downregulated genes, red indicates the upregulated genes, and blue indicates genes that are inconsistent in invasive or non-invasive NFPAs.

growth factor receptors, intracellular molecules, and integrins. This pathway played important roles in the regulation of cell behavior and tumor cell survival, and might be cancer therapeutic targets (27). Thus, clarification of molecular processes of focal adhesion signaling might offer better insights into signal bypass and molecular mechanism of resistance, and help to develop reasonable multiple options of treatments. One of the important protein families in the pathway was the integrin family. FAK was a core mediator in the integrin signaling (28). FAK had three domains, including (i) focal adhesion targeting (FAT) region in the C-terminal, (ii) kinase domain in the central region, and (iii) band 4.1, ezrin, radixin and moesin (FERM) sequence in the N-terminal (29). Binding of integrin to ECM resulted in phosphorylation of FAK at several tyrosine residues including Tyr397 to increase kinase activities and promote the interaction of FAK with other proteins including SRC (30–32). One study found that FAK directly bond to cortactin (an actin regulator), which was not only a key force movement and focal adhesion conversion, but also affected cell survival (33). This study found 35 molecules (DEGs; proteins) distributed in this pathway (**Supplemental Table 9**), which suggested that the biological behavior of NFPA should be similar to that of other tumors, and that there should be a huge difference in cell adhesion between NFPAs and normal pituitaries. Previous studies examined the expression of FAK with immunohistochemistry in 49 human pituitary adenomas, and analyzed the relationship of FAK and invasiveness of pituitary adenomas. The results showed that there were 36 cases (73.5%) with FAK expression, and the expression level of FAK was highly correlated with invasiveness of pituitary adenomas, which clearly indicated that the integrin-focal adhesion kinase signaling pathway played a role in the invasion of pituitary adenomas (34). It also provided new ideas for one to study the pathogenesis and treatment of targeted drugs in pituitary adenomas.

The cGMP/PKG pathway played complex roles in cancer, and differed in different tumor types and even in different model systems (32). This study found 23 molecules (DEGs; proteins) distributed in cGMP/PKG pathway (**Figure 13**, **Supplemental Table 10**). It has been reported that cGMP promoted tumorigenesis and anticancer effects. For example, the activated cGMP/PKG pathway induced multiple cancers (33, 35–37). Studies found specifically activated protein kinase G1 (PKG1) triggered MAPK signaling pathway to promote growth of melanoma (38). GMP analogs that activated PKG were a novel molecular strategy that interferes with tumor progression, and had attracted interest in oncology (32). Some studies demonstrated that cGMP/PKG pathway-targeted therapeutic potentials for multiple cancers (39, 40). This signaling was also involved in NFPA pathogenesis, with a wide distribution of DEGs from GEO database and of proteins identified with TMT-quantitative proteomics in human NFPAs. Generally NFPAs grow slowly, with low rate of invasiveness, it may be associated with activation of cGMP-PKG pathway. However, no cGMP/PKG pathway had been studied previously in NFPA

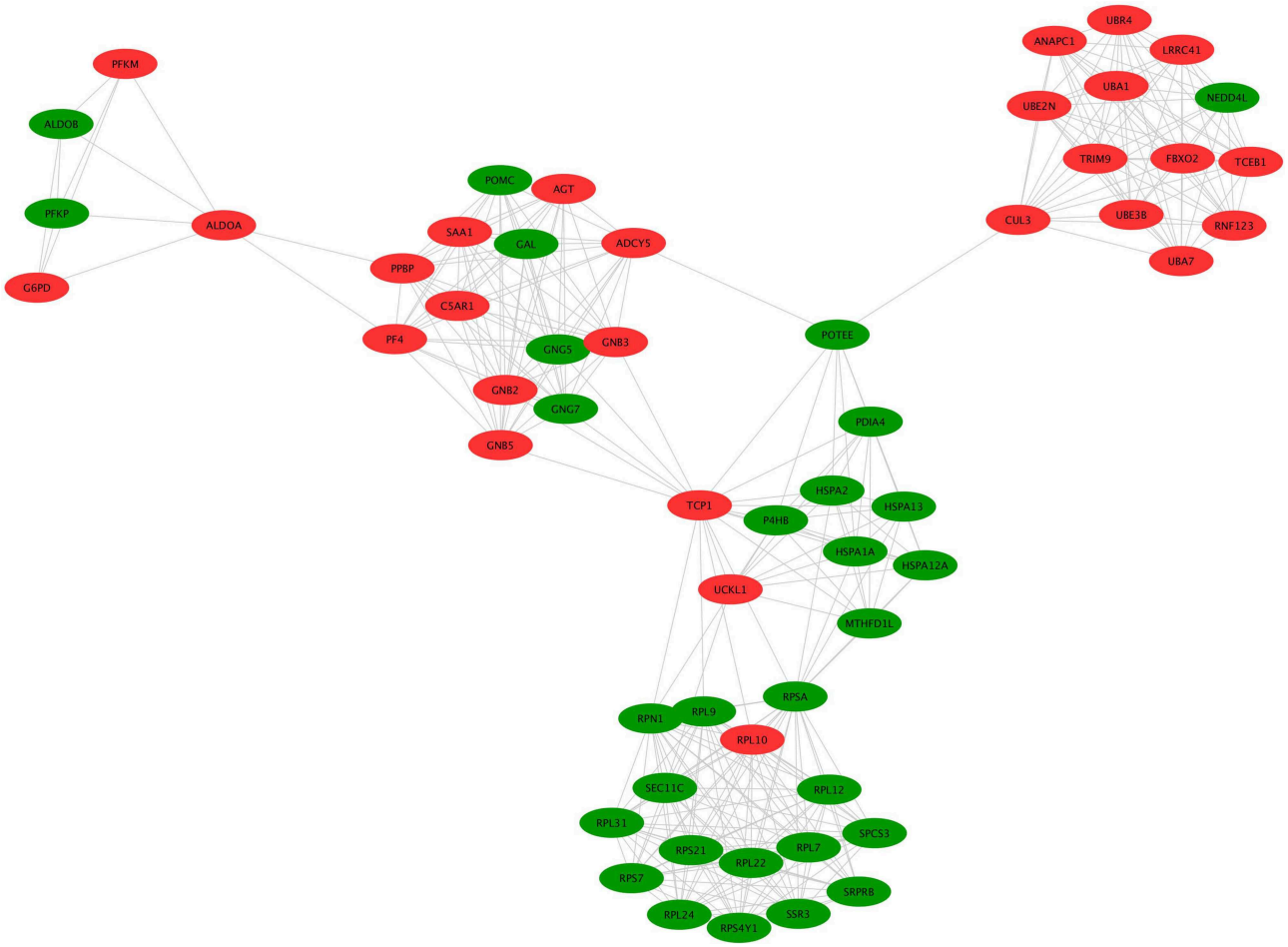

FIGURE 8 | MCODE identification of the most significantly enriched module. The module with the highest MCODE score was selected from the PPI network. Green indicates the downregulated genes and red indicates the upregulated genes.

yet. This present study provided a basis for further in-depth investigation of cGMP/PKG pathway in pituitary adenomas.

The platelet activation pathway was always in a prominent position in the list of enriched KEGG pathways (**Figure 14**, **Supplemental Table 11**). In recent years, the change of tumor microenvironment has become a research hotspot. Different tumor microenvironments were formed in each progression step of cancer and had multiple abilities to induce adverse and beneficial consequences of tumorigenesis (41). The roles of platelets in hemostasis and thrombosis were well-recognized. Platelets were also looked as multi-functional cells; for example, it recruited and regulated monocytes and granulocytes in tumor tissues, which indicated that platelet played important roles in production of tumor-associated macrophages/neutrophils (42). Many studies revealed that platelets were relevant to cancer biology as a hallmark of cancer, and that platelets participated in multistep processes of tumorigenesis (43, 44). In addition to its traditional role in hemostasis and thrombosis, platelets involved in hemostasis, thrombosis, inflammation and cancer interactions are complex and important in every disease process. Our study for the first time reported a correlation between platelet activation and the development of NFPAs.

Comparison of GEO transcriptomics data (DEGs) and proteomics data found that not all DEGs were expressed at the protein level. For many upregulated DEGs, the corresponding proteins were not detected. It reminded one not all DEGs in this study were transcribed into proteins to exert their functions. However, the molecular mechanisms of these DEGs without expressions at the protein level have not been fully understood yet. Among 1088 overlapped molecules (DEGs; proteins), the highest change in the GEO database was GH ($\log_2$FC = −12.56.). This means that GH was most significantly downregulated in NFPAs compared to normal pituitary tissues. It is consistent with previous research results (8, 13). Also, pituitary adenoma itself often results in the development of hypopituitarism, including GH deficiency (GHD). GHD has been reported in up to 85% of NFPA patients (45, 46).

The 1088 overlapped molecules (DEGs; proteins) were analyzed with String and Cytoscape software, and the hub molecules were obtained according to the degree, including

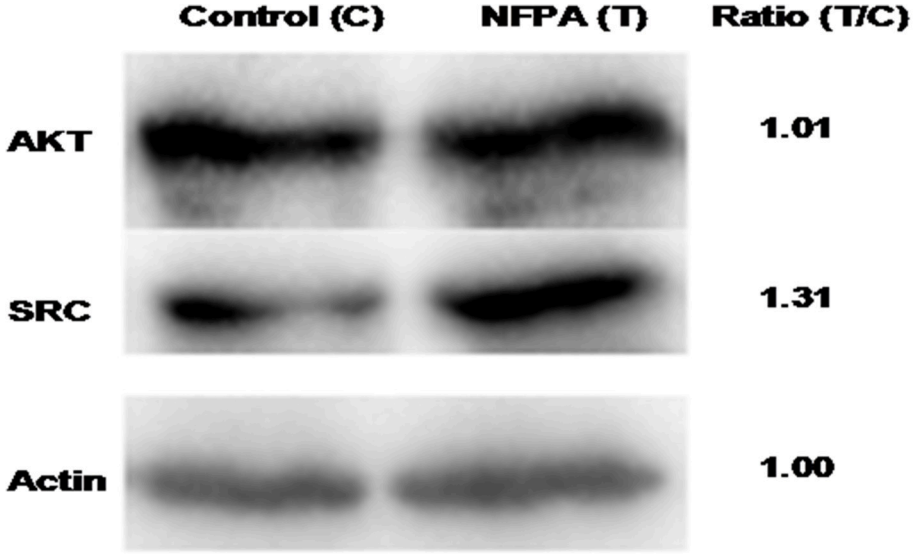

FIGURE 9 | Western blotting analysis of overlapped molecules (AKT and SRC) between NFPAs and controls. T, tumor (NFPAs); C, control (pituitary tissues). Ratio (T/C) means the ratio of the optic density (OD) values between NFPAs and controls ($n = 3$). The internal reference actin was no difference between NFPAs and controls.

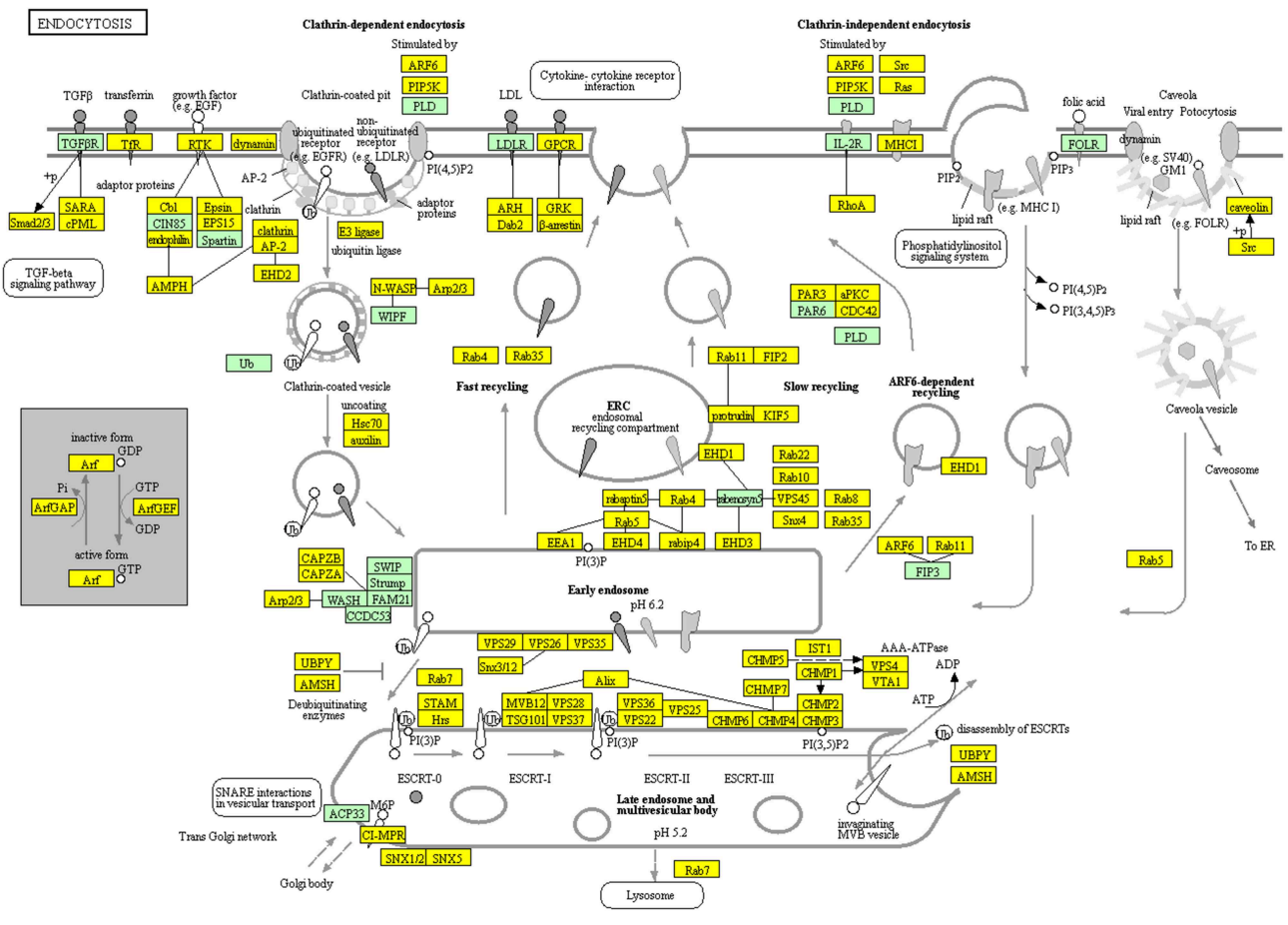

FIGURE 10 | Endocytosis pathway altered in an NFPA. Yellow means the identified proteins.

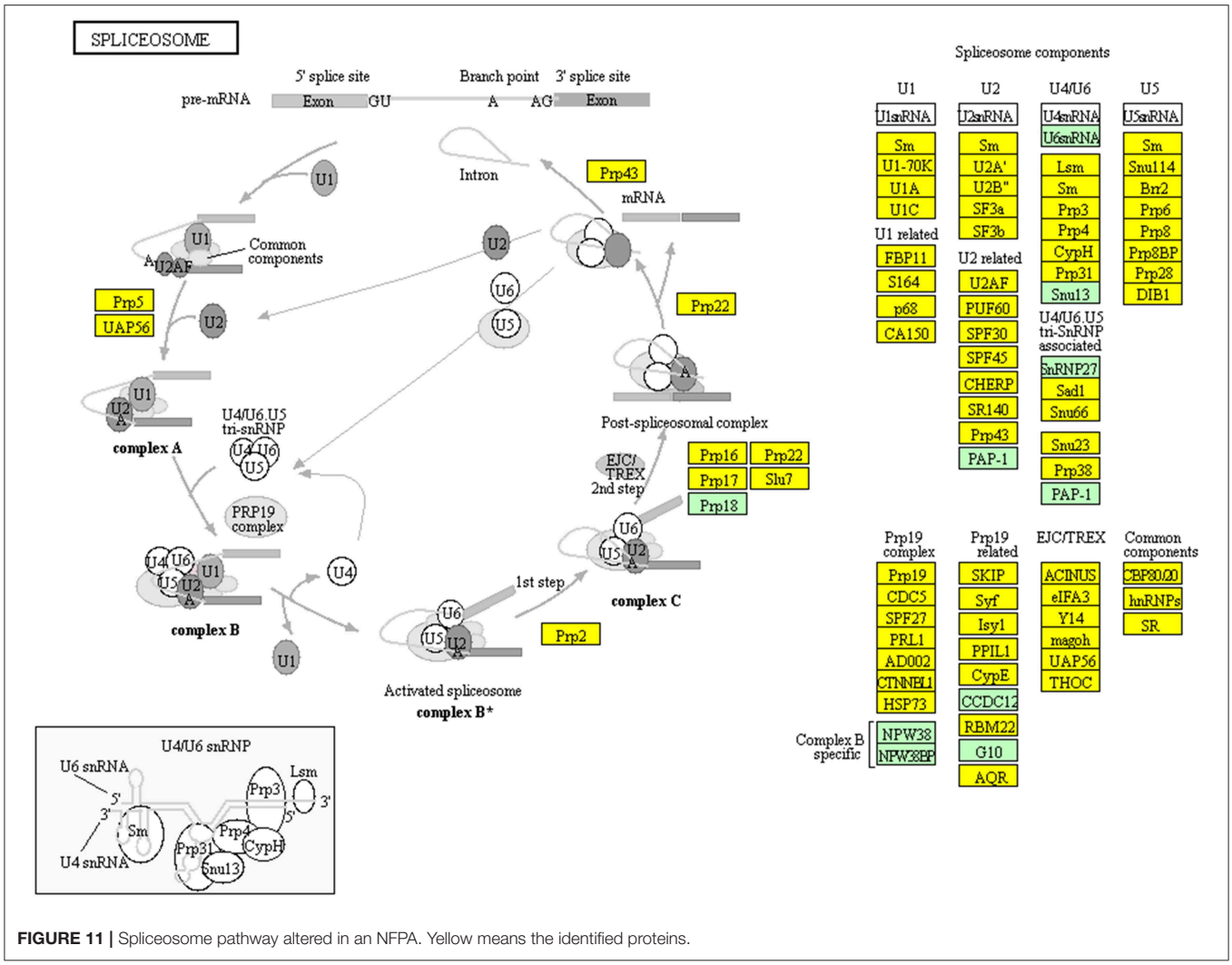

FIGURE 11 | Spliceosome pathway altered in an NFPA. Yellow means the identified proteins.

GAPDH (degree = 148), ALB (degree = 143), ACACA (degree = 137), SRC (degree = 115), and AKT1 (degree = 114). GAPDH is glyceraldehyde-3-phosphate dehydrogenase, an enzyme in the glycolysis process. The gene encoding this enzyme is a housekeeping gene, which is highly expressed in almost all tissues. ALB is the main substance that maintains the body's nutrition and osmotic pressure. SRC is activated by different classes of receptors. The activated SRC regulates multiple biological processes such as cell adhesion, cell cycle, cell migration, immune response, cell transformation, and cell apoptosis (47). Studies found that when the SRC/FAK pathway was disturbed, FAK began to be depleted, and the isolation of FAK-high-efficiency cells or the expression of non-phosphorylated FAK proteins resulted in the active SRC to be isolated from focal adhesions into intracellular sites (48), and inhibition of autophagy recovered active SRC in the peripheral adhesion process to cause the death of cancer cells. Therefore, these proteins were considered to be the main targets of cancer treatment (49). In fact, SRC family kinases (SFKs) were overexpressed/overactivated in various malignancies, which was associated with poor disease progression and poor prognosis in patients with various cancers (50); for example, SRC was overexpressed in lung cancers (51). Some SFK inhibitors had successfully entered clinical trials, and were considered as the most potential drugs. For example, an SRC inhibitor BMS-354825 (aka Dasatinib) targeted all SFKs to inhibit the SRC signaling pathway (52). This present study also showed that SRC was a hub molecule and participated in multiple pathways in NFPAs. SRC inhibitors might be also potential target genes for the treatment of NFPA patients, which provided new ideas for treatment of NFPAs. Another hub molecule, acetyl-CoA carboxylase (ACACA) was a rate-limiting enzyme and upregulated in fatty acid synthetic pathway. ACACA was traditionally recognized as target of metabolic syndrome. However, studies found that malignant tumors had a strong capability for fatty acids synthesis (53), that ACACA was overexpressed in malignant cancers, and that the inhibition of ACACA resulted in cell-cycle arrest and apoptosis of cancer cells (54, 55). Thus, ACACA and some fatty acids might play important roles in cancer cell survival. Cancer

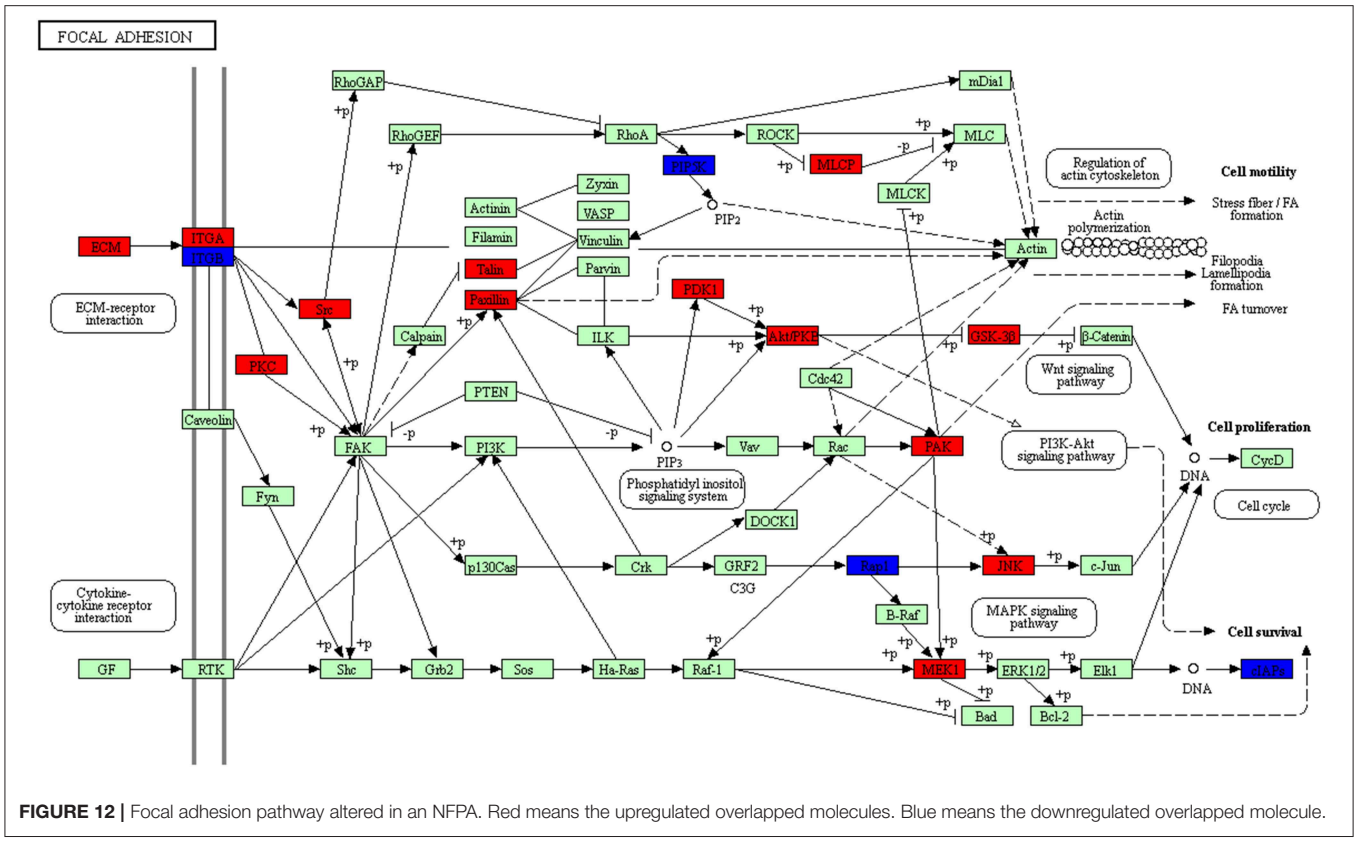

FIGURE 12 | Focal adhesion pathway altered in an NFPA. Red means the upregulated overlapped molecules. Blue means the downregulated overlapped molecule.

cells could re-connect metabolic pathways from glycolysis-dependent patterns to lipogenesis-dependent patterns. AMPK was phosphorylated by an ACACA, which maintained cellular energy homeostasis to play an important role, while the cells were under stress (56, 57). Highly expressed lipogenic enzymes such as ACACA were integrated with certain signaling pathways that triggered tumorigenesis, invasion, and metastasis (58). The effects of abnormal metabolism on malignant transformations in cancer research have been underestimated for decades and may become another hallmark of anti-cancer and an attractive target for intervention. Akt kinase was an important protein in the PI3K-AKT-mTOR pathway and was activated by PI3K (phosphoinosidite-3-OH kinase). It was dysregulated in various tumors. Studies found that AKT was an important regulator in cell proliferation and apoptosis in the tumorigenesis process (59). Several studies demonstrated that AKT activation was associated with several tumor invasions (60). The PI3K-AKT pathway has been proposed to play an important role in the metabolic pathway of pituitary tumors, and future clinical studies should focus on the PI3K-AKT pathway for drug research and individualized treatment (61), which was consistent with our results regarding the overlapped molecule (DEG; protein)—AKT gene was upregulated in NFPAs compared to controls. Furthermore, this study used western blotting analysis to confirm that the expression of AKT1 protein in NFPA and control tissues although it was not changed significantly between NFPAs and controls. However, in our research group, another study found phosphorylated AKT1 in NFPA was significantly increased (62), which might lead to the activation of PI3K-AKT-mTOR pathway. In addition, studies also showed that low levels of APAF-1 were inversely related to invasiveness, and cathepsin B expression was positively related to invasiveness in pituitary adenomas (63). This TMT-quantitative proteomics identified multiple cathepsin family members, including cathepsin L1, cathepsin B, cathepsin G, cathepsin D, cathepsin Z, cathepsin S, cathepsin F, cathepsin W, and pro-cathepsin H, in human NFPA tissues (**Supplemental Table 1**). It clearly demonstrated that cathepsin family might play important roles in NFPA pathogenesis. Vascular endothelial growth factor (VEGF) and basic-fibroblast growth factor (bFGF) were significantly elevated in sera of pituitary adenoma patients (64). This TMT-quantitative proteomics found that FGF receptor 4 (FGFR4) and FGFR1 oncogene partner 2 (FGFR1OP2) were expressed in NFPA tissues. These findings demonstrated that these hub molecules (DEGs; proteins) were potential biomarkers for NFPAs.

For AKT1, western blotting results showed that AKT1 protein was expressed in NFPAs, but did not have significant difference between NFPAs and controls. This result indicated that AKT1 was a DEG at the level of transcriptome, but it was not a DEP at the level of proteome, between NFPAs and controls. It might be derived from different protein PTMs to produce different AKT1 proteoforms (65–68), which was confirmed by our another PTMScan experimental study that the phosphorylation levels at residues Ser473, Thr308, or Thr312 in AKT1 were significantly increased by at least 3 folds in NFPAs compared to controls (62). Therefore,

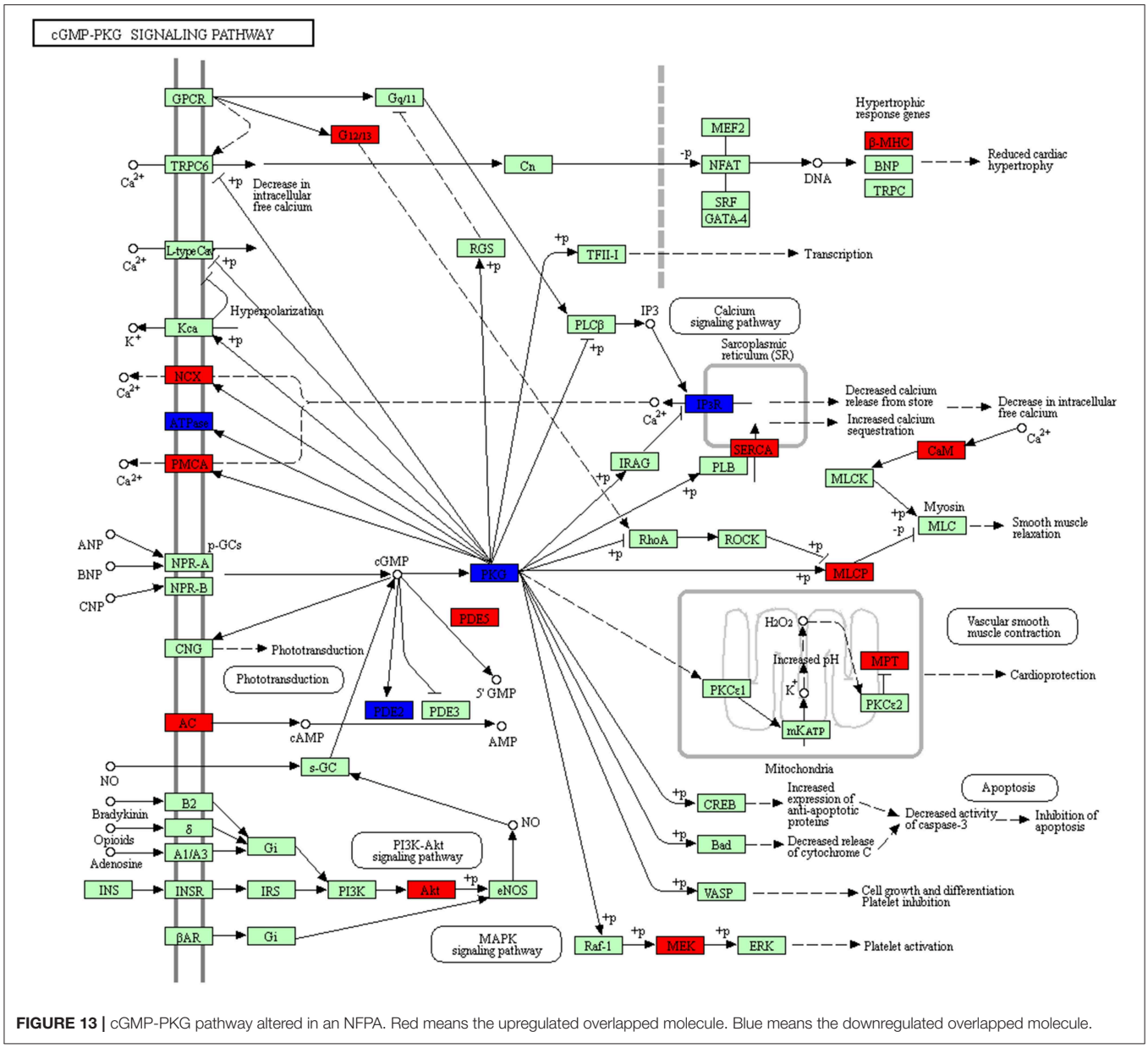

FIGURE 13 | cGMP-PKG pathway altered in an NFPA. Red means the upregulated overlapped molecule. Blue means the downregulated overlapped molecule.

the phosphorylated AKT1 (pAKT1) might contribute to NFPA pathogenesis.

Furthermore, a total of 6076 proteins identified from human NFPA tissues with TMT-based quantitative proteomics in this study (**Supplemental Table 1**) were compared to a total of 2175 proteins identified from human anterior pituitary gland with SDS-PAGE-LC-MS/MS and LC-LC-MS/MS (**Supplemental Table 12**) (69). A total of 1933 proteins were identified in both NFPAs and anterior pituitary gland, 242 proteins were only identified in anterior pituitary gland but not in NFPAs, 4143 proteins were only identified in NFPAs but not in anterior pituitary gland. It clearly demonstrated that much more proteins (n = 3,901 6,076–2,175) were identified in NFPAs compared to anterior pituitary gland. The main reason might be because we used more peptide fractions, longer LC gradient, and more sensitive mass spectrometer. Anyway, those two mapping proteomic data-sets from the corresponding NFPA tissues and anterior pituitary gland were precious resource to establish proteomic databases for human NFPA tissues and anterior pituitary glands, study the physiological functions of anterior pituitary glands and pathogenesis of NFPAs, and discover potential protein pattern biomarkers for NFPAs.

STRENTHS AND LIMITATIONS

Strengths

NFPNA is involved in a series of molecule changes at the levels of DNAs (genome), RNAs (transcriptome), proteins (proteome), and metabolites (metabolome). Of them, transcriptome and proteome are the functional performers of genome. This study

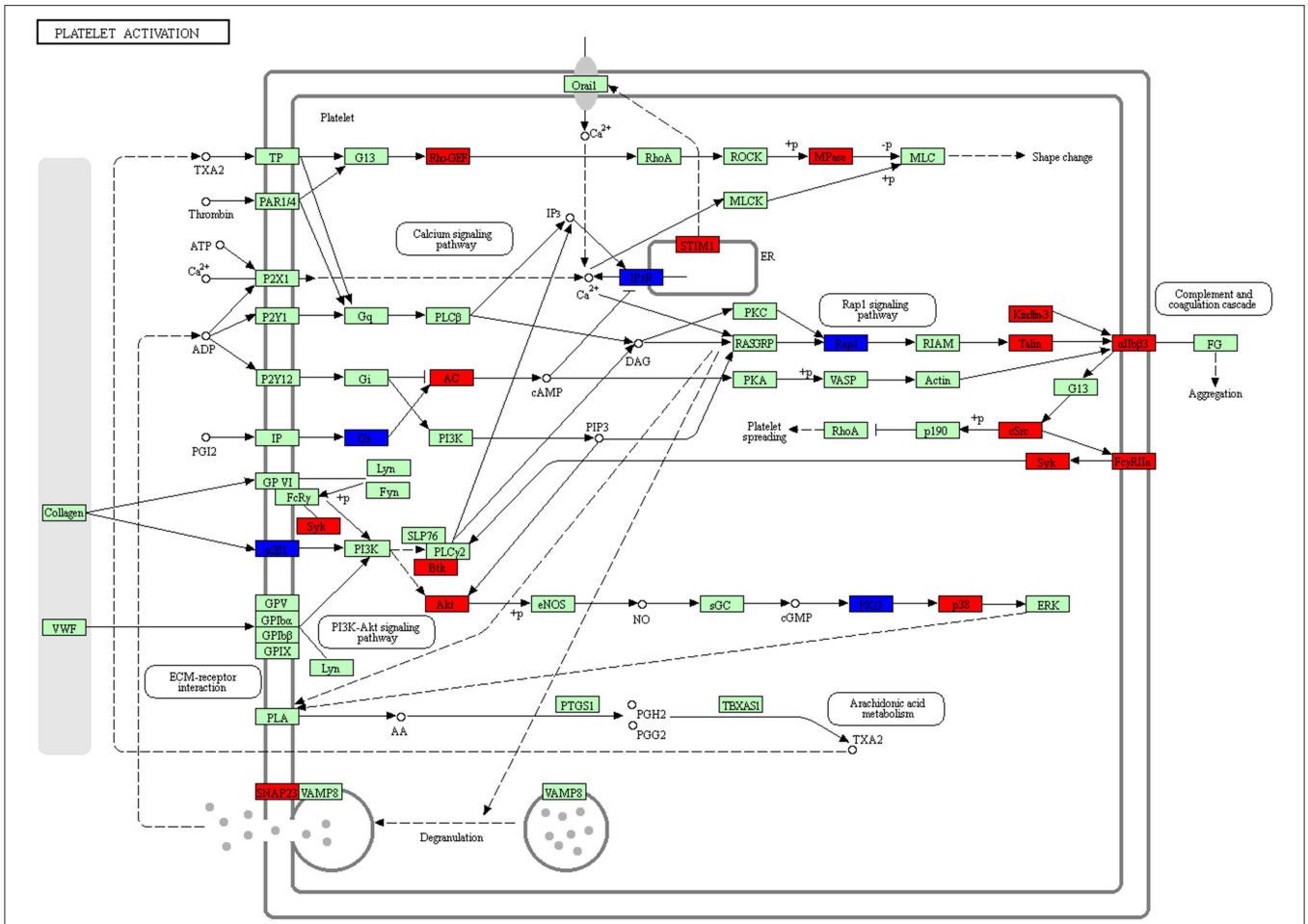

FIGURE 14 | Platelet activation pathway altered in an NFPA. Red means the upregulated overlapped molecule. Blue means the downregulated overlapped molecule.

performed a large-scale of proteomics analysis of NFPAs (n = 6), and integrated the transcriptomics data in NFPAs (n = 8) vs. controls (n = 3) from GEO database, which found 6076 proteins in NFPA tissues, and 3598 DEGs in NFPAs vs. controls. Overlapping analysis obtained 1088 overlapped molecules (proteins; DEGs). Moreover, a set of data about signaling pathway network alterations were obtained based on those 1088 overlapped molecules. Those data are currently the biggest protein database and molecule network changes for NFPA tissues, which is precious resource to discover reliable biomarker pattern and explore in-depth molecular mechanisms for NFPAs.

Limitations

One must note that for proteomics and transcriptomics analyses in this study, the sample size was not big, only 6 NFPA tissues for proteomics, and 8 NFPA tissues and 3 control tissues for transcriptomics. In future, it is necessary to significantly expand the tissue sample size for biomarker studies. Also, one must note that NFPA tissue is relative pure cell type in cell origin, while control pituitary tissue contains multiple pituitary cell types, which might cause bias when comparison is performed between NFPA and control pituitary tissues. However, this is a common problem for any researchers who study human pituitary adenoma tissues. In this study, more experiments such as western blotting among different NFPA and control tissues, and different omics methods were used to versify mutually the results, achieving the consistent results.

CONCLUSION AND OUTLOOK

NFPA is a type of complex disease involved in multiple molecule changes at the levels of genome, transcriptome, and proteome. This study identified 6076 proteins with quantitative information in NFPAs with TMT-based quantitative proteomics, which was the large-scale quantitative protein reference map for human NFPA tissue proteome. Also, 3598 DEGs were identified between NFPAs and controls with the transcriptomic data from GEO database. Further, 1088 overlapped molecules (DEGs; proteins) between 6076 proteins and 3598 DEGs were analyzed to confirm that NFPAs differed from normal pituitary tissues in terms of FAK, cGMP/PKG, and platelet activation signaling pathways. In addition, the hub molecules derived from PPI network of those overlapped molecules (DEGs; proteins) were obtained and verified in NFPAs, which confirmed the

differences between NFPA and normal pituitary tissues. These proteomic and transcriptomic data were the important resource to screen out new tumor biomarkers to form a pattern biomarker for diagnosis and target treatments, which is emerging as a great promise for NFPAs (19, 20) to achieve predictive, preventive, and personalized medicine (PPPM) for NFPA future research and clinical practice (70). These overlapped molecules are the important biomarker resource for sample stratification and clinical significance analysis (71). Thereby, in clinical applications, patients can be classified according to changes in these important molecules, providing better treatment options and predicting patient outcomes.

ETHICS STATEMENT

The NFPA tissues were obtained from the Department of Neurosurgery, Xiangya Hospital, Central South University, and was approved by the Medical Ethics Committee of Xiangya Hospital of Central South University. Control pituitary glands were post-mortem tissues obtained from the Memphis Regional Medical Center, which were approved by University of Tennessee Health Science Center Internal Review Board (UTHSC-IRB). Consent was obtained from each patient or the family of control pituitary subject after full explanation of the purpose and nature of all procedures used.

AUTHOR CONTRIBUTIONS

TC analyzed data, performed Western blot experiment, prepared figures and tables, and wrote the manuscript. YW, ML, TZ, and BL participated in Western blot experiment and partial data analysis. XiaohanZ participated in language revisions and partial data analysis. XianquanZ conceived the concept, designed experiments and manuscript, collected the samples, obtained TMT quantitative proteomic data, instructed experiments and data analysis, supervised results, coordinated, critically revised and wrote the manuscript, and was responsible for its financial supports and the corresponding works. All authors approved the final manuscript.

FUNDING

This work was supported by the grants from the China 863 Plan Project (Grant No. 2014AA020610-1 to XianquanZ), National Natural Science Foundation of China (Grant Nos. 81572278 and 81272798 to XianquanZ), Hunan Provincial Hundred Talent Plan (to XianquanZ), the Xiangya Hospital Funds for Talent Introduction (to XianquanZ), and the Hunan Provincial Natural Science Foundation of China (Grant No. 14JJ7008 to XianquanZ).

ACKNOWLEDGMENTS

Authors acknowledged the assistances of Dr. Dominic M. Desiderio in collection of control pituitary tissues and of Dr. Xuejun Li in collection of pituitary adenoma tissues.

SUPPLEMENTARY MATERIAL

The Supplementary Material for this article can be found online at: https://www.frontiersin.org/articles/10.3389/fendo.2019.00854/full#supplementary-material

REFERENCES

1. Daly AF1, Rixhon M, Adam C, Dempegioti A, Tichomirowa MA, Beckers A. High prevalence of pituitary adenomas: a cross-sectional study in the province of Liege, Belgium. *J Clin Endocrinol Metab*. (2006) 91:4769–75. doi: 10.1210/jc.2006-1668
2. Fernandez A, Karavitaki N, Wass JAH. Prevalence of pituitary adenomas: a community-based, cross-sectional study in Banbury (Oxfordshire, UK). *Clin Endocrinol*. (2010) 72:377–82. doi: 10.1111/j.1365-2265.2009.03667.x
3. Raappana A, Koivukangas J, Ebeling T, Pirilä T. Incidence of pituitary adenomas in Northern Finland in 1992–2007. *J Clin Endocrinol Metab*. (2010) 95:4268–75. doi: 10.1210/jc.2010-0537
4. Karavitaki N, Collison K, Halliday J, Byrne JV, Price P, Cudlip S, et al. BWhat is the natural history of nonoperated nonfunctioning pituitary adenomas? *Clin Endocrinol*. (2007) 67:938–43. doi: 10.1111/j.1365-2265.2007.02990.x
5. Dekkers OM, Hammer S, de Keizer RJ, Roelfsema F, Schutte PJ, Smit JW, et al. The natural course of non-functioning pituitary macroadenomas. *Eur J Endocrinol*. (2007)156:217–24. doi: 10.1530/eje.1.02334
6. Melmed S. Pituitary tumors. *Endocrinol Metab Clin North Am*. (2015) 44:1–9. doi: 10.1016/j.ecl.2014.11.004
7. Zhan X, Long Y. Exploration of molecular network variations in different subtypes of human non-functional pituitary adenomas. *Front Endocrinol*. (2016) 7:13. doi: 10.3389/fendo.2016.00013
8. Zhan X, Wang X, Cheng T. Human pituitary adenoma proteomics: new progresses and perspectives. *Front Endocrinol*. (2016) 7:54. doi: 10.3389/fendo.2016.00054
9. Liuzzi A, Tassi V, Pirro MT, Zingrillo M, Ghiggi MR, Chiodini I, et al. Nonfunctioning adenomas of the pituitary. *Metabolism*. (1996) 45(8 Suppl. 1):80–2. doi: 10.1016/S0026-0495(96)90090-6
10. Ramírez C, Cheng S, Vargas G, Asa SL, Ezzat S, González B, et al. Expression of Ki-67, PTTG1, FGFR4, and SSTR 2, 3, and 5 in nonfunctioning pituitary adenomas: a high throughput TMA, immunohistochemical study. *J Clin Endocrinol Metab*. (2012) 97:1745–51. doi: 10.1210/jc.2011-3163
11. Hu X, Zhang P, Shang A, Li Q, Xia Y, Jia G, et al. A primary proteomic analysis of serum from patients with nonfunctioning pituitary adenoma. *J Int Med Res*. (2012) 40:95–104. doi: 10.1177/147323001204000110
12. Zhan X, Long Y, Zhan XH, Mu Y. Consideration of statistical vs. biological significances for omics data-based pathway network analysis. *Med One*. (2017) 1:e170002. doi: 10.20900/mo.20170002
13. Zhan X, DM Desiderio. Comparative proteomics analysis of human pituitary adenomas: current status and future perspectives. *Mass Spectrom Rev*. (2005) 24:783–813. doi: 10.1002/mas.20039
14. Thompson A, Schäfer J, Kuhn K, Kienle S, Schwarz J, Schmidt G, et al. Tandem mass tags: a novel quantification strategy for comparative analysis of complex protein mixtures by MS/MS. *Analyt Chem*. (2003) 75:1895–904. doi: 10.1021/ac0262560
15. Corthals GL, Wasinger VC, Hochstrasser DF, Sanchez JC. The dynamic range of protein expression: a challenge for proteomic research. *Electrophoresis*. (2015) 21:1104–15. doi: 10.1002/(SICI)1522-2683(20000401)21:6<1104::AID-ELPS1104>3.0.CO;2-C

16. Jiang X, Zhang X. The molecular pathogenesis of pituitary adenomas: an update. *Endocrinol Metab*. (2013) 28:245–54. doi: 10.3803/EnM.2013.28.4.245
17. Du Q, Hu B, Feng Y, Wang Z, Wang X, Zhu D, et al. circOMA1-Mediated miR-145–5p suppresses tumor growth of nonfunctioning pituitary adenomas by targeting TPT1. *J Clin Endocrinol Metab*. (2019) 104:2419–34. doi: 10.1210/jc.2018-01851
18. Barbieri F, Bajetto A, Stumm R, Pattarozzi A, Porcile C, Zona G, et al. Overexpression of stromal cell-derived factor 1 and its receptor CXCR4 induces autocrine/paracrine cell proliferation in human pituitary adenomas. *Clin Cancer Res*. (2008) 15:5022–32. doi: 10.1158/1078-0432.CCR-07-4717
19. Lu M, Zhan X. The crucial role of multiomic approach in cancer research and clinically relevant outcomes. *EPMA J*. (2018) 9:77–102. doi: 10.1007/s13167-018-0128-8
20. Cheng T, Zhan X. Pattern recognition for predictive, preventive, and personalized medicine in cancer. *EPMA J*. (2017) 8:51–60. doi: 10.1007/s13167-017-0083-9
21. Bader GD, Hogue CW. An automated method for finding molecular complexes in large protein interaction networks. *BMC Bioinformatics*. (2003) 13:2. doi: 10.1186/1471-2105-4-2
22. Ferreli F, Turrizanoni M, Canevari FR, Battaglia P, Bignami M, Castelnuovo P, et al. Endoscopic endonasal management of non-functioning pituitary adenomas with cavernous sinus invasion: a 10-year experience. *Rhinology*. (2015) 53:308. doi: 10.4193/Rhin14.309
23. Boucrot, E, Kirchhausen T. Endosomal recycling controls plasma membrane area during mitosis. *Proc Natl Acad Sci USA*. (2007) 104:7939–44. doi: 10.1073/pnas.0702511104
24. Lehtonen S, Shah M, Nielsen R, Iino N, Ryan JJ, Zhou H, et al. The endocytic adaptor protein ARH associates with motor and centrosomal proteins and is involved in centrosome assembly and cytokinesis. *Mol Biol Cell*. (2008) 19:2949–61. doi: 10.1091/mbc.e07-05-0521
25. El Marabti E, Younis I. The cancer spliceome: reprograming of alternative splicing in cancer. *Front Mol Biosci*. (2018) 5:80. doi: 10.3389/fmolb.2018.00080
26. Ikeda K, Horieinoue K, Inoue S. Identification of estrogen-responsive genes based on the DNA binding properties of estrogen receptors using high-throughput sequencing technology. *Acta Pharmacologica Sinica*. (2015) 36:24. doi: 10.1038/aps.2014.123
27. Eke I, Cordes N. Focal adhesion signaling and therapy resistance in cancer. *Semin Cancer Biol*. (2015) 31:65–75. doi: 10.1016/j.semcancer.2014.07.009
28. Schaller MD, Borgman CA, Cobb BS, Vines RR, Reynolds AB, Parsons JT. pp125FAK a structurally distinctive protein-tyrosine kinase associated with focal adhesions. *Proc Natl Acad Sci USA*. (1992) 89:5192–6. doi: 10.1073/pnas.89.11.5192
29. Parsons JT. Focal adhesion kinase: the first ten years. *J Cell Sci*. (2003) 116:1409–16. doi: 10.1242/jcs.00373
30. Polte TR, Hanks S. Interaction between focal adhesion kinase and Crk-associated tyrosine kinase substrate p130Cas. *Proc Natl Acad Sci USA*. (1995) 92:10678–82. doi: 10.1073/pnas.92.23.10678
31. Tomar A, Lawson C, Ghassemian M, Schlaepfer DD. Cortactin as a target for FAK in the regulation of focal adhesion dynamics. *PLos ONE*. (2012) 7:e44041. doi: 10.1371/journal.pone.0044041
32. Fajardo AM, Piazza GA, Tinsley HN. The role of cyclic nucleotide signaling pathways in cancer: targets for prevention and treatment. *Cancers*. (2014) 6:436–58. doi: 10.3390/cancers6010436
33. Alamolhodaei NS, Tsatsakis AM, Ramezani M, Hayes AW, Karimi G. Resveratrol as MDR reversion molecule in breast cancer: an overview. *Food Chem Toxicol*. (2017) 103:223–32. doi: 10.1016/j.fct.2017.03.024
34. Wang F, Shu K, Lei T, Xue D. The expression of integrinbeta1 and FAK in pituitary adenomas and their correlation with invasiveness. *J Huazhong Univ Sci Technolog Med Sci*. (2008) 28:572–5. doi: 10.1007/s11596-008-0518-6
35. Karakhanova S, Golovastova M, Philippov PP, Werner J, Bazhin AV. Interlude of cGMP and cGMP/protein kinase G type 1 in pancreatic adenocarcinoma cells. *Pancreas*. (2014) 43:784–94. doi: 10.1097/MPA.0000000000000104
36. Wang Y, Chen Y, Wu M, Lan T, Wu Y, Li Y, et al. Type II cyclic guanosine monophosphate-dependent protein kinase inhibits Rac1 activation in gastric cancer cells. *Oncol Lett*. (2015) 10:502–8. doi: 10.3892/ol.2015.3173
37. Tuttle TR, Mierzwa ML, Wells SI, Fox SR, Ben-Jonathan N. The cyclic GMP/protein kinase G pathway as a therapeutic target in head and neck squamous cell carcinoma. *Cancer Lett*. (2016) 370:279–85. doi: 10.1016/j.canlet.2015.10.024
38. Abusnina A, Keravis T, Yougbaré I, Bronner C, Lugnier C. Anti-proliferative effect of curcumin on melanoma cells is mediated by PDE1A inhibition that regulates the epigenetic integrator UHRF1. *Mol Nutrit Food Res*. (2011) 55:1677–89. doi: 10.1002/mnfr.201100307
39. Whitt JD, Li N, Tinsley HN, Chen X, Zhang W, Li Y, et al. A novel sulindac derivative that potently suppresses colon tumor cell growth by inhibiting cGMP phosphodiesterase and β-catenin transcriptional activity. *Cancer Prev Res*. (2012) 5:822–33. doi: 10.1158/1940-6207.CAPR-11-0559
40. Fallahian F, Karami-Tehrani F, Salami S, Aghaei M. Cyclic GMP induced apoptosis via protein kinase G in oestrogen receptor-positive and-negative breast cancer cell lines. *FEBS J*. (2011) 278:3360–9. doi: 10.1111/j.1742-4658.2011.08260.x
41. Jurasz P, Alonso-Escolano D, Radomski MW. Platelet–cancer interactions: mechanisms and pharmacology of tumour cell-induced platelet aggregation. *Br J Pharmacol*. (2004) 143:819–26. doi: 10.1038/sj.bjp.0706013
42. Sierko E, Wojtukiewicz MZ. Wojtukiewicz. Platelets and angiogenesis in malignancy. *Semin Throm Hemostasis*. (2004) 30:95–108. doi: 10.1055/s-2004-822974
43. Lal I, Dittus K, Holmes CE. Platelets, coagulation and fibrinolysis in breast cancer progression. *Breast Cancer Res*. (2013) 15:207. doi: 10.1186/bcr3425
44. Labelle M, Begum S, Hynes RO. Platelets guide the formation of early metastatic niches. *Proc Natl Acad Sci USA*. (2014) 111:E3053–61. doi: 10.1073/pnas.1411082111
45. Corneli G, Baldelli R, Di Somma C, Rovere S, Gaia D, Pellegrino M, et al. Occurrence of GH deficiency in adult patients who underwent neurosurgery in the hypothalamus–pituitary area for non-functioning tumour masses. *Growth Horm IGF Res*. (2003) 13:104–8. doi: 10.1016/S1096-6374(03)00010-8
46. Dekkers O, Pereira A, Romijn J. Treatment and follow-up of clinically nonfunctioning pituitary macroadenomas. *J Clin Endocrinol Metab*. (2008) 93:3717–26. doi: 10.1210/jc.2008-0643
47. Parsons SJ, Parsons JT. Src family kinases, key regulators of signal transduction. *Oncogene*. (2004) 23:7906. doi: 10.1038/sj.onc.1208160
48. Sandilands E, Serrels B, McEwan DG, Morton JP, Macagno JP, McLeod K, et al. Autophagic targeting of Src promotes cancer cell survival following reduced FAK signalling. *Nat Cell Biol*. (2012) 14:51. doi: 10.1038/ncb2386
49. Gelman IH. Src-family tyrosine kinases as therapeutic targets in advanced cancer. *Front Biosci*. (2011) 3:801–7. doi: 10.2741/e287
50. Gebregiworgis T, Marshall CB, Kano Y, Radulovich N, Tsao M-S, Ohh M, et al. Altering the regulation of KRAS GTPase cycle via Src and SHP2 creates a potential therapeutic vulnerability for pancreatic cancer. *Cancer Res*. (2018) 78:4360. doi: 10.1158/1538-7445.AM2018-4360
51. Masaki T, Igarashi K, Tokuda M, Yukimasa S, Han F, Jin Y, et al. pp6oc-src activation in lung adenocarcinoma. *Eur J Cancer*. (2003) 39:1447–55. doi: 10.1016/S0959-8049(03)00276-4
52. Olivieri A, Manzione L. Dasatinib: a new step in molecular target therapy. *Ann Oncol*. (2007) 18(Suppl.6):vi42–6. doi: 10.1093/annonc/mdm223
53. Wang C, Ma J, Zhang N, Yang Q, Jin Y, Wang Y. The acetyl-CoA carboxylase enzyme: a target for cancer therapy? *Expert Rev Anticancer Ther*. (2015) 15:667–76. doi: 10.1586/14737140.2015.1038246
54. Fang W, Cui H, Yu D, Chen Y, Wang J, Yu G. Increased expression of phospho-acetyl-CoA carboxylase protein is an independent prognostic factor for human gastric cancer without lymph node metastasis. *Med Oncol*. (2014) 31:15. doi: 10.1007/s12032-014-0015-7
55. Menendez JA, Lupu R. Fatty acid synthase and the lipogenic phenotype in cancer pathogenesis. *Nat Rev Cancer*. (2007) 7:763. doi: 10.1038/nrc2222
56. Hardie DG, Ross FA, Hawley SA. AMPK: a nutrient and energy sensor that maintains energy homeostasis. *Nat Rev Mol Cell Biol*. (2012) 13:251. doi: 10.1038/nrm3311
57. Currie E, Schulze A, Zechner R, Walther TC, Farese RV Jr. Cellular fatty acid metabolism and cancer. *Cell Metab*. (2013) 18:153–161. doi: 10.1016/j.cmet.2013.05.017
58. Hardie DG. The AMP-activated protein kinase pathway–new players upstream and downstream. *J Cell Sci*. (2004) 117:5479–87. doi: 10.1242/jcs.01540
59. Saglam O, Garrett CR, Boulware D, Sayegh Z, Shibata D, Malafa M, et al. Activation of the serine/threonine protein kinase AKT during the

progression of colorectal neoplasia. *Clin Colorectal Cancer*. (2007) 6:652–6. doi: 10.3816/CCC.2007.n.034
60. Ren D, Jia L, Li Y, Gong Y, Liu C, Zhang X, et al. ST6GalNAcII mediates the invasive properties of breast carcinoma through PI3K/Akt/NF-κB signaling pathway. *IUBMB Life*. (2014) 66:300–8. doi: 10.1002/iub.1268
61. Tanase C, Neagu M, Albulescu R. Key signaling molecules in pituitary tumors. *Expert Rev Mol Diagn*. (2009)9:859–77. doi: 10.1586/erm.09.60
62. Long Y, Lu M, Cheng T, Zhan XH, Zhan X. Multiomics-based signaling pathway network alterations in human nonfunctional pituitary adenomas. *Front Endocrinol*. (2019) 10:835. doi: 10.3389/fendo.2019.00835
63. Tanase C, Albulescu R, Codrici E, Calenic B, Popescu ID, Mihai S, et al. Decreased expression of APAF-1 and increased expression of cathepsin B in invasive pituitary adenoma. *Oncol Targets Ther*. (2014) 8:81–90. doi: 10.2147/OTT.S70886
64. Tanase C, Codrici E, Popescu ID, Cruceru ML, Enciu AM, Albulescu R, et al. Angiogenic markers: molecular targets for personalized medicine in pituitary adenoma. *Per Med*. (2013) 10:539–48. doi: 10.2217/pme.13.61
65. Zhan X, Long Y, Lu M. Exploration of variations in proteome and metabolome for predictive diagnostics and personalized treatment algorithms: Innovative approach and examples for potential clinical application. *J Proteomics*. (2018) 188:30–40. doi: 10.1016/j.jprot.2017.08.020
66. Zhan X, Yang H, Peng F, Li J, Mu Y, Long Y, et al. How many proteins can be identified in a 2DE gel spot within an analysis of a complex human cancer tissue proteome? *Electrophoresis*. (2018) 39:965–80. doi: 10.1002/elps.201700330
67. Qian S, Yang Y, Li N, Cheng T, Wang X, Liu J, et al. Prolactin variants in human pituitaries and pituitary adenomas identified with two-dimensional gel electrophoresis and mass spectrometry. *Front Endocrinol*. (2018) 9:468. doi: 10.3389/fendo.2018.00468
68. Zhan X, Huang Y, Long Y. Two-dimensional gel electrophoresis coupled with mass spectrometry methods for an analysis of human pituitary adenoma tissue proteome. *J Vis Exp*. (2018) 2018:134. doi: 10.3791/56739
69. Yelamanchi SD, Tyagi A, Mohanty V, Dutta P, Korbonits M, Chavan S, et al. Proteomic analysis of the human anterior pituitary gland. *OMICS*. (2018) 22:759–69. doi: 10.1089/omi.2018.0160
70. Janssens JP, Schuster K, Voss A. Preventive, predictive, and personalized medicine for effective and affordable cancer care. *EPMA J*. (2018) 9:113–23. doi: 10.1007/s13167-018-0130-1
71. Golubnitschaja O, Polivka J Jr, Yeghiazaryan K, Berliner L. Liquid biopsy and multiparametric analysis in management of liver malignancies: new concepts of the patient stratification and prognostic approach. *EPMA J*. (2018) 9:271–85. doi: 10.1007/s13167-018-0146-6

Conflict of Interest: The authors declare that the research was conducted in the absence of any commercial or financial relationships that could be construed as a potential conflict of interest.

frontiers in Endocrinology

ORIGINAL RESEARCH
published: 17 December 2019
doi: 10.3389/fendo.2019.00835

Multiomics-Based Signaling Pathway Network Alterations in Human Non-functional Pituitary Adenomas

Ying Long[1,2,3], *Miaolong Lu*[1,2,3], *Tingting Cheng*[1,2,3], *Xiaohan Zhan*[1,2,3] *and Xianquan Zhan*[1,2,3,4,5]*

[1] *Key Laboratory of Cancer Proteomics of Chinese Ministry of Health, Xiangya Hospital, Central South University, Changsha, China,* [2] *Hunan Engineering Laboratory for Structural Biology and Drug Design, Xiangya Hospital, Central South University, Changsha, China,* [3] *State Local Joint Engineering Laboratory for Anticancer Drugs, Xiangya Hospital, Central South University, Changsha, China,* [4] *Department of Oncology, Xiangya Hospital, Central South University, Changsha, China,* [5] *National Research Center for Geriatric Disorders, Xiangya Hospital, Central South University, Changsha, China*

Non-functional pituitary adenoma (NFPA) seriously affects hypothanamus-pituitary-target organ axis system, with a series of molecule alterations in the multiple levels of genome, transcriptome, proteome, and post-translational modifications, and those molecules mutually interact in a molecular-network system. Meta analysis coupled with IPA pathway-network program was used to comprehensively analyze nine sets of documented NFPA omics data, including NFPA quantitative transcriptomics data [280 differentially expressed genes (DEGs)], NFPA quantitative proteomics data [50 differentially expressed proteins (DEPs)], NFPA mapping protein data (218 proteins), NFPA mapping protein nitration data (9 nitroproteins and 3 non-nitrated proteins), invasive NFPA quantitative transriptomics data (346 DEGs), invasive NFPA quantitative proteomics data (57 DEPs), control mapping protein data (1469 proteins), control mapping protein nitration data (8 nitroproteins), and control mapping phosphorylation data (28 phosphoproteins). A total of 62 molecular-networks with 861 hub-molecules and 519 canonical-pathways including 54 cancer-related canonical pathways were revealed. A total of 42 hub-molecule panels and 9 canonical-pathway panels were identified to significantly associate with tumorigenesis. Four important molecular-network systems, including PI3K/AKT, mTOR, Wnt, and ERK/MAPK pathway-systems, were confirmed in NFPAs by PTMScan experiments with altered expression-patterns and phosphorylations. Nineteen high-frequency hub-molecules were also validated in NFPAs with PTMScan experiment with at least 2.5-fold changes in expression or phosphorylation, including ERK, ERK1/2, Jnk, MAPK, Mek, p38 MAPK, AKT, PI3K complex, p85, PKC, FAK, Rac, Shc, HSP90, NFκB Complex, histone H3, AP1, calmodulin, and PLC. Furthermore, mTOR and Wnt pathway-systems were confirmed in NFPAs by immunoaffinity Western blot analysis, with significantly decreased expression of PRAS40 and increased phosphorylation levels of p-PRAS40 (Thr246) in mTOR pathway in NFPAs compared to controls, and with the decreased protein expressions of GSK-3β and GSK-3β, significantly increased phosphorylation levels of p-GSK3α (Ser21) and p-GSK3β (Ser9), and increased expression level of β-catenin in Wnt pathway in NFPAs compared to

OPEN ACCESS

Edited by:
Fabienne Langlois, Centre Hospitalier Universitaire de Sherbrooke, Canada

Reviewed by:
Ulrich Renner, Max Planck Institute of Psychiatry (MPI), Germany
José Miguel Hinojosa-Amaya, Universidad Autónoma de Nuevo León, Mexico

***Correspondence:**
Xianquan Zhan
yjzhan2011@gmail.com

Specialty section:
This article was submitted to Pituitary Endocrinology, a section of the journal Frontiers in Endocrinology

Received: *20 February 2019*
Accepted: *15 November 2019*
Published: *17 December 2019*

Citation:
Long Y, Lu M, Cheng T, Zhan X and Zhan X (2019) Multiomics-Based Signaling Pathway Network Alterations in Human Non-functional Pituitary Adenomas. Front. Endocrinol. 10:835. doi: 10.3389/fendo.2019.00835

controls. Those findings provided a comphrensive and large-scale pathway network data for NFPAs, and offer the scientific evidence for insights into the accurate molecular mechanisms of NFPA and discovery of the effective biomarkers for diagnosis, prognosis, and determination of therapeutic targets.

Keywords: non-functional pituitary adenoma, integrative omics data, PTMScan, immunoaffinity, signaling pathways, molecular networks, biomarkers

INTRODUCTION

Human non-functional pituitary adenoma (NFPA) is a common disease that occurs in the central regulatory organ pituitary, and seriously impacts on physiological functions and human health (1). Compared to functional pituitary adenomas (FPAs), NFPA has a very challenging clinical problem in early diagnosis and treatment because of the lack of the corresponding hormone elevation in NFPA patients (2, 3). NFPA is a complex whole-body disease that alters in the levels of gene (genome), RNA (transcriptome), protein (proteome), and metabolite (metabolome), and that involves multi-factors, multi-processes, and multi-consequences (4–6). Individual variations are involved in prediction/prevention, early-stage diagnosis/therapy, and late-stage diagnosis/therapy. Moreover, omics (genomics, transcriptomics, proteomics, peptidomics, metabolomics, and radiomics) and systems biology are promoting one to change paradigms from traditional single-factor strategy to multi-parameter systematic strategy in pituitary adenoma studies and clinical practice (4, 7), in the model of predictive screening and prognostic assessment, which traditionally only depended on the changes of serum single-hormone change and pituitary imaging, and in the therapeutic model of cancer from the general radiotherapy and chemotherapy to personalized strategy (8, 9). From multi-parameter systematic strategy opinion, it is necessary to systematically study the changes in genome, transcriptome, proteome, peptidome, and metabolome in individual pituitary adenoma tissue and body-fluid (cerebrospinal fluid, CSF; serum/plasma) (7). Systems biological technologies are able to integrate all experimental data and clinical information of individuals to identify key molecular networks specific to individual NFPA (10, 11). However, the data from genome, transcriptome, proteome, peptidome, metabolome, and radiome are much different among individual tumors, and between tumors and normals; and molecular networks alter among individuals, and between tumors and normals. Therefore, it is necessary to construct multiple omics data-based molecular networks for clarification of accurate molecular mechanisms of NFPAs, and discovery of tumor-specific biomarker pattern for efficient prediction screening, early diagnosis, prognostic assessment, and individualized prevention and therapy (12).

Molecular-network alterations are the hallmark in complex cancer disease (4, 7, 12). The molecules in the levels of gene (genome), RNA (transcriptome), protein (proteome), and metabolite (metabolome) are mutually regulated and form dynamically associated systems. Each molecule change is associated with the changes of other molecules in a pathway system. One molecule in a signaling pathway system might also trigger the effects of other signaling pathways in a tumor biological system. Thus, if only a single-one molecule is targeted or only a single-level of omics studies is focused on, then it must result in obvious limitations. A globally systematic and comprehensive recognition of molecular networks based on multi-omics data has an important scientific merit to understand the molecular mechanisms of NFPAs and discover really useful biomarkers for NFPAs. However, it is difficulty for a single research team to perform all studies in each level of genome, transcriptome, proteome, and metabolome commonly, due to the limited experimental conditions, expertise, and financial support in a single research team. The single and independent experimental data from different omics studies under a given condition can only explain and represent a certain aspects of a tumor because of tumor heterogeneity and plasticity (13, 14). The experimental subjects are also not same among different research groups. Thus, the experimental results from different research group have their own strengths and limitations. The concept and principle of Meta analysis (15), which is a secondary analysis based on multiple center published experimental data, offers one a new strategy to integrate and analyze different levels of NFPA omics data that were published by different research groups. Moreover, Ingenuity Pathway Analysis (IPA) system is an extensively used and classic pathway analysis system to construct pathway networks with different omics data from large-scale IPA knowledge base database (>6 million scientific findings and >800 canonical pathways) (16, 17). Meta analysis in combination with IPA pathway network analysis can construct integrative molecular networks to in-depth understand NFPA pathogenesis and discover accurate and reliable biomarkers for NFPAs (5).

The present study collected all published omics data about NFPAs (**Supplemental Table 1**), including mapping protein data in NFPAs and controls, quantitatively transcriptomic data and proteomic data between NFPAs and controls, mapping protein-nitration data in NFPAs and controls, mapping protein-phosphorylation data in controls, and quantitatively transcriptomic data and proteomic data between invasive and non-invasive NFPAs. IPA pathway analysis program (17) was used to reveal signaling networks, canonical pathways, and biological functions with each set of omics data. The important signaling pathways and the corresponding molecules were confirmed with PTMScan experiments and immunoaffinity Western blot in the real NFPA samples compared to control samples. Then, these data were comprehensively analyzed to reveal integrative molecular networks that function in an NFPA biological system. The experimental flow chart was shown

to construct and validate pathway-network systems in NFPAs (**Figure 1**).

MATERIALS AND METHODS

Omics Datasets

All documented omics data regarding NFPAs were collected from Pubmed and Google Scholar databases. Those omics data from NFPAs were classified into nine datasets (**Figure 1** and **Supplemental Table 1**): (i) *Dataset 1*—NFPA quantitative transcriptomics data, including 280 differentially expressed genes (DEGs) (114 upregulated and 166 downregulated) (**Supplemental Materials 1.1**). (ii) *Dataset 2*—NFPA quantitative proteomics data: including 50 differentially expressed proteins (DEPs) (21 upregulated and 29 downregulated) (**Supplemental Materials 2.1**). (iii) *Dataset 3*—NFPA mapping protein data, including 218 proteins (**Supplemental Materials 3.1**). (iv) *Dataset 4*—NFPA mapping protein nitration data, including 9 nitroproteins and 3 non-nitrated proteins (**Supplemental Materials 4.1**). (v) *Dataset 5*—Invasive NFPA quantitative transriptomics data, including 346 DEGs (233 upregulated and 113 downregulated) (**Supplemental Materials 5.1**). (vi) *Dataset 6*—Invasive NFPA quantitative proteomics data, including 57 DEPs (30 upregulated and 27 downregulated) (**Supplemental Materials 6.1**). (vii) *Dataset 7*—Pituitary control mapping protein data, including 1,469 proteins (**Supplemental Materials 7.1**). (viii) *Dataset 8*—Pituitary control mapping protein nitration data, including 8 nitroproteins (**Supplemental Materials 8.1**). (ix) *Dataset 9*—Pituitary control mapping phosphorylation data, including 28 phosphoproteins (**Supplemental Materials 9.1**).

IPA Analysis

Each dataset was analyzed with IPA analysis program (http://www.ingenuity.com). Briefly, the ID numbers of genes and proteins in each dataset were used as the identifiers, and input into the IPA analysis program with the Core analysis platform. For DEG and DEP data, the ID numbers and corresponding fold-change values were input simultaneously into the IPA analysis system to automatically search the matched genes/molecules, and generate a two-dimensional table that includes the matched and unmatched genes/proteins. Five subdatasets were automatically generated, including (i) All IDs that contained all input IDs, (ii) Unmapped IDs that were without the matched molecules in the IPA system, which did not enter the next-step pathway analysis, (iii) Mapped IDs that were the matched molecules with

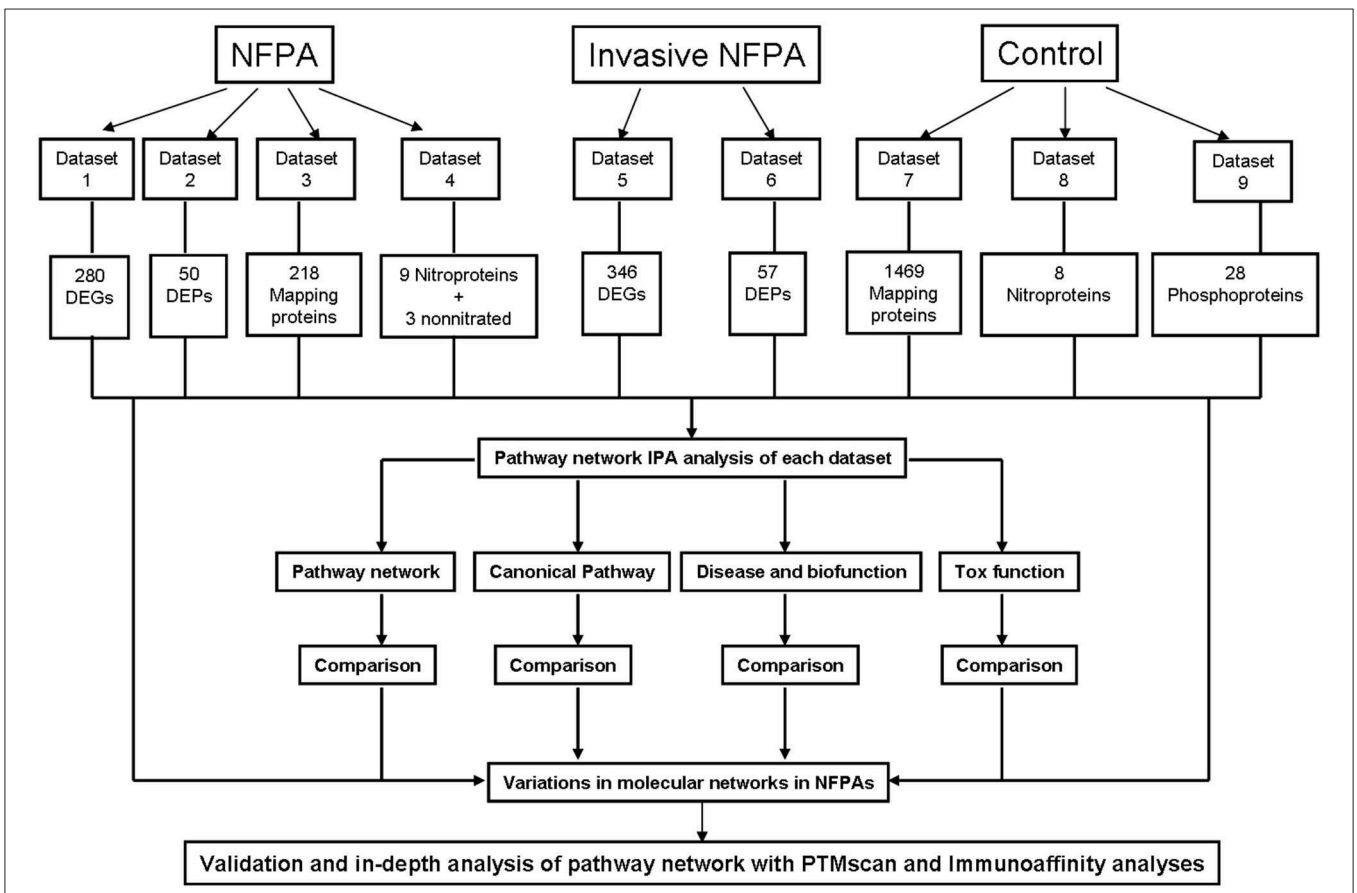

FIGURE 1 | Scheme to construct molecular networks based on an integrative analysis of the documented omics data in NFPAs. DEG, differentially expressed gene; DEP, differentially expressed protein.

duplicated IDs, (iv) Network-eligible IDs that were the mapped IDs without duplicated IDs, and (v) Functions/Pathways/List-eligible IDs. For the duplicated IDs for the same gene/protein, the identifier with the highest fold-change was used in the pathway analysis; or, the first appeared gene/protein was used in the pathway analysis without an expression value such as mapping proteomic data, nitroprotein data, and phosphorylation data. The Network-eligible IDs were proceeded into the pathway network analysis with comparison of network-eligible molecules (genes; proteins) with the IPA knowledge base (IPAKB); and IPAKB contains over 6 million scientific findings and over 800 canonical pathways (2, 17). The significances (p-values) of the associations between the dataset and the canonical pathways in the IPAKB were measured with comparison of the number of use-specific genes/proteins of interest that participate in a given pathway to the total number of occurrences of these genes in all pathway annotations that are stored in the IPAKB. The Benjamini-Hochberg for multiple testing was used to calculate each p-value to determine the probability that the association between genes in the dataset and the canonical pathways in IPAKB was explained only by chance, with a statistical significance of $p < 0.05$. Each IPA analysis generated statistically significant networks, canonical pathways, biofunctions, and tox functions. A toxic pathway is defined as a canonical pathway that is significantly associated with toxicity lists that describe adaptive, defensive, or reparative responses to xenobiotic insult, and could be used to understand biological responses.

Analysis of Molecular Networks

All IPA data (networks, canonical pathways, biofunctions, and tox functions) from different datasets together with the original gene/protein data were comprehensively analyzed in combination with literature-based bioinformatics and clinical features, to clarify molecular pathway-network alterations in NFPAs. Those common networks, canonical pathways, biofunctions, and tox functions derived from multiple datasets were important molecular events that occurred in NFPAs. Moreover, an important role of network is to find hub-molecules. All of those hub-molecules with at least five linked molecules among those networks identified from nine datasets were further analyzed to find hub-molecule panels. Each hub-molecule panel was further rationalized in NFPAs. Each canonical-pathway panel derived from nine datasets was also rationalized in NFPA biological processes.

Pituitary Tumor and Control Tissues

Pituitary adenoma tissue samples were obtained from Department of Neurosurgery, Xiangya Hospital, Central South University, and were approved by Xiangya Hospital Medical Ethics Committee of Central South University. Control pituitary glands were post-mortem tissues obtained from the Memphis Regional Medical Center, and were approved by University of Tennessee Health Science Center Internal Review Board (UTHSC-IRB). The written informed consent was obtained from each patient or the family of control pituitary subject, after full explanation of the purpose and nature of all used procedures. The tissues were removed during neurosurgery or autopsy, frozen immediately in liquid nitrogen, and stored (−80°C) until processed.

PTMScan Direct Multi-Pathway Analysis of Mined Signaling Pathways

Pituitary tissue samples from NFPA patients ($n = 4$) and control pituitaries ($n = 4$) (**Supplemental Table 2-1**) were analyzed with PTMScan® Direct Test (Cell Signaling Technology Company, Danvers, MA, USA) to experimentally investigate the roles of multiple pathways including PI3K/AKT, mTOR, Wnt, and ERK/MAPK signaling pathways derived from nine sets of omics data in NFPAs.

Tissue Lysate Preparation

An amount (100 mg) of pituitary tissue samples were added in a volume (1 ml) of urea lysis buffer (20 mM 2-hydroxyethyl (HEPES), 9 M urea, 2.5 mM sodium pyrophosphate, 1 mM sodium orthovanadate, and 1 mM β-glycerophosphate, pH 8.0), and homogenized with refiner on the ice. The lysates were sonicated (30 s x 3 times at 15 W output, chilled on ice with 1-min intervals), and centrifuged (20,000 g, 4°C, 15 min). The supernatant was collected, and its protein concentration was measured with Bio-Rad 2-D Quant assay using bovine serum albumin (BSA) as standard. Each sample was mixed with the equal protein amount in NFPA group and in control group, respectively.

Protein Digestion and Purification

Equal amount (10 mg/sample) of protein mixture (NFPAs; and controls) was reduced (55°C, and 30 min) with a final concentration of 4.5 mM dithiothreitol (DTT) in an incubator. After the solution was cooled on ice to room temperature, an appropriate volume (1 ml) of 100 mM iodoacetamide was added to 40 mg of protein extract, mixed well, and incubated (dark, 15 min, and room temperature). The reduced and alkalized samples were diluted (1:4) with 20 mM HEPES buffer at pH 8.0. The diluted samples were digested (overnight, room temperature, and gentle mixing) with 10 μg/ml trypsin-TPCK (TPCK = tosyl-phenylalanine chloromethyl-ketone) in 1 mM hydrochloric acid (HCl). After digestion, the tryptic peptides were acidified with 1% trifluoroacetic acid (TFA) to reach pH < 3, and then stood on ice for 15 min to be precipitated. The acidified peptide solution was centrifuged (1,780 g, 15 min, and room temperature), followed by desalination through a C18 Sep-Pak cartridge (Waters) and elution by 40% acetonitrile in 0.1% TFA. The eluted peptides were lyophilized.

Immunoprecipitation Through PTMScan Direct Multi-Pathway Reagents and Purification

PTMScan Direct Multipathway V2.0 (18) antibody mixture was incubated (overnight; 4°C) with 30 μl protein G agarose beads (Roche). The beads with antibodies were washed four times with 1X phosphate buffered saline (PBS). Lyophilized peptides were resuspended in 1.4 ml 1X IAP buffer (50 mM MOPS, 50 mM sodium chloride, 10 mM sodium phosphate, pH 7.2), and centrifuged (10,000 g, 5 min, 4°C). The resupended peptides were added into the beads with PTMScan antibodies,

and incubated (4°C, 2 h); and a mixture of tryptic peptides of various cell lysates was used as a positive control (18). After immunoaffinity reaction, the supernatant was removed, and beads with antibody-peptides were washed with 1 ml 1X IAP buffer for three times, then followed by wash with 1 ml high-performance liquid chromatography (HPLC)-grade water for three times. Enriched peptides were eluted (25°C, 10 min, and gentle mixing) from the beads with 50 μl 0.15% TFA, repeat the elution step, and all of the eluents were combined. The combined peptide solution was desalted through Stagetip by laying two layers of C18 Empore™ materials into a 10-μl pipette tip (Cell Signaling Technology), passed with 50 μl 50% acetonitrile in 0.1% TFA (1,500 g, 2 min; 2 x), and followed by rinsing with 50 μl 0.1% TFA by centrifuging the tip (1,500 g, 1 min; 2 x). The peptides were eluted from the Stagetip through passing 10 μl 40% acetonitrile in 0.1% TFA and centrifuging (750 g, 1 min; 2 x). The eluted peptides were vacuum-dried.

LC-MS/MS

The PTMScan antibody-enriched peptides were resuspended in 12 μl of 0.125% formic acid for each sample, and separated through a reversed-phase C18 column (75 μm i.d. x 10 cm length) which packed into a PicoTip emitter (∼8 μm i.d.) with a Magic C18 AQ (100 Å x 5 μm). Each sample was divided into two equal portions for liquid chromatography-tandem mass spectrometry (LC-MS/MS) analysis to increase the number of identifications and perform analytical reproducibility. Each sample was spiked with a standard peptide mixture [MassPREP™ Protein Digestion Standard Mix 1; an overall quantity of 100 fmol (33 fmol per injection)] ahead of LC-MS/MS analysis on an Easy-nLC 1000 hyphened Q-Exactive™ mass spectrometer. Peptides were separated by a linear gradient from 2 to 32% acetonitrile over 120 min. Both MS and MS/MS data were acquired in centroid mode. For precursor ion scan, resolution was set at 70,000 with an automatic gain control (AGC) target of 1×10^6, and scan range was from *m/z* 300 to 1,500. For product ion scan, resolution was set at 17,500 with AGC target of 1×10^5, and scan range was from *m/z* 200 to 2,000. The top 10 intensive precursor ions in each MS scan were selected for MS/MS analysis with normalized collision energy of 25.

Database Searching and Label-Free Quantification

SEQUEST and the core platform from Harvard University were used to evaluate MS/MS spectra. MS/MS data were used to search against Swiss-Prot *homo sapiens* FAST database (updated on April 29, 2015; 42,104 forward and 42,104 reverse sequences, and isoform messages). A mass accuracy of ±0.02 Da was used for product ions and ±5 ppm for precursor ions. Enzyme was selected as trypsin with at least one tryptic (K- or R-containing) terminus required and up to four miscleavages allowed per peptide. Carboxamidomethylation at cysteine residues was set as a fixed modification; and oxidation at methionine residues and the appropriate PTMs were set as variable modifications. All searches included reverse decoy database was used to value false discovery rates (FDR), and the linear discriminant module of core was screened with 5% FDR. Progenesis V4.1 (Waters Cooperation) and Skyline Version 3.1 (MacCoss Lab, University of Washington) were used to generate quantitative data and to extract the whole peal area of the corresponding peptide assignments. Extracted ion chromatograms of peptide ions with abundance variations between samples were manually assessed to make sure the accurate quantification in Skyline.

West Blot Evaluation of Key Molecules in Signaling Pathways

Equal amount of tissue lysates (20 μg) were mixed (v:v = 1:1) with 2x loading buffer that mixed 50 μl β-mercaptoethanol (β-ME) and 950 μl Laemmli sample buffer (Bio-Rad, Cat#: 1610737), boiled (95–100°C, 5 min), and then chilled on the ice. The boiled protein samples were separated with 10% sodium dodecyl sulfate polyacrylamide gel electrophoresis (SDS-PAGE) (Bio-Rad, Cat#: 4561033), transferred to a polyvinylidene fluoride (PVDF) membrane (Merck Millipore, Cat#: INCP00010), and blocked (1 h, room temperature) with 5% BSA in Tris buffered saline (TBS) containing 0.1% Tween 20 (TBST). The blocked proteins on the PVDF membrane were incubated (4°C, overnight) with primary antibodies, washed in TBST, and incubated (2 h, room temperature) with anti-mouse or anti-rabbit HRP-conjugated secondary antibodies. Each primary or secondary antibody was prepared (**Supplemental Table 2-2**). The membranes were washed and developed with chemiluminescence reaction (SuperSignal™ West Pico Chemiluminescent Substrate, Thermo Fisher Scientific, Cat#: 34077; or Clarity Max Western ECL Substrate, Bio-Rad, Cat#: 1705062s). The digital images were acquired with a scanner (FLURCHEM FC3, ProteinSimple), and optical density (O.D.) values were quantified with a specific densitometric software (Quantity One, Bio-Rad). Each targeted protein was analyzed with Western blot for at least three times. Student *t*-test with $p < 0.05$ was used to determine statistically significant difference between NFPAs and controls.

Statistical Analysis

For IPA analysis of multi-omics data, Benjamini-Hochberg for multiple testing with significance level of $p < 0.05$ was used to determine statistically significant molecular-networks, and canonical pathways. For PTMScan experiments, 5% FDR with reverse decoy database search using Progenesis V4.1 (Waters Cooperation) and Skyline Version 3.1 (MacCoss Lab, University of Washington) was used to quantitatively determine a reliable peptide, protein, and phosphorylation. For Western blot analysis, Student *t*-test with $p < 0.05$ and at least repetition three times were used to determine statistically significant difference in each protein or phosphorylation in NFPAs relative to controls.

RESULTS

Data Characteristics of Nine Sets of Omics Datasets

Nine sets of omics data (**Supplemental Materials 1.1, 2.1, 3.1, 4.1, 5.1, 6.1, 7.1, 8.1, 9.1**) were input into the IPA, respectively. Each set of omics data was classified into unmatched, matched, duplicated, and network-eligible IDs (**Supplemental Table 3**). Only network-eligible IDs were processed into network analysis.

Among them, there were two sets of DEG data (Datasets 1 and 5), two sets of DEP data (Datasets 2 and 6), and one set of nitroprotein data (Dataset 4), from NFPAs or invasive NFPAs (**Figure 1**, **Supplemental Table 1**). Analyses of those DEG, DEP, and nitroprotein data from NFPAs or invasive NFPAs directly resulted in clarification of molecular profiling variations in NFPAs relative to controls. Four sets of mapping data (proteins, nitroproteins, and phosphoproteins) from controls (Datasets 7, 8, and 9) or NFPAs (Dataset 3) provided the baseline data for NFPA molecular profiling variations. Moreover, the data characteristics of nine sets of omics data were summarized (**Supplemental Table 4**), of which four types of common molecules were present in NFPA datasets 1 (DEGs) and 2 (DEPs), and invasive NFPA datasets 5 (DEGs) and 6 (DEPs), including growth factors, kinases/enzymes, transcriptional regulators, and transporters.

Molecular Network Alterations in NFPAs

IPA system compared and associated the network-eligible molecules (genes; proteins) in each omics dataset with the large-scale IPAKB to link molecules with direct or indirect relationship into a biological function group, and further generate the complicated interactive molecular-network diagrams. This study identified 62 statistically significant molecular-networks from nine sets of omics data, including 15 networks from NFPA DEGs (**Supplemental Materials 1.2**), 4 from NFPA DEPs (**Supplemental Materials 2.2**), 12 from NFPA mapping proteins (**Supplemental Materials 3.2**), 1 from NFPA nitroproteins (**Supplemental Materials 4.2**), 13 from invasive NFPA DEGs (**Supplemental Materials 5.2**), 3 from invasive NFPA DEPs (**Supplemental Materials 6.2**), 10 from control mapping proteins (**Supplemental Materials 7.2**), 1 from control nitroproteins (**Supplemental Materials 8.2**), and 3 from control phosphoproteins (**Supplemental Materials 9.2**). Each network performed the corresponding biological functions. The functions, nodes, molecules, and statistical score of each network were collected in **Supplemental Materials 1.2–9.2**. Two networks from NFPA DEP data (Dataset 2) were taken as representative examples (**Figure 2**). Network 1 mainly functioned in cancer, organismal development, and vascular system development and function, which contained 35 nodes (genes; proteins), 23 nodes (66%) were identified in this network, and ERK1/2, STAT5a/b, GH1, PRL, PLC, growth hormone, LH, ADCY, proinsulin, FSH, Cg, cytochrome C, LDL, GNAO1, and estrogen receptor were the key molecules in this network. Network 2 mainly functioned in drug metabolism, protein synthesis, and hereditary disorder, which contained 35 nodes (genes; proteins), 18 nodes (51%) were identified in this network, and Jnk, Hsp90, Akt, IL12 (complex), p38 MAPK, Ap1, HSP90B1, CD3, Mek, Tgf beta, ubiquitin, caspase, Hsp27, 14-3-3, YWHAQ, TCR, p85 (pik3r), VIM, Rock, Ige, IL15, IgG, Nos, HSP, HSPB1, HSPB8, and immunoglobulin were the key molecules in this network. Similarly, the rest 60 networks were present in **Supplemental Materials 1.2–9.2**. Comprehensive analysis of all 62 networks clearly found that some functional items of networks were present in different networks across nine different omics datasets.

To reveal the significance of overall variations in molecular networks from different datasets in NFPAs relative to controls, the frequencies of top functional items occurred among networks were counted and analyzed. The results revealed that top network-function items from control pituitary group were mainly related to essential biological processes of normal cell life, including RNA-transcriptional modifications, protein synthesis, carbohydrate metabolism, molecular transport, cell morphology, cell cycle, and cell growth and proliferation (**Supplemental Figure 1A**). Whereas, top network-function items from NFPA group were mainly related to the biological processes of endocrine and nervous system tumors, including cancer, cell signaling and interaction alteration, endocrine and nervous system disorder, inflammatory response, immunological response, cell death and survival, cell growth and proliferation, metabolism abnormalities, free radical and oxidative stress, and protein synthesis and degradation abnormalities (**Supplemental Figure 1B**). These results demonstrated that much different network-function variations were occurred between NFPAs and controls.

Molecular Network-Based Hub-Molecule Panels in NFPAs

Each network containing multiple node molecules (genes; proteins) formed a web to participate in the biological functions. However, different node molecules in a given network did not equally contribute to the biological functions of that given network. Some node molecules in a network were in the hub position, namely hub molecule that connected with many other node molecules in a direct or indirect way, and played key roles in that network. Some node molecules were at the boundary position in a network, and interacted with a relatively less number of other node molecules; such a boundary node molecule could only contribute a relatively weak role in a network. Furthermore, some hub molecules were present in multiple networks that were derived from nine different datasets, which clearly revealed that different networks were interacted mutually in an NFPA biological system. Therefore, the detailed analysis of all hub-molecules in 62 networks from nine sets of omics datasets might reveal and discover key molecules, molecule-panels, and corresponding biological functions that operate in an NFPA biological system, which benefits the discovery of biomarkers for NFPAs.

In this study, a hub-molecule was defined as a node molecule that directly or indirectly connected at least five other node molecules in a network. Thus, a total of 861 hub-molecules were identified from 62 networks, and the primary function annotation of each hub-molecule was obtained from UniProt annotation page, NCBI database, and extensive literature analysis (**Supplemental Table 5**). A total of 42 hub-molecule panels were generated from 861 hub-molecules according to primary functions of hub-molecules. Each hub-molecule panel was displayed with the number of hub-molecules originated from different dataset. Those 42 hub-molecule panels were further grouped into 16 functional categories, and each functional category was described in detail (**Supplemental Figure 2**). Here,

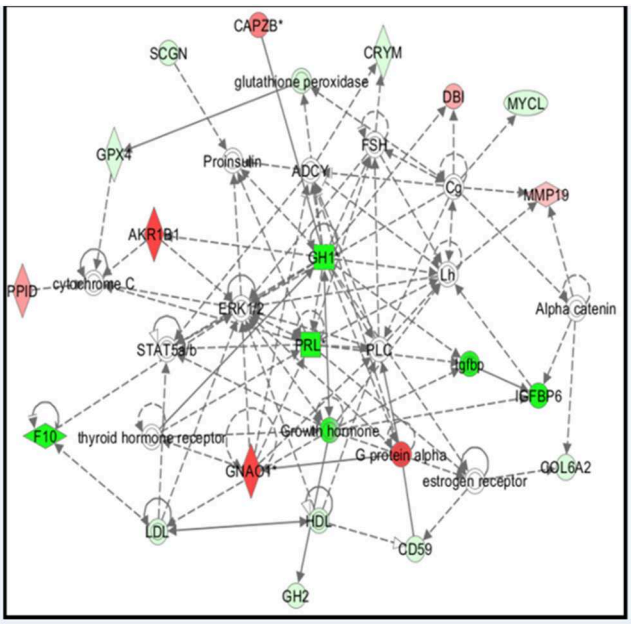

Network 1_NFPA DEGs

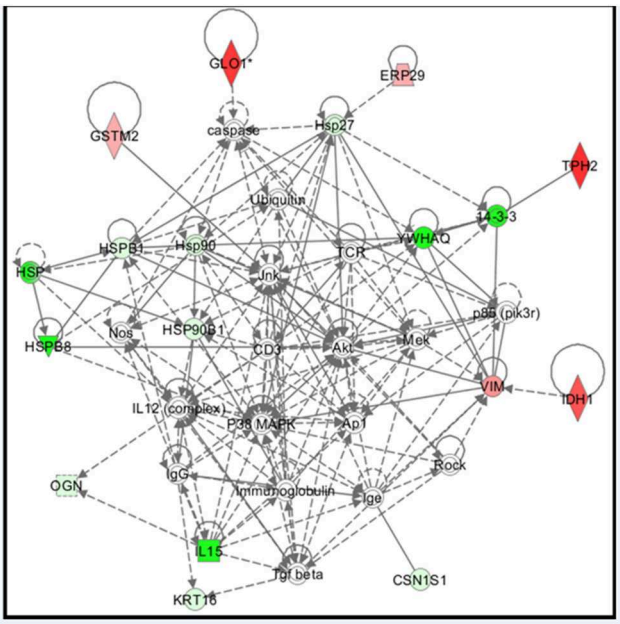

Network 2_NFPA DEGs

Networks ID	Molecules in Network	Score	Nodes	Focus Molecules	Top Diseases and Functions	Hub Molecules
1	ADCY, AKR1B1, Alpha catenin, CAPZB, CD59, Cg, COL6A2, CRYM, cytochrome C, DBI, ERK1/2, estrogen receptor, F10, FSH, G protein alpha, GH1, GH2, glutathione peroxidase, GNAO1, GPX4, Growth hormone, HDL, Igfbp, IGFBP6, LDL, Lh, MMP19, MYCL, PLC, PPID, PRL, Proinsulin, SCGN, STAT5a/b, thyroid hormone receptor	37	35	23	Cardiovascular System Development and Function, Organismal Development, Cancer	ERK1/2, STAT5a/b, GH1, PRL, PLC, Growth hormone, Lh, ADCY, Proinsulin, FSH, Cg, cytochrome C, LDL, GNAO1, estrogen receptor
2	14-3-3, Akt, Ap1, caspase, CD3, CSN1S1, ERP29, GLO1, GSTM2, HSP, Hsp27, Hsp90, HSP90B1, HSPB1, HSPB8, IDH1, Ige, IgG, IL15, IL12 (complex), Immunoglobulin, Jnk, KRT16, Mek, Nos, OGN, P38 MAPK, p85 (pik3r), Rock, TCR, Tgf beta, TPH2, Ubiquitin, VIM, YWHAQ	32	35	18	Drug Metabolism, Protein Synthesis, Hereditary Disorder	Jnk, Hsp90, Akt, IL12 (complex), P38 MAPK, Ap1, HSP90B1, CD3, Mek, Tgf beta, Ubiquitin, caspase, Hsp27, 14-3-3, YWHAQ, TCR, p85 (pik3r), VIM, Rock, Ige, IL15, IgG, Nos, HSP, HSPB1, HSPB8, Immunoglobulin

FIGURE 2 | The representative molecular networks derived from NFPA DEG dataset.

the hub-molecule panel regarding GF, GFR, and related proteins from functional category A (**Supplemental Figure 2A**) was taken as an example for detailed description (**Supplemental Figure 3**). In this panel, those hub-molecules were GF, GFR and related molecules, and 9 hub-molecules (ANGPT1, FDF, FGF2, FGFR, FGFR1, PDGF BB, PTN, Tgf beta, and VEGF) from NFPA DEGs (Dataset 1), 6 (FLT4, GFR, PDGF BB, PDGFR, Tgf beta, and VEGF) from NFPA DEPs (Dataset 2), 5 (PDGF complex, PDGF BB, Tgf beta, TGFB1, and VEGF) from NFPA mapping proteins (Dataset 3), 6 (EGFR, FGFR1, PDGF BB, Tgf beta, TGFB1, and VEGF) from invasive NFPA DEGs (Dataset 5), 2 (EGFR, and Tgf beta) from invasive NFPA DEPs (Dataset 6), 3 (ACVRL1, EGFR, and FGFR1) from control mapping proteins (Dataset 7), and 1 (VEGF) from control nitroproteins (Dataset 8).

Comprehensive analysis of those 42 hub-molecule panels revealed 16 hub-molecule functional categories (**Supplemental Figure 2**). In each category, those hub-molecules derived from NFPA DEGs and DEPs (Datasets 1 and 2), nitroprotein data (Dataset 4), and invasive NFPA DEGs, and DEPs (Datasets 5 and 6) were directly associated with NFPA pathogenesis, compared to hub-molecules from mapping data (datasets 3, 7, 8, and 9). For cell movement, angiogenesis, invasion, and metastasis (**Supplemental Figure 2A**), the important hub-molecules included actin, F-actin, a-actin, cofilin, EZR, VIM, FLNA, Rar, Rxr, Rock, ANGPT1, FDF, FGF2, FGFR,

FGFR1, PDGF BB, PDGFR, PTN, TGF beta, TGFB1, EFGR, VEGF, FLT4, GFR, CDH2, COL2A1, collegens, collegen type I, collegen type IV, integrin, Laminin, SELL, VCAN, ICAM3, and MMP, which were significantly associated with NFPAs. For kinase signaling pathways-related proteins (**Supplemental Figure 2B**), the important hub-molecules included DUSP4, ERK, ERK1/2, JNK, MAPK, MEK, p38 MAPK, MAP2K1/2, Shc, Rac, Ras, Ras homolog, K-Ras, Rsk, Sos, Akt, PI3K (complex), PI3K (family), p85, p70 S6k, PKA, PKC(s), PKG, PRKAA, PRKACA, PRKAR1A, TK, FAK, FYN, CK2, and PDPK1, which were significantly associated with NFPAs. For protein synthesis and degradation (**Supplemental Figure 2C**), the important hub-molecules included FBXO6, UBC, ubiquitin, PSMA2, 26s proteasome, CAND1, MDM2, EEF1A1, and KARS, which were significantly associated with NFPAs. For stress response (**Supplemental Figure 2D**), the important hub-molecules included P4HB, HSP, HSP27, HSP70, HSP90, HSP90B1, HSP90AA1, HSP90AB1, HSPB1, HSPB8, HSPA5, NOS, nitric oxide, SOD, MT1L, and CAT, which were significantly associated with NFPAs. For Notch-Wnt signaling pathway (**Supplemental Figure 2E**), the important hub-molecules included GSK3, LGR4, CTNNB1, Notch, NOTCH3, and ATXN1, which were significantly associated with NFPAs. For cell-cycle regulation (**Supplemental Figure 2F**), the important hub-molecules included 14-3-3, YWHAQ, YWHAG, CDC2, cyclin A, CCND1, CDH1, and CDKN1A, which were significantly associated with NFPAs. For transcription and its regulation (**Supplemental Figure 2G**), the important hub-molecules included C/ebp, CREB, CREM, ETV5, FOXO1, HES1, NFAT (complex), NFAT (family), ARNT2, CEBPA, E2F, XBP1, NFYB, NFkB (complex), NANOG, GATA3, NEUROD1, N-cor, BHLHE40, SAFB, and SMAD3, which were significantly associated with NFPAs. For DNA/RNA regulation and metabolism (**Supplemental Figure 2H**), the important hub-molecules included ZFP36, TARDBP, HDAC, histone, histone H3, histone H4, CBX5, TIP60, and RNA polymerase II, which were significantly associated with NFPAs. For immune and inflammation-related proteins and cytokines (**Supplemental Figure 2I**), the important hub-molecules included BCR (complex), BSG, IgE, IgG, IgM, immunoglobulin, LGALS3, CD1, CD3, TCR, Fc gamma receptor, CXCR4, IL1, IL12 (complex), IL12 (family), IL15, interferon-a, IFNG, TNF, TNF (family), and pro-inflammatory cytokines, which were significantly associated with NFPAs. For hormones and related proteins (**Supplemental Figure 2J**), the important hub-molecules included ADM, β-estradiol, CGA, CYP11A1, estrogen receptor, FSH, GH1, GRB2, GH, IGFBP3, insulin, LH, POMC, PRL, proinsulin, ADRB, ESR1, ESR2, IGFBP5, progesterone, EDNRA, and GAST, which were significantly associated with NFPAs. For energy metabolism (**Supplemental Figure 2K**), the important hub-molecules included cytochrome C, cytochrome-c oxidase, COX4I1, COX6C, POR, AMPK, ATP5B, and LDH, which were significantly associated with NFPAs. For proteins involved in tumorigenesis (**Supplemental Figure 2L**), the important hub-molecules included Ap1, FOS, JUN/JUNB/JUND, STAT5a/b, SKI, SNAI2, SRC (family), TP53, and Rb, which were significantly associated with NFPAs. For apoptosis-related proteins (**Supplemental Figure 2M**), the important hub-molecules included BCL2, caspase, BAX, BBC3, PARP, and CASP1, which were significantly associated with NFPAs. For Ca^{2+}-related proteins (**Supplemental Figure 2N**), the important hub-molecules included calpain, CACNA1B, calmodulin, SLC8A1, S100A1, and TRPC6, which were significantly associated with NFPAs. For G protein-related signaling pathway (**Supplemental Figure 2O**), the important hub-molecules included ADCY, PLC, PLC gamma, RGS2, GNAO1, and Gpcr, which were significantly associated with NFPAs. Moreover, the hub-molecules, Nr1h, NR4A1, NR4A2, HNRNPU, PP1 protein complex group, PP2A, Ppp2c, LDH, LDL, SREBF1, and APOA1, were also significantly associated with NFPAs (**Supplemental Figure 2P**). Those NFPA-associated hub-molecules offered an important resource to determine reliable biomarkers for NFPAs.

High-Frequency Hub-Molecules Among Datasets in NFPAs

Some hub-molecules appeared multiple times in different NFPA dataset groups. For example, integrin, VEGF, PDGF BB, Ras, Mek, p38 MAPK, PKA, FAK, Creb, histone h3, estrogen receptor, growth hormone, cytochrome C, AP1, and ADCY appeared four times; TGF-β, ERK, Jnk, MAPK, Akt, PI3K complex, NFκB complex, immunoglobulin, LH, insulin, and LDL appeared five times; PKC, and UBC appeared six times. In this study, a hub-molecule that appeared at least three times among 42 hub-molecule panels across nine datasets was defined as a high-frequency hub-molecule. A total of 57 high-frequency hub-molecules were obtained (**Table 1**). Among them, 25 (43.8%) high-frenquency hub-molecules were also found with PTMScan experiment in NFPAs, including ERK, ERK1/2, Jnk, MAPK, Mek, p38 MAPK, AKT, PI3K complex, p85, PKC, FAK, Rac, Shc, HSP90, NFκB Complex, histone H3, AP1, calmodulin, and PLC, which were differentially expressed or modified at least 2.5-fold changes in NFPAs compared to controls; and actin, rock, PKA, creb, STAT5a/b, and caspase, which were differentially expressed with a fold-change of 1∼2.5. Most of these high-frequency hub-molecules were kinases and signaling transduction-related molecules, which might contribute to oncogenesis and tumor development. Thereby, high-frequency hub-molecules did play essential roles in the progression of an NFPA. Those high-frequency hub-molecules might be used as targets for NFPA diagnostic indicators.

Canonical Pathway Alterations in NFPAs

A total of 519 statistically significant canonical pathways were mined from nine datasets, including 68 canonical pathways from NFPA DEGs (Dataset 1), 25 from NFPA DEPs (Dataset 2), 89 from NFPA mapping proteins (Dataset 3), 29 from NFPA nitroproteins (Dataset 4), 30 from invasive NFPA DEGs (Dataset 5), 28 from invasive NFPA DEPs (Dataset 6), 174 form control mapping proteins (Dataset 7), 33 from control nitroproteins (Dataset 8), and 43 from control phosphoproteins (Dataset 9) (**Supplemental Materials 1.3–9.3**). Of them, some statistically significantly canonical pathways were mined from only one dataset, such a type of canonical pathways had 30

TABLE 1 | High-frequency hub-molecules that were present in multiple datasets of NFPA group.

Hub molecule	Frequency	Dataset serial number	PTMScan detection	Fold change ≥ 2.5 or ≤ −2.5
PKC	6	1, 2, 3, 4, 5, 6	Y	Y
UBC	6	1, 2, 3, 4, 5, 6		
TGF-β	5	1, 2, 3, 5, 6		
ERK	5	1, 2, 3, 5, 6	Y	Y
ERK1/2	5	1, 2, 3, 5, 6	Y	Y
Jnk	5	1, 2, 3, 5, 6	Y	Y
MAPK	5	1, 2, 3, 5, 6	Y	Y
Akt	5	1, 2, 3, 5, 6	Y	Y
PI3K complex	5	1, 2, 3, 5, 6	Y	Y
NFκB Complex	5	1, 2, 3, 5, 6	Y	Y
Immunoglobulin	5	1, 2, 3, 5, 6		
Lh	5	1, 2, 3, 5, 6		
Insulin	5	1, 2, 3, 5, 6		
LDL	5	1, 2, 3, 5, 6		
Integrin	4	1, 2, 3, 5		
VEGF	4	1, 2, 3, 5		
PDGF BB	4	1, 2, 3, 5		
Ras	4	1, 2, 3, 5		
Mek	4	1, 2, 3, 5	Y	Y
p38 MAPK	4	2, 3, 5, 6	Y	Y
PKA	4	2, 3, 5, 6	Y	N
FAK	4	2, 3, 5, 6	Y	Y
Creb	4	1, 2, 3, 5	Y	N
Histone h3	4	2, 3, 4, 5	Y	Y
Estrogen receptor	4	1, 2, 3, 5		
GH1	4	1, 2, 3, 6		
Growth hormone	4	1, 2, 3, 5		
Cytochrome C	4	1, 2, 3, 5		
AP1	4	1, 2, 3, 5	Y	Y
ADCY	4	1, 2, 3, 6		
Actin	3	1, 3, 5	Y	N
F-Actin	3	1, 3, 5		
Rock	3	1, 2, 3	Y	N
Collagens	3	1, 3, 5		
Collagen type I	3	2, 3, 5		
Laminin	3	1, 3, 5		
p85	3	2, 3, 5	Y	Y
p70S6K	3	1, 3, 5		
Rac	3	1, 5, 6	Y	Y
Shc	3	2, 3, 5	Y	Y
Ubiquitin	3	2, 3, 5		
HSP90	3	2, 3, 5	Y	Y
Cyclin A	3	1, 3, 5		
IgG	3	2, 3, 6		
TCR	3	2, 3, 5		
IgE	3	1, 2, 3		
IFNG	3	3, 5, 6		
IFN-α	3	3, 4, 5		
B-estradiol	3	1, 3, 5		
FSH	3	1, 2, 5		
Proinsulin	3	1, 2, 3		
AMPK	3	1, 3, 5		
STAT5a/b	3	1, 2, 3	Y	N
Caspase	3	2, 3, 5	Y	N
Calmodulin	3	3, 5, 6	Y	Y
Calpain	3	1, 3, 5		
PLC	3	2, 3, 6	Y	Y

Among 57 hub-molecules that were present in at least 3 datasets, a total of 25 hub-molecules (25/57 = 43.9%) were detected by PTMScan experiments, 19(19/57 = 33.3%) of which were changed more than 2.5 times in NFPAs compared to controls. Y, yes; N, no.

canonical pathways from dataset 1, 4 from dataset 2, 8 from dataset 3, 15 from dataset 4, 5 from dataset 5, 3 from dataset 6, 49 from dataset 7, 1 from dataset 8, and 3 from dataset 9 (**Supplemental Table 6**). Meanwhile, a total of 139 statistically significantly canonical pathways were mined from at least two datasets (**Supplemental Table 7**). After extensive literature analysis of these 139 canonical pathways, a total of 68 canonical pathways were found to obviously associate with the occurrence and development of a tumor in direct and indirect ways (**Supplemental Table 8**). Moreover, for those 68 cancer-related canonical pathways, 14 canonical pathways were not mined from any DEGs or DEPs datasets, and 54 canonical pathways involved in any DEGs or DEPs were divided into nine canonical-pathway panels according to the similar cellular functions and biological processes (**Supplemental Table 8**; **Supplemental Figure 4**). Nine canonical-pathway panels associated significantly with NFPA pathophysiological processes were addressed in detail (**Supplemental Figure 4**), and differentially expressed hub-molecules (DEGs, or DEPs) in those 54 significantly cancer-related canonical pathways among nine canonical-pathway panels were summarized (**Table 2**). Those important canonical-pathway panels with differentially expressed hub-molecules (DEGs; DEPs) in NFPAs benefited for in-depth understanding of NFPA molecular mechanisms and discovery of reliable biomarkers for NFPAs. For example, (i) Gao and CDK5 were upregulated in CDK5 signaling. Nectin and myosin were upregulated, and CLDN was downregulated in tight junction signaling. Notch, N-cadherin, and FGFR1 were upregulated in epithelial adherens junction signaling. Dysregulation of these molecules in those pathways might promote cytoskeleton, cell adhesion, and movement imbalance in pituitary cells (**Table 2**: Panel A). (ii) NDUFS8, COX6B, ATP5B, CAT, and β-secret 2 were upregulated in mitochondrial dysfunction pathway, which might cause mitochondrial dysfunction and energy metabolism abnormality in NFPAs (**Table 2**: Panel B). (iii) ESR1

TABLE 2 | Differentially expressed hub-molecules (DEGs, or DEPs) in 54 significantly cancer-related canonical pathways among nine canonical-pathway panels in NFPAs.

Canonical-pathway panel		Pathway name	Upregulated hub-molecules (DEGs; DEPs)	Downregulated hub-molecules (DEGs; DEPs)	Nitroproteins and nitroprotein-related proteins
Panel A: Cytoskeleton, cell adhesion and movement pathways	1.	Actin Cytoskeleton Signaling	Dataset 1: PI3K, Talin, and Myosin	Dataset 1: TIAM, PIR121, TMSB4 and ERM	_
	2.	CDK5 Signaling	Dataset 6: Gao and CDK5	_	_
	3.	ILK Signaling	Dataset 5: FILAMIN (FLNA) and SLUG	Dataset 5: PI3K, PDK1 and MSK1/2 (RPS6KA5)	_
	4.	Inhibition of Matrix Metalloproteases	Dataset 6: ADAM	Dataset 6: MMP19	_
	5.	RhoA Signaling	_	_	Dataset 4: RHOGAP and Rhophilin are nitrated
	6.	Tight Junction Signaling	Dataset 1: NECTIN and MYOSIN	Dataset 1: TIAM1, CLDN and AP-1	_
	7.	Epithelial Adherens Junction Signaling	Dataset 1: Nectin, NOTCH, N-cadherin, FGFR1 and Myosin	_	_
Panel B: Mitochondrial dysfunction and energy metabolism related pathways	1.	Mitochondrial Dysfunction	Dataset 2: NDUFS8, COX6B and ATP5B; Dataset 6: CAT and β-secret2, ATP5B	Dataset 2: GPX4; Dataset 6: ATP5A1	_
	2.	Oxidative Phosphorylation	Dataset 2: NDUFS8, COX6B, ATP5B	_	_
	3.	AMPK Signaling	Dataset 5: PP2C and PFK	Dataset 5: PI3K, PKA and PDK1	_
Panel C: Angiogenesis, invasion, and metastasis related pathways	1.	CXCR4 Signaling	Dataset 1: Gβ, PI3K and IP3R	Dataset 1: CXCR4 and c-FOS	_
	2.	eNOS Signaling	Dataset 5: ESR1 and HSP90 (HSPCA and HSPCB)	Dataset 5: PI3K, PDK1, PKA and ESR2; Dataset 6: HSP70	_
	3.	Nitric oxide signaling in the cardiovascular system	Dataset 1: PI3K, CaM, IP3R and SERCA; Dataset 5: HSP90 (HSPCA and HSPCB)	Dataset 5: PI3K and PKA	_
	4.	Ephrin B Signaling	Dataset 1: EPHB, EFNE and Gβ	Dataset 1: CXCR4	_
	5.	Ephrin Receptor Signaling	Dataset 1: EPHB, EFNE and Gβ	Dataset 1: CXCR4 and ANGPT1	_
	6.	Hypoxia signaling in the cardiovascular system	Dataset 5: HSP90 (HSPCA and HSPCB)	Dataset 5: UBE2	_
	7.	Role of Tissue Factor Cancer	Dataset 2: Src	Dataset 2: FX (FXα)	_
Panel D: Toxin metabolism and oxidative stress related pathways	1.	Aryl hydrocarbon receptor signaling	Dataset 2: GST (GSTM2); Dataset 5: HSP90 (HSPCA and HSPCB), ESR1 and Bax	Dataset 2: HSP27, HSP90 and TGM2; Dataset 5: ESR2	_
	2.	Corticotropin Releasing Hormone Signaling	Dataset 1: CALM and IP3R	Dataset 1: ACTH, Nur77 and c-FOS	_
	3.	Glucocorticoid Receptor Signaling	Dataset 1: PI3K	Dataset 1: HSP70, c-Fos, CCL2, BCL2, PRL and POMC	_
	4.	Glutathione redox reactions I	_	Dataset 2: GPX4	_
	5.	Melatonin signaling	_	_	Dataset 4: PKA are nitrated
	6.	Methylglyoxal Degradation III	Dataset 2: AKR1B1	_	_

(Continued)

TABLE 2 | Continued

Canonical-pathway panel		Pathway name	Upregulated hub-molecules (DEGs; DEPs)	Downregulated hub-molecules (DEGs; DEPs)	Nitroproteins and nitroprotein-related proteins
	7.	NRF2-mediated Oxidative Stress Response	Dataset 2: GST (GSTM2) and ERP29	Dataset 2: HSP22, HSP27 and HSP90	_
	8.	Superoxide Radicals Degradation	Dataset 6: CAT	_	_
Panel E: Protein synthesis, degradation and amino acid metabolism related pathways	1.	EIF2 signaling	Dataset 5: 60S ribosomal subunit (RPL10 and RPL32)	Dataset 5: PI3K, PDK1, 40S ribosomal subunit (RPS2 and RPS2) and 60S ribosomal subunit (RPL18A)	_
	2.	Polyamine Regulation in Colon Cancer	Dataset 1: ODC1 and SSAT (SAT1)	_	_
	3.	Putrescine Degradation III	Dataset 1: MAOB	Dataset 1: ALDH2 and SSAT (SAT1)	_
	4.	Protein Ubiquitination Pathway	Dataset 5: HSP (HSPCA and HSPCB)	Dataset 2: HSP (HSPB8, GRP94 and HSPB1); Dataset 5: E2	Dataset 4: PSMA2 is nitrated, Ub is nitroprotein-interacted protein
Panel F: Cell cycle, proliferation and apoptosis related pathways	1.	14-3-3-mediated Signaling	Dataset 2: VIM	Dataset 2: 14-3-3	_
	2.	Calcium Signaling	Dataset 1: CALM, IP3R, PMCA, NCX (SLC8A2), SERCA and Myosin; Dataset 5: nACHR, NCX (SLC8A1) and Tropomyosin (TPM3, TPM4)	Dataset 1: DSCR1; Dataset 5: PKA	_
	3.	Cardiac β-adrenergic Signaling	Dataset 5: PPM1K, PPP1R11 and NCX	Dataset 5: IPKA, AKAP, PKA and PKI(PKIG)	_
	4.	ERK/MAPK Signaling	Dataset 1: PI3K, Talin and cPLA2; Dataset 2: FYN; Dataset 5: 14-3-3(YWHAG), PPM1K, PPP1R11 and ESR1	Dataset 1: MKP2; Dataset 2: 14-3-3(YWHAQ) and HSP27; Dataset 5: PI3K, PKA, PPM1A, ESR2 and RPS6KA5	_
	5.	IGF-1 Signaling	Dataset 1: PI3K; Dataset 5: IGFBP (IGFBP5) and 14-3-3 (YWHAG)	Dataset 1: IGFBP (IGFBP3), FKHR and c-FOS; Dataset 2: IGFBP (IGFBP6) and 14-3-3 (YWHAQ); Dataset 5: PI3K, PDK1 and PKA	_
	6.	mTOR Signaling	Dataset 5: PROTOR (PRR5)	Dataset 5: PI3K, PDK1, RSK (RPS6KA5) and 40S Ribosome(RPS2 and RPS2)	_
	7.	p53 signaling	Dataset 1: PI3K; Slug, Dataset 5: PUMA(BBC3) and BAX	Dataset 1: GADD45, NOXA, Bcl-2 and ZAC1; Dataset 5: PI3K	_
	8.	PEDF signaling	Dataset 1: PI3K and DOCK3; Dataset 5: GDNF	Dataset 1: BCL-2; Dataset 5: PI3K, TCF	_
	9.	PI3K/Akt signaling	Dataset 5: HSP90 (HSPCA and HSPCB) and 14-3-3 (YWHAG)	Dataset 2: HSP90 (GRP94) and 14-3-3 (YWHAQ); Dataset 5: PI3K p110 and PDK1	_
	10.	Sonic Hedgehog Signaling	_	_	Dataset 4: PKA is nitrated
	11.	Tec kinase signaling	Dataset 2: Gα and SRC(FYN)	_	_
	12.	Telomerase Signaling	Dataset 5: HSP90 (HSPCA, HSPCB)	Dataset 5: PI3K and PDK1	_
	13.	β-Adrenergic Signaling	Dataset 1: Gβ, Calm, IP3R and NCX	_	_

(Continued)

TABLE 2 | Continued

Canonical-pathway panel		Pathway name	Upregulated hub-molecules (DEGs; DEPs)	Downregulated hub-molecules (DEGs; DEPs)	Nitroproteins and nitroprotein-related proteins
Panel G: Immunity related pathways	1.	IL-1 Signaling	_	_	Dataset 4: IRAK-2 and PKA are nitrated
	2.	Role of NFATRegulation of the Immune Response	Dataset 1: PI3K, Gβ, CALM, CSP (CSPG5) and IP3R	Dataset 1: c-FOS	_
Panel H: ER stress related pathways	1.	Endoplasmic Reticulum Stress Pathway	_	Dataset 2: GRP94; Dataset 6: BIP (HSPA5 and HSPA6)	_
	2.	Unfolded protein response	Dataset 1: SREBP (SREBF1)	Dataset 1: PDI (P4HB), c/EBP, BCL2 and HSP70 (HSPA2)	_
Panel I: Others	1.	Aldosterone Signaling Epithelial Cells	Dataset 5: HSPCA and HSPCB	Dataset 2: HSPB8, HSP90B1 (GRP94) and HSPB1; Dataset 5: DNAJB6, PI3K and PDK1	_
	2.	Docosahexaenoic acid (DHA) signaling	Dataset 1: PI3K; Dataset 5: BAX	Dataset 1: FKHR and BCL2; Dataset 5: PI3K and PDK1	_
	3.	Endometrial Cancer Signaling	_	Dataset 5: PI3K, PDK1 and E-cadherin	_
	4.	Growth Hormone Signaling	Dataset 1: PI3K; Dataset 5: CEBPA	Dataset 1: GH, c-FOS and IGFBP3; Dataset 2: GH; Dataset 5: PI3K and PDK1	_
	5.	Hereditary Breast Cancer Signaling	Dataset 1: PI3K	Dataset 1: BLM, Wee1 and GADD45	Dataset 4: Ub is nitroprotein-interacted protein
	6.	PPARα/RXRα Activation	_	Dataset 2: GH, HSP90 (GRP94) and APOA1	_
	7.	PXR/RXR Activation	_	_	Dataset 4: PKA is nitrated
	8.	TR/RXR Activation	Dataset 1: PI3K, ZAKI4 and SREBP; Dataset 6: F10	Dataset 1: GH1 and FASN; Dataset 2: F10 and GH1; Dataset 6: GH1	_

Dataset 1: NFPA DEGs. Dataset 2: NFPA DEPs. Dataset 5: invasive NFPA DEGs. Dataset 6: NFPA DEPs. Dataset 4: NFPA nitroproteins.

was upregulated in eNOS signaling. CaM, IP3R, and SERCA were upregulated in nitric oxide signaling in the vascular system. EPHB, EFNE, and Gβ were upregulated in ephrin b/ephrin receptor signaling. The expression abnormalities of these molecules facilitated angiogenesis, and invasion abilities of NFPAs (**Table 2**: Panel C). (iv) AKR1B1 was upregulated in methylglyoxal degradation III pathway. GST (GSTM2) was upregulated in nrf2-mediated oxidative stress response pathway. This situation might convert toxin metabolism and oxidative stress response in pituitary to benefit the tumor progression (**Table 2**: Panel D). (v) VIM was upregulated, and 14-3-3 was downregulated, in 14-3-3-mediated signaling. CALM, NCX (SLC8A2), and tropomyosin (TPM3, TPM4) were upregulated in calcium signaling. Talin, FYN, and PPM1K were upregulated, and MKP2, PPM1A, and ESR2 were downregulated, in ERK/MAPK signaling. Various IGFBPs (IGFBP3, IGFBP5, and IGFBP6) were differentially expressed in IGF-1 signaling from multiple datasets (**Table 2**: Panel F). These changed molecules and pathways might cause the imbalance of many important processes such as cell cycle, and proliferation, and apoptosis to promote NFPA progression.

Validations of Networks and Canonical Pathways With PTMScan® Direct Test

PTMScan® Direct test that combined immunoaffinity enrichment and LC-MS/MS was used to identify and quantify phosphorylated peptides/proteins within multiple key canonical pathways (18). This study analyzed a total of 1006 unique phosphorylated-sites within 409 proteins that participated in more than 19 pathways. Moreover, many hub-molecules in multiple important canonical pathways including PI3K/Akt, mTOR, Wnt, NFκB, ERK/MAPK, p38, and JNK signaling pathways in NFPAs were identified with PTMScan® Direct test; and PI3K/AKT, mTOR, Wnt, NF-κB, ERK/MAPK, p38, and JNK signaling pathways were confirmed excessively activated in NFPAs with PTMScan experiments-based phosphorylation analysis (**Table 3**). From PTMScan® Direct results in NFPAs compared to controls, the phosphorylated sites and levels were identified and quantantified for proteins PI3K, SHIP, GAB2, SHC, SOS, HSP90, AKT, IKK, NFκB, GSK3, β-CATENIN, BAD, MEK1/2, and ERK1/2 in PI3K/Akt signaling pathway (**Figure 3**); for proteins PKC, p90RSK, mTOR, PRAS40, RICTOR, 4EBP, and RPS6 in the downstream mTOR signaling (**Figure 4A**);

TABLE 3 | PI3K/AKT, mTOR, Wnt, and ERK/MAPK signaling pathways confirmed with PTMScan experiments and phosphorylation sites.

Pathway	Symbol	Hub molecules	Gene name	Protein name	Phospho-site	Peptide	Tumor: normal ratio	Reported reference
PI3K/AKT pathway	HSP90	Y	HSP90B1	GRP94		EAESSPFVER	−2.5	
						FAFQAEVNR	−2.5	
						FQSSHHPTDITSLDQYVER	−3.0	
						GTTITLVLK	−2.6	
						GVVDSDDLPLNVSR	−4.3	
						IKEDEDDKTVLDLAVVLFETATLR	−3.0	
						NLLHVTDTGVGM#TR	−2.7	
						TVWDWELM#NDIKPIWQRPSK	−2.5	
			HSP90B2P; HSP90B1	HSP90B2P; GRP94		GLFDEYGSKK	−2.8	
	IKK	Y	IKBKG	IKKG; IKKG iso 2; IKKG iso 3	§374; 442; 275	HVEVSQAPLPPAPAY*LSSPLALP SQR	2.8	
					§376; 444; §277	HVEVSQAPLPPAPAYLS*SPLAL PSQR	2.8	
					§377; 445; 278	HVEVSQAPLPPAPAYLSS*PLAL PSQR	5.2	
	NFKB	Y	NFKB2	NFkB-p100; NFkB-p100 iso4 iso 4		DSGEEAAEPSAPSR	6.1	
	SHIP	N	INPPL1	SHIP-2; SHIP-2 iso 2	§886; 644	ERLY*EWISIDKDEAGAK	33.7	
	GAB2	N	GAB2	GAB2; GAB2 iso2 iso 2	§476; 438	AGDNSQSVY*IPM#SPGAHHFDSL GYPSTTLPVHR	4.8	
PI3K/AKT pathway, mTOR pathway	PI3K (P85)	Y	PIK3R2	PIK3R2		VYHQQYQDK	−2.9	
			PIK3R4	PIK3R4	§926, 932	KPVIPVLSS*TILPST*YQIR	−5.8	
	AKT	Y	AKT1; AKT2; AKT1; AKT3; AKT3; RPS6KB1; RPS6KB1; RPS6KB1; RPS6KB1; RPS6KB1; RPS6KB2; SGK1; SGK2; SGK3; SGK1; SGK1; SGK1; SGK1; SGK2; SGK2; SGK3	Akt1; Akt2; Akt1 iso 2; Akt3; Akt3 iso 2; p70S6K; p70S6K iso2 iso 2; p70S6K iso2 iso 3; p70S6K iso2 iso 5; p70S6K iso2 iso 4; P70S6KB; SGK1; SGK2; SGK3; SGK1 iso 2; SGK1 iso3 iso 3; SGK1 iso 4; SGK1 iso 5; SGK2 iso2 iso 2; SGK2 iso 3; SGK3 iso 2		ITDFGLCK	3.3	Phospho-Akt (Ser473), and Akt (Total), increased (19).
			AKT1; AKT2; AKT1; AKT3; AKT3	Akt1; Akt2; Akt1 iso 2; Akt3; Akt3 iso 2	§308; §309; §246; §305; §305	T*FCGTPEYLAPEVLEDNDYGR	3.1	
					§312; §313; 250; §309; §309	TFCGT*PEYLAPEVLEDNDYGR	3.1	
			AKT2	Akt2	§313	EGISDGATM#KTFCGT*PEYLA PEVLEDNDYGR	34.0	
			AKT2	Akt2; Akt2 iso 2	§475; 432	THFPQFSY*SASIRE	3.7	
			AKT3	Akt3	§472	RPHFPQFS*YSASGR	6.6	
			AKT3	Akt3	§472, §476	RPHFPQFS*YSAS*GRE	9.9	
			AKT3	Akt3	§474, §476	RPHFPQFSYS*AS*GRE	9.9	
			AKT3	Akt3; Akt3 iso 2		EGITDAATM#K	4.3	
	mTOR	Y	mTOR	mTOR	§2444	T*RTDSYSAGQSVEILDGVELGEPA HKK	2.6	Phospho-mTOR (Ser2448), and mTOR (Total), no significant change (20).
					§2446	TRT*DSYSAGQSVEILDGVELGEP AHK	3.0	

(Continued)

TABLE 3 | Continued

Pathway	Symbol	Hub molecules	Gene name	Protein name	Phospho-site	Peptide	Tumor: normal ratio	Reported reference
					§2446, §2449	T*DSY*SAGQSVEILDGVELGE PAHK	5.8	
					§2448	TRTDS*YSAGQSVEILDGVELGEPA HK	2.5	
					§2449	TRTDSY*SAGQSVEILDGVELGEPA HKK	2.6	
					§2450	TRTDSYS*AGQSVEILDGVELGEPA HKK	2.6	
					§2454	TRTDSYSAGQS*VEILDGVELGEPA HKK	5.1	
					§2471	T*GTTVPESIHSFIGDGLVKPEALNK	23.3	
	PRAS40	N	AKT1S1	PRAS40; PRAS40 iso3 iso 2; PRAS40 iso3 iso 3	§246; 116; 266	LNT*SDFQK	22.7	
	S6	N	RPS6	S6	§235, §236, §240	RLS*S*LRAS*TSKSESSQK	55.8	
					§235, §241, §244	LS*SLRAST*SKS*ESSQK	34.2	
					§236, §240	RLSS*LRAS*TSK	10.1	
					§236, §241, §242	RLSS*LRAST*S*KSESSQK	7.8	
					§236, §241, §244	RLSS*LRAST*SKS*ESSQK	55.8	
					§236, §242, §244	RLSS*LRASTS*KS*ESSQK	7.8	
	RICTOR	Y	RICTOR	RICTOR; RICTOR iso3 iso 3		DAFGYATLK	3.9	
	VEGFR	N	FLT1	VEGFR1; VEGFR1 iso2 iso 5; VEGFR1 iso2 iso 6; VEGFR1 iso2 iso 7; VEGFR1 iso2 iso 8	1295; 513; 420; 300; 318	ESGLSDVSRPSFCHS*SCG HVSEGK	2.8	
PI3K/AKT pathway, mTOR pathway, ERK/ MAPK signaling	ERK	Y	MAPK1	ERK2; ERK2 iso 2	§185, §187; §185, §187	VADPDHDHTGFLT*EY*VATR	90.6	Phospho-ERK1/2(Thr183), increased; ERK1/2(Total), no significant change (20).
					§185; §185	VADPDHDHTGFLT*EYVATR	114.5	
					§187; §187	VADPDHDHTGFLTEY*VATR	114.5	
						VADPDHDHTGFLTEYVATR	4.9	
			MAPK1; MAPK1; MAPK3; MAPK3; MAPK3	ERK2; ERK2 iso 2; ERK1; ERK1 iso2 iso 2; ERK1 iso2 iso 3		APEIM#LNSK	6.5	
			MAPK3	ERK1; ERK1 iso2 iso 2; ERK1 iso2 iso 3	§198, §204; 198, 204; 198, 204	IADPEHDHT*GFLTEY*VATR	385.0	
					§202, §204; 202, 204; 202, 204	IADPEHDHTGFLT*EY*VATR	24.9	
					§202, §207; 202, 207; 202, 207	IADPEHDHTGFLT*EYVAT*R	24.9	
					§202; 202; 202	IADPEHDHTGFLT*EYVATR	62.4	
					§204; 204; 204	IADPEHDHTGFLTEY*VATR	62.4	
	RSK	Y	RPS6KA1; RPS6KA3; RPS6KA6; RPS6KA1; RPS6KA1; RPS6KA1; RPS6KA6	p90RSK; RSK2; RSK4; p90RSK iso2 iso 2; p90RSK iso 3; p90RSK iso 4; RSK4 iso 2	§220; §226; §231; 229; 128; 204; §231	KAY*SFCGTVEYM#APEVVNR	2.8	
					§221; §227; §232; 230; 129; 205; §232	KAYS*FCGTVEYM#APEVVNR	2.8	
					§225; §231; §236; 234; 133; §209; §236	KAYSFCGT*VEYMAPEVVNR	7.7	
			RPS6KA4	MSK2; MSK2 iso2 iso 2	§360, §365; 360, 365	IFQGYS*FVAPS*ILFDHNNAVM#TD GLEAPGAGDRPGR	−3.0	
					§360; 360	IFQGYS*FVAPSILFDHNNAVM#TD GLEAPGAGDRPGR	12.1	

(Continued)

TABLE 3 | Continued

Pathway	Symbol	Hub molecules	Gene name	Protein name	Phospho-site	Peptide	Tumor: normal ratio	Reported reference
			RPS6KA5	MSK1; MSK1 iso 2; MSK1 iso 3	§376; §376; 297	LFQGYS*FVAPSILFK	184.0	
						EFVADETER	7.5	
	4EBP	N	EIF4EBP1	4E-BP1	§34, §37	VVLGDGVQLPPGDY*STT*PGGTLF STTPGGTR	61.1	
					§34, §41	VVLGDGVQLPPGDY*STTPGGT*LF STTPGGTR	61.1	
					§35, §41	VVLGDGVQLPPGDYS*TTPGGT*LF STTPGGTR	61.1	
					§35, §44	VVLGDGVQLPPGDYS*TTPGGTLF S*TTPGGTR	61.1	
					§35, §46	RVVLGDGVQLPPGDYS*TTPGGTL FSTT*PGGTR	3.3	
					§36	VVLGDGVQLPPGDYST*TPGGTLF STTPGGTR	9.7	
					§37, §45	VVLGDGVQLPPGDYSTT*PGGTLF ST*TPGGTR	61.1	
					§41	VVLGDGVQLPPGDYSTTPGGT*LF STTPGGTR	9.7	
					§41, §44	VVLGDGVQLPPGDYSTTPGGT*LF S*TTPGGTR	61.1	
					§44	VVLGDGVQLPPGDYSTTPGGTLFS *TTPGGTR	9.7	
					§46	VVLGDGVQLPPGDYSTTPGGTLFS TT*PGGTR	7.1	
						DLPTIPGVTSPSSDEPPM#EASQSHLR	35.2	
						FLM#ECR	20.5	
			EIF4EBP1; EIF4EBP2	4E-BP1; 4E-BP2	§44; §44	TPGGTLFS*TTPGGTR	94.0	
					§45; §45	TPGGTLFST*TPGGTR	94.0	
					§46; §46	TLFSTT*PGGTR	2.9	
			EIF4EBP2	4E-BP2	§25, §44	TVAIS*DAAQLPHDYCTTPGGTLFS *TTPGGTR	61.3	
					§25, §45	TVAIS*DAAQLPHDYCTTPGGTLFS T*TPGGTR	61.3	
					§25, §46	TVAIS*DAAQLPHDYCTTPGGTLFS TT*PGGTR	41.7	
					§34, §45	TVAISDAAQLPHDY*CTTPGGTLFS T*TPGGTR	61.3	
					§34, §46	TVAISDAAQLPHDY*CTTPGGTLFS TT*PGGTR	61.3	
					§36	TVAISDAAQLPHDYCT*TPGGTLFS TTPGGTR	6.9	
					§36, §46	TVAISDAAQLPHDYCT*TPGGTLFS TT*PGGTR	61.3	
					§37	TVAISDAAQLPHDYCTT*PGGTLFS TTPGGTR	6.9	
					§37, §45	TVAISDAAQLPHDYCTT*PGGTLFS T*TPGGTR	61.3	
					§37, §46	TVAISDAAQLPHDYCTT*PGGTLFS TT*PGGTR	61.3	
					§44	TVAISDAAQLPHDYCTTPGGTLFS* TTPGGTR	6.9	
					§45	TVAISDAAQLPHDYCTTPGGTLFST *TPGGTR	6.9	
					§46	TVAISDAAQLPHDYCTTPGGTLFST T*PGGTR	6.9	
						TVAISDAAQLPH	74.7	
						VEVNNLNNLNNHDR	33.4	
			EIF4EBP3	4E-BP3	§23	DQLPDCYSTT*PGGTLYATT PGGTR	19.3	
					§23, §32	DQLPDCYSTT*PGGTLYATT*PGGTR	84.7	

(Continued)

TABLE 3 | Continued

Pathway	Symbol	Hub molecules	Gene name	Protein name	Phospho-site	Peptide	Tumor: normal ratio	Reported reference
					§27	DQLPDCYSTTPGGT*LYATT PGGTR	67.4	
					§31	DQLPDCYSTTPGGTLYAT*T PGGTR	67.4	
					§32	DQLPDCYSTTPGGTLYATT*P GGTR	67.4	
					22	DQLPDCYST*TPGGTLYATT PGGTR	67.4	
PI3K/AKT pathway, mTOR pathway, ERK/MAPK signaling, Noncanonical Wnt pathway	PKC	Y	PRKCA	PKCA	§651	IANIDQS*DFEGFSYVNPQFVHPILQ SAV	24.4	
			PRKCA; PRKCB; PRKCB	PKCA; PKCB; PKCB iso2 iso 2	§48; §48; 48	QPT*FCSHCTDFIWGFGK	−33.1	
			PRKCA; PRKCB; PRKCB; PRKCG; PRKCG	PKCA; PKCB; PKCB iso2 iso 2; PKCG; PKCG iso 2	§497; §500; 500; §514; 401	T*FCGTPDYIAPEIIAYQPYGK	−3.1	
					§501; §504; 504; §518; 405	TFCGT*PDYIAPEIIAYQPYGK	−3.6	
					§504; §507; 507; §521; 408	TFCGTPDY*IAPEIIAYQPYGK	−3.1	
			PRKCD	PKCD; PKCD iso2 iso 2	§664; 695	NLIDSM#DQSAFAGFS*FVNPK	−3.7	
						FEHLLED	−4.5	
PI3K/AKT pathway, Wnt pathway	GSK3	Y	GSK3A	GSK3A	§19	T*SSFAEPGGGGGGGGGPGGS ASGPGGTGGGK	17.1	
					§19, §39	T*SSFAEPGGGGGGGGGPGGS* ASGPGGTGGGK	17.8	
					§21	TSS*FAEPGGGGGGGGGPGGS ASGPGGTGGGK	17.1	
					§21, §39	TSS*FAEPGGGGGGGGGPGGS* ASGPGGTGGGK	22.1	
	CTNNB1	Y	CTNNB1	CTNNB1	§551	T*SMGGTQQQFVEGVR	5.0	No significant change of total β-catenin (21), nuclear accumulation of β-catenin (22).
					§552	RTS*M#GGTQQQFVEGVR	5.0	
					§556	TSM#GGT*QQQFVEGVR	4.7	
					§675, §679	RLS*VELT*SSLFR	4.7	
					§675, §680	KRLS*VELTS*SLFR	7.7	
					§675, 681	RLS*VELTSS*LFR	10.0	
					§718	S*FHSGGYGQDAL	19.1	
					§721	SFHS*GGYGQDALGM#DPM#	28.4	
						GGTQQQFVEGVR	17.8	
						GTQQQFVEGVR	49.5	
						QDDPSYR	4.0	
						RTSM#GGTQQQFVEGVR	67.3	
						SFHSGGYGQD	4.2	
						SFHSGGYGQDA	6.8	
						SFHSGGYGQDAL	3.2	
						TQQQFVEGVR	23.9	
						TSM#GGTQQQFVEGVR	5.3	
						TSMGGTQQQFVEGVR	18.0	
			CTNNB1; JUP; CTNNB1	CTNNB1; CTNNG; CTNNB1 iso 2		M#EEIVEGCTGALH	2.5	
						M#EEIVEGCTGALHI	41.9	
						MEEIVEGCTGALH	52.8	
Wnt pathway	BCL9	N	BCL9	Bcl-9		TVASSDDDSPPAR	2.9	
Noncanonical Wnt pathway	JNK	Y	MAPK8; MAPK10; MAPK8; MAPK8; MAPK8;	JNK1; JNK3; JNK1 iso2 iso 2; JNK1 iso2 iso 3; JNK1 iso2 iso 4; JNK1 iso2 iso 5; JNK3 iso2 iso 2; JNK3	§183, §185; §221, §223; §183, §185; §183, §185; §183, §185; §183, §185; §221, §223;	TAGTSFM#M#T*PY*VVTR	12.2	

(Continued)

TABLE 3 | Continued

Pathway	Symbol	Hub molecules	Gene name	Protein name	Phospho-site	Peptide	Tumor: normal ratio	Reported reference
			MAPK8; MAPK10; MAPK10; MAPK10	iso2 iso 3; JNK3 iso2 iso 4	183, 185; 76, 78			
			MAPK9	JNK2; JNK2 iso2 iso 2; JNK2 iso3 iso 3; JNK2 iso3 iso 4; JNK2 iso3 iso 5	§183, §185; 183, §185; 183, 185; 183, 185; 183, 185	TACTNFM#M#T*PY*VVTR	8.3	
					175, §185; 175, §185; 175, 185; 175, 185; 175, 185	T*ACTNFM#M#TPY*VVTR	8.3	
	CDC42	N	CDC42	CDC42; CDC42 iso1 iso 1		IGGEPYTLGLFDTAGQEDYDR	−28.6	
ERK/ MAPK signaling, Noncanonical Wnt pathway	PLC	Y	PLCG1	PLCG1; PLCG1 iso2 iso 2	§1248; 1249	AREGS*FESR	22.4	
PI3K/AKT pathway, ERK/ MAPK signaling	SHC	Y	SHC4	SHC4; SHC4 iso 2	§424; 181	CSSVY*ENCLEQSR	21.2	
	SOS	Y	SOS2	SOS2; SOS2 iso 2	§1132; 1099	SFFSS*CGSLHK	11.9	
	BAD	N	BAD	BAD	§71	S*RHSSYPAGTEDDEGM#GEEPSPFR	−26.9	
					§74	SRHS*SYPAGTEDDEGM#GEEPSPFR	−26.9	
					§75	SRHSS*YPAGTEDDEGM#GEEPSPFR	−26.9	
					§76	SRHSSY*PAGTEDDEGM#GEEPSPFR	−332.1	
					§80	HSSYPAGT*EDDEGMGEEPSPFR	7.5	
	MEK	Y	MAP2K1; MAP2K2; MAP2K1	MEK1; MEK2; MEK1 iso 2 iso 2	§218; §222; 192	LCDFGVSGQLIDS*M#ANSFVGTR	339.6	Phospho-MEK1/2 (Ser217/221), increased; MEK1/2 (Total), no significant change (20).
					§222; §226; 196	LCDFGVSGQLIDSM#ANS*FVGTR	339.6	
ERK/ MAPK signaling	FAK	Y	PTK2	FAK; FAK iso2 iso 2; FAK iso2 iso 3; FAK iso2 iso 4; FAK iso5 iso 5; FAK iso2 iso 7	§575, §577; 423, 425; 423, 425; 423, 425; 575, 577; 575, 577	YMEDST*YY*K	16.3	
					§575; 423; 423; 423; 575; 575	YMEDST*YYK	233.4	
					§576; 424; 424; 424; 576; 576	YMEDSTY*YK	233.4	
			PTK2; PTK2; PTK2; PTK2; PTK2; PTK2; PTK2B; PTK2B	FAK; FAK iso2 iso 2; FAK iso2 iso 3; FAK iso2 iso 4; FAK iso5 iso 5; FAK iso2 iso 7; Pyk2; Pyk2 iso2 iso 2		LGDFGLSR	7.1	
	PAK	N	PAK6	PAK6; PAK6 iso 2	§132; §132	AQSLGLLGDEHWATDPDM#YLQS*PQSER	27.1	
	RAF	Y	BRAF	BRAF	§446	RDS*SDDWEIPDGQITVGQR	1193.2	B-Raf mRNA, increased, B-Raf protein (Total), variable expression, increased, decreased or no significant change (23).
					§447	RDSS*DDWEIPDGQITVGQR	1193.2	

(Continued)

TABLE 3 | Continued

Pathway	Symbol	Hub molecules	Gene name	Protein name	Phospho-site	Peptide	Tumor: normal ratio	Reported reference
	MKP	Y	DUSP1	MKP-1	§359	GTSTTTVFNFPVSIPVHSTNSALSY LQS*PITTSPSC	−2.8	
	HSP27	Y	HSPB1	HSP27		GPSWDPFR	−5.6	
						LFDQAFGLPR	−18.1	
	MYC	N	MYC	Myc; Myc iso2 iso 2		NYDLDYDSVQPY	4.6	Phospho-c-myc (Thr58/Ser62), decreased; Phospho-c-myc (Ser62), no significant change; c-myc (total), no significant change (20) or increased (21, 22).
	MYCT1		MYCT1	MYCT1	112, 114	S*RS*SYTHGLNR	590.0	
					114	S*SYTHGLNR	12.5	
					115	SRSS*YTHGLN	189.3	
	NFAT	Y	NFATC3	NFAT4;NFAT4 iso 2;NFAT4 iso 3;NFAT4 iso 4;NFAT4 iso 5;NFAT4 iso 6		LVFGEDGAPAPPPPGSR	−2.8	
	Histone h3	Y	H3F3A	H3F3A		FQSAAIGALQEASEAYLVGLFEDTN LCAIHAK	−23.2	
			HIST3H3; HIST1H3A; HIST2H3C; H3F3A; H3F3C	HIST3H3; H3; HIST2H3A/C/D; H3F3A; H3F3C		YRPGTVALR	−6.4	
	Jun	Y	JUN	Jun	§58, §63	AKNS*DLLTS*PDVGLLK	14.4	
					§63	NSDLLTS*PDVGLLK	16.1	
						NSDLLTSPDVGLLK	19.1	
			JUND	JunD	§90	ADGAPSAAPPDGLLAS*PDLGLLK	56.7	
						AAALKPAAAPPPTPLR	16.8	
						ADGAPSAAPPDGLLASPDLGLLK	182.4	
						KDALTLSLSEQVAAALKPAAAPPPTPLR	40.8	
			JUND; JUN	JunD; Jun	§100; §73	LAS*PELER	14.4	
	ATF	N	ATF2	ATF-2; ATF-2 iso 3; ATF-2 iso 5; ATF-2 iso 7	§69, §71; §69, §71; 51, 53; 51, 53	NDSVIVADQT*PT*PTR	8.1	
					§71; §71; 53; 53	NDSVIVADQTPT*PTR	23.5	
			ATF7	ATF7; ATF7 iso2 iso 2; ATF7 iso6 iso 3; ATF7 iso6 iso 4; ATF7 iso6 iso 6	§424, §434; 392, 402; 403, 413; 237, 247; 413, 423	TQGYLES*PKESSEPTGS*PAPVIQ HSSATAPSNGLSVR	20.9	
					§424; 392; 403; 237; 413	TQGYLES*PKESSEPTGSPAPVIQH	7.1	
					§428, §434; 396, 402; 407, 413; 241, 247; 417, 423	TQGYLESPKES*SEPTGS*PAPVIQ H	25.1	
					§429; 397; 408; 242; 418	TQGYLESPKESS*EPTGSPAPVIQH	7.1	
					§432; 400; 411; 245; 421	ESSEPT*GSPAPVIQHSSATAPSNG LSVR	213.7	
					§434; 402; 413; 247; 423	ESSEPTGS*PAPVIQHSSATAPSNG LSVR	213.7	
						ESSEPTGSPAPVIQH	20.8	
						ESSEPTGSPAPVIQHSSATAPSNGLSVR	2.5	
						SSATAPSNGLSVR	6.9	
				ATF7;ATF7 iso2 iso 2;ATF7 iso6 iso 3;ATF7 iso6 iso 4;ATF7 iso6 iso 6;ATF7 iso5 iso 5	§53; 53; 53; 53; 53; 53	TDSVIIADQTPT*PTR	80.0	
P38 MAPK signaling	P38 MAPK	Y	MAPK14	P38A; P38A iso2 iso 2; P38A iso2 iso 3; P38A iso2 iso 4; P38A iso2 iso 5	§180, §182; 180, §182; 180, §182; 180, §182; 180, §182	HTDDEM#T*GY*VATR	3.0	Phospho-p38 MAPK (Thr180/Tyr182) and p38 MAPK (total), no significant change (20).
					§182, §185; §182, 185; §182, 185; §182, 185	HTDDEM#TGY*VAT*R	3.0	

*N, Not exist in this category; Y, Exist in this category. §, the phospho site was confirmed by literature. *, phosphorylation, #, oxidized methionine.*

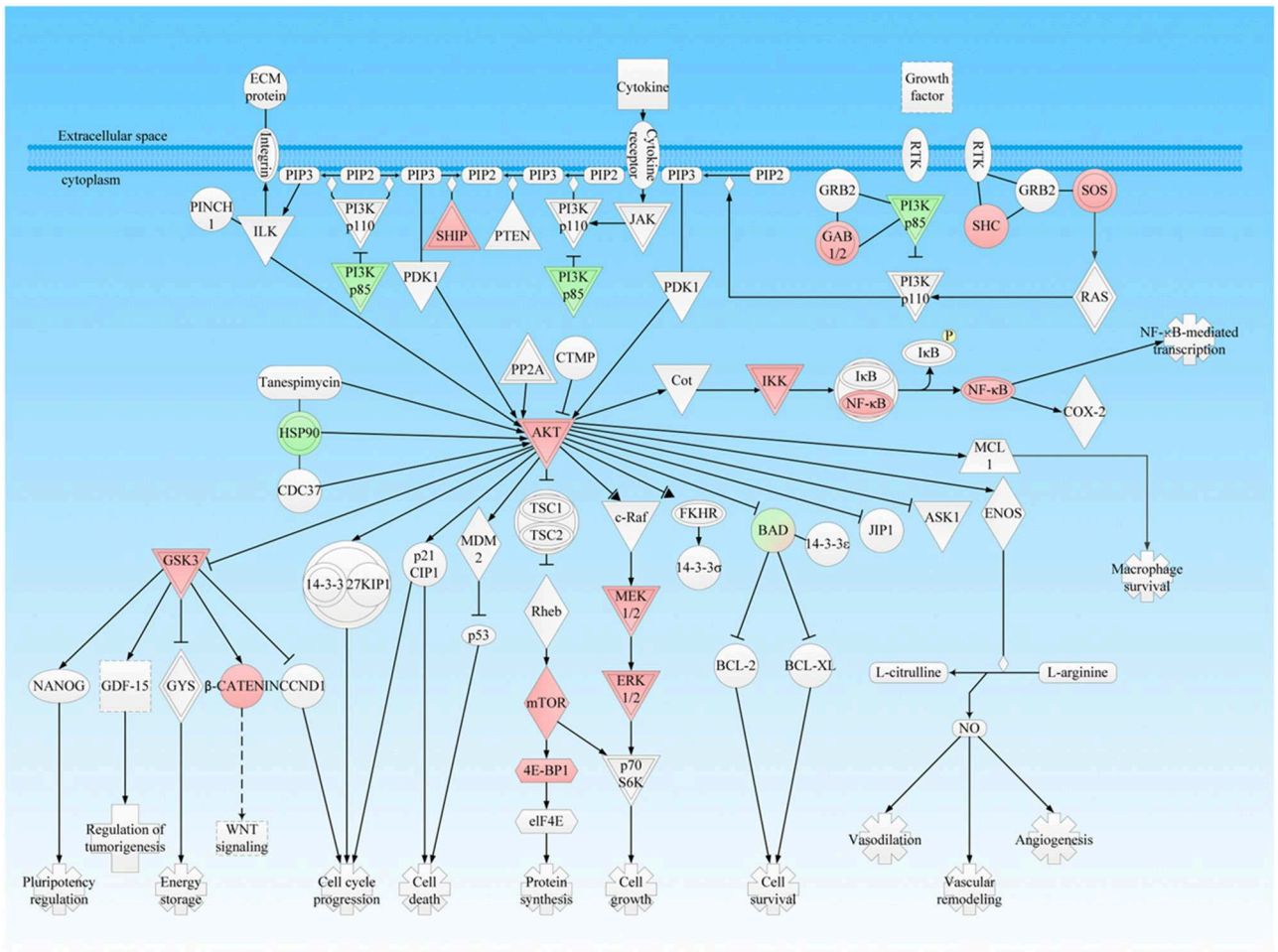

FIGURE 3 | PI3K-AKT signaling pathway was involved in NFPA. This pathway was derived from the IPA analysis results of multi-omics, and then it was modified and verified according to the PTMScan results of NFPAs compared to controls. The red color means upregulation of a molecule in NFPAs, and the green color means downregulation of a molecule in NFPAs. The gradient color degree means slightly different expression tendency of that molecule.

for proteins GSK3, β-catenin, Bcl-9, PLC, NFkB, JNK, AP-1, and ATF2 in Wnt pathways (**Figure 5A**); and for proteins SHC, SOS, PI3K, PKC, MEK1/2, ERK1/2, BAD, p90RSK, 4EBP1, PLC, PAK, B-RAF, FAK, MKP, HSP27, MSK1/2, c-Myc, NFATc, CREB, Histone H3, and Jun in ERK/MAPK signaling (**Figure 6**), and some of these proteins were also found in PI3K/Akt/mTOR signaling (**Table 3**). PTMScan experiments revealed the significantly increased phosphorylation levels at residues Thr308/309/305 in Akt1/2/3, Ser472 in Akt3, Ser2448 in mTOR, Ser246 in PRAS40; Thr37 and Thr46 in both 4E-BP1 and 4E-BP2, Thr23 in 4E-BP3; Ser235, Ser236, Ser240, Thr241 and Ser244 in S6, Ser376 in IKKγ, Ser21 in GSK3α, and Ser552 and Ser675 in β-Catenin (**Table 3**), which might stimulate and magnify PI3K/Akt signaling, and its downstream mTOR, NFκB, and canonical Wnt pathways to contribute to tumor progression. Moreover, the significantly increased phosphorylation levels were also found at residues Ser446 or Ser447 in B-Raf, Ser218 or Ser222 in MEK1, Thr202 and Tyr187 in both ERK1 and ERK2, Tyr220, Ser221, and Thr225 in RSK1, Tyr226, Ser227, and Thr231 in RSK2, Tyr231, Ser232, and Thr236 in RSK4, Ser376 in MSK1, Ser360 in MSK2, Thr575 and Tyr577 (Thr575 and/or Tyr576) in FAK, Thr180 and Tyr182 (Tyr182 and Thr185) in p38a, Thr183 and Tyr185 in JNK1, Thr221 and Tyr223 in JNK3, Thr183 and Tyr185 (Thr175 and Tyr185) in JNK2, and Thr69 and Thr71 in ATF2; whereas the decreased phosphorylation level was found at residue Ser359 in MKP1, and Ser71, Ser74, Ser75, and Tyr76 in BAD (**Figure 6** and **Table 3**). Those findings demonstrated that ERK/MAPK and its related p38 and Jnk pathways were activated to significantly affect NFPA development. Thereby, PTMScan® experiment confirmed clearly PI3K/Akt, mTOR, Wnt, ERK/MAPK, p38, and Jnk pathways derived from IPA pathway network and bioinformatic analyses of multi-omics data, and further revealed the functions of those pathway-networks in NFPA tumorigenesis.

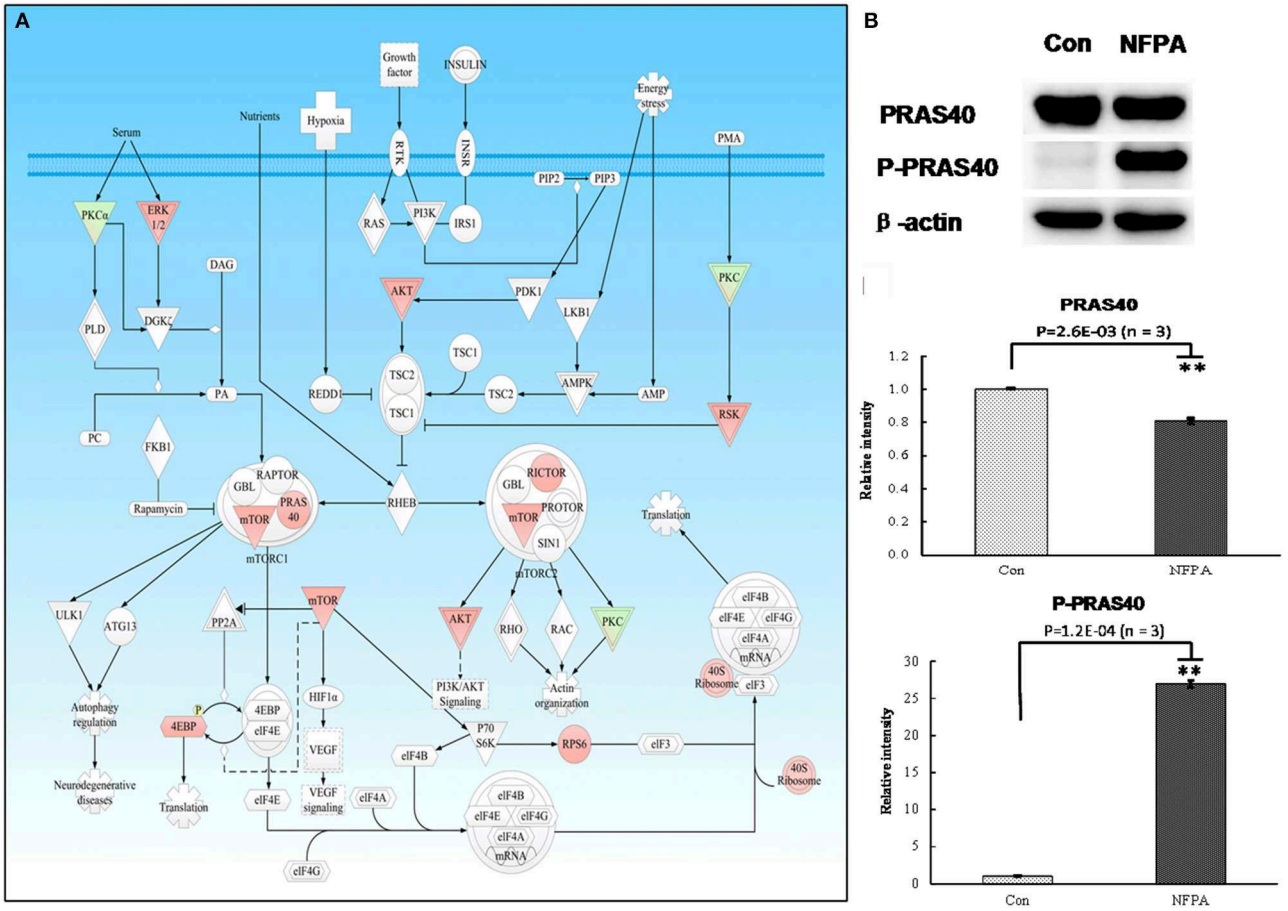

FIGURE 4 | mTOR signaling pathway was involved in NFPA. **(A)** mTOR signaling pathway was derived from the IPA analysis results of multi-omics, and then it was modified and verified according to the PTMScan results of NFPAs compared to controls. The red color means upregulation of a molecule in NFPAs, and the green color means downregulation of a molecule in NFPAs. The gradient color degree means slightly different expression tendency of that molecule. **(B)** Immunoaffinity Western blot analyses of PRAS40 and p-PRAS40 (Thr246) confirmed. mTORC1 signaling was involved in NFPAs ($n \geq 3$). The relative intensity was the ratio of absorbance units of NFPAs compared to controls. $^{**}p < 0.01$.

mTORC1 Signaling and Canonical Wnt Pathway Are Activated in an NFPA

For mTOR signaling pathway (**Figure 4A**), PRAS40 was the pivotal modulator of the mTOR complex 1 (mTORC1)**.** The total protein expression level of PRAS40 and its phosphorylation level at residue Thr246 in PRAS40 were the switch of mTORC1 pathway to decide the initiation of the downstream protein synthesis and metabolism enhancement (24). Western blot analysis found that PRAS40 was significantly downregulated in NFPAs (**Figure 4B**), while the phosphorylation level at residue Thr246 in p-PRAS40 was significantly increased in NFPAs relative to controls. For canonical Wnt pathway (**Figure 5A**), GSK3α and GSK3β were key inhibitors of canonical Wnt pathway. The enhanced phosphorylation level at residue Ser21/9 in GSK3α/β would remove the inhibition of Wnt pathway. The total protein expression levels of GSK3α and GSK3β were decreased slightly in NFPAs relative to controls (**Figure 5B**). Whereas, the phosphorylation levels at residues Ser21 in p-GSK3α and Ser9 in p-GSK3β were significantly increased in NFPAs relative to controls. In addition, the main effector β-catenin in Wnt pathway was significantly upregulated in NFPAs compared to controls. Therefore, the expression and phosphorylation levels of GSK3α/β could reflect the state of canonical Wnt pathway. These Western blot experiments further validated IPA pathway-network analysis results and PTMScan experimental results; namely, the canonical Wnt pathway and mTORC1 signaling were activated in NFPAs, and contributed to NFPA pathogenesis.

DISCUSSION

Molecular network changes are the hallmark in human pituitary adenoma pathogenesis, which is involved in multiple molecule alterations in different levels of genes (genome), RNAs (transcriptome), proteins (proteome), metabolites (metabolome), and imaging features (radiome), and those different levels of molecules are mutually interacted. Multiomics data-based pathway network analysis benefits for the complete

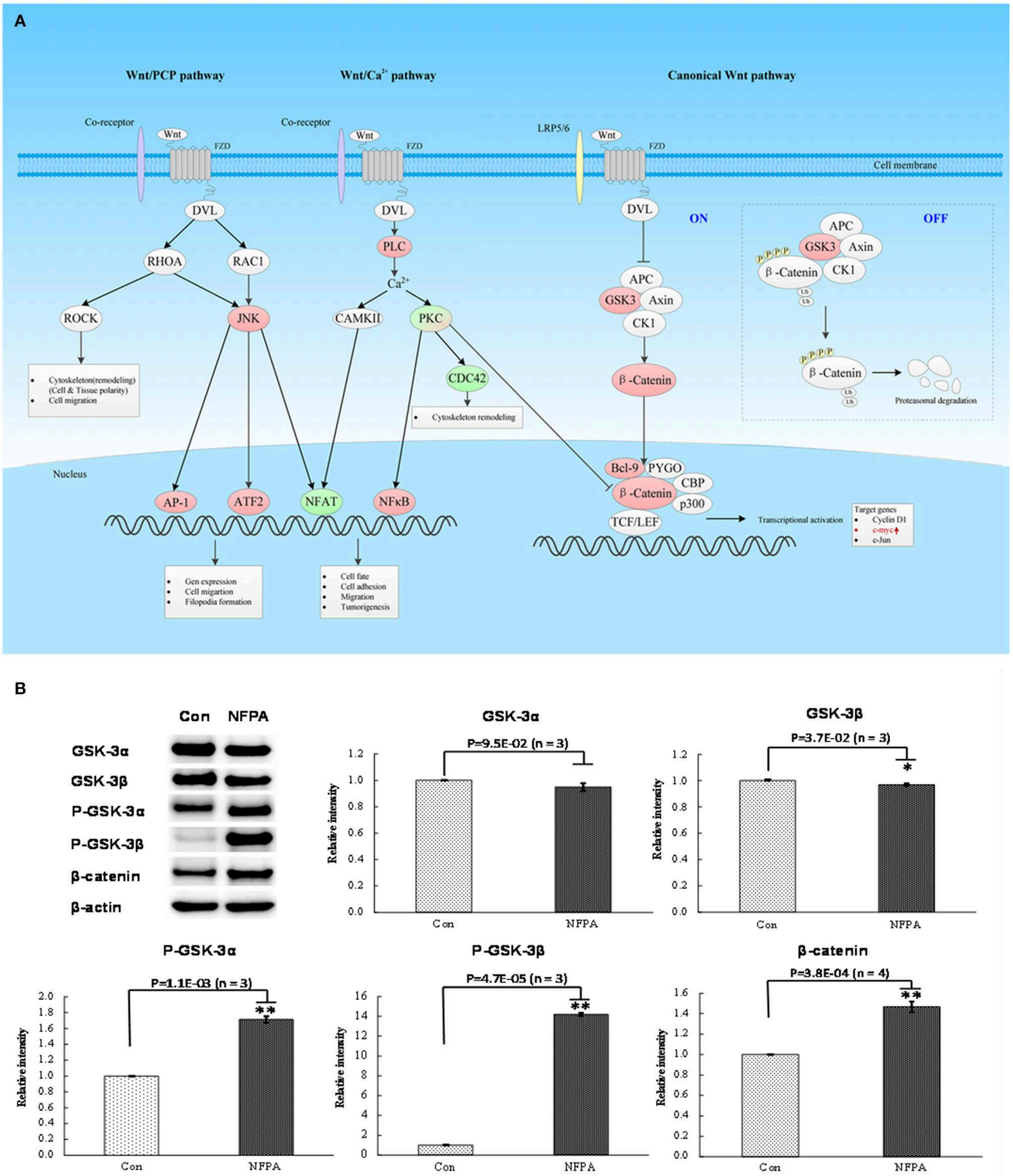

FIGURE 5 | Wnt signaling pathway was involved in NFPA. **(A)** Wnt signaling pathway was derived from PTMScan results of NFPAs compared to controls. The red color means upregulation of a molecule in NFPAs, and the green color means downregulation of a molecule in NFPAs. The gradient color degree means slightly different expression tendency of that molecule. **(B)** Activation of canonical Wnt pathway in NFPAs was verified by Western blot results of GSK-3α, GSK-3β, p-GSK-3β (Ser9), p-GSK-3α/β (Ser21/9), β-catenin and β-actin in control pituitaries (Con) and NFPAs ($n \geq 3$). The relative intensity was the ratio of absorbance units of NFPAs compared to Con. $^{*}p < 0.05$, $^{**}p < 0.01$.

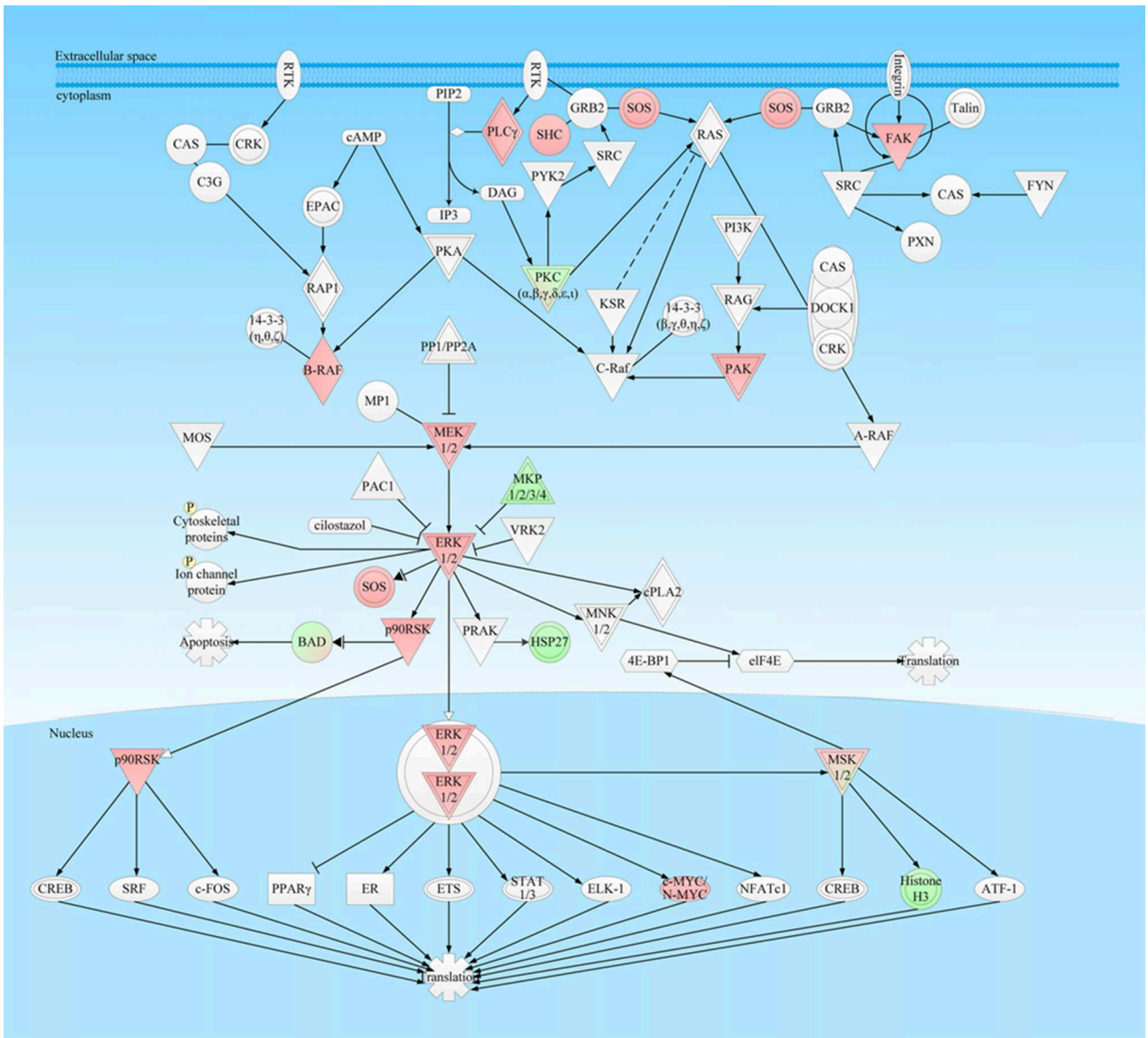

FIGURE 6 | ERK-MAPK signaling pathway was involved in NFPA. This pathway was derived from the IPA analysis results of multi-omics, and then it was modified and verified according to the PTMScan results of NFPAs compared to controls. The red color means upregulation of a molecule in NFPAs, and the green color means downregulation of a molecule in NFPAs. The gradient color degree means slightly different expression tendency of that molecule.

and comprehensive understanding of molecular mechanisms and discovery of reliable pathway-network-based biomarkers for pituitary adenomas. This study collected nine sets of omics data from different research groups in the world, including DEG and DEP data in NFPAs compared to controls, DEG and DEP data in invasive NFPAs compared to non-invasive NFPAs, nitroproteins in NFPAs, mapping proteins in NFPAs, and mapping proteins/nitroproteins/phosphoproteins in control pituitaries. Each omics data was performed by pathway-network analysis and related bioinformatics analysis, and hub-molecules were identified from pathway-networks. Those pathway networks derived from mapping proteins in NFPAs and mapping proteins/nitroproteins/phosphoproteins in controls were the base line data, which provided the reference for determination of reliable NFPA-related pathway-networks. Those pathway networks derived from DEGs and DEPs in NFPAs and invasive NFPAs, and nitroproteins in NFPAs, were directly associated with NFPAs pathophysiological changes. Thus, a total of 62 molecular networks and 861 hub-molecules were identified. According to the primary functions of 861 hub-molecules, 42 hub-molecule panels that were grouped into 16 functional categories were identified (**Supplemental Figure 2**); and 57 high-frequency hub-molecules were identified. Moreover, among 519 statistically significant

canonical pathways derived from nine sets of omics data, 54 significantly cancer-related canonical pathways were identified to involve differentially expressed hub-molecules (DEGs, or DEPs), and were further grouped into 9 canonical-pathway panels (**Table 2**). Many of these altered canonical pathways interact with each other through hub-molecules to form pathway networks. Comprehensive analysis of all these networks, hub-molecule panels, cancer-related canonical pathways, and canonical pathway panels, the PTMScan experiment (multiple antibodies-based enrichment and LC-MS/MS) that contained 1006 phosphorylated sites with 409 proteins within 19 important signaling pathways were carried out in NFPAs compared to control pituitaries, which confirmed the important pathway-networks and the corresponding hub-molecules in NFPAs and further investigate the functional roles of those pathway network and hub-molecules, including PI3K/Akt signaling, mTOR signaling, Wnt pathway, NFκB signaling, apoptosis-regulated pathways, ERK/MAPK signaling, p38 MAPK, and JNK pathways, and the corresponding hub-molecule changes (**Table 3**). Furthermore, differentially expressed hub-molecules and differentially phosphorylated hub-molecules in mTOR pathway and Wnt pathway were confirmed and validated with immunoaffinity Western blot in NFPAs compared to control pituitaries (**Figures 4B**, **5B**). One might note that those important pathway-systems and hub-molecules were not directly further confirmed and validated in invasive NFPAs compared to non-invasive NFPAs to identify NFPA invasiveness-related pathways and hub-molecules, because there were not enough clinical information in our laboratory to distinguish those NFPA samples used for PTMScan experiment into invasive and non-invasive groups. However, NFPA samples used for PTMScan experiment included invasive and non-invasive NFPA tissues. Those solid data including 42 hub-molecule panels, 57 high-frequency hub-molecules, 9 canonical-pathway panels, and PTMScan and Western blot-valued pathway-systems and hub-molecules in NFPAs provided overall and large-scale pathway-network alteration profiles for NFPAs, which benefited for discovery of novel drug targets and tumor molecular biomarkers, and development of more specific and comprehensive diagnosis and target treatment strategies for NFPAs.

Based on multi-omics data, PTMScan experimental data, and immunoaffinity Western blot data of key hub-molecules within important signaling pathway systems, PI3K/Akt signaling pathways (mTOR signaling, Wnt pathway, NFκB signaling, and apoptosis-regulated pathways), and MAPK signaling pathways (ERK/MAPK signaling, and p38 and JNK pathways), were significantly associated with NFPA pathogenesis, and were further discussed in details below.

PI3K/Akt Signaling Pathways Were Activated in NFPAs

The PI3K/Akt cascade is an essential downstream effector of many protein-kinase signaling pathways, including receptor tyrosine kinases (RTKs) and G protein-coupled receptors (GPCRs), and its excessive activation often leads to genomic instability, tumor formation, progression, angiogenesis, and multidrug resistance (25). This study found that many abnormal protein expressions in the PI3K/Akt canonical pathway and mTOR pathway, including upregulated SHIP, GAB1/2, SHC, SOS, AKT, IKK, NFkB, MEK1/2, ERK1/2, mTOR, 4E-BP1, GSK3, and β-catenin, and downregulated PI3K p85, HSP90, and BAD, in PI3K/Akt pathway (**Figure 3**); upregualted ERK1/2, AKT, RSK, mTOR, PRAS40, RICTOR, 4EBP, RPS6, and 40S ribosome, and downregulated PKC, PKCa, and p-4EBP in mTOR pathway (**Figure 4**). These data indicated multi-level dysfunctions in PI3K/Akt signaling pathway in NFPA. Moreover, mTOR signaling abnormality was found with abnormally expressed proteins RSK, mTORC1 that regulated ATG13 and 40S ribosomes, and RICTOR in mTORC2 (**Figure 4A**). These findings demonstrated that mTOR pathway as the downstream signaling of PI3K/Akt was also dysregulated. Furthermore, the abnormally expressed 14-3-3 and HSP90 in PI3K/Akt signaling pathway played an important role in the aberrantly activated PI3K/Akt signaling.

Akt is also known as PKB, a serine/threonine kinase, and belongs to protein kinase A/G/C family. Akt modulates many important cellular processes. Aberrant activation of Akt often leads to multiple diseases including cancers (26). Three Akt isoforms (Akt1, Akt2, and Akt3) exist in mammals, and phosphorylation at two residues Thr308 and Ser473 in Akt1, Thr309 and Ser474 in Akt2, and Thr304 and Ser472 in Akt3 are needed for their full activation. The residues Thr308 in Akt1, Thr309 in Akt2, and Thr304 in Akt3 were located in the activation loop, and were phosphorylated by PDK1. Whereas, the residues Ser473 in Akt1, Ser474 in Akt2, and Ser472 in Akt3 were located in C-terminal regulatory domain, and were regulated by mTORC2, which were critical to stabilize their active conformation (27). This study found that Akt1, Akt2, and Akt3 were upregulated in NFPAs relative to controls, and phosphorylation levels at residues Thr308 in Akt1, Thr309 in Akt2, and Thr305 and Ser472 in Akt3 were upregulated in NFPAs relative to controls, which demonstrated Akt was overexpressed and fully activated in NFPAs. Furthermore, Akt can regulate the functions of more than 100 substrates in a cell, which suggests a possibility for PI3K/Akt to build crosstalk with other pathways, including ERK, JNK, p38, NFκB, and Wnt signaling (26). This study demonstrated that the activated PI3K/Akt signaling was substantially involved in stimulation of multiple cascades in NFPAs through the following pathways (**Figure 3**): (i) The activated Akt phosphorylated TSC2 and residue Thr246 in PRAS40 to inactivate these proteins and subsequently stimulated mTORC1 signaling; (ii) The functional loss of Akt consequentially activated canonical Wnt pathway by phosphorylation at residue Ser21 in GSK3α, and Ser9 in GSK3β; (iii) Akt activated NF-κB signaling through phosphorylating the upstream IκB kinase α; (iv) Akt blocked pro-apoptotic activity of BAD through phosphorylation and promoted cell survival; (v) PI3K/Akt signaling could interact with ERK, JNK, and p38 signaling from multiple levels; and (vi) Akt lead to degradation of the transcription factors NFAT and inhibited migration and invasion of a cancer.

The mTOR Signaling Pathway Was Activated in NFPAs

The mTOR was a conserved serine/threonine kinase, and belongs to the PI3K superfamily, which can integrate multiple signals such as pressure, oxygen content, nutrient availability, and mitogenic signals to regulate growth and homeostasis. The mTOR functioned in two functionally distinct complexes, including mTORC1 (mTORC1), and mTOR complex 2 (mTORC2) (**Figure 4A**). The core components mainly included mTOR, Raptor, PRAS40, and mLST8 in mTORC1, and mTOR, RICTOR, mSIN1, and mLST8 in mTORC2 (24). When stimulated by stress, oxygen, nutrition, energy and growth factors, mTORC1 regulated protein translation, autophagy and metabolism including adipogenesis, ketone formation and glucose homeostasis. The mTORC2 that can be activated by extracellular growth factors phosphorylated downstream kinases such as Akt, PKC and SGK to enhance signal cascade and regulate biological effects including cell survival, cytoskeleton, and metabolism (28). The activated mTORC1 phosphorylated S6K and eIF-4E binding proteins (4E-BPs), and mTORC2 was necessary for the maximal activation of Akt through phosphorylation of its residue Ser473 (29). Upon stimulation, mTOR was commonly phosphorylated at its residues Thr2446, Ser2448, and Ser2481, and the region of its residues 2430–2450 was important for function regulation of mTOR (29). The residue Ser2448 in mTOR was phosphorylated by S6K, and this phosphorylation increased associations of mTOR with Raptor in mTORC1 and Rictor in mTORC2. The phosphorylation status of mTOR Ser2448 was correlated with mTORC1 activity (30). In this study, PTMScan results demonstrated that phosphorylation levels at residues Thr2446 or Ser2448 in mTOR were significantly increased, which demonstrated that mTOR was activated in NFPAs, and contributed to the initiation and development of NFPAs. As a substrate, AKT-phosphorylated PRAS40 negatively regulated mTORC1 Rheb-GTP-dependent activation in normal state. When residue Thr246 in PRAS40 was phosphorylated by Akt, PRAS40 could not inhibit the activity of mTORC1 (24), thus activated mTORC1 phosphorylated downstream eIF4E-binding proteins (4E-BPs) and ribosomal S6 kinase (p70RSK) to enhance protein synthesis and regulate energy metabolism (31). Moreover, this study found that phosphorylation of residue Thr246 in PRAS40 was significantly increased in NFPAs with Western blot and PTMScan experiment, while the overall expression of PRAS40 was significantly decreased in NFPAs. These results demonstrated that the suppressions of PRAS40 on mTORC1 were dramatically relieved in NFPAs.

There are three kinds of 4E-BPs, including 4E-BP1, 4E-BP2, and 4E-BP3 in mammals. In quiescent state, 4E-BPs tightly interact eIF4E to prevent the initiation of translation (24, 32). Phosphorylation at residues Thr37 and Thr46 in 4E-BP2 by mTOR significantly decreased the affinity capability between 4E-BP2 and eIF4E by100 folds (33). 4E-BP3 had similar functional characteristics with 4E-BP1 and 4E-BP2 (34). In this study, PTMScan experiment found that many peptides derived from 4E-BPs were significantly increased in NFPAs, and phosphorylations at residues Thr37 and Thr46 in both 4E-BP1 and 4E-BP2, and Thr23 in 4E-BP3 were increased in NFPAs. The increased phosphorylation in 4E-BPs benefited for disassociation of 4E-BPs from eIF4E to promote the initiation of protein translation in NFPAs. Moreover, the highly conserved phosphorylation at residues Ser235, Ser236, Ser240, Ser244, and Ser247 in 40S ribosomal protein S6 played an important role in protein translation initiation. These phosphorylations especially at residues Ser235 and Ser236 in 40S ribosomal protein S6 could effectively facilitate the assembly of translational pre-initiation complex (35). In this study, PTMScan experiments found that phosphorylations at residues Ser235, Ser236, Ser240, Thr241 and Ser244 in 40S ribosomal protein S6 were obviously increased in NFPAs. In addition, Rictor was a scaffolding protein to regulate the localization, assembly, and substrate binding in mTORC2, and its overexpression was highly related to metastatic process (36). PTMScan experiment found the upregulated Rictor in NFPAs and increased phosphorylations at residues Ser472 in Akt3, which suggested that activation of mTORC2 contributed to the tumor progression in NFPAs.

Those findings clearly demonstrated that mTOR signaling, including mTORC1 and mTORC2 complexes, was involved in NFPA pathogenesis, including cell survival, protein synthesis, and metabolism.

Wnt Pathways Were Involved in NFPAs

Wnt pathways are pivotal to modulate many cellular and physiological processes such as cell polarity, motility, adhesion, proliferation, survival, stem cells self-renewal, and tissue homeostasis, and include canonical and non-canonical Wnt pathways according to different ligands and downstream effectors (37) (**Figure 5A**).

Canonical Wnt Pathway Was Activated in NFPAs

Canonical Wnt pathway mainly regulated the stability of β-catenin to modulate transcriptions of Wnt-targeted genes, and control cell fate, growth and differentiation (38). (i) β-catenin was the key effector in canonical Wnt pathway. There was a destruction complex containing two kinases [glycogen synthase kinase 3 (GSK3) and casein kinase I (CKI)], and two scaffold proteins [adenomatous polyposis coli (APC) and Axin 1/2] that controlled the stability of cytoplasmic β-catenin through phosphorylation and ubiquitylation on specific sites and then degraded it through proteasome. Without Wnt ligand stimulation, the destruction complex could keep cytoplasmic β-catenin in a low level (37). When canonical Wnt pathway was activated by Wnt ligand, the destruction complex was inhibited by the activated disheveled-protein (DVL or DSH), which lead to the cellular accumulation and nuclear import of β-catenin (39). In the nucleus, β-catenin acted as a co-activator for T-cell factor/lymphoid enhancer factor (TCF/LEF), and then recruited various transcriptional cofactors including B-cell CLL/lymphoma 9 protein (Bcl9), Pygopus (PYGO), CREB-binding protein (CBP), and histone acetyltransferase p300 (p300) to activate transcription of target genes such as FGF20, JUN, MYC, and CCND1. In order to degrade β-catenin, β-catenin should be initially phosphorylated at its residue Ser45 by CK1, and subsequently be phosphorylated at its residues Ser33, Ser37, and Thr41 by GSK3. The E3-ubiquitin ligase β-TrCP could

bind to a short region containing phosphorylated residues Ser33 and Ser37 in β-catenin to result in its followed ubiquitylation and degradation (40); and phosphorylation at N-terminal in β-catenin regulated its degradation, while phosphorylation at C-terminal in β-catenin regulated its function. Phosphorylation at residues Ser552 and Ser675 in β-catenin, which was regulated by PI3K/Akt, Camp/PKA and/or GPCR/PKD, caused β-catenin to be accumulated in nucleus for stimulating its transcriptional activity to increase expressions of cyclin D1 and c-Myc (41, 42), and enhanced the ability of β-catenin to recruit many transcriptional coactivators such as CBP or TBP (TATA binding protein) to bind to its C-terminal tail (43). In this study, PTMScan experiment found that all detected peptides derived from β-catenin were dramatically elevated about 2.5 to 65.3-fold. No phosphorylation was found at residues Ser33, Ser37, Th41, and Ser45 in β-Catenin, which indicated that N-terminal of β-catenin was barely phosphorylated, thus degradation complex might be inhibited. However, PTMScan found that phosphorylations at residues S552 and S675 in β-catenin C-terminal were significantly increased, which might improve stability and transcriptional functions of β-catenin. These results were also confirmed by Western blot in its overall expression level of β-catenin (**Figure 5**). (ii) GSK3 was a highly conserved and multifunctional serine/threonine kinase to participate in various cellular processes (44), which was inactivated through phosphorylating residues Ser21 in GSK-3α and Ser9 in GSK-3β. In this study, Western blot found slightly decreased expression levels of GSK3α and GSK3β, and increased phosphorylation levels at residues Ser21 in GSK3α and Ser9 in GSK3β in NFPAs compared to controls; and PTMScan experiment also found increased phosphorylation at residue Ser21 in GSK3α. These findings clearly demonstrated that GSK3α was inhibited in NFPAs, which might cause differential expressions of many target genes that regulate apoptosis, proliferation, differentiation, and motility. (iii) Bcl9 was an important downstream transcriptional co-activator, which can augment and diversify the transcriptional output of canonical Wnt pathway. Bcl9 could also modulate interactions of β-catenin to improve EMT and invasion, and was associated with poor outcome in cancer (45). In this study, PTMScan experiment found the increased level of Bcl9 in NFPAs, and upregulations of many target genes such as c-Myc and c-Jun in canonical Wnt pathway. Moreover, some studies clearly demonstrated that β-catenin was accumulated in the nucleus of NFPAs (22), several Wnt target genes such as Cyclin D1 and c-MY were upregulated in NFPAs (21, 22), and the inhibitor of Wnt pathway including Wnt inhibitory factor 1 (WIF1) and secreted frizzled related protein (sFRP) were significantly decreased in NFPAs (22, 46). All these data revealed that canonical Wnt pathway was activated in NFPAs to participate in cell apoptosis, proliferation, differentiation, and motility.

Non-canonical Wnt Pathway Might Be Involved in Regulation of NFPAs

Non-canonical Wnt pathways were independent of β-Catenin, and involved many downstream signal transduction effectors, including multiple small GTPases (RAC, RHOA, and CDC42), G proteins, calmodulin/calcium, PKC, Src, and JNK (37). Among them, Wnt/planar cell polarity (Wnt/PCP) pathway and Wnt/Ca^{2+} pathway had been characterized (47) (**Figure 5A**). Wnt/PCP pathway mainly engaged GTPases to activate downstream targets such as JNK or rho-related kinase ROCK, which played important roles in reconfiguration of cytoskeleton, cell movement, polarity, and patterning in tissue (37, 38). When activated by a Wnt ligand, Wnt/Ca^{2+} pathway exerted its function by activating G proteins, phospholipase C (PLC) and phosphodiesterase (PDE), then invoked calcium-sensitive enzymes such as calcium–calmodulin-dependent kinase II (CaMK II) and PKC, which subsequently activated the corresponding transcription factor NFAT and CDC42 to cause a wide range of cellular effects, including cell adhesion, migration, inflammation, and tumorigenesis (47). In addition, non-canonical Wnt pathways could regulate canonical Wnt pathway through GTPases, PKC or other mechanisms. PKC especially PKCa could negatively regulate Wnt/β-catenin pathway through directly phosphorylating residues Ser33, Ser37, and Ser45 in β-catenin (48). This study found that JNK, Jun, ATF2, NFAT, PLC, PKC, CDC42, and NFκB were differentially expressed in non-canonical Wnt pathway in NFPAs compared to controls, which demonstrated non-canonical Wnt pathways were closely related to NFPAs. Moreover, this study also found that Rho/Rac-related proteins such as ARHGAP18 and ARHGEF17 were upregulated in NFPAs, and that canonical pathways were involved in cytoskeleton rearrangement and cell mobility, including Gaq signaling, RhoGDI signaling, Rho family GTPase signaling, and RhoA signaling, and in calcium modulation-related signaling, including calcium signaling, and calcium-induced T lymphocyte apoptosis. Those findings indicated that PCP signaling and calcium-related signaling might be involved in NFPA tumorgenesis. Also, Ephs and Ephrins signaling regulated activation of Rho GTPases such as RAC, RHO, CDC42, and JNK through PCP signaling (37). Ephrin B and Ephrin receptor signaling were identified as canonical pathway in this study, with upregulations of Ephrin B and Ephrin receptor in NFPAs, which means Ephrin B and Ephrin receptor signaling were activated in NFPAs. In this study, PTMscan experiment found most (80%) peptides derived from cPKCs were decreased in NFPAs. Only one peptide derived from PKCα was increased and its phosphorylation at residue Ser651 in PKCα was not involved in its own activation. All peptides derived from PKCδ are decreased in NFPAs, which means the decreased function of PKC to attenuate inhibition of β-catenin and improve apoptosis-resistance in NFPAs. Therefore, dysregulated non-canonical Wnt pathway might reduce inhibition of canonical Wnt pathway, and be involved in NFPA pathogenesis.

NFκB Signaling Was Provoked in NFPAs

Nuclear factor kappa B (NFκB) family members were critical transcription factors, and were involved in numerous cellular processes including cancer (49). After cellular stimulation, phosphorylation of IkBs by IκB kinase (IKK) complex resulted in ubiquitination and subsequent degradation to cause activation of NFκB signaling. The IKK complex was composed of two catalytic IκB kinases (IKKα and IKKβ) and one scaffold/adaptor protein

IKKγ (49). Phosphorylation at residue Ser376 in IKKγ was required for signal dependent activation of IKKβ and regulated NFκB signaling. In this study, PTMScan experiment found the increased phosphorylation at residue Ser376 in IKKγ and the upregulated NFκB in NFPAs compared to controls, which indicated the activation of NFκB signaling in NFPAs. Moreover, NFκB signaling and Wnt pathway had crosstalk in multiple levels and modulated the activities and functions of other signaling pathways (50), such as the activation of NFκB signaling could infect Wnt pathway in NFPAs.

Apoptosis-Regulated Pathway Was Involved in NFPAs

BAD was a proapoptotic member in Bcl-2 family, and was phosphorylated by many upstream kinases to control apoptosis. BAD could inhibit Ras/MEK/ERK and JNK signaling, and EMT. Studies found that downregulated p-BAD and BAD in cancer cells promoted tumor invasion and migration (26, 51). The dysregulated expressions and phosphorylation of BAD might lead to imbalance of programmed cell death and immortalized cancer cells. In this study, PTMScan experiment found most of peptides derived from BAD were dramatically decreased to cause significantly reduced binding among BAD, Bcl-2, and Bcl-xL, and promote cell survival and invasion in NFPAs. Thus, PI3K/Akt signaling and its related pathways including *mTOR,* Wnt, and NFκB signalings were dysregulated in NFPAs, and multiple molecules in these signaling pathways were further abnormally modulated in invasive relative to non-invasive NFPAs.

MAPK Pathways Were Dysregulated in NFPAs

MAPKs can regulate many biological processes, including proliferation, apoptosis, stress responses, and immune defense, and include four independent MAPK cascades: Extracellular signal-regulated kinase1/2 (ERK1/2) pathway (canonical ERK/MAPK pathway), c-Jun N-terminal kinase (JNK) pathway, p38 pathway, and ERK5 pathway (52) (**Figure 6**). In this study, mRNA expressions of PI3K, Talin, and cPLA2 in NFPA DEG data were significantly upregulated in ERK/MAPK signaling (PI3K: 2.26-fold; Talin: 2.9-fold; and cPLA2: 2.44-fold), while MKP1/2/3/4 was significantly downregulated (MKP2: −2.52 fold). For NFPA DEP data, FYN was significantly upregulated (3.9-fold), and 14-3-3 (β, γ, θ, η, ζ) and HSP27 were downregulated (14-3-3: −1,000-fold; HSP27: −4.7-fold). For invasive NFPA DEG data, PI3K, PKA, PP1/PP2A, 14-3-3 (β, γ, θ, η, ζ), MSK1/2 and ER were expressed abnormally [PI3K: −1.85-fold; PKA: −1.56-fold; PP1/PP2A (PPM1A −1.85-fold; PPM1K 1.66-fold; PPP1R11 1.59-fold); 14-3-3 (2.06-fold); MSK1 (−1.92-fold); and ER (ERα 2.12-fold; ERβ −3.7-fold)]. The abnormal expressions of key molecules in ERK/MAPK signaling pathway in NFPAs clearly demonstrated that ERK/MAPK signaling were dysregulated in NFPAs, and could intensely promote occurrence and development of an NFPA.

ERK/MAPK Signaling Was Stimulated at Multiple Levels in NFPAs

Extracellular signals were transducted to intracellular targets through phosphorylation cascade reactions in Ras-Raf-Mek-ERK1/2 activation pattern. The ectopic activation of this signaling could result in tumorigenesis, progression, and metastasis; and Ras-Raf-Mek-ERK1/2 signaling can interact with Ras-PI3K-Akt signaling to amplify signal regulation range and mutually modulate tumorigenesis (53). (i) In mammalian cells, Raf family includes A-Raf, B-Raf, and C-Raf (Raf-1). The constitutive phosphorylation at residues Ser446 and/or Ser447 and the presence of two aspartates acids at residues 448/449 in B-Raf promoted its activation, and activated ERK/MAPK pathway. In this study, PTMScan experiment found that phosphorylations at residues Ser446 or Ser447 in B-Raf were dramatically increased over 1,000-fold in NFPAs, which clearly demonstrated that B-Raf was utmostly invoked in NFPAs to constantly abnormally activate ERK/MAPK pathway. Thus, B-Raf might act as one of potential biomarkers or therapy targets for NFPA patients. (ii) Phosphorylations at residue Ser218 and Ser222 in human MEK1 were needed for its full activation. MEKs modulated the activation of ERKs through phosphorylations at residues Thr202 & Tyr204 and Thr185 & Tyr187 in human ERK1 and ERK2 in their activation loop Thr-Glu-Tyr motif (54). In this study, PTMScan experiment found phosphorylations at residues Ser218 or Ser222 in MEK1 were significantly increased over 300-fold in NFPAs, and phosphorylations at residues Thr202 in ERK1 and Tyr187 in ERK2 were also significantly increased in NFPAs. These data revealed that the phosphorylation cascade in ERK/MAPK pathway was full stimulated in NFPAs. (iii) As bispecific protein phosphatases, MKP proteins can inactivate the phosphorylated MAPK through dephosphorylation at residues Ser and Tyr of TXY motif. Among them, MKP1 and MKP2 can dephosphorylate ERK, JNK, and p38, which negatively regulated MAPK cascades (55). Phosphorylation at residues Ser359 and Ser364 in MKP1 by ERK1 and ERK2 enhanced MKP1 stability and protected it from proteasome-mediated degradation (56). Therefore, downregulated expressions of MKP1 and MKP2 might attenuate their inhibitory effect to promote tumorigenesis. Moreover, MKP1 with pSer359 was reduced, and MKP2 was decreased in NFPA DEG data, these findings demonstrated that the inhibition of MKPs to ERK1/2, JNK and p38 are decreased to further augment the MAPK signaling in NFPAs. (iv) PPM1A was a member of the protein phosphatase 2C family and an important tumor suppressor, which was involved in regulation of multiple pathways, such as TGFβ/Smad, JNK/p38, Cdk2, Cdk6, and Akt/ERK signaling (57). Its low expression can enhance NF-κB-dependent tumor invasion, tumor poor differentiation and prognosis. The invasive NFPA DEG data demonstrated that the downregulation of PPM1A might contribute to tumor invasion of NFPAs. Moreover, PPM1K was a highly conserved serine/threonine protein phosphatise, and mainly targeted mitochondrial matrix to regulate mitochondrial permeability transition pore (MPTP), which played important roles in cell survival, and nervous system development (58). The invasive NFPA DEG data found that PPM1K was increased in NFPAs. (v) Human p90 ribosomal S6 kinases (RSKs) are a family

of Ser/Thr kinases that comprises of four isoforms (RSK1–4) and two structurally related homologs of RLPK (MSK1) and RSKB (MSK2) (59). RSKs are directly phosphorylated by ERK1/2 and PDK1, and RSKs are potently activated by ERK1/2 and p38 pathways to regulate various biological processes through phosphorylating numerous transcription factors, such as CREB, CBP, p300, SRF, c-Fos, ETV1, estrogen receptor-α (ERα), NF-κB, and NFATc4. Moreover, RSKs inhibit the tumor-suppressor TSC2 through phosphorylation at its residue Ser1798. MSKs predominantly resided in the nucleus and were required for phosphorylating histone H3, CREB, ATF1, and HMG-14. Phosphorylations at residues Ser221 in RSK1-3 and Ser376 in MSK1 were required for its catalytic activity (60). In this study, PTMScan experiment found phosphorylations at residues Tyr220, Ser221 and Thr225 in RSK1, Tyr226, Ser227, and Thr231 in RSK2, and Tyr231, Ser232, and Thr236 in RSK4 were significantly increased in NFPAs. Moreover, phosphorylations at resides Ser376 in MSK1 and Ser360 in MSK2 were also increased in NFPAs. Those data clearly demonstrated most of RSK family members were overexpressed and activated in NFPAs. (vi) Focal adhesion kinase (FAK) was a cytoplasmic non-receptor tyrosine kinase (61). When FAK was stimulated by integrin, FAK was autophosphorylated at its residue Tyr397 to result in subsequent phosphorylations at residues Tyr576 and Tyr577, and Tyr861 and Tyr925 in the C-terminal domain of FAK by Src. The activations of FAK and Src can exert their catalytic activities through promoting gene expressions of VEGF and MMPs (61). In this study, PTMScan experiment found that phosphorylations at residues Thr575, Tyr576, and Tyr577 in FAK are significantly increased in NFPAs (**Table 3**), which clearly demonstrated that FAK was strongly activated in NFPAs to further stimulate multiple cascades including Akt, MAPKs, p53, VEGF, and IGF-1 pathways in NFPAs. (vii) Many proteins associated with modulation of MAPK signaling were also downregulated in NFPAs, including SHC, SOS, PLC, PAK, HSP27, c-Myc, NFATc, histone H3, and Jun. In this study, PTMScan experiment found that peptides derived from SHC, SOS, PLC, PAK, c-Myc, Jun, ATF2, ATF7, GRB2-associated-binding protein 2 (GAB2), and Myc target protein 1 (MYCT1) were significantly increased in NFPAs, whereas derived from HSP27, NFATc, and Histone H3 were downregulated in NFPAs. Therefore, those findings clearly demonstrated that ERK/MAPk signaling pathway was changed in multiple levels in NFPAs.

The p38 and JNK Pathways Were Involved in NFPAs

p38 signaling primarily participated in responses to environmental stress, and also answers to immune response and inflammation. p38 MAPKs included four homologous members p38α, p38β, p38γ, and p38δ. p38α and p38β were ubiquitously expressed in human body, whereas p38γ and p38δ were restricted expressed in muscle, and lung and kidney, respectively (62). Upon stimulation, p38 MAPKs controlled cell fate by regulating activities of heat shock proteins and transcription factors (ATF2, CHOP, ELK1, and MEF2C). In addition, p38 signaling was also involved in modulation of eIFs function and protein synthesis (62). p38a was activated through dual phosphorylations at its residues Thr180 and Tyr182 in the activation loop Thr-Gly-Tyr motif (54). Another important stress-activated MAPK cascade was JNK signaling that has been involved in cell fate decisions responding to various stress stimulations. JNK regulated and activated the functions of its targets including transcription factors (Elk1, c-Myc, c-Jun, JunB, ATF2, and p53), and factors related to cell death such as the members of Bcl-2 family to modulate many cellular processes (54). JNK family included JNK1, JNK2, and JNK3. JNK1 and JNK2 were ubiquitously expressed in human body, and JNK3 was mainly expressed in the brain (63). JNKs were activated by phosphorylations at residues Thr183 and Tyr185 in JNK1 and JNK2, and Thr221 and Tyr223 in JNK3. Moreover, JNK and p38 cascades shared synergistically many components and functions. JNK and p38 contributed to AP-1 activities through phosphorylations at residues Thr69 and Thr71 in ATF2, and these two phosphorylations in ATF2 enhanced its histone acetyltransferase (HAT) activity (64). JNK and p38 played pivotal roles in coordination of immune and inflammatory responses through various cytokines including interleukin-1 (IL-1), IL-10, IL-12, and tumor necrosis factor α (TNFα). Cytokines, especially TNFα, contributed to the generation of reactive oxygen species/reactive nitrogen species (ROS/RNS) (65) to activate JNK and p38 signaling, thus continuously activated JNK and p38 signaling facilitated abnormal synthesis of ROS and chronic inflammation (63). In this study, PTMScan experiment found that phosphorylations at residues Thr180 & Tyr182 and/or Tyr182 & Thr185 in p38a, Thr183 & Tyr185 in JNK1, Thr221 & Tyr223 in JNK3, Thr183 & Tyr185 and/or Thr175 & Tyr185 in JNK2, and Thr69 & Thr71 in ATF2 were significantly increased in NFPAs. Those results strongly supported that activations of JNK and p38 signaling were involved in development of NFPAs, and were most likely responsible for the high oxidative stress state, immune and inflammatory disorders in NFPAs.

This present study used the systems biology opinion to find out the key pathological mechanisms commonly existing in NFPA through Meta analysis. The IPA system was used to further analyze different omics data of NFPA and extract important data such as molecular networks, canonical signaling pathways, and high-frequency hub molecules closely related to the occurrence and development of NFPAs, providing effective data to promote individualized precise treatment. Many studies have shown that targeting some high-frequency hub-molecules in Table 1 has achieved good results in other types of pituitary adenomas. For example, TGFβ1 is used as a novel therapeutic target to treat resistant prolactinomas (66); the microRNA-145 inhibits the activation of the mTOR signaling by targeting AKT3 to suppress the proliferation and invasion of invasive pituitary adenoma cells (67); lncRNA H19 inhibits mTORC1 by disrupting 4E-BP1/Raptor interaction in pituitary tumors (68); and MAPK Pathways act as therapeutic targets in pituitary tumors (69). Because PI3K/Akt/mTOR and ERK/MAPK signaling pathways are significantly dysregulated in NFPA, and these two essential signaling pathways are not only related to rapid proliferation and apoptosis resistance of tumor cells, but also can regulate the activities of many other pathways and then regulate tumor growth in the multiple levels. Therefore, these two pathways can act as the most convenient and effective therapeutic target in

pituitary adenomas. Moreover, since NFPA is a multifactorial and multifaceted disease, it is reasonable to infer that the combination therapy targeting multiple pathways and hub-molecules based on the patient's tumor molecular subtype can achieve better therapeutic results. Researchers have shown that the combination treatment targeting AMPK and PI3K/Akt/mTOR pathway at the same time in GH-secreting pituitary tumors achieved a better treatment effect than the single medication alone (70). This study found that AMPK was a high-frequency hub-molecule in NFPA, and PI3K/Akt/mTOR signaling pathway was highly maladjusted in NFPA. Thus, has laterally proved that this kind of drug combination also achieved a good therapeutic effect in NFPA. In future studies, multiple combinations of drugs targeting different high-frequency hub-molecules and important signaling pathways would provide new hope for improving the therapeutic effects of NFPAs.

CONCLUSIONS

Pituitary adenoma is a common pituitary disease, with a series of molecule alterations in DNAs (genome), RNAs (transcriptome), proteins (proteome), metabolites (metabolome), and imaging characteristics (radiome) that resulted from exogenous and endogenous carcinogens, and those molecules associate mutually and function in a molecular network system. Molecular network-based molecule pattern has important scientific merits in clarification of molecular mechanisms and discovery of effective biomarkers and therapeutic targets for pituitary adenomas. This study used the Meta-analysis strategy and integratively analyzed all documented NFPA omics data (a total of nine sets of omics data) with IPA pathway network program. A total of 62 molecular-networks and 519 canonical-pathways were revealed with statistical significance from nine sets of NFPA omics data. A total of 861 hub-molecules were derived from those molecular-networks and were classified into 42 hub-molecule panels to associate with pituitary tumorigenesis. A total of 139 canonical-pathways were found from at least two sets of omics data, which generated 68 cancer-related canonical-pathways to obviously associate with the occurrence and development of tumor, and of them 54 canonical pathways involved in any DEGs or DEPs were divided into 9 canonical-pathway panels according to the similar cellular functions and biological processes. Those molecular networks, hub molecules, hub-molecule panels, canonical pathways, and canonical-pathway panels formed the overall pathway-network characterization of NFPAs. The important pathway-networks and hub-molecules were further validated and in-depth studied with PTMScan experiments and immunoaffinity Western blot analysis to quantify the alterations in the protein expressions and specific phosphorylation status. Comprehensive analysis of all data including multi-omics data, PTMScan experimental data, and immunoaffinity Western blot data revealed several important signaling pathway systems that operate in NFPA biological system, including PI3K/Akt signaling pathways (mTOR signaling, Wnt pathway, NFκB signaling, and apoptosis-regulated pathways), and MAPK signaling pathways (ERK/MAPK signaling, and p38 and JNK pathways). These findings are the solid scientific evidence and molecular targets to discover molecular-network-based biomarkers and effective therapeutic targets for the accurate diagnosis and treatment of the different types and different development stages of NFPAs. Here we specially emphasize that, NFPAs are very complex diseases, involving a series of molecule changes and pathway-network changes. One should change our thinking and working models from mono-targeting pharmacological treatment concept to the multi-targeting pharmacological treatment concept, from mono-molecule biomarker to multi-molecule-panel biomarker for insights into its molecular mechanism, patient stratification, diagnosis, and prognostic assessment. This present multi-omics data exactly offer the scientific data for multi-targeting pharmacological treatment concept and multi-molecule-panel biomarker for pituitary adenomas including NFPAs.

DATA AVAILABILITY STATEMENT

All datasets generated for this study are included in the article/**Supplementary Material**.

ETHICS STATEMENT

Pituitary adenoma tissue samples were obtained from Department of Neurosurgery, Xiangya Hospital, Central South University, and were approved by Xiangya Hospital Medical Ethics Committee of Central South University. Control pituitary glands were post-mortem tissues obtained from the Memphis Regional Medical Center, and were approved by University of Tennessee Health Science Center Internal Review Board (UTHSC-IRB). The written informed consent was obtained from each patient or the family of control pituitary subject, after full explanation of the purpose and nature of all used procedures.

AUTHOR CONTRIBUTIONS

YL analyzed the documented omics data, IPA-mined result data and PTMScan experimental result data, performed Western blot experiments, and wrote partial manuscript draft. ML and TC participated in Western blot experiments. XiaoZ participated in the critical revision. XianZ conceived the concept, designed the entire project, collected the documented omics data, performed IPA analysis, designed and coordinated the entire experiments, designed and wrote manuscript, critically revised the manuscript, trained YL regarding omics, systems biology, molecular networks, and pathway analysis, and was responsible for its financial supports and the corresponding works. All authors approved the final manuscript.

FUNDING

The authors acknowledge the financial supports from China 863 Plan Project (Grant No. 2014AA020610-1 to XianZ), the National Natural Science Foundation of China (Grant No. 81272798 and 81572278 to XianZ), the Xiangya Hospital Funds for Talent Introduction (to XianZ), the Hunan Provincial Hundred Talent program (to XianZ), the Hunan Provincial Natural Science Foundation of China (Grant No. 14JJ7008 to XianZ),

and Ingenuity for the Ingenuity Pathway Analysis free-trial program, and the constructed canonical pathways. The scientific contributions of Dominic M. Desiderio, Nelson M. Oyesiku, and Chanson P are acknowledged. The authors also acknowledge the USA CST company performed the PTMScan experiments.

SUPPLEMENTARY MATERIAL

The Supplementary Material for this article can be found online at: https://www.frontiersin.org/articles/10.3389/fendo.2019.00835/full#supplementary-material

REFERENCES

1. Zhan X, Wang X, Cheng T. Human pituitary adenoma proteomics: new progresses and perspectives. *Front Endocrinol.* (2016) 7:54. doi: 10.3389/fendo.2016.00054
2. Zhan X, Wang X, Long Y, Desiderio DM. Heterogeneity analysis of the proteomes in clinically nonfunctional pituitary adenomas. *BMC Med Genomics.* (2014) 7:69. doi: 10.1186/s12920-014-0069-6
3. Melmed S. Pathogenesis of pituitary tumors. *Nat Rev Endocrinol.* (2011) 7:257–66. doi: 10.1038/nrendo.2011.40
4. Grech G, Zhan X, Yoo BC, Bubnov R, Hagan S, Danesi R, et al. EPMA position paper in cancer: current overview and future perspectives. *EPMA J.* (2015) 6:9. doi: 10.1186/s13167-015-0030-6
5. Cheng T, Zhan X. Pattern recognition for predictive, preventive, and personalized medicine in cancer. *EPMA J.* (2017) 8:51–60. doi: 10.1007/s13167-017-0083-9
6. Lu M, Zhan X. The crucial role of multiomic approach in cancer research and clinically relevant outcomes. *EPMA J.* (2018) 9:77–102. doi: 10.1007/s13167-018-0128-8
7. Hu R, Wang X, Zhan X. Multi-parameter systematic strategies for predictive, preventive and personalised medicine in cancer. *EPMA J.* (2013) 4:2. doi: 10.1186/1878-5085-4-2
8. Zhan X, Desiderio DM. Editorial: systems biological aspects of pituitary tumors. *Front Endocrinol.* (2016) 7:86. doi: 10.3389/fendo.2016.00086
9. Golubnjitschaja O, Costigliola V, EPMA. General report & recommendations in predictive, preventive and personalized medicine 2012: White Paper of the European Association for Predictive, Preventive and Personalised Medicine. *EPMA J.* (2012) 3:14. doi: 10.1186/1878-5085-3-14
10. Hood L, Tian Q. Systems approaches to biology and disease enable translational systems medicine. *Genomics Proteomics Bioinformatics.* (2012) 10:181–5. doi: 10.1016/j.gpb.2012.08.004
11. Chen R, Snyder M. Promise of personalized omics to precision medicine. *Wiley Interdiscip Rev Syst Biol Med.* (2013) 5:73–82. doi: 10.1002/wsbm.1198
12. Zhan X, Long Y. Exploration of molecular network variations in different subtypes of human nonfunctional pituitary adenomas. *Front Endocrinol.* (2016) 7:13. doi: 10.3389/fendo.2016.00013
13. Meacham CE, Morrison SJ. Tumour heterogeneity and cancer cell plasticity. *Nature.* (2013) 501:328–37. doi: 10.1038/nature12624
14. Zhan X, Desiderio DM. Heterogeneity analysis of the human pituitary proteome. *Clin Chem.* (2003) 49:1740–51. doi: 10.1373/49.10.1740
15. NSCLC Meta-analysis Collaborative Group. Preoperative chemotherapy for non-small-cell lung cancer: a systematic review and meta-analysis of individual participant data. *Lancet.* (2014) 383:1561–71. doi: 10.1016/S0140-6736(13)62159-5
16. Zhan X, Long Y, Lu M. Exploration of variations in proteome and metabolome for predictive diagnostics and personalised treatment algorithms: innovative approach and examples for potential clinical application. *J Proteomics.* (2018) 188:30–40. doi: 10.1016/j.jprot.2017.08.020
17. Zhan X, Desiderio DM. Signaling pathway networks mined from human pituitary adenoma proteomics data. *BMC Med Genomics.* (2010) 3:13. doi: 10.1186/1755-8794-3-13
18. Stokes MP, Farnsworth CL, Moritz A, Silva JC, Jia X, Lee KA, et al. PTMScan direct: identification and quantification of peptides from critical signaling proteins by immunoaffinity enrichment coupled with LC-MS/MS. *Mol Cell Proteomics.* (2012) 11:187–201. doi: 10.1074/mcp.M111.015883
19. Musat M, Korbonits M, Kola B, Borboli N, Hanson MR, Nanzer AM, et al. Enhanced protein kinase B/Akt signalling in pituitary tumours. *Endocr Relat Cancer.* (2005) 12:423–33. doi: 10.1677/erc.1.00949
20. Dworakowska D, Wlodek E, Leontiou CA, Igreja S, Cakir M, Teng M, et al. Activation of RAF/MEK/ERK and PI3K/AKT/mTOR pathways in pituitary adenomas and their effects on downstream effectors. *Endocr Relat Cancer.* (2009) 16:1329–38. doi: 10.1677/ERC-09-0101
21. Formosa R, Gruppetta M, Falzon S, Santillo G, DeGaetano J, Xuereb-Anastasi A, et al. Expression and clinical significance of Wnt players and survivin in pituitary tumours. *Endocr Pathol.* (2012) 23:123–31. doi: 10.1007/s12022-012-9197-8
22. Wu Y, Bai J, Hong L, Liu C, Yu S, Yu G, et al. Low expression of secreted frizzled-related protein 2 and nuclear accumulation of β-catenin in aggressive nonfunctioning pituitary adenoma. *Oncol Lett.* (2016) 12:199–206. doi: 10.3892/ol.2016.4560
23. Ewing I, Pedder-Smith S, Franchi G, Ruscica M, Emery M, Vax V, et al. A mutation and expression analysis of the oncogene BRAF in pituitary adenomas. *Clin Endocrinol.* (2007) 66:348–52. doi: 10.1111/j.1365-2265.2006.02735.x
24. Haar EV, Lee SI, Bandhakavi S, Griffin TJ, Kim DH. Insulin signalling to mTOR mediated by the Akt_PKB substrate PRAS40. *Nat Cell Biol.* (2007) 9:316–23. doi: 10.1038/ncb1547
25. Toulany M, Rodemann HP. Phosphatidylinositol 3-kinase/Akt signaling as a key mediator of tumor cell responsiveness to radiation. *Semin Cancer Biol.* (2015) 35:180–90. doi: 10.1016/j.semcancer.2015.07.003
26. Manning BD, Cantley LC. AKT/PKB signaling: navigating downstream. *Cell.* (2007) 129:1261–74. doi: 10.1016/j.cell.2007.06.009
27. Risso G, Blaustein M, Pozzi B, Mammi P, Srebrow A. Akt/PKB: one kinase, many modifications. *Biochem J.* (2015) 468:203–14. doi: 10.1042/BJ20150041
28. Xu K, Liu P, Wei W. mTOR signaling in tumorigenesis. *Biochim Biophys Acta.* (2014) 1846:638–54. doi: 10.1016/j.bbcan.2014.10.007
29. Copp J, Manning G, Hunter T. TORC-specific phosphorylation of mammalian target of rapamycin (mTOR): phospho-Ser2481 is a marker for intact mTOR signaling complex 2. *Cancer Res.* (2009) 69:1821–7. doi: 10.1158/0008-5472.CAN-08-3014
30. Rosner M, Siegel N, Valli A, Fuchs C, Hengstschläger M. mTOR phosphorylated at S2448 binds to raptor and rictor. *Amino Acids.* (2010) 38:223–8. doi: 10.1007/s00726-008-0230-7
31. Robbins HL, Hague A. The PI3K/Akt pathway in tumors of endocrine tissues. *Front Endocrinol.* (2016) 6:188. doi: 10.3389/fendo.2015.00188
32. Tsukumo Y, Sonenberg N, Alain T. Transcriptional induction of 4E-BP3 prolongs translation repression. *Cell Cycle.* (2016) 15:3325–6. doi: 10.1080/15384101.2016.1224786
33. Bah A, Vernon RM, Siddiqui Z, Krzeminski M, Muhandiram R, Zhao C, et al. Folding of an intrinsically disordered protein by phosphorylation as a regulatory switch. *Nature.* (2015) 519:106–9. doi: 10.1038/nature13999
34. Martineau Y, Azar R, Bousquet C, Pyronnet S. Anti-oncogenic potential of the eIF4E-binding proteins. *Oncogene.* (2013) 32:671–7. doi: 10.1038/onc.2012.116
35. Roux PP, Shahbazian D, Vu H, Holz MK, Cohen MS, Taunton J, et al. RAS/ERK signaling promotes site-specific ribosomal protein S6 phosphorylation via RSK and stimulates cap-dependent translation. *J Biol Chem.* (2007) 282:14056–64. doi: 10.1074/jbc.M700906200
36. Sakre N, Wildey G, Behtaj M, Kresak A, Yang M, Fu P, et al. RICTOR amplification identifies a subgroup in small cell lung cancer and predicts response to drugs targeting mTOR. *Oncotarget.* (2017) 8:5992–6002. doi: 10.18632/oncotarget.13362
37. Sedgwick AE, D'Souza-Schorey C. Wnt signaling in cell motility and invasion: drawing parallels between development and cancer. *Cancers.* (2016) 8:E80. doi: 10.3390/cancers8090080

38. Chambers TJ, Giles A, Brabant G, Davis JR. Wnt signalling in pituitary development and tumorigenesis. *Endocr Relat Cancer.* (2013) 20:R101–11. doi: 10.1530/ERC-13-0005
39. Niehrs C. The complex world of WNT receptor signalling. *Nat Rev Mol Cell Biol.* (2012) 13:767–79. doi: 10.1038/nrm3470
40. Stamos JL, Weis WI. The β-catenin destruction complex. *Cold Spring Harb Perspect Biol.* (2013) 5:a007898. doi: 10.1101/cshperspect.a007898
41. Wang J, Han L, Sinnett-Smith J, Han LL, Stevens JV, Rozengurt N, et al. Positive cross talk between protein kinase D and β-catenin in intestinal epithelial cells: impact on β-catenin nuclear localization and phosphorylation at Ser552. *Am J Physiol Cell Physiol.* (2016) 310:C542–57. doi: 10.1152/ajpcell.00302.2015
42. Chowdhury MK, Wu LE, Coleman JL, Smith NJ, Morris MJ, Shepherd PR, et al. Niclosamide blocks glucagon phosphorylation of Ser552 on β-catenin in primary rat hepatocytes via PKA signalling. *Biochem J.* (2016) 473:1247–55. doi: 10.1042/BCJ20160121
43. Taurin S, Sandbo N, Qin Y, Browning D, Dulin NO. Phosphorylation of beta-catenin by cyclic AMP-dependent protein kinase. *J Biol Chem.* (2006) 281:9971–6. doi: 10.1074/jbc.M508778200
44. Shahab L, Plattner F, Irvine EE, Cummings DM, Edwards FA. Dynamic range of GSK3α not GSK3β is essential for bidirectional synaptic plasticity at hippocampal CA3-CA1 synapses. *Hippocampus.* (2014) 24:1413–6. doi: 10.1002/hipo.22362
45. Moor AE, Anderle P, Cantù C, Rodriguez P, Wiedemann N, Baruthio F, et al. BCL9/9L-β-catenin signaling is associated with poor outcome in colorectal cancer. *EBiomedicine.* (2015) 2:1932–43. doi: 10.1016/j.ebiom.2015.10.030
46. Elston MS, Gill AJ, Conaglen JV, Clarkson A, Shaw JM, Law AJ, et al. Wnt pathway inhibitors are strongly down-regulated in pituitary tumors. *Endocrinology.* (2008) 149:1235–42. doi: 10.1210/en.2007-0542
47. Liu LJ, Xie SX, Chen YT, Xue JL, Zhang CJ, Zhu F. Aberrant regulation of Wnt signaling in hepatocellular carcinoma. *World J Gastroenterol.* (2016) 22:7486–99. doi: 10.3748/wjg.v22.i33.7486
48. Gwak J, Cho M, Gong SJ, Won J, Kim DE, Kim EY, et al. Protein-kinase-C-mediated beta-catenin phosphorylation negatively regulates the Wnt/beta-catenin pathway. *J Cell Sci.* (2006) 119 (Pt 22):4702–9. doi: 10.1242/jcs.03256
49. Mitchell S, Vargas J, Hoffmann A. Signaling via the NFκB system. *Wiley Interdiscip Rev Syst Biol Med.* (2016) 8:227–41. doi: 10.1002/wsbm.1331
50. Ma B, Hottiger MO. Crosstalk between Wnt/β-catenin and NF-κB signaling pathway during inflammation. *Front Immunol.* (2016) 7:378. doi: 10.3389/fimmu.2016.00378
51. Yang J, Li JH, Wang J, Zhang CY. Molecular modeling of BAD complex resided in a mitochondrion integrating glycolysis and apoptosis. *J Theor Biol.* (2010) 266:231–41. doi: 10.1016/j.jtbi.2010.06.009
52. Burotto M, Chiou VL, Lee JM, Kohn EC. The MAPK pathway across different malignancies: a new perspective. *Cancer.* (2014) 120:3446–56. doi: 10.1002/cncr.28864
53. McCubrey JA, Steelman LS, Chappell WH, Abrams SL, Wong EW, Chang F, et al. Roles of the Raf/MEK/ERK pathway in cell growth, malignant transformation and drug resistance. *Biochim Biophys Acta.* (2007) 1773:1263–84. doi: 10.1016/j.bbamcr.2006.10.001
54. Keshet Y, Seger R. The MAP kinase signaling cascades: a system of hundreds of components regulates a diverse array of physiological functions. *Methods Mol Biol.* (2010) 661:3–38. doi: 10.1007/978-1-60761-795-2_1
55. Haagenson KK, Zhang JW, Xu Z, Shekhar MP, Wu GS. Functional analysis of MKP-1 and MKP-2 in breast cancer tamoxifen sensitivity. *Oncotarget.* (2014) 5:1101–10. doi: 10.18632/oncotarget.1795
56. Wang J, Zhou JY, Wu GS. ERK-dependent MKP-1-mediated cisplatin resistance in human ovarian cancer cells. *Cancer Res.* (2007) 67:11933–941. doi: 10.1158/0008-5472.CAN-07-5185
57. Geng J, Fan J, Ouyang Q, Zhang X, Zhang X, Yu J, et al. Loss of PPM1A expression enhances invasion and the epithelial-to-mesenchymal transition in bladder cancer by activating the TGF-β/Smad signaling pathway. *Oncotarget.* (2014) 5:5700–11. doi: 10.18632/oncotarget.2144
58. Lu G, Ren S, Korge P, Choi J, Dong Y, Weiss J, et al. A novel mitochondrial matrix serine/threonine protein phosphatase regulates the mitochondria permeability transition pore and is essential for cellular survival and development. *Genes Dev.* (2007) 21:784–96. doi: 10.1101/gad.1499107
59. Anjum R, Blenis J. The RSK family of kinases: emerging roles in cellular signalling. *Nat Rev Mol Cell Biol.* (2008) 9:747–58. doi: 10.1038/nrm2509
60. McCoy CE, Campbell DG, Deak M, Bloomberg GB, Arthur JS. MSK1 activity is controlled by multiple phosphorylation sites. *Biochem J.* (2005) 387(Pt 2):507–17. doi: 10.1042/BJ20041501
61. Schaller MD. Cellular functions of FAK kinases: insight into molecular mechanisms and novel functions. *J Cell Sci.* (2010) 123(Pt 7):1007–13. doi: 10.1242/jcs.045112
62. Takeda K, Ichijo H. Neuronal p38 MAPK signalling: an emerging regulator of cell fate and function in the nervous system. *Genes Cells.* (2002) 7:1099–111. doi: 10.1046/j.1365-2443.2002.00591.x
63. Hotamisligil GS, Davis RJ. Cell signaling and stress responses. *Cold Spring Harb Perspect Biol.* (2016) 8:a006072. doi: 10.1101/cshperspect.a006072
64. Ouwens DM, de Ruiter ND, van der Zon GC, Carter AP, Schouten J, van der Burgt C, et al. Growth factors can activate ATF2 via a two-step mechanism: phosphorylation of Thr71 through the Ras-MEK-ERK pathway and of Thr69 through RalGDS-Src-p38. *EMBO J.* (2002) 21:3782–93. doi: 10.1093/emboj/cdf361
65. Baregamian N, Song J, Bailey CE, Papaconstantinou J, Evers BM, Chung DH. Tumor necrosis factor-alpha and apoptosis signal-regulating kinase 1 control reactive oxygen species release, mitochondrial autophagy, and c-Jun N-terminal kinase/p38 phosphorylation during necrotizing enterocolitis. *Oxid Med Cell Longev.* (2009) 2:297–306. doi: 10.4161/oxim.2.5.9541
66. Recouvreux MV, Camilletti MA, Rifkin DB, Graciela DT. The pituitary TGFβ1 system as a novel target for the treatment of resistant prolactinomas. *J Endocrinol.* (2016) 228:R73–83. doi: 10.1530/JOE-15-0451
67. Zhou K, Fan Y, Wu P, Duysenbi S, Feng Z, Du G, et al. MicroRNA-145 inhibits the activation of the mTOR signaling pathway to suppress the proliferation and invasion of invasive pituitary adenoma cells by targeting AKT3 *in vivo* and *in vitro*. *Onco Targets Ther.* (2017) 10:1625–35. doi: 10.2147/OTT.S118391
68. Wu Z, Yan L, Liu Y, Cao L, Guo Y, Zhang Y, et al. Inhibition of mTORC1 by lncRNA H19 via disrupting 4E-BP1/Raptor interaction in pituitary tumours. *Nat Commun.* (2018) 9:4624. doi: 10.1038/s41467-018-06853-3
69. Lu M, Wang Y, Zhan X. The MAPK pathway-based drug therapeutic targets in pituitary adenomas. *Front Endocrinol.* (2019) 10:330. doi: 10.3389/fendo.2019.00330
70. Tulipano G, Faggi L, Cacciamali A, Spinello M, Cocchi D, Giustina A. Role of AMP-activated protein kinase activators in antiproliferative multi-drug pituitary tumour therapies: effects of combined treatments with compounds affecting the mTOR-p70S6 kinase axis in cultured pituitary tumour cells. *J Neuroendocrinol.* (2015) 27:20–32. doi: 10.1111/jne.12231

Conflict of Interest: The authors declare that the research was conducted in the absence of any commercial or financial relationships that could be construed as a potential conflict of interest.

Advantages of publishing in Frontiers

OPEN ACCESS
Articles are free to read for greatest visibility and readership

FAST PUBLICATION
Around 90 days from submission to decision

HIGH QUALITY PEER-REVIEW
Rigorous, collaborative, and constructive peer-review

TRANSPARENT PEER-REVIEW
Editors and reviewers acknowledged by name on published articles

Frontiers
Avenue du Tribunal-Fédéral 34
1005 Lausanne | Switzerland

Visit us: www.frontiersin.org
Contact us: info@frontiersin.org | +41 21 510 17 00

REPRODUCIBILITY OF RESEARCH
Support open data and methods to enhance research reproducibility

DIGITAL PUBLISHING
Articles designed for optimal readership across devices

FOLLOW US
@frontiersin

IMPACT METRICS
Advanced article metrics track visibility across digital media

EXTENSIVE PROMOTION
Marketing and promotion of impactful research

LOOP RESEARCH NETWORK
Our network increases your article's readership